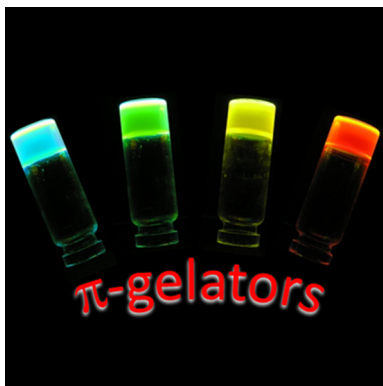


Functional π -Gelators and Their Applications

Sukumaran Santhosh Babu, Vakayil K. Praveen,[†] and Ayyappanpillai Ajayaghosh*

Photosciences and Photonics Group, Chemical Sciences and Technology Division, CSIR-National Institute for Interdisciplinary Science and Technology (CSIR-NIIST), Trivandrum 695019, India



CONTENTS

1. Introduction
 - 1.1. Gelator and the Solvent
 - 1.2. Mechanistic Considerations
 - 1.3. Structural Requirements
 - 1.4. π -Gelators vs Liquid Crystals
2. Photoresponsive Gelators
 - 2.1. Azobenzenes
 - 2.2. Stilbenes
 - 2.3. Butadienes
 - 2.4. Dithienylethenes
 - 2.5. Spiropyrans and Spirooxazines
 - 2.6. 2H-Chromenes
 - 2.7. Diacetylenes
 - 2.8. Cinnamic Acid Derivatives
 - 2.9. Miscellaneous Photoresponsive Gelators
3. Functional Dye Derived Gelators
 - 3.1. Merocyanines
 - 3.2. Naphthalimides
 - 3.3. Perylene Bisimides
 - 3.4. BODIPY Dyes
 - 3.5. Phthalocyanines
 - 3.6. Porphyrins
 - 3.7. Squaraines
 - 3.8. Azo Dyes
 - 3.9. Coumarins
 - 3.10. Dye Doped Gels
 - 3.11. Miscellaneous Dye Based Gelators
4. Gelators Based on Fused Aromatics
 - 4.1. Pyrenes
 - 4.2. Triphenylenes
 - 4.3. *n*-Acenes
 - 4.3.1. Naphthalenes
 - 4.3.2. Anthracenes and Anthraquinones
 - 4.3.3. Tetracenes and Pentacenes
 - 4.4. Fluorenes
5. Heterocycles as Gelators

5.1. Pyrrole	CE
5.2. Indole	CF
5.3. Adenines, Guanines, and Guanosines	CG
5.4. Pyridine Derivatives	CI
5.4.1. Bipyridines	CI
5.4.2. Terpyridines	CJ
5.4.3. Phenanthrolines	CJ
5.4.4. Miscellaneous Pyridine Based Gelators	CK
5.5. Quinolines	CL
5.6. Phenazines	CM
5.7. Riboflavins	CN
5.8. Carbazoles	CN
5.9. Oxadiazoles, Benzoxazoles, and Phenylisoxazoles	CN
5.10. Benzofurans, Benzimidazoles, and Benzo-thiadiazoles	CP
5.11. Tetraphiafulvalenes	CQ
5.12. Miscellaneous Gelators	CT
6. Oligomeric π -Systems Based Gels	CW
6.1. Thiophenes	CX
6.2. Phenylenevinylenes	DC
6.3. Phenyleneethynylennes	DK
6.4. Phenyles	DN
7. Carbon Allotrops and Related Gelators	DS
7.1. Fullerenes (C_{60} s)	DS
7.2. Carbon Nanotubes	DS
7.3. Graphenes	DV
7.4. Coronenes	DW
8. Gels Formed by Miscellaneous Chromophores	DX
9. Applications of π -Gels	DY
9.1. Organic Electronics	DZ
9.1.1. Field Effect Transistors (FETs)	EA
9.1.2. Photovoltaic Devices (PVDs)	EA
9.2. Imaging and Sensing Applications	EB
10. Conclusion and Outlook	ED
Appendix	ED
Author Information	ED
Corresponding Author	ED
Present Address	ED
Notes	ED
Biographies	EE
Acknowledgments	EE
Abbreviations	EE
References	EF

Received: April 10, 2013

1. INTRODUCTION

Supramolecular chemistry originally defined by Lehn as “chemistry beyond molecules” exploits noncovalent interactions between molecules to form 1D, 2D, and 3D architectures.^{1–3} Molecular self-assembly is an offshoot of supramolecular chemistry, which originated as a laboratory curiosity among chemists.^{4,5} Over the years, the study of molecular self-assembly has grown to a matured field of interdisciplinary research by which both biology and material sciences have benefited.^{6–8} When molecules with certain structural features self-assemble, the resulting supramolecular architectures can immobilize a large volume of solvents leading to gelation of the solvent mass.^{9–24} Such molecules can gelate both organic as well as aqueous solvents. In recent years, this area of research has been aggressively pursued by chemists and materials scientists resulting in a wide variety of soft materials.^{25–31} A large number of review articles have appeared in the literature pertaining to general aspects and mechanisms of gelation,^{9–24,32–49} different types of gelators,^{50–78} and their applications.^{25–31,79–111} The basic principles, the structural features of gelators, influence of solvents and role of noncovalent interactions, properties of gels, and their characterization have been discussed in many of those reviews. Readers are advised to refer to previous reviews for a general understanding of the gel chemistry. Even though in many of those reviews chromophore based gels and their properties have been discussed, a comprehensive analysis of the progress with different types of π -systems is not available. Therefore, the main purpose of this review is to bring together a detailed discussion of organogelators based on π -systems, which are named as “ π -gelators”.^{28,44,57} Organogels derived from “ π -gelators” are called “ π -gels” which are soft, nonflowing materials derived from gelators with more than one aromatic π -unit which are either fused as in the case of naphthalene, anthracene, pyrene, etc. or conjugated as in the case of *p*-phenylenevinylenes, *p*-phenyleneethynylens, thiylenevinylenes, etc.

π -systems, by virtue of their delocalized π -electrons,¹¹² have inherent electronic properties such as luminescence,¹¹³ charge carrier mobility, and electronic conductivity.¹¹⁴ Therefore, π -conjugated molecules are extensively used in organic electronic devices such as, LEDs,¹¹⁵ FETs,^{116,117} and PVDs.^{118,119} When π -systems are used in devices by deposition or coating, they exist as aggregates of different size and shape which have influence on electronic properties.¹²⁰ Therefore, controlling the size and shape of molecular aggregates are important for optimum electronic properties.¹²¹ One way to control the size and shape of aggregates is by the “bottom-up” self-assembly approach, utilizing weak forces such as hydrogen bonding and π -stacking interactions.¹²² In this context, gel chemistry has been recognized as a convenient strategy to exploit molecular self-assembly for the creation of supramolecular architectures of nano to microscale dimensions. However, the judicious choice of the molecular components plays a significant role in the design of functional π -gels with controlled size and shape.

1.1. Gelator and the Solvent

In an organogels, solvent is the major component which gets gelled by the gelator which is the minor component. Therefore, nature of the solvent is a crucial factor in the gelation process. For example, polarity, functional groups, hydrophobic–hydrophilic character, viscosity etc. are influential in deciding the net property of the resultant gel. The balance of gelator–solvent and gelator–gelator interactions is determined by the solvent

polarity and temperature.^{41,123,124} Ability of the solvent to disrupt the hydrogen bonding between the gelator molecules can severely retard the gelation of solvents. Solvents have a critical role in assisting the nucleation and growth processes of the self-assembly¹²⁵ and the consequent gelation.^{41,126} For a homogeneous solution of the gelator, the solvent should have the ability to compete with the intergelator interaction whereas in the case of gelation, solvents favor the intergelator interactions.⁴¹ Hence the dielectric constants¹²⁷ and the Hansen solubility parameters^{128–130} for the gelator as well as for the solvent are important.^{131,132} Recent studies revealed that once the gelation is complete, the solvent trapped inside the gel fibrous structures becomes mechanically passive.^{133–136} The mechanical strength of gels and the ability to reset could be varied with the volume fraction of the solvent used.^{133–136} The importance of the chemical structure of the gelator and the type of solvent molecules used in gelation have been established in a recent study.¹³⁷ In the case of most of the π -gelators, nonpolar or lowpolar hydrocarbon solvents have been found to be suitable for gelation. Nevertheless, the nature of the gelator is also a deciding factor on the choice of the appropriate solvent for the preparation of the gels.

1.2. Mechanistic Considerations

Even though, there are numerous approaches toward the design of supramolecular gelators, in the earlier period most gelators are found rather by serendipity than by design. However, the following features of gelation are considered to be important in the design of new organogelators: (1) formation of 1D aggregates via anisotropic growth process, (2) intertwining of these 1D aggregates to form a 3D network, and (3) the prevention of crystallization or precipitation of the self-assembled aggregate through a delicate balance between order and disorder (Figure 1). Hence, the design of new

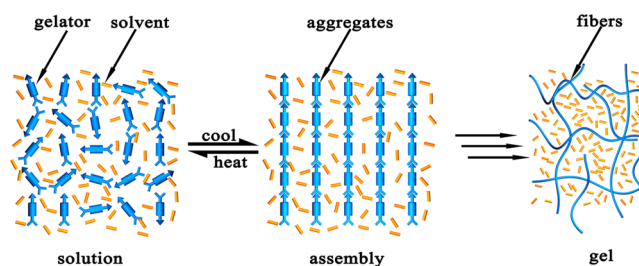
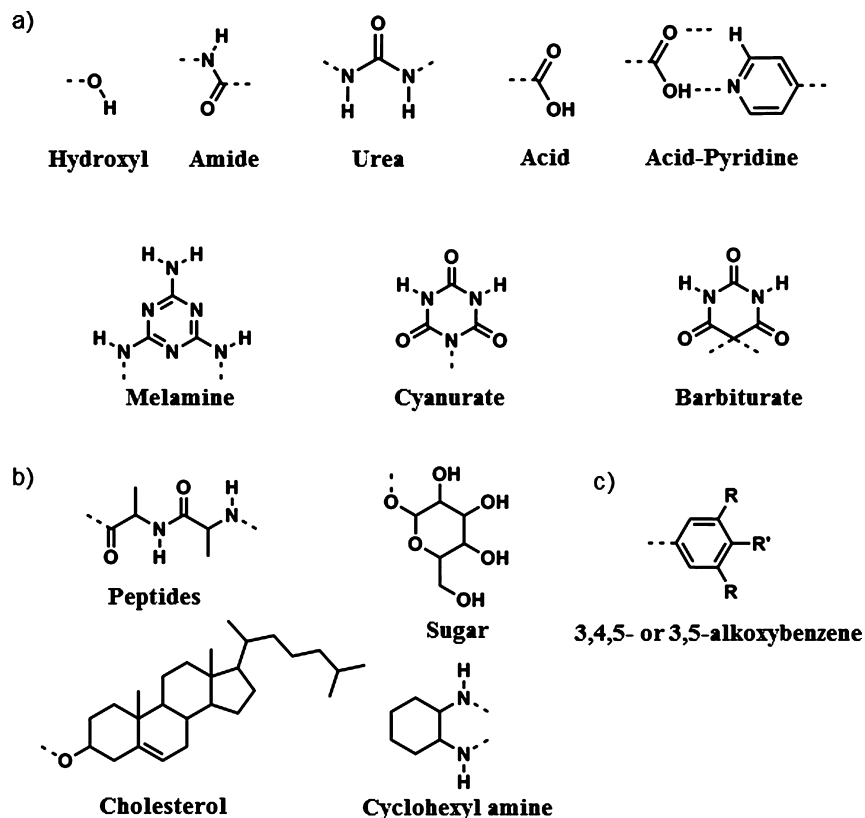


Figure 1. Schematic representation of the self-assembly of low molecular weight gelators into one-dimensional aggregates and the subsequent formation of an entangled network.

gelling agents continues to be a challenging task. The knowledge gained from the aggregation of gelator molecules during the past decade, has enabled gelators to be “designed” through the incorporation of structural features that are known to promote aggregation. This novel class of supramolecular materials exhibits striking properties with respect to self-assembly phenomena leading to diverse architectures.

Gelation is normally observed when a homogeneous solution of the gelator, obtained by heating a required amount in a suitable solvent, is cooled to room temperature or below. Supersaturation-mediated nucleation and growth is found to be the driving force for the gel nanostructure formation.⁴¹ As evidenced in the recent studies of chiral and achiral perylene bisimide gelators, a marked difference is observed in the aggregation process at low and high concentration of the

Chart 1. Structural Requirements for the Design of Gelators



gelator upon slow cooling.¹³⁸ At a lower concentration thermodynamically stable aggregates are formed, whereas the kinetically favored products are preferably formed at higher concentrations, especially for organogels upon cooling. The fast nucleation and growth process at the initial stages of aggregation rapidly converts to kinetically stable fibrous aggregates, which hold a large excess of solvent molecules to form organogels.

1.3. Structural Requirements

Even though the chemical structure of many of the gelators looks rather simple, it is difficult to precisely predict the structural requirements for molecules to show gelation property. However, the information gained from a variety of different types of gelators helped in rationalizing the general structural requirements of molecular gelators. In majority of the cases, presence of functional groups such as hydroxyl, amide, urea and carboxylic acid that are capable of forming hydrogen bonded assemblies has been proved to be essential for gelation. The directionality, specificity and rigidity of multiple hydrogen bonding interactions help spatial arrangement of functional chromophores in achieving efficient gelation. For example, the complexation between ditopic *N,N'*-disubstituted melamine type DAD module and barbiturate or cyanurate type ADA modules as well as the complementary interactions of acid-pyridine derivatives have also been widely used for gelation (Chart 1a). Molecules with structural motifs such as amino acids, peptides, cholesterol, sugar, cyclohexyl amine, chiral/achiral aliphatic/oligoethylene chains (Chart 1b), etc. have been found to facilitate gelation of a variety of solvents.

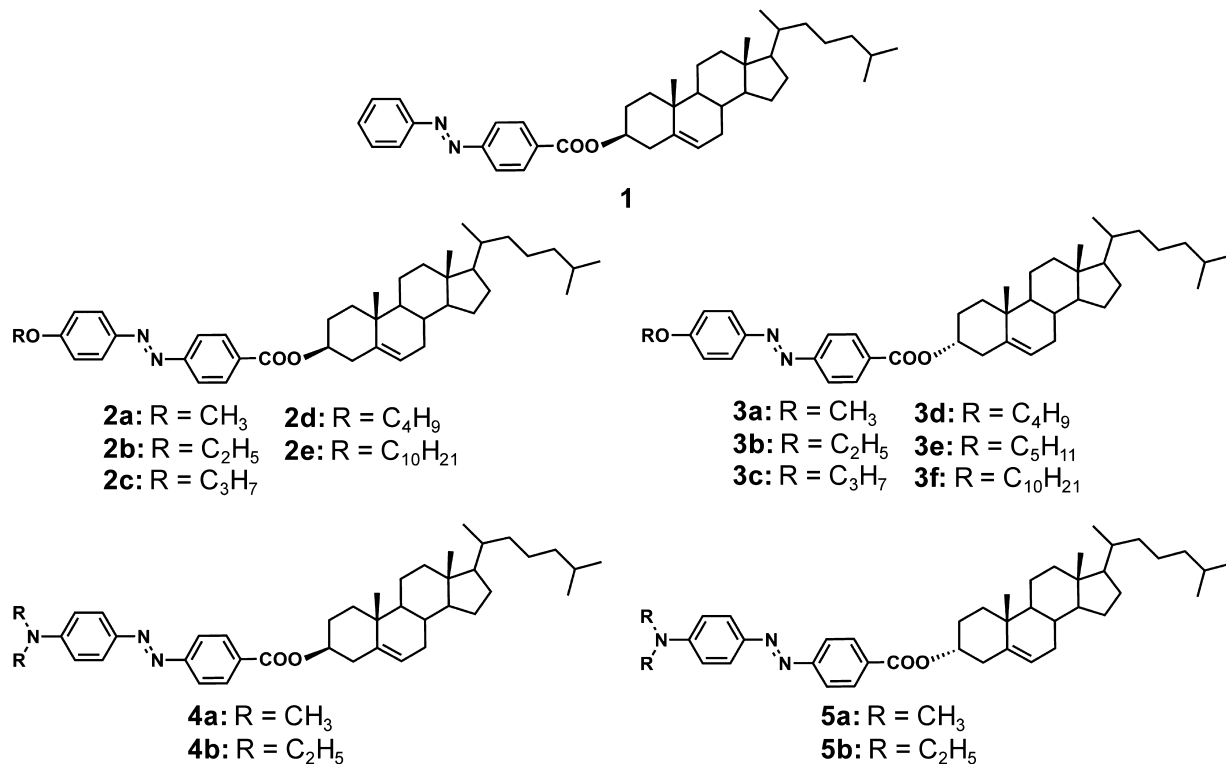
Presence of an aromatic core that helps $\pi-\pi$ stacking is another requirement for the design of organogelators. Molecules that facilitate dipole-dipole and donor-acceptor

interactions can also lead to the gelation of solvents. Another important structural requirement for molecules to assist gelation is the presence of long hydrocarbon chains with a certain optimum chain length. For example, functionalization of molecules with 3,4,5- or 3,5-alkoxy substituted benzene (Chart 1c) moieties helps to induce gelation. The presence of alkoxy chains maintains the subtle balance between solubility and precipitation of the gelator molecules in a given solvent. The presence of hydrocarbon chains also facilitates van del Waals interaction of gelator molecules. In a majority of cases, more than one such structural requirement is essential for the design of gelator molecules, even though there are exceptions.

1.4. π -Gelators vs Liquid Crystals

π -gelators and liquid crystals (LCs) are a significantly different class of soft materials with distinct properties. They have important applications in certain domains of advanced materials. In this respect LCs have an advantage over π -gelators due to the proven application history of the former whereas π -gelators are still waiting for a major breakthrough in application. However, π -gelators have advantages over LCs in terms of the diversity of the architectural shape and size with tunable properties. Apart from the aesthetic architectural features, chromophore based gelators are interesting from the viewpoint of their electronic properties which can be significantly modulated by self-assembly and gelation. After discussing the gelation, morphology, and associated properties of π -gelators derived from a different class of molecules, we briefly review their application, mainly in organic electronic devices, sensing, and imaging. Even though a large number of gelators have already been investigated for their functional properties, these soft materials are yet to be exploited for advanced applications. It is an emerging area, and therefore

Chart 2



viable strategies with innovative ideas and immense care need to be implemented to improve the quality and efficiency of the devices based on π -gelators.

The progress achieved in gel chemistry has been tremendous and almost every class of molecules has been touched so far in search of new gelators. Atleast one new molecule may be getting added everyday as judged from the frequency of reports appearing in various scientific journals. Therefore, it is difficult to discuss all of them at one place. Due to this reason, while discussing different types of π -gelators, we have excluded gelators based on metallo supramolecular assemblies, hydrogels, and ionic gels derived from simple amino acids, peptides, and carbohydrates since several recent reviews are available on these topics. We rather focus on π -gelators based on photoresponsive chromophores, functional dyes, fused polyaromatics, heterocycles, functional dyes, oligomeric conjugated π -systems, and carbon allotrops. We have minimized discussions related to gelators obtained from simple functional derivatives of aromatic molecules such as benzene, pyrrole, or thiophene. However, we have included peptide and sugar based gelators having fused aromatics and functional dyes attached to them as borderline cases of π -gelators for the benefit of readers. The nonaromatic diacetylenes and several miscellaneous systems such as DNA bases and riboflavines are also included in this review to give a wider perspective of the topic to readers. For a better understanding, we have classified gelators discussed in this review into different categories according to the general nomenclature of molecules.

2. PHOTORESPONSIVE GELATORS

Organogels based on photoresponsive chromophores are of great interest since their properties can be modulated using light as an external trigger.^{139–149} For example, upon photoradiation, gel can be transformed into a viscous liquid

or a solution. In many cases, the size and shape of the xerogel morphology can be manipulated with light, leading to a change in their electronic properties. Such change in photoinduced physical processes can be achieved by trans–cis isomerization, 2 + 2 dimerization, photoscission, or photopolymerizations of the chromophore derived gelators. The most commonly used photoresponsive chromophores for the design of photoresponsive gels are azobenzene, stilbene, diarylethene, and spiropyran.^{139–151}

2.1. Azobenzenes

Azobenzene derivatives have been studied for the design of photoresponsive gels. The reversible photoinduced trans–cis isomerization of azobenzene unit^{140,150–152} significantly influence the gelation ability of the associated gelators. A major limitation of the azobenzene systems is the thermal back isomerization under dark conditions. Moreover, a complete conversion of the trans to the cis isomer cannot generally be accomplished. However, the large volume and polarity changes associated with the trans to the cis isomerization can induce considerable variation in the properties even with partial isomerization yield. Due to the large steric repulsion of the cis isomers, they have relatively weak association constants resulting in the destruction of the self-assembly.

Shinkai and co-workers have made significant contributions to azobenzene derived gelators. In their first report, gelation of two types of gelators 1–6 (Chart 2 and Figure 2) with steroid skeletons having either the natural (*S*) configuration or the inverted (*R*) configuration have been studied.^{153,154} Among them, the gelator with a *p*-alkoxy azobenzene moiety is the most efficient and can gelate either nonpolar solvents (*S* derivatives, 2a–e) or polar solvents (*R* derivatives, 3a–f). It is possible to “read-out” the sol–gel phase transition as well as the chirality of the supramolecular stacks using CD spectroscopy.

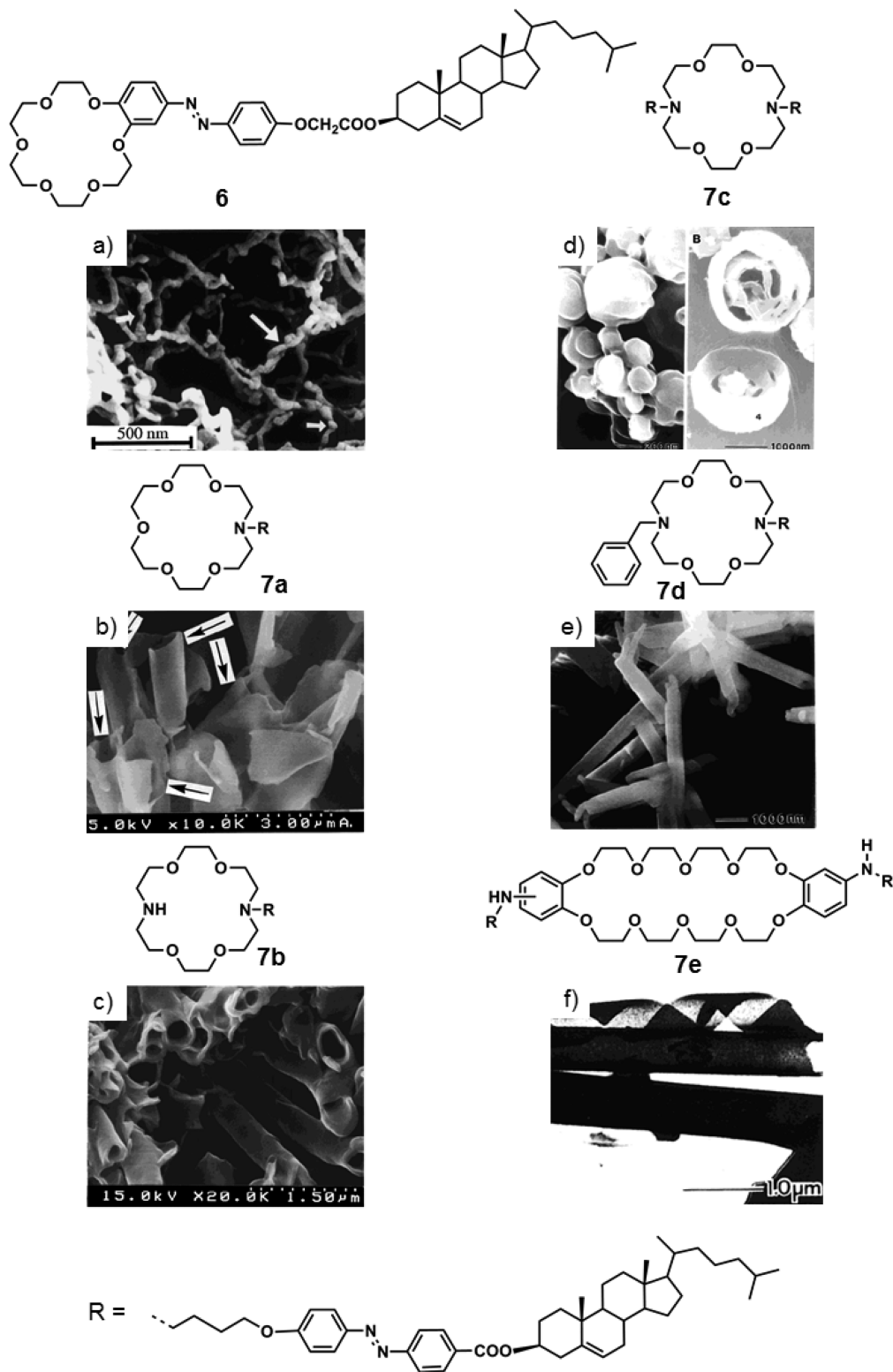


Figure 2. SEM and TEM images of gel nanostructures of azacrown appended cholesterol gelators. (Panels a–c, reprinted with permission from ref 157. Copyright 2000 American Chemical Society. Panels d and e reprinted with permission from ref 159. Copyright 2000 American Chemical Society. Panel f, reprinted with permission from ref 161. Copyright 2001 American Chemical Society.)

py.^{153,154} For example, the 1-butanol gel of **2a** showed a positive exciton coupling whereas methanol gel of **3b** showed a negative exciton coupled band characteristic of the clockwise and anticlockwise orientation of the azobenzene dipoles in the

gel state, respectively. The SEM pictures of the xerogels showed helical fibers that complement the observed CD spectra.

Detailed morphological studies of a variety of azacrown appended cholesterol gelators, have revealed the formation of supramolecular architectures of different shape and size.^{153–162}

Chart 3

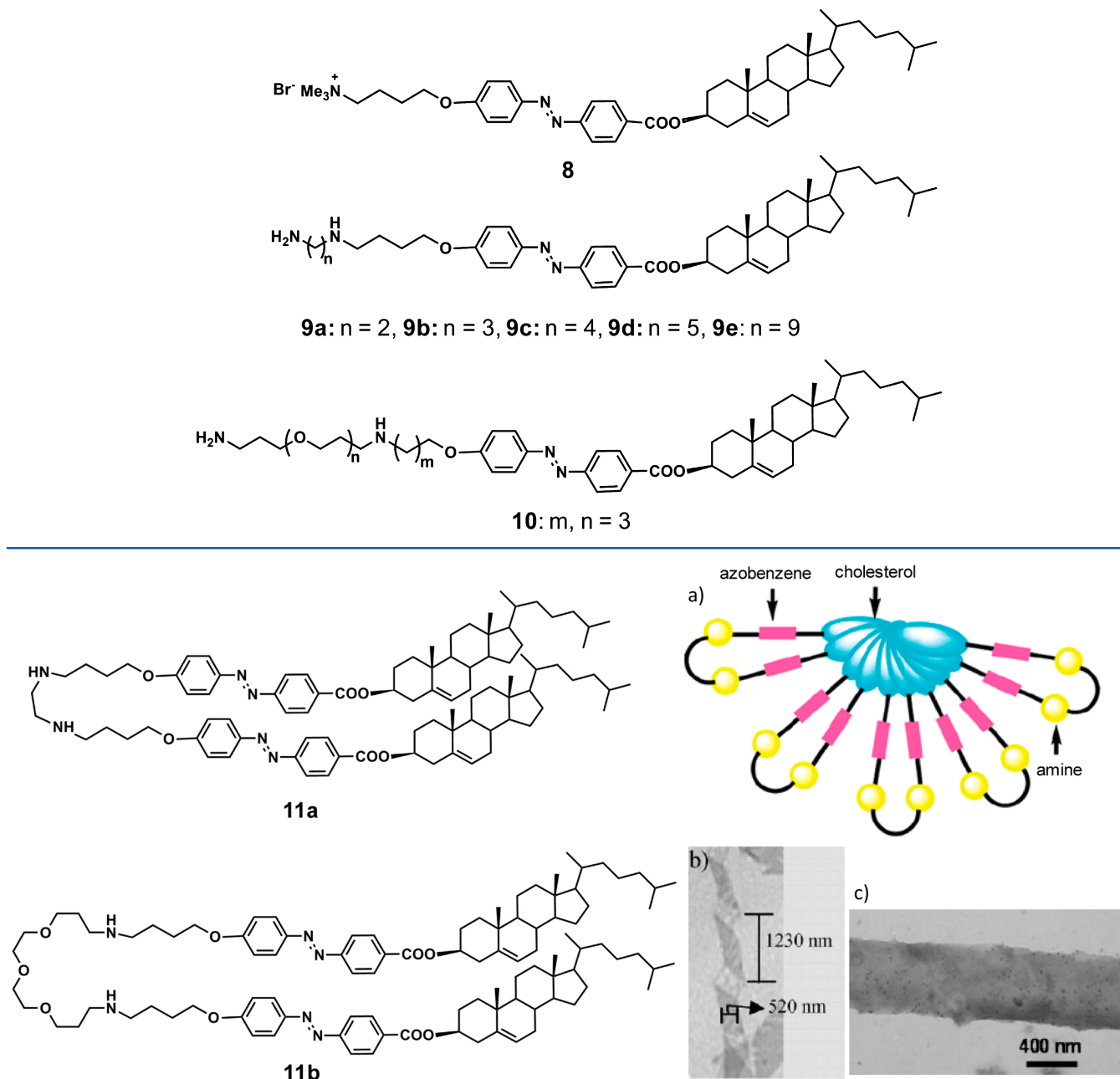


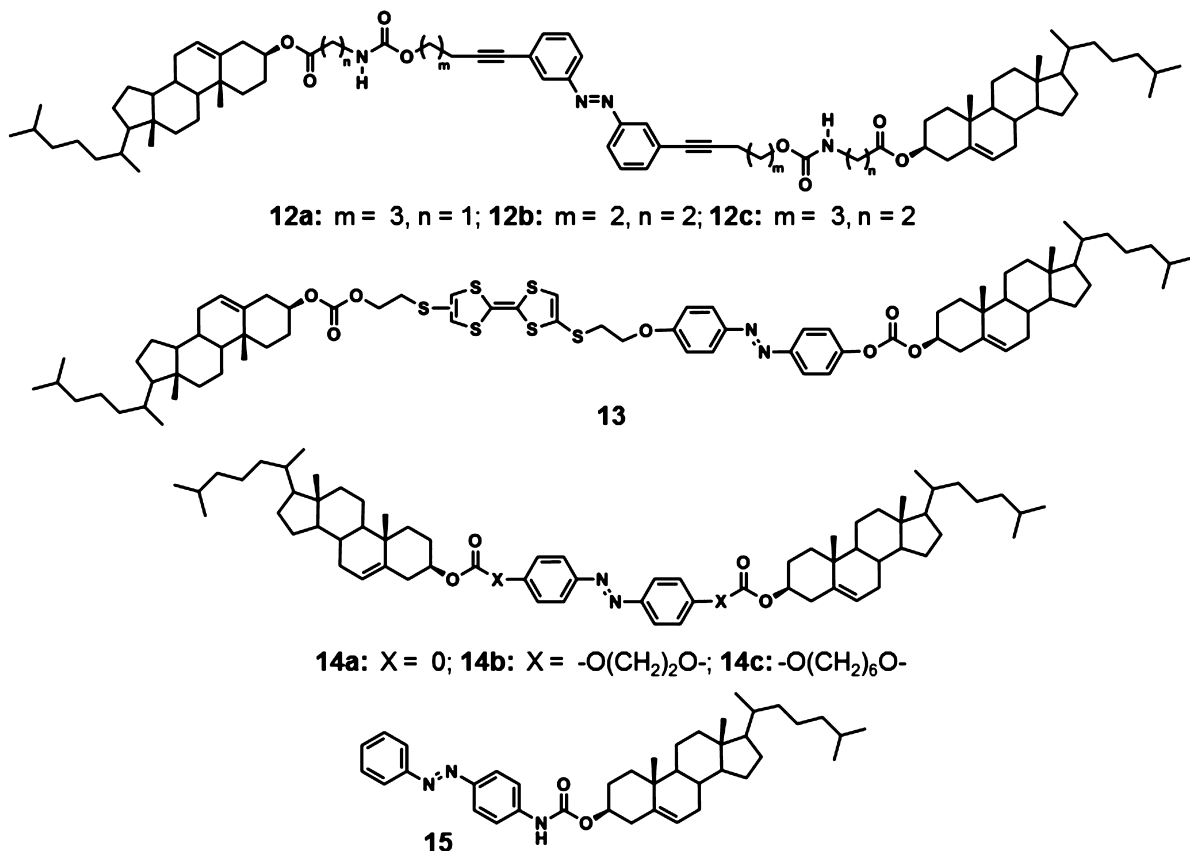
Figure 3. (a) Schematic representation of 1D molecular stacking of **11a**. TEM images of (b) helical ribbon and (c) tubular structure of self-assembled **11b** in the absence and presence of Pd metal ion. (Panel a reprinted with permission from ref 170. Copyright 2003 American Chemical Society. Panels b and c reprinted with permission from ref 171. Copyright 2005 The Royal Society of Chemistry.)

The xerogel of **6** in cyclohexane showed the fibrous network structure with 25–62 nm diameter, which were partially twisted in a helical fashion (Figure 2a).¹⁵⁷ The SEM pictures of the dried samples of **7a** (Figure 2b) showed curved film like aggregates with 30–40 nm thickness.^{157,158} As shown in Figure 2c, the xerogel of **7b** exhibited a tubular structure with 45–75 nm wall thickness and 170–390 nm inside tube diameter.¹⁵⁷ The growth of a few layered and curved lamellae is observed in the case of **7a** (Figure 2b) whereas continuous growth of multilayered “paper like roll” structure is observed for **7b** (Figure 2c). In contrast to the common fibrous or plate like aggregates of organogels, a multilayered spherical morphology was observed for the xerogel of **7c** (Figure 2d) whereas a

cyclohexane gel of **7d** showed the presence of rolled film-like structure (Figure 2e).^{159,160} The xerogel of **7e** exhibited a tubular structure with 520 nm outer diameter and also showed the presence of linear and the helical ribbons with 1700–1800 nm pitch (Figure 2f).^{161,162} Observation of such a wide variety of self-assembled structures indicate the feasibility of preparing diverse architectures with controlled morphology which are otherwise difficult to obtain.

An interesting aspect of the above studies is the use of the self-assembled architectures as templates for the creation of exotic inorganic silica structures which are difficult to obtain by conventional methods.¹⁶⁴ For example the sol–gel polymerization of TEOS in the presence of various supramolecular

Chart 4



structures of the gelators resulted in spherical, tubular and rolled-paper-like silica structures.^{163–166} SAXS studies revealed that the gel fibers of the ionic gelator **8** (Chart 3) is amorphous whereas that of the nonionic gelator **3c** (Chart 2) is crystalline.¹⁶⁴ An important finding of these studies is that ionic as well as amorphous nature of the fiber is essential for silica transcription by template reaction.^{163–166}

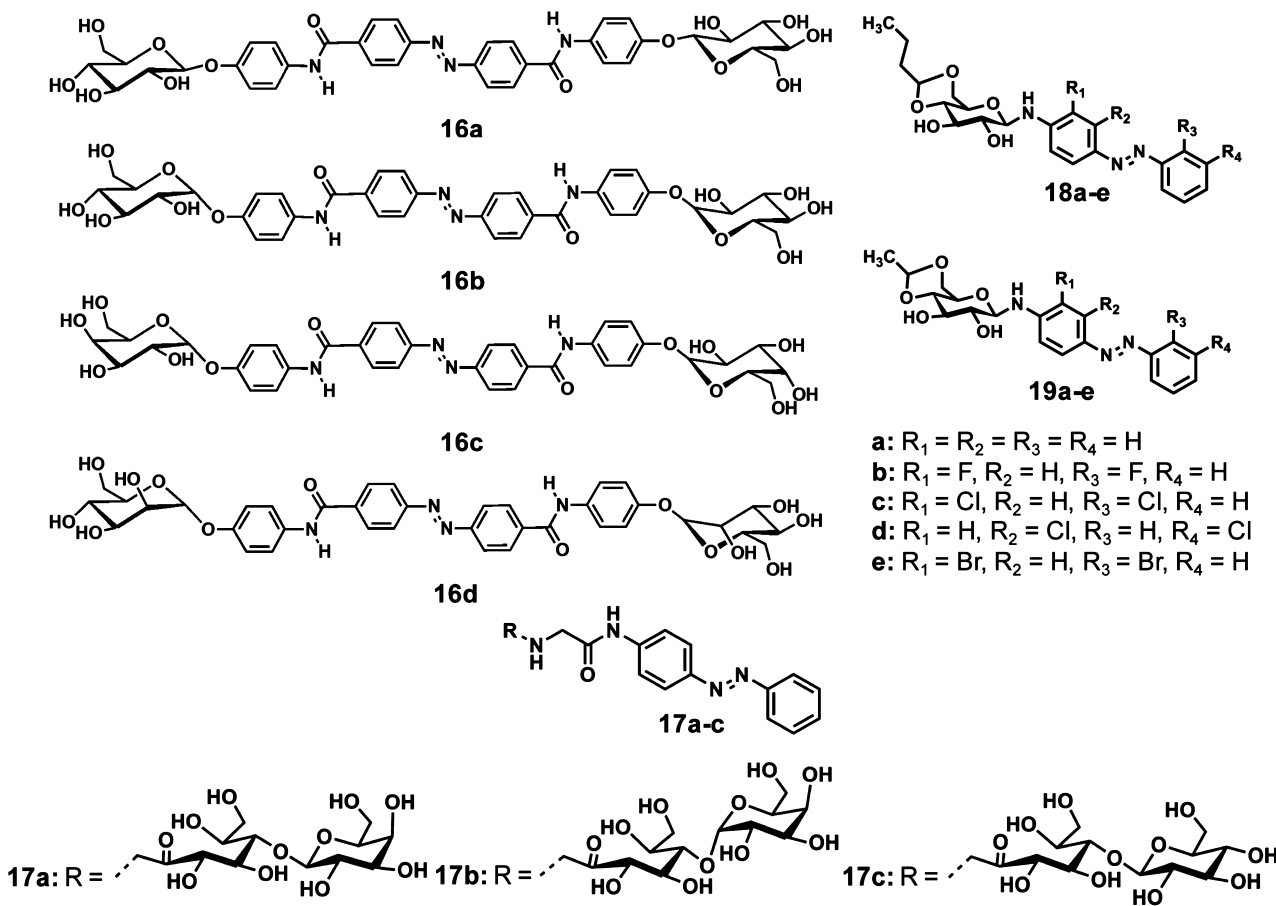
The “Gemini” type azobenzene functionalized cholesterol based gelators **9a–e** (Chart 3) exhibit an odd–even effect in gelation.^{167,168} Compounds **9a** and **9c** having an even number of methylene units between NH and NH_2 formed translucent organogels. The SEM images showed lamellar structured film-like aggregates with 60–330 nm thickness and a few micrometer lengths. The gelators **9b** and **9d** having an odd number of methylene units formed transparent organogels having fibrous structures of diameters 20–50 and 10–70 nm, respectively. In another study, it has been demonstrated that the morphologies of the self-assembled azobenzene-cholesterol gelators could be controlled by the balance of the solvophilic and solvophobic groups in organic solvents.¹⁶⁹ The self-assembled gelator **9e** (Chart 2) showed a fibrous structure with 200–300 nm diameters, whereas the gelator **10** (Chart 3) exhibited a tubular structure with a uniform external diameter of ca. 560 nm, with a wall thicknesses of 50 nm.¹⁶⁹

The dimeric azobenzene appended cholesterol based organogelator **11a** (Figure 3) adopts a folded conformation in the self-assembled state to have an efficient intramolecular and intermolecular cholesterol-cholesterol and azobenzene-azobenzene interactions (Figure 3a).¹⁷⁰ Compound **11b** (Figure 3) is found to form helical ribbon and tubular structures in the absence and presence of Pd metal ion,

respectively (Figure 3b,c).¹⁷¹ This is attributed to the change in the balance between hydrophobicity and hydrophilicity in **11b** upon complexation with metal ions. Using this gelator, the sol–gel transcription method has been shown to be effective to the formation of palladium-doped double-walled silica nanotubes.¹⁷²

Azobenzenes **12a–c** (Chart 4), functionalized with two urethane moieties linked to two cholesterol ester units form gels that exhibit sol–gel phase transitions upon photo-irradiation as a result of trans–cis isomerization of the azobenzene units. During the sol–gel phase transitions, hydrogen bonds, which are partly responsible for stabilizing the gels are broken or reformed.¹⁷³ In a bischolesterol functionalized gelator **13** (Chart 4), in addition to the photoresponsive property of the azobenzene moiety, a redox activity has been introduced by adding a TTF moiety. Therefore, this gelator allows both photo and redox control of the electronic properties.¹⁷⁴ Recently, a series of photo-responsive dicholesterol linked azobenzene gelators **14a–c** (Chart 4) with different spacer lengths have been reported.¹⁷⁵ Detailed studies revealed that spacer groups dramatically affect the gelation properties. Accordingly, **14b** with a spacer of two methylene units is found to be the best gelator. In addition to the effect of spacer groups, the effect of methanol as a cosolvent on the gelation of cyclopentanone by **14b** has been studied.¹⁷⁶ The addition of methanol is found to modulate the speed of gelation, photoresponsive property and the morphology of the gel nanostructures. This study highlights the importance of the solvent-gelator interaction in tuning the properties of the resultant gel. A cholesterol imide appended azobenzene gelator **15** (Chart 4) exhibited reversible sol–gel transition via

Chart 5



photoisomerization of the azobenzene moiety upon irradiation with UV and visible lights.¹⁷⁷

A family of hydrogelators based on azobenzene appended sugar bolaamphiphiles, **16a–d** (Chart 5), has been reported jointly by Shinkai and Reinhoudt.¹⁷⁸ These bolaamphiphiles consist of two solvophilic aminophenyl sugar skeletons as the chiral aggregate forming site and a solvophobic azobenzene moiety as the $\pi-\pi$ stacking site. Compound **16a** is found to be a “super” hydrogelator, as it can form gels even at concentrations as low as 0.05 wt %, whereas compound **16b** could gelate only a 1:1 (v/v) DMSO-water solvent mixture. On the otherhand, **16c** and **16d** could not gelate any of the solvents investigated. These observations reveal that the conformation of the sugar moieties has significant influence on the gelation property.

The sugar derivatives **16a** and **16b** were reported to form right handed helical aggregates in 1:1 (v/v) DMSO-water, whereas **16c** and **16d** formed left handed helical aggregates as is evident from the corresponding exciton coupled CD spectra. TEM studies revealed right handed helical fibrillar structures (Figure 4b) for the aggregates of **16a** and **16b**, reflecting the microscopic 1D columnar orientation of azobenzene chromophores. However **16c** and **16d** tend to aggregate into vesicular structures as a result of their 2D aggregation mode and failed to form gels. Addition of boronic acid appended poly(L-lysine) (Figure 4a) to the gel phase of **16b** resulted in the formation of sol phase with a morphological transition from fibrous aggregate (Figure 4b) to vesicular aggregate (Figure 4c,d).¹⁷⁹ These macroscopic and microscopic level changes are due to

the specific boronic acid-sugar interaction and can be reverted using D-fructose, which has high affinity toward the boronic acid group.

The sugar coated nanofibers formed by a combination of azobenzene and disaccharide lactones **17a–c** (Chart 5) provided a bioactive interface for cell attachment and exhibited lectin binding.¹⁸⁰ In addition, the hydrogels exhibited a reversible sol–gel transition in response to temperature and UV irradiation. The latest report on a photoresponsive gelator pertains to a sugar based amphiphilic system containing an azobenzene moiety **18** and **19** (Chart 5).¹⁸¹ The partial trans–cis isomerization of the azobenzene moiety allows photo-induced chopping of the entangled long fibers to short fibers, resulting in controlled fiber length and gel–sol transition. These gelators facilitate phase selective gelation of aromatic solvents from aqueous emulsion. Such a phase selective gelation is useful for the removal of small amounts of toxic solvents from water.

Feringa and co-workers have reported chiral recognition in hybrid gel assemblies of alkyl substituted 1,2-bis-(uridocyclohexane) derivatives (*S*)-**20**, (*R*)-**20**, and the azobenzene incorporated derivatives (*S*)-**21** and (*R*)-**21** (Figure 5).¹⁸² The CD spectra of (*R*)-**21** in 1-butanol gel of (*S*)-**20** showed a slightly more intense bisignate CD signal than that of a solution of (*R*)-**21** in 1-butanol, indicating that the environment of (*R*)-**21** is less polar when it is incorporated into aggregates of (*S*)-**20** than in 1-butanol (Figure 5a). However, incorporation of (*R*)-**21** in a gel of (*R*)-**20** results in a strong positive Cotton effect, which is not exciton coupled,

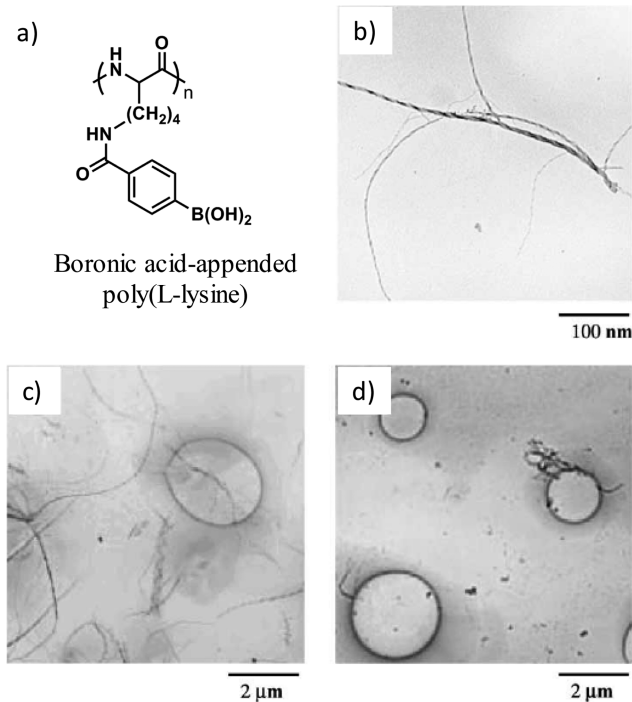


Figure 4. (a) Structure of a boronic acid appended poly(L-lysine) used as an additive to the gelator **16b**. TEM images of **16b** (b) alone and (c and d) with increasing concentration of boronic acid appended poly(L-lysine). (Reprinted with permission from ref 179. Copyright 2002 The Royal Society of Chemistry.)

indicating that the azobenzene groups are no longer stacked but incorporated between the closely packed alkyl chains of (*R*)-**20** aggregate as shown in Figure 5b.

The simple bisurea appended azobenzene derived organogelators **22a** and **22b** (Figure 5) are reported to show distinct gelation behavior.¹⁸³ For example, the 4,4'-disubstituted derivative (**22a**) is found to be a poor gelator, whereas the 2,2'-disubstituted derivative (**22b**) is an excellent gelator of a variety of organic solvents at concentrations as low as 0.2 mM. Interestingly, **22b** showed remarkable polymorphism in their gel state leading to two different types of supramolecular aggregates, which differ in the stacking of chromophore moiety as well as in their hydrogen bonding patterns, as evident from the differences in the UV/vis absorption and IR spectra. This novel observation of polymorphism in organogels was found to depend on the solvent polarity and kinetic factors.

Use of a liquid crystal (LC) as a medium to self-assemble azobenzene derivatives **23** and **24** (Chart 6) is a facile way of preparing an LC gel with aligned gelator molecules.^{184–188} Thus, the anisotropic LC physical gels can be prepared in the absence of any external effect, by slowly cooling a nematic LC/**23** mixture, cast as a thin film on a glass surface or calcium fluoride crystal windows from the isotropic phase.¹⁸⁴ It has been found that the LC environment has strong influence on the gelation properties of **24**.¹⁸⁵ By utilizing the light induced structural reorganization of **23** in the LC gel state, electrically switchable volume gratings can be prepared without using patterned electrodes.¹⁸⁶ The photoluminescence intensity of CdSe/ZnS QDs dispersed in a cholesteric LC can be switched using the gel network of **23** in presence of a covalently cross-linked polymer to configure the changes in the LC orientational state in response to an electric field.¹⁸⁷ In addition, using the

gelator **24** and a ferroelectric LC, gels showing interesting electrooptical properties could be designed.¹⁸⁸

Ikeda, Kato and co-workers have reported a chiral azobenzene **25** (Chart 6) containing a cyclic *syn*-carbonate moiety that self-assembles via dipole–dipole interactions to form a photoswitchable organogel.¹⁸⁹ They have also demonstrated photoresponsive properties of anisotropic physical gels (Figure 6) composed of **26** (Chart 6) and a room temperature nematic LC 4-cyano-4'-pentyl-biphenyl.¹⁹⁰ The photoinduced gel–sol transition of the physical gel upon UV irradiation at room temperature leads to the trans–cis photoisomerization which induces the transition from nematic LC gel (Figure 6b) to a cholesteric sol phase (Figure 6c). Subsequent visible light irradiation or keeping the sol at room temperature causes cis–trans photoisomerization of the azobenzene moiety leading to regelation. During this process, the cholesteric molecular alignment in the sol phase (Figure 6c) behaves as a template for the aggregation of gelators into cholesteric LC gel (Figure 6d). The polarity change of the azobenzenes in **26** should be a key factor to the induction of photo stimulated on–off switching of the hydrogen bonding which eventually led to the gel–sol transition.^{191,192} Light induced complex structural changes were also reported for LC gels consisting of **26** and a discotic LC 2,3,6,7,10,11-hexahexyloxytriphenylene.¹⁹¹

Another series of azobenzene based photoresponsive organogelators functionalized with semicarbazide groups **27a–e** (Chart 6) as hydrogen bonding motifs have been reported by Zentel and co-workers.^{193–195} Compounds **27c** and **27e** were found to gelate smectic phase of a chiral smectic C* LC material and stabilize the LC director pattern present during the gel formation upon application of a DC electric field.¹⁹⁴ The photoinduced gel to sol transition of the LC physical gel of **27c** and **27e** could be monitored by using magnetic polymer colloids entrapped in the gel fibers. Upon irradiation, the magnetic polymer colloids start to move and align in the direction of the external magnet, indicating collapse of the gel nanostructures.¹⁹⁵

The azobenzene appended melamine (**28**) and the complementary H-bonding barbiturate (**B1**) or cyanurate (**C1**) derivatives (Figure 7) have been exploited for the preparation of photoresponsive rosette assemblies.¹⁹⁶ In aliphatic solvents, a rosette possessing the sterically bulky tridodecyloxyphenyl substituent in the barbiturate component **B1** does not hierarchically organize into higher order columnar aggregates. However, the sterically nondemanding *N*-dodecyl-cyanurate **C1** results hierarchically organized elongated columnar fibrous aggregates in cyclohexane, which eventually leads to the formation of an organogel (Figure 7). Dynamic light scattering and UV/vis studies revealed that the dissociation and the reformation of columnar aggregates could be controlled by the trans–cis isomerization of the azobenzene moiety. The molecular modeling study indicates that the rosette possessing azobenzene side chains loses its planarity upon irradiation resulting in the disruption of the aggregates and hence the dissociation of the organogel.

Due to tight molecular packing in the supramolecular polymeric gel fibers of the coassembled azobenzene tethered melamine dimer **29** (Chart 7) and cyanurate/barbiturates (**C1/B1** and **B2**; Figure 7 and Chart 7), the azobenzene moiety in the gel state showed resistance to photoisomerization.¹⁹⁷ Therefore, this system loses the photoresponsive character of the assembly. On the other hand, the azobenzene-function-

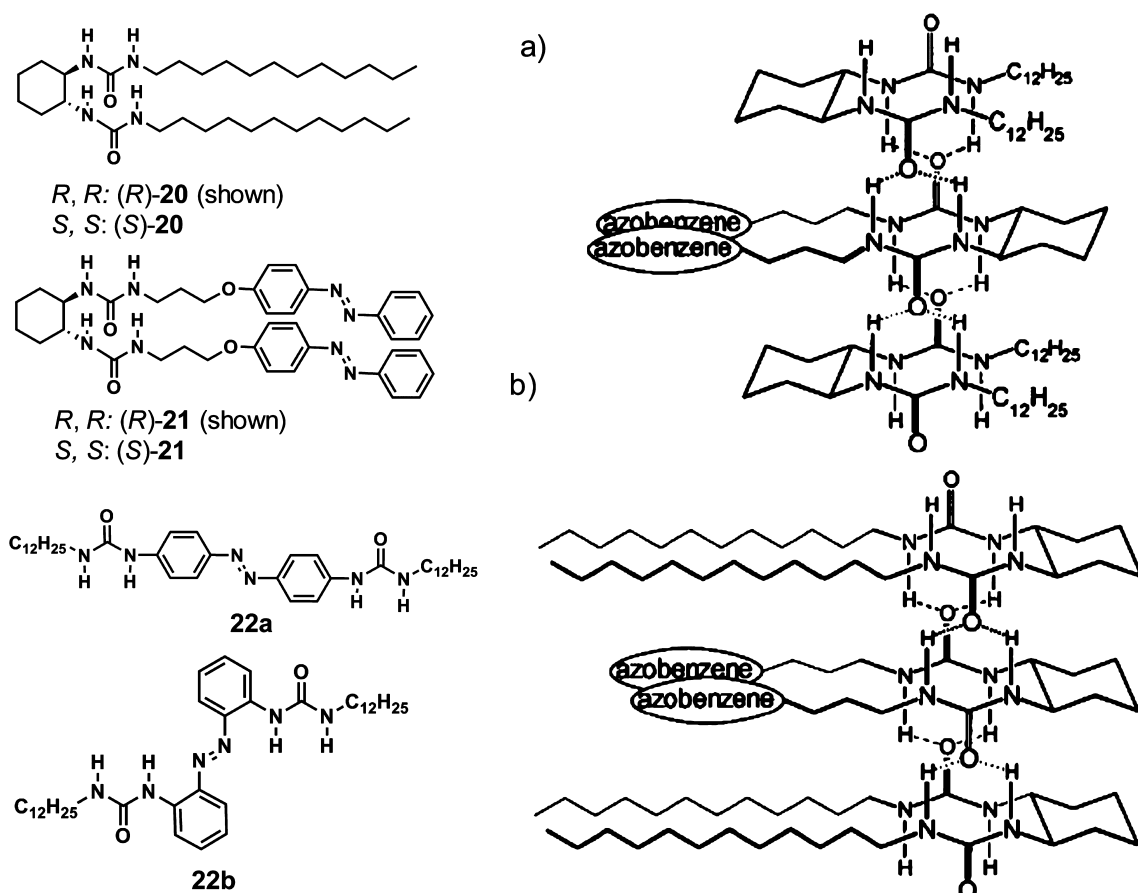
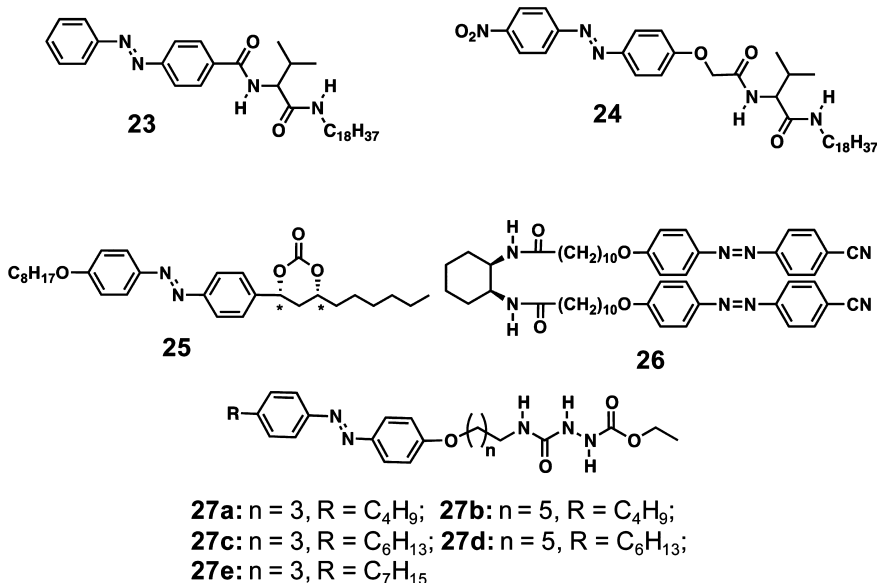


Figure 5. Model for the incorporation of (R)-21 in (a) an aggregate of (S)-20 with opposite configuration and (b) an aggregate of (R)-20 with the same configuration, showing the distinct environments for the azobenzene groups. (Reprinted with permission from ref 182. Copyright 2001 Wiley-VCH.)

Chart 6



alized diaminopyrimidinone derivatives **30a** and **30b** (Chart 7) hierarchically organize into lamellar superstructures to form organogels in nonpolar media, which undergo photoinduced disruption and reformation as demonstrated by the photochemically reversible sol–gel transition.¹⁹⁸ Irradiation with UV

light (350 nm) slowly dissolves the macroscopic aggregates, resulting in the collapse of the gel into soluble supramolecular tapes. A zinc complex prepared from the cyclen (1,4,7,10-tetraazacyclododecane) based ligand **31** functionalized with

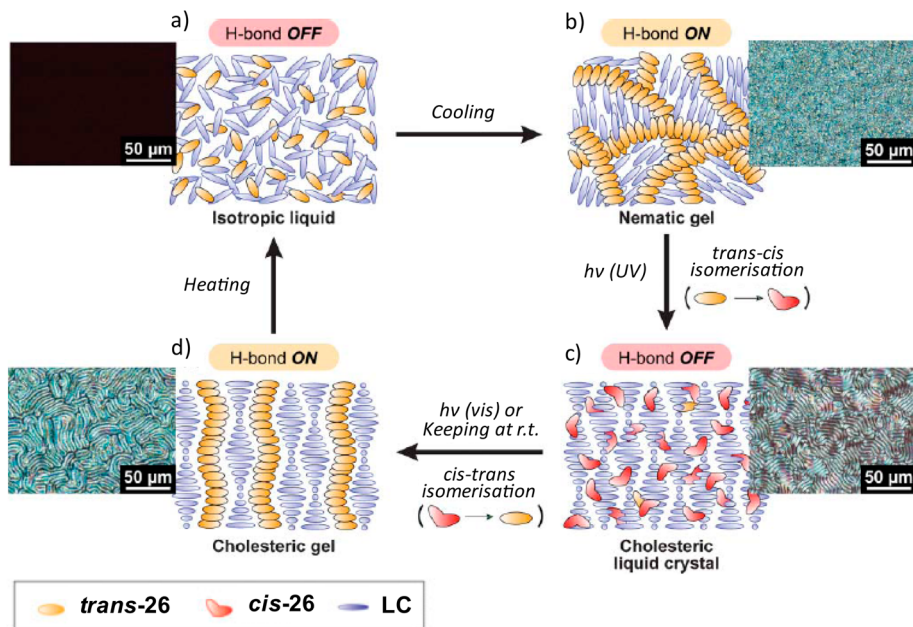


Figure 6. POM pictures and the respective schematic illustration of photoinduced structural changes in LC physical gels consisting of 4-cyano-4'-pentyl-biphenyl containing 3 wt % of **26**: (a) isotropic liquid state at 120 °C; (b) nematic gel state at room temperature; (c) cholesteric LC phase (LC sol state) at room temperature after UV irradiation of the nematic gel for 15 min; (d) cholesteric gel state at room temperature after keeping the cholesteric LC phase. (Reprinted with permission from ref 190. Copyright 2003 Wiley-VCH.)

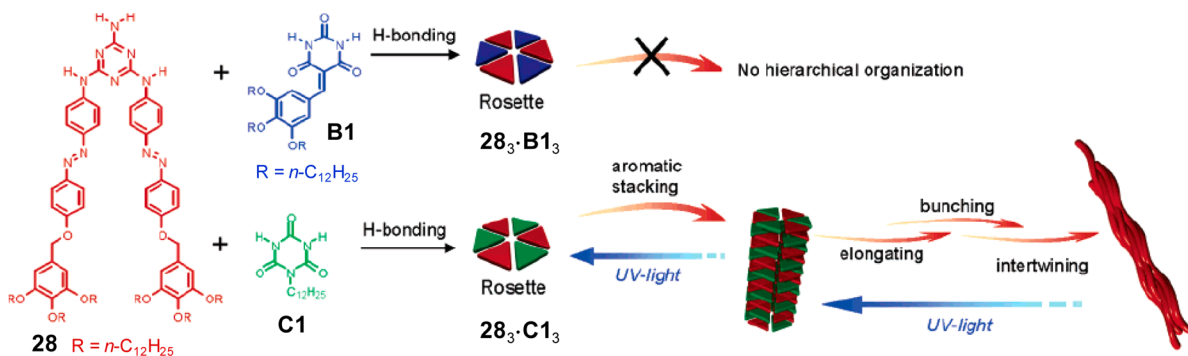


Figure 7. Schematic representation showing aggregation of the melamine–azobenzene conjugate (**28**) with barbiturate (**B1**) and cyanurate (**C1**) derivatives. Rosette $28_3 \cdot B1_3$ can hierarchically organize into intertwined fibers (red arrows). The fiber formation can be regulated by light (blue arrows). (Reprinted with permission from ref 196. Copyright 2005 American Chemical Society.)

1,3,5-triazine featuring azobenzene with long alkyl chains (Chart 7) is reported to form organogels.¹⁹⁹

Amino acids and peptides are versatile building blocks to create functional helical assemblies and supramolecular gels when integrated with an appropriate chromophore.^{81,82,84,90,93} For example, the gelators based on *p*-nitro-azobenzene-coupled bis-alanines **32a–c** (Chart 8)²⁰⁰ and the glycine (**33e–35e**), L-alanine (**33d–35d**), L-leucine (**33c–35c**), L-valine (**33b–35b**), and L-isoleucine (**33a–35a**) functionalized azobenzenes (Chart 8) form gels in many solvents including oils.²⁰¹ The 4-substituted benzoic acid derivatives **34a** and **34b** and the disubstituted azobenzene derivatives **35a** and **35b** showed better gelation abilities than the monosubstituted azobenzene derivative **33a** and **33b**.

The photoresponsive gel formed by **36** (Chart 9) is the first example of an enzymatic reaction catalyzed generation of photoresponsive hydrogelator.²⁰² A large number of amino acids based photoresponsive gelators **37–39** (Chart 9) have been reported which upon trans–cis photoisomerization induce breaking and forming of hydrogen bonds resulting in gel–sol

transition.^{203–206} Zhang and co-workers have conducted comprehensive studies on the gelation properties of a large variety of short peptide functionalized azobenzene derivatives **38a–d** (Chart 9).²⁰⁵ These studies revealed that gelation ability can be modulated by the amino acid residues, pH, and by salt effect. The presence of aromatic amino acids such as phenylalanine and tyrosine was found to favor gelation of water at an appropriate pH range whereas cationic amino acid residues such as arginine and lysine showed adverse effect. The different strength of intermolecular interactions in the gel matrix was found to influence the sensitivity of the hydrogel toward light. The potential of the hydrogel matrix for biological application is demonstrated by the controlled photoresponsive release of vitamin B12. Huang and co-workers have reported the salt promoted hydrogelation of the dipeptide functionalized azobenzene amphiphiles **39a,b** (Chart 9).²⁰⁶ Upon UV irradiation, the laminated ribbon-like morphology of the gel nanostructures was found to undergo a morphological transition to short fibers, which revert to nanoribbons by visible light exposure.

Chart 7

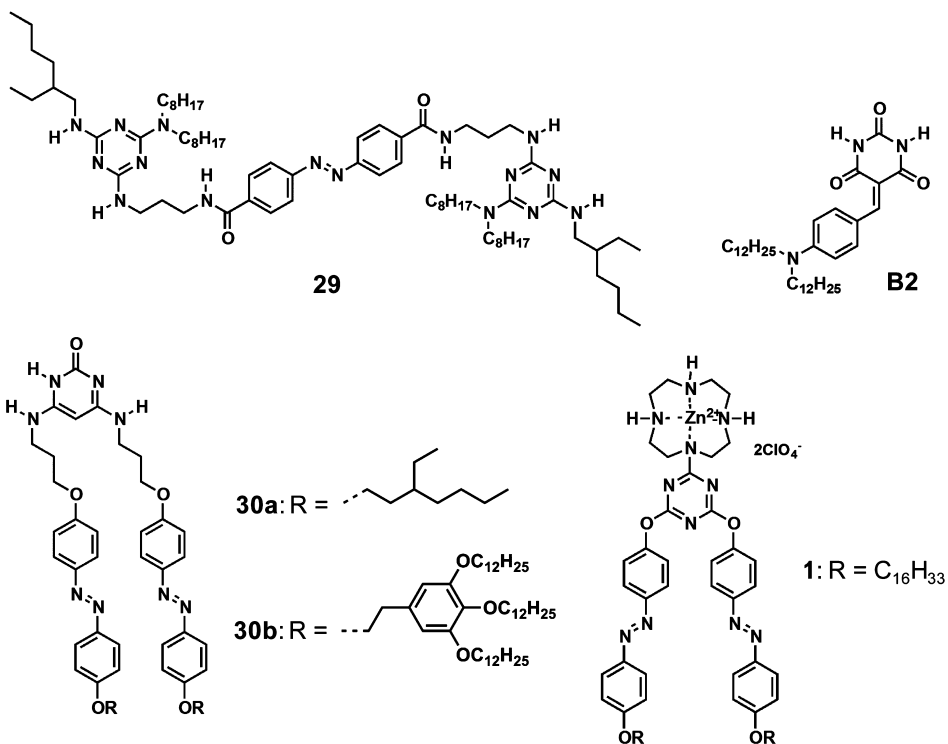
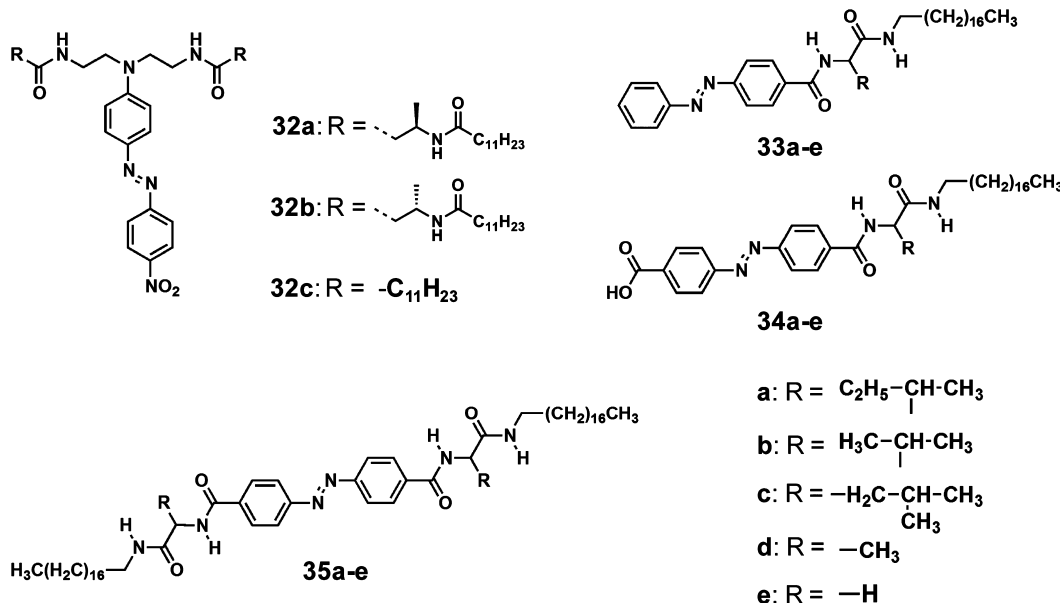


Chart 8



The chiroptical properties of a coassembled gel formed from a mixture of an azobenzene containing lipid molecule **40a** and a simple L-glutamate derivative **40b** (Figure 8) is reported by Ihara and co-workers.²⁰⁷ The gelator **41** showed a positive CD spectrum in polar solvents while it is inverted to a negative one in nonpolar solvents (Figure 8).²⁰⁸ This is rationalized in terms of the difference in interchromophoric interaction under the respective conditions. Detailed chiroptical studies and semi-empirical quantum mechanical calculations revealed that the gelator self-assembled into H-type aggregates with strong interchromophoric interaction in polar solvents. In nonpolar solvents also, the gelator forms H-type aggregates but with

weak interchromophoric interactions and strong hydrogen bonding interactions by an interdigitated stacking mode. The gelation is found to be responsive to temperature, photo-irradiation and polarity of the solvents (Figure 8). The chiroptical switching properties of a gel with nanotubular morphology formed by the coassembly of a lipid gelator and an azobenzene derivative is also reported in the literature.²⁰⁹

Lee et al. reported the gelation properties of small peptides with laterally grafted azobenzene. The photoresponsive hydrogels formed by **42a** and **42c** (Chart 10) showed morphological switching from long nanofibers to discrete spherical aggregates whereas the gel of **42b** remained unchanged upon photo-

Chart 9

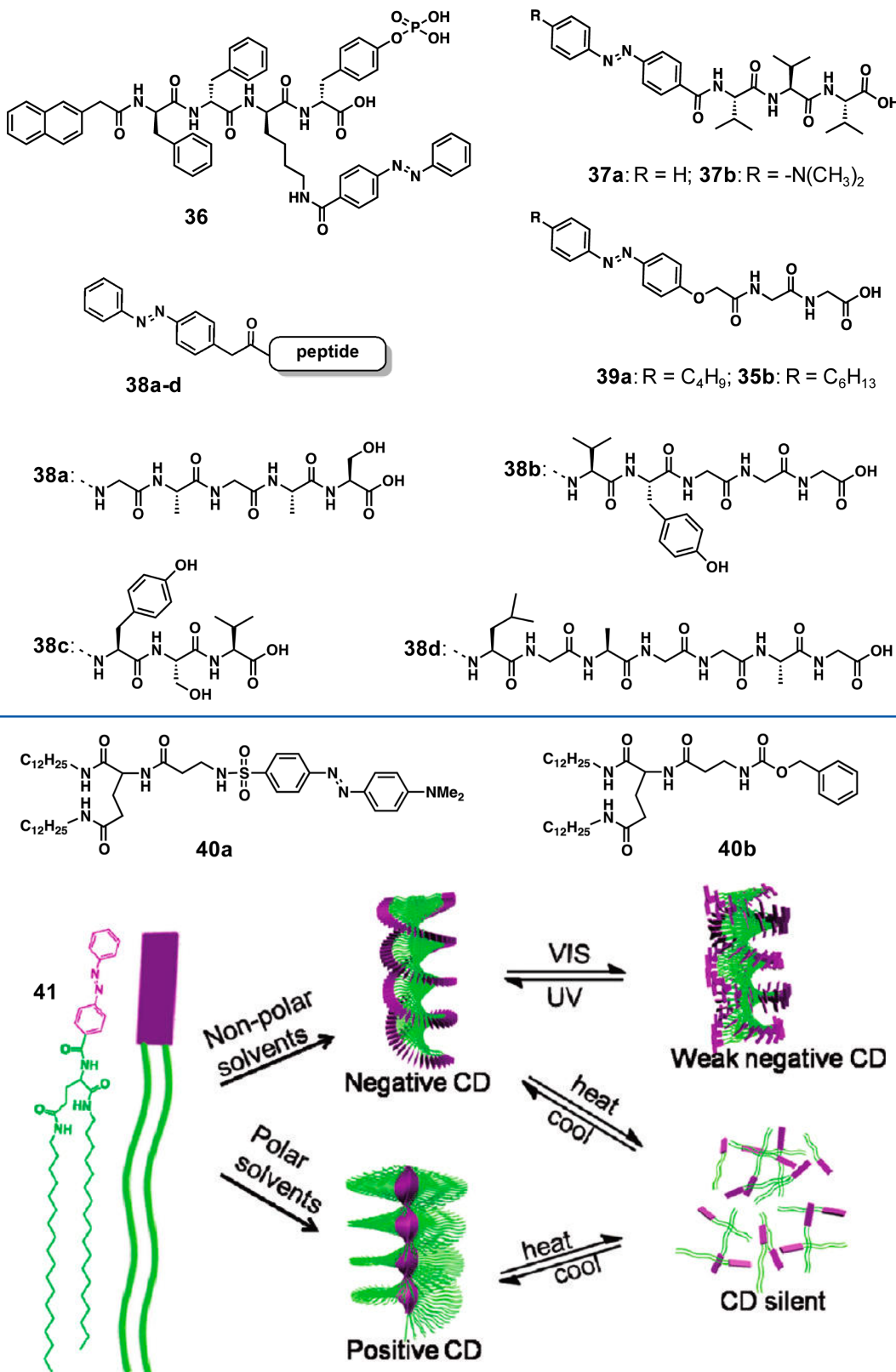
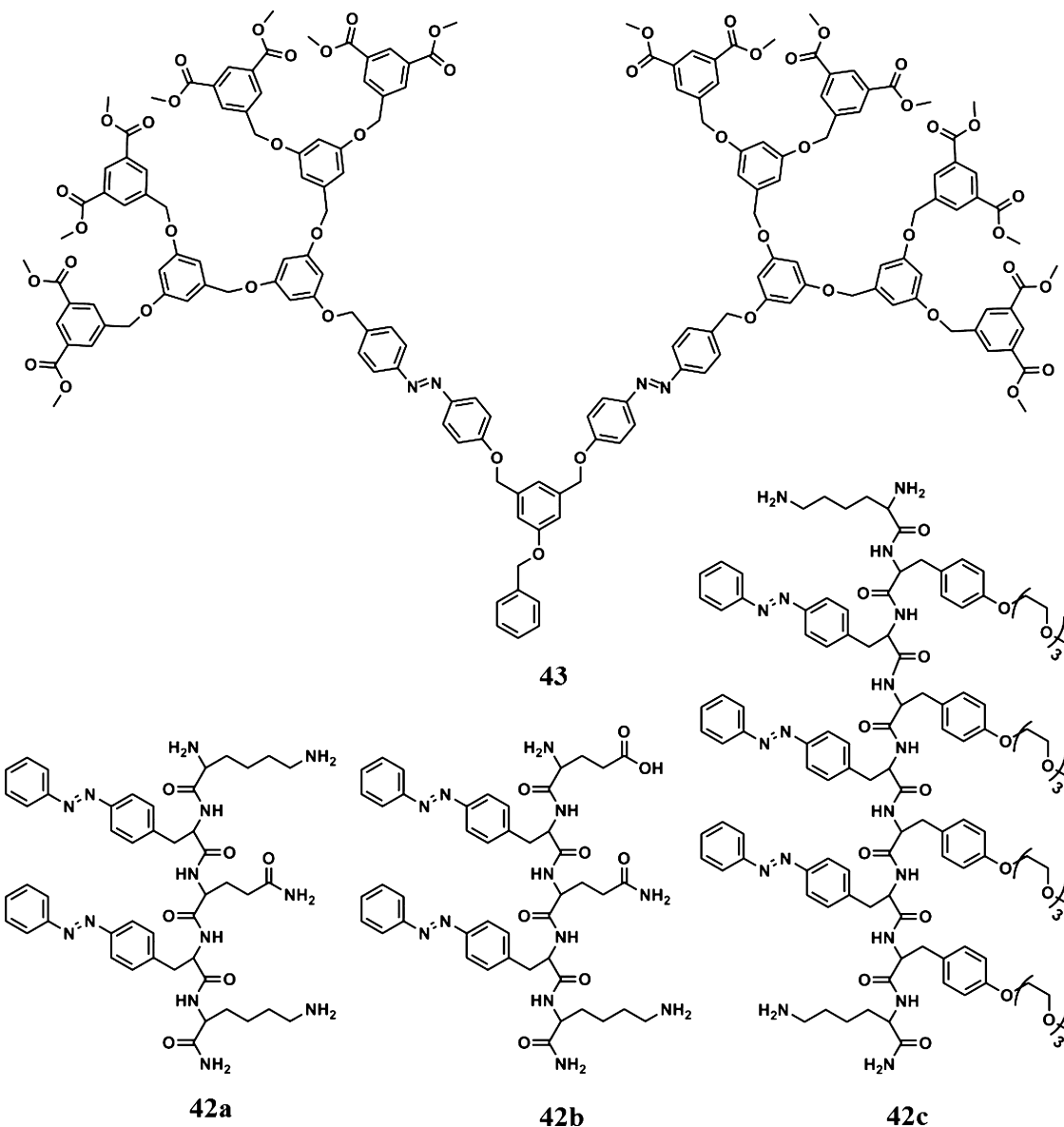


Figure 8. Illustration of the multichannel supramolecular chiroptical switches composed by 41. (Reprinted with permission from ref 208. Copyright 2011 American Chemical Society.)

irradiation.²¹⁰ The gel matrix of 42a has been tested for the controlled encapsulation and release of dye molecules such as rhodamine B. Several photoreversible dendritic organogelators

such as 43–47 (Chart 10 and 11) are known in the literature.^{211–216} A poly(benzyl ether) dendritic supergelator 43 (Chart 10) containing azobenzene moiety exhibited multi

Chart 10



stimuli responsive gelation.²¹¹ Microsphere morphology in the solution was changed to nanofibers, by sonication which triggered the gelation processes.

Pauli and Banerjee have reported fluorescent organogels from self-assembly of an azobenzene molecule appended with four amino acid (isoleucine) residues **45a** (Chart 11). The structurally analogous **45b,c** (Chart 11) failed to gelate any of the solvents tried suggesting the crucial role of amino acid side chain in the self-assembling process.²¹³ Kim and co-workers have reported self-assembly and gelation of an asymmetric bis-dendritic gelator consisting of an azobenzene dendron and an aliphatic amide dendron **46** (Chart 11).²¹⁴ Sterically bulky azobenzene groups at the periphery of the dendron allowed a rapid and reversible gel–sol transition by light through disruption of hydrogen bonds between the aromatic and aliphatic secondary amides in the molecule. Hydrogel formed from the tetrameric sugar derivative **47** (Chart 11) showed resistance toward photoinduced isomerization due to the strong packing of the molecules assisted by π – π stacking and hydrogen bonding.²¹⁵

Yi, Huang and co-workers have reported the gelation property of the tripodal gelators **48** and **49**, functionalized with azobenzene bearing long alkyl chains (Chart 12).^{216,217} The gelator **48** is capable of forming anisotropic bilayers which are hydrophilic along the plane but hydrophobic near the rim.²¹⁶ The xerogels formed by **48** displayed morphologies and surface properties that are strongly depend on the nature of the gelling solvent. A cabbage-like topography and super hydrophobicity were observed in the xerogel formed from a low polar aromatic solvent such as xylene. The wettability of the xerogel of **48** could be turned from hydrophobicity to hydrophilicity by applying a sol–gel process with different solvents. The C₃-symmetrical photoresponsive trisurea compounds connected with three azobenzene moieties through flexible alkyl spacers (**50a** or **50b**) when mixed with another trisamide gelator (TG) formed a stable gel in 1,4-dioxane (Chart 12).²¹⁸ Since the azobenzene moiety is present at the rim of the packing, the two-component gel exhibits reversible photoisomerization from trans–cis without the breakage of the gel state.

Chart 11

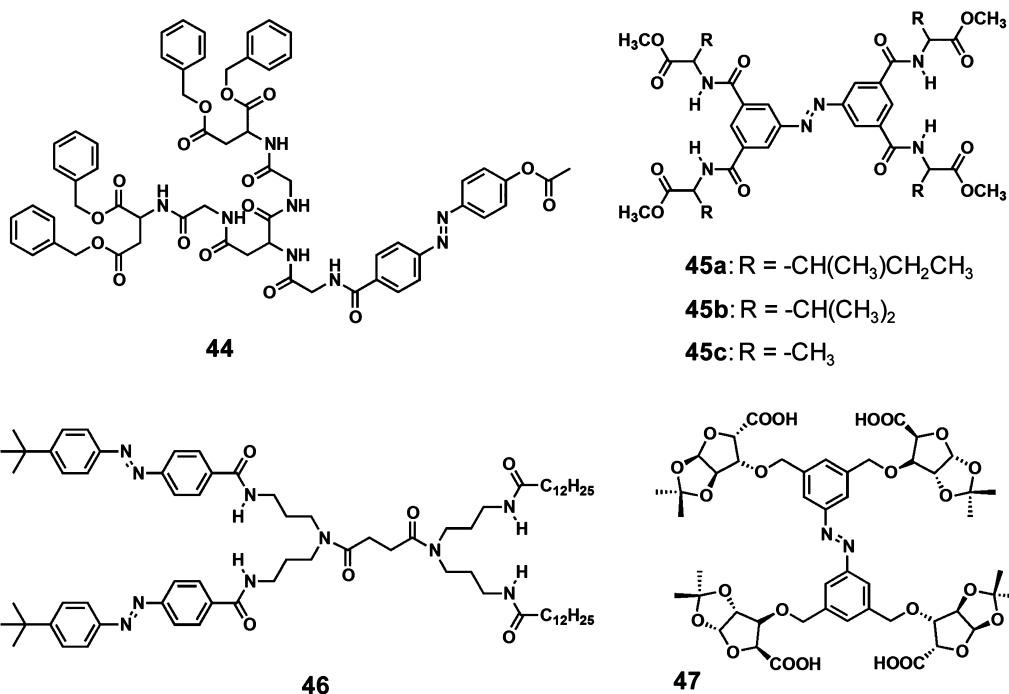
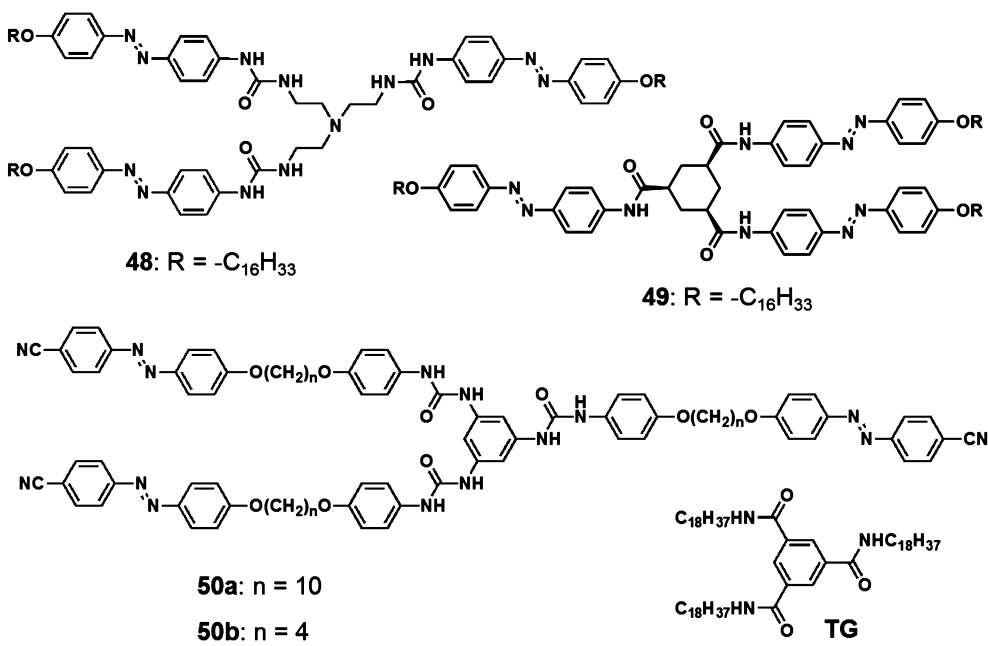


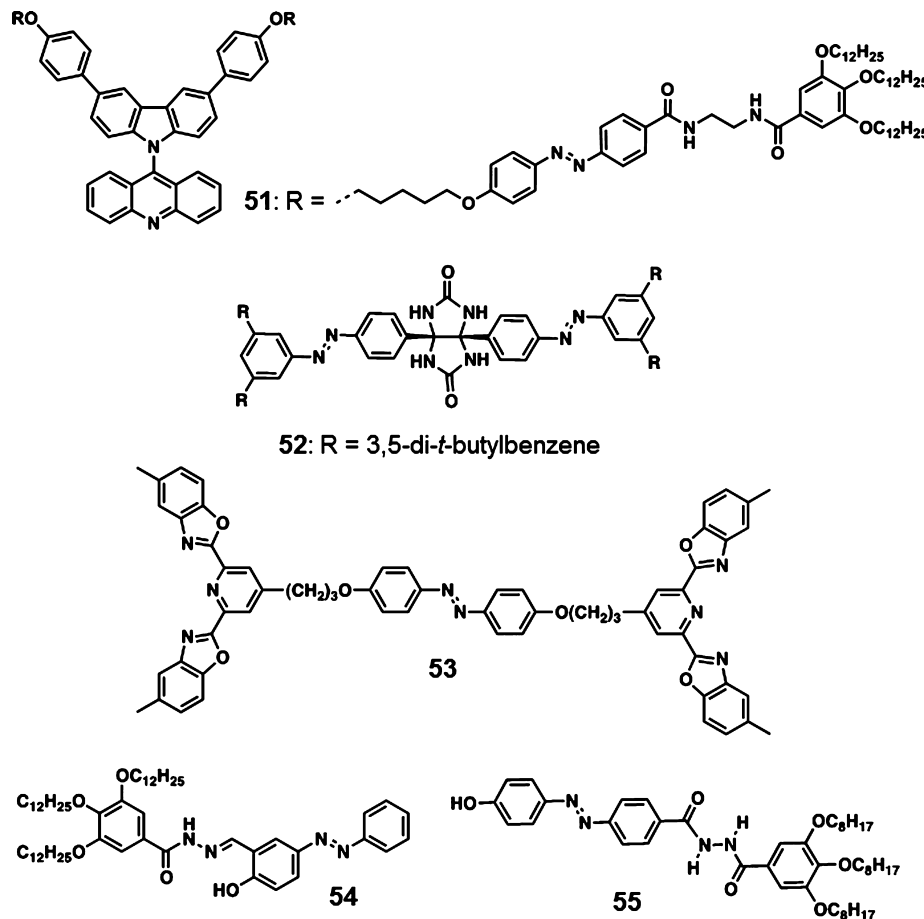
Chart 12



Some of the interesting photoresponsive gelators are shown in Chart 13. The gelator **51** (Chart 13) is based on a twisted intramolecular charge transfer probe 9-(9'-acridyl)carbazole and an azobenzene unit that shows photoinduced reversible fluorescence wavelength shift between the gel and the sol state.²¹⁹ Rebek and co-workers have demonstrated the photoresponsive properties of organogels prepared from an azobenzene appended glycoluril derivate **52** (Chart 13).²²⁰ The gel–sol transition of **52** occurred in the presence of UV light, fluoride ions or a suitable guest such as *n*-tetradecane. The photoresponsive supramolecular gel prepared from a 1:1 hydrogen bonded complex of an azobenzene appended 2,6-

bis(benzoxazol-2-yl)pyridine ligand **53** (Chart 13) and a polymeric secondary dialkyl ammonium salt exhibited increase in the fluidity upon illumination due to trans–cis isomerization driven gel–sol phase transition.²²¹ A rotaxane composed of azobenzene chromophore and α -CD dispersed in an amphoteric thermoreversible hydrosol gels showed fluorescent binary signals when compared to that in solution state.²²² Tuning of amphiphilic properties of **54** (Chart 13) by complexation with α -CD was found to enhance its gelation ability which can be reversibly modulated by photoirradiation.²²³ Photoinduced fiber to vesicle morphological transition was exhibited by an organogelator bearing azobenzene and

Chart 13



hydrazide groups **55** (Chart 13).²²⁴ A lipophilic azobenzene functionalized 2,2,4-triazole Fe(II) complex reported by Kimizuka and co-workers formed molecular wires and gels in organic solvents.²²⁵ Organogels formed by primary ammonium dicarboxylate salts of azobenzene-4,4'-dicarboxylic acid and primary alkyl amines exhibited reverse-thermal gelation.²²⁶ A 1:3 molar ratio mixture of 12-hydroxystearic acid and an azobenzene amine derivative was reported to show light triggered gel to sol transition in toluene and sol to gel transition in chloroform, which is a very rare observation for a given photoresponsive system.²²⁷

Apart from the above-mentioned systems, a large variety of azobenzene containing polymers have been reported to show gelation behavior under suitable experimental conditions.^{228–243} Most of these systems show interesting reversible property change upon UV-vis light irradiation. An interesting case is the photoinduced anisotropic bending and unbending behavior of a LC gel prepared by the polymerization of mixtures containing azobenzene monomers and cross-linkers with azobenzene moieties, reported by Ikeda et al.^{230–232} The difference in the association constants of trans and cis azobenzene inclusion complex with cyclodextrin has been exploited to the design of a variety of smart gels having reversible gel–sol property.^{234–241} The viscosity of a gel prepared from a mixture of hydrophobically modified PAA and a cationic photosensitive surfactant, azobenzene trimethylammonium bromide, can be controlled reversibly by UV and visible light irradiation.²⁴² In response to the photoswitching of azobenzene moiety, an azobenzene containing heteropolymer

gel in an ionic liquid exhibited thermally reversible volume phase transition.²⁴³

2.2. Stilbenes

Stilbenes are recognized as one of the thoroughly studied photochemical systems.^{146,244} Upon direct excitation of stilbenes, photoisomerization is confined entirely to the singlet excited state and competes with fluorescence on the trans side and photocyclization on the cis side. Stilbenes in the cis-form are not thermally stable and return to the trans-form in the dark. For most of the stilbene derivatives, the thermal activation barrier is around 154 kJ mol⁻¹. Owing to their photoresponsive conformational changes, stilbenes are suitable moieties for the design of “smart” gelators. However, the thermal back isomerization is the limitation of stilbene based systems which does not allow a photochemical control on the properties. Despite this limitation, the photochemical properties and self-assembly of stilbenes have been the subjects of numerous studies.

The stilbene appended cholesterol derivative **56** (Figure 9), reported by Whitten and co-workers, self-assembles to form organogels in appropriate solvents.²⁴⁵ Time dependent evolution of the gel nanostructures of **56** has been studied using AFM technique, in order to get a direct observation on the role of solvent during the gel formation (Figure 9).²⁴⁶ The gel formation was initiated by a change in the gelator–solvent interaction, resulting in dewetting of the sol phase from a solid support. Time transient AFM images of **56** in 1-octanol on HOPG revealed that at first the solution is dewetted from the surface, forming circular and elongated droplets (Figure 9b),

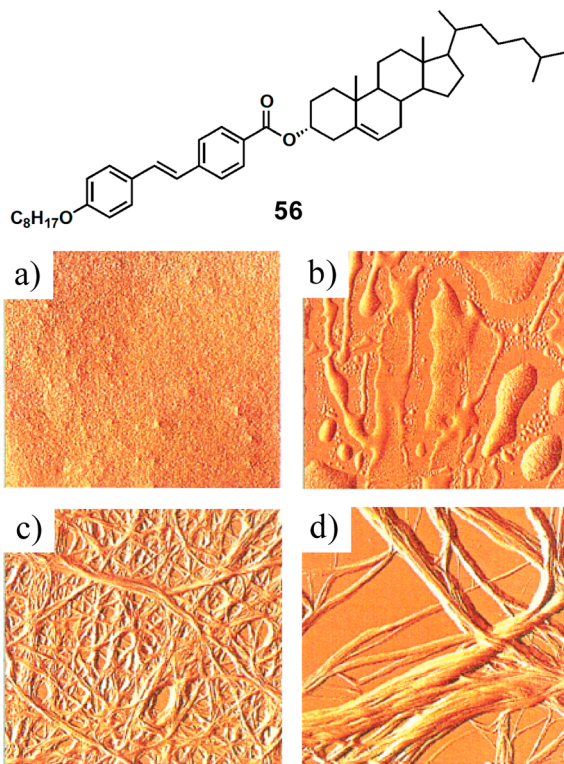
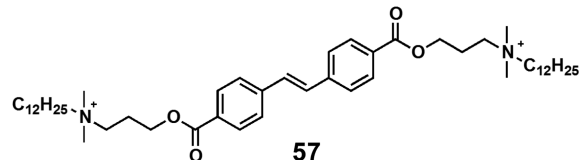


Figure 9. Time transient AFM images (in amplitude mode) of sol–gel phase transition of the gelators **56**. Images were acquired after the heated sol phase was cooled to room temperature for (a) 0, (b) 10, (c) 21, and (d) 31 min. The scale of all images is $12 \times 12 \mu\text{m}$. (Reprinted with permission from ref 246. Copyright 2000 American Chemical Society.)

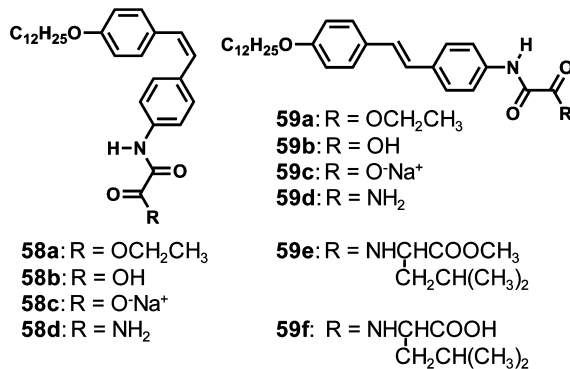
followed by the formation of fine fibers (Figure 9c), with average length of $250 \pm 5 \text{ nm}$ and width as thin as $6.5 \pm 0.5 \text{ nm}$. Further, the growth process was continued through the combination of the neighboring fine fibers into thicker ones (Figure 9d). Detailed ^1H NMR investigation on the composition, structure and dynamics of the stilbene-cholesterol gels were also reported by the same research group.¹³³

Eastoe et al. have made a photoresponsive organogel system by refluxing stilbene-containing photosurfactant **57** (Figure 10), and *N,N'*-dimethyldodecylamine in toluene-*d*₈ for several hours followed by cooling to room temperature.²⁴⁷ Upon exposure to UV light, this gel transformed to sol phase with a spatial control and has been demonstrated within the sample as showed in Figure 10.



As in the case of azobenzene derivatives, gelation ability of stilbene derivatives becomes weak upon photoisomerization. The cis stilbene derivatives, **58a-d** (Chart 14) showed poor

Chart 14



gelation ability when compared to the corresponding *trans*-stilbenes **59a-f** (Chart 14).^{248,249} However, a concentrated solution of the cis isomer turns into a gel upon exposure to irradiation. Detailed studies revealed that, apart from the hydrogen bonding between the oxalyl amide units, the lipophilic interactions between long alkyl chains and the π -stacking between the *trans*-stilbene units are responsible for the gelation.

The polycondensation of silsesquioxanes in the organogel phase of the diureido stilbene derivative bearing triethoxysilane end functional group **60** (Chart 15) allowed the transcription and fixation of the gel nanostructures stabilized by weak intermolecular interactions to a rigid hybrid network frozen by covalent siloxane linkages.²⁵⁰ Hydrogen bonded complexes of L-tartaric acid and alkoxy substituted stilbazoles **61a-c** (Chart 15) form organogels with strongly enhanced fluorescence property.²⁵¹ Similarly, a H-bonded complex of 3-cholesteryl 4-(*trans*-2-(4-pyridinyl)vinyl)phenyl succinate and 3-cholesteryloxycarbonylpropanoic acid **62** (Chart 15) showed very efficient gelation as well as thermotropic LC properties.²⁵²

AIEE is an interesting property of several modified stilbene derivatives.²⁵³ A series of such organogelators **63-65** (Chart 16) has been reported by Park and co-workers.²⁵⁴⁻²⁶⁰ The gelation of **63a** and **63b** is attributed to the cooperative effect of the π -stacking interactions of the rigid rod-like aromatic segments and the intermolecular interactions induced by the four CF₃ units.²⁵⁴⁻²⁵⁷ Organogels formed from **63b** was found to undergo proton induced gel–sol phase transition with the concomitant fluorescence intensity modulations.²⁵⁶ The fibrous

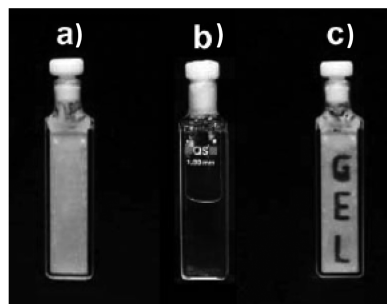


Figure 10. Photoinduced gel-to-sol transition of **57**–*N,N'*-dimethyldodecylamine organogel in toluene-*d*₈: (a) initial gel state, (b) after irradiation, and (c) after irradiation through a mask. (Reprinted with permission from ref 247. Copyright 2004 The Royal Society of Chemistry.)

Chart 15

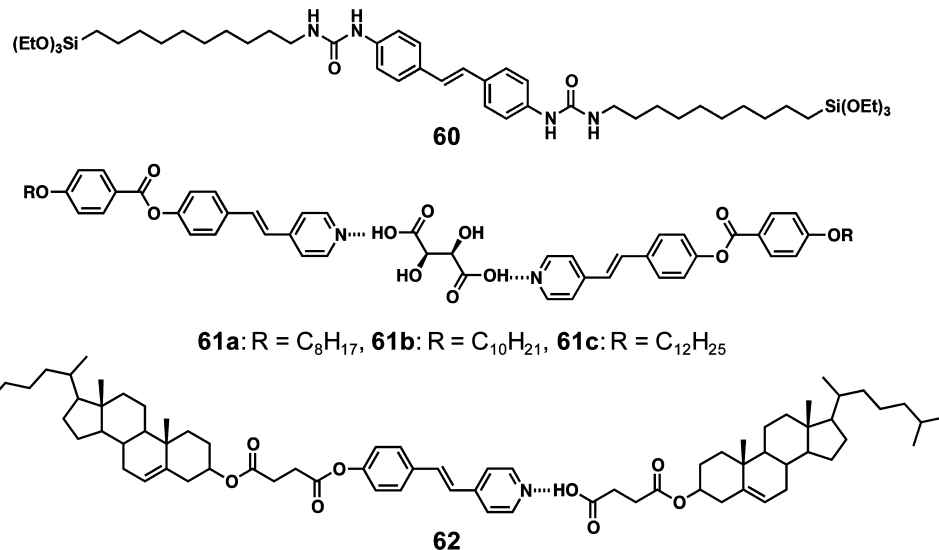
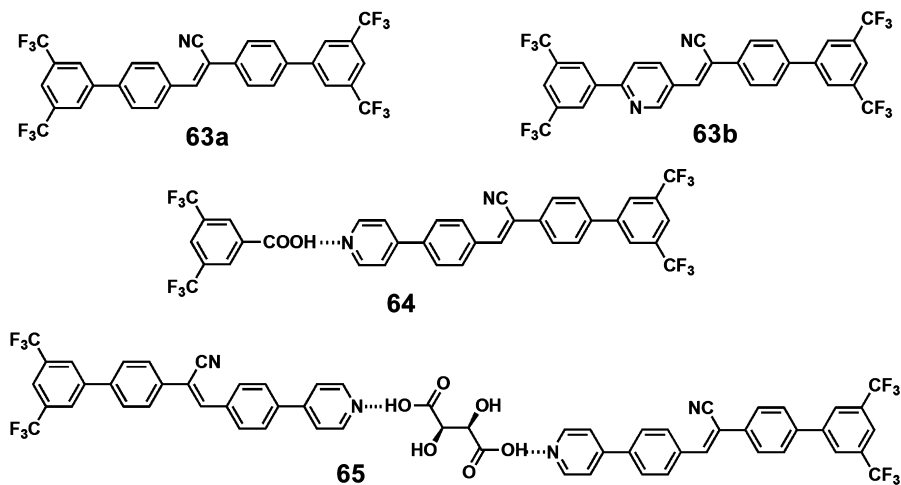


Chart 16



self-assembly of **63a** and **63b** is highly emissive when compared to that of the isotropic solution (Figure 11).^{254–256} AIEE in the gel state is attributed to the synergistic effect of intramolecular planarization and J-type aggregate formation (restricted excimer formation). The photoluminescence, arising from the fibrous aggregates of **63a** can be repeatedly switched by an electric

field.²⁵⁷ Modulation of the excitation wavelength through electric field induced LC orientation offers new ways to achieve and explore electrically controllable photoluminescence. Aggregation of **63a** confined in the LC droplets resulted in circular and highly folded nanoscale fibers, in contrast to the extended ones formed in the bulk LC gel.²⁵⁸ This confinement was found to influence the switching times and contrast of single LC gel droplets which is largely determined by the droplet size. The organogel of the hydrogen bonded complex **64** (Chart 16), formed from the nonfluorescent 2-(3',5'-bis(trifluoromethyl)biphenyl-4-yl)-3-(4-pyridin-4-yl-phenyl)-acrylonitrile monomer and 3,5-bistrifluoromethyl benzoic acid, was found highly transparent and fluorescent.²⁶⁰ The complexation of the monomer **65** with a chiral dicarboxylic acid L- or D-tartaric acid (Chart 16) also resulted in a stable gel, accompanied by a drastic fluorescence enhancement as well as chirality induction.²⁶⁰

The D- π -A type organogelators **66a** and **66b** (Chart 17) exhibited AIEE during the sol–gel phase transformation.²⁶¹ Interestingly, **66b** showed solvent dependent gelation and emission properties, such as yellow fluorescence from THF–water gel, orange emission from acetone gel and red fluorescence from DMSO gel. A gel like material obtained

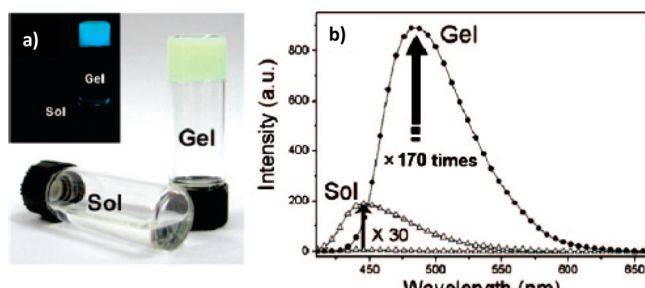


Figure 11. (a) Photographs of gel and sol states of **63b**; inset shows the fluorescence emission of the sol and gel states of **63b**. (b) Fluorescence spectra of **63b** in the sol and gel states. (Reprinted with permission from ref 256. Copyright 2008 American Chemical Society.)

Chart 17

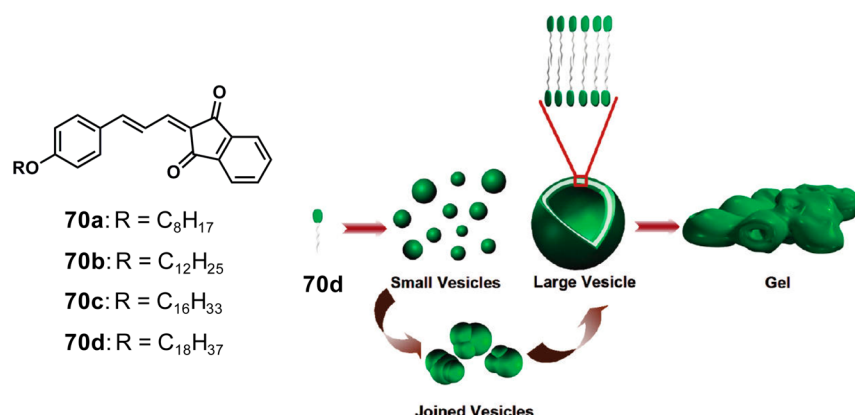
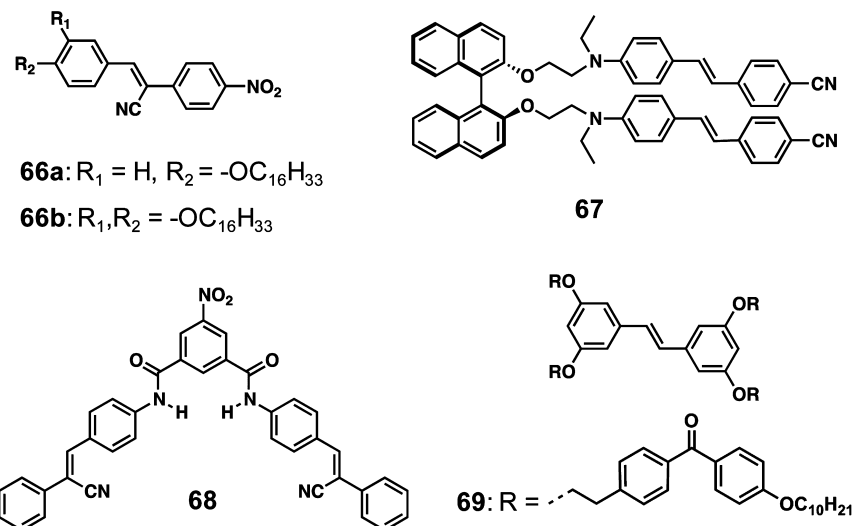
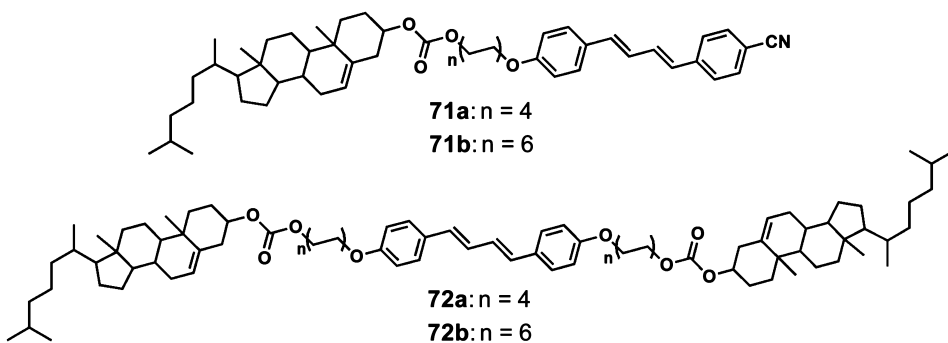


Figure 12. Chemical structure of **70** and schematic representation of the hierarchical organization of **70d** from small to large vesicles and finally to gels. (Reprinted with permission from ref 267. Copyright 2006 Wiley-VCH.)

Chart 18



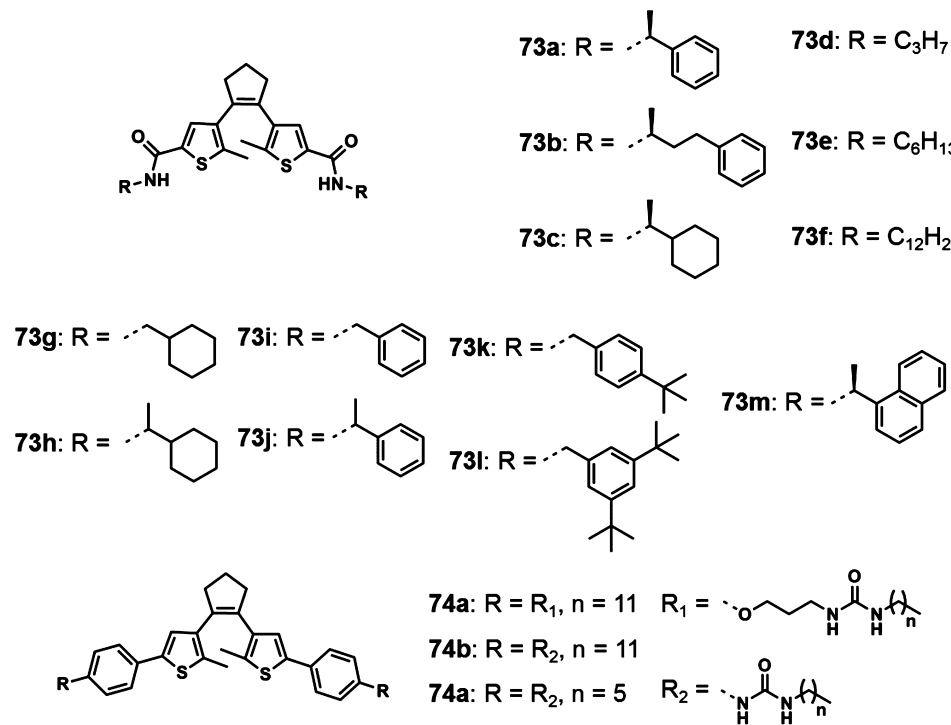
from the self-assembly of the stilbene functionalized binaphthyl derivative **67** (Chart 17) has shown enhanced sensitivity toward the detection of DNT and TNT vapors in comparison to the solution state.²⁶² Compound **68** (Chart 17) is an example of multistimuli responsive organogelator which showed ultrasound induced gelation as well as fluoride and proton controlled reversible gel to sol transition.²⁶³ The stilbene-cored gelator **69** (Chart 17) having benzophenone peripheries with alkyl chains self-assembles to form a gel in methylcyclohexane.²⁶⁴ A photoresponsive hydrogel has been reported from a cucurbit[7]uril derivative in the presence of a

small amount of 4,4'-diaminostilbene dihydrochloride as a guest.²⁶⁵ The cyanostilbene derivative switches the fluorescence intensity in the gel matrix through AIEE, enabled the quantitative determination of enantiomer composition.²⁶⁶

2.3. Butadienes

The D-A substituted amphiphilic butadienes **70a–d** undergo concentration dependent hierarchical self-assembly from vesicles to gels due to the formation of globular aggregates with entrapped solvent within them (Figure 12).^{146,267} The self-assembly process was associated with unique changes in the

Chart 19



fluorescence of the system.²⁶⁷ At room temperature, the solution of **70d** exhibited a weak fluorescence at 540 nm with a very low quantum yield whereas upon aggregation at a lower temperature of 7 °C, nearly 40-fold enhancement in fluorescence accompanied by a shift in the maximum to 602 nm was observed. This AIEE effect can be attributed to the formation of H-type aggregates, which involves a parallel interaction mode of the chromophores. Apart from this observation, the presence of a photoisomerizable butadiene chromophore makes these materials photoresponsive.

Functionalization of the butadiene core with a cholesterol moiety (Chart 18) resulted in the gelation with interesting morphological features.^{146,268} The correlation of the morphology with absorption and emission spectral studies as a function of concentration and temperature revealed that the mono-cholesterol derivatives **71a,b** form J-type aggregates and the bischolesterol derivatives **72a,b** form H-type aggregates.²⁶⁸ The slipped stacking of the monocholesterol J-type aggregate resulted in the formation of helically twisted fibers, whereas the cofacial arrangement in the bischolesterol H-type aggregate resulted in agglomerated spheres.

2.4. Dithienylethenes

Dithienylethenes are a distinct class of photochromic system that can undergo a reversible ring-closure reaction upon irradiation with UV and visible light, respectively.^{142,150,151,269–273} A pronounced change of the electronic properties and conformational flexibility occurs by this transformation. In the open form, the two thienyl moieties are not conjugated and can rotate around the bond connecting them with the cyclopentene ring. However, in the ring-closed form, the conjugation extends throughout the molecule and the rotational freedom is lost.

The research groups of van Esch and Feringa have conducted extensive studies on photoresponsive as well as chiroptical properties of organogels derived from dithienylethene based molecules **73** and **74** (Chart 19).^{274–279} For instance, they have

demonstrated the reversible optical transcription of supramolecular chirality into molecular chirality using an organogelator **73a**.^{275,279} The dithienylethene molecule **73a** exists in two antiparallel interconvertible open forms with *P*- and *M*-helicity, which cyclize in a fully reversible manner upon irradiation with UV light to form two diastereomers of the ring closed product of **73a**. The open form **73a** is found to be an efficient organogelator of nonpolar solvents. CD and TEM studies of the toluene gels revealed that the molecule **73a** self-assemble to helical fibers, owing to the expression of the *M*- or *P*-chirality of the open form at the supramolecular level.

The photocyclization of **73a** in the gel state showed nearly absolute stereocontrol though there is no stereoselectivity in the nongelled solution. Both the open and closed forms of **73a** exist in two different chiral gel states, denoted as α and β , leading to a four-state chiroptical supramolecular switch, since these four states can be cycled by a sequence of photochemical reactions as shown in Figure 13. A stable gel of (α)-**73a** (*P*-helicity) is obtained on cooling the isotropic solution of the open form **73a**. Photocyclization results in the formation of the metastable gel (α)-**73a**, which converts into the thermodynamically stable gel (β)-**73a** (*M*-helicity) upon the heating–cooling cycles. Irradiation of the gel (β)-**73a** closed form with visible

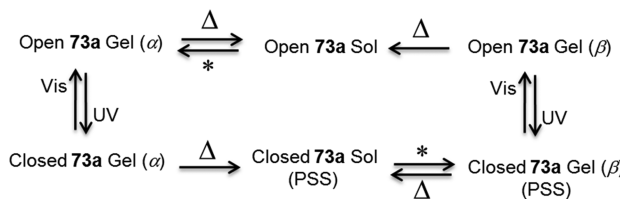


Figure 13. Four different chiral aggregated states and the switching processes of the chiroptical supramolecular switch consisting of the open form **73a** and the closed form of **73a**. UV, $\lambda = 313$ nm; visible (Vis), $\lambda > 460$ nm; * = cooling; Δ = heating.

Chart 20

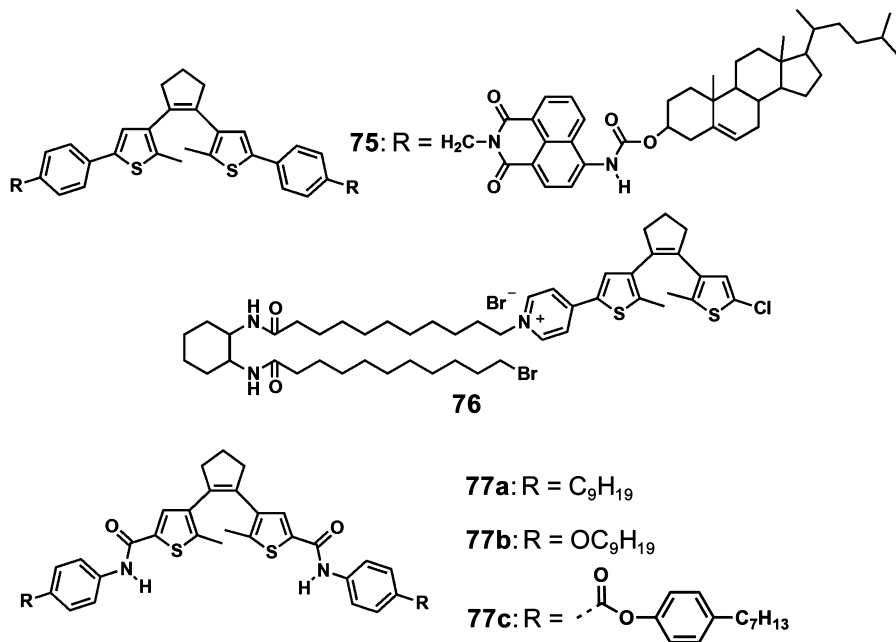
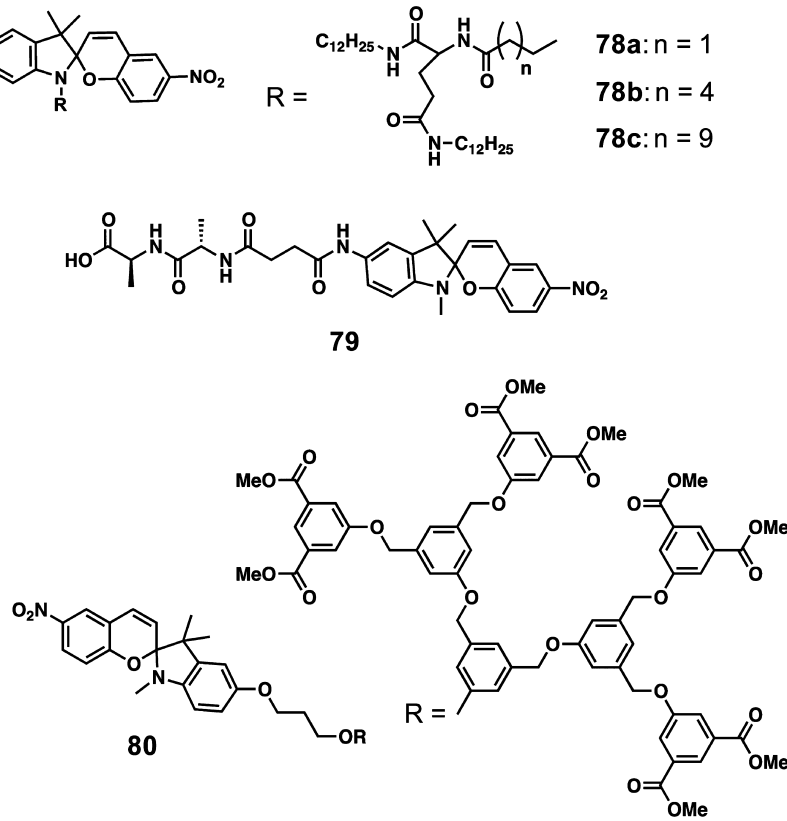


Chart 21



light results in the metastable gel (β)-73a open form, which then change into the original stable gel (α)-73a open form via an isotropic solution of 73a, after a heating–cooling cycle. The optical switching between different supramolecular chiral aggregates and the interplay of molecular and supramolecular chirality in these systems is attractive for designing molecular memory systems and smart functional materials. Later, by manipulating the delicate balance between the solution and self-

assembling properties of these molecules, dynamic and reversible pattern formation was realized.²⁷⁶

The coassembly of chiral and achiral gel forming dithienylethene molecules results in induction and amplification of chirality via sergeant and soldier principle.^{278–281} During the aggregation, the chiral molecules (73a–c, sergeants) select only one of the photoactive conformers and controlled the stereochemistry of the achiral molecules (73d–j,

soldiers).^{278,279} The supramolecular chirality of the assembly was found to be essential in transferring the chirality of the chiral sergeant molecules to the achiral soldiers. Apart from this, the solvents used for the coassembly and gelation were also found to play a crucial role in transferring the supramolecular chirality and decide whether four- or two-gel states are accessible.

Dithienylethenes are found in a variety of π -gelators 75–77 (Chart 20) which show reversible photoinduced changes in the gelation and electronic properties.^{282–285} For example, Tian and co-workers have reported a photochromic fluorescent organogel based on bisthiene-ethene-bridged naphthalimides 75.²⁸² The presence of naphthalimides on the photochromic unit enables the photoswitching of fluorescence with high contrast whereas the cholesterol group leads to a chiral assembly of the chromophores. The dithienylethene having the 2,1,3-benzothiadiazole unit as the center ethene bridge shows good photochromic performance, with a high cyclization quantum yield and moderate fatigue resistance in an organogel media.²⁸³

2.5. Spiropyrans and Spirooxazines

The photochromic reaction of spiropyans and closely related spirooxazines involves reversible photochemical cleavage of the C–O bond of the spiro unit.^{139,150,151,286–288} Because of their interesting photochromic properties, spiroheterocyclic compounds have been investigated for the design of optical memories, switches, and displays.^{286–288} The first report about the spiropyran based organogel system is reported by Hachisako et al.²⁸⁹ They have determined the critical aggregation concentrations of organogelators by following the kinetics of the thermal merocyanine-spiropyran isomerization of L-glutamic acid-derived lipids with spiropyran head groups, 78a–c (Chart 21). Similar observations are also made when spiropyran doped into organogels formed from L-glutamic acid-derived lipids.²⁹⁰

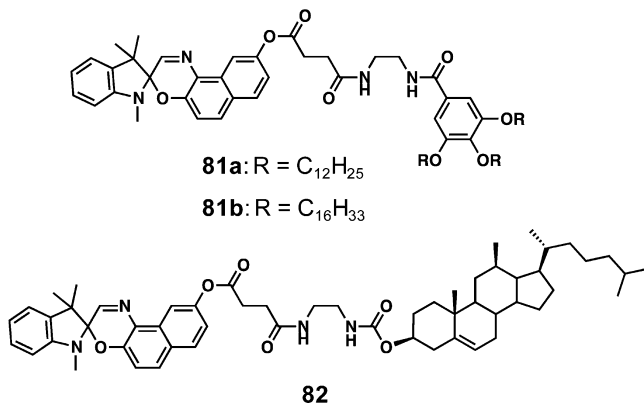
The spiropyran linked dipeptide molecule 79 (Chart 21) is reported to form a hydrogel upon photoisomerization into a merocyanine form.²⁹¹ In addition, the hydrogel is found to undergo gel to sol transition upon interaction with vancomycin due to the strong interaction of the later with peptide unit of the gelator thereby weakening the supramolecular interactions responsible for the gelation. The spiropyran derived dendron molecule 80 (Chart 21) shows different self-assembling properties depending upon the processing conditions.²⁹² For instance, cooling of a hot solution of 80 to 30 °C followed by UV irradiation to the open merocyanine leads to the formation of nano/microsized particles, while cooling into 0 °C results in fibrous morphology and gel. Visible light irradiation of the gel caused merocyanine-spiropyran isomerization and gel-to-sol transition. Apart from this, aggregation of 80 was found to enhance the fluorescence property of the photomerocyanine by minimizing the nonradiative decay pathways of the excited state.

Doping of spiropyran into an organogel system based on 4-*tert*-butyl-1-phenylcyclohexanol was found to increase the lifetime of the photomerocyanine and also stabilize the organic photochromic material.²⁹³ Recently, Raghavan and co-workers have reported photorheological properties of a gel prepared from a lecithin/sodium deoxycholate reverse micelles doped with spiropyran.²⁹⁴ The gel consisting of long worm like reverse micelles changed its dimension upon UV induced isomerization of spiropyran to merocyanine and caused about 10-fold

decrease in the viscosity. When the UV irradiation was switched off, merocyanine was reverted back to spiropyran form, and the viscosity recovered its initial value. This cycle can be repeated several times without loss of response.

Spironaphthoxazines appended to gallic acid 81a,b and cholesterol 82 form photoresponsive gels (Chart 22).²⁹⁵ In the

Chart 22



presence of *p*-toluenesulfonic acid, the gelation ability of these molecules is further enhanced owing to an acid mediated ring-opening of the photochromic moiety. Kinetic studies revealed that the rate of bleaching of the open to closed form is much slower in the gel state when compared to that in the solution.

2.6. 2H-Chromenes

2H-Chromenes are known to display interesting photochromic properties based on their photoirradiation induced fatigue resistant reversible color change.^{151,296} The closed form is colorless, whereas its photoisomerized open form is colored. The latter is thermally unstable and reverts back to its original form by an electrocyclization process. Pozzo and co-workers reported light and pH sensitive properties of organogels of 2H-chromene derivative 83 (Chart 23).²⁹⁷ The neutral carboxylic acid form was found to be readily soluble in polar organic solvents which upon addition of NaOH turned to gel. Furthermore, on irradiation at 366 nm, a yellow color was developed and the gel started to flow upon inversion. In the dark, a colorless viscous solution was formed, which on heating followed by cooling regenerated the original gel. These transitions were caused by the photoinduced ring-opening of the colorless cyclic form to the colored acyclic form, which partially disrupts the gel structure due to its incompatibility with the network. The acyclic form is, however, thermally unstable and returns to the cyclic form upon heating and cooling, resulting in the formation of a gel. A series of 2H-chromene derivatives functionalized with N-acyl-1, ω -amino acids 84a–i (Chart 23) and dipeptide 84j (Chart 23) also reported to form gels in presence of sodium salts.²⁹⁸

2.7. Diacetylenes

In the recent past, there has been considerable interest in the self-assembly of diacetylene derivatives as they allow the covalent fixation of supramolecular assemblies through photopolymerization reactions to give polydiacetylenes, which are attractive candidates as conducting nanowires.^{143,299–302} Gel forming diacetylenes are particularly interesting because the gel network which is stabilized by the noncovalent interactions can be permanently supported by strong covalent bonds under

Chart 23

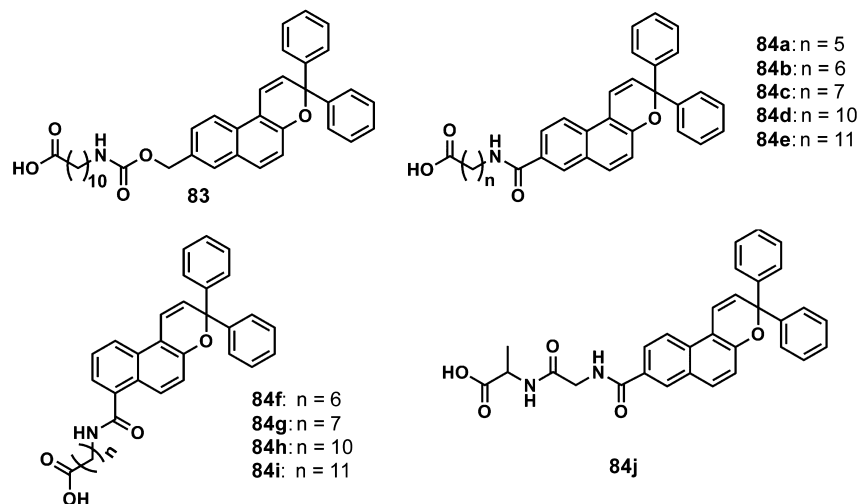
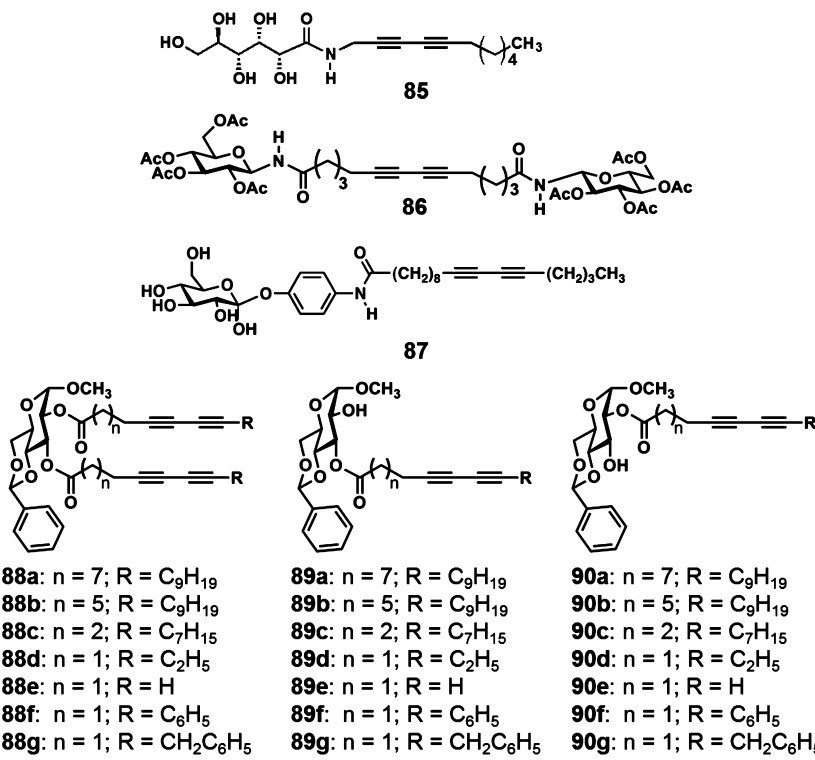


Chart 24



photolytic conditions, thereby retaining the morphological characteristics with increased thermal stability.^{143,299–302}

The diacetylene-1-glucosamide derivatives 85 and 86 (Chart 24) have been reported to form nanofibres upon UV irradiation leading to the gelation of organic solvents.^{303–305} UV or γ -ray polymerization of the nanofibers of 86 by utilizing gel state as a template resulted in the formation of insoluble fibers. UV irradiation of the hydrogel derived helical ribbons of 87 (Chart 24) at 254 nm resulted in the polymerization of self-assembled gelators leading to a red coloration.³⁰⁶ Stimuli responsive polydiacetylenes were prepared by the cross-linking of the diacetylene-containing glycolipids 88–90 (Chart 24).^{307,308} The diacetylene amide derivatives 91–93 (Figure 14) form gels which upon UV irradiation undergo polymerization.^{309–311} Interestingly, the gelators 93a–f, exhibited odd–even effect on

the color of the polymer obtained.³¹⁰ The odd–even effect in the carbon atoms of the aliphatic chains controls the planarity of the polymers and hence the color of the odd chain gels is red and that of the even chain is blue (Figure 14). In addition, the resulted gel derived polymers showed electric field emission characteristics.

The diacetylene dicholesteryl ester derivative 94j (Chart 25) undergo photopolymerization in the organogel state resulting in nanowires.³¹² TEM images of the unstained specimens revealed that the fibril structure formed in the gel did not show any change even after polymerization. A series of diacetylene cholesteryl esters 94a–m, and 95a,b (Chart 25) having two urethane linkages have been reported and the relationship between their gelation properties and chemical structures has been established.³¹³ Most of these gelators could be

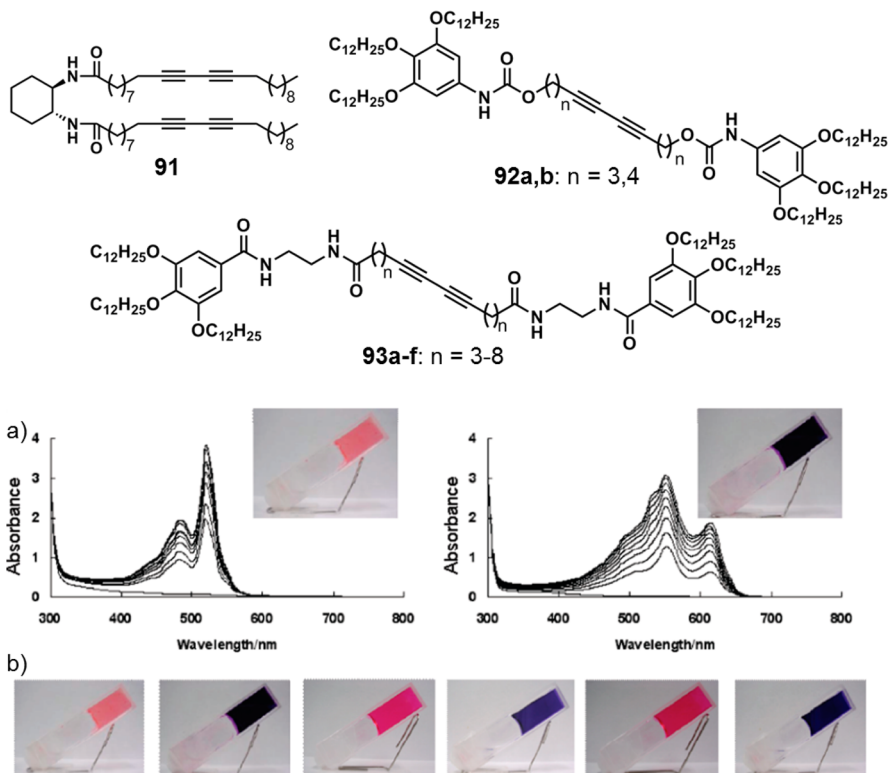
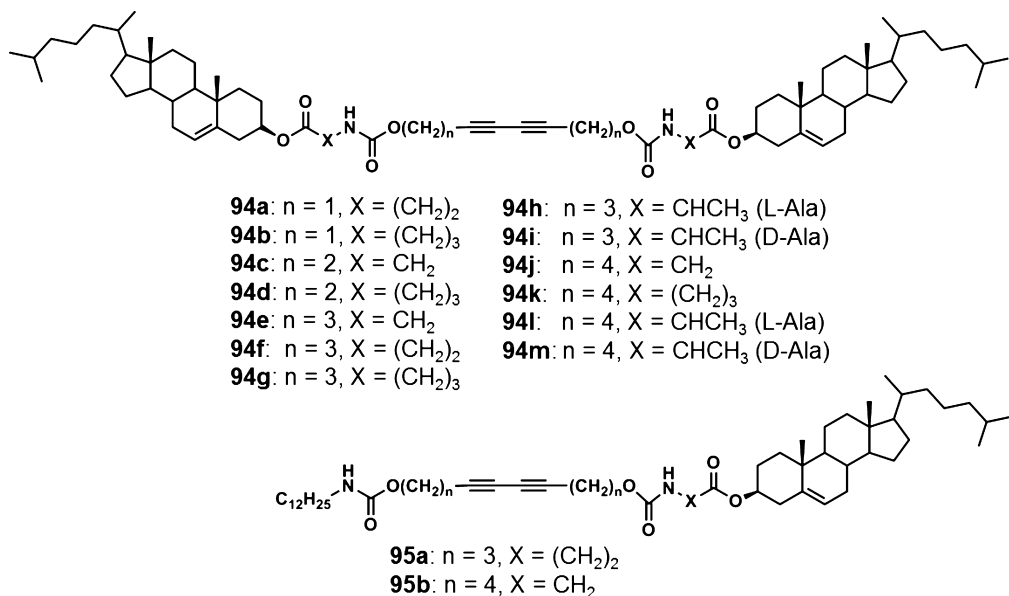


Figure 14. (a) Time dependence (0–180 min) of UV–vis spectral change on photoirradiation of the *n*-hexane gels prepared from 93c (left) and 93d (right). Insets show the photographs of the irradiated gels. (b) Photographs of *n*-hexane gels of 93c–93f after photoirradiation for 3 h. (Reprinted with permission from ref 310. Copyright 2007 American Chemical Society.)

Chart 25



polymerized to give polydiacetylenes upon UV irradiation, with concomitant change in the absorption properties. The compounds with excellent gelation ability exhibited high polymerization rate and yield, as in the case of the cyclohexane gel of 94f, with a polymerization yield of 52%.

The diacetylene based gelators 96a–f (Figure 15) exhibit interesting odd–even effect in the color of the resulted photopolymers.³¹⁴ The cyclohexane gels of 96a, 96c, and 96e, with odd numbers of carbon atom spacers, showed remarkable

color changes to either orange (96a) or blue-violet (96c and 96e) upon photoirradiation, whereas in the case of gels with even number of methylene units (96b, 96d, and 96f), photopolymerization was not observed. Gelation properties of macrocyclic dimers and linear derivatives of diacetylene containing L-glutamic acid units 97 and 98 (Figure 15) have also been investigated.³¹⁵ Macrocylic compounds with a long spacer length 97b–e and 98b–e formed stable gels and hence undergone photoirradiation with a significant color change

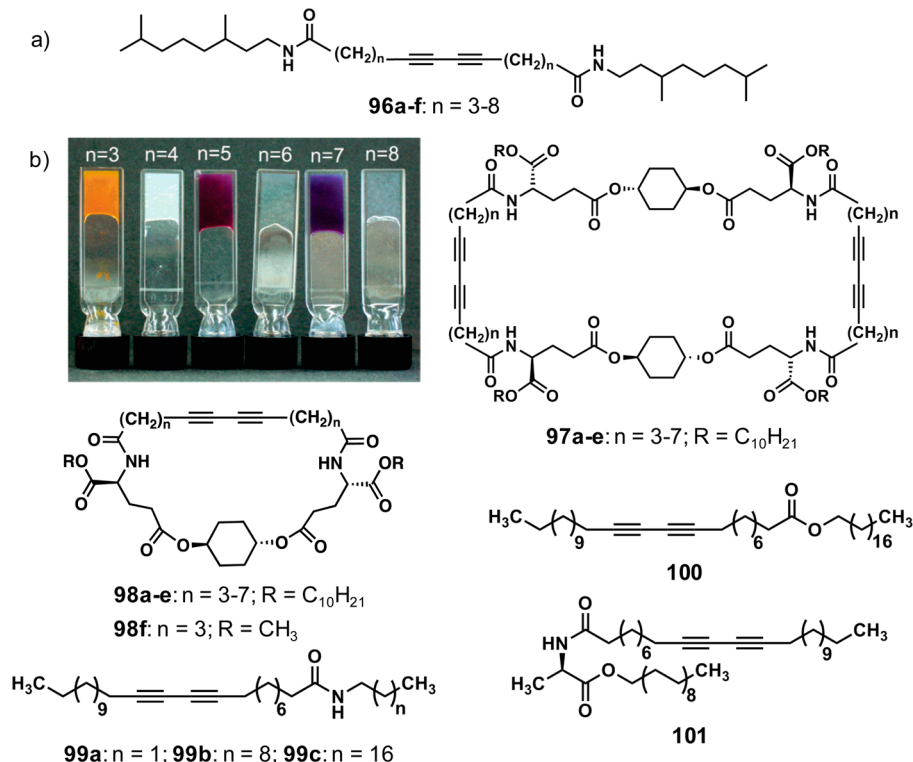


Figure 15. (a) Structures of different diacetylene gelators; (b) Photographs of the photoirradiated cyclohexane gels of 96a–f. (Reprinted with permission from ref 314. Copyright 2004 American Chemical Society.)

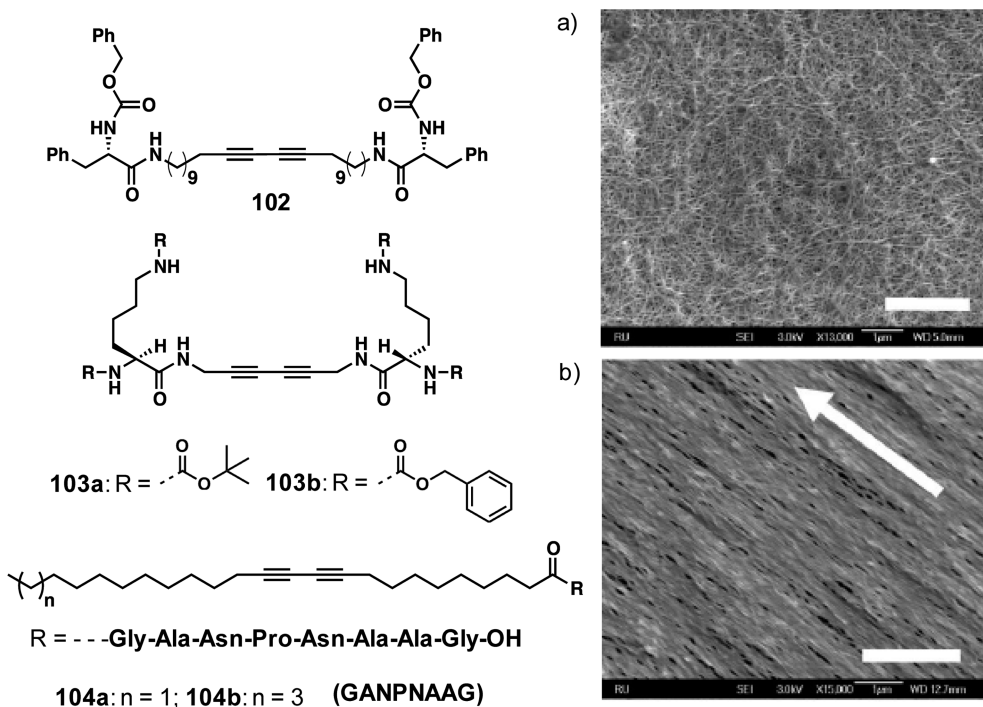


Figure 16. SEM images of self-assemblies of 104b (a) in the absence and (b) in the presence of an applied magnetic field of 20 T. The arrow indicates the direction of the magnetic field. The scale bar is 2 μ m. (Reprinted with permission from ref 320. Copyright 2007 Wiley-VCH.)

from colorless to red or orange. On the other hand, for compounds with a relatively short spacer length 97a, 98a, and 98f, no change in the visible color upon irradiation was observed. It indicates the inability to undergo photopolymerization due to the slight difference in the optimum arrangement of the diacetylene moieties for polymerization. Weiss et al. have

reported the gelation and polymerization of 10,12-pentacosadienoic acid derived amides 99a–c, ester 100 and the chiral amidoester 101 (Figure 15).^{316,317} Photopolymerization and subsequent heating led to significant changes in the absorption spectrum and also change of the visible color from blue to red.³¹⁶

Chart 26

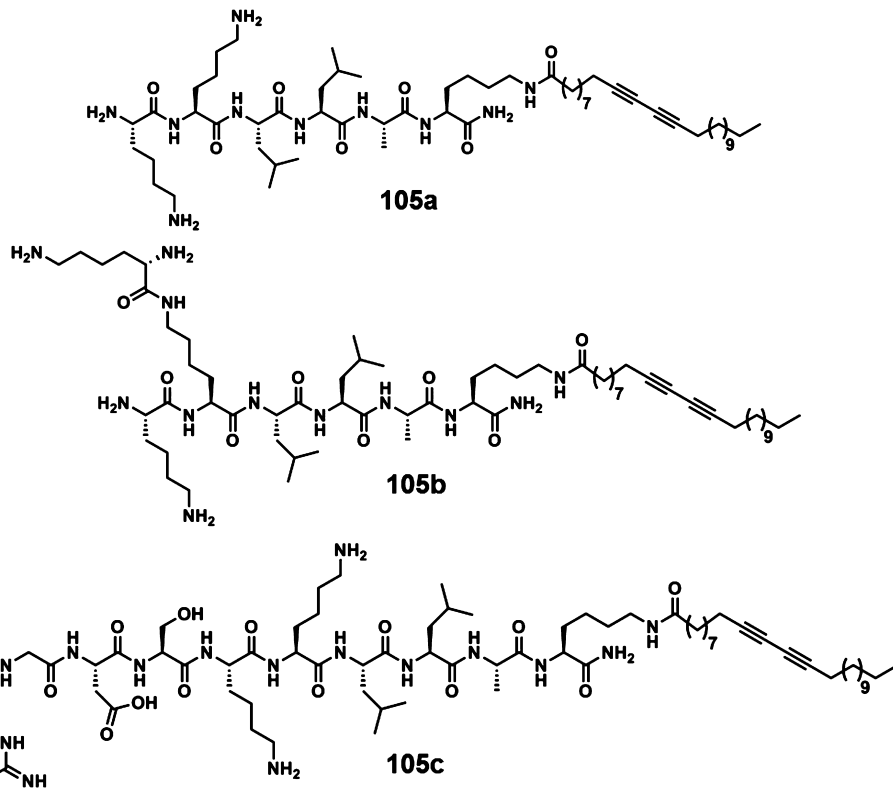
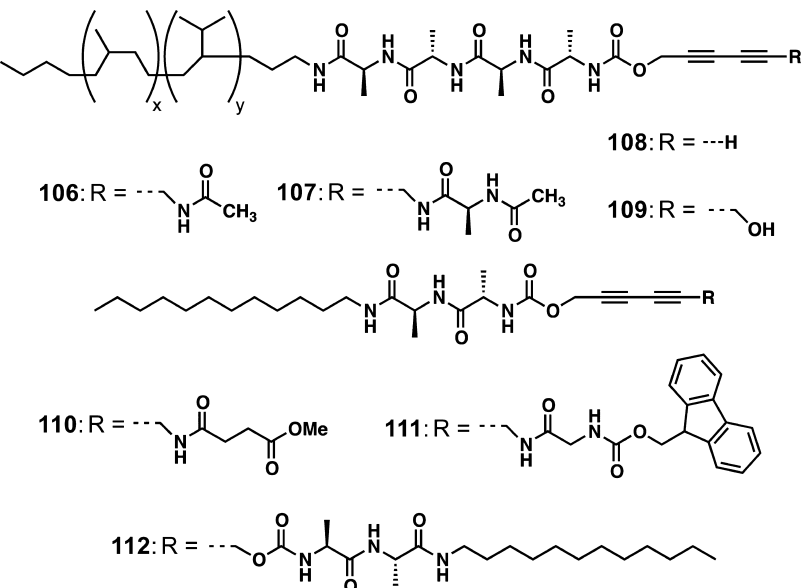


Chart 27



There are several reports of gelators based on peptide amphiphiles containing photopolymerizable diacetylenes 102–114 (Figure 16 and Charts 26 and 27).^{318–330} The presence of amino acid units direct the self-assembly and gelation, enabling the diacetylene moieties to ideally position for photopolymerization. UV irradiation of gels of 103a and 103b (Figure 16) at 254 nm produced red colored gels with straight and tightly packed fibers due to cross-linking.³¹⁹ Studies on the fiber forming properties and polymerization characteristics of two peptide amphiphile based gelators 104a,b revealed that the peptide sequence GANPNAAG allowed remarkably stable and

twisted ribbons to be prepared which can be aligned with the help of an applied magnetic field (Figure 16).^{320,321} The stable, aligned β-sheet fibers formed by the diyne containing peptide amphiphiles did not change the fiber structure, even after the polymerization.

Stupp et al. have reported the preparation of supramolecular nanofibers of 105a and 105b (Chart 26) having β-sheet structures.³²² As a clear indication of the effect of molecular order on the efficiency of polymerization, 105b with branched architectures exhibited less efficient polymerization. The topographical patterns obtained from peptide amphiphiles

Chart 28

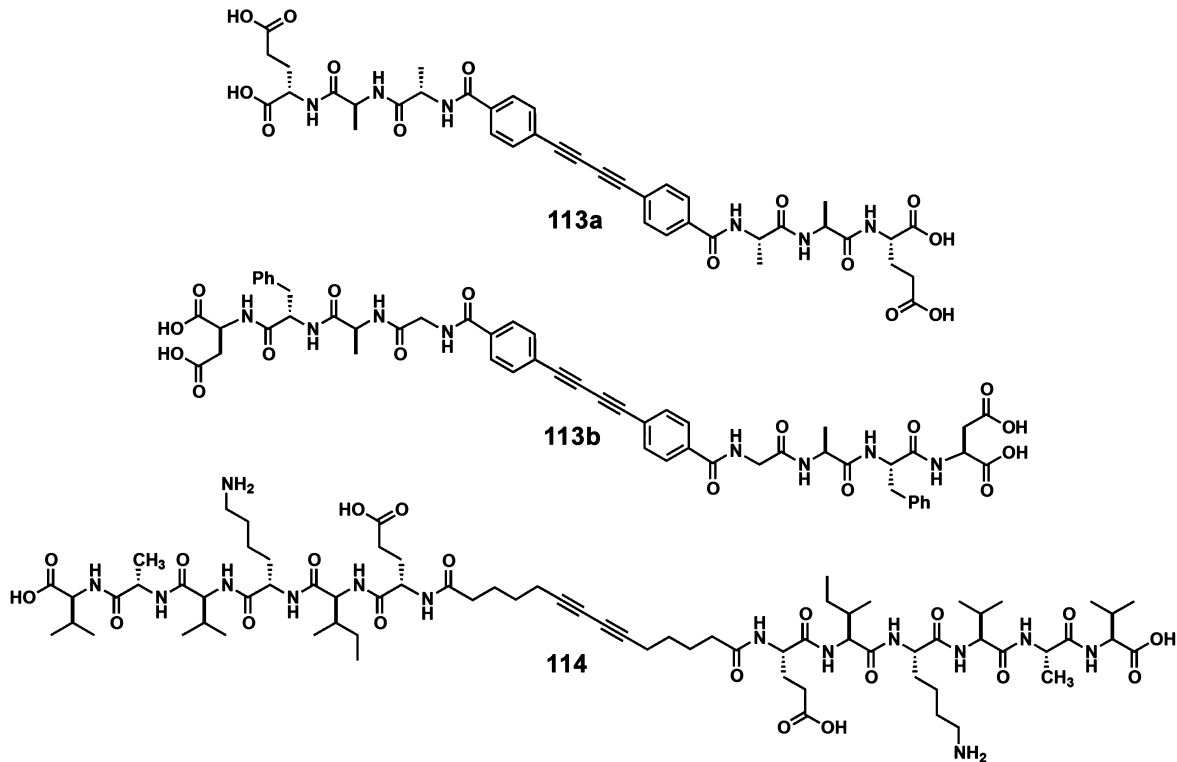
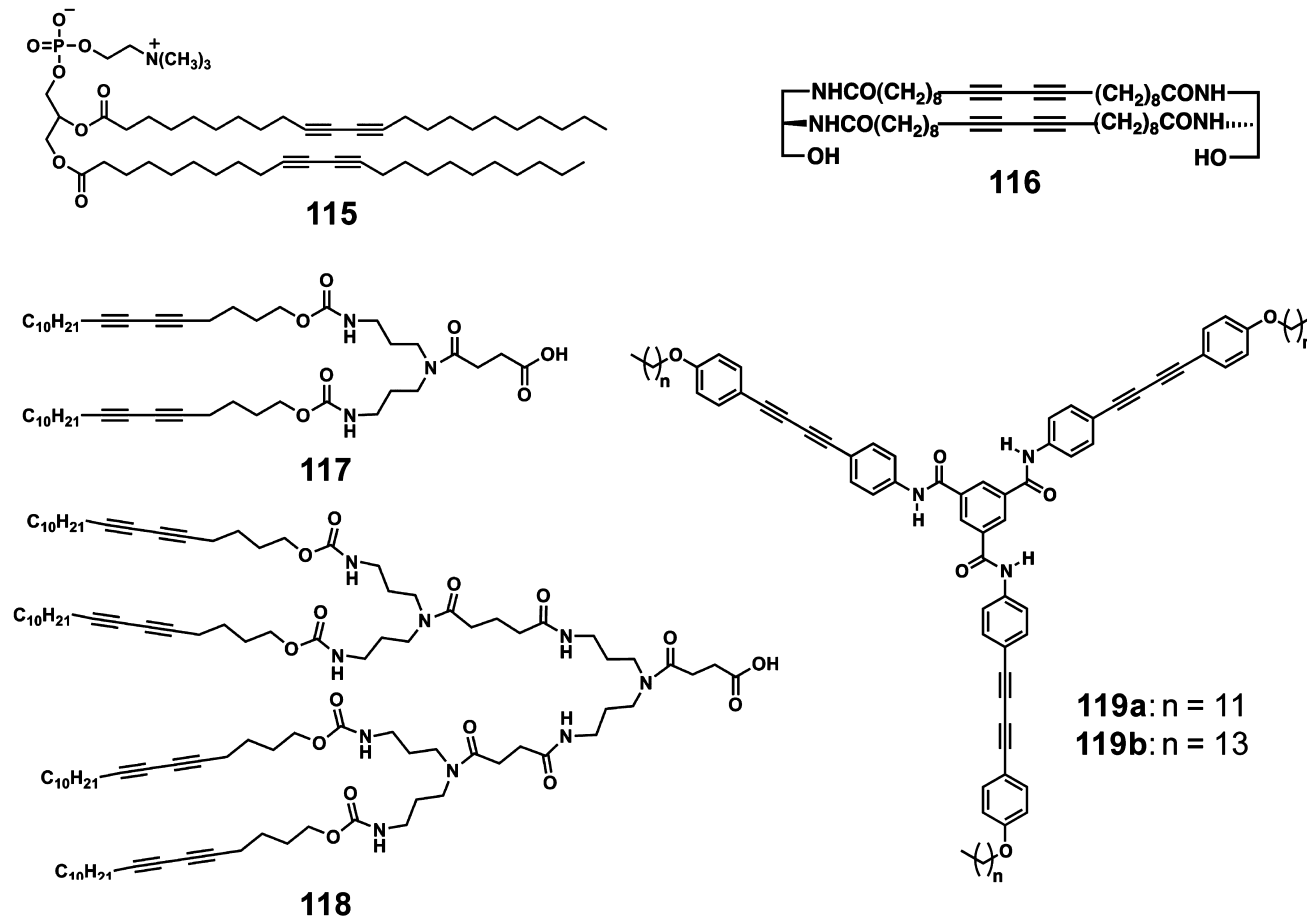


Chart 29



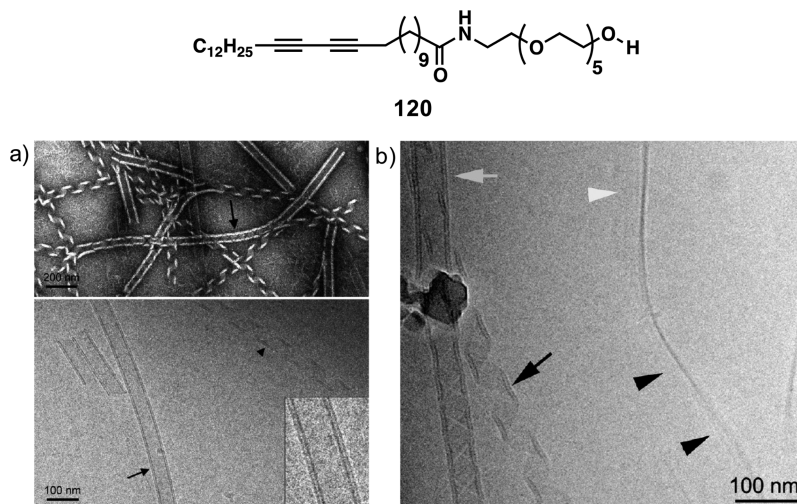


Figure 17. (a) TEM (0.1% aqueous solution) (top) and cryo-TEM of the self-assembled nanotubes formed by **120** (0.05% aqueous solution) (bottom). (b) Corresponding cryo-TEM of polymerized nanotubes (0.05% aqueous solution). (Reprinted with permission from ref 335. Copyright 2011 American Chemical Society.)

105a and **105c** (Chart 26) have been used to create cell environments with microtextures and well-defined nanoscale bioactivity.³²³ The photopolymerization of diacetylene macromonomers **106** and **107** (Chart 27) consisting of hydrogenated poly(isoprene) and β -sheet forming oligopeptide upon UV irradiation gave supramolecular polymers with a double-helical topology.^{302,324–329} In these structures, the degree of order in the parallel β -sheets is governed by the number of hydrogen bonds at the end group that controls degree of diacetylenes polymerization. This is clear from the successful photopolymerization of supramolecular polymers of macromonomers **106** and **107** and organogels of amphiphilic diacetylene model compounds **110–112** (Chart 27). However, gels obtained from **108** and **109** failed to do so.^{328,329} The peptide-diacetylene-peptide molecules **113** and **114** (Chart 28) are shown to form aligned macroscopic hydrogels consisting of 1D nanostructures in acidic water.³³⁰ The internal diacetylene unit of **113b** can be photopolymerized into polydiacetylenes that run parallel to the nanostructure long axis and the resulting polydiacetylenes exhibited ambipolar charge transport.

Photopolymerization of nanotubes and ribbons of phospholipid diacetylene conjugate **115** (Chart 29) revealed that nanotubes are spontaneously transformed to helical ribbons.³³¹ In the case of the gelator **116** (Chart 29), helical ribbons were formed which are responsible for the 3D network of the photopolymerized gel.³³² Polymerization and stabilization of the supramolecular nanostructures formed by the urethane-amide dendrons **117** and **118** (Chart 29) with diacetylenes moieties at the alkyl periphery have been reported.³³³ Tris[4-(4-alkyloxyphenyl) butadiynylphenyl]-1,3,5-benzenetricarboxamides **119a,b** (Chart 29) form stable gels in THF/cyclohexane mixture.³³⁴ However, the diacetylenic groups in **119a** exhibits poor photoreactivity in the gel state due to the inappropriate alignment for polymerization.

The amphiphilic diacetylene **120** self-assembles into helical tapes or nanotubes (Figure 17a) with a bilayer structure.³³⁵ Photopolymerization enabled the conversion of the nanotubes to helical tapes and flat ribbons as indicated by the TEM images (Figure 17b).

The heterobifunctional molecules **121a–c** (Figure 18) form gels in hexyl methacrylate as the gelling solvent.^{336,337} The

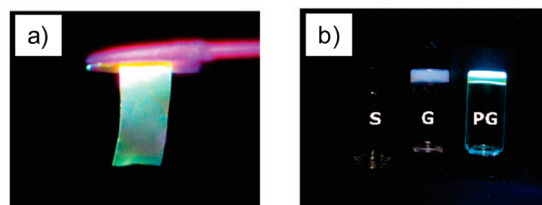
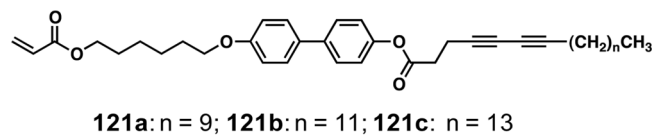
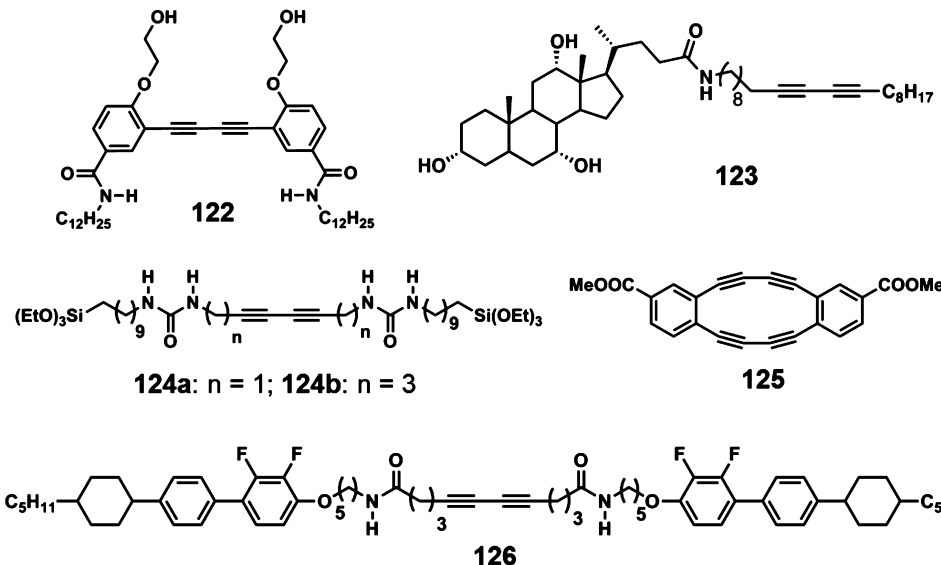


Figure 18. (a) Photographs of the free-standing film of the polymerized gel of **121a** and (b) photographs of vials containing a sol in *n*-decane at 50 °C (left), a gel in *n*-decane at room temperature (middle), and a polymerized gel (right) under 365 nm UV light. (Reprinted with permission from ref 337. Copyright 2008 American Chemical Society.)

photopolymerization of the acryloyl and diacetylene groups of the gelator resulted in nanofibers with a cross-linked structure whereas the simultaneous polymerization of hexyl methacrylate formed a polymer matrix. Interestingly, polymerization occurred in the bulk of the monomeric solvent, inside the self-assembled nanofibers and at the interface between the nanofibers and the solvent. Thus, free-standing films of the polymerized gels could be obtained as shown in Figure 18a. The nonfluorescent sol state of **121a** showed enhanced emission properties in the gel state due to AIEE phenomenon (Figure 18b).

High molecular weight polydiacetylenes ($M_n = 27.9$ kDa) with low polydispersity index ($PI = 1.8$) has been achieved in good yield from a butadiyne derivative **122** (Chart 30) having sterically demanding phenyl groups, using a light-promoted topochemical reaction.³³⁸ A cholic acid derivative with a diacetylene functionality **123** (Chart 30) is found to be a good gelator but failed to undergo photopolymerization in the gel state.³³⁹ Photopolymerization of the diacetylene-urea-trialkoxysilyl gelators **124a,b** (Chart 30) gave thermochromic ureido-polydiacetylene gels.³⁴⁰ The multichromic assemblies could be

Chart 30

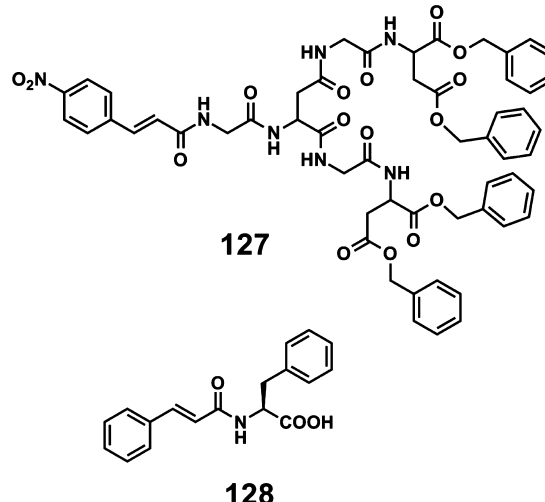


further stabilized by the covalent siloxane network through polycondensation of the trialkoxysilyl groups. This study provided a clear insight about the molecular mechanism of the blue to red color transition and of the reversibility of the purple to red color transition as generally observed in polydiacetylene thermochromism. The dehydrobenzoannulenes **125** (Chart 30) with methyl ester groups was designed in such a way to have boomerang shape with highly polarized substituents in the periphery that could help to align the molecules anisotropically to form stable organogel.³⁴¹ The parallelly aligned fibers of **126** (Chart 30) bridging two gold electrodes were obtained under an electric field.³⁴² The negative dielectric anisotropy of fluorinated rod-shaped LC side groups of **126** is considered to assist the alignment of fibers. In situ photopolymerization enabled to get the macroscopic orientation of the aligned fibers. Optically active polydiacetylenes were prepared by UV-irradiation of the xerogel of the achiral diacetylene 10,12-pentacosadiynoic acid and a chiral LMOG *N,N*-9-bis(octadecyl)-Boc-glutamic diamide.³⁴³ Mechanistic pathway of the formation of helical microtubules from an initial solution of nanoscale vesicles in real time was investigated.³⁴⁴ An aqueous mixture of achiral components such as single tailed diacetylenic surfactant, 10,12-pentacosadiynoic acid and a short chain alcohol, geraniol formed vesicles and gels which changed to microtubules with time.

2.8. Cinnamic Acid Derivatives

A photoresponsive reversible gel–sol transition has been observed in *p*-nitrocinnamate containing amino acid-based dendron gelator **127** (Chart 31).³⁴⁵ A similar observation was reported by Xu and co-workers using cinnamic acid functionalized amino acid derivative **128** (Chart 31).³⁴⁶ Raghavan and co-workers have investigated combinations of surfactants and cinnamic acid derivatives to tune the gelation properties.^{347–349} They have used combinations of cationic surfactant cetyl trimethylammonium bromide and *o*-methoxy-cinnamic acid,³⁴⁷ zwitterionic surfactant erucyl dimethyl amidopropyl betaine and *o*-methoxy-cinnamic acid,³⁴⁸ and phospholipid lecithin and *p*-coumaric acid.³⁴⁹ Upon irradiation by UV light (<400 nm), photoisomerization of cinnamic acid from its trans to cis form

Chart 31

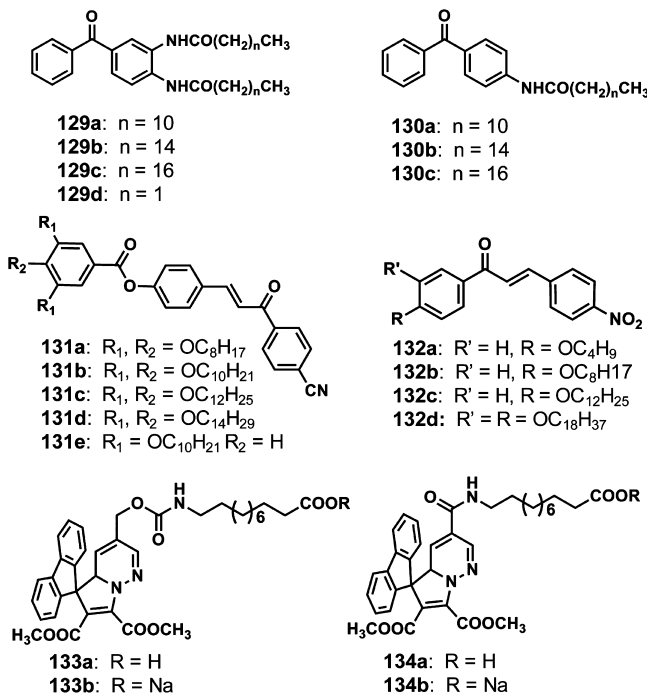


changes the molecular packing significantly and thereby decrease viscosity. In another report, the aqueous solutions of cationic surfactant cetyltrimethylammonium bromide and sodium cinnamate exhibited higher viscosity and gel formation.³⁵⁰ UV irradiation of the aqueous gel resulted in a remarkable decrease in its viscosity and finally converted to sol. Gel formation in polar and nonpolar organic solvents including commercial fuels and edible oils has also been observed in primary or secondary ammonium salt of cinnamic acid derivatives.^{351–353}

2.9. Miscellaneous Photoresponsive Gelators

A series of photoreactive gelators based on benzophenone alkylamide derivatives **129** and **130** (Chart 32) which undergo photoreaction in the gel state affording solutions of the corresponding pinacols has been reported.³⁵⁴ Photoresponsive organogels of polycatenar type organogelators comprising of a cyanochalcone unit **131a–e** (Chart 32) undergo [2 + 2] addition of the chalcone units upon photoirradiation, inducing a gel–sol transition.³⁵⁵ A series of 4-alkoxynitrochalcones **132a–d** (Chart 32) exhibited organogelation in polar organic solvents.³⁵⁶ Photoinduced ring-opening of the chromene

Chart 32



subunit disrupted supramolecular gel network of **133** and **134** (Chart 32) and can be reverted back by using temperature, light, or pH as external stimuli.³⁵⁷

Compounds **135** and **136** (Chart 33) are examples of photoresponsive gelators that exhibit photochromism upon irradiating with UV light.^{358,359} The cholesterol appended salicylideneaniline derivatives **137** and **138a** (Chart 33) undergo isomerization of salicylideneaniline and keto-enol tautomerism under UV-light, accompanied by gel-sol transition.^{360,361} Interestingly, replacement of the cholesterol group and ester linkage with 3,4,5-tridodecyloxybenzoic acid unit and amide linkage resulted in a gelator **138b** (Chart 33) that showed thermochromic/nonphotochromic behavior in the self-assembled state.³⁶² In addition, these molecules showed AIEE in the gel state due to J-aggregation and inhibition of nonradiative

decay via intramolecular rotation.^{360–362} In addition, photoresponsive gelators based on maleic and fumaric acids are also reported.^{363–368}

3. FUNCTIONAL DYE DERIVED GELATORS

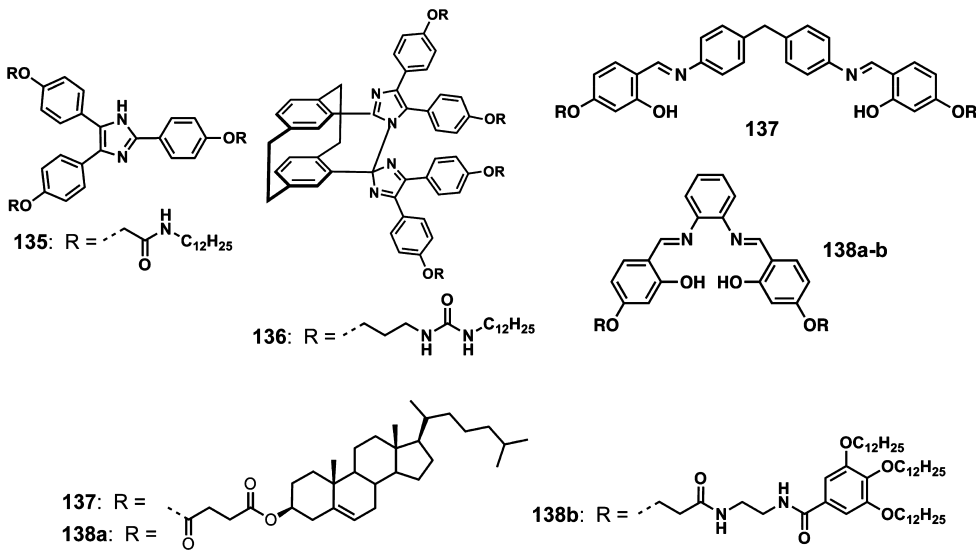
Organic dyes are widely exploited in materials as well as biological applications.^{369–371} Since most of the dyes have a strong tendency to aggregate and to exhibit solvatochromic behavior, self-assembly and gelation of dyes have generated interests among chemists. Synthetic modification of organic dyes with suitable functional groups has resulted in a large number of gelators exhibiting interesting optoelectronic properties. In addition, there has been interest in dye doped gels in which the encapsulated dyes undergo absorption and emission changes depending upon the nature of the gel. A large number of organic functional dyes have been exploited for the design of organogel that are discussed in this section.

3.1. Merocyanines

Merocyanines are intensely colored fluorescent dyes with large extinction coefficients, dipole moments and polarizabilities. Due to the tunable optoelectronic properties, merocyanine dyes have attracted much attention in photovoltaic devices (PVDs).³⁷² In addition, merocyanines are used in nonlinear optics and as photorefractive materials. Due to the strong tendency to form higher order aggregates, merocyanines are known for their gelation properties when suitably functionalized.

Würthner and co-workers have reported the hierarchical self-organization of the merocyanine dye **139** (Figure 19) to supramolecular polymers and organogels, through antiparallel H-type aggregate formation, thus minimizing the electrostatic energy.^{373–375} Based on the detailed optical as well as morphological studies, a structural model for the gelation of **139** has been suggested as depicted in Figure 19. This molecule exists as monomeric units in polar solvents at low concentrations. Increasing concentration or changing the solvent polarity leads to the formation of a well-defined helical polymer with a uniform pitch of about 5 nm. Six of these preorganized strands of the initially formed supramolecular helical polymer further intertwined to form rods laminated with

Chart 33



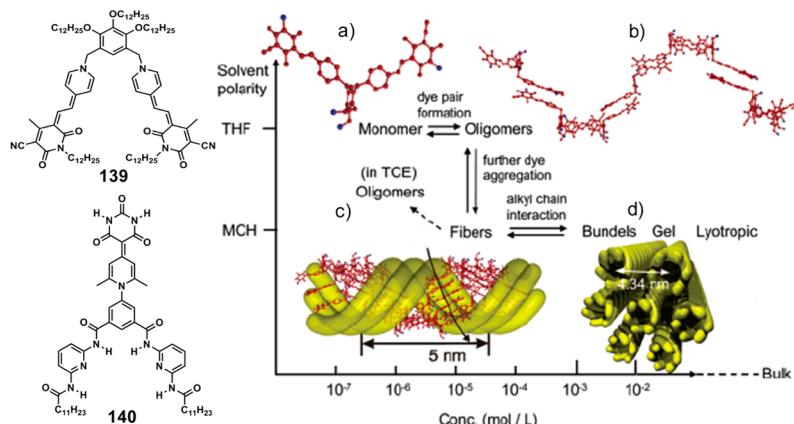
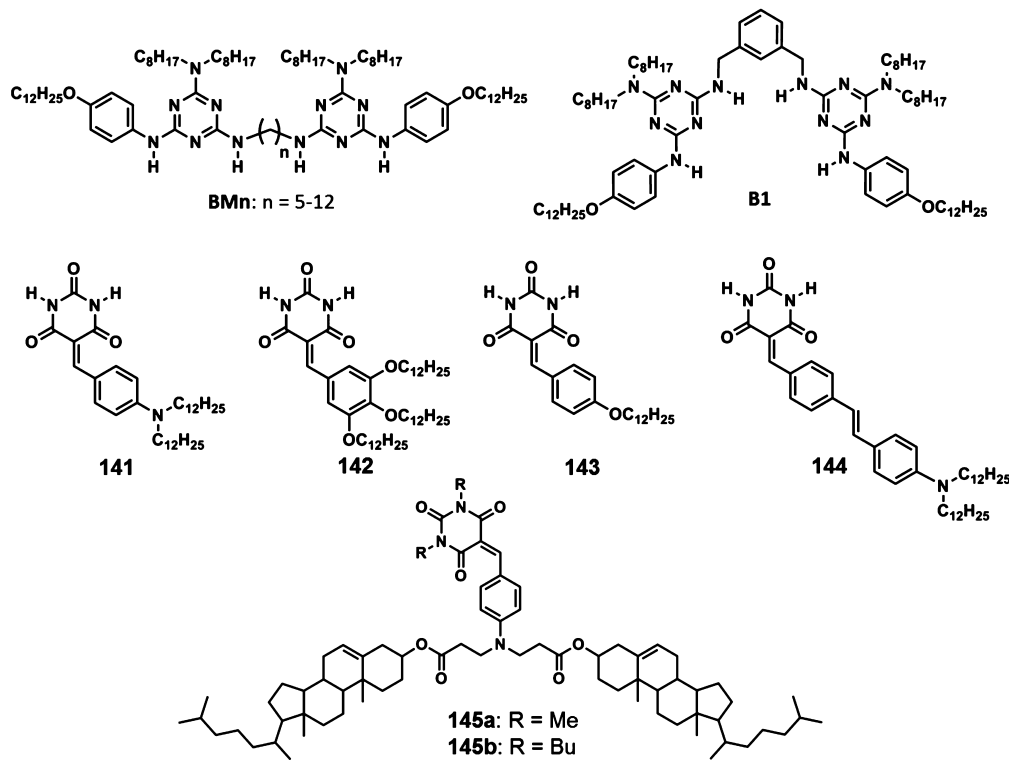


Figure 19. Chemical structures of **139** and **140**. Structural models for the different levels of organization observed for bis(merocyanine) dye **139** in dependence on the solvent polarity and the concentration. (a) Monomer, (b) polymeric chain constituted by antiparallel pairing of merocyanine dyes, and (c) tubular fiber consisting of H-type aggregate dyes. The arrow around the fiber indicates the direction of H-aggregation with a closer and a more distant antiparallel dye neighbor and (d) hexagonal packing of the rods. In methylcyclohexane/THF mixtures, all processes can be controlled in a reversible manner at ambient temperature. (Reprinted with permission from ref 375. Copyright 2004 American Chemical Society.)

Chart 34



alkyl chains. In aliphatic solvents, increase in concentration allowed alkyl chains at the periphery to entangle, resulting in an increase in viscoelastic and gelation properties and a lyotropic mesophase formation. A self-complementary Hamiltion receptor functionalized merocyanine dye **140** (Figure 19) self-assembles in a h-t fashion through six hydrogen bonds, exhibiting enhanced emission in the gel state.³⁷⁶

Complementary hydrogen bonding interaction between flexible bismelamine receptors **BM_n** with different alkyl linker lengths ($n = 5-12$) and the barbituric acid type merocyanine dyes **141-143** (Chart 34) is a good way of creating supramolecular assemblies and gels.³⁷⁷⁻³⁷⁹ The merocyanine dyes **141-143** exhibit efficient gelation in the presence of an equimolar amount of bismelamine receptor **BM₁₂** in nonpolar

organic solvents.³⁷⁷⁻³⁷⁹ **141.BM₁₂** exhibited an entangled fibrous network whereas **143.BM₁₂** showed a 2D sheet-like structure.³⁷⁸ By varying the alkyl linker lengths, columnar structures with and without 2D ordering have been obtained.³⁷⁹ In addition, hierarchical organization afforded phase separated crystalline nanofibers for $n = 5, 7$ and soft nanofibrils, agglomerating into worm-like objects for $n = 8$, gel-forming continuous globular networks for $n = 10$, and nanofibers for $n = 11, 12$ (Figure 20). Barbituric acid functionalized merocyanine dye **144** (Chart 34) forms vesicular aggregates (deformed to coffee-bean-like ellipsoidal morphology upon solvent evaporation) through J-type aggregates.³⁸⁰ The aggregation mode is changed to H-type through dipolar interactions in presence of the barbituric acid receptor **B1** (Chart 34) through the

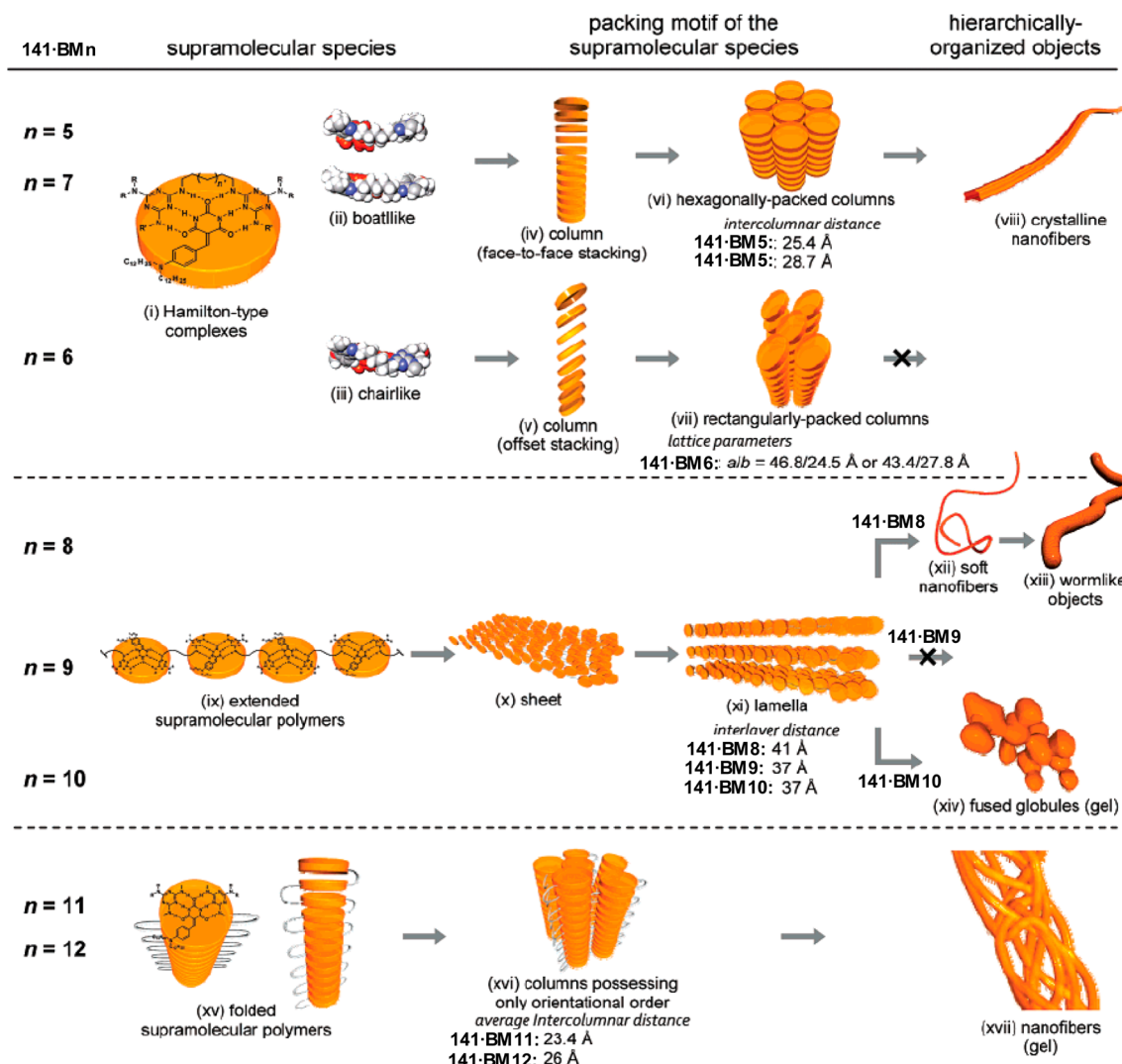


Figure 20. Schematic representation of the hierarchical organization of 141.BMn. (Reprinted with permission from ref 379. Copyright 2007 American Chemical Society.)

formation of hydrogen bonded complex, leading to gelation and ribbon-like aggregates.

Aggregation and gelation properties of cholesterol appended merocyanines **145a,b** (Chart 34) in various organic solvents with dramatically different chromophore packing and distinct optical properties were reported by Yagai and co-workers.³⁸¹ Interestingly, morphological transition from kinetically formed nanofibers to thermodynamically stable globules with the disappearance of excitonic interactions between the chromophoric units is also observed. α -Aminoalkyloyl L-glutamic acid amphiphiles form chiral assemblies and induce chirality to achiral cyanine dye which is bonded through specific binding sites.³⁸²

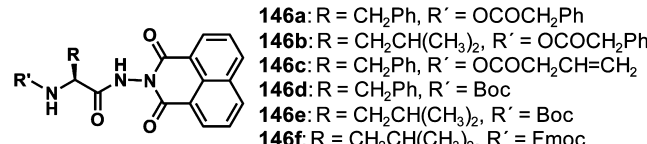
3.2. Naphthalimides

Naphthalene mono- and diimides have attracted much attention due to their tendency to form n-type semiconductor materials.^{383–385} The naphthalimides belong to electron deficient class of aromatic compound and found to be versatile due to easy functionalization through the imide nitrogen or via core substitution.^{383–385} Naphthalimides exhibit good electron transport properties, and hence their self-assembly and gelation

have significance with respect to the creation of supramolecular structures of different size and shape.

A systematic investigation of the organogelation behavior of the amino acid functionalized naphthalene monoimides **146a–f** (Chart 35) in a wide range of solvents to establish a

Chart 35



relationship between the nature of the solvent and the gel formation has been reported.^{134,135,386–389} The side chains of **146a** and **146b** influence the organization of the aggregates, in such a way to form a J-type aggregate for **146b** and an H-type for **146a** in toluene.³⁸⁷ IR and ¹H NMR experiments enabled to understand the aggregation behavior of **146a,b** and found that the preformed hydrogen bonded h-t stacks, resulting in self-assembled columns. Further, small aggregates and gels are formed through inter columnar $\pi-\pi$ stacking.³⁸⁸ The

Chart 36

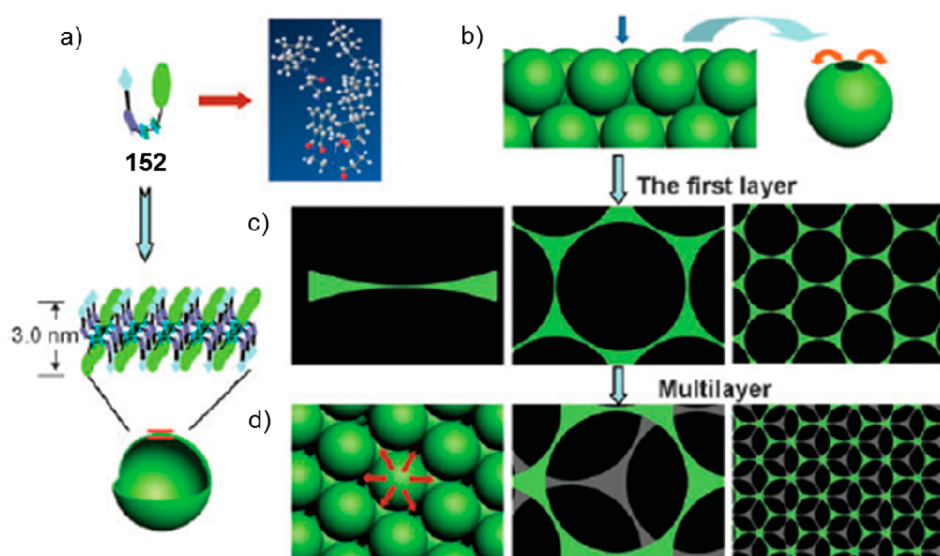
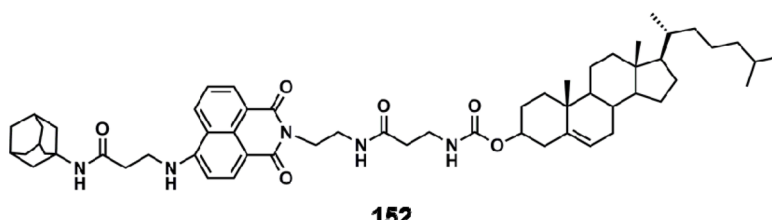
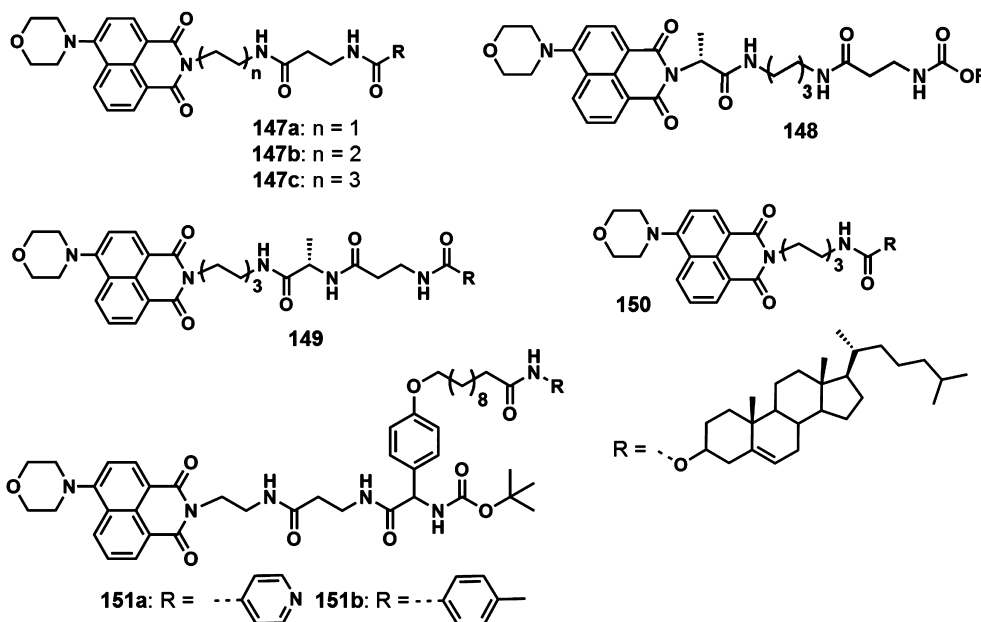


Figure 21. Schematic representation of the mechanism of formation of a regular pattern; (a) vesicle structure; (b) arrangement of the vesicles in solution, the red arrow indicates the direction of molecular movement with evaporation; formation of the porous pattern on (c) the first layer and (d) multilayer. (Reprinted with permission from ref 394. Copyright 2010 The Royal Society of Chemistry.)

importance of hydrogen bonding, Hansen parameter and Hildebrand parameter pertaining to the gelation was also investigated.³⁸⁹ The dynamical behavior of solvent in a gel phase of **146a** and intermolecular structural features of gelator in the gel nanofiber have been investigated using NMR spin relaxation and diffusion experiments.^{134,135}

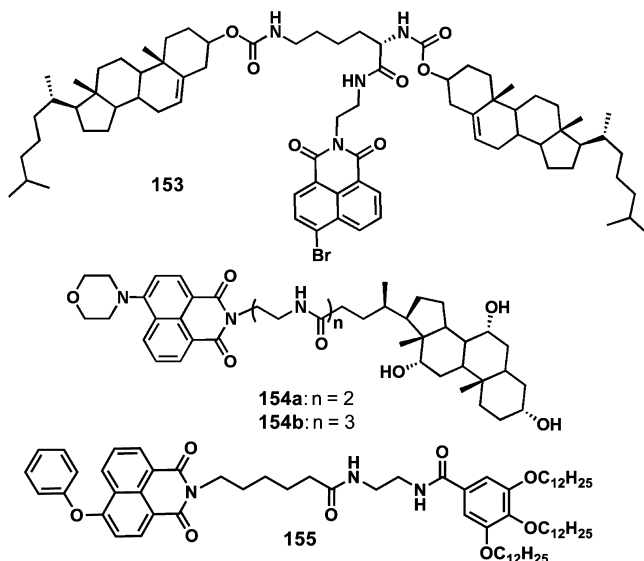
Yi and co-workers have made significant contribution in the area of naphthalimide based organogelators.^{390–399} External stimuli such as heat and ultrasound have been used to achieve a thermodynamic balance between hydrogen bonding, hydrophobic interactions, and $\pi-\pi$ interactions, to control the solubility, gelation, and morphological features of a family of asymmetric cholesterol containing naphthalimide based orga-

nogelators **147–150** (Chart 36) having different alkyl chain spacers.^{390–392} Comparison of the gelation studies of **148** and **149** indicate that the presence of a chiral center at the middle position of the linker facilitate the gelation of the latter.³⁹² Moreover, upon sonication, an instantaneous gel-to-gel transition occurred with morphological change from micelle structure of **148** and the core–shell microsphere of **149** to entangled fibers. The gelator **151b** formed a vesicular structure whereas the gelator **151a** having a heteroatom showed a spherical morphology (Chart 36).³⁹³

A self-assembly approach has been utilized to generate large area honeycomb patterned films of the gelator **152** (Figure 21), by casting the solution onto solid substrates followed by evaporation.³⁹⁴ As shown in Figure 21, a model was proposed to explain these results. At the beginning, quasi amphiphilic character of the folded structure of **152** allowed the formation of vesicles in CH_2Cl_2 , which was then deposited on the surface of a substrate (Figure 21a). As the solvent began to vaporize, these structures started to break around the surface of the solvent due to the pressure difference between the inside and outside of the vesicle. With further evaporation of solvent, the molecules moved to the more diluted area and reaggregated (Figure 21b). On reaching the surface of the liquid to the bottom of the vesicles, the molecules moved from the upper part of the vesicles and aggregated in the gap between adjacent vesicles to form a hexagonal grid-like pattern (Figure 21c). In addition, in the case of multilayer structure, cross bed pattern was also found (Figure 21d). These studies indicate that the preorganization of deposited vesicles in a packed and ordered manner is essential to obtain such a regular hexagonal pattern.

A cross-linked ring structure with nanoscale to microscale pores has been obtained from thixotropic, self-healing organogel of **153** (Chart 37).³⁹⁵ The reversible rheological switching

Chart 37



was observed with respect to alternate shaking and resting due to ring disintegration and reconstitution of the gel network. A variety of up conversion nanoparticle (UCNP)-organogel nanocomposites of cholic acid-based tripeptide containing naphthalimide fluorophore **154a,b** (Chart 37) with different UCNPs, such as NaYF_4 :20 mol % Yb, 2% Er (UCNP-Red), NaYF_4 :25 mol % Yb, 2% Er (UCNP-Green), and NaYF_4 :20

mol % Yb, 1% Tm (UCNP-Blue) have been reported.³⁹⁶ These hybrid gels show different colors under normal light and on excitation with a near IR light.

White a light emitting two component gel was obtained when phenol substituted 1,8-naphthalimide derivative **155** (Chart 37) was mixed with an orange emitting iridium(III) complex.³⁹⁷ In addition, the gel composite has been used for the naked eye detection of cysteine. The naphthalimide based gelators **156** and **157** (Figure 22) form blue and green emitting

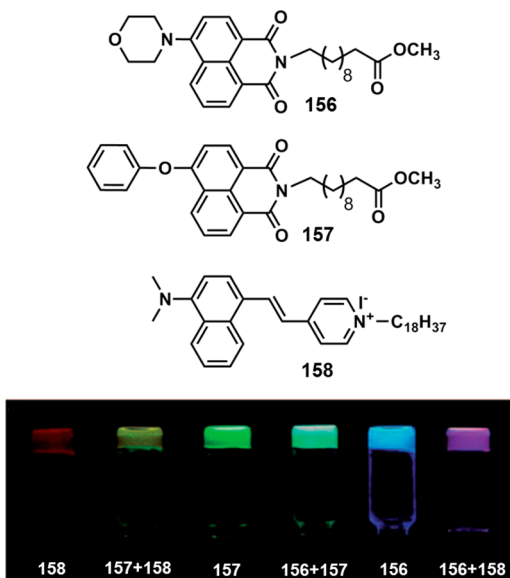


Figure 22. Images of mixed gels which emit six different colors upon illumination with a single wavelength (365 nm). (Reprinted with permission from ref 398. Copyright 2008 The Royal Society of Chemistry.)

gels respectively.³⁹⁸ Intermolecular energy transfer has been observed with these gels and a red emitting hemicyanine dye based gelator **158** (Figure 22).³⁹⁸ Thus, six different emission colors are obtained by a single excitation wavelength (365 nm) of the mixed gels (Figure 22).

Yi et al. have studied the fluorescence, morphology and surface wettability of naphthalimide gelator **159** (Figure 23) by UV-light irradiation in the presence of melamine group containing the photochromic diarylethene unit DTE.³⁹⁹ The flaky texture (Figure 23a) of the gelator was changed to film-like morphology (Figure 23b), when it was complexed with diarylethene and further to aggregated flakes (Figure 23c) when the complex was irradiated by UV light. The change of the surface morphology resulted in switchable wettability of the film surface upon alternate irradiation of UV/vis light.

Near IR chiroptical switching has been reported in the redox-active gels of a sugar appended NDI based gelator **160** (Chart 38).⁴⁰⁰ Shinkai and co-workers have reported a NDI based stimuli responsive gelator **161** (Chart 38) which can be used for the colorimetric detection of various naphthalene derivatives.⁴⁰¹ These thixotropic organogelators exhibit self-healing process to regenerate the disintegrated 1D fibers with time.⁴⁰² Moreover, the addition of a molecular adhesive 1,3-dihydroxynaphthalene to the disintegrated gel, regenerated the fibers. However, when 1,6-dihydroxy naphthalene was added, 2D sheet-like structures were formed.

In the case of the NDI derived gelators **162a–c** (Chart 39), the morphology showed a drastic variation from entangled

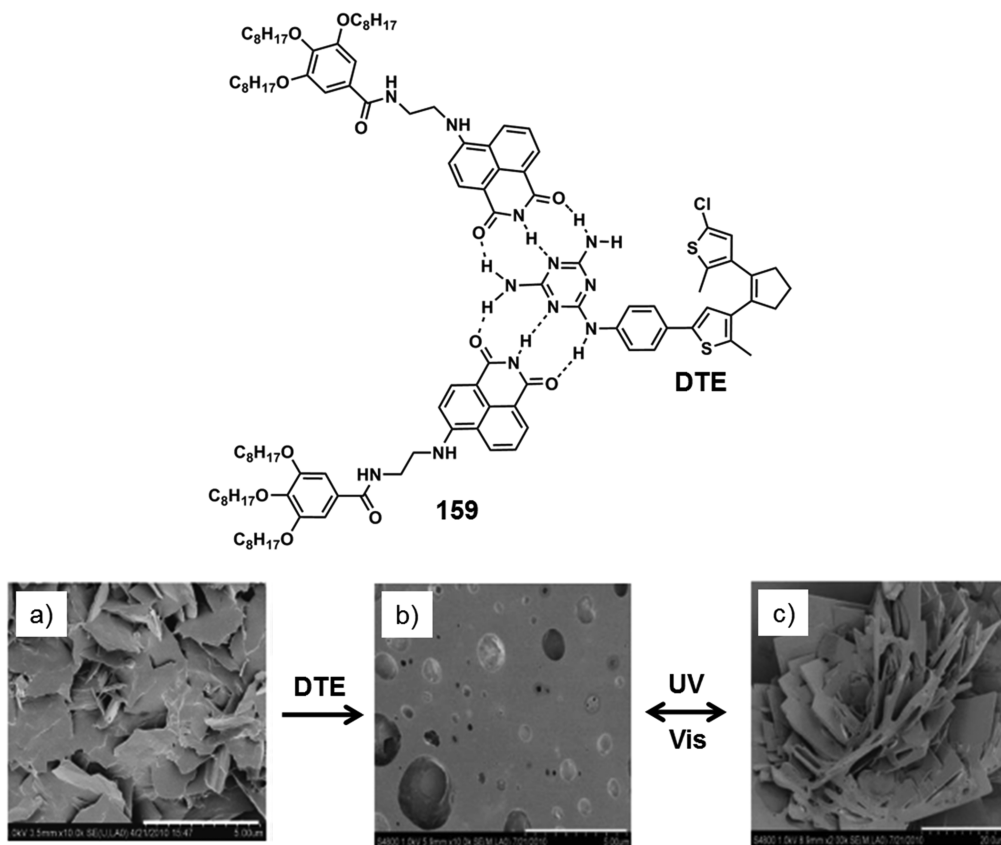
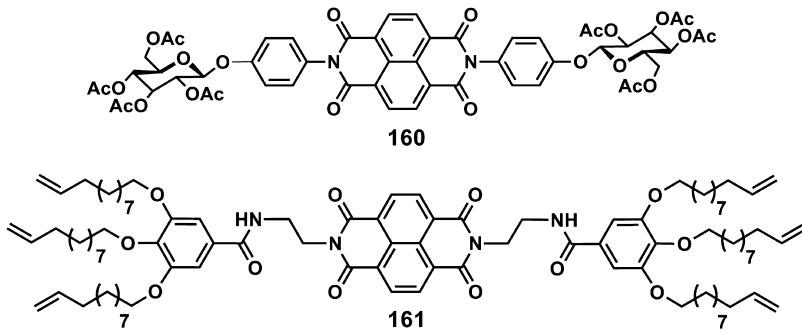


Figure 23. Molecular structures of the naphthalimide gelator **159** and diarylethene unit (DTE). SEM images of (a) ethyl acetate gel of **159**, complex **159+DTE**, (b) before and (c) after UV irradiation. (Reprinted with permission from ref 399. Copyright 2011 American Chemical Society.)

Chart 38

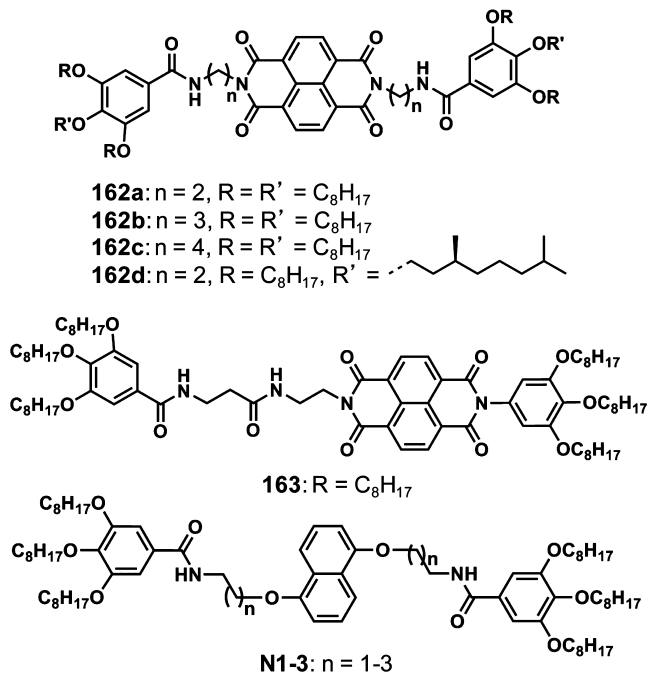


micrometer long nanowires for **162a** to relatively less entangled nanoribbons with much higher aspect ratio for **162b** to discontinuous hairy nanofibers for **162c** when the number of methylene units between the bis(trioctyloxybenzene) and the NDI units was varied systematically.⁴⁰³ The sergeant and soldiers effect has been used to induce supramolecular chirality from helical fibers of **162d** to achiral dialkoxy naphthalene **N1** (Chart 39) fibers due to the hydrophobic interaction among the peripheral alkyl chains.⁴⁰⁴ Self-sorting has been observed when **163** and **N3** (Chart 39) were mixed in 1:1 ratio due to the absence of molecular mixing among the donor and acceptor units, whereas coassembly of **162a** and **N3** produced an intense red gel due to a CT-interaction.⁴⁰⁵ Self-sorting was observed in the coassembly of **162a** and **163** also.⁴⁰⁶ Coassembled gels of D–A mixtures of **162a–c** and **N1–3** exhibited two distinct modes such as alternate D–A coassembly as well as self-sorted assembly upon variation in the structure of the chromophores

and/or solvent polarity.^{407,408} In the case of strong hydrogen bonding, a kinetically controlled CT-state has been reorganized to form more stable self-sorted state whereas when the CT interaction is dominated and long-lived CT-state has been observed.

The NDI based bolaamphiphile **164** (Figure 24) forms vesicular assembly in aqueous conditions by using synergistic effects of hydrogen bonding and π – π stacking.⁴⁰⁹ Interestingly, addition of pyrene resulted in a time dependent CT mediated morphological transition from vesicle to fiber and finally gelation at higher concentration (Figure 24). Detailed absorption and FT-IR studies revealed that the morphological transition is driven by the intercalation of electron rich pyrene donor in between the electron-deficient NDI based bolaamphiphile without disrupting the hydrogen bonding between the hydrazide units of NDI bolaamphiphiles. Detailed time-dependent morphological studies using AFM showed that

Chart 39



alternatively stacked NDI-pyrene assembly substantially increased the radius of curvature of vesicles, thereby leading to intervesicular fusion and rupturing of membrane to form fibrous structure.

Parquette et al. have reported that the antiparallel β -sheet structure of 165 (Figure 25a) facilitates dimer formation and flat nanobelt assemblies, stabilized by the intermolecular π - π interaction of the NDI and fluorene units, thereby resulting in hydrogels (Figure 25c).⁴¹⁰ The bolaamphiphile 166 (Figure 25b) was found to form stable hydrogel composed of 1D n-type nanotubes (Figure 25d).⁴¹¹ Detailed morphological and optical studies revealed that these nanotubes are formed via

stacking of a monolayer of preformed nanorings. Time resolved fluorescence studies revealed that these systems show energy migration properties. The nanotubular system with homogeneity in the structure and well-defined conformation of constituent NDI chromophoric units ensured rapid migration of excitation energy which makes them very attractive for application in light harvesting devices.

3.3. Perylene Bisimides

Perylene is a polycyclic aromatic hydrocarbon having unique optical and redox properties and stability, hence enable to use in electrophotography (xerographic photoreceptors) and as a blue emitting dopant material in LEDs.⁴¹² Due to the excellent photoconductive properties, perylenes are now used in PVDs and FETs.⁴¹³⁻⁴¹⁶ In recent times, core modified PBIs have been used for the creation of supramolecular assemblies and gels. An interesting case is the organogels of cholesterol functionalized PBI derivatives 167a-d (Figure 26) with tunable optical properties, reported by Shinkai and co-workers.⁴¹⁷ These gels showed cascade energy transfer when mixed together. Various binary, ternary, and quaternary perylene gels were prepared and subjected to energy transfer studies. Selective excitation of 167a at 457 nm resulted in the quenching of its emission at $\lambda_{em} = 544$ nm with efficiencies of 68% for 167b, 53% for 167c, and 34% for 167d, consistent with decreasing D-A spectral overlap (Figure 26). These trends are visually shown in the inset of Figure 26. Addition of the corresponding thiophene derivative into 167a resulted in a self-sorting organogel of two different π -conjugated molecules with p-n heterojunctions.⁴¹⁸ The dissociation temperatures of the gelators monitored by temperature dependent absorption studies of the gel match well with that of the individual gelators indicating that aggregation-dissociation processes are independent of each other.

The gelation properties of a PBI dye 168 (Chart 40) functionalized with long aliphatic chains through urea moieties was reported by Würthner and co-workers.⁴¹⁹ The urea units provide the self-complementary directional hydrogen bonding

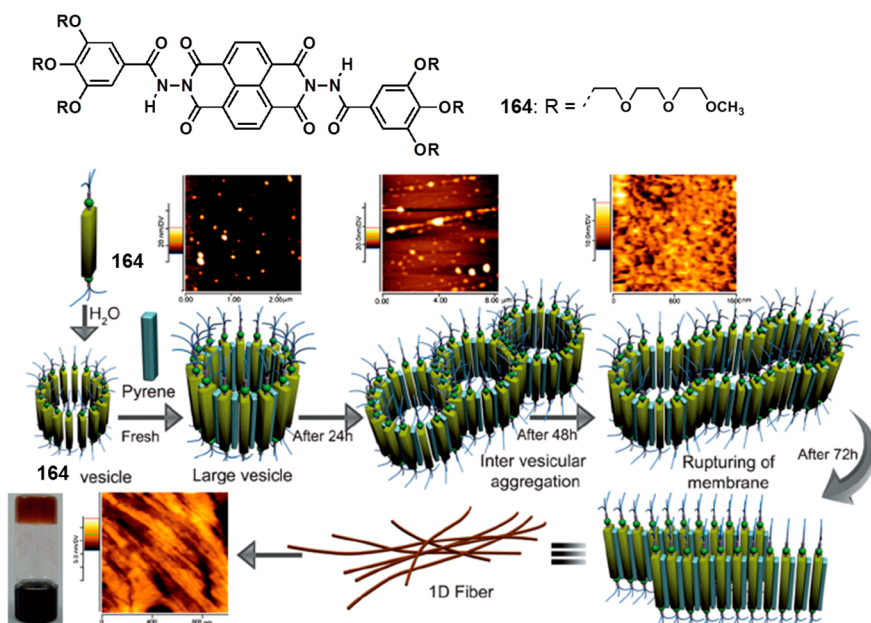


Figure 24. Proposed model for the pyrene (electron rich) induced stepwise morphological transition from vesicles to fibers for 164 (electron deficient), thereby leading to gelation. (Reprinted with permission from ref 409. Copyright 2012 Wiley-VCH.)

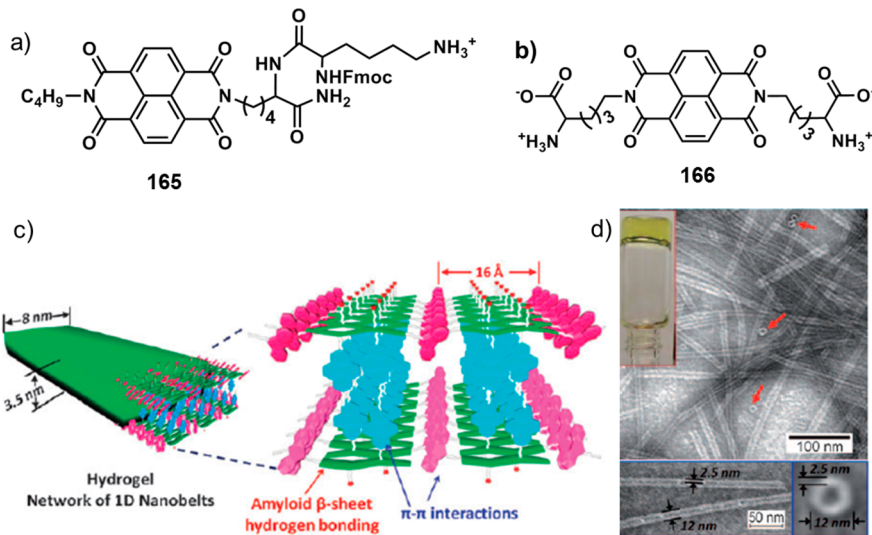


Figure 25. Molecular structures of (a) dipeptide-NDI gelator, **165** and (b) lysine-based bolaamphiphilic gelator, **166**. (c) Schematic representation of the self-assembly of **165** into nanobelts. (d) TEM image of nanotubes formed by **166** in water; inset shows picture of the corresponding gel. The inset in the bottom part of the figure shows two nanotubes and one nanoring. (Panel c reprinted with permission from ref 410. Copyright 2010 The Royal Society of Chemistry. Panel d reprinted with permission from ref 411. Copyright 2010 Wiley-VCH.)

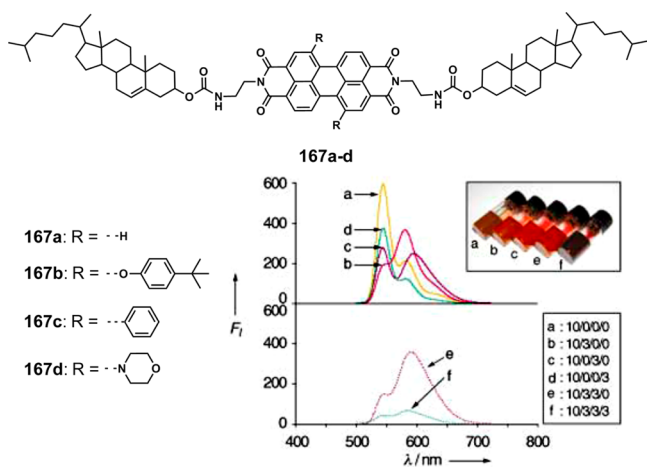
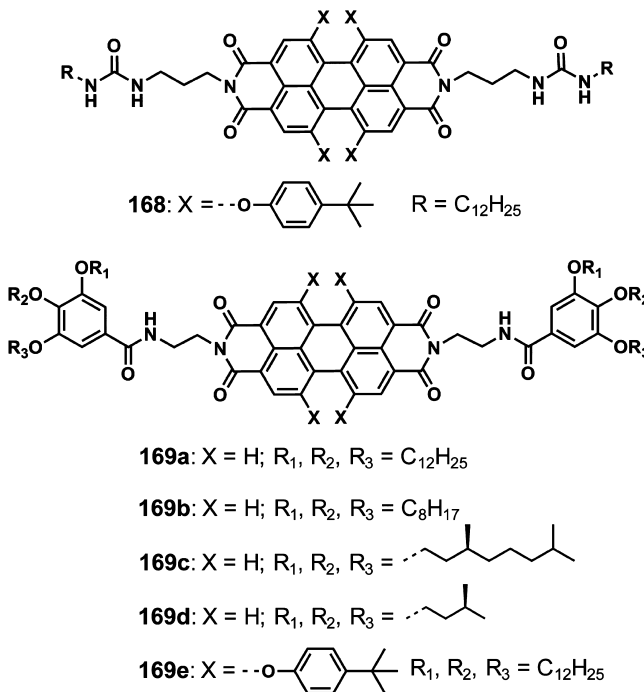


Figure 26. Fluorescence spectra of mixed PBI-cholesterol gels. The numbers in inset denote the molar ratios for **167a**/**167b**/**167c**/**167d**. The corresponding photographs of the mixed gels are also shown in the inset. (Reprinted with permission from ref 416. Copyright 2004 Wiley-VCH.)

to give stacks separated by the $\pi-\pi$ stacking of the PBI core. The replacement of the hydrogen bonding moiety from urea to amide **169a** (Chart 40) also resulted in the self-assembly and gelation in a variety of organic solvents.⁴²⁰ The characteristic optical spectral features of the aggregates of **169a** indicated a close face to face stacking of the rotationally displaced chromophores along the direction of the π -stack. The intense absorbance of **169c** (Chart 40) over the whole visible range resulted in a black colored gel.⁴²¹ PVDs were fabricated using **169c** as an acceptor in combination with a hole transporting polymer poly{N,N'-bis(4-methoxyphenyl)-N-phenyl-N'-4-vinylphenyl-[1,1'-biphenyl]-4,4'-diamin}.⁴²²

An interesting observation regarding the aggregation properties of the PBI based organogelators, **169a-d** (Chart 40), is that the peripheral alkyl side chains influence the mode of $\pi-\pi$ stacking between PBI units and thereby changing the aggregation mode from H- to J-type (Figure 27). Detailed

Chart 40



gelation as well as optical studies revealed that PBI derivatives bearing linear alkyl side chains (**169a,b**) form H-type aggregates and red gels, whereas those with branched alkyl chains (**169c,d**) form J-type aggregates and green gels (Figure 27). The helical bias of achiral PBI aggregates is successfully tuned by using chiral solvents such as (R)- or (S)-limonene. In addition, vortex flow is also found to be useful for the macroscopic chiral orientation of the aggregates of achiral PBI molecules.

The introduction of bulky *tert*-butylphenoxy substituents at the bay positions of the perylene dye exhibited a distorted core and led to a change in aggregation mode from H-type for **169a** to J-type for **169e** (Chart 40).⁴²⁴ As inferred from the

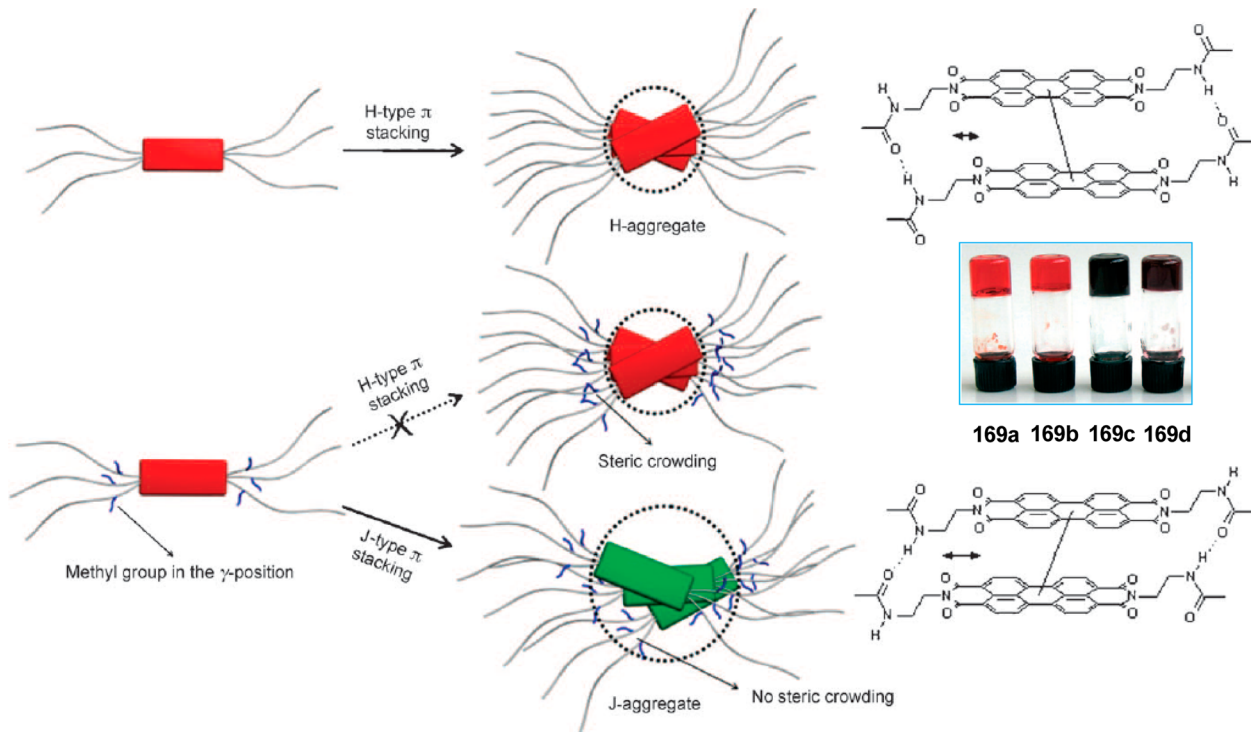
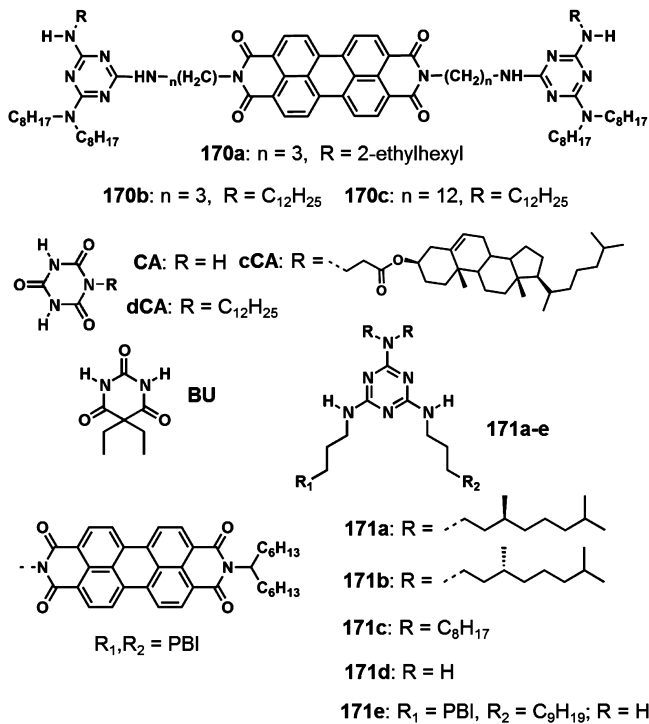


Figure 27. Schematic representation of PBI chromophores with linear (top) and branched (bottom) alkyl substituents (left). The transition from H- (top) to J-type (bottom) π -stacking with increasing steric demand of the peripheral alkyl side chains (middle). Packing model for H- (top) and J-type (bottom) π -stacking (right). In both cases additional rotational offsets are needed to enable close $\pi-\pi$ contact and hydrogen bonding. The inset shows photographs of the red gels of 169a,b that form H-type aggregates and green gels of 169c,d that form J-type aggregates. (Reprinted with permission from ref 423. Copyright 2008 Wiley-VCH.)

absorption studies in apolar solvents, 169e strongly aggregated due to intermolecular π -stacking and hydrogen bonding while in polar solvents aggregation tendency is diminished due to competing hydrogen bonding with solvent molecules, however impose gelation at higher concentrations.

Yagai and co-workers have utilized the complementary interaction between cyanurates and melamines for the gelation-induced fabrication of 1D aggregates of PBI derivatives 170a–c (Chart 41).^{425,426} The 1:1 complexation of 170a with complementary hydrogen bonding components such as N-dodecylcyanurate dCA (Chart 41) resulted in the formation of flexible hydrogen bonded supramolecular polymers.⁴²⁵ Similarly, 1:1 mixture of 170b with dCA and a cholesterol appended cyanurate cCA (Chart 41) as well as a mixture of 170c and dCA could gelate many of the aliphatic nonpolar solvents tested.⁴²⁶ Very recently, they have reported that 3:1 complexation between melamines functionalized with two PBI chromophores and two 3,7-dimethyloctyl chiral handles 171a–c (Chart 41) with cyanuric acid CA (Chart 41) form helical columnar assemblies (Figure 28) which eventually lead to gelation.⁴²⁷ CD and TRMC studies have revealed the presence of extended chiral stacks of PBI chromophores within the columnar assemblies. Detailed CD studies indicated that “majority-rules”, where a slight excess of an enantiomer dictates the overall helical sense, is operative in the mixed columnar assemblies prepared from varying molar ratios of the melamine-PBI derivative having R and S chiral handles (171b and 171a, respectively). Organogels of 171d in combination with barbiturate BU (Chart 41) having complementary hydrogen bonding motifs, formed multilayer terraced morphologies with perpendicular lamellar periodicity with the axis of semi-

Chart 41



conductive PBI stacks parallel to the substrate.⁴²⁸ FET measurements of the lamellar structures exhibited an electron mobility value of $1 \times 10^{-4} \text{ cm}^2 \text{ V}^{-1} \text{ s}^{-1}$. The melamine derivative functionalized with only one PBI unit 171e (Chart

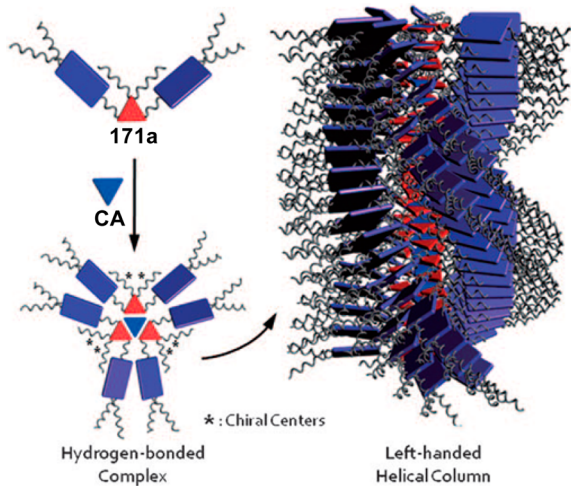


Figure 28. Schematic representation of a proposed helical columnar structure formed from hydrogen bonded complex **171a**·**CA**. (Reprinted with permission from ref 427. Copyright 2011 Wiley-VCH.)

41) was reported to form organogel upon self-aggregation, also in the presence of **dCA**.⁴²⁹ However, hydrogen bonded complex of **171d-dCA** and **171e-BU** failed to gelate any of the solvents tested.

The aggregation of **172a** (dimer) and **172b** (hexamer) resulted in folded conformation with the two PBI units through an intramolecular process and formed large molecular aggregates via an intermolecular process (Figure 29).⁴³⁰ In the case of **172a**, bundles of long fibers are formed whereas **172b** formed small rod-like aggregates (Figure 29c,d).

The PBI-bipyridine system **173** (Figure 30) decorated with polyethyleneglycol chains self-assembles to form extended supramolecular fibers and aqueous gels with excellent light absorption and exciton mobility characteristics.⁴³¹ These gels were stable up to 70 °C, however further heating to 100 °C led to expulsion of solvents and shrinkage of the gel without damaging the morphology. It shows the robustness of the gel fibers (Figure 30). This is a unique observation when compared to other supramolecular gels where heating at higher temperature normally lead to gel–sol transition and the disintergration of the self-assembled fibers. The shrinkage of gel is due to a complex interplay between the hydrophobic

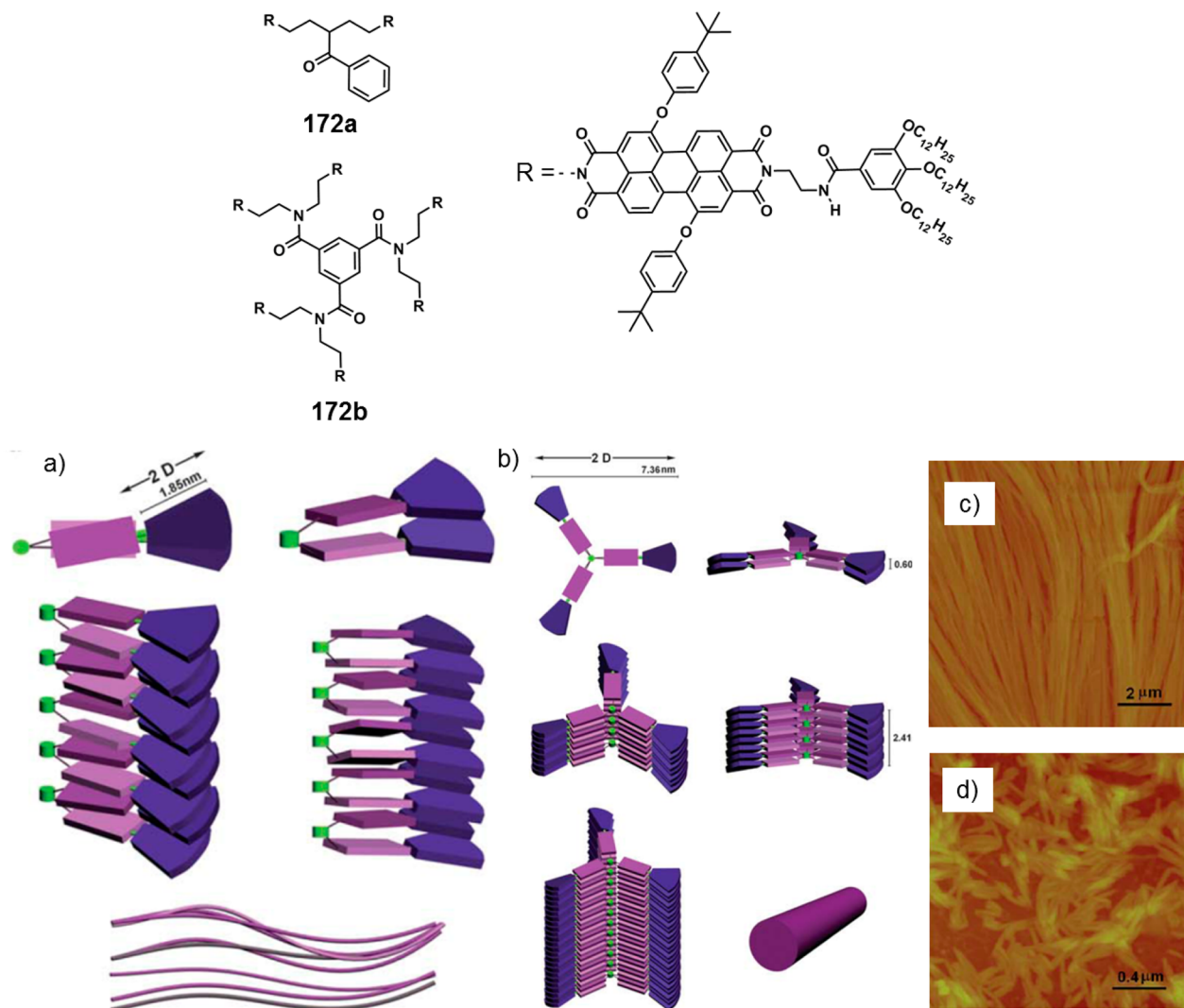


Figure 29. Chemical structures of **172a,b**. Proposed aggregation modes of (a) **172a** and (b) **172b**. AFM images of diluted methylcyclohexane gel of (c) **172a** and (d) **172b**. (Reprinted with permission from ref 430. Copyright 2011 The Royal Society of Chemistry.)

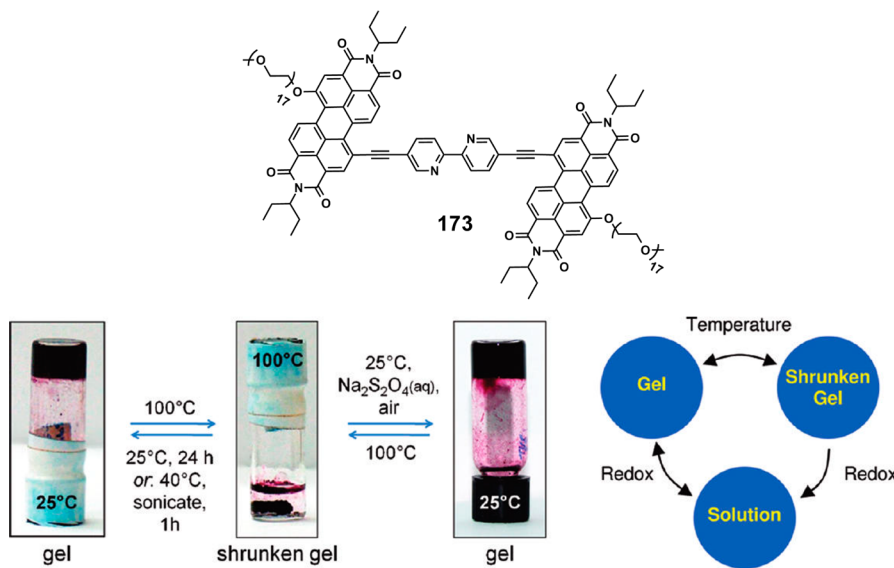
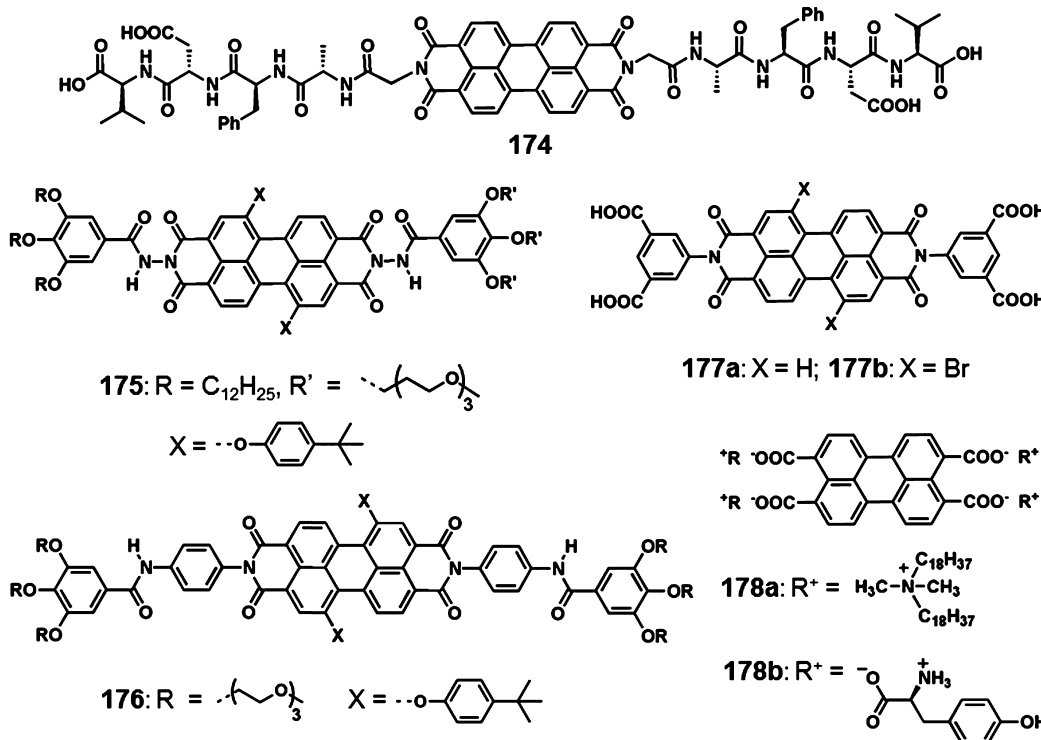


Figure 30. Chemical structure of the gelator 173. Left: shrinkage of the gel of 173 (water/THF, 80:20, v/v) in response to the rise in temperature. The completely swollen gel is obtained back after 24 h at room temperature. It can be obtained more rapidly by either sonicating at 40 °C for 1 h or by addition of 1 equiv. of Na₂S₂O₄(aq) in the presence of air. Right: reversible switching between swollen gel, shrunken gel, and solution by exploiting response to temperature and reversible charging. (Reprinted with permission from ref 431. Copyright 2009 American Chemical Society.)

Chart 42



effect and solvation of glycol chains at higher temperatures. The shrinkage is reversible in several ways. Swelling of the shrunken gel took place on slow cooling of a hot gel to room temperature over a period of ~24 h. However, sonication for 1 h at 40 °C accelerated the swelling process. The fastest way for swelling is reduction induced gel to sol transition by adding a reducing agent Na₂S₂O₄, followed by gelation within several minutes due to oxidation by atmospheric oxygen. Detailed optical and electron spin resonance studies indicate stimuli responsiveness

of the gel on reduction and oxidation due to the reversible charging of 173 and the resultant solubility changes.

The controlled assembly of the PBI 174 (Chart 42) has been achieved by symmetrically substituting with a peptide scaffold.⁴³² Li et al. reported the gelation of amphiphilic PBI derivative 175 (Chart 42) and bolaamphiphilic 176 (Chart 42) through the formation of J- and H-type aggregates, respectively.⁴³³ The hydrogelators 177a,b (Chart 42) form H-type aggregates of the perylene core which can be cross-linked by hydrogen bonding with melamine units resulting in

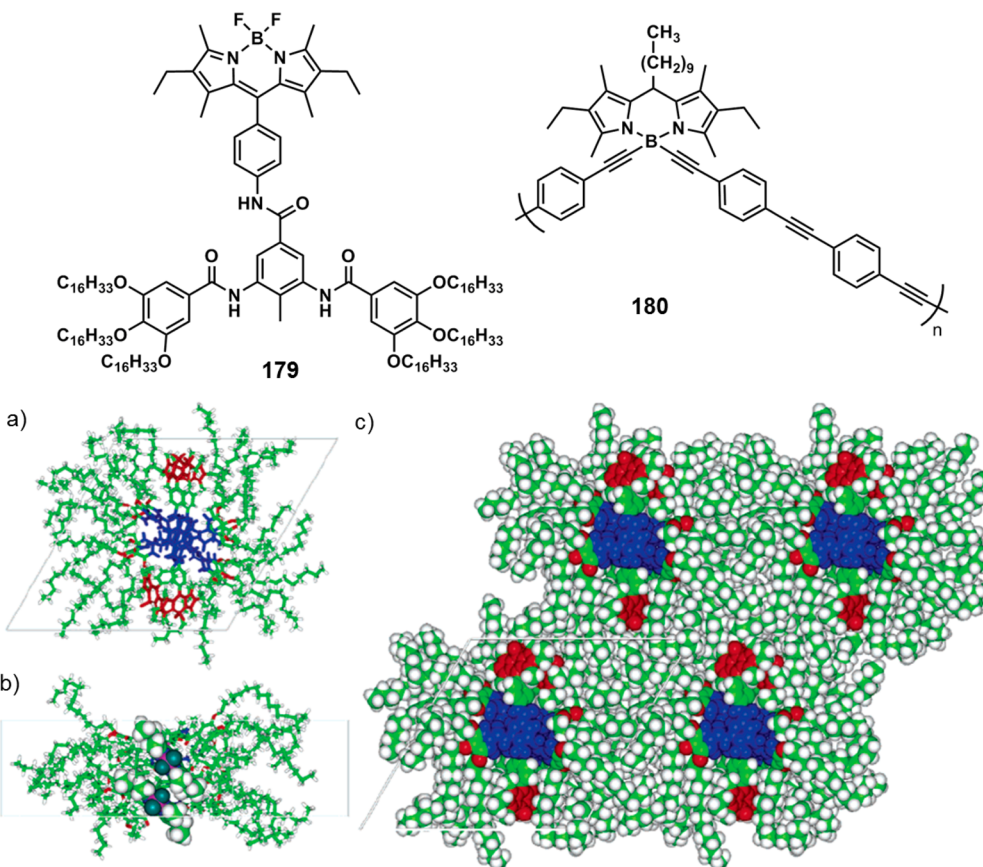


Figure 31. (a) Top view of the formation of hydrogen bonded dimers of **179** (central core in blue, BODIPY in red). (b) Side view showing the stacking of four **179** molecules. (c) Self-assembled hexagonal lattice of the Col_h phase of **179**. (Reprinted with permission from ref 443. Copyright 2006 American Chemical Society.)

luminescent gels.⁴³⁴ The perylene-3,4,9,10-tetracarboxylate ion is capable of forming fluorescent gels with cationic surfactants such as dioctadecyldimethylammonium bromide **178a** (Chart 42)⁴³⁵ as well as L-tyrosine **178b** (Chart 42).⁴³⁶ A two component organogel consisting of perylene dye and bis carbamate-based organogelator has been reported by Khan and Sundarajan.⁴³⁷ A color tunable gelation induced fluorescence enhancement upon varying the concentration of doped PBI was observed in dendron substituted tetraphenylethene gel.⁴³⁸

3.4. BODIPY Dyes

4,4-Difluoro-4-bora-3a,4a-diaza-s-indacene (BODIPY or boron-dipyrromethene) dyes are known to have high molar absorption coefficients and fluorescence quantum yields.^{439–441} Negligible triplet state formation, narrow emission bandwidths with high peak intensities, good solubility, excitation/emission wavelengths in the visible spectral region, and fluorescence lifetimes in the nanosecond range are the special features of this class of dyes.^{439–441} BODIPY dyes are widely used to label proteins and DNA as well as for imaging applications. The applications of BODIPY dyes are limited for a certain extent due to small Stokes shift. There are a few reports related to BODIPY dyes as gelators.^{442–445} Ziessel and co-workers have reported that the attachment of BODIPY unit to 3,5-diacylamidotoluene with sufficient aliphatic chains **179** (Figure 31) results in strong fluorescence in the gel state as well as in columnar mesophases.^{442,443} The formation of a dimer stabilized by tight hydrogen bonded network and stacking of

the BODIPY part led the self-assembly to thermotropic and fluorescent columnar mesophases with a hexagonal symmetry. The BODIPY based rod-coil polymer **180** (Figure 31) consisting of a *p*-phenyleneethynylene as a rod segment and decyl chain as a coil is a good gelator of organic solvents.⁴⁴⁴ Morphological studies revealed that the gelator **180** self-assembles to form nano- to micrometer sized particles and also fibers. Photoluminescence studies indicated that efficient energy transfer is possible from the π -conjugated polymer linkers to the BODIPY moieties. A methacrylic polymer based hydrogelator containing BODIPY dye exhibited thermosensitive fluorescence properties.⁴⁴⁵ A hybrid material of supramolecular hydrogel, enzymes, and aminoethyl modified mesoporous silica particles containing encapsulated anionic BODIPY dyes have been used for the fluorescence sensing of biologically relevant polyanions.⁴⁴⁶ The use of BODIPY derivative as a suitable energy-acceptor, enabled the FRET based detection of polyanions.

3.5. Phthalocyanines

Phthalocyanines are intensely blue-green colored macrocyclic dyes that are widely used in dyeing due to their chemical and thermal stability and very strong characteristic optical absorption in the visible region.^{447–453} Phthalocyanines form planar coordination complexes with most elements of the periodic table. Phthalocyanines have been used as components in photoconductors, photomemory systems, PVDs, electrochromic displays, deodorizers, and sensors.^{447–453} The phthalocyanine derivative **181a** (Figure 32a) exhibits thermo-

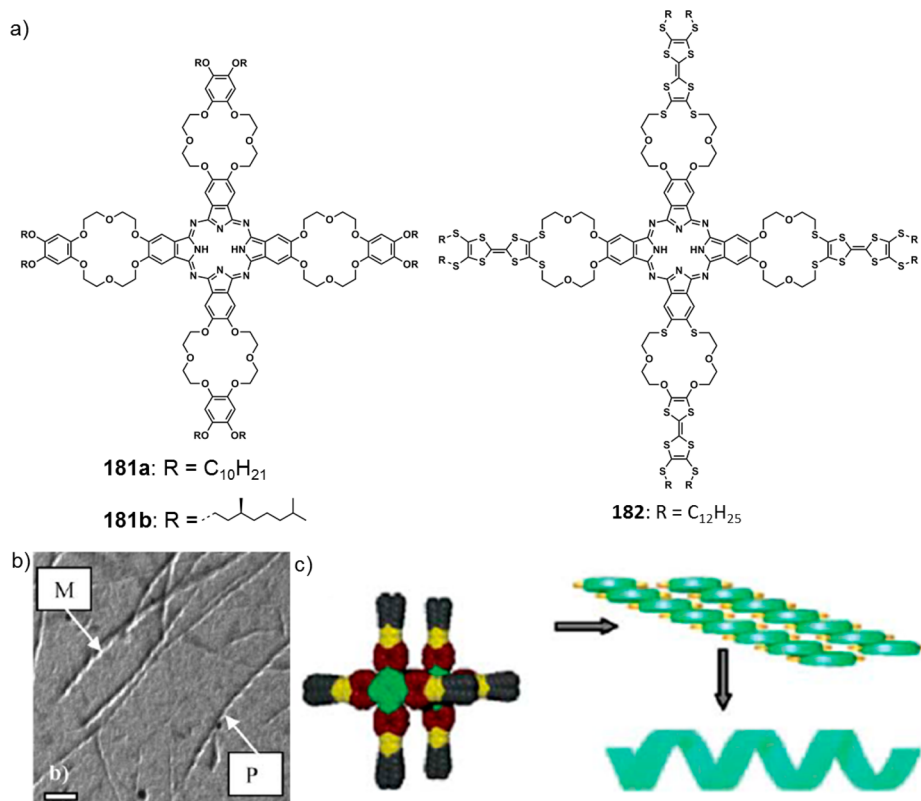


Figure 32. (a) Chemical structures of **181a,b** and **182**. (b) TEM image of the gel fibers of **182** showing an equal distribution of both left and right helical structures (scale bar = 200 nm). (c) Molecular model (phthalocyanine moiety in green, crown-ether in red, TTF in yellow, alkyl chains in gray) showing the stacking mode of **182** in which phthalocyanines-TTF and TTF-TTF interactions dominate resulting in initial bilayer type structures which scroll into helical tapes. (Reprinted with permission from ref 458. Copyright 2005 The Royal Society of Chemistry.)

tropic mesophase and self-assembles in chloroform solution to yield an extremely long supramolecular cables leading to gelation.^{454,455} Each fiber is composed of bundles of single parallel strands having $\sim 10^4$ molecules packed in eclipsed conformation. These fibers can be considered as molecular cables, containing a central electron wire, four ion channels, and a surrounding insulating hydrocarbon mantle. As evident from polarization absorption spectroscopic studies, application of high magnetic field is found to be effective for the alignment of molecular aggregates of **181a**.⁴⁵⁶ In the gel state, this alignment can be retained even after the removal of the magnetic field which highlight the role of a gel state in preserving an induced property.

The disk-shaped phthalocyanine molecule **181b** with chiral tails (Figure 32a) forms micrometer-long fibers and organogels in chloroform.^{455,457} The gelator molecules within a fiber are organized into a right handed helix, which further self-assemble into left handed twisted bundles. Upon addition of alkali metal ions, the helices are transformed into straight fibers as a consequence of the cofacial arrangement of crown ether moieties for the cooperative binding to metals. STM study of **181b** indicated that the molecular arrangement comprises two face-on phases and one edge-on lamellar phase.⁴⁵⁷ The gelation of a TTF-crown ether functionalized phthalocyanine **182** (Figure 32a) was observed by the slow addition of dioxane to a chloroform solution.⁴⁵⁸ This is attributed to the presence of a combination of TTF-TTF and TTF-phthalocyanine interactions leading to the formation of helical fibers (Figure 32b,c).

Photoactive organogels of the mesogenic octakis(alkyloxy)-substituted Zn(II)-phthalocyanines **183a–c** (Figure 33) have

been prepared by mixing into fibrous organogel network of *(1R,2R)-trans-1,2-bis(dodecanoylamino)cyclohexane* in a ratio of 1:10.⁴⁵⁹ Similarly, a series of organogels were prepared by using a combination of well-known gelators such as *5 α -cholestane-3 β -ylN-(2-anthryl)carbamate or *(1R,2R)-trans-1,2-bis(dodecanoylamino)cyclohexane* with corresponding Zn(II)-phthalocyanine containing analogues **184** and **185** (Figure 33).⁴⁶⁰ The thermal/mechanical stability of the gel could be improved by Cu^I-catalyzed azide–alkyne [3 + 2] cycloaddition mediated cross-linking of a suitable complementary diacetylene and a linear diazide incorporated into the multicomponent hybrid gel network. In addition, there are some reports related to gelation properties of phthalocyanine doped polymers,^{461–463} or peptide nanofibers.⁴⁶⁴*

3.6. Porphyrins

Porphyrins are a class of macrocyclic dyes exhibiting intense absorption bands in the visible region and are deeply colored.^{452,453,465–470} In general, porphyrins have tunable electronic properties depending on the exocyclic modifications and coordinated metal ion.^{468–470} Photosynthetic antenna complexes consisting of self-assembled arrays of porphyrinic and carotenoid pigments have been a motivation for chemists to design and develop new molecules and assemblies to mimic the natural photosynthetic processes.^{452,467} Porphyrins have been used as building blocks for the construction of a variety of functional photonic devices, especially in conjugation with fullerene derivatives.⁴⁵³ In addition, metalloporphyrins are widely used as host molecules for fullerenes, taking advantage of the physical interaction between the two.⁴⁷⁰

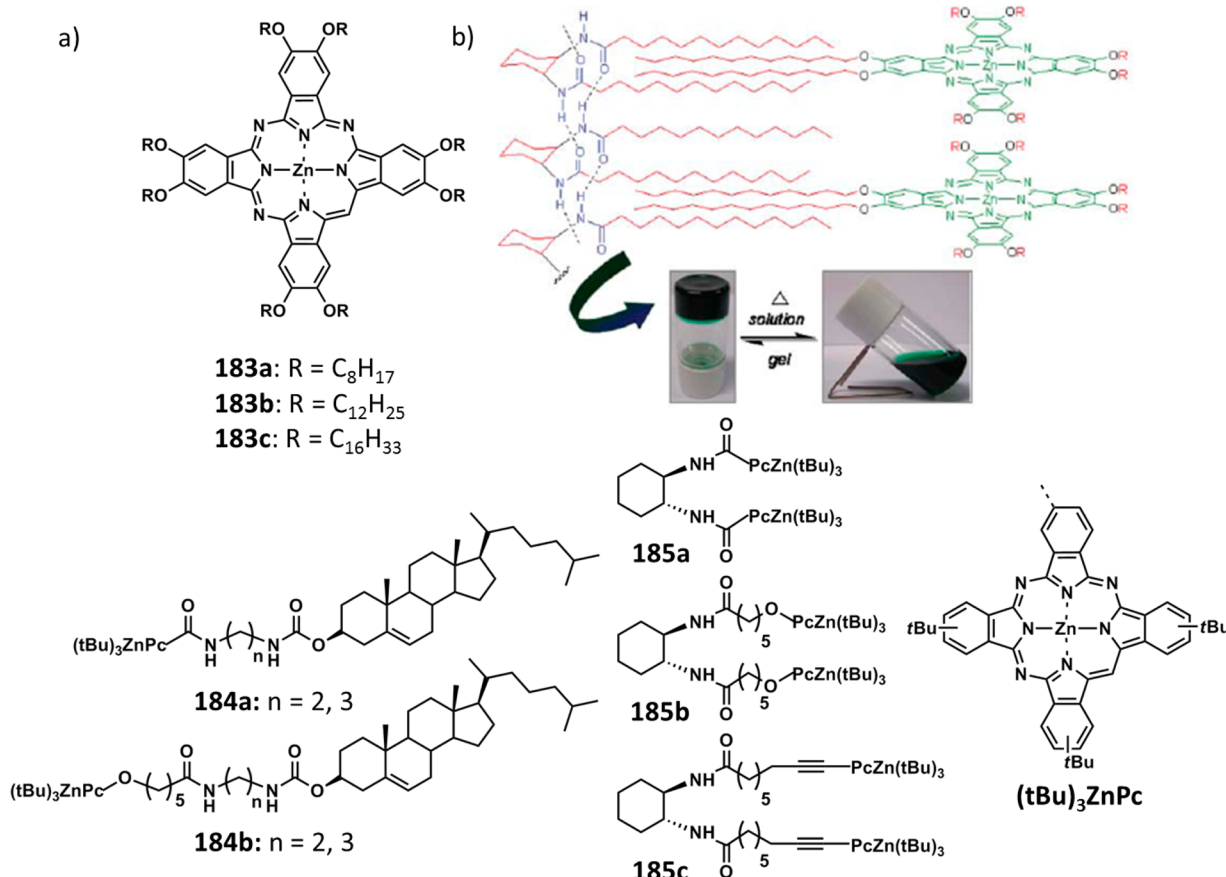


Figure 33. (a) Chemical structures of phthalocyanine derivatives 183a–c, 184a,b, and 185a–c. (b) Top: proposed interaction pattern for formation of stable gels. Zones of main possible interactions are colored: hydrogen bonds (blue), hydrophobic forces (red), π–π interactions (green). Bottom: thermally induced phase transition of the dark-green organogel made with (1*R*, 2*R*)-*trans*-1,2-bis(dodecanoylamino)cyclohexane + 183b with a molar ratio of 10:1. (Reprinted with permission from ref 459. Copyright 2007 The Royal Society of Chemistry.)

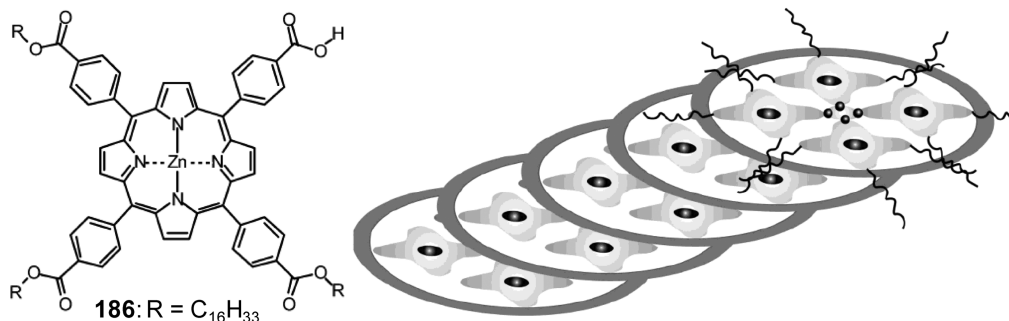


Figure 34. Schematic representation of tetrameric association of 186 in a rod section. (Reprinted with permission from ref 472. Copyright 2003 American Chemical Society.)

Terech et al. have shown that *meso*-tetrakis(*p*-carboxyphenyl) porphyrin 186 (Figure 34), forms thixotropic gel in hydrocarbon solvents.^{471–473} A cyclohexane solution of 186 exhibited a broad and red-shifted Soret exciton absorption band associated to the formation of J-type aggregates. This gelator self-assembles to form supramolecular nanorods consisting of four molecules laterally associated with a slipped arrangement of the consecutive layers in a tilted columnar fashion (Figure 34).

Kimura et al. reported that a mixture of the zinc porphyrin dimer 187 (Chart 43) and an optically active (1*R*,2*R*)-*trans*-1,2-bis(akylamide)cyclohexane form an optically transparent gel with well resolved fibrous assemblies.⁴⁷⁴ The organogelation of

L-glutamic acid derived porphyrin systems 188–190 (Chart 43) through hydrogen bonding interactions was reported by Ihara and co-workers.^{475–482} TEM images of the fibrous networks of 188 and 189 showed several tens to hundreds of nanometers in width and hundreds of micrometers in length.^{475–478} In addition, in the coassembly of 188 and 189 with a pyrene functionalized L-glutamide derivative, energy transfer was observed from the pyrene excimer to the porphyrin moiety.^{475–477} In the case of the tetraphenylporphyrin derivative 189, nanofibrillar aggregates with both R- (H-type aggregate) and S- (J-type aggregate) chiral stacking structures were observed.^{477,478} The gelator 190 exhibited a drastic change of morphology from globular aggregate to needle-like

Chart 43

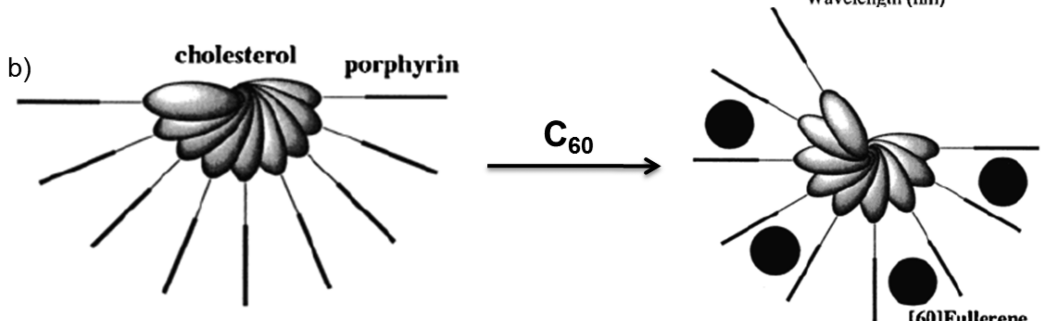
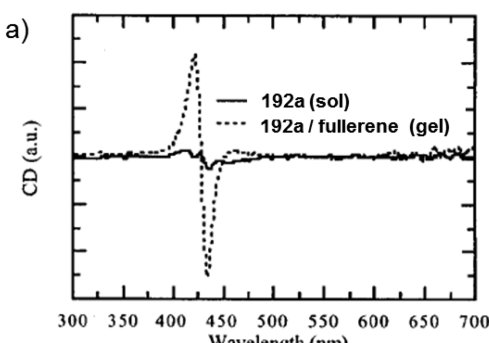
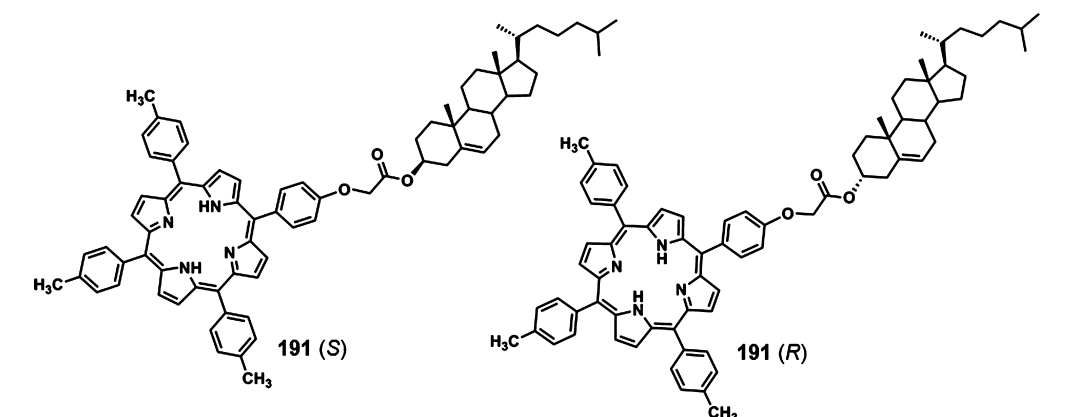
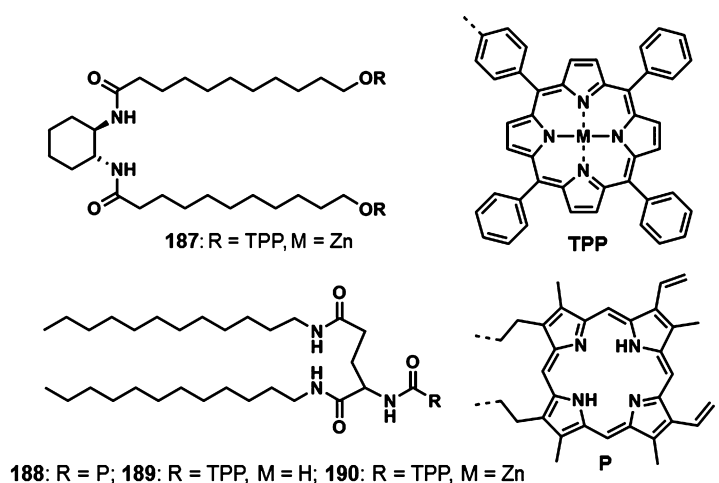


Figure 35. (a) CD spectra of **192a** sol phase and **192a**/C₆₀ complex (2:1 molar ratio) gel phase, both in toluene. (b) Schematic representation of the sandwich complex formation of a Zn(II) porphyrin and C₆₀ in (2:1) molar ratio. (Reprinted with permission from ref 485. Copyright 2001 American Chemical Society.)

structures upon complexation with pyridine.⁴⁷⁹ A remarkable quenching of fluorescence and significant enhancement in the

binding constant due to the ordered aggregate formation was observed upon complexation with pyridyl fullerene deriva-

Chart 44

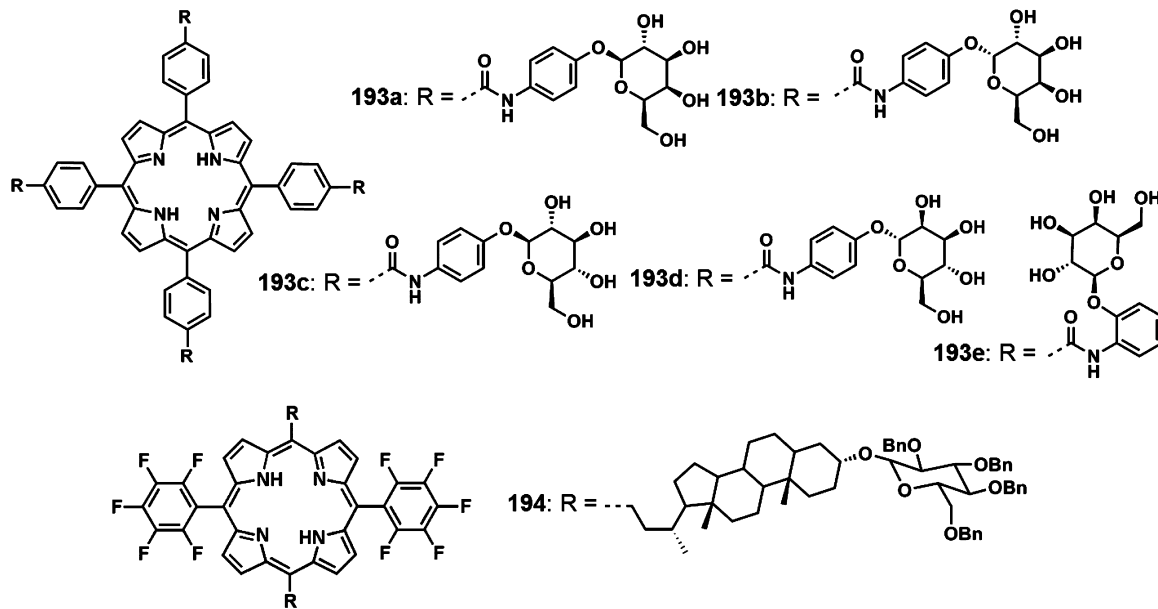
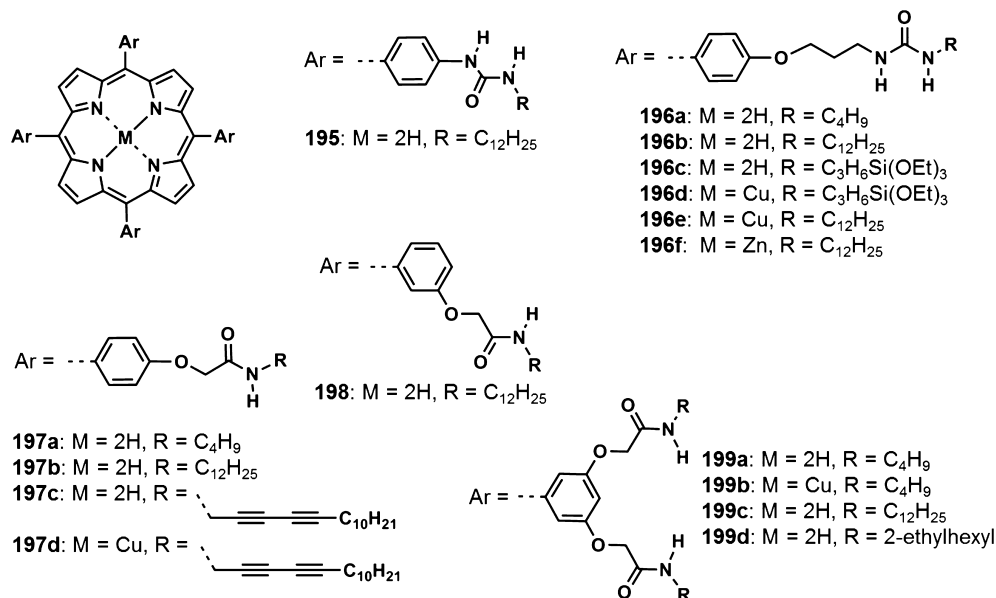


Chart 45



tive.⁴⁸⁰ An organogel based enantioselective recognition system for various amino acid methyl ester racemates has been achieved by an ordered assembly of glutamide functionalized porphyrin 190.^{481,482} The enantioselectivity was determined by monitoring the changes in the CD spectra and by fluorescence quenching.

Shinkai and co-workers have conducted an extensive investigation on the gelation properties of a variety of porphyrins (Chart 43).^{483–489,491–499,502,503} The gelator 191 (*S*) with *S*-configuration at the C-3 position was found to form stable gel in organic solvents with flake like fiber morphology, whereas the one with inverted configuration *R*, 191 (*R*) was failed to gelate all of the solvents tested.

A study of the ground state intermolecular interaction between Zn(II) porphyrin appended cholesterol gelator 192a–d (Figure 35) and fullerene (C₆₀) in an organogel system

revealed that the sandwich complexation of a Zn(II) porphyrin/C₆₀ (2:1) enhances the gelation ability of 192a,c having an even number of methylene units in their spacer between porphyrin and cholesterol units but not with 192b,d having an odd number of methylene units (Figure 35).^{484,485} A bathochromic shift of the Soret absorption band and enhancement in the negative exciton coupled CD signal in the presence of C₆₀ established intermolecular interaction between 192a and C₆₀ in the gel phase (Figure 35a). In order to study the DNA mimetic properties in a gel medium, the CD spectral studies of the gelator containing cholesterol and DNA base pairs, especially the uracil moiety and 0.2 equiv. of 192a have been carried out.⁴⁸⁶ The enhancement in the CD signal indicated the incorporation of 192a into the gel fibers.

A variety of porphyrin based gelators 193a–e (Chart 44) that form hydrogen bonded 1D assemblies were created by

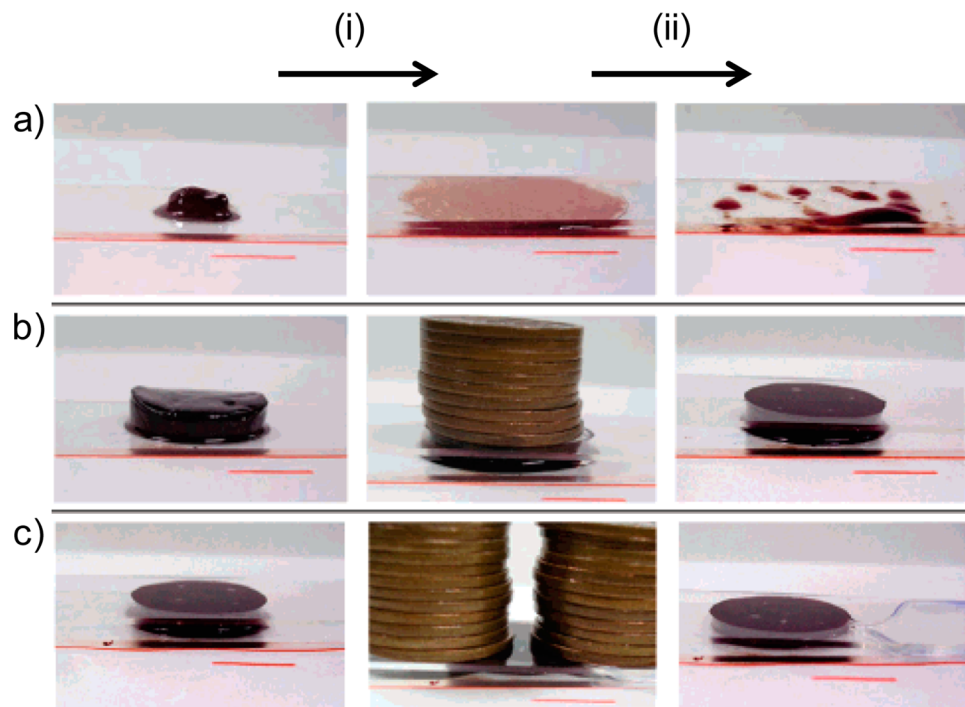


Figure 36. Photographs of the anisole gel of **196d**, (a) before sol–gel polycondensation, which collapses by putting on only a glass plate, (b) after sol–gel polycondensation, a glass plate and ten 10-yen coins were put on, and (c) after sol–gel polycondensation, in which the solvent was squeezed out by putting on a glass plate and twenty four 10-yen coins; (i) a plate and/or 10-yen coins were put on the anisole gel and (ii) they were taken off from the anisole gel. (Reprinted with permission from ref 495. Copyright 2005 American Chemical Society.)

substituting the periphery of the porphyrin chromophores with sugar moieties, connected through amide groups.^{487–489} It is interesting to note that slight variation in the structure of sugars drastically changed the solubility as well as the gelation ability. Hence porphyrins **193a–c** were found to be efficient gelators and **193d** formed weak gels whereas **193e** was completely soluble in most of the solvent systems tried.⁴⁸⁹ The 1D helical assemblies of the porphyrin chromophores are stabilized by the synergistic effect of the π – π stacking interaction among the porphyrin cores and the hydrogen bonding interactions between the sugar moieties. This is facilitated by the sugar moiety with the equatorial OH groups rather than axial OH groups; hence, **193c** is a much better gelator than **193a**. These organogelators are found to be versatile for creating helical silica structures by a sol–gel transcription process.^{488,489} The solvent promoted aggregation and modulation of supramolecular chirality of a porphyrin based organogelator **194** (Chart 44) containing glucosylated steroidal moiety has been reported by Monti and co-workers.⁴⁹⁰

The stability of the porphyrin based gel assemblies has been significantly increased when the peripheral sugar moieties are replaced with urea groups, **195** and **196** (Chart 45).^{491,492} The synergistic effect of porphyrin-porphyrin π – π stacking and urea–urea hydrogen bonding interactions increase the gelation efficiency of **195** when compared to that of the corresponding amide derivatives **197b** and **198** (Chart 45).⁴⁹² Chiral urea derivatives such as (*R*) and (*S*) enantiomers of *N*-(1-phenylethyl)-*N'*-dodecyl urea were able to bind with the 1D porphyrin stacks of **195** to twist them in a helical sense, which is evident from the resultant exciton coupled CD spectra.⁴⁹¹

The 2D sheet structure obtained from the self-assembly of **196c** (Chart 45) by the hydrogen bonding interaction among the peripheral urea groups was immobilized by *in situ* sol–gel

polycondensation of the end triethoxysilyl groups.^{493–495} In a similar way, 1D molecular assembly created by the stacked H-type aggregates of **196d** (Chart 45) was also immobilized, without a morphological change.^{494,495} The resultant reinforced gel after polycondensation showed a very high thermal stability and mechanical strength. The gel melting temperature values for **196d** after the sol–gel polycondensation were enhanced up to 160 °C. As observed in the rheological measurements, the elasticity of the gel was also considerably increased. The improved elasticity of the gel after sol–gel polycondensation was demonstrated by putting weight (thirteen 10-yen coins, 4.5 g) over the gel as shown in Figure 36.^{494,495}

Comparison of the gelation properties of **196b** and its Cu(II) and Zn(II) complex **196e** and **196f** (Chart 45) revealed that the presence of Zn metal considerably reduces the gelation properties.^{495,496} Complexation **196f** with piperazine resulted in the formation of gels with thixotropic property.⁴⁹⁶ Moreover, the morphology of **196f** is found to vary with the equivalence of added piperazine, spherical structure at 0 equiv., 1D fibrous structure at 0.5 equiv. and 2D sheet-like structure at 1.0 equiv. In addition, absorption studies revealed that J-type aggregates of **196f** turned into H-type aggregates in the presence of 0.5 and 1.0 equiv. of piperazine. Self-assembled transparent and thixotropic gel of porphyrin derivative **197c** (Chart 45) has been used as a photopolymerization template to create unimolecularly segregated polydiacetylenes nanowires.⁴⁹⁷ AFM observations strongly suggest that the polymerized polydiacetylene fiber was elongated to more than several micrometers in length without any defect.

Appropriate positioning of the peripheral hydrogen bonding amide motifs could facilitate the formation of one of the aggregates (J or H) preferentially. Shinkai and co-workers have synthesized the amide appended porphyrin organogelators

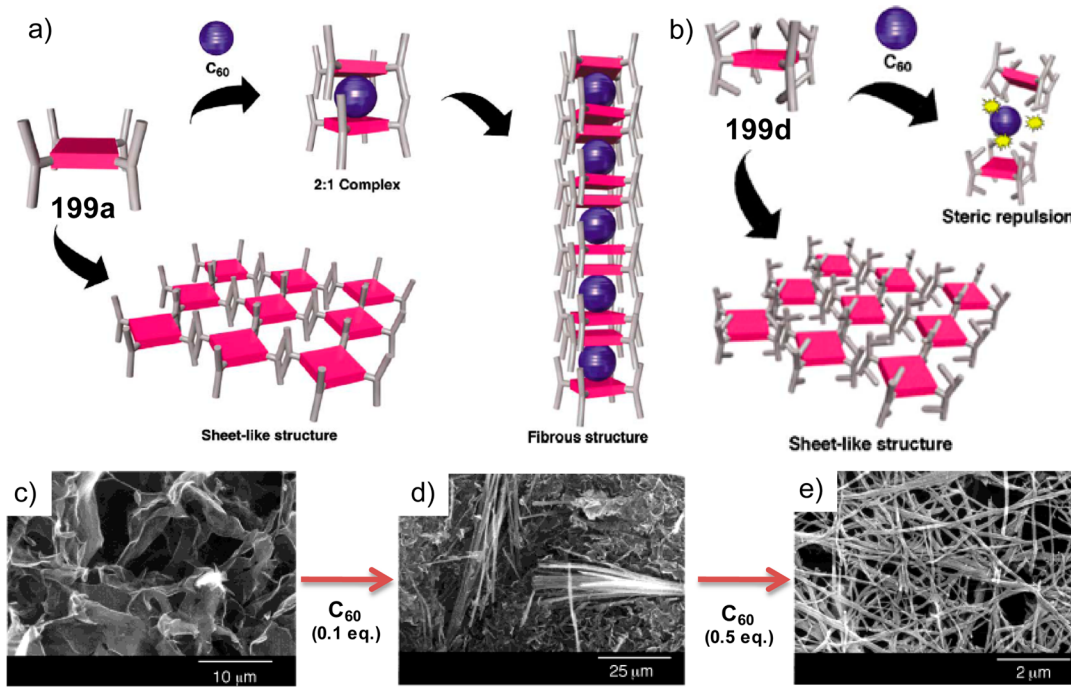
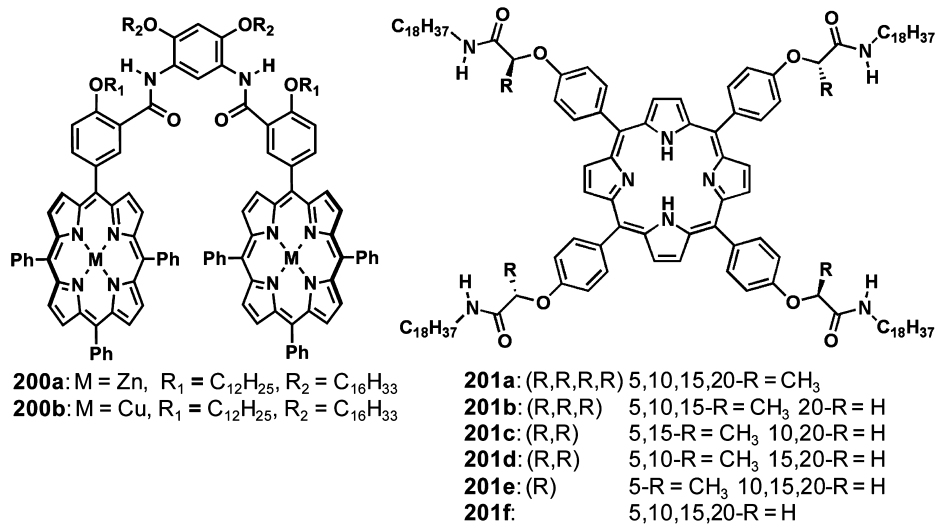


Figure 37. Aggregation modes of (a) 199a and (b) 199d. SEM pictures of the xerogels in benzene containing (c) 199a, (d) 199a + 0.10 equiv. of C₆₀, and (e) 199a + 0.50 equiv of C₆₀. (Panels a and b reprinted with permission from ref 499. Copyright 2006 Elsevier Ltd. Panels c–e reprinted with permission from ref 498. Copyright 2003 American Chemical Society.)

Chart 46



197a,b (Chart 45) substituted with amide groups at the 3,5 positions of the *meso*-phenyl groups, whereas for 199a,b at the 4-position (Chart 45).⁴⁹² Spectroscopic and XRD analyses revealed that the porphyrins in 197a,b adopt the H-aggregation mode resulting in columnar stacks, whereas those in 199a,b adopt the J-aggregation mode resulting in 2D planar assemblies. The difference in the microscopic hydrogen bonded organization of the porphyrin chromophores was reflected in gelation and was further confirmed by SEM analysis of the cyclohexane gels.

The self-assembly of porphyrin appended gelator 199a resulted in a cavity by adjusting the distance between the two adjacent porphyrin units connected through the π-π stacking and the hydrogen bonding interactions.^{498,499} UV-vis absorption

elemental analysis, XRD, IR, and computer modeling studies have shown that four amide groups from two adjacent porphyrins form a circular hydrogen bonding array, which can easily encapsulate a C₆₀ molecule to give a 1:2 complex. These “capsules” will further grow into a 1D multicapsular structure. The sheet-like morphology of 199a undergoes a drastic change to a fibrous network on increasing the concentration of the C₆₀ from 0 to 0.5 equivalents, due to a strong porphyrin-C₆₀ interaction (Figure 37). Gelation properties of 199b could be improved by the addition of C₆₀, implying that 199b also possesses versatile gelation ability comparable to that of 199a.⁴⁹⁹ On the other hand, when bulky alkyl substituents such as ethylhexyl groups were present as in 199d, the gelator could not accept C₆₀ as a guest, leading to the formation of 2D

sheet structures in the absence or even in the presence of C₆₀ molecules (Figure 37b).

The hydrogen bonding driven preorganized, "U" shaped bisporphyrin receptors **200a,b** (Chart 46) efficiently complex with C₆₀ derivatives that could gelate alkanes.⁵⁰⁰ The bisporphyrins and their C₆₀ complexes also form smectic LC phase. Lazzaroni, De Feyter, Amabilino, and co-workers have investigated the effect of the number of stereogenic centers on gelation of **201a–f** (Chart 46).⁵⁰¹ The interactions between molecules were disturbed by the methyl group attached to the stereogenic center that increased solubility and hence decreased the gelation ability. Moreover, the presence of only one stereogenic center was sufficient to induce chirality in the self-assembled structures.

Significant modulation of the 1D aggregation properties of porphyrins, and thereby the overall gelation property was possible by functionalizing the porphyrin core with hydrogen bond donating carboxylic acid and hydrogen bond accepting pyridine substituents at the peripheral positions of **202a–e** (Chart 47).^{502,503} Detailed study revealed that, in **202a**, the

decalin whereas **204b** and **204c** (Chart 48) displayed vesicular aggregates in methanol–chloroform mixtures. The role of azulene moiety in determining the orientation of the molecules during the self-assembling process was revealed by detailed optical and morphological studies in comparison with naphthalene bridged porphyrin gelator **204d** (Chart 48).

Elemans and co-workers have reported the formation of highly periodic patterns at macroscopic length scales, by combining self-assembly of disk-like porphyrin trimers **205a,b** with physical dewetting phenomenon upon drop casting a solution of the molecules on to a mica surface (Figure 39).^{507,509} The strong self-assembly of porphyrin trimers is governed by a balanced combination of hydrogen bonding and π–π stacking interactions and is essential for the growth of columnar stacks of almost millimeter in length. The pattern formation was found to be highly dependent on the nature of solvent and concentration of porphyrin trimer. In chloroform, up to concentrations of 0.2 mM, porphyrin trimers mainly existed as molecularly dissolved species and started to self-assemble during the spinodal dewetting. Irrespective of the concentration range, due to preorganization of molecules, only entangled fibers were observed when the solvent was changed to hexane.

Hori and Osuka have reported the gelation of the corrole derivatives **206a** and **206b** (Chart 49) in hydrocarbon solvents through H-type aggregation.⁵⁰⁹ The doping of porphyrins to various gelators resulted in improved stability and enhancement in the chiroptical response and photophysical properties.^{510,511}

3.7. Squaraines

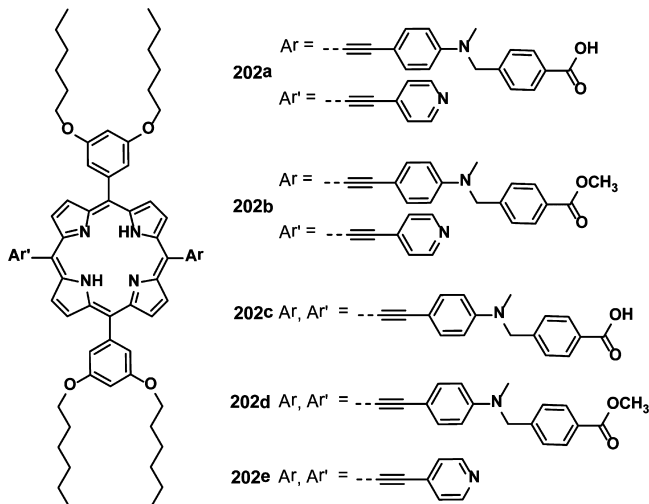
Squaraine dyes that show intense absorption and emission properties in the visible to near-IR region have been at the center stage of organic materials research for the past several years.^{512,513} The characteristic feature of squaraine dyes is the availability of a highly electron deficient four membered cyclobutene ring.^{512,513} Since the optical properties of squaraines are sensitive to the surrounding medium, they are widely used as chemosensors.^{513,514} The electronic properties of squaraine dyes have made them attractive for a number of applications such as xerography, PVDs, optical recording, diode lasers, laser printing, photolabeling, and DNA sequencing.^{512–514} However, when compared to other organic dyes, squaraines have been least exploited in gel chemistry.

One of the early reports on the gelation of squaraine dye is based on the cholesterol appended derivative **207** (Chart 50).^{245,515} Upon gelation, this dye exhibited a blue shift in the absorption spectrum, loss of fluorescence and the appearance of an exciton coupled CD spectrum, indicating that the dye molecules are arranged in a helical "H"-type aggregate fashion. The combination of hydrophilic squaraine with a hydrophobic steroid imparts a reasonable amphiphilic character to the molecule. Another steroid-squaraine combination based on a naphthalimide platform **208** (Chart 50) reported by Yi and co-workers also formed stable gels in toluene in the presence of organic amines.⁵¹⁶ The gradual release of the gelling solvent resulted in the gel shrinkage which was found reversible.

3.8. Azo Dyes

Azo dyes have been exploited for the design of gelators that could gelate water and organic solvents. Hamada et al. have found that the monoazo sulfonic dye **209** (Chart 51) containing a trifluoromethyl group at the meta position formed aggregates in aqueous solutions, eventually turned into a hydrogel when the concentration of the gelator was

Chart 47



acid–base interaction suppresses the crystal growth and enables the aggregation and gel formation. Sheet-like 2D structures derived from cyclohexane gel of **202a** transformed to fibrous aggregates upon addition of a small amount of pyridine or N,N-(dimethylamino)pyridine due to the suppression of the acid–pyridine interaction. While the gelators **202a,b** and **202d** could gelate organic solvents, **202c** and **202e** precipitated from most of the aliphatic nonpolar solvents and alcoholic solvents due to their poor solubility.⁵⁰³

The gelation properties of the porphyrins **203a,b** (Chart 48) functionalized with four quaternized brucines on the periphery were studied using vibrational CD spectroscopy which provided insights on the involvement of specific segments of molecules in the formation of chiral self-assemblies.^{504,505} The vibrational CD analysis revealed information on the parts of molecules whose optical activity could be influenced by the organogel formation. The azulene bridged porphyrins have been reported to form 1D aggregates that further entangled into 3D network structures to form organogels, or self-assembled into vesicular structures, depending on the number of porphyrin units and solvents (Figure 38).⁵⁰⁶ Self-assembly of **204a** (Chart 48) resulted in entangled fibrils formation and gelation in *trans*-

Chart 48

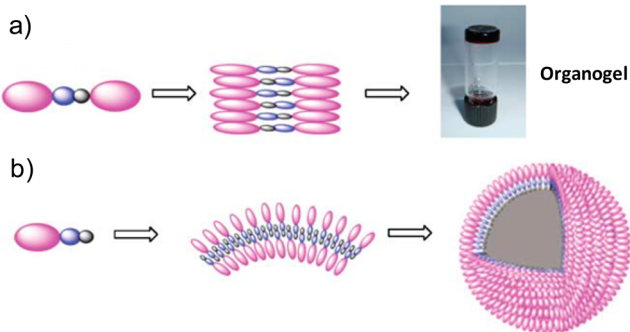
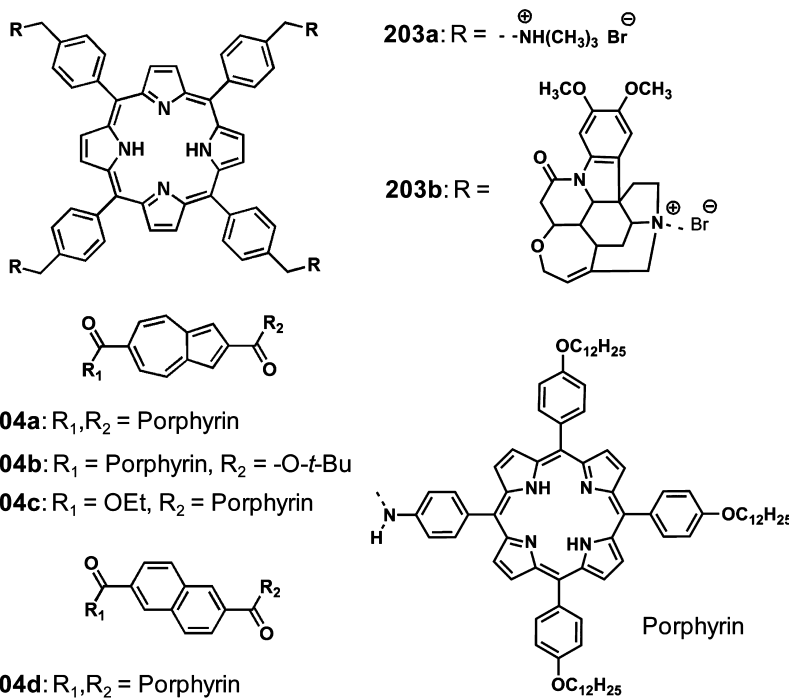


Figure 38. (a) Proposed mode for the formation of nanowires from 204a or 204d and (b) vesicles from 204b or 204c. (Reprinted with permission from ref 506. Copyright 2009 The Royal Society of Chemistry.)

increased.⁵¹⁷ A viscoelastic gel of 210 (Chart 51) in a water/methanol system displayed stationary birefringence with herringbone texture as well as fibrils having linear molecular arrangement and at high methanol content, ordered bundles were also formed.⁵¹⁸ The azonaphthol gelators of 211a–d (Chart 51) have been used as a measure of the microscopic solvent polarity due to the switchable azo and hydrazone tautomers indicating that the micropolarity of the gelator aggregates is less polar than that of the gelation medium.⁵¹⁹ The control over the inner diameter of silica nanotubes has been achieved by the variation of the concentrations of the sugar appended azonaphthol gelators 211a and 211d.⁵²⁰ The hydrogen bonding interactions between the template gel fiber and the silica precursor led to well-defined silica nanotubes with inner diameters in the meso/macroscale. The sugar azonaphthol gelator 211a tends to orient on the surface of SWCNTs and exhibits intense fluorescence due to the suppression of molecular freedom of the corresponding hydrazone in the gel phase.⁵²¹

The azo dye 212a–c (Chart 51), in the presence of a surfactant, formed organized supramolecular architectures and thereby LC gels.^{522,523} This could be attributed to the formation of highly ordered arrays of the dye assemblies in the alkyl matrix by the balanced hydrophobic, electrostatic and π - π interactions. Hydrogels of the anionic azo dye 213 (Figure 40) was formed on cationic surfaces even at concentrations 50 times below the minimal gelation concentration and exhibited a broccoli-like structure originated from the water filled channels of the honeycomb-like architecture.^{524–526} An anisotropic supramolecular gel was formed when the azo dye was complexed with γ -CD through a specific host–guest interaction.⁵²⁷

3.9. Coumarins

Coumarins belong to the class of benzopyrone and are a naturally occurring organic dye that often found in many plants. During the last few decades, coumarin derivatives have been intensely studied because of their possible applications in material as well as biological fields. The nature and position of the substituents on coumarin ring have profound influence on the photophysical behavior.⁵²⁸ The first coumarin based organogelator was reported by Takenaka and co-workers. Gelation of 214a,b (Chart 52) and 215a,b (Chart 52) in various organic solvents was controlled by intermolecular interactions around the lactone moiety and by the large dipole moment of the gelator molecule.⁵²⁹ Gel fibers of 216a,b (Chart 52) in cyclohexane were observed to have distinct helical sense.⁵³⁰ The reversible and stereoselective photodimerization of coumarin in 217a–i (Chart 52) occurred without disrupting the gel phase, however resulted in a drastic change of the gel morphology.⁵³¹ Upon irradiation at >300 nm, the gel fibers were merged into lumps whereas when the wavelength was changed to <280 nm, the morphology was changed from the lumps to sponge-like aggregates. Small molecules like 218 (Chart 52), having a long alkenyl chain at position 3, exhibited excellent organogelation properties due to hydrogen bonded

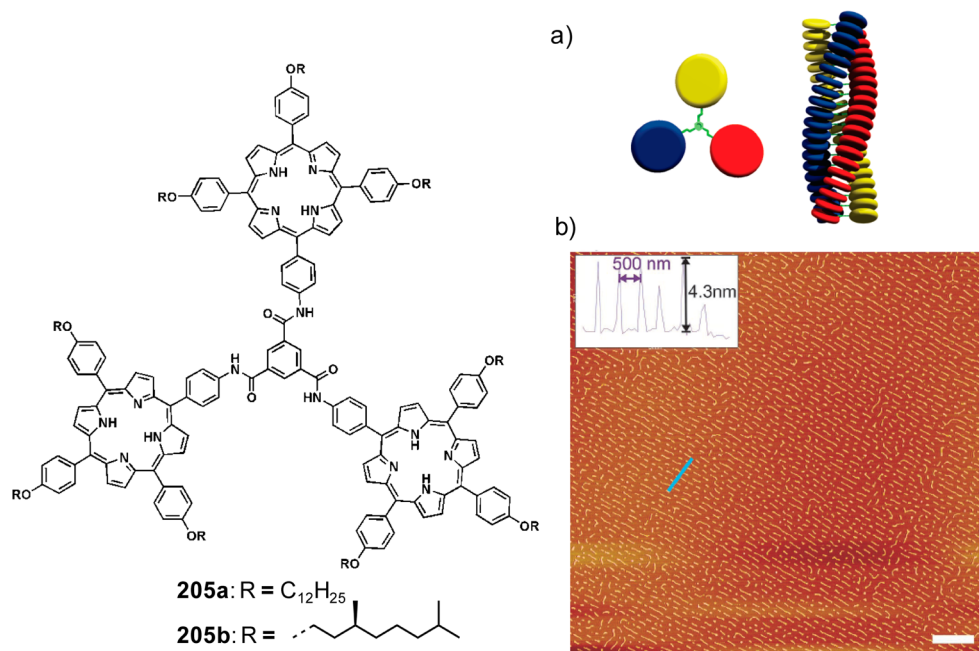
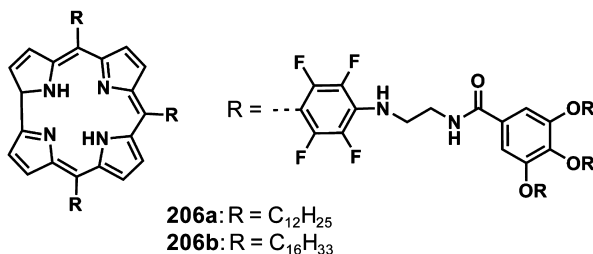


Figure 39. (a) Schematic representation of porphyrin trimers and their self-assembly into columnar stack. (b) AFM images of patterns formed after drop casting a solution of **205b** in chloroform (scale bar = 1 μ m). (Reprinted with permission from ref 508. Copyright 2008 American Chemical Society.)

Chart 49



aggregate formation.⁵³² A chemodosimetric gelation system that turns into a fluorescent gel in the presence of fluoride anions has been developed.⁵³³ The selective cleavage of a silyl ether protecting group on the gelators **219a,b** (Chart 52) by a fluoride anion enhanced the fluorescence with a sol–gel phase transition. However the gelator **219c** (Chart 52) without a silyl ether group was able to form gel in the absence of fluoride ions. PEGs having a coumarin moiety as the pendent group exhibit

photoreversible hydrogelation.⁵³⁴ In addition, several coumarin doped gels are also reported in the literature.^{535–537}

3.10. Dye Doped Gels

There are several interesting reports on gels doped with different organic dyes. Stable and efficient two photon lasing has been achieved by doping a two photon upconverting 4-(dimethylamino)-N-methylstilbazoliumtosylate dye into a gelatin based organogel medium.⁵³⁸ The gelation process of bile acid gelators was probed by accommodating a hydrophobic fluorescent dye ANS into the hydrophobic cavities of the gel networks.⁵³⁹ The sol–gel transition was visualized using a sodium salt of bromophenol blue dye which exhibited a color change from yellow in the solution phase to green upon gelation. Ultrafast time-resolved fluorescence measurements revealed that dyes get encapsulated more tightly in the gel network than into micellar aggregates, throwing insights to the dynamics of the dyes between hydrophobic pockets and the bulk aqueous phase in the hydrogel medium.⁵⁴⁰ The gelation kinetics monitored by the ultrafast dynamics of the dyes inside the gel matrix revealed the progressive increase in the aggregate

Chart 50

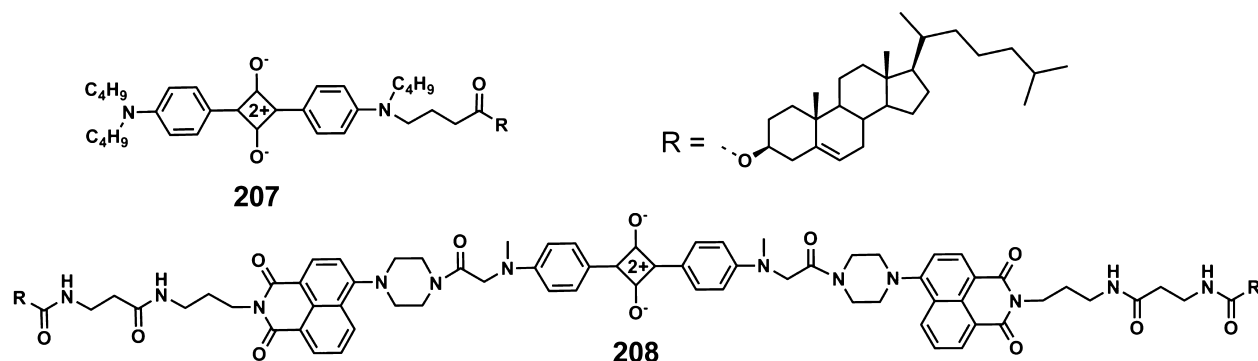


Chart 51

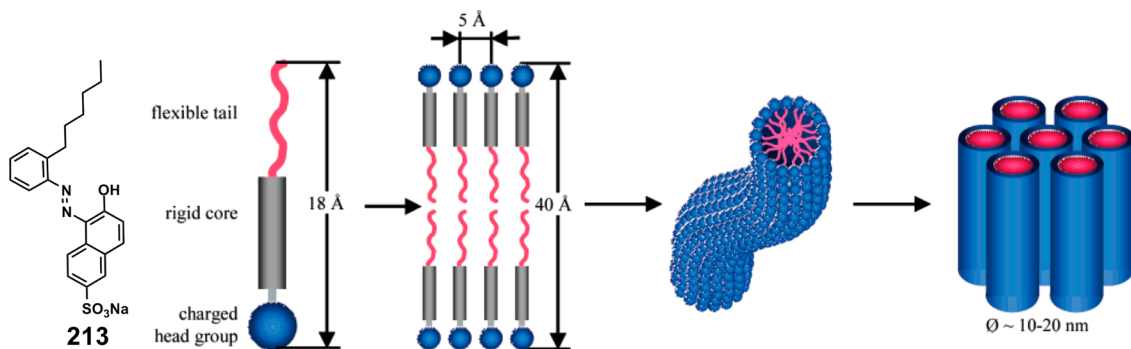
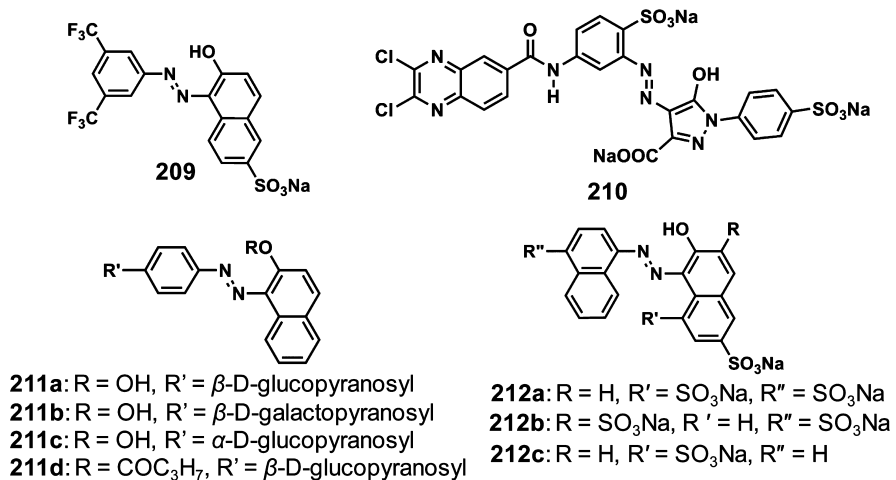
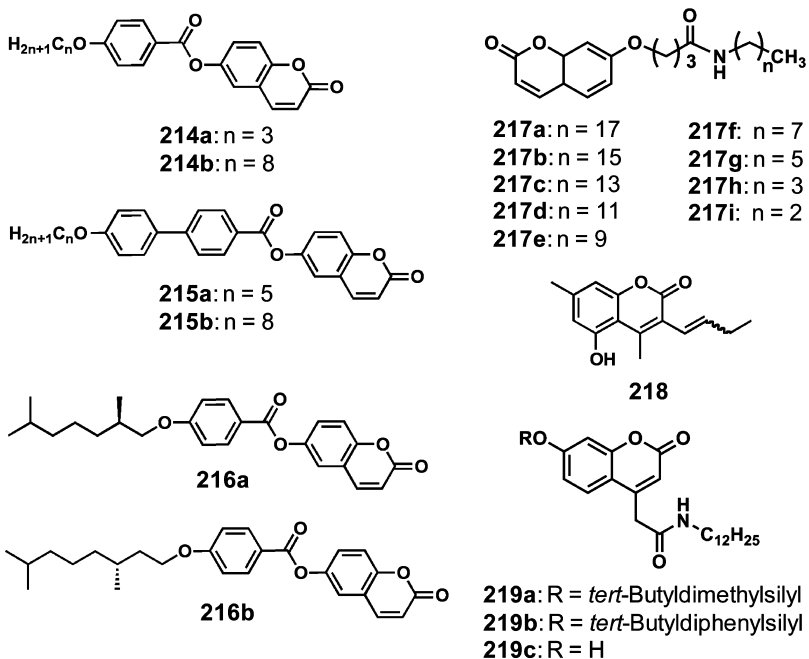


Figure 40. Representation of formation of tail-to-tail arrangement and rod-shaped micelle of 213 leading to hexagonal array. (Reprinted with permission from ref 525. Copyright 2007 American Chemical Society.)

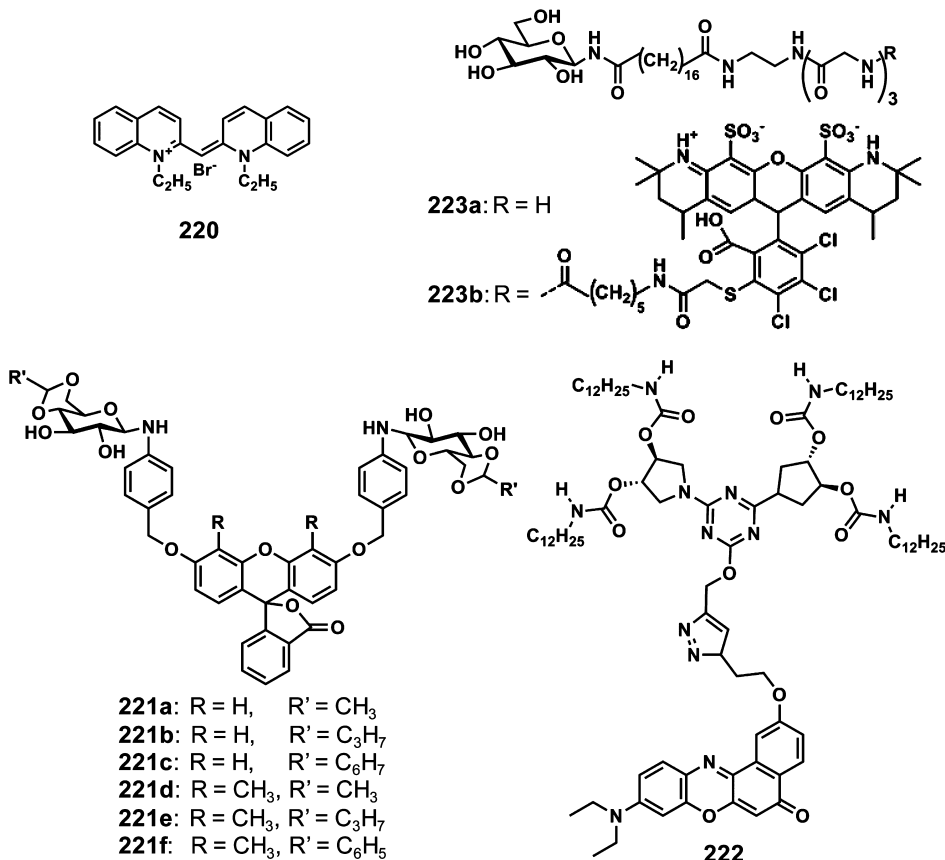
Chart 52



size and the microviscosity due to the formation of fibrillar network.⁵⁴¹ The orthogonal self-assembly of 1,3,5-trisamide cyclohexane based gelators and surfactants is probed using ANS revealed the independent formation of gel fibrillar network with

encapsulated micelles of surfactants.⁵⁴² Amino acid based amphiphilic hydrogelators has been used in the pH triggered release of entrapped vitamin B12 and cytochrome c.⁵⁴³

Chart 53



Hamachi et al. have used cooperative interaction of artificial receptors with semiwet glycosylated amino acid hydrogels for efficient molecular recognition and sensing applications.^{544–547}

The gel matrix of glycosylated amino acid scaffold was able to accommodate hydrophobic dyes such as ANS and (*S*-dimethylaminonaphthalene-1-(*N*-2-aminoethyl)sulphonamide) in the hydrophobic domains of the gel fibers and found to be useful for monitoring semiwet enzyme reactions.⁵⁴⁴ Similarly, the dye doped hydrogel based semiwet supramolecular sensor chip has been used for mixed sample analysis of various analytes.⁵⁴⁵ The dynamic redistribution of the receptor molecule between the aqueous microcavity and the dye doped hydrophobic gel nanofibers, upon guest binding, has been used for molecular recognition based on fluorescence resonance energy transfer type of fluorescent signal change.⁵⁴⁶

The altering equilibrium position between the two chromophoric forms of congo red dye has been utilized to prepare a thermochromic gel exhibiting violet color in the gel and magenta-red in the sol.⁵⁴⁸ A significant fluorescence enhancement was reported for fluorescent hydrophilic antibiotic, norfloxacin, when it was trapped in the hydrophilic core of the micellar assembly formed by an imidazole based amphiphilic gelator.⁵⁴⁹ A Schiff base doped *N,N'*-bis{octadecyl-L-Boc-glutamic diamide} organogel exhibited fluorescence enhancement as well as chirality induction from the gelator to the doped dye.⁵⁵⁰ The J/H-type aggregate ratio of fluorescein has been controlled by regulating the properties of a bile salt hydrogel medium.⁵⁵¹ Thermally controlled fluorescence enhancement of acridine orange has been achieved in supramolecular hydrogels formed by self-assembly of the gelator 3-{[(2R)-2-(octadecylamino)-3-phenylpropanoyl]-

amino}butyrate and 1,3:2,4-di-*O*-benzylidene-*D*-sorbitol.⁵⁵² 5-Fluorouracil doped supramolecular gels of 1,3:2,4-di-*O*-benzylidene-*D*-sorbitol were reported.⁵⁵³ The mobility of 4-dicyanomethylene-2-methyl-6-*p*-dimethyl aminostyryl-4*H*-pyran dye in the gel phase of a lipid was studied by fluorescence correlation spectroscopy.⁵⁵⁴ Hydrogels of achiral oligoamide embedded with rhodamine B dye showed stirring induced circularly polarized luminescence and the sense of which can be controlled by switching the stirring direction from clockwise to counter clockwise with slow cooling from the sol to gel states.⁵⁵⁵ The self-assembled vesicular gels formed by a medicinally important 6-6-6-6-6 pentacyclotriferpenoid, oleanolic acid gelator could entrap fluorophores such as rhodamine B and anticancer drug doxorubicin.⁵⁵⁶ The tris(hydroxymethyl)aminomethane doped sodium deoxycholate hydrogel microstructures have been used as templates for cyanine based fluorescent nanoparticles synthesis.⁵⁵⁷

3.11. Miscellaneous Dye Based Gelators

The aqueous solution of 1,10-diethyl-2,20-quinocyanine bromide **220** (Chart 53) formed J-type aggregate gel upon cooling.⁵⁵⁸ Gel nano fibers could be oriented under an applied magnetic field and the alignment has been preserved even in the absence of magnetic field. Fluorescein based *N*-glycosylamines formed 3D fibrous networks, which hold the solvent molecules to form stable gel.⁵⁵⁹ Similar glycosylamine molecules **221a–f** (Chart 53) exhibited anticancer property via exclusive localization in the cytoplasm. A triazine nucleus substituted with pyrrolidine rings connected to the nile red **222** (Chart 53) formed transparent gel in toluene.⁵⁶⁰ The nanotube hydrogels of asymmetric amphiphilic monomers **223a** and

223b (Chart 53) containing Alexa Fluor 546 could encapsulate chemically denatured proteins such as green fluorescent protein, carbonic anhydrase, and citrate synthase in the 1D channel of the nanotubes.⁵⁶¹ By varying the pH, the partially refolded and encapsulated proteins were smoothly released into the bulk solution in a completely refolded state.

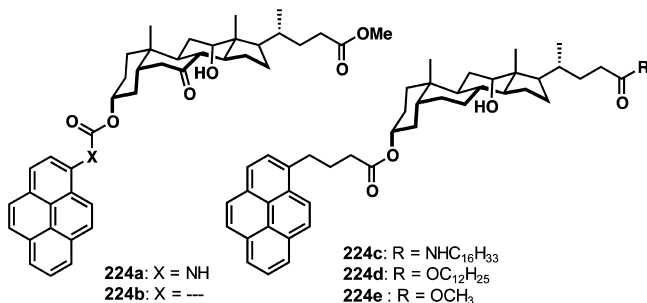
4. GELATORS BASED ON FUSED AROMATICS

4.1. Pyrenes

Pyrene is a fluorescent polycyclic aromatic hydrocarbon which is amenable for a variety of functional group modifications.⁵⁶² High fluorescence quantum yield and its sensitivity toward microenvironmental changes enabled the use of pyrene in labeling and sensing applications. The interesting photophysical properties such as excimer formation as well as exceptional distinction of the fluorescence bands for monomer and excimer are advantageous for structural studies of biological molecules and their self-assembly.

The two component system consisting of pyrene appended bile acid derivatives **224a–e** as the donor (Chart 54) and TNF

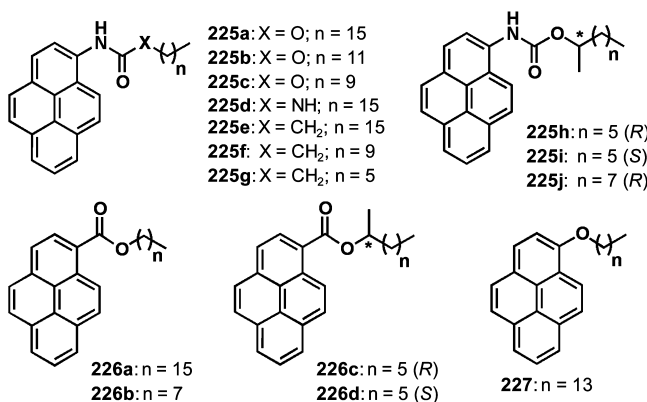
Chart 54



as the acceptor when mixed together gave organogels in a variety of alcoholic and hydrocarbon solvents through CT interactions.^{563,564} The colored gels obtained from colorless precursors indicate the CT interaction between the components.

Later, a new class of pyrene derived organogelators in which the bile acid part was replaced by alkyl chains through a variety of linkers have been reported.^{565–567} Compounds with hydrogen bond D–A linkers such as urethane, urea, and amide **225a–j** (Chart 55) undergo 1D self-assembly to form gels through hydrogen bond and π -stack interactions.^{565–567}

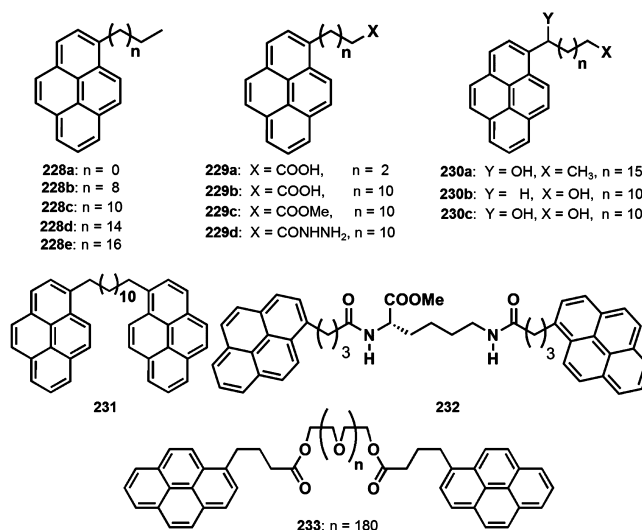
Chart 55



However, compounds with no hydrogen bonding D–A functionality such as ester or ether linkages as in **226** and **227** (Chart 55) resulted in colored gels in the presence of TNF in a 1:1 stoichiometry through CT interaction.⁵⁶⁶ Gel–sol transition monitored by variable temperature UV/vis and fluorescence studies revealed the existence of stacking and destacking of pyrene units in the gel fibers.

Many of the pyrene based LMOG were able to gelate solvents even in the absence of hydrogen bonds, by using weaker bonding mechanism in presence of a suitable co-gelator and appropriate solvents.^{566–568} For example, detailed gelation tests have indicated that compounds **228–231** (Chart 56) do

Chart 56



not form gels alone in any of the organic solvents tested whereas form stable gels in the presence of TNF. Optically transparent dark red or brown gels were formed at lower concentrations whereas at higher concentration, the obtained gels were translucent. Moffat and Smith have reported another D–A complexation driven gel composed of **232** (Chart 56) and TNF, reinforced by D–A and hydrogen bond interactions.⁵⁶⁹ With time, similar to Ostwald ripening, homogeneous red transparent metastable gels become inhomogeneous and crystals were directly formed from the gel. The 1:1 complex formed between the bispyrene derivative **233** (Chart 56) and an octafluoronaphthalene was reported to gelate water due to cross-linked networks formed through alternating stacks of arenes and perfluoroarenes.⁵⁷⁰ Polymerization of the pyrene functionalized gelator **234** (Chart 57) in DMSO/styrene/divinylbenzene mixtures resulted in the migration and accumulation of fluorescent gelator nanostructures at one face of the polymer wafer, giving rise to a two-faced material.⁵⁷¹

Ihara and co-workers studied the gelation and photophysical properties of pyrene based L-glutamic acid derivative.^{475–477,572–576} Pyrene functionalized with dialkyl L-glutamic acid **235a–c** (Chart 57) has been used as a donor in the energy transfer studies with dodecyl chain functionalized L-glutamic acid appended porphyrin derivatives **188** or **189** (Chart 43).^{475–477} Since the emission band of pyrene excimer show partial overlap with absorption band of the acceptor, energy transfer occurs from the pyrene excimer to the porphyrin moiety. The efficiency of energy transfer was found to depend upon the alkyl chain attached to L-glutamic acid part of the

Chart 57

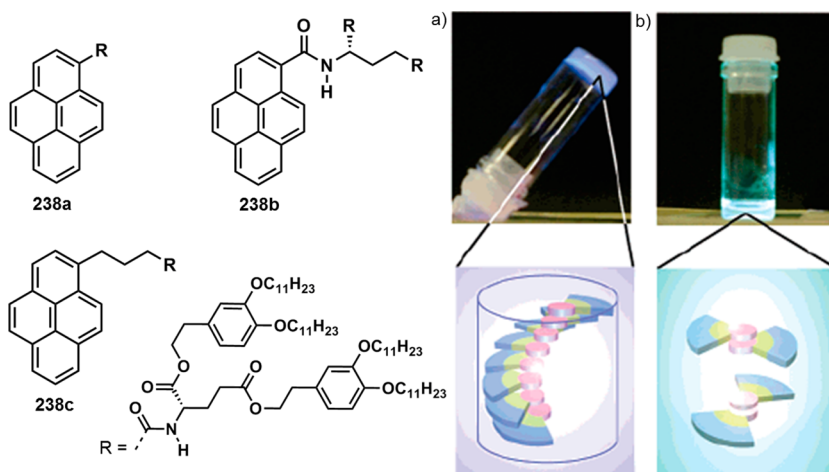
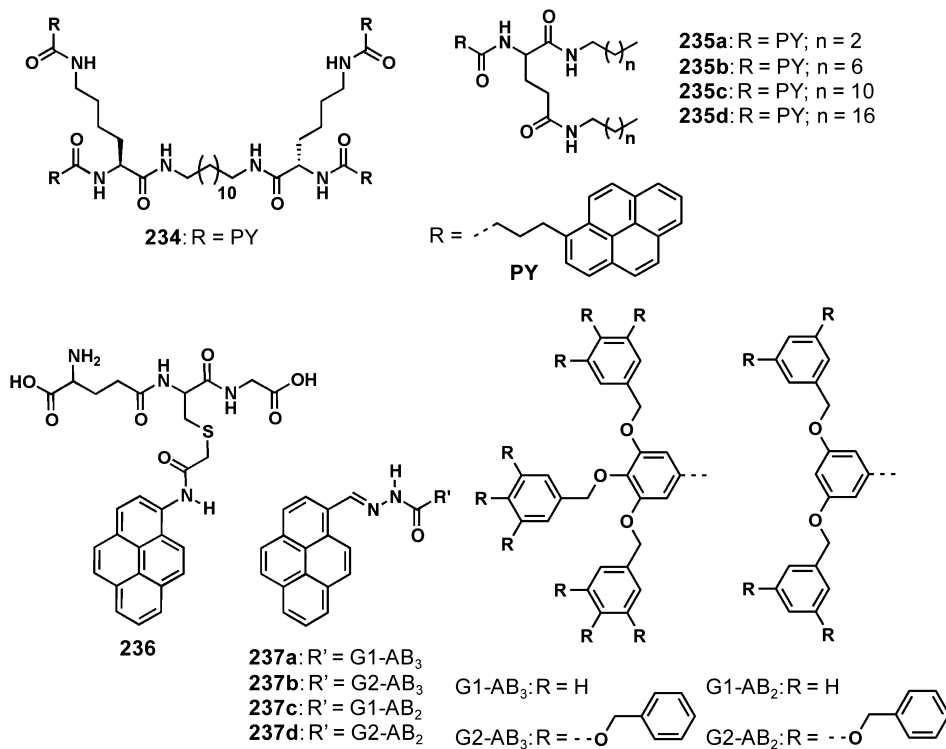


Figure 41. Chemical structures of oligopeptide functionalized pyrene gelators 238a–c. (a) Photograph of the fluorescent gel of 238a and schematic illustration of the self-assembly in the gel state. (b) Photograph of the sol of 238a and schematic illustration of excimer formation in the sol state. (Reprinted with permission from ref 580. Copyright 2007 American Chemical Society.)

pyrene gelator.⁴⁷⁶ The porphyrin acceptor 189 coassembled with 235a showed distinct emission enhancement when compared to that assembled with 235c. Apart from energy transfer, coassembly of 235c and the corresponding L-glutamide *N,N*-dimethylaniline analogue resulted in the formation of exciplex gel due to the charge transfer from *N,N*-dimethylaniline to pyrene.⁵⁷² Polymerizable monomer solvent such as methyl methacrylate, methyl acrylate, styrene and divinyl benzene has been used for the gelation of 235c.^{573,574} The photoinduced polymerization of methyl methacrylate retained the chiral microenvironment formed by 235c in methyl methacrylate and enabled to develop polymer sheets with stable as well as enhanced optical activity.^{573,574} Polymer films prepared from a benzene gel composed of 235c and polymethyl

methacrylate or polystyrene were also showed similar properties.⁵⁷⁵ Polymer films doped with achiral organic dyes showed CD signals from dyes due to induction of supramolecular chirality.⁵⁷⁵ Molecular gel-mediated power-conversion enhancement of solar cells was achieved by utilizing the excimer emission of nanofibrillar assembly of 235c embedded in a transparent and colorless polystyrene film.⁵⁷⁶

The interaction of pyrene moiety of 235d (Chart 57) with SWCNTs significantly decreased the critical gelation concentration of the gelator, depressed the sol–gel transition temperature as well as prolonged the time required to form a gel.⁵⁷⁷ Attaching a hydrophobic pyrene moiety to a glutathione tripeptide 236 (Chart 57) enabled gelation of DMSO/water mixtures.⁵⁷⁸ The transparent gels thus obtained exhibited the

Chart 58

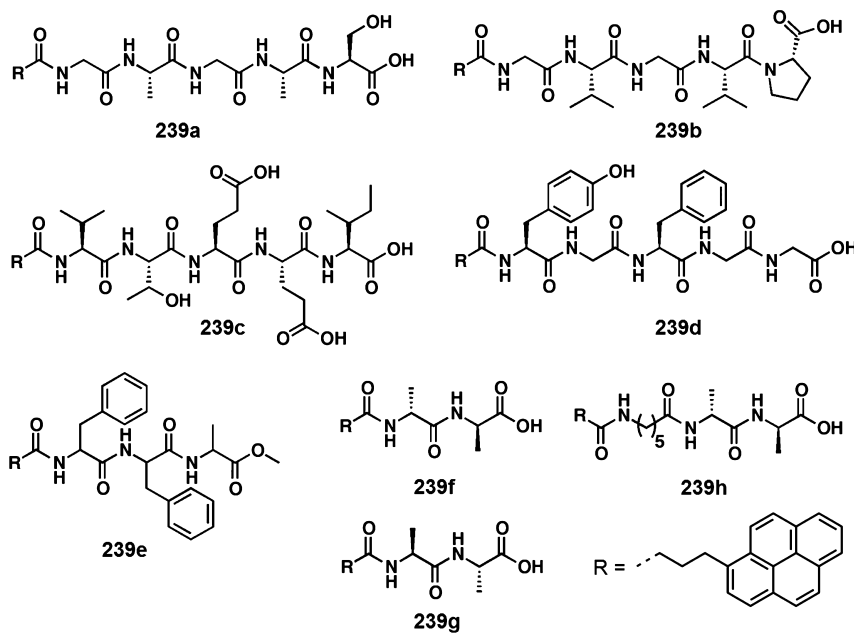
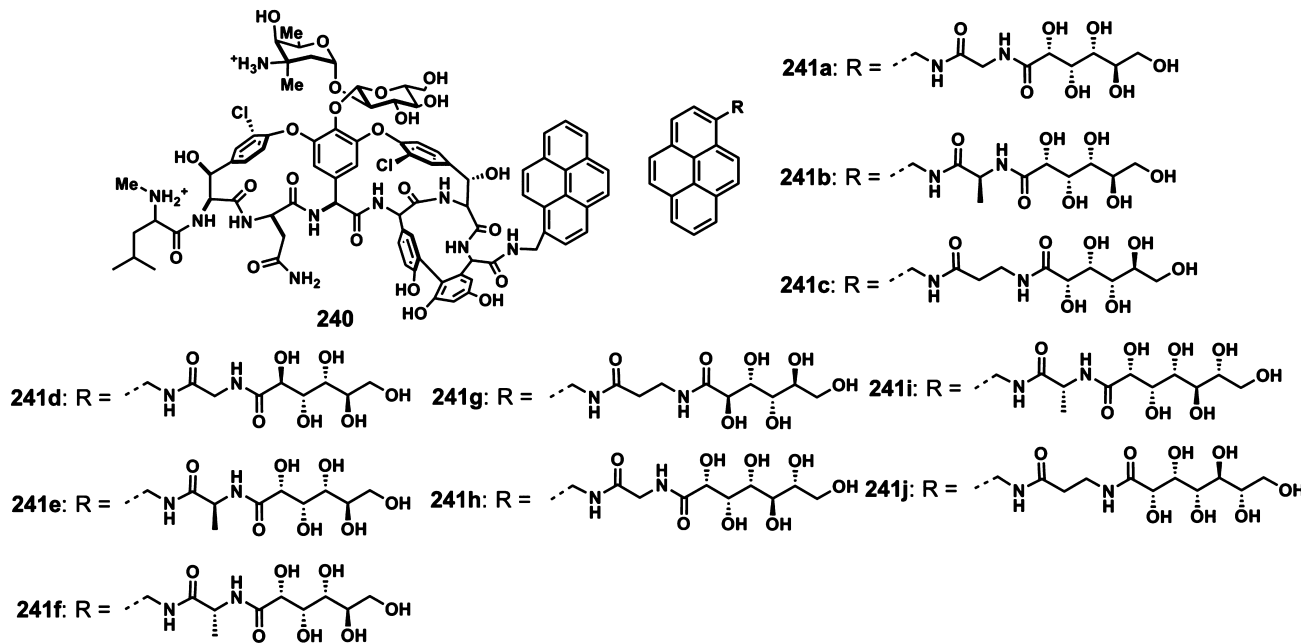


Chart 59



blue pyrene excimer fluorescence and strong CD bands characteristic of chiral pyrene stacks. Gelators based on nonamphiphilic pyrene functionalized poly(aryl ether) dendrons 237a-d (Chart 57) exhibited tunable fluorescence, morphology and sensing properties.⁵⁷⁹ In mixed solvent conditions, 237b,d formed nano sized vesicles at lower concentrations, which further aggregate to micro sized vesicles and finally ended up with entangled fibrous aggregates. The gels composed of different nano/micro aggregates exhibited gelation induced enhanced emission (GIEE) with tunable emission wavelength due to the controlled “excimer” and “exciplex” formation of the pyrene moiety.

Reverse mode fluorescence color switching of the oligopeptide functionalized pyrene gelators 238a-c (Figure 41) is an

interesting phenomenon.⁵⁸⁰ The cyclohexane gel of pyrene monoglutamate derivatives 238a,b showed monomer like emission because of the hydrogen bonded arrays of the oligopeptide moieties which suppress the formation of pyrene excimers. The reverse way is encountered in the case of 238c that exhibited excimer emission of pyrene. Xu and co-workers have reported the synthesis and hydrogelation properties of a series of pyrene end functionalized pentapeptides 239a-d (Chart 58).⁵⁸¹ Detailed CD studies revealed that the self-assembly of the hydrogelators affords helical or β -sheet-like structures. Optical and morphological studies indicated that a synergic effect of the intermolecular aromatic–aromatic interaction and the hydrogen bonds are responsible for the gelation. The pyrene conjugated tripeptide 239e (Chart 58)

reported by Banerjee and co-workers was found to form fluorescent organogels and hybrid gels with graphene.⁵⁸²

The molecular recognition between vancomycin and the gelator **239f** (Chart 58) was shown to enhance the storage modulus of the coassembled hydrogels to 10^6 fold.⁵⁸³ Addition of vacomycin to **239g,h** (Chart 58) showed only a marginal enhancement in the storage modulus due to weak recognition and interaction. In another interesting observation, the first antibiotic hydrogel based on a vancomycin-pyrene conjugate **240** (Chart 59) that forms a helical polymer has been reported.^{584,585} The h-t organization of the gelator leads to the helical packing of the biphenyl and pyrene moieties in the assembly. The vancomycin pyrene conjugate **240** was found to self-assemble on cell surfaces in a phosphate buffer.⁵⁸⁵ Moreover, the presence of pyrene moiety allowed probing of in situ dimerization and membrane anchoring through optical spectroscopy. Kim et al. have synthesized a library of amphiphilic pyrene carbohydrate conjugates **241a–j** (Chart 59) which form hydrogels.⁵⁸⁶ Since insulin interacts strongly with D-glucose in biological systems, D-gluconolactone derived **241b** was found to be a sensor of insulin at very low concentrations in aqueous media.

Hamachi et al. have reported the gelation properties of galactoside attached pyrene glutamic acid derivative **242** (Chart 60).⁵⁸⁷ The gelation properties of the pyrene functionalized

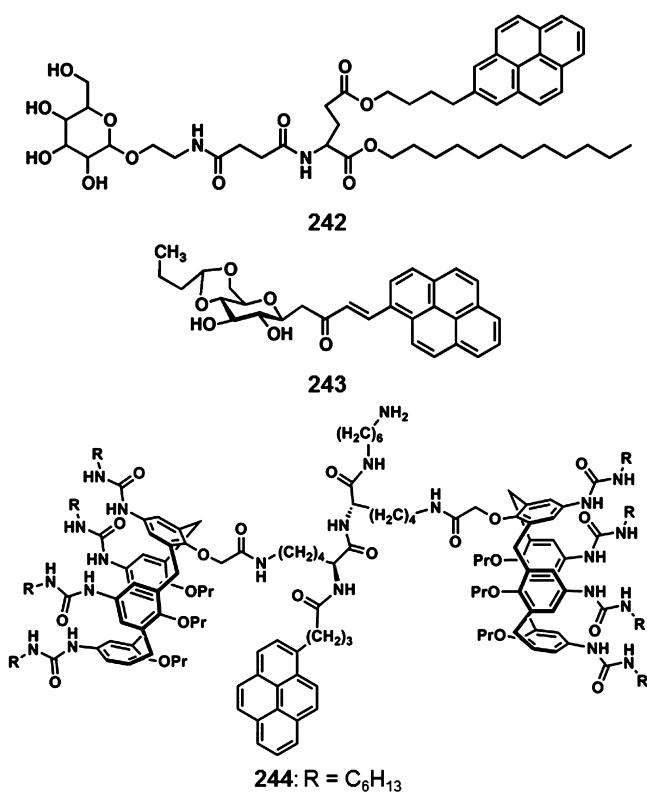
(Chart 60) cross-links the chains to form 3D polymeric network and finally stable gels with switchable fluorescence.

Aggregation of an amphiphilic pyrene molecule **245** (Chart 61) in water/methanol mixture produced a gel. The strong $\pi-\pi$ interaction capability of pyrene based gelators with SWCNTs surface can be utilized for improving the strength of gels.⁵⁹⁰ The freely moving peripheral amphiphilic chains lead to the accumulation of oligomeric silica species around SWCNTs, resulting in the formation of organic-inorganic nanoscopic fibers resembling electronic cables composed of a conductive SWCNT and an insulating silica wall. The cationic pyrene dendrons **246** and **247** (Chart 61) formed hydrogels under basic conditions and showed large fluorescence enhancements in the presence of NaOH due to favorable formation of pyrene excimers in the aqueous phase.⁵⁹¹ Amabilino and co-workers have reported gelator **248** (Chart 61) composed of electron rich and deficient units such as TTF and pyrene.^{592,593} The solvent used for the xerogel preparation played a crucial role in the conducting properties of the fibers after doping with iodine. Addition of a small amount of SWCNTs was found to assist the formation of a fibrous structure in the gel together with improvement in the conducting properties.⁵⁹³ Muccini, Ziessel and co-workers have designed a pyrene substituted 4-ethynylphenylaminoacyl derivative **249** (Chart 61), which formed organogel with distinct morphologies of a 3D network of interlocked thin fibers in both cyclohexane and toluene, whereas in DMF, a dense network of entangled rope like fibers were formed.⁵⁹⁴ The FET characteristics of such gels as the active layer exhibited good electron and hole transport properties from source to drain electrodes as well as light emission in the high source-drain voltage region.

The gelation properties of a set of hydrazide based foldamers end functionalized with pyrene, naphthalene, and anthracene units **250a–e** (Figure 42) have been reported by Li and co-workers.⁵⁹⁵ Based on detailed optical and morphological investigations, a dislocated “tail-to-tail” stacking was proposed. The van der Waals forces of the decyl chains of the foldamers drive them further to aggregate into bundles of fibrils, which gelate the solvent molecules (Figure 42). The addition of octylated glucose considerably enhanced the gelation ability of foldamers and resulted in dynamic helicity induction (Figure 42) as inferred from the detailed CD studies. Furthermore, CD studies have revealed a nucleation elongation mechanism for the self-assembling process.

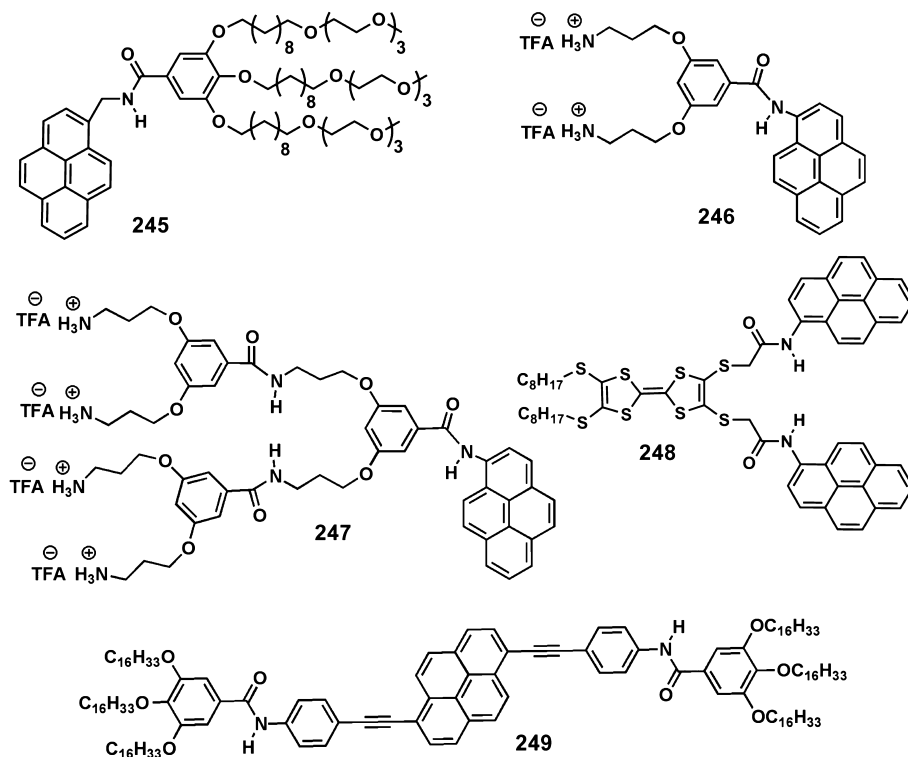
Apart from the above-mentioned studies, a pyrene group end functionalized helical poly(γ -benzyl-L-glutamate)-poly(ethyleneglycol) random coil diblock copolymer was reported to show gelation behavior in toluene.⁵⁹⁶ Pyrene was used to determine the critical aggregation concentration of the tripodal cholamide hydrogelator.⁵⁴¹ Doping of pyrene into a Eu-cholate gel was found to sensitize Eu(III) emission through an energy transfer process.⁵⁹⁷ Pyrene has also been incorporated into styrene based polymer hydrogels.⁵⁹⁸ Zhang and co-workers have reported the reversible modulation of the monomer/excimer emission of a bispyrene molecule coassembled with *trans*-dodecyl-3-[2-(3-dodecyl-ureido)cyclohexyl]urea gelator through a sol-gel phase transition.⁵⁹⁹ A saccharide derived hydrogelator has been used as a medium to study the release mechanism of a pyrene based saccharide derivative, facilitated by the presence of cysteine.⁶⁰⁰ An ethynylpyrene labeled molecular beacon has been used as an oligonucleotide signal unit in biotin based hydrogels.⁶⁰¹ A coassembled system consisting of homoadenine self-duplexes of pyrene appended

Chart 60



sugar derivative **243** (Chart 60) has also been reported.⁵⁸⁸ However, the addition of SWCNTs was found to negatively affect the gelation by preventing the interaction between the pyrene moieties which are responsible for gelation. Xu and Rudkevich have used the chemistry between CO₂ and primary amine to develop switchable, supramolecular gels.⁵⁸⁹ The carbamate salt bridges created by the reaction of CO₂ with **244**

Chart 61



deoxyadenosine base and a biotin based hydrogel was utilized to recognize streptavidin.⁶⁰² Moreover, a pyridyl disulfide derivative of pyrene has been used as a model hydrophobic drug in hyaluronan based hydrogels.⁶⁰³ Analysis of a pyrene based microporous polymer indicated that the porous fluorescent frameworks exhibit gelation and undergo swelling in the presence of hydrophobic and aromatic guests.⁶⁰⁴ Hence the porous polymer has been used for the phase selective removal of oil from water and guest induced fluorescence modulation.

4.2. Triphenylenes

Triphenylene, a member of a polycyclic aromatic hydrocarbon family, is a disc shaped molecule with a planar structure.^{605,606} The thermal stability and the synthetic feasibility for functionalization make them appealing for the design of soft materials having interesting opto-electronic properties.^{605,606} Shinkai and co-workers have reported the organogelation of the triphenylene derivatives **251a,b** (Chart 62) substituted with six amide groups and six hydrocarbon side chains.⁶⁰⁷ A staggered lateral rectangular arrangement was observed for the triphenylene core of **251a** in the gel state whereas an eclipsed hexagonal columnar arrangement was observed for **251b**, which led to an unusual excimer emission. Triphenylenes bearing six peripheral chiral amide units **252a–c** (Chart 62) were found to stabilize 1D stacking of triphenylene core leading to self-assembled nanofibers and gels.⁶⁰⁸ Stable gels of an ion-bonded discotic complex **253** (Chart 62) were prepared from the cationic triphenylene derivative and 4'-dodecyloxybiphenyl-4-carboxylic acid.⁶⁰⁹ A combination of ionic bonds, hydrogen bonds, $\pi-\pi$ stacking and van der Waals interactions in the complex resulted in the formation of elongated gel nanofibers. A triphenylene derivative functionalized with a triazole moiety containing alkyl chain **254** (Chart 62) was found to self-assemble in bulk as well as in solution.⁶¹⁰ Furthermore, fluorescent organogels obtained

from the electron rich triphenylene derivative **254** was utilized as a chemosensor to detect electron deficient nitroaromatics.

Gels formed by the thermotropic discotic LC organogelator **255** (Chart 62) exhibited distinct elastic modulus depending on the gelation temperature.⁶¹¹ The transition from a discotic columnar to a plastic crystal and to a crystalline phase were observed. These transitions led to harder gels at lower temperatures, composed of partly crystalline gelator fibrils, and softer gel formed at higher temperatures having a fairly low ordering. Triphenylene derivatives **256a–d** (Chart 62) containing amide groups at 2,7-positions were reported to form gels in a wide range of solvents due to intermolecular hydrogen bonding assisted stabilization of columnar organization and assembly.⁶¹² Compound **257a** (Figure 43) formed a turbid gel whereas the presence of an imidazole group in **257b** (Figure 43) resulted a transparent gel.⁶¹³ A rotation bias provided by the steric hindrance of the imidazole group induced a helical stack in the assembly of the achiral gelator **257b** (Figure 43). A thermotropic LC assembly has been formed by the complexation of **257b** with benzene-1,3,5-tricarboxylic acid. Kato and co-workers have investigated the enhanced hole mobility of a semiconducting discotic LC 2,3,6,7,10,11-haxaalkoxytriphenylene derivative by encapsulating in the hydrogen bonded fibrous gel aggregates of L-valine.^{614,615} Due to the presence of gel networks, the hexagonal columnar phases have a control on the molecular dynamics of the LCs, which suppress the LC molecular fluctuation, leading to enhancement of hole transporting behavior.

The tetrabenzopentaphene mesogens **258a,b** (Chart 63) form organogels that exhibit a hexagonal columnar mesophase.⁶¹⁶ The presence of a larger flat core enables effective $\pi-\pi$ stacking which assist self-organization in the LC state as well as the organogel formation.

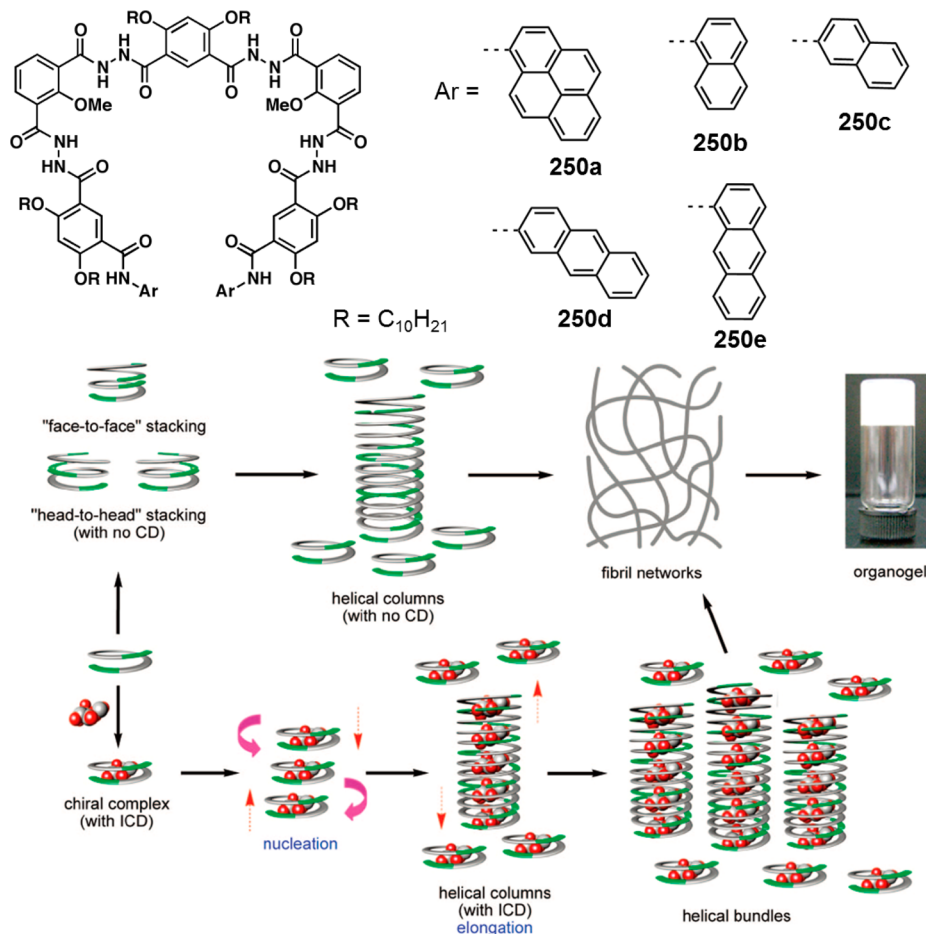
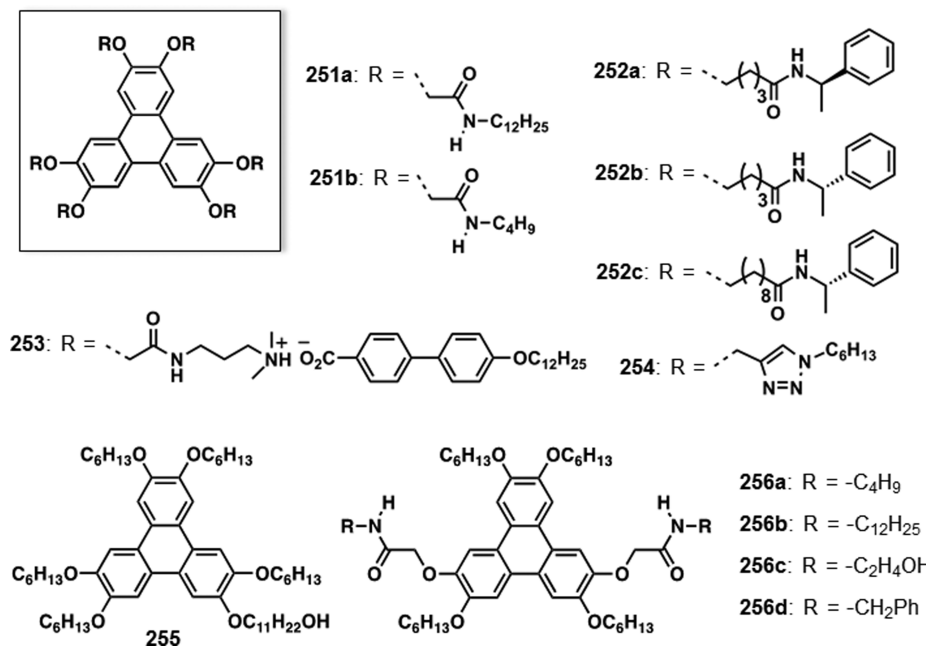


Figure 42. Chemical structures of polyaromatic hydrocarbons and functionalized achiral hydrazide heptamers 250a–e. Schematic representation of the self-assembly of foldamer gels and glucose initiated helicity induction. (Reprinted with permission from ref 595. Copyright 2008 American Chemical Society.)

Chart 62



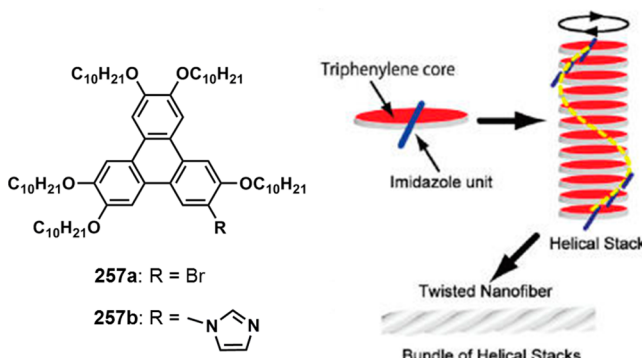
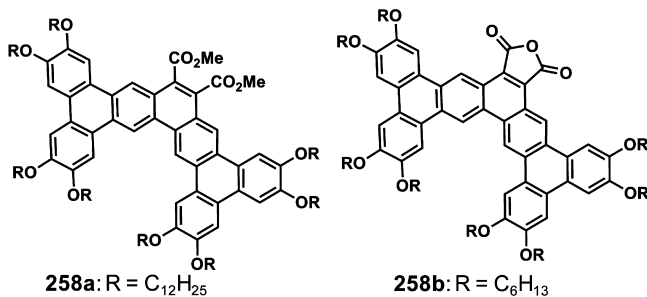


Figure 43. Chemical structures of imidazole functionalized triphenylene gelators **257a,b** and schematic representation of self-organization process of **257b** into twisted nanofibers. (Reprinted with permission from ref 613. Copyright 2010 American Chemical Society.)

Chart 63



4.3. *n*-Arenes

4.3.1. Naphthalenes. Naphthalene is a simple fused aromatic molecule exhibiting interesting optical properties. Since the fluorescence properties are dependent upon the environments, naphthalenes have found wide interest in the gel chemistry.^{29,80–84,87,90,617–619} Whitesides and co-workers studied the self-assembly and gelation assisted polymeric nanorod formation (Figure 44) from a combination of naphthalene linked bismelamine **259** and a bisisocyanuric acid **260** derivatives.⁶²⁰

SANS measurements of the gels formed by 2,3-di-*n*-hexadecyloxy naphthalene **261** (Chart 64) indicated characteristic well resolved oscillation related to the monodispersed thickness of the ribbon-like fibers.⁶²¹ The presence of nodal zones or merging points of fibers lead to 3D opened pores with fibrillar boundaries to entrap the bulk volume of solvents. There are several other reports on gelators such as **262–265** having alkoxy naphthalene groups (Chart 64).^{622–624} The role of functional groups in directing the assembly formation in these gelators was demonstrated by bisamide and bisurea functionalized naphthalene derivatives **265a,b** (Chart 64).^{624,407,408} Distinctly different packing modes were observed during the gelation of these bisamide and bisurea functionalized alkoxy naphthalenes as the result of the high propensity J-aggregates of **265a** and thermally/mechanically stable H-aggregates of **265b**.

The intensity of the weak fluorescence due to the excited state intramolecular proton transfer in the gelator **266** (Chart 65) in solution could be significantly increased upon gelation due to the prevention of intramolecular rotation in the gel state.⁶²⁵ Bisurea functionalized naphthalene organogelators **267a–c** (Chart 65) showed excellent gelation with enhanced

and red-shifted fluorescence in the gel state. In 1,4-dioxane, xerogel of **267a** has shown a smooth belt structure whereas **267b** and **267c** exhibited a morphology of regular wool balls connected by thin ribbons.⁶²⁶ A binaphthalene chiral gelator appended with urea moieties **268** (Chart 65) exhibited CD signal upon gel formation indicating chiral ordering of the chromophores.⁶²⁷ Steed and co-workers studied the gelation of naphthalene functionalized chiral bisurea derivative **269** (Chart 65). Shaking a solution of the gelator **269** initiates nucleation of assembly accompanied by a red shift and intensity increase of fluorescence which highlights the importance of kinetic nucleation in the gelation process.⁶²⁸

The intra site reaction between neighboring cysteine residues in **270a–c** with disulfide bonds (Chart 66) has been shown to lead organogelation.^{629–631} For example, a convenient and portable triacetone triperoxide sensor was developed utilizing a thiol-to-disulfide oxidation triggered gelation of **270a**.⁶³⁰ The dendritic L-glutamic acid functionalized naphthalene based gelator **271a** (Chart 66) in solution forms precipitates which could be converted to a stable organogel by applying ultrasound, indicating rearrangement of the molecular assemblies in favor of gelation.⁶³² Hydrogels and organogels (ambidextrous) formed by naphthyl containing L-glutamate dendrons **271a,b** (Chart 66) showed strong fluorescence enhancement in the gel state.⁶³³ The immobilization of propyldansylamide based energy acceptor into the 1,3,5-cyclohexyltricarboxamide based LMOG **272** containing a hydrophobic fluorophore (Chart 66) resulted in an efficient energy transfer.⁶³⁴ Moreover, 75% of the photons absorbed by **272** has been funneled to the acceptor when approximately five dansyl molecules were incorporated into every 100 molecules of **272**. An acyclic chiral L-phenylalanine based receptor **273** (Chart 66) has been used to recognize enantiomers of mandelic acid and α-amino acid derivatives through enantioselective gel formation.⁶³⁵ The receptor selectively formed gel with R enantiomer of tetrabutylammonium salts of mandelic acid whereas no gel was observed with S enantiomer.

Jia and co-workers have investigated the polymorphic properties of two naphthyl dendrons **274a–b** (Chart 67).⁶³⁶ In cyclohexane, **274a** formed a gel with β-sheet architecture and spherulitic networks in chloroform/petroleum ether whereas **274b** self-organized to form intertwined nanobelts in chloroform, and crystalline microbelts in acetone and alcohols. The C₃ symmetric 1-aza-adamantanetrione containing naphthalene **275** (Chart 67) formed translucent gels consisting of lamellar sheet architectures with layers of uniform thickness.⁶³⁷ Compound **276** (Chart 67) formed organogels in cyclohexane with enhanced CD signals in the gel phase.^{638,639} Coassembled gels of **276** and a nitrobenzofuran derivative showed efficient energy transfer at different D–A ratios.⁶⁴⁰

The kinetics of the gel formation via instantaneous nucleation and 1D growth of 5α-cholestane-3β-yl N-(2-naphthyl)-carbamate **277a** (Chart 68) was reported by Weiss and co-workers.⁶⁴¹ In this case, two types of SAFINs were observed. For example, at incubation temperatures of ≤28 °C or concentrations above 1.5 wt %, thixotropic gels with spherulitic SAFINs were observed. At concentrations of ca. 0.9–1.0 wt % and incubation temperatures of 30–40 °C, gels with fiber like SAFINs were formed. A small variation in the molecular structure of **277a** by introducing a double bond at C5 as shown in the derivative **277b** (Chart 68) has resulted in a significantly different self-assembly and gelation.⁶⁴² In addition, at lower temperatures, the gelation of **277b** followed a

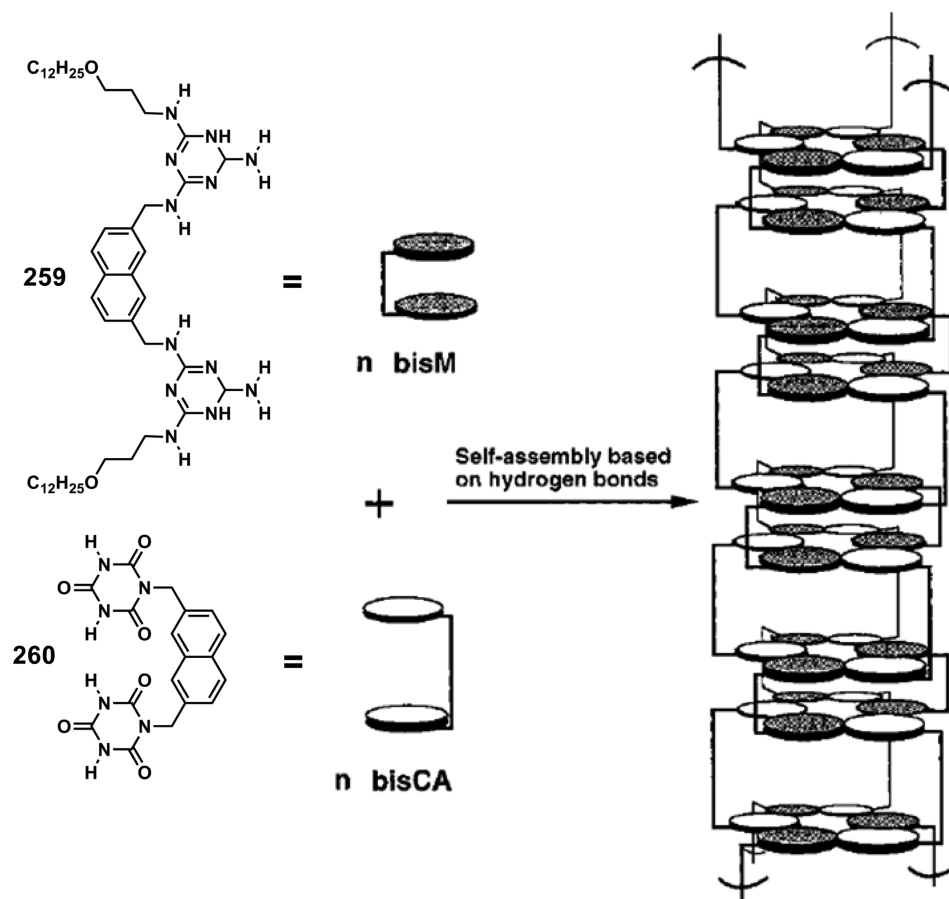


Figure 44. Self-assembly pathways of the bismelamine **259** and the bisiscyanurate **260** to form polymeric nanorods. (Reprinted with permission from ref 620. Copyright 1999 American Chemical Society.)

Chart 64

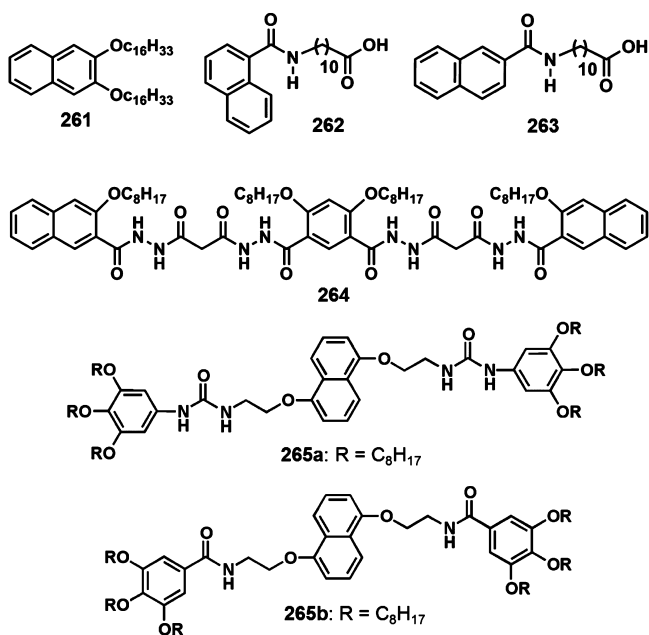
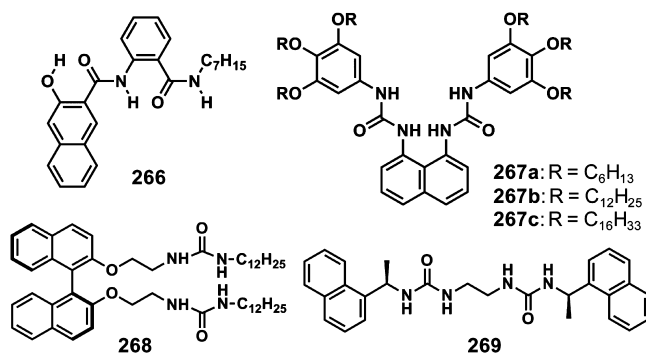


Chart 65



mixed solvent systems.⁶⁴³ The drop cast samples self-organize to form layered droplet superstructures consisting of a stack of concentric discs with increasing size.⁶⁴⁴ Ultrasound induced growth of helical fibers of **279** (Chart 68) resulted in a chiral fluorescent organogel at relatively high temperatures or low concentrations.⁶⁴⁵

The glucose based naphthalene derivatives **280a-e** (Chart 69) exhibited interesting gelation behavior (Figure 45).⁶⁴⁶ In support of a direct correlation between the gelator–solvent interaction, Fang et al. found a transition from hydrogelators (**280a**) to an ambidextrous gelator (**280b**) and then to organogelators (**280c-e**) in a series of LMOGs when the spacer length was marginally increased. AIEE and supramolecular chiroptical switching were observed during the self-

heterogeneous nucleation mechanism whereas above 0.5 °C, it has been changed to a homogeneous nucleation. Stoddart et al. have reported the gelation of a cholesterol stoppered dumbbell containing 1,5-dioxynaphthalene as well as a bistable rotaxane **278** (Chart 68) and cyclobis(paraquat-*p*-phenylene) rings in

Chart 66

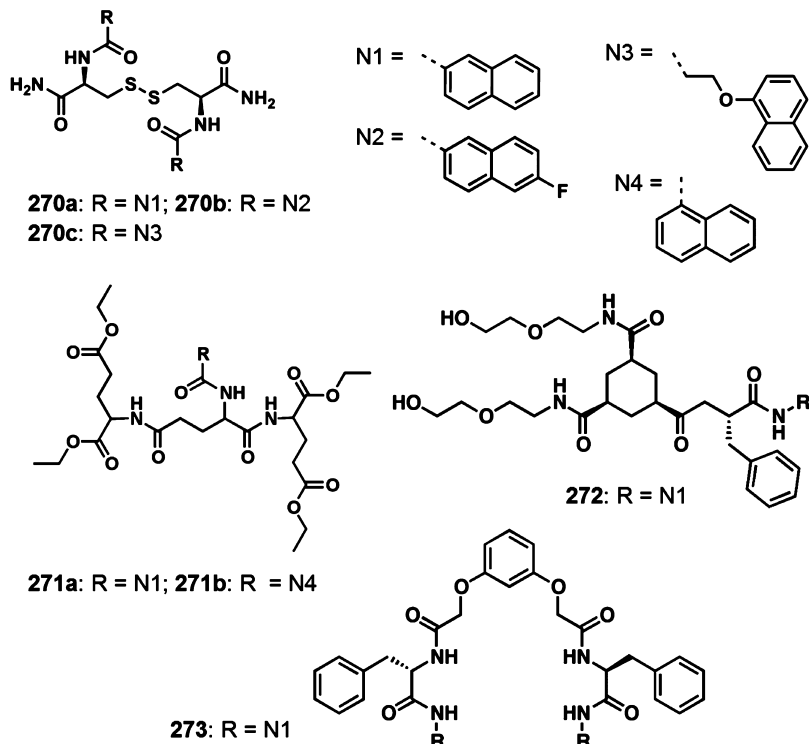
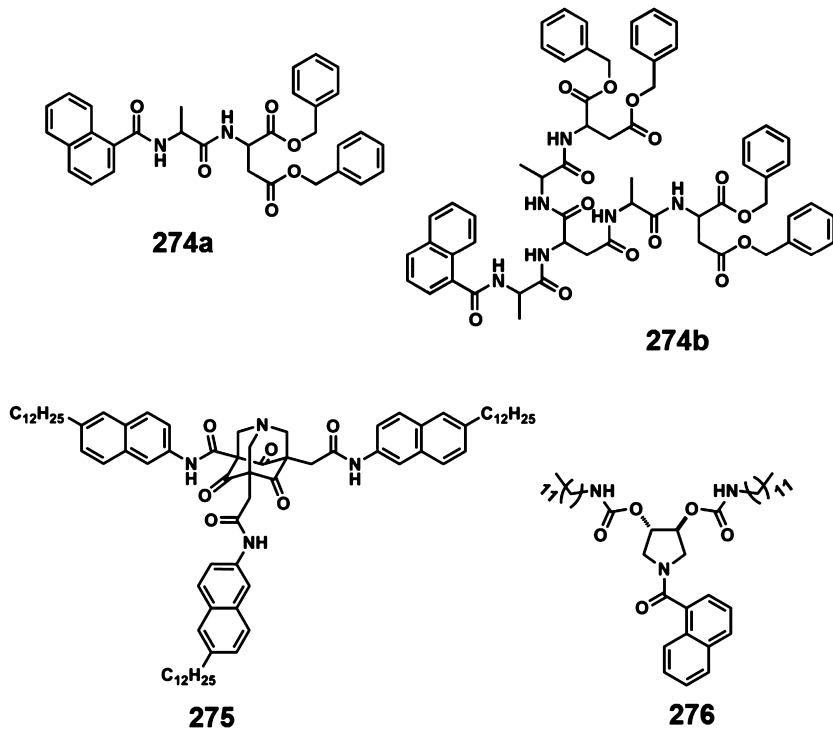


Chart 67



assembly process of these gelators. The chiral pyrano[2,3-b]naphtho[1,2-e]-pyrans **281** (Chart 69) is a good organogelator which forms micro tubular assembly through intermolecular C–H···O and C–H··· π (arene) hydrogen bonding interactions.^{647,648} A monosaccharide derived carbamate derivative containing naphthyl moiety **282a** (Chart 69) was able to form gel only in DMSO/water mixtures,⁶⁴⁹ whereas

naphthalene containing 1-deoxysugar derived ester **282b** (Chart 69) was found to gelate organic solvents.³⁰⁸ However, the gelation efficiency of the 1-deoxysugar gelator was less when compared to the α -methoxy analogs. The nanotube forming glycolipid naphthalene gelator **283** (Chart 69) exhibited strong fluorescence and efficient energy transfer to

Chart 68

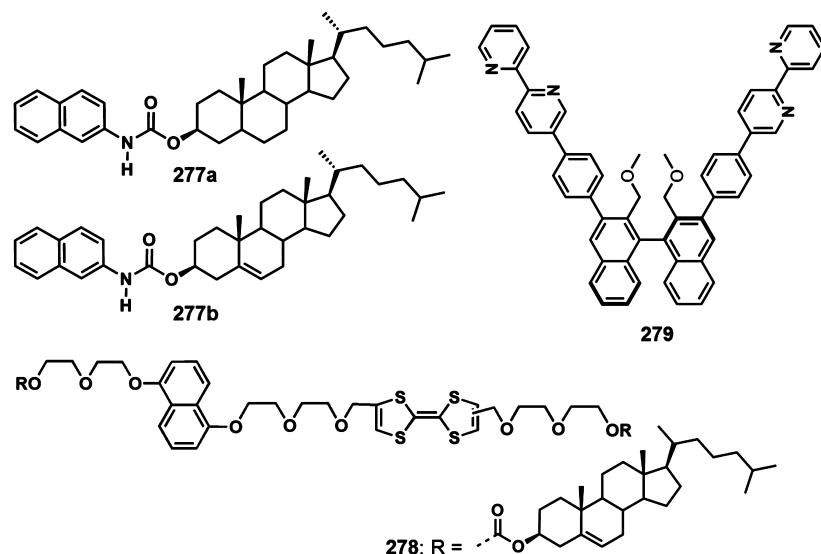
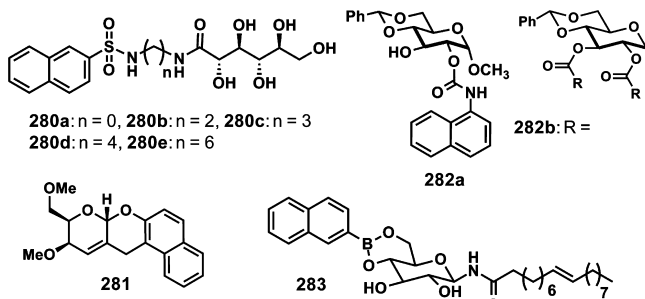


Chart 69



anthracene when encapsulated into nanochannels (Figure 46).⁶⁵⁰

Adams et al. have investigated the gelation properties of a library of naphthalene dipeptides 284a–s (Chart 70) by varying both the amino acid sequence and the substituents on the naphthalene ring.^{651–653} Many of these gelators form self-supporting hydrogels at high pH on addition of salts. Energy transfer was observed from the gelator 284d to dansylamides as

well as to anthracene diphenylalanine derivatives.⁶⁵⁴ Incorporation of dextran into a hydrogel of the dipeptide conjugated gelator 284f leads to modification of the material properties as well as gelation time.⁶⁵⁵ Transparent gels were formed with 33 wt % dextran and 0.5 wt % of the dipeptide 284f. Dextran increases the solution viscosity and acts as a physical barrier, resulting in a decrease in the gelation time. The effect of polymeric additives such as dextran, poly(vinylpyrrolidone), PEG, glycerol, PAA, etc. on the gelation of *N*-functionalized dipeptide 284h was also investigated.⁶⁵⁶ High concentrations of polymer additives can be incorporated into hydrogels, and they have significant influence on the rheological properties. UV irradiation of a series of dipeptide gelators 284a, 284d, 284h, 284p, and 285 (Chart 70) in the presence of a photoacid generator diphenyliodonium nitrate resulted in the formation of a hydrogel.⁶⁵⁷ Upon adding diphenyliodonium nitrate followed by UV irradiation, pH of the solution was found reduced below the apparent pK_a and hence induced self-assembly to form hydrogels. The gelation in the presence of a photoacid generator finds application in UV photopatterning of gels using a UV mask.

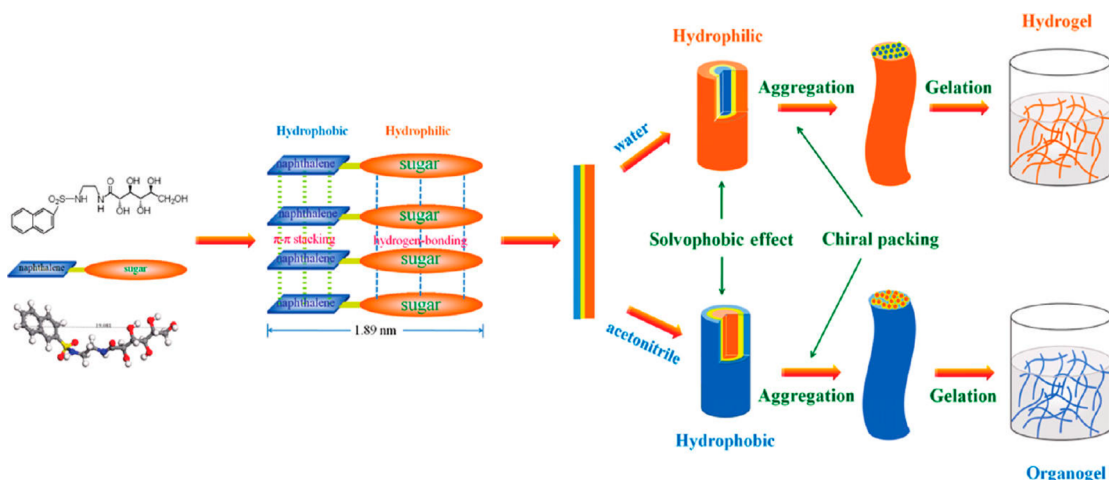


Figure 45. Schematic representation of the formation mechanism of the aggregates of naphthalene-sugar gelator in water and in acetonitrile. (Reprinted with permission from ref 646. Copyright 2010 American Chemical Society.)

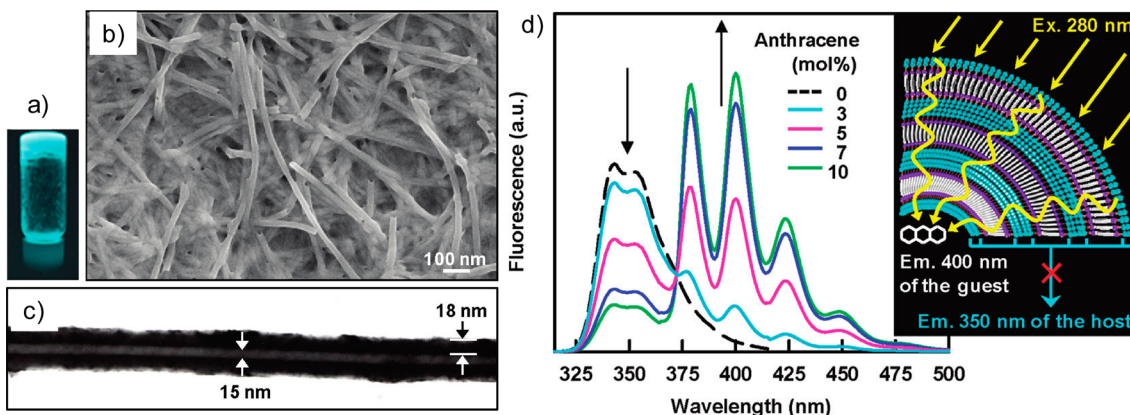
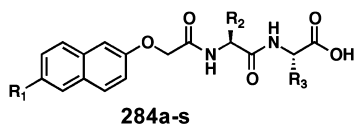
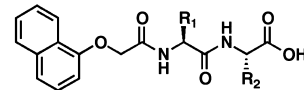
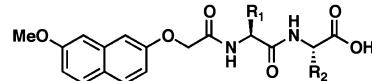


Figure 46. (a) Photograph of the nanotube organogel. (b) SEM and (c) TEM images of the nanotubes of **283**. (d) Fluorescence spectra of the anthracene encapsulated nanotube (solid lines) and the nanotube alone (dotted line). Schematic illustration of the energy transfer from naphthalene to the encapsulated anthracene. (Reprinted with permission from ref 650. Copyright 2012 American Chemical Society.)

Chart 70



284a:	$R_1 = H$,	$R_2 = CH_3$,	$R_3 = CH_3$
284b:	$R_1 = H$,	$R_2 = CH_2Ph$,	$R_3 = H$
284c:	$R_1 = H$,	$R_2 = CH_2Ph$,	$R_3 = CH(CH_3)_2$
284d:	$R_1 = H$,	$R_2 = CH_2Ph$,	$R_3 = CH_2Ph$
284e:	$R_1 = H$,	$R_2 = CH(CH_3)_2$,	$R_3 = H$
284f:	$R_1 = Br$,	$R_2 = CH_3$,	$R_3 = H$
284g:	$R_1 = Br$,	$R_2 = CH_3$,	$R_3 = CH_3$
284h:	$R_1 = Br$,	$R_2 = CH_3$,	$R_3 = CH(CH_3)_2$
284i:	$R_1 = Br$,	$R_2 = CH_2Ph$,	$R_3 = H$
284j:	$R_1 = Br$,	$R_2 = CH_2Ph$,	$R_3 = CH(CH_3)_2$
284k:	$R_1 = Br$,	$R_2 = CH_2Ph$,	$R_3 = CH_2Ph$
284l:	$R_1 = CN$,	$R_2 = CH_3$,	$R_3 = H$
284m:	$R_1 = CN$,	$R_2 = CH_3$,	$R_3 = CH_3$
284n:	$R_1 = CN$,	$R_2 = CH_2Ph$,	$R_3 = H$
284o:	$R_1 = CN$,	$R_2 = CH_2Ph$,	$R_3 = CH(CH_3)_2$
284p:	$R_1 = CN$,	$R_2 = CH_2Ph$,	$R_3 = CH_2Ph$
284q:	$R_1 = H$,	$R_2 = H$,	$R_3 = H$
284r:	$R_1 = H$,	$R_2 = H$,	$R_3 = CH_3(D/L)$
284s:	$R_1 = H$,	$R_2 = H$,	$R_3 = CH_2OH$



286a:	$R_1 = CH(CH_3)_2$,	$R_2 = H$
286b:	$R_1 = CH(CH_3)_2$,	$R_2 = CH(CH_3)_2$
286c:	$R_1 = CH_2Ph$,	$R_2 = H$
286d:	$R_1 = CH_2Ph$,	$R_2 = CH(CH_3)_2$
286e:	$R_1 = CH_2Ph$,	$R_2 = CH_2Ph$

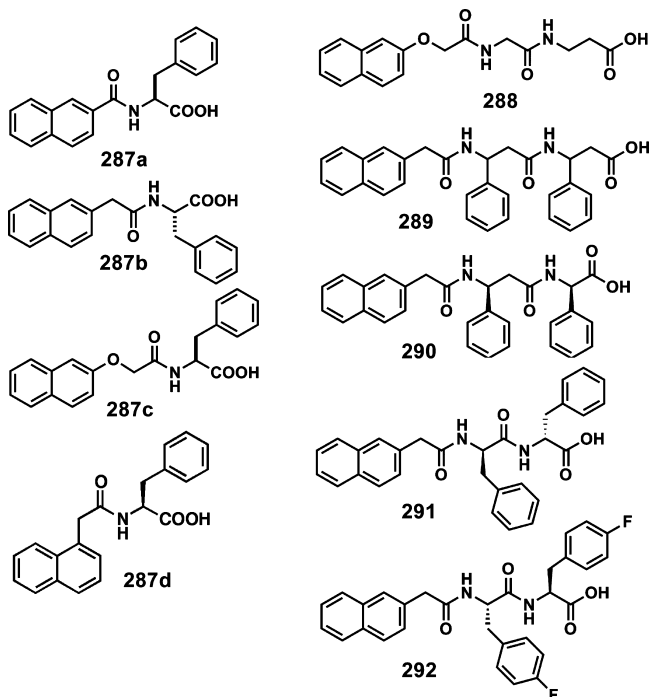
In order to understand the relationship between the fiber phase and the crystal structure of gelators, self-assembly as well as crystal structures of dipeptides **284a–e** and **286a–e** (Chart 70) were studied systematically.⁶⁵⁸ The gelator **284a** crystallized directly from the gel phase and found that the molecular packing of the crystal structure differs from the gel/fiber phase. A significant rearrangement of the molecules in the fibers promotes 1D assembly whereas in the crystals, 3D growth is favored. Cameron et al. have utilized the pH drop associated with a sugar-boronic acid interaction to initiate the gelation process in the dipeptide gelator **284h**.⁶⁵⁹ The interaction of D-fructose with boronic acid brings pH below the pK_a of **284h** and hence led to gelation whereas due to the weaker binding constant of D-glucose to boronic acids, no gelation was observed.

Xu et al. have enzymatically converted samogens (simple samogen contained two phenylalanine residues and a naphthyl group) to prepare biologically active hydrogels.^{29,80–84,87,90} This strategy was based on the ability of the precursor molecule to convert into molecular hydrogelators that self-assemble in water resulting in nanofibers. The capability of the aminoacid residue of the samogen to form multiple hydrogen bonding interactions and the aromatic–aromatic interaction of the naphthalene part in water, have been used to generate functional hydrogels. Interestingly, several chemical or enzymatic paths such as dephosphorylation were used to convert precursors containing enzymes such as phosphatase, thermolysin, β -lactamase, and phosphatase/kinase to less soluble amphiphilic hydrogelators. These hydrogels exhibited

promising applications such as drug release, bacterial typing, wound healing, cell inhibition and catalysis.

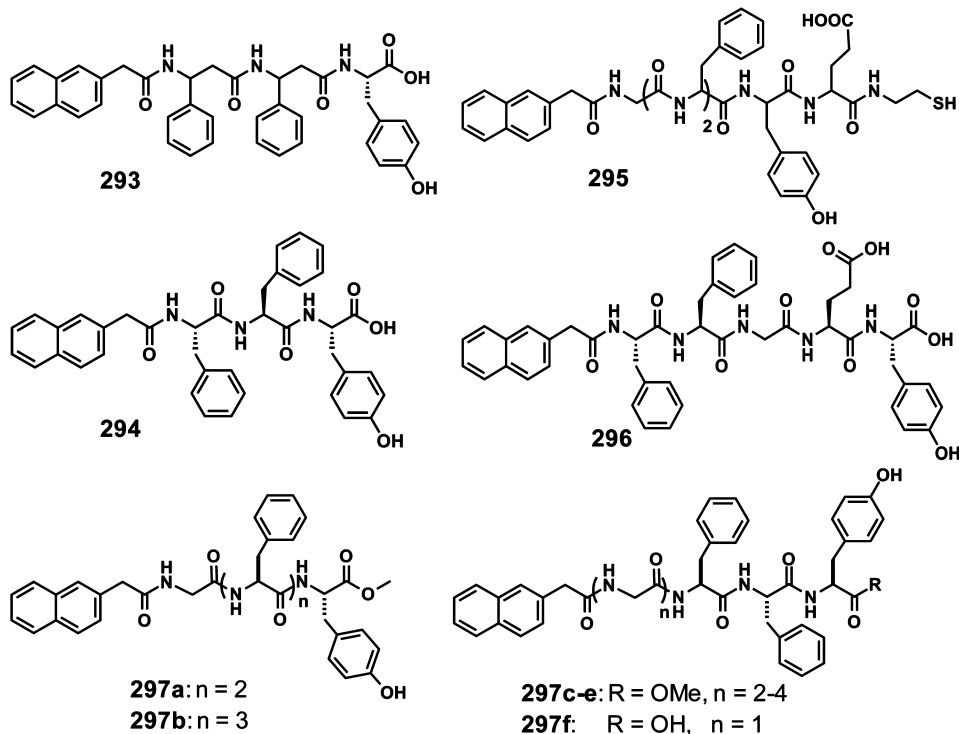
Xu et al. reported the gelation properties of molecules **287a–c** (Chart 71) consisting of an aromatic naphthyl and

Chart 71



naphthalenoxyl moieties covalently attached to phenylalanine.³⁴⁶ The naphthalene-1-acetamide derivative of L-phenylalanine **287d** (Chart 71) is a super gelator which could gelate

Chart 72



water even with 0.025 wt %.⁶⁶⁰ The entrapment of water-soluble dye afforded chiral fluorescent gels owing to the formation of J-type aggregates of the dye within the gel. The naphthalene based hydrogelators **288** and **289** (Chart 71) containing α - and β -amino acids formed dimers and oligomers even in dilute solutions with characteristic asymmetric shapes for the red-shifted emission peaks with long wavelength tails.⁶⁶¹ This could be attributed to the excimer emission by the oligomers formed by π -stacking which led to gel formation. Compounds **284q–s** (Chart 70) form biocompatible hydrogels with helical nanostructures associated with the chirality of the alanine moiety.⁶⁶²

The *in vivo* enzymatic hydrogelation experiments indicated no long-term toxicity of the hydrogelator in mice. The first *in vivo* imaging experiments using hydrogels of **284d** and **290–292** (Chart 70 and 71) have been characterized by isotope encapsulation and single photon emission computed tomography imaging.⁶⁶³ The biostability of three unnatural D amino acid based hydrogelators **290–292**, which exhibited resistance toward proteinase K catalyzed hydrolysis and offered long-term biostability as well as controlled *in vivo* release. A magneto-rheological hydrogel was prepared by incorporating surface modified Fe₃O₄ nanoparticles into hydrogel of **284d** and found that nanoparticles were exclusively localized inside the hybrid nanofibers.⁶⁶⁴ In addition, hydrogelation of naphthalene and azobenzene functionalized dipeptide **36** (Chart 9) catalyzed by the enzymatic reaction of phosphatase has also been reported.²⁰² The hydrogel of **36** exhibited gel–sol transition upon photoirradiation.

Supramolecular hydrogels with long lifetimes in biological environments were prepared by an enzymatic conversion of a precursor into the corresponding β -peptide hydrogelator **293** (Chart 72).⁶⁶⁵ Phosphatase converts the precursor to **293** in aqueous and phosphate buffered saline solution, and even in

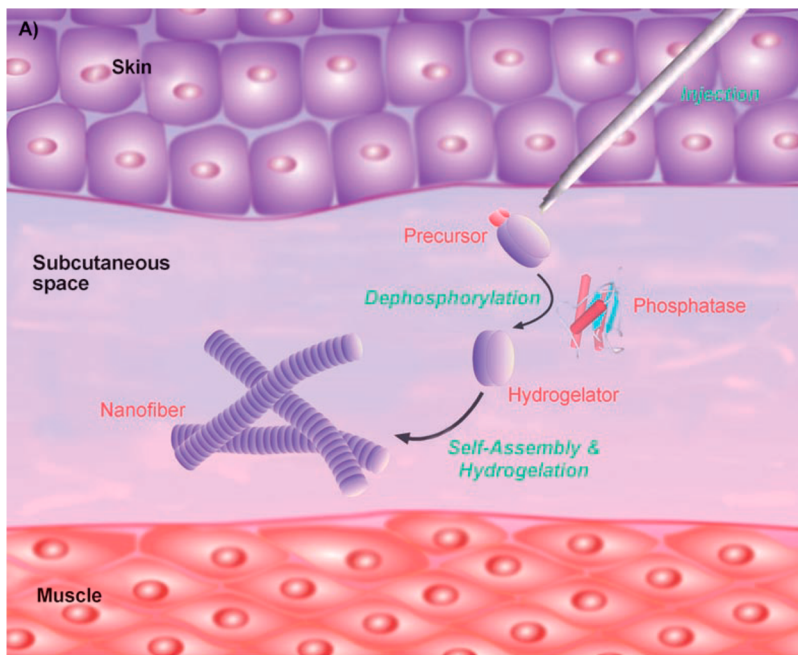
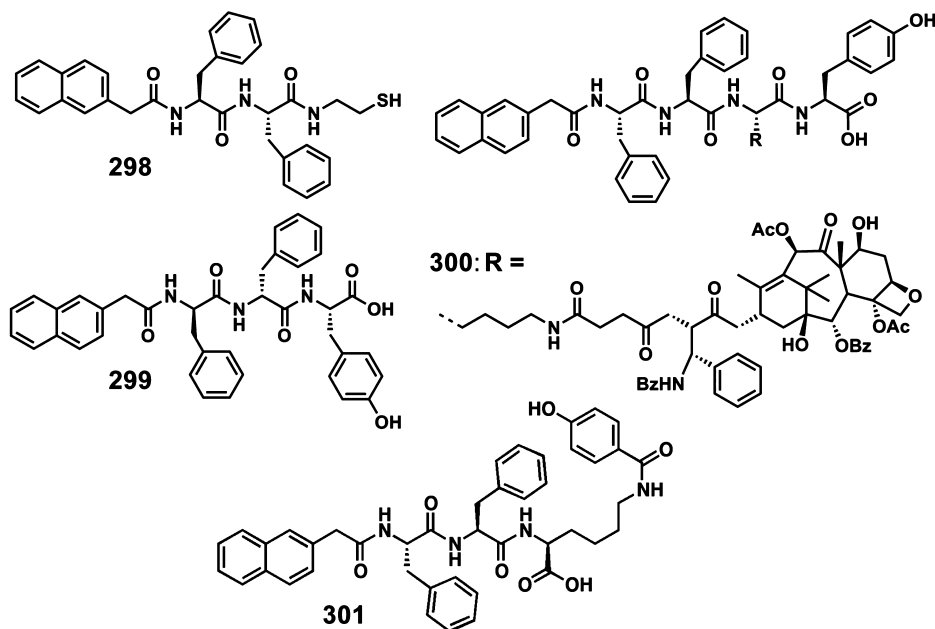


Figure 47. Illustration of the process of using enzyme to control the balance of hydrophilic and hydrophobic interactions to form a supramolecular hydrogel *in vivo*. (Reprinted with permission from ref 665. Copyright 2007 Wiley-VCH.)

Chart 73



complex biological fluids such as blood, which self-assembles into nanofibers and results in hydrogel formation (Figure 47). Detailed studies have indicated that β -amino acid derivatives can serve as the substrate of an enzyme and afford hydrogels with longer biostability than that of α -amino acid derivative based hydrogels 294 (Chart 72). Intracellular hydrogelation of 294 in the cytoplasm of the bacteria *E. coli*, resulted in the inhibition of multiple cellular processes including the growth of *E. coli*.⁶⁶⁶ Yang et al. have used a disulfide bond as a cleavable linker to control molecular self-assembly and hydrogelation of 295 (Chart 72).⁶⁶⁷

Enzymatic reaction can be used to convert a precursor into a hydrogelator as in the case of the gelator 296 (Chart 72) or vice

versa.⁶⁶⁸ Enzymes such as kinase/phosphatase were used to control the phosphorylation as well as dephosphorylation and thereby to regulate hydrogelation of a biocompatible gelator 296.⁶⁶⁹ A gel–sol phase transition could be achieved for the gelator 296 in the presence of adenosine triphosphate. Dephosphorylation in the presence of phosphatase has also been used to prepare biocompatible pentapeptidic hydrogelators 297a–f (Chart 72) from the precursor molecules.^{670,671} A detailed investigation has been carried out to understand the relationship between the chemical structure and the gelation ability of short peptide-based gelators 297a–f after enzymatic conversion from the precursors.⁶⁷¹

Chart 74

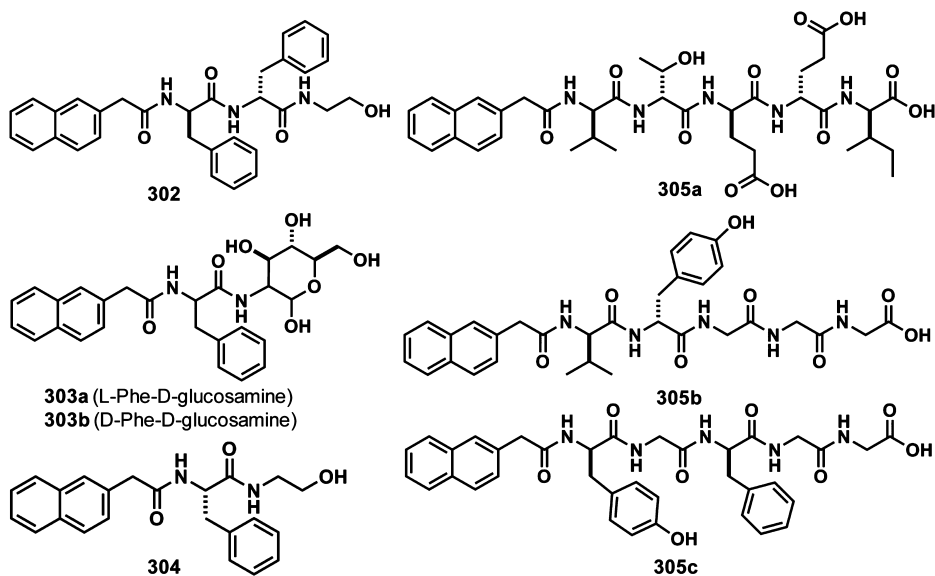
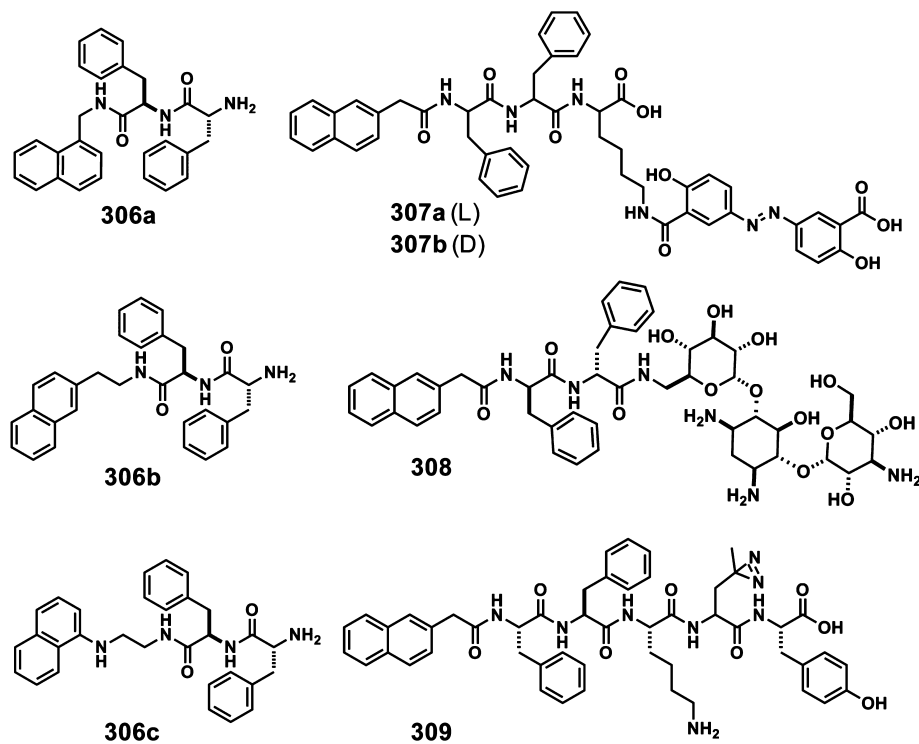


Chart 75

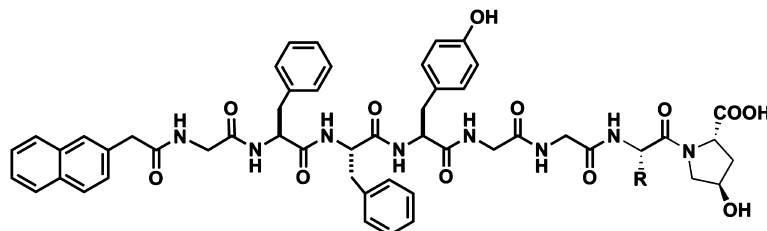


β -Lactamase hydrolyze the four membered β -lactam ring in the precursor molecule (lysates of bacteria) to yield the naphthalene based hydrogelator 298 (Chart 73) and thereby catalyzed the formation of supramolecular hydrogel.⁶⁷² The lysates of *E. coli* containing different kinds of β -lactamases were also found to efficiently trigger supramolecular hydrogelation. The immobilization of an enzyme, acid phosphatase, has been achieved by the enzymatic hydrogelation of 299 (Chart 73).⁶⁷³ Enzymatic reaction of alkaline phosphatase has been used to release taxol derivative 300 (Chart 73) and thereby to self-assemble in water to form nanofibers that resulted in a supramolecular hydrogel.⁶⁷⁴ β -Galactosidase, an enzyme that catalyzes the hydrolysis of glycosidic linkages in saccharides and

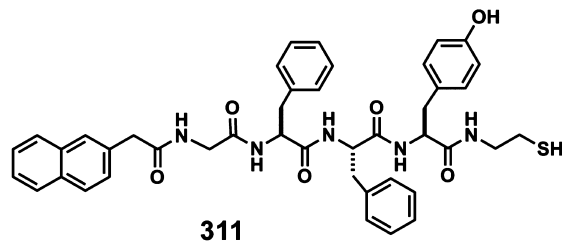
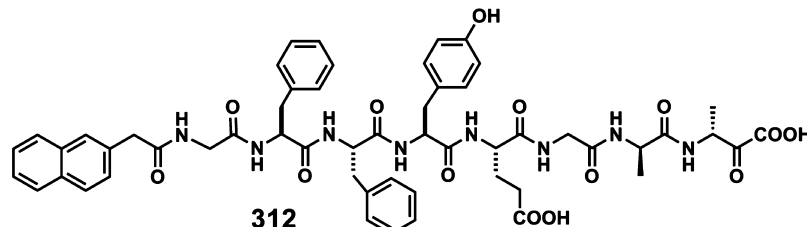
glycoconjugates has been utilized to trigger the cell compatible formation of supramolecular nanofibers. Upon hydrolysis with β -galactosidase, the precursor molecule of the gelator 301 (Chart 73) was converted into a glycane, which triggers the self-assembly and gelation of water.⁶⁷⁵

Hydrogels have been found useful for biological applications.^{676–694} The hydrogelator 302 (Chart 74) generated by an enzyme catalyzed reaction from its precursor formed hydrogel inside cancer cells and inhibit cell growth.⁶⁷⁶ The gelator 302 was found to be less cytotoxic toward fibroblast cells (NIH3T3), when compared to HeLa cells. Because of the higher expression of esterases in HeLa cells than that in the NIH3T3 cells, the intracellular nanofibers formed after

Chart 76



310a: R = Lys; **310b:** R = Ala; **310c:** R = Glu;
310d: R = Pro; **310e:** R = Ser

**311****312**

hydrogelation resulted in the death of HeLa cells. Congo red serves as extra- and intracellular assay to stain the peptide based supramolecular hydrogels of **294** and **302**.⁶⁷⁷ This staining method has initiated a convenient method to explore molecular self-assembly inside cells such as HeLa cells and *E. coli*. Biocompatible hydrogels consisting of the naturally occurring aminosaccharide, D-glucosamine **303a,b** (Chart 74) were found to act as biomaterials for wound healing.⁶⁷⁸ The controlled hydrolysis of the carboxylic ester bond by a base or catalyzed by an enzyme under weak basic conditions, is a simple trigger to form the gelator **304** (Chart 74) which self-assembles to form anisotropic supramolecular hydrogels that are stable over a wide pH range.⁶⁷⁹ The balance between intermolecular aromatic–aromatic interactions and hydrogen bonds enabled the self-assembly, nanofiber formation and hydrogelation of naphthalene containing pentapeptides **305a–c** (Chart 74) under acidic conditions in water.⁵⁸¹

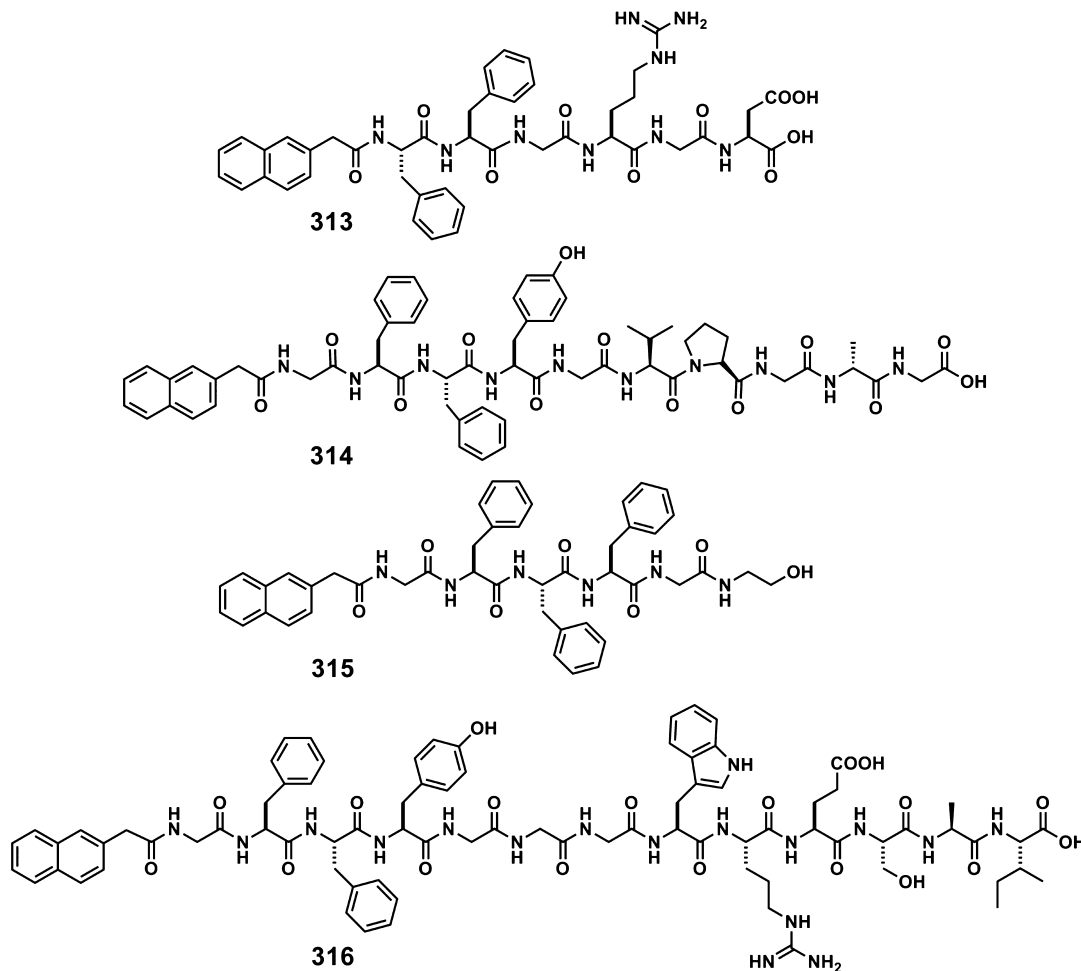
N-Terminated diphenylalanines containing naphthalene **306a–c** (Chart 75) formed supramolecular hydrogels within a narrow pH window due to the balance of protonation/deprotonation of the N-terminal amine and exhibited significantly high cytotoxicity to HeLa cells.⁶⁸⁰ Tripeptide conjugated anti-inflammatory prodrug olsalazines **307a,b** (Chart 75), self-assembled to form biostable supramolecular hydrogels.⁶⁸¹ A gel–sol phase transition upon reduction lead to the controlled release of 5-aminosalicylic acid as the anti-inflammatory agent. The hydrogelator **308** (Chart 75) derived from an antibiotic aminoglycoside, kanamycin, exhibited specific interaction with their macromolecular targets such as 16S rRNA.⁶⁸² The diminished fluorescence intensity indicated that two molecules of the gelator bind to the same A-site of 16S rRNA. A diazirine based photoreactive analog of leucine has

been incorporated to the hydrogelator **309** (Chart 75) backbone to increase the interaction of the gelator molecules with proteins.⁶⁸³ Detailed studies have indicated that after UV irradiation, dense nano fiber networks were formed and a coexistence of the protein particles and the hydrogel nanofibers were confirmed. The molecular structure of the gelator molecule plays a crucial role in the binding specificity of the nanofibers for a particular protein.

A small library of gelators **297f** and **310a–e** (Chart 76), having similar chemical structures to that of collagen, containing tripeptide units, have been used for tissue engineering.⁶⁸⁴ Multicomponent molecular hydrogelator systems consisting of **297a+312**, **297f+312**, and **311 + 312** (Chart 76) have been reported.⁶⁸⁵ Both the bioactive molecule and the gelator exhibited excellent stability against proteinase K digestion. The unstable gels formed by the hydrophobic gelator **311**, obtained from the precursor using reductants such as dithiothreitol, have been stabilized by adding bovine serum albumin to the gel medium.⁶⁸⁶ Bovine serum albumin interacts with the gelator, stabilizing the self-assembled hydrophobic nanofibers, which enhanced the intensity of the emission peak of the naphthalene moiety.

A bioactive surface of **313** (Chart 77) created on poly(3-caprolactone) fibers has been used to promote cell adhesion and proliferation.⁶⁸⁷ The pentapeptide of the protein elastin was incorporated as a part of **314** (Chart 77) to develop a biocompatible hydrogel system.⁶⁸⁸ The cleavage of a disulfide carbonate linker by reductants, followed by a self-cyclization process resulted in a gelator **315** (Chart 77).⁶⁸⁹ Even though a total conversion was not achieved, stable hydrogel formation occurred. A stable hydrogel has been prepared by enhancing the interaction between self-assembled fibers through a protein-

Chart 77



peptide interaction by mixing the peptide with solutions of 316 (Chart 77).⁶⁹⁰

A supramolecular hydrogelator 317 (Chart 78) with a nitrilotriacetic acid motif afforded hydrogels, which can act as an efficient absorber of various metal ions.⁶⁹¹ Magneto rheological hydrogels were formed upon interacting with nickel particles. Significant enhancement in the elasticity of hydrogels was observed in the case of gelators 318a–c (Chart 78) in the presence of calcium ions.⁶⁹² The presence of calcium ions cross-link the gel fibers to form stable supramolecular nanofibers and hydrogels. A post self-assembly cross-linking process using Belousov–Zhabotinsky reaction has been utilized to make a composite hydrogel of 319 and ruthenium(II) tris(bipyridine) complex ($\text{Ru}(\text{II})\text{-}(\text{bipy})_3\text{Cl}_2$; Chart 78) for chemical oscillation.⁶⁹³ The polymerized hydrogelator nanofibers exhibited concentration oscillations, spiral waves, and concentric waves. Stupp et al. have reported that the hydrazide containing peptide 320 (Chart 78) can be used to store ketone-containing, nonsteroidal anti-inflammatory drug nabumetone within the fibrous gel matrix, which can be slowly released from the gel into aqueous solution.⁶⁹⁴

The transformation between organogel 321a–d (Chart 79) in alkaline medium and hydrogel 322–324 (Chart 79) in acidic medium has been achieved using a simple method of protection and deprotection of a Boc moiety.⁶⁹⁵ Quaternary ammonium amphiphiles containing L-amino acids with nonpolar naphthalene residue and hexadecyl alkyl chain 325a,b (Chart 79) are

good hydrogelators.⁶⁹⁶ The tryptophan containing amphiphilic hydrogelator 325a has been utilized for the synthesis of Ag nanoparticles in the absence of any external reducing agent.

The fluorescence behavior and the CT properties of naphthalene based organic dyad-phase of nonionic polyoxyethylene-polyoxypropylene based $(\text{PEO})_{20}\text{-}(\text{PPE})_{70}\text{-}(\text{PEO})_{20}$ copolymer was investigated by using steady state, time-resolved spectroscopic techniques and fluorescence anisotropy decay profiles.⁶⁹⁷ Similarly, fluorescence properties of nonsteroidal anti-inflammatory drug naproxen in the self-assembled fibrillar network of a LMOG has been probed by means of time-resolved fluorescence spectroscopy.⁶⁹⁸ A novel magnetic organogel was reported by doping ferrite particles into the gel network of anionic sodium bis(2-ethylhexyl)-sulfosuccinate reverse micelles with 2,6-dihydroxynaphthalene.^{699,700} Dynamic and stimuli-responsive supramolecular ternary complexes of cucurbit[8]uril and viologen, naphthoxy polymers (1:1:1) formed stimuli responsive hydrogels.⁷⁰¹ Harada et al. have prepared gel assemblies from inclusion complexes of polyacrylamide gels modified with cyclodextrin and methylnaphthalenes.⁷⁰²

4.3.2. Anthracenes and Anthraquinones. Anthracene, a polycyclic aromatic hydrocarbon, shows interesting photo-physical properties and reversible photodimerization in the presence of UV light through a [4 + 4] cycloaddition reaction.^{54,703} During the photochemical investigations of anthracene derivatives, Weiss and co-workers have noticed

Chart 78

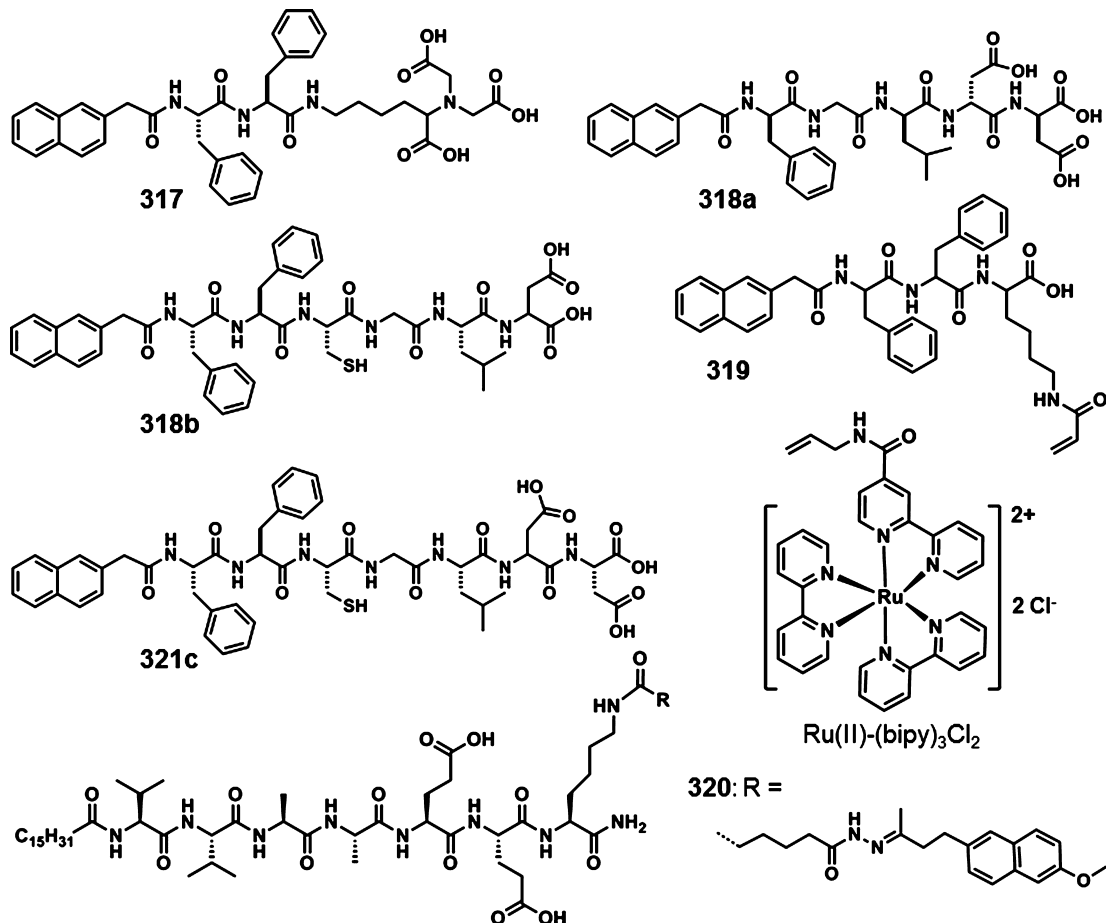


Chart 79

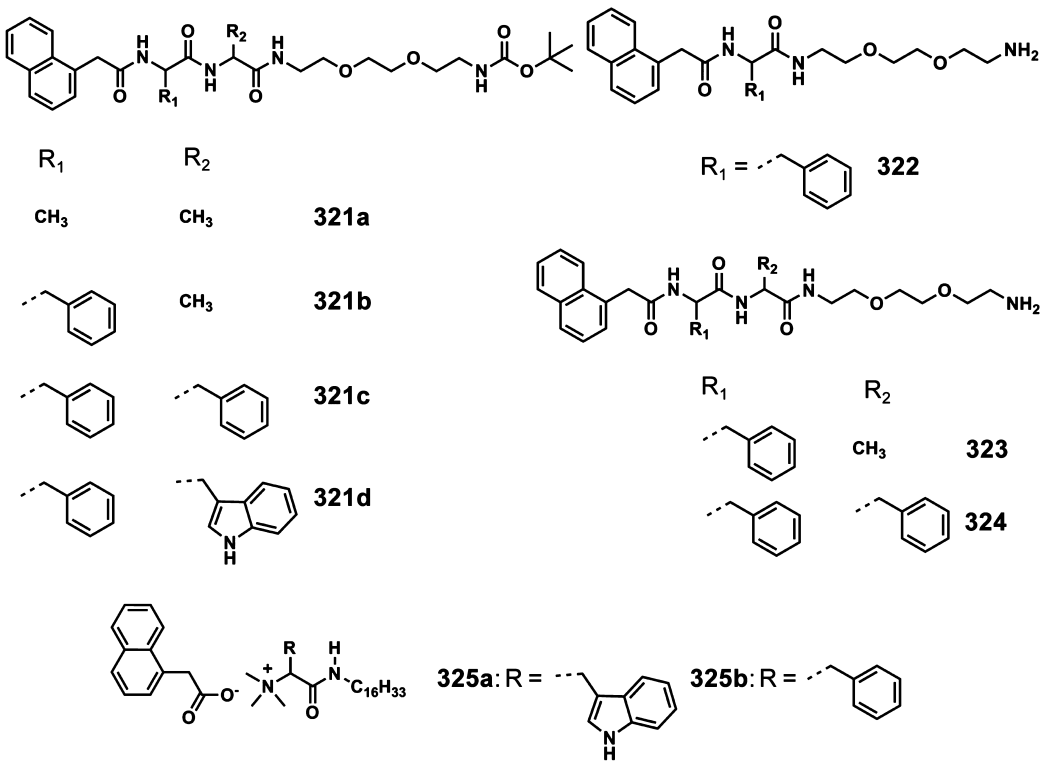
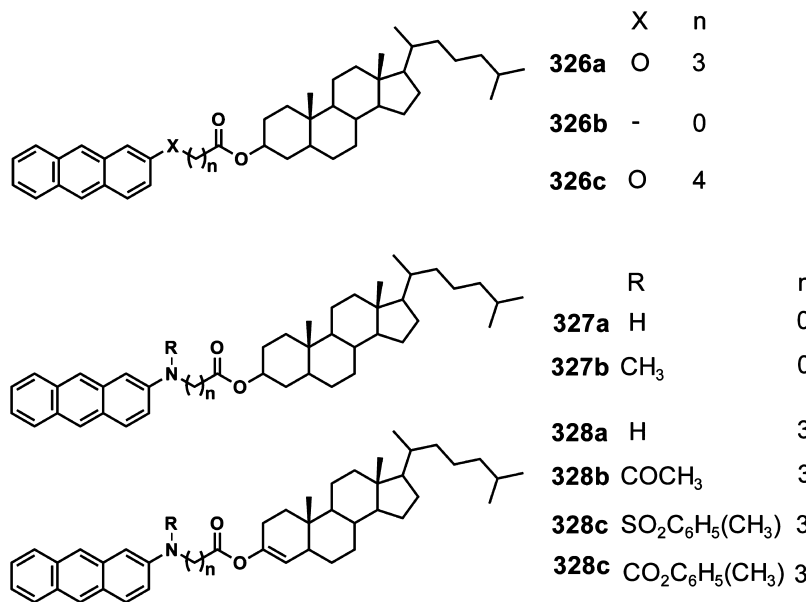


Chart 80



that some of these derivatives solidify organic solvents. For instance, they have reported the gelation of cholestryl 4-(2-anthryloxy)butyrate **326b** (Chart 80) in which the anthracene part was found to be helically stacked by the assistance of the dipolar and van der Waals interactions induced by the cholesterol moiety.⁷⁰⁴ The detailed understanding of the gelation properties of a series of gelators established the relationship between the solvent/gelator interaction, chemical structure of the gelator and the kinetics of gel formation through absorption, fluorescence and CD spectral changes.^{705,706} A series of anthracene based gelators **326a–c** (Chart 80) have been prepared and the aggregation behavior was monitored by scattering techniques.⁷⁰⁸ SAN/XS investigations of **326b** revealed that the diameter of fibers formed was sensitive to the solvent type.^{707,708} The derivatives with amide linkages **327a,b** and **328a–d** (Chart 80) were less efficient gelators than their oxa analogues.⁷⁰⁹ Detailed gelation studies showed that **327a** is a better gelator than the analogous **327b**, methylated at the carbamate nitrogen. The other derivatives **328a–d** were found to be less efficient gelators than **326b**.

Desvergne, Del Guerzo, Terech, and others have reported the gelation and thermoreversible viscoelastic behavior of 2,3-di-*n*-alkyloxyanthracenes **329a–h** (Figure 48).^{708,710–712} Later, Pozzo et al. have developed a different synthetic route for the preparation of 2,3-substituted anthracenes which allowed them to introduce a variety of substituents as side arms to study their influence on gelation properties.⁷¹³ The detailed understanding of the influence of alkyl chain length on the gelation of **329a–h** was investigated and found that *n*-undecyl and *n*-decyl chains (**329c** and **329d**) were most effective.⁷¹⁴ The h-t arrangement and the partial overlap between aromatic rings resulted in significant changes in the absorption and fluorescence properties.^{712,714} IR and fluorescence linear dichroism experiments have also been used to monitor the molecular organization of **329d** in the gel fibers.⁷¹⁵ The long axis of **329d** was uniaxially oriented around the fiber axis and the molecules were arranged along the helicoidal coils in concentric cylinders. Also the hydrocarbon chains favor a 2D molecular arrangement^{715,716} initiating the formation of hollow filaments and fibres.^{715,716}

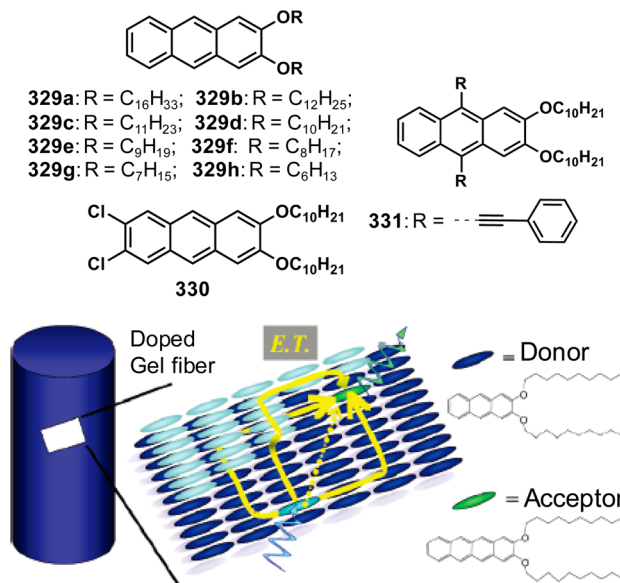
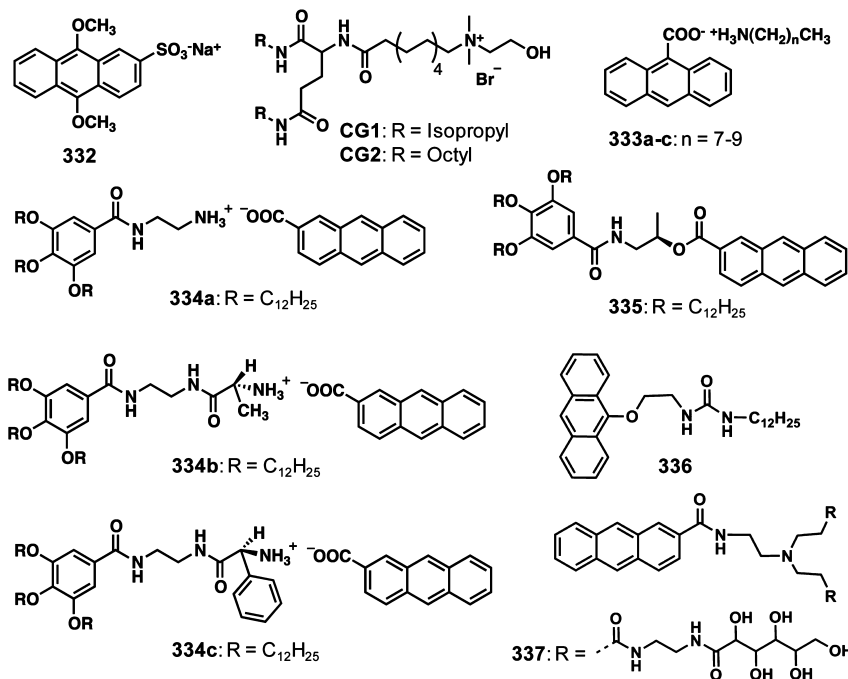


Figure 48. Chemical structures of 2,3-di-*n*-alkyloxyanthracene based gelators and a schematic representation of the energy transfer process in **329d** gel fiber. Energy transfer pathways are depicted by yellow arrows. (Reprinted with permission from ref 729. Copyright 2005 American Chemical Society.)

Mesoporous SiO₂ fibers were fabricated through sol–gel process using **329d**.^{717–719} In another report, aerogels of **329d** have been prepared by either drying ethanol gels of **329d** with supercritical CO₂ or in situ aerogel formation in supercritical CO₂.^{720,721} The incorporation of tetraalkylammonium salts in **329d** propylene carbonate gels enabled to evaluate the performances of the gel electrolyte in carbon double-layer capacitor.⁷²² The cooling rate in the case of propylene carbonate-**329d** gel was found to be crucial in the microscopic structure and the network formation by a nucleation growth mechanism.⁷²³ In addition, the number of junctions and the viscoelastic behavior of the gel could be tuned by the variation of the cooling rate. A hybrid gel of **329d** and AlCl₃ has been used as a template to direct the growth of high-surface alumina-

Chart 81



based fibers with anisotropic porosity.⁷²⁴ Colin, Pozzo and co-workers used POM and TEM to monitor the shear-induced structural changes of **329d** leading to long-range oriented mesoscopic fibrous structures.⁷²⁵ A controlled anisotropic 1D $\pi-\pi$ stacking assisted gelation of **329d** was observed by using biphenyl based nematic and smectic LC as templates.⁷²⁶

The organogelation of **329d** was monitored in the presence of high magnetic field, which oriented the self-assembled gel fibers with parallel aromatic anthracene moiety in a direction perpendicular to the magnetic field.^{727,728} The alignment of fibers was stable even after removal of the magnetic field and exhibited a large linear birefringence as well as fluorescence dichroism. An efficient energy transfer organogel system was obtained by using **329d** as the excitation energy donor and 1 mol % 2,3-*n*-dialkoxytetracene derivatives as the acceptors, indicating that the efficiency is due to the fast energy migration along the self-assembled fibers (Figure 48).^{729–734} Detailed energy transfer studies revealed that the efficiency of the process is also influenced by the structural and chemical similarity between tetracene acceptors and **329d**.^{729–731} The incorporation of green- and red-emitting tetracenes to a blue emitting gel medium of **329d** resulted in white-light-emission through an excitation energy transfer process involving anthracene donor and tetracene acceptors, while inter tetracene energy transfer also takes place.^{733,734} Moreover, multicolor emission is also possible to achieve by energy transfer from blue emitting donor **329d** to green as well as red emitting tetracene acceptors.⁷³⁴ Apart from these studies, the interaction between gel nanofibers of **329d** and an electron deficient 1,3,5-trinitrobenzene has also been studied with time-resolved confocal fluorescence microscopy.⁷³⁵

Morphological as well as photophysical properties of a hybrid gel composed of **329d** and thiol capped Au nanoparticles have been reported.⁷³⁶ The formation of hybrid material was facilitated by the supramolecular interaction of the ligands on the nanoparticles and the gelator. A hybrid gel consisting of **329d** and 2,3-di(6-oxy-*n*-hexanoic acid)-anthracene capped

ZnO nanoparticle was reported.⁷³⁷ The structural similarity between the capping agent and the gelator resulted in a robust self-assembled hybrid material. In both of these cases, **329d** gel acted as a matrix to harvest light energy leading to a photoinduced process even in the presence of very small amount of inorganic nanoparticles, facilitated by the efficient energy migration within the gel scaffold.^{736,737} Terech, Desvergne and co-workers have reported the gelation of 6,7-dichloro-2,3-didecyloxyanthracene **330** (Figure 48) mainly in higher molar mass solvents such as propionitrile and 1-hexanol.⁷³⁸ The polymorphic gelator **331** (Figure 48) formed kinetically metastable and thermodynamically stable gel states.⁷³⁹ Ostwald ripening upon aging drives the nanofibers to a dispersion of nanoribbons or -crystals with J-type aggregate features.

The amphiphilicity created by the complex formation of anionic anthracene sulfonate **332** and cationic L-glutamate **CG1** (Chart 81) reduced the electrostatic repulsion between the fibers and thereby resulted in hygrogelation.⁷⁴⁰ Doping of anthracene sulfonate (acceptor) into a donor gel comprised of naphthalene sulfonate and cationic L-glutamate **CG2** (Chart 81) resulted in an efficient energy harvesting hydrogel.⁷⁴⁰ The gelation ability of a series of alkylammonium anthracene carboxylates **333a–c** (Chart 81) prepared from equimolar amounts of 9-anthracenecarboxylic acid and alkylamines ($C_nH_{2n+1}NH_2$) where $n = 8, 9$, and 10 , were reported.⁷⁴¹ The gelation properties of a series of ionic complexes **334a–c** (Chart 81) prepared from 2-anthracenecarboxylic acid and 3,4,5-tris(*n*-dodecyloxy)-benzoylamine derivatives were also reported.^{742,743} The photodimerization of 2-anthracenecarboxylic acid in the presence of D-alanine appended 3,4,5-tris(*n*-dodecyloxy)-benzoylamine **334b** enabled to get a significant enantiomeric excess ($ee = 10\%$) in the h-h photocyclo-dimer.^{742,743} The product selectivity can be inverted by using bulky L-2-phenylglycine chiral substituent **334c**, producing h-t photodimers as major products. In the case of an organogel obtained from **335** (Chart 81) in enantiomeric glycidyl methyl

Chart 82

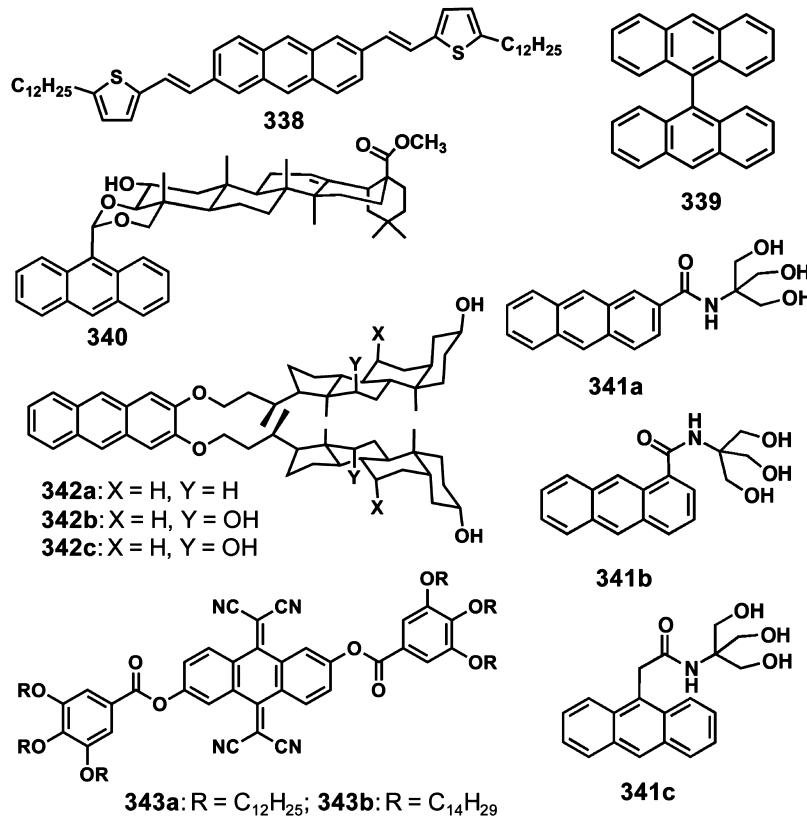
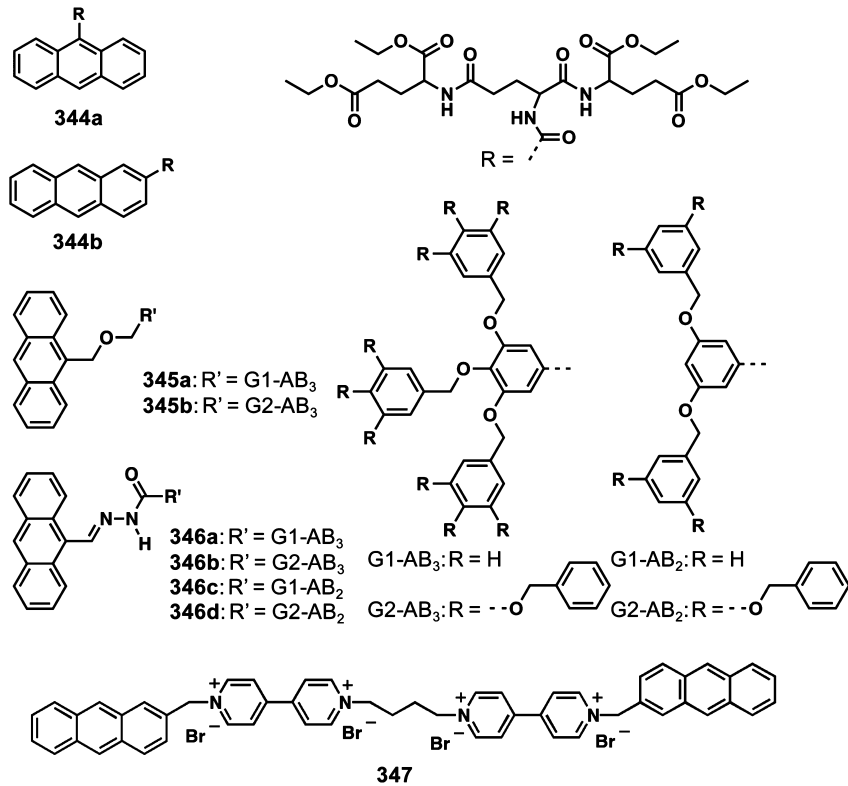


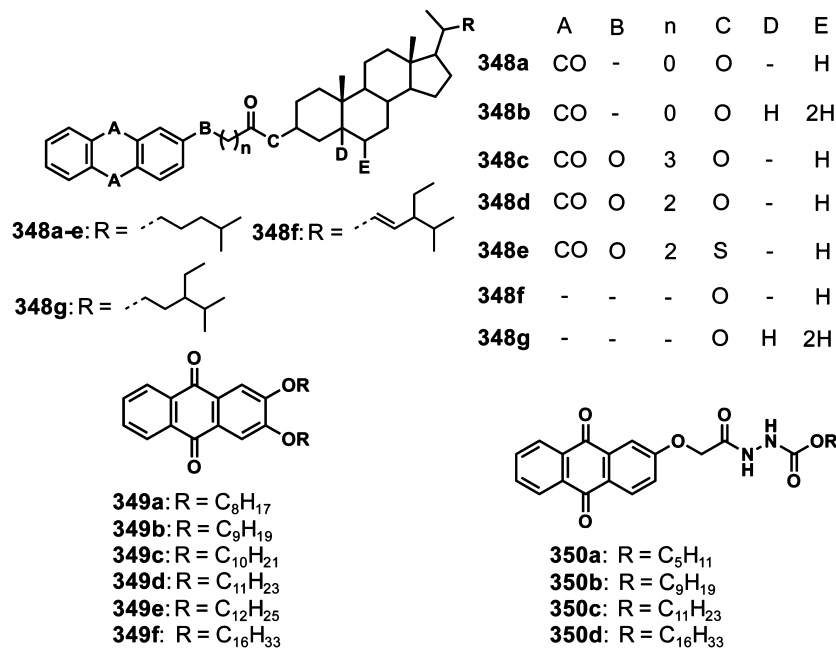
Chart 83



ethers, *ee* values of the major h-h photodimers reached as high as 56%.⁷⁴⁴ The h-t dimers form thermoresponsive gel as indicated by the frequency independent elastic and viscous

moduli whereas h-h dimers remained fluidlike.⁷⁴⁵ Furthermore, the photoresponsive nature of the gel which depends upon the choice of the gelator, was established by the phase transition

Chart 84



among gel, sol, and precipitate, controlled by light and temperature.^{741–745}

The organogel of 336 (Chart 81) is an example of a thermally driven molecular fluorescence switch which exhibits a 10-fold fluorescence enhancement due to the intermolecular anthracene excimer emission.⁷⁴⁶ Photodimerization reaction of 336 in THF solution yielded h-t photodimers exclusively and the organogels of these photodimers are found to be fairly stable, which show resistance toward light irradiation and temperature. A photoresponsive hydrogel, whose gel–sol transition triggered by the regioselective photodimerization of the anthracene moiety of 337 (Chart 81), was reported by Sako and Takaguchi.⁷⁴⁷ A photoresponsive PEG based hydrogel was realized by using the photodimerization reaction of anthracene linked PEG.⁷⁴⁸ The hydrogels formed from alginate covalently modified with PEG-conjugated anthracene molecule was found to be a photosensitive cross-linker that stabilizes the alginate as well.⁷⁴⁹

The gel nanofiber of a thienylvinylene anthracene 338 (Chart 82) has been used to develop organic single nanofiber transistors.⁷⁵⁰ Organogelation of 9,9'-bianthryl gelator 339 (Chart 82) was observed in haloalkanes and hydrocarbons, especially in chlorocycloheptane.⁷⁵¹ This is a rare example for a π -gelator without any alkyl chains or hydrogen bonding motif. As in the case of naphthalenes, CT interaction between anthracene and electron deficient molecules is a promising strategy for the design of gelators.^{752–755} Lev, Melman and co-workers have reported the CT assisted two component D–A organogel of electron deficient dinitrobenzoate gelators and anthracene.⁷⁵² Arjunolic acid conjugated anthrylidene derivative 340 (Chart 82) formed organogels in the presence of an electron deficient guest (picric acid) and exhibited a color change due to CT complex formation.⁷⁵³ Maitra and co-workers have demonstrated the formation of two component CT mediated organogels derived from the anthracene derivatives 341a–c (Chart 82) and 2,3-di-n-alkyloxyanthracenes (Figure 48) and TNF.⁷⁵⁴ The properties of CT gels were found to depend on the subtle structural changes of the

anthracene donor as well as the composition of the D–A mixtures. CT assisted two component organogels were formed when bile acid anthracene conjugates 342a–c (Chart 82) were used as donor and TNF as the acceptor.⁷⁵⁵ The hydrophobicity–hydrophilicity balance imparts thermal stability as well as mechanical strength to the CT supported composite gels. Kato and co-workers have reported that the intermolecular dipole–dipole interaction in electrochromic tetracyanoanthraquinone dimethane derivatives 343a,b (Chart 82) lead to the formation of hexagonal columnar LC having fan-like textures and organogels consisting of birefringent fibrous aggregates.⁷⁵⁶

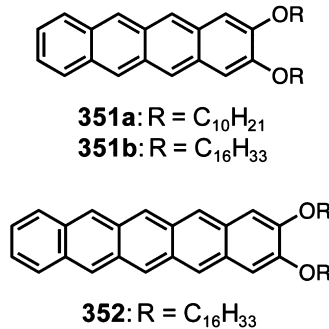
Hydrogels and organogels of anthracene derivatives with L-glutamate based dendrons 344a,b (Chart 83) are examples of thermally driven chiroptical switches.⁶³³ Gels of 344a exhibited strong fluorescence enhancement upon gelation. The gelation of poly(aryl ether) dendrons 345a,b and 346a–d (Chart 83) functionalized with anthracene moieties at the focal point has been reported.^{757,758} Detailed studies revealed that the gelation process could be controlled by using partial polar solvent environment which enhances the π – π interaction between the aryl units. In the case of 346a–d, GIEE has been observed in anthracene excimers.⁷⁵⁸ Furthermore, these gels were found to be useful for naked eye detection of fluoride ions, signaled with a color change as well as gel–sol transition. A diffusion controlled photoinduced electron transfer reaction between the anthracene and the amine moieties has been observed for the self-organized organogel.⁷⁵⁹ Multiple host stabilized CT interaction has been used for fabricating supramolecular polymers and gelators.⁷⁶⁰ The double host stabilized CT interactions by using viologen moieties as electron acceptors and two anthracene moieties as electron donors as in the case of 347 (Chart 83) enabled the monomers to join together in h-t fashion when encapsulated in cucurbit[8]uril.

A series of anthraquinone linked steroid based gelators 348a–g (Chart 84) were developed to understand the influence of the α/β stereochemistry at C-3 position, the nature of the alkyl chains on C-17 of the steroid, and the length and functionality of the linking group, on organogel formation.

It has been found that the gelation is facilitated when the stereochemistry at C-3 position of the steroid unit is β . Minor structural variation on the sterol chain at C-17, such as introduction of an unsaturated unit and/or an ethyl substituent, is not enough to limit the gelation properties. In addition, the length of the chain and the functionality play an important role in the gelation efficiency.^{705,761,762} The polymorphism in the packing of molecules within fibers was established using 348a as an example and found that the polymorphs obtained from the gel fibers are not identical with that from the normal crystallization method.⁷⁶³ The understanding of the molecular organization of the gel structure of 348a consisting of long and rigid fibers has revealed the presence of junction zones of the 3D network.⁷⁶⁴ In addition to dialkoxy anthracenes, 2,3-dialkoxy anthraquinone derivatives 349a–f (Chart 84) form stable organogels which entrap solvent molecules.^{710,765} The comparison of the gelation studies of 2,3-di-*n*-alkyloxyanthracenes and anthraquinone organogels indicated a reduced stability for the later ones. Chen, Ma and co-workers have reported that smart anion responsive supergelators 350a–d (Chart 84) composed of an anthraquinone unit, a hydrazide group, and long alkyl chains showed selective gelation of an oil in the presence of water.^{766,767} Ultrasound radiation induced gelation as well as morphology transition from flower-like ball to rod shaped fibrillar network was observed.

4.3.3. Tetracenes and Pentacenes. Tetracenes and pentacenes are well-known for their significant charge mobility, intense colored absorption and emission, and photochromism. They are extensively used in optoelectronic devices.⁷⁶⁸ In this context, preparation of 1D self-assembly of these molecules by gelation approach is of particular interest. However, there are only a very few reports on gelators based on these systems. For example, Hopf, Desvergne and co-workers have reported the synthesis and gelation properties of 2,3-di-*n*-alkyloxytetracenes and pentacenes 351a,b and 352 (Chart 85). For

Chart 85



tetracene and pentacene based gelators, hexadecyl side chains were found to be more efficient due to the best balance between the chain length and the aromatic core size. As in the case of 2,3-di-*n*-alkyloxyanthracenes, van der Waals and π – π stacking interactions mainly drive the gelation. Apart from this, tetracene derivatives were found as very good energy acceptors when doped in the gel matrix of 2,3-di-*n*-decyloxyanthracenes (Figure 48).^{729–734}

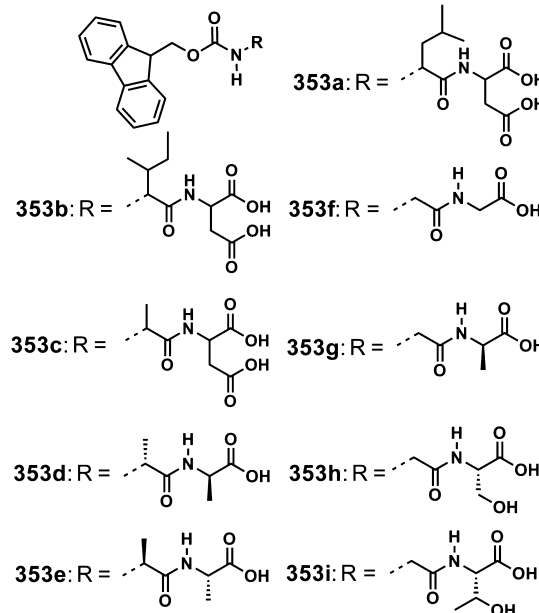
4.4. Fluorenes

Fluorene is a polycyclic aromatic hydrocarbon and has been used for the preparation of hydrogels.^{25,29,80–84,87,88,90,772–774}

In most of the cases, fluorene has been used as a part of the protecting agent Fmoc along with peptide backbones.⁷⁷⁵

The Fmoc hydrogelators 353a–c (Chart 86) have been used for biological applications.⁷⁷⁶ For example, the nonantigenic

Chart 86

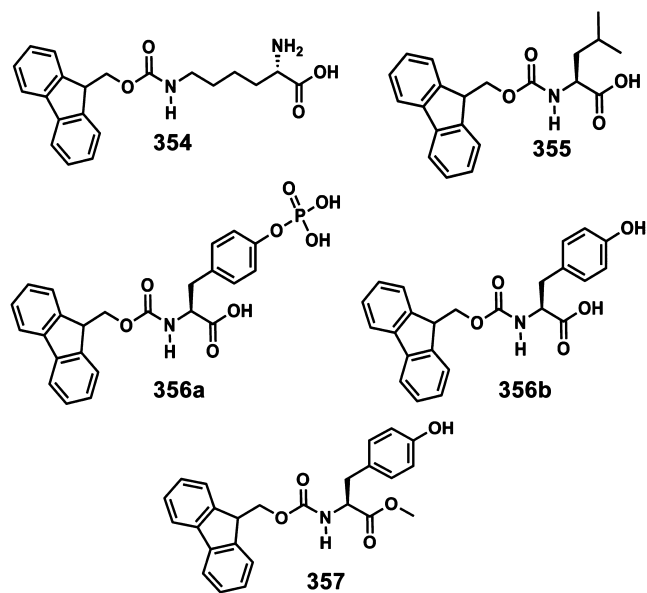


antiviral drugs, adamantanamine derivatives incorporated hydrogels of 353a produced high titer specific antibodies when injected into rabbits. Xu et al. have reported a series of Fmoc dipeptides 353d–i (Chart 86) based hydrogels.⁷⁷⁷ The antiparallel overlap of the fluorenes 353d and 353e assisted by hydrogen bonding interactions facilitate superhelical arrangements of the gelator molecules as indicated by the CD signals. In addition, the D-Ala-D-Ala has strong ligand receptor interaction and hence results in the gel–sol transition with significant change in the morphology upon addition of 1 equiv. of vancomycin. The hydrogel scaffold of a combination of amphiphilic anti-inflammatory agent Fmoc-L-lysine 354 and N-Fmoc amino acid 355 (Chart 87), has been used as carriers for an antineoplastic agent 5-fluoro-2A-deoxyuridine⁷⁷⁸ and as a self-delivery biomaterial to reduce the toxicity of uranyl oxide at the wound sites.⁷⁷⁹

The hydrogelator 356a (Chart 87) facilitates the gelation of the molecule 356b (Chart 87) in the presence of acid phosphatase. This two component hydrogelator has been used as a simple visual assay for screening the activities of inhibitors such as pamidronate disodium, Zn²⁺ and sodium orthovanadate for an enzyme acid phosphatase.⁷⁸⁰ An enzymatic dephosphorylation reaction triggers the self-assembly of *N*-Fmoc tyrosine 356b and results in hydrogelation at physiological temperatures.⁷⁸¹ In a similar way, enzymatic (phosphatase) hydrogelation assisted by the formation of 3D fiber networks (Figure 49) with antiparallel oriented fluorene moiety has been observed in the case of the gelator 357 (Chart 87).⁷⁸²

A series of pentapeptide based hydrogels 358a–e (Chart 88) have been reported as potential biomaterials.⁵⁸¹ Supramolecular hydrogel based artificial enzymes obtained by the encapsulation of hemin chloride into a combination of 354 and 359 (Chart 88) are effective carrier to minimize the dimerization and

Chart 87



oxidative degradation of free hemin in the peroxidation reaction.^{783,784} Hydrogels of 356b obtained by enzymatic dephosphorylation of 356a has been used as a matrix for calcium phosphate mineralization.⁷⁸⁵ Confining of heme proteins and a luminol within the coassembled hydrogel nanofibers of 354 and 359 has shown enhanced quantum yield of chemiluminescence.⁷⁸⁶ Banerjee and co-workers have utilized stable and transparent hydrogel of 359 to prepare and stabilize few-atom Ag nanoclusters without the use of any reducing agent.⁷⁸⁷ They have also used hydrogel matrix of 359 to incorporate and disperse functionalized SWCNTs within the gel phase.⁷⁸⁸ Conductivity of the hybrid hydrogel has been found to be 3.12 S cm^{-1} , which is less than that of functionalized SWCNTs. A hydrogelator 360 (Chart 88) with a functional epitope of K^+ channels forms tunable hierarchical nanostructures with respect to the concentration of K^+ .⁷⁸⁹

The spontaneous hydrogelation of a series of Fmoc-dipeptides 361a–g (Chart 89) and its dependence on amino acid sequence of the peptide building blocks was reported by Ullig and co-workers.^{790–792} An interesting observation is that 361f with a reverse kind of peptide sequence of 361e formed only crystals under any of the conditions tested for gelation. This finding emphasizes that the slight variation in the molecular structures of the building block could substantially influence the final self-assembled materials.⁷⁹⁰ A coassembly of 361a and 361g and Fmoc-Lysine also formed stable, self-supporting and transparent gels.⁷⁹⁰ The gel matrix has been used for cell proliferation and retention of phenotype bovine chondrocytes.^{790,791} The molecular packing of the supramolecular hydrogels of 361g consisted of antiparallel β -sheets and antiparallel π -stacked fluorenyl groups (Figure 50).⁷⁹² Detailed morphological studies revealed the self-assembly mechanism of aromatic short peptide derivative 361g leading to the formation of entangled network of flexible fibrils at high pH, and flat rigid ribbons at intermediate pH values.⁷⁹³ A novel approach of an enzyme catalyzed reverse hydrolysis has been used to produce amphiphilic Fmoc-tripeptide hydrogelators from Fmoc amino acids 359 and 362a–c (Chart 89).⁷⁹⁴

Thermolysin catalyzed condensation reaction between the precursors Fmoc protected serine or threonine and the methyl ester of phenylalanine or leucine (Chart 90) leading to aromatic dipeptide amphiphile gelators 363a–d (Chart 90) indicated sequence specificity.⁷⁹⁵ Depending upon the relative thermodynamic stability of the resulting self-assembling structures, differences in the yield of the reaction was observed.

Xu et al. used aromatic–aromatic interaction to produce nanofibers and hydrogels from gelator 359.³⁴⁶ A 1:1 complex of Fmoc-phenylalanine 359 and aminoanthracene or 2-amino-naphthalene resulted in a coassembled organogel.⁷⁹⁶ When compared to phenylalanine gels, the coassembled gels exhibited different morphologies, improved mechanical stiffness and conductivity. Polymeric additives influence the gelation and rheological properties of the dipeptide gelator 361g.⁶⁵⁶ The gels formed were found to be sensitive to the presence of dextran, glycerol, poly(vinylpyrrolidone), poly(ethylene glycol), and poly(acrylic acid). Depending on the nature of the polymer

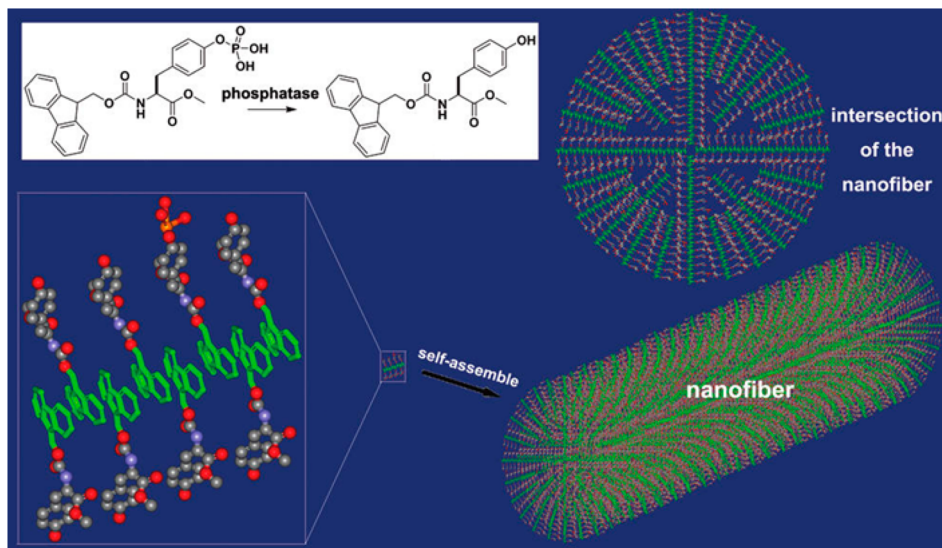


Figure 49. Schematic illustration of enzymatic conversion and proposed molecular arrangements of 357 in nanofibers. (Reprinted with permission from ref 782. Copyright 2009 American Chemical Society.)

Chart 88

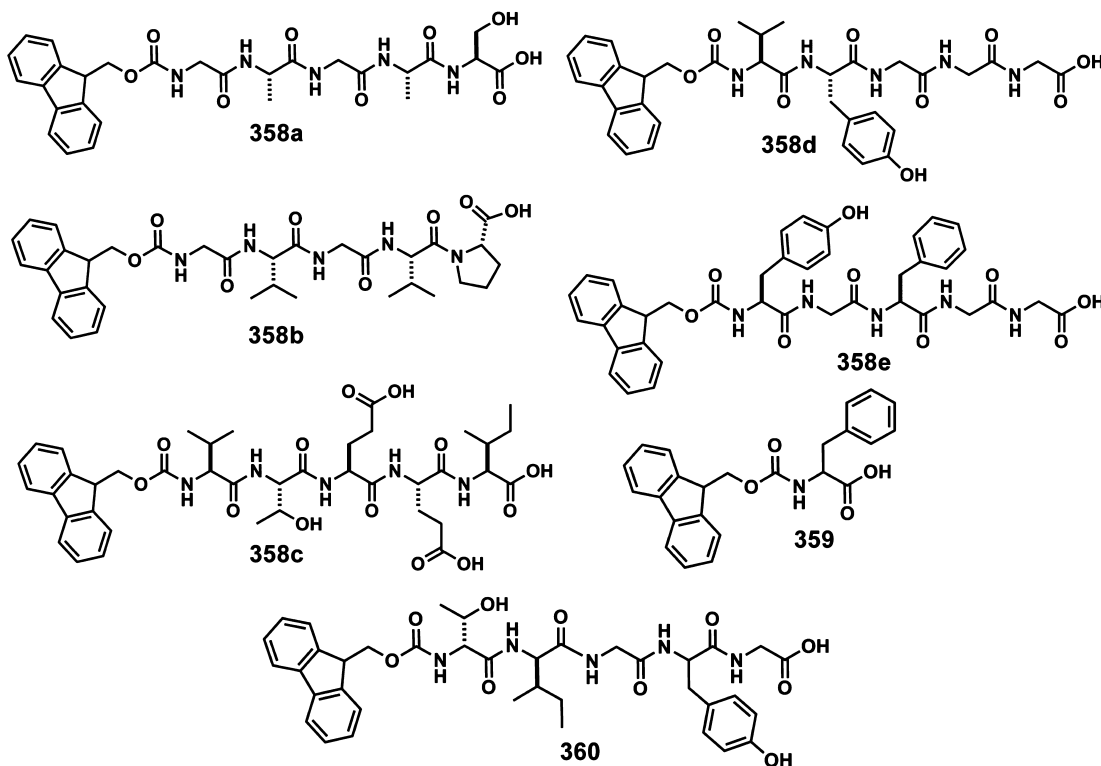
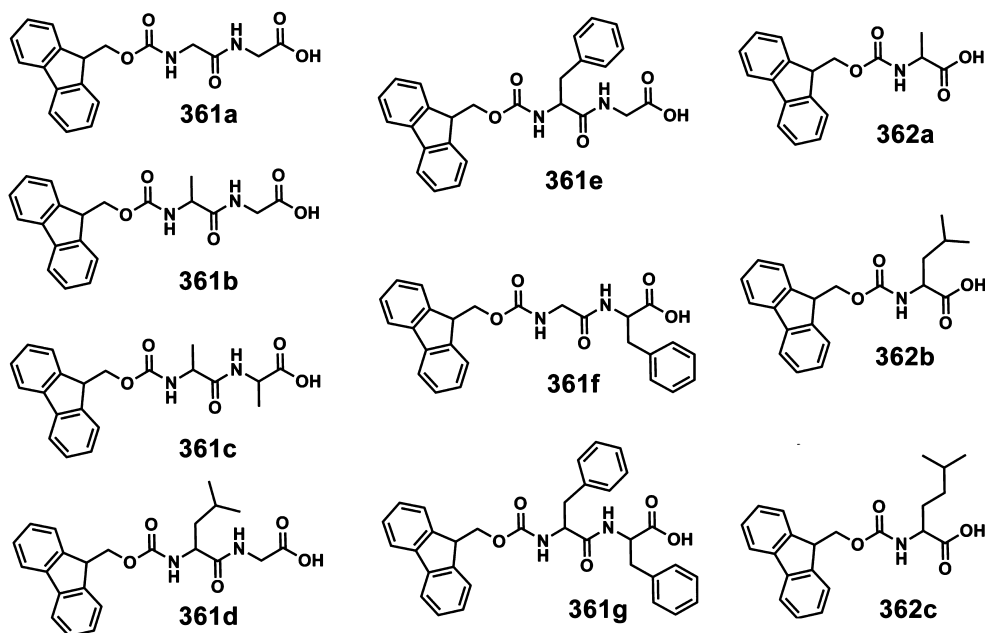


Chart 89



used, crowding of the gelator accelerates the rate of fiber formation, thereby leading to gelation. UV irradiation of the dipeptide gelator **361d** in presence of a photoacid generator diphenyliodonium nitrate resulted in the formation of a hydrogel.⁶⁵⁷ As the first example of nonenzymatic dephosphorylation assisted hydrogelation, hybrid supramolecular hydrogels were prepared from *N*-fluorenlymethoxy carbonyl tyrosine-(*O*)-phosphate **356a** using catalytic cerium oxide nanoparticles.⁷⁹⁷ The coassembled hydrogel matrix of **354** and **359** has been used for the immobilization of enzymes such as

horseradish peroxidase or α -chymotrypsin which catalyze reactions and exhibit superactivity and exceptional stability.⁷⁹⁸ The mixed gels of *N*-Fmoc-L-lysine and **359** formed in the presence of sodium carbonate exhibited exceptional rheological properties.⁷⁹⁹

An enzyme driven dynamic supramolecular peptide system **364** (Chart 91) displays multiple reversible pathways leading to hydrogelation.⁸⁰⁰ Using a combination of biocatalysis and molecular self-assembly, higher order structures are formed via enzymatic hydrolysis of the precursor ester moiety leading to

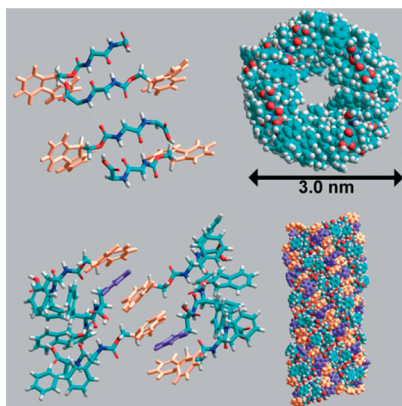


Figure 50. Model of the antiparallel β -sheet pattern created by **361g** upon self-organization and gelation. (Reprinted with permission from ref 792. Copyright 2008 Wiley-VCH.)

amphiphilic dipeptide hydrogelators **361g** and **365a-d** (Chart 91).⁸⁰¹ The modification of the chemical functionality of **361g** hydrogels by adding Fmoc protected amino acids with varying side groups exhibited significantly different compatibility with cell culture of bovine chondrocytes, mouse 3T3 fibroblasts and human dermal fibroblasts.⁸⁰² The transition metal phosphate nanotubes prepared by using hydrogelator **361g** as a template has been used as a cathode material for rechargeable lithium ion batteries.⁸⁰³ Kinloch and Uljin have demonstrated that the nanotubular network formed by enzyme triggered self-assembly of Fmoc-trileucine **366** (Chart 91) produced by subtilisin catalyzed hydrolysis of the corresponding methyl ester derivative shows significant charge transport properties as indicated by the impedance spectroscopy studies.⁸⁰⁴

The endoprotease enzyme thermolysin has been used for the reversible formation of Fmoc-protected peptide building blocks in a reversible and spatially confined manner, thereby leading to gelation.⁸⁰⁵ The thermolysin catalyzed condensation of Fmoc protected hydrophilic amino acid (serine) and a hydrophobic amino acid ester (phenylalanine) resulted in **367** (Chart 91) that can form extended 2D peptide nanostructures.⁸⁰⁶ Coassembly and gels of **361a** and **361g** formed under different agitation conditions exhibited drastic differences in the mechanical properties due to the mechanical and physicochemical differences in the fibrillar elements.⁸⁰⁷ Gelation studies of **361a** and **361e-g** showed that replacement of phenylalanine by glycine significantly affects self-assembly properties.⁸⁰⁸ The reversible assembly/disassembly of molecular gelator **359** has been achieved in response to spatiotemporally imposed electrical signals.⁸⁰⁹ Another study reports that salts induce a

dramatic effect on the gelation as well as functional properties of aromatic dipeptide amphiphiles **365b**, **365c**, **365e**, and **353e** following the Hofmeister trend of anions.⁸¹⁰ Depending upon the type of anions used, drastic morphological changes from fibrous (phosphate and chloride) to spherical aggregates (thiocyanate) were formed by **365b**.

Gazit et al. have reported that a hydrogel of **361g** exhibits the ability to encapsulate and release drugs.⁸¹¹ In addition, hydrogels have also been used for tissue engineering and regeneration experiments. Hydrogels of Fmoc-peptides containing natural and synthetic amino acids **368-371** (Chart 92) exhibited excellent biological activity.⁸¹² The hydrogel matrix of **368** and **369** provided a cell adhesive biomedical scaffold. The self-assembly process during the gelation of **368-371** and **361g** indicated that the aromatic moieties contributed mainly to free energy of formation as well as given order and directionality leading to defined organization.⁸¹³ An increase in the number of aromatic content in the gelator caused faster self-assembly kinetics and higher yield of self-organized structures. Interestingly, the formation of a quantum confined structure^{814,815} within the self-assembled hydrogel nanotubes composed of the gelator **361g** has also been investigated.⁸¹⁶ As the concentration increases, a peak at the red edge of the absorption spectrum due to strong exciton effect was observed, indicating the creation of quantum well structures representing the small crystalline regions.⁸¹⁷

The 3D fibrous network of a short peptide **372** (Chart 93) hydrogel has been successfully utilized by Banerjee et al. to make and stabilize fluorescent Ag nanoclusters in the absence of any reducing agents.⁸¹⁸ Similarly, nano templates of peptide nanofibers of **373** (Chart 93) has been used by Liu and co-workers for the production of monodispersed and stable Ag nanoparticles.⁸¹⁹ Ag-peptide nanocomposite exhibited highly effective and long-term antibacterial activity against both Gram-positive and Gram-negative bacteria. Coassembly of racemic and equimolar mixtures of **374a,b** (Chart 93) and lysine formed hydrogels.⁸²⁰ The equimolar mixture of two L-isomers and two D-isomers formed left and right handed helical nanofibers, respectively. In addition to nanoparticle synthesis, the successful incorporation of rGO into the hydrogel matrix of **375a,b** (Chart 93) has resulted in a stable hybrid hydrogel.⁸²¹ Banerjee et al. reported proteolitically stable hydrogels of N-terminally protected dipeptides with a β -amino acid residue **376a,b** (Chart 93).⁸²² The gelator **376a** exhibited better gelation efficiency due to enhanced hydrophobicity and $\pi-\pi$ interaction. Moreover, efficient encapsulation and sustained release of vitamins (B2 and B12) over a period of about three days has been achieved.

Chart 90

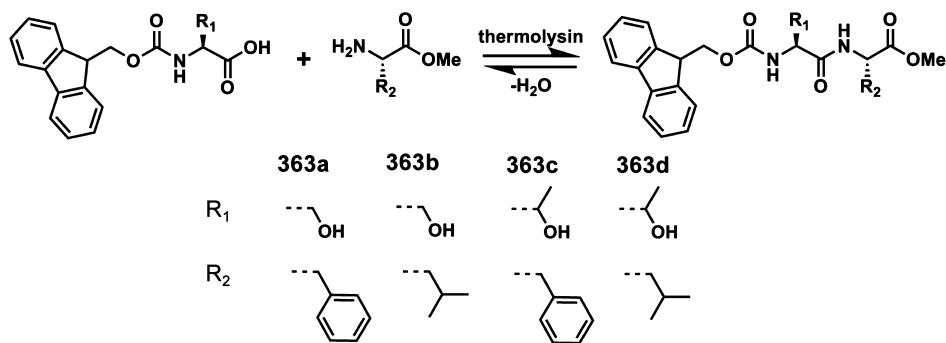


Chart 91

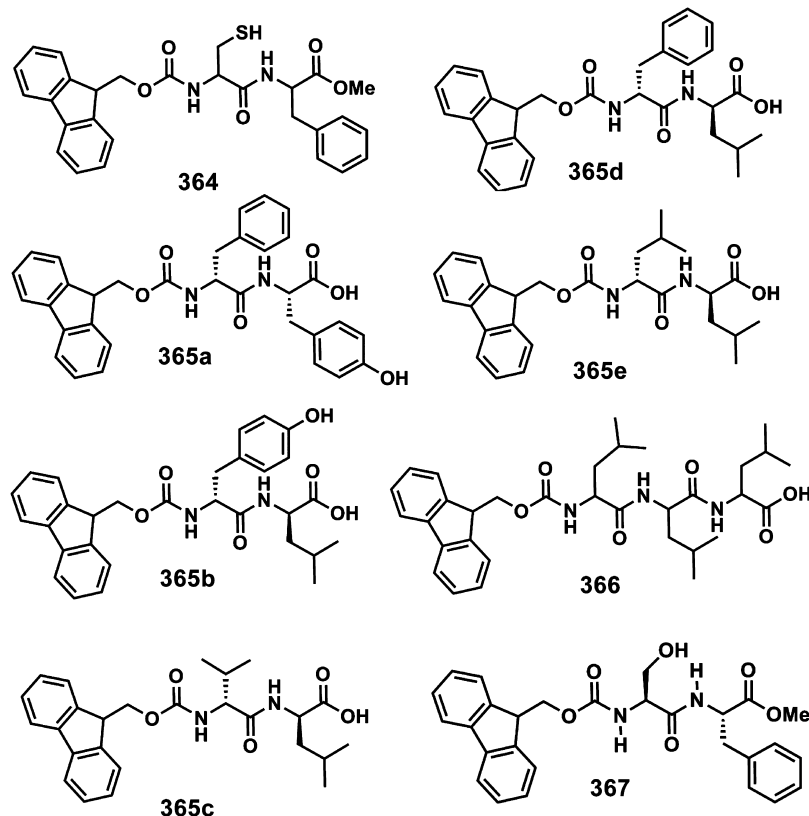
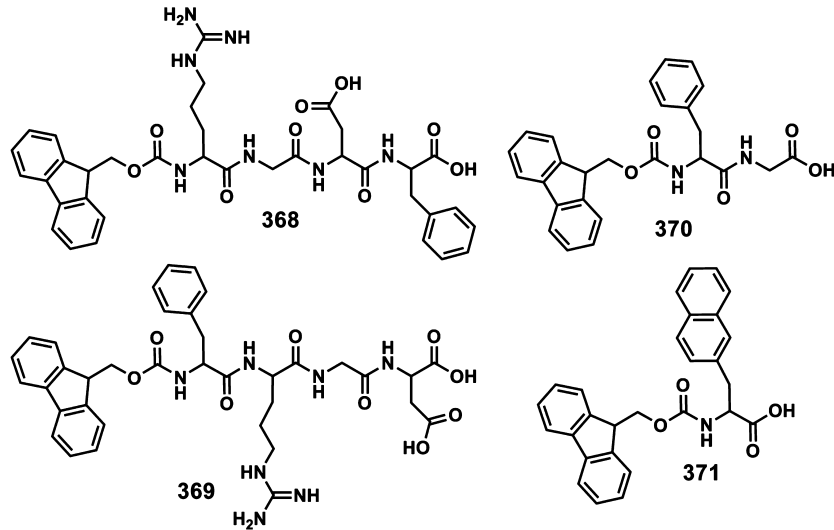


Chart 92



Sonication has been used to trigger the gelation of Fmoc-dipeptide 377 (Chart 94) with a drastic change of morphology from sheets structure in *n*-hexane to extended fibrous network.⁸²³ Ultrasound induced nanocomposite gel of CdSe/ZnS QDs with the gelator 377 has bright luminescence under UV light which is useful for sensing application.⁸²⁴ MacPhee et al. have investigated the energy migration and excimer formation within the fibrils of Fmoc-amyloid fibril forming peptide (TTR_{105–115}) from the protein *trans*-thyretin 378 (Chart 94) by using time-resolved fluorescence spectroscopy.⁸²⁵ A two component gel of anti-inflammatory agents 379a or 379b (Chart 94) and neurotransmitter γ -amino butyric acid

through molecular recognition and self-aggregation has been reported.⁸²⁶

A large number of biocompatible F-moc protected β -helical peptide hydrogels have been used for cell culture.⁸²⁷ For example, the Fmoc diphenylalanine 361g dipeptide hydrogel has been used for the *in situ* patterned 3D cell culturing.⁸²⁸ In another report, lipase has been used to link an Fmoc-Phe amino acid to the dipeptide diphenylalanine to form a gelator 380 (Chart 94) leading to a noncytotoxic porous hydrogel matrix that enabled cell and nutrient mobility, suitable for tissue engineering.⁸²⁹ Entrapped dyes such as Naphthol Yellow and Direct Red, inside the hydrogel matrices of Fmoc-phenylalanine

Chart 93

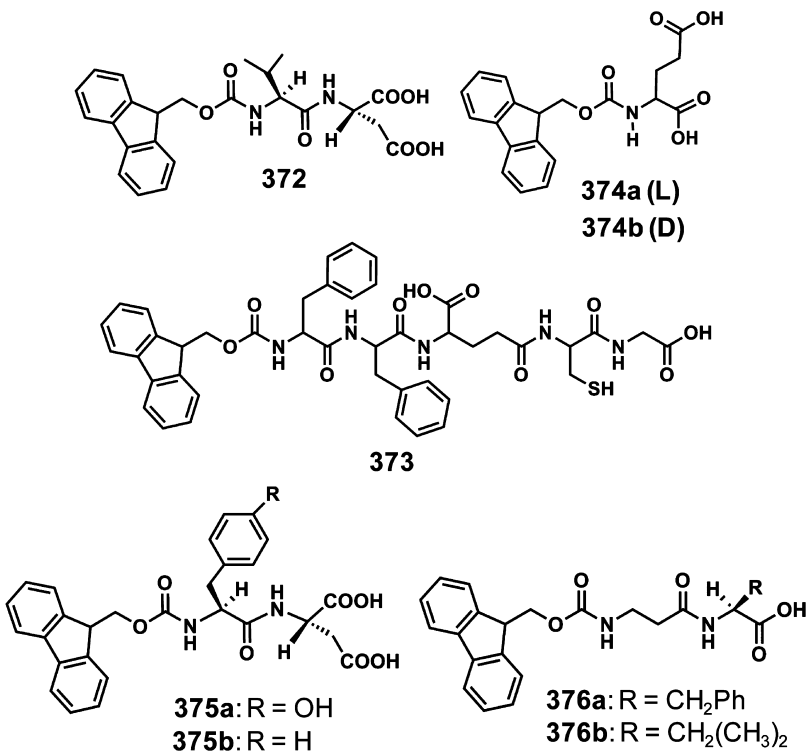
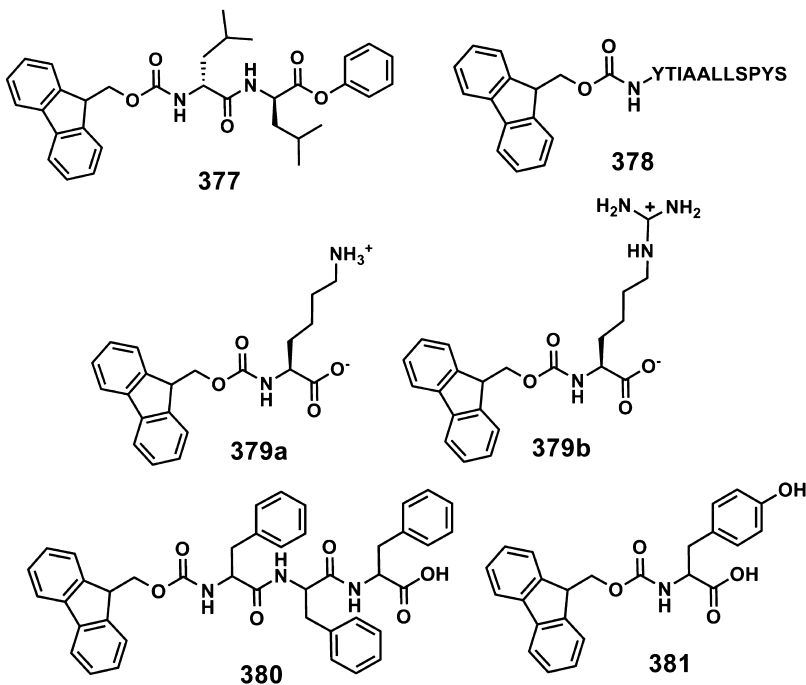


Chart 94



359 or Fmoc-tyrosine 381 (Chart 94) exhibited similar diffusion rates.⁸³⁰ A series of Fmoc-dipeptides 382a–e (Chart 95), 353c, 353d, 361c, 361d, and 361g have been investigated for a deeper understanding of the effect of molecular structure and the overall hydrophobicity on the gelation behavior.^{831,832} Self-assembled hydrogel membranes of controlled thickness obtained from the dipeptide amphiphile 361d resembled a dense mat of entangled fibers, which could be reversibly dried and reswollen back to the gel.⁸³³ The tunable mechanical

properties and the ability to recover after shear has been achieved by controlling the volume fraction of the cosolvent and the temperature cycle used.⁸³⁴ Systematic variations of the gelation conditions of 361g through various experimental protocols indicated that the mechanical properties of the gels depend upon conditions such as pH and solvent combinations.⁸³⁵

Nilsson et al. have reported that the gelator 383a (Chart 95) displayed a rapid hydrogelation at lower concentrations when

Chart 95

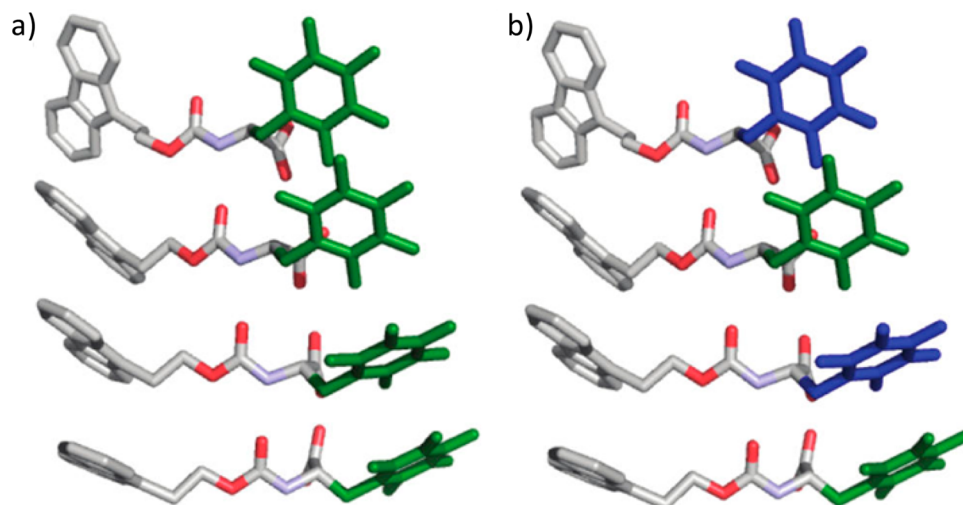
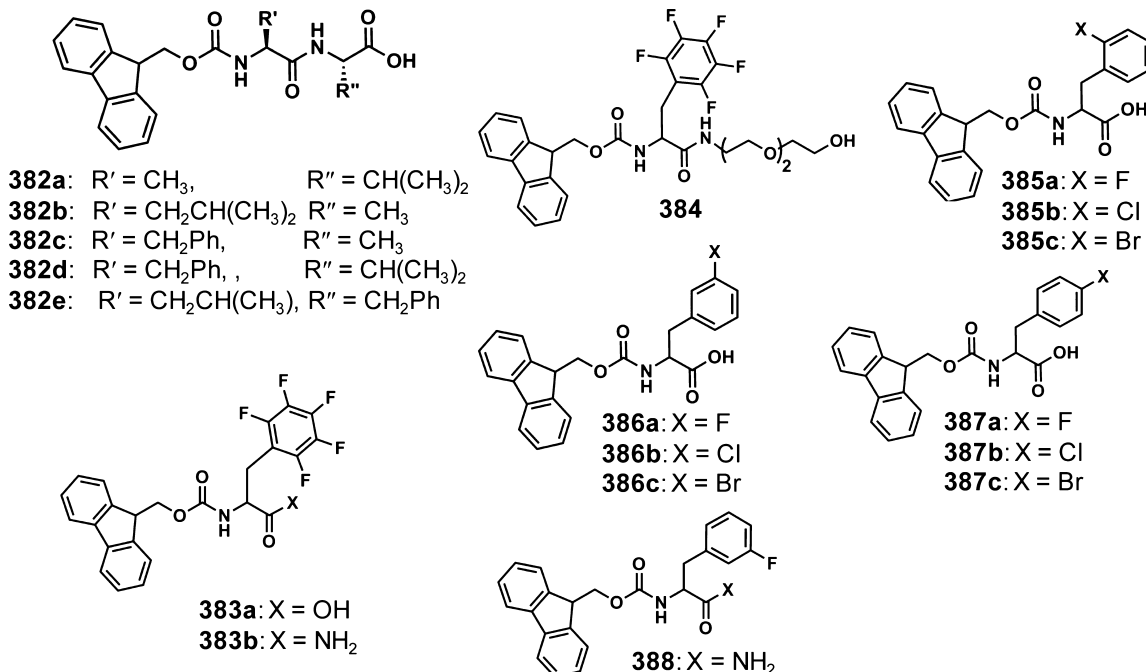


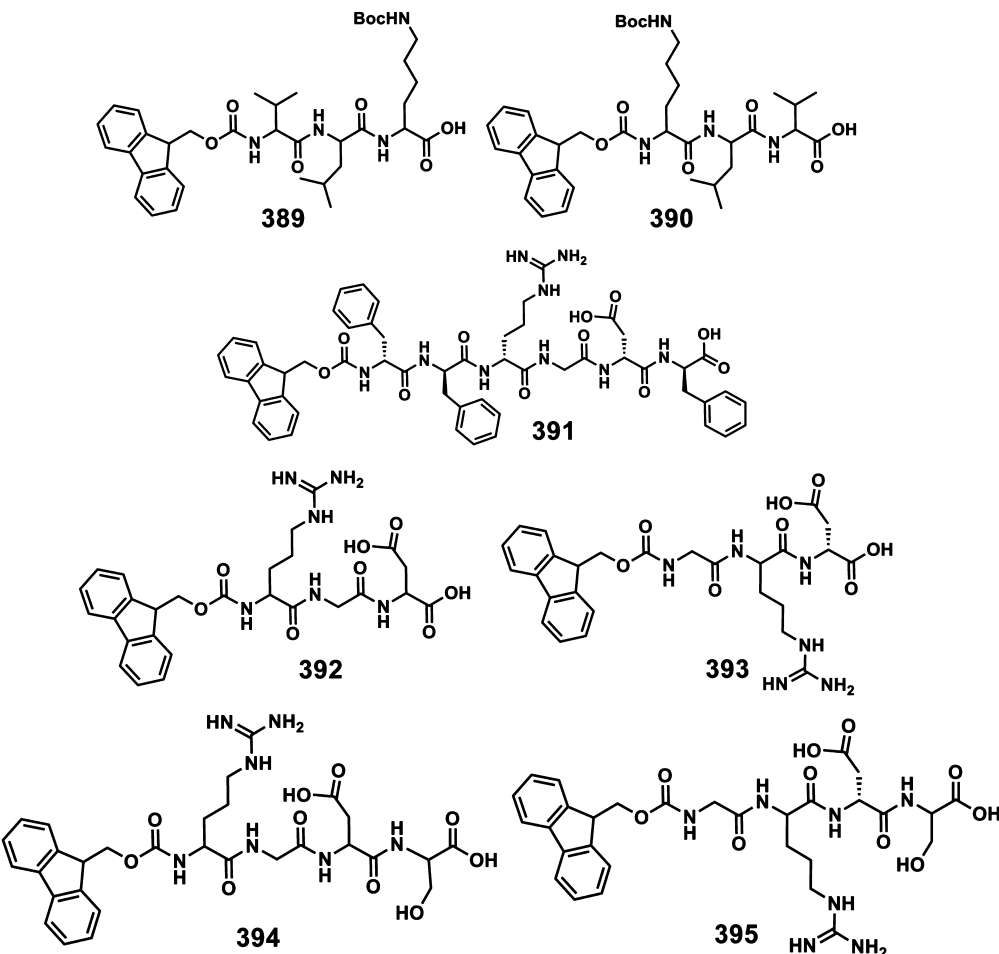
Figure 51. Proposed packing model of (a) 383a self-assembly and (b) coassembly of 359 (blue) and 383a (green). (Reprinted with permission from ref 840. Copyright 2011 American Chemical Society.)

compared to that of the corresponding phenyl and trifluoromethylphenyl derivatives as well as Fmoc-Tyrosine.⁸³⁶ The replacement of the Fmoc group with carboxybenzyl and Boc groups revealed significant influence of the former in the hydrogelation of 383a. Coassembly of 383a with a C-terminal PEG functionalized derivative 384 (Chart 95) exhibited remarkable enhancement in the CD signals.⁸³⁷ A detailed study has been carried out to understand the electronic and steric role of the benzyl side chain on the self-assembly and hydrogelation of the Fmoc-Phe derivatives by incorporating a single halogen substituent on the benzyl side chain in either the ortho, meta, or para positions of 385–387 (Chart 95).⁸³⁸ The gelators 383a and 386a formed rigid hydrogels under suitable pH conditions whereas 383b and 388 (Chart 95) were weak gelators.⁸³⁹ Most of these gelators could enter into comple-

mentary aromatic $\pi-\pi$ interactions in the presence of other suitable gelators (Figure 51).⁸⁴⁰

The hydrogels of Fmoc-tripeptides 389 and 390 (Chart 96) exhibited significantly different assembly properties.⁸⁴¹ For example, the gelator 389 formed highly anisotropic fibrils with flow aligning properties whereas 390 formed isotropic hydrogels with highly branched fibrils. A biocompatible hydrogel scaffold of 391 (Chart 96) has been used to load antiproliferative model drug and also used in the filtering surgery of rabbit eyes.⁸⁴² Hydrogels of 392 and 393 (Chart 96) formed amyloid fibrils through π -stacking interactions of the Fmoc moiety and found that hydrogels of 392 supported bovine fibroblast cells.⁸⁴³ The hydrogel of 394 (Chart 96) was less stable to shear when compared to the hydrogel of 395 (Chart 96).⁸⁴⁴ In the case of 394, self-assembly was stabilized through intramolecular interactions via salt bridges between the

Chart 96



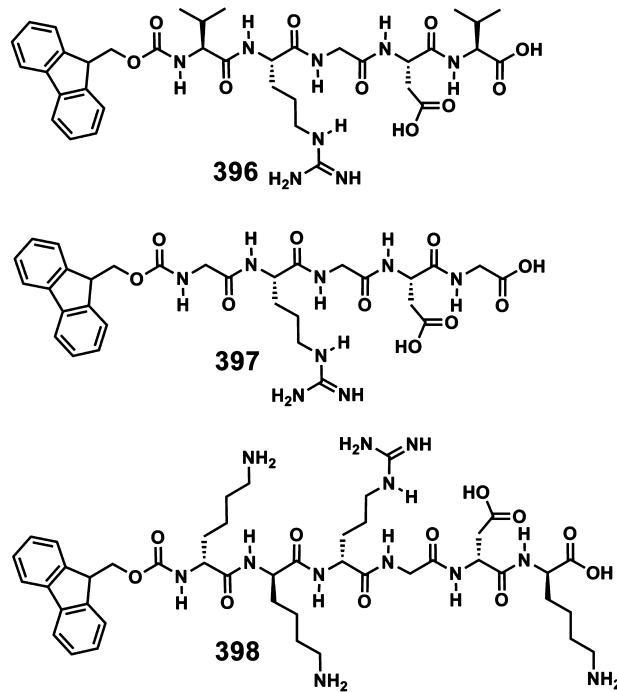
Arg and Asp side chain residues. On the other hand, assembly of 395 was mainly stabilized through intermolecular hydrogen bonds.

Monoliths of Fmoc-RGD 394 hydrogel are found to be stable in water for nearly 40 days without much detachment of peptide fibers.⁸⁴⁵ The fibrillar structure of the monolith enabled encapsulation and release of thioflavin T, methylene blue, riboflavin, and salicylic acid. The incorporation of multicomponent supramolecular hydrogels of 354, 355, 358b, 359, and 362a into agarose hydrogels has been used to create novel hybrid hydrogels.⁸⁴⁶ The mechanically stable hybrid gels could be fabricated into different shapes and used as potential drug delivery carriers.

The electrostatic attraction of the gelators 396 and 397 (Chart 97) at higher pH has been used as a trigger to form supramolecular hydrogels.⁸⁴⁷ The coassembly of 396 and 398 (Chart 97) and 397 and 398 at neutral pH also resulted in hydrogelation. Das et al. have reported a series of Fmoc-dipeptide functionalized cationic amphiphiles 399 and 400 (Chart 98) containing a pyridinium moiety at the C-terminus, exhibiting efficient antibacterial activity against both Gram-positive and Gram-negative bacteria.⁸⁴⁸ A phenylalanine based cationic amphiphile 401 (Chart 98) could impart hydrophobicity and facilitated gelation due to the strong $\pi-\pi$ interaction.⁸⁴⁹

In recent years several interesting F-moc based gelators containing different functional groups have been reported. Some of the applications of these gelators involve stem cell

Chart 97



delivery⁸⁵⁰ and excited-state proton transfer studies.⁸⁵¹ The gelators based on F-moc functionalized carbohydrates 402a,b

Chart 98

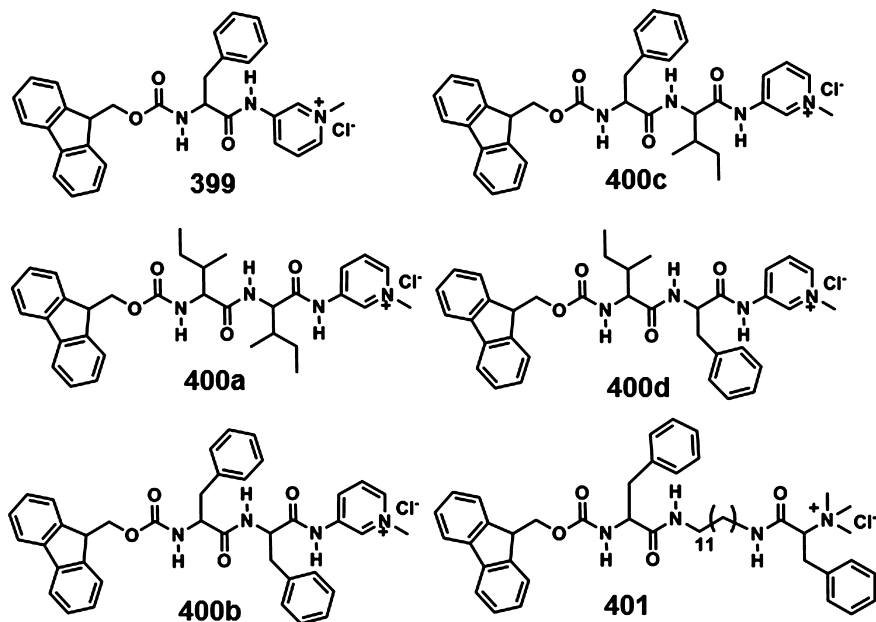
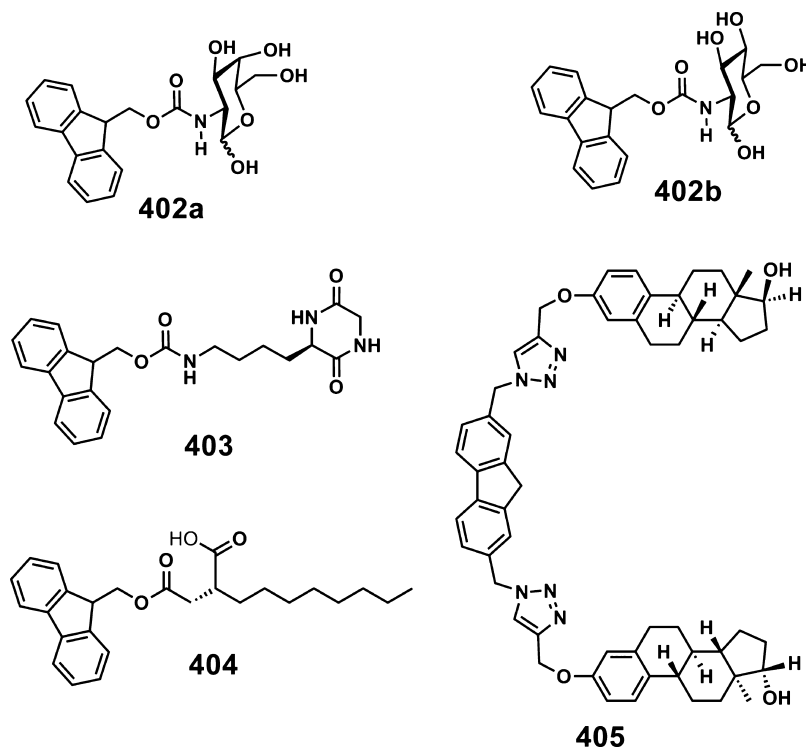


Chart 99



(Chart 99) were shown to form hydrogels via CH– π interactions as inferred from the optical and computational studies.⁸⁵² The cyclic dipeptide based gelator 403 (Chart 99) exhibited initial J-type aggregation in solution, which turned to excimer emission in the self-assembled microporous gel nanostructures.⁸⁵³ (R)-N-Fmoc-octylglycine 404 (Chart 99) formed organogels exclusively when ultrasound was used as an external stimulus.⁸⁵⁴ Click chemistry has also been applied to design F-moc based gelators. For example, Lopes and Sierra have reported a clicked estradiol containing fluorene based gelator 405 (Chart 99).⁸⁵⁵

π -gels in which conjugated fluorenes are present as the backbone have been reported by Schenning and co-workers.⁸⁵⁶ White light emission has been observed in a coassembled gels of the blue emissive molecule 406a, red emissive 406b (Figure S2) doped with corresponding green and yellow emissive nongelators. In addition to these reports, gelation and photophysical properties of polyfluorenes such as poly(9,9-diethylfluorene-2,7-diyl),^{857,858} and poly(9,9-dialkylfluorene)s^{859–862} have also been reported.

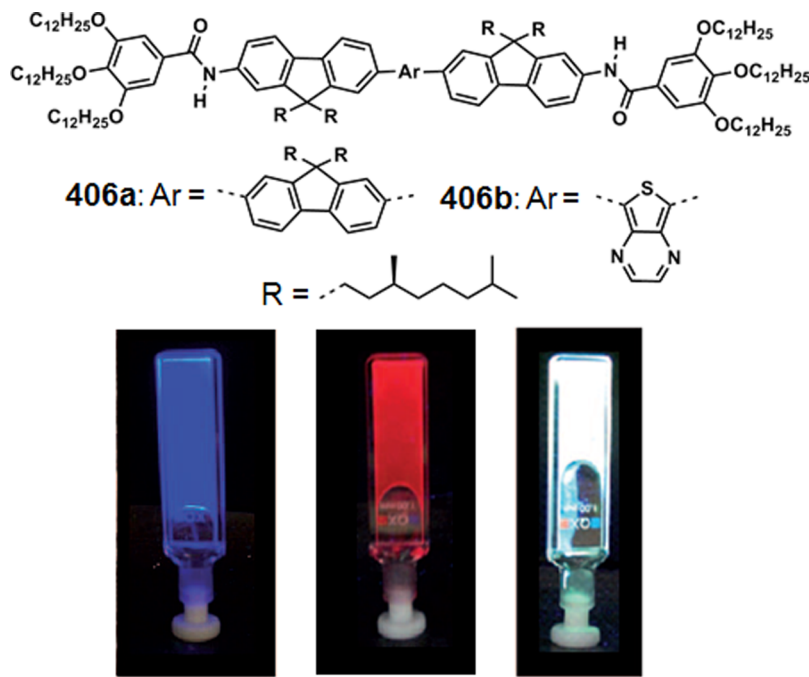


Figure 52. Photographs of the organogels formed by **406a** (blue) and **406b** (red) and the coassembled gel (white) under UV light. (Reprinted with permission from ref 856. Copyright 2009 Wiley-VCH.)

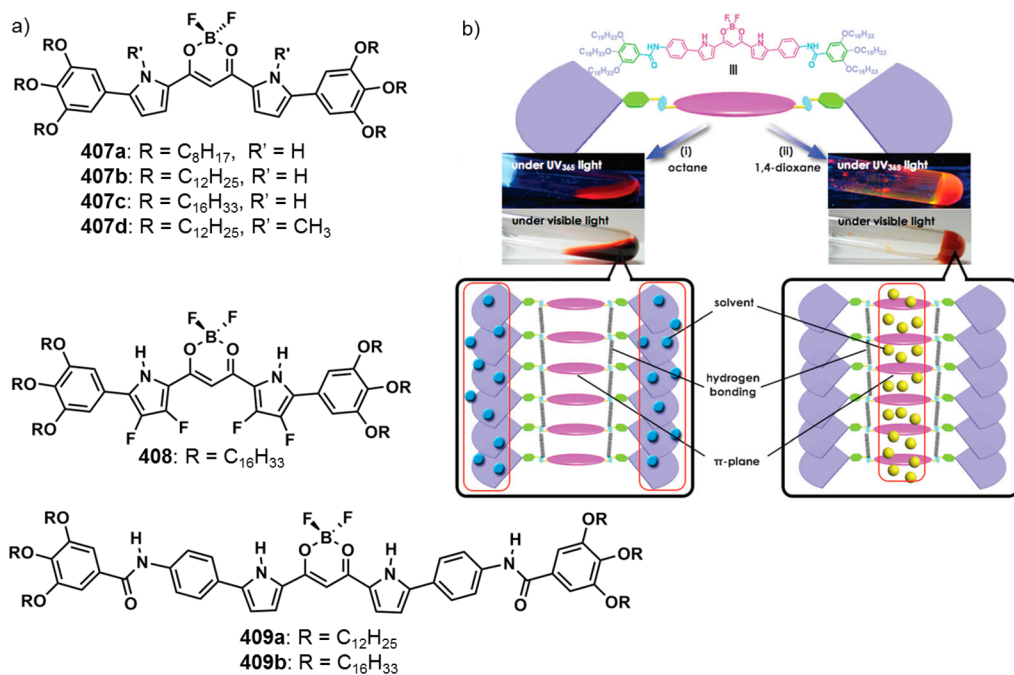


Figure 53. (a) Chemical structures of **407–409** and (b) graphical representation of the possible self-assembly modes of **409b** in different solvents. (Reprinted with permission from ref 869. Copyright 2011 The Royal Society of Chemistry.)

5. HETEROCYCLES AS GELATORS

Fused heterocyclic compounds have received considerable attention in the recent past due to their extensive use in organic electronics. When compared to the fully carbon based parent molecules, the heteroatom substituted analogues show efficient bandgap tuning. Therefore, preparation of self-assembled architectures and gels of heterocyclic compounds has gained much attention. In this section we discuss the gelation properties of different heterocyclic derivatives.

5.1. Pyrrole

Pyrrole is a five membered heterocyclic aromatic compound and is a component of a number of naturally found complex macrocycles, including the porphyrins of heme, chlorins, bacteriochlorins, chlorophyll and porphyrinogens.^{468,863,864} Maeda et al. have reported that BF₃ complexes of aryl substituted dipyrrolyldiketones with long alkoxy chains at 3,4,5-positions of the substituent aryl rings **407a–d** (Figure 53) form emissive gels through slipped H- and J-aggregation modes indicating incomplete parallel orientation of the mole-

Chart 100

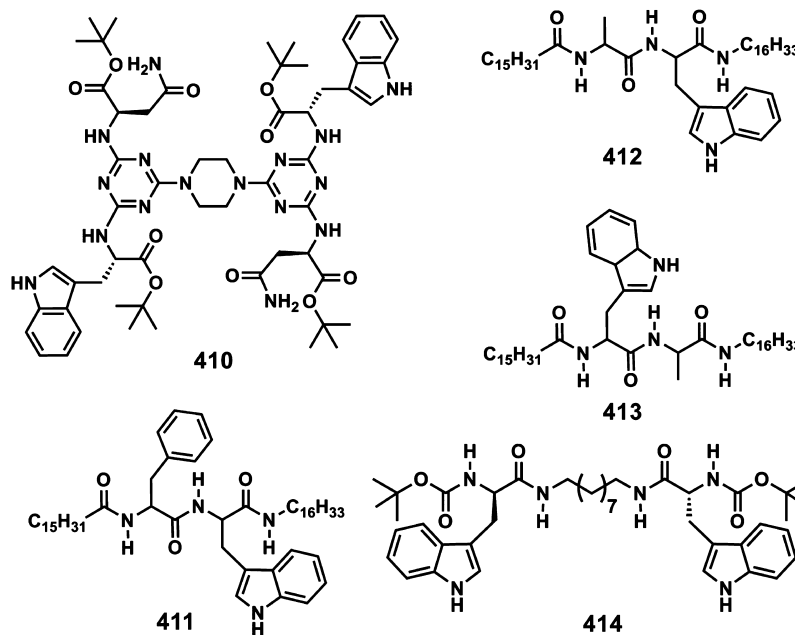
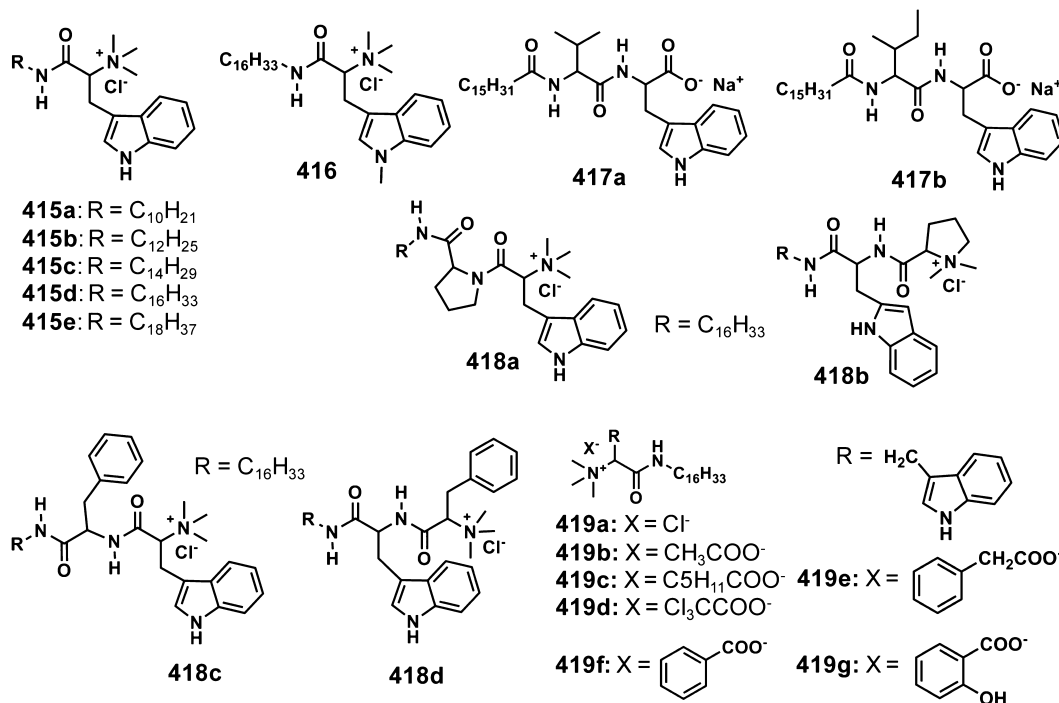


Chart 101



cules.^{865,866} A stable gel of **407c** (Figure 53) was obtained in the presence of Cl⁻ salts of planar 4,8,12-trialkyl-4,8,12-triazatriangulenium (TATA) cation due to the formation charge-by-charge assembly of **407c**·Cl⁻(TATA)⁺ complex.⁸⁶⁷ The β-fluorinated pyrrole receptor **408** (Figure 53) gave stable supramolecular gels even in the presence of tetraalkylammonium chloride.⁸⁶⁸ The amide functionalized pyrrole based anion receptors **409a,b** (Figure 53) also provide supramolecular gels with tunable stabilities.⁸⁶⁹

5.2. Indole

Indole, the bicyclic aromatic heterocyclic compound consisting of a benzene ring fused to a pyrrole ring has been widely used

for the preparation of gelators. In recent years, there is a growing interest to the study of tryptophan, an indolic amino acid which is the precursor of the neurotransmitter serotonin, based gelators with a view to exploit their inherent optical and biological properties. For example, the organogelator **410** (Chart 100) has been designed by incorporating asparagine and tryptophan residues at the outer core of a central piperazine with two 1,3,5-triazine units.⁸⁷⁰ The xerogels of **411–413** (Chart 100) were potentially active to adsorb crystal violet dyes from water and hence projected for wastewater treatment.⁸⁷¹ Thermally stable gels of **414** (Chart 100) consist of nanoscale

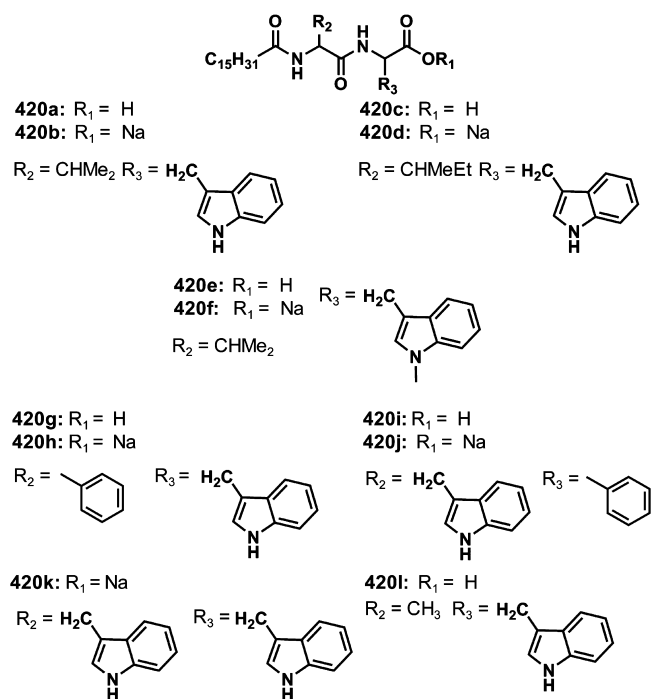
interpenetrating fiber network exhibiting thermoresponsive optical and chiroptical properties.⁸⁷²

Das and co-workers have investigated the effect of hydrophobic chain length of L-tryptophan based cationic amphiphiles **415a–e**⁸⁷³ and **416**⁸⁷⁶ (Chart 101) on gelation efficiency as well as biological activities.^{873–877} The minimum condition for gelation is a chain length of 12 carbons, the gelation ability increases with chain length. The gelator **415e** with 18 carbon atoms was found to be the best hydrogelator. These cationic amphiphilic hydrogelators exhibited remarkable bactericidal activity against Gram-positive and Gram-negative bacteria.⁸⁷⁴ The systematic variation of the counteranion of the amphiphilic hydrogelator **415d**^{696,875} enabled modulation of the gelation, antimicrobial activity, and biocompatibility. In addition, in situ synthesis of Ag nanoparticle within the hydrogel network has been achieved using hydrogelators **415d** and **417a,b** (Chart 101).^{696,875,876} The Ag nanoparticle composite also exhibited antibacterial activity and considerable cytocompatibility to mammalian cells.^{875,876} A series of cationic dipeptide amphiphilic hydrogelators **418a–d** (Chart 101) were also reported and the bioinspired nanocages of **418d** were used for the release of the entrapped hydrophilic biomolecules such as vitamin B₆ and B₁₂.⁸⁷⁸

The gel network of tryptophan based peptide amphiphiles **418a–d** (Chart 101) has been used for the in situ synthesis of Au nanoparticles having different shapes such as sheet, wire, octahedral, and decahedral shapes by the reduction of HAuCl₄ without using any reducing or capping agents.⁸⁷⁹ L-Tryptophan containing amphiphiles **419a–g** (Chart 101) are good hydrogelators.⁶⁹⁶ Ag nanoparticles were synthesized from AgNO₃ within the hydrogel medium of gelators **419b–g** and **325a** (Charts 101 and 79) without assistance from temperature, alkaline medium, and external reducing agent.

The amphiphilic dipeptide based carboxylic acids/salts **420a–l** (Chart 102) exhibit excellent gelation behavior.^{880,881} Au nanoparticles were in situ synthesized by dropwise addition

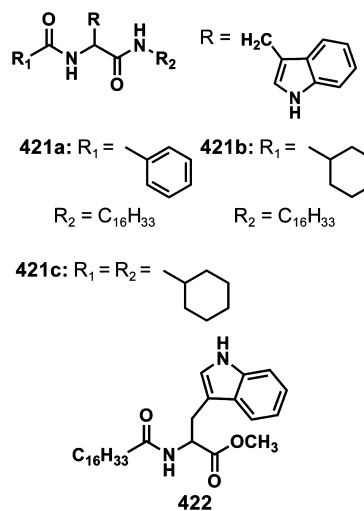
Chart 102



of aqueous HAuCl₄ solution to the hydrogel of amphiphiles **420a–d**.⁸⁸⁰ The gel network of the amphiphile hydrogelators functioned as reducing as well as capping agents for the synthesis of nanoparticles. Gelators **420a** and **420g** showed phase selective gelation of organic solvents from water mixture and the gel showed dye absorption.⁸⁸¹

Amino acid based molecules **421a–c** (Chart 103) are efficient gelators of ionic liquids.⁸⁸² An ionogel template has

Chart 103



been utilized for the synthesis of TiO₂ nanoparticles with different sizes and shapes from titanium tetraisopropoxide and adsorption of both cationic and anionic dyes from aqueous solution. Acid functionalized SWCNTs played remarkable role in the improvement of mechanical strength and gelation of amphiphilic molecules **420a** and **420g**.⁸⁸³ The interconnected network of self-assembled nanofibers led to gelation at a minimal amount of the gelator. Gelator **422** (Chart 103) exhibited gelation ability in vegetable oil through hydrogen bonding and van der Waals interactions.⁸⁸⁴

5.3. Adenines, Guanines, and Guanosines

Nucleobases, a group of nitrogen containing heterocyclic molecules, are essential for the formation of nucleotides. Nucleobases provide the molecular structure necessary for the hydrogen bonding of complementary DNA and RNA strands. Due to the biological relevance of nucleobases, a series of nucleobase derived gelators have been designed and synthesized, which were used as gel phase biomaterials.^{885–887}

Xu et al. have reported that the connection of a nucleobase to the dipeptide segment affords a series of nucleopeptides **423** and **424** (Chart 104) which are biocompatible hydrogelators.⁸⁸⁸ The gelators **425** and **426** (Chart 104), which are combinations of a nucleobase, an amino acid and a glycoside, form hydrogels at suitable pH with excellent biocompatibility and biostability toward enzymatic digestion.⁸⁸⁹ The dephosphorylation of adenosine monophosphate using alkaline phosphatase enzyme afforded the adenosine derivative **427** (Chart 105), which formed supramolecular nanofibers and hydrogels.⁸⁹⁰

Oda and co-workers developed a cationic gemini surfactant **428** (Chart 105) having adenine 5'-monophosphate as the counterion that formed hydrogels upon the addition of complementary nucleoside bases such as adenosine.⁸⁹¹ A combination of gemini surfactant (**GS**; Chart 105) and

Chart 104

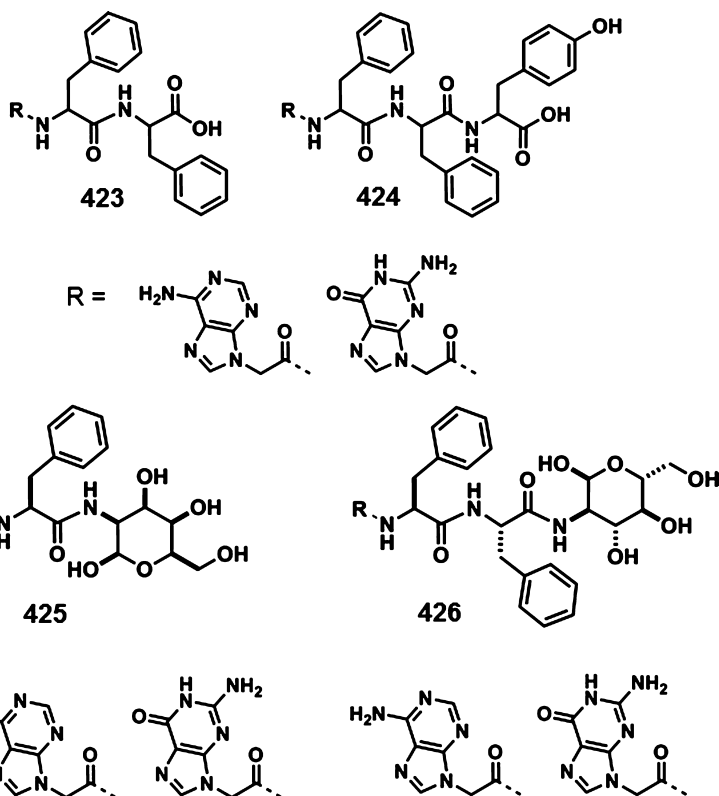
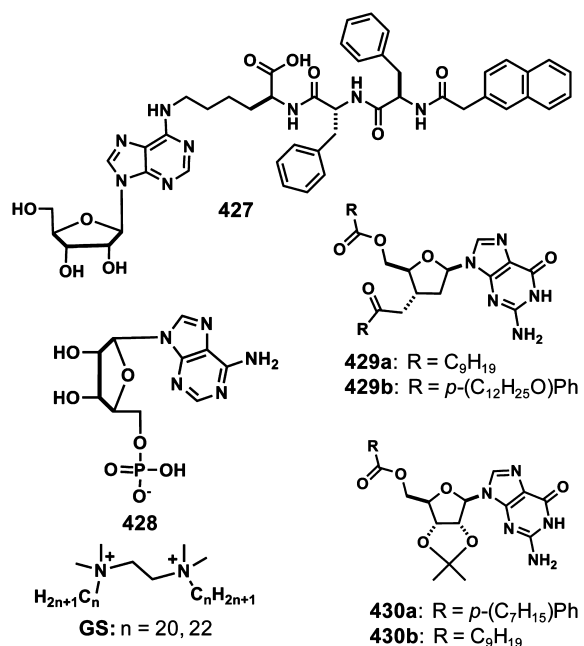


Chart 105



nucleotide 428 formed hydrogels in the presence of adenosine. The lipophilic deoxyguanosine derivative 429 (Chart 105)^{892–896} formed an ordered lyotropic LC phase and organogels whereas the self-assembly of guanosine 430 (Chart 105)⁸⁹⁴ resulted in birefringent gels. In the case of 429, gel phases in hydrocarbon solvents exhibited a 2D square packing of the molecules as observed from the spacing of the small angle reflections. In chloroform, a different structure

consisted of rods formed from multiple stacked ribbons, packed in a 2D cell was confirmed.⁸⁹⁴

A conjugate of adenine with oleanic acid 431 (Chart 106) is reported to form gels in solvent mixtures of THF and water in which the complementary interaction between the gelator and uracil derivatives have an impact on the gel stability and morphology.⁸⁹⁵ 2'-Deoxyadenosine based gelators 432a,b (Chart 106) with an alkyl chain containing a urea linker formed a stable gel under ultrasound due to the formation of the oxidized species.⁸⁹⁶

Xu et al. developed biostable and biofunctional hydrogelators 433 and 434 (Chart 106) based on a combination of nucleobases, tetra/pentapeptides, and glucosamine in a single molecule for applications that require long-term biostability.⁸⁹⁷ The guanosine base pair formation promoted gelation of alkylsilylated guanosine derivatives 435a–c (Chart 106).⁸⁹⁸ Dinucleosides 436a–e (Chart 107) form thermoreversible gels in organic solvents due to base pairing assisted linear aggregate formation followed by desolvation of the nucleobases.^{899,900}

The binary mixtures of 5'-guanosine monophosphate and guanosine form stable gels at neutral pH over a temperature range that can be tuned by varying the relative proportions of the hydrophobic guanosine and the hydrophilic 5'-guanosine monophosphate in the mixture.⁹⁰¹ The transformation of gel fibres into precipitates upon aging was accompanied by a change in the photoluminescence intensity and was ascribed to as a consequence of Ostwald ripening process. A hydrogelator based on selective molecular interaction of adenine and 1,3,5-benzenetricarboxylic acid, has been reported.⁹⁰² The morphology of dried composite gel revealed the presence of belt-like thick fibers composed of network of nanofibers. Supramolecular blends of polymers with guanosine urea and 2,7-diamido-1,8-naphthyridine moieties was reported to form gels through

Chart 106

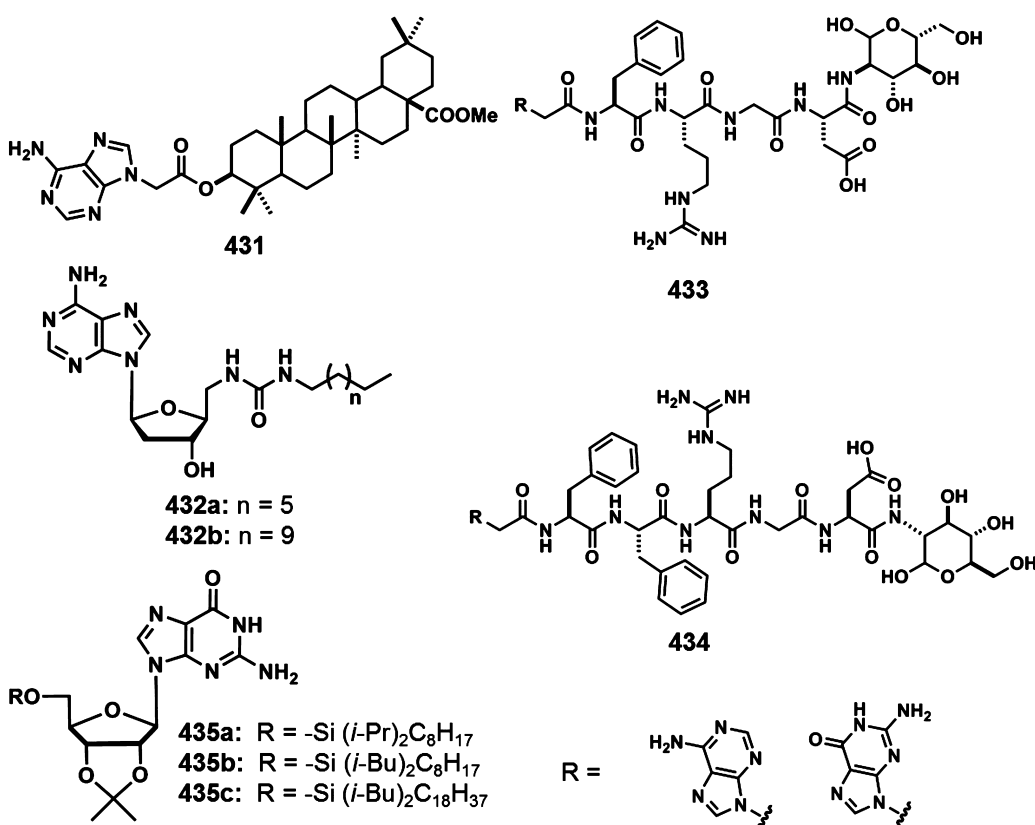
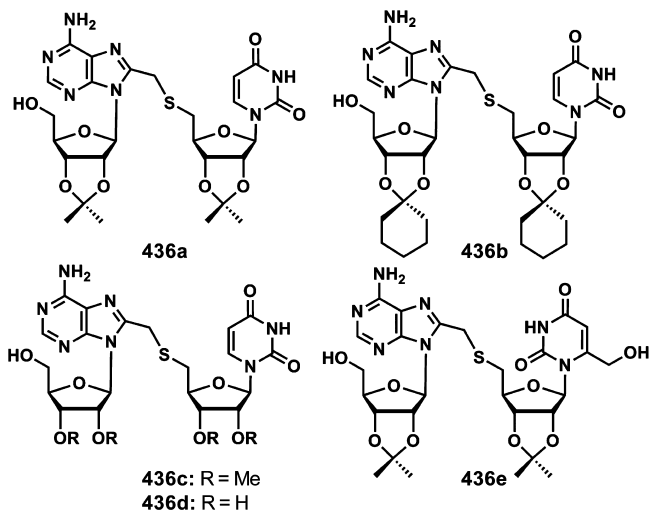


Chart 107



quadruple hydrogen bonded heterocomplex formation.⁹⁰³ In addition to the above-mentioned studies, reports pertaining to gelation of other kinds of nucleobases are also available.^{904–912}

5.4. Pyridine Derivatives

5.4.1. Bipyridines. Bipyridines are known to complex with a variety of transition metal ions. Therefore, properties of bipyridine based gelators can be significantly controlled by cation complexation. For example, the molecular receptor 437 (Chart 108) that complexes with transition metal ions exhibits solvent gelation.⁹¹³ Each of the trisbipyridine ligand binds with approximately 8000 molecules of toluene, thereby resulting in gel formation. The ligand in the gel phase binds with iron(II)

and undergoes a gel–sol phase transition. Meijer et al. studied the gelation properties of urea linked C_3 -symmetrical chiral 438a and achiral 438b (Chart 108) molecules.^{914,915} SANS studies indicated the presence of cylindrical aggregates, formed via hydrogen bonding and π -stacking. As shown in Figure 54, through urea helical aggregates, micrometer long strands consisting of thousands of molecules were formed. Detailed understanding of the assembly behavior of the gelator 438 suggested that independent of the linear or branched alkane used, lyotropic LC phase was observed.⁹¹⁵ In addition, distance between the stacks can be tuned by adding solvent to the system, through a swelling process. SAXS measurements of the lyotropic LC structures of 438b revealed that at higher concentrations, swelling of the aggregates in the plane perpendicular to the column axis occurs in two dimensions whereas at lower concentrations, 3D swelling facilitates the columns to fragments. A cholesterol linked viologen derivative 439 (Chart 108) forms stable gel in 1-butanol, and a dipole moment assisted clockwise orientation of the assemblies tend to form thick fibers composing of thin fibrils.⁹¹⁶ The sol–gel polycondensation of tetraethoxysilane in the gel phase allowed the transcription of the fibrous structures into silica fibers having 20–30 nm outer diameter and a unique hollow inner diameter of 15 nm.

Self-complexation of a pillar[5]arene derivative 440 (Chart 108) carrying a viologen side chain led to the formation of supramolecular daisy chain polymers at lower concentrations, eventually leading to organogel formation at higher concentrations.⁹¹⁷ Gelation and morphological studies of a series of amphiphilic L-glutamic acid derivatives having various saturated alkyl chains in the presence of 4,4'-bipyridine revealed the transformation of 3D networks of worm-like nanofibers to

Chart 108

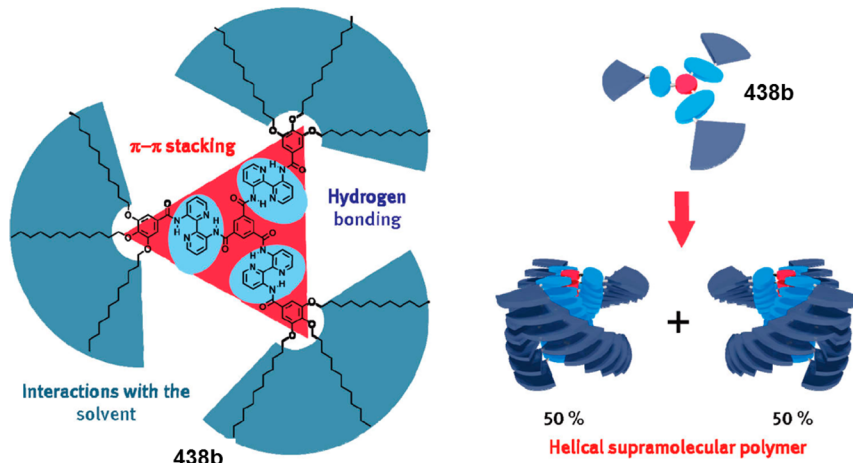
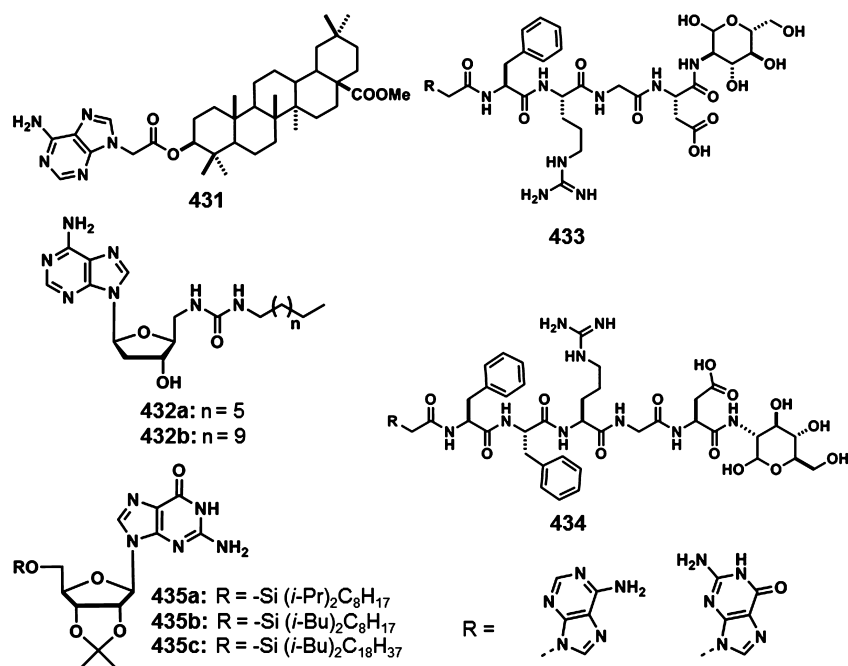


Figure 54. Schematic representation of the self-assembly of **438b** in hydrocarbon solvents. (Reprinted with permission from ref 915. Copyright 2009 American Chemical Society.)

twisted chiral ribbons.⁹¹⁸ A cyanurate derivative possessing three carboxylic acid groups and 4,4-bipyridine has been reported to form a supramolecular two component fluorescent gel.⁹¹⁹

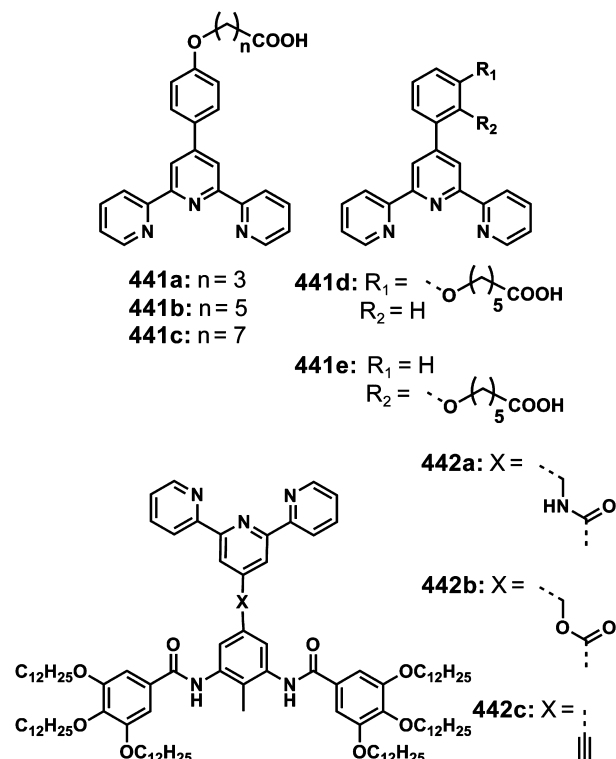
5.4.2. Terpyridines. Terpyridine containing carboxylic acid gelators **441a–e** (Chart 109) formed transparent hydrogels in NaOH solution.⁹²⁰ Ziessel et al. studied the gelation and LC properties of a series of terpyridine ligands **442a–c** (Chart 109).^{921,922} When the functional moiety connecting terpyridine and 3,5-diacylamino toluene platform containing two alkoxy phenyl rings was varied from amide (**442a**) to ether (**442b**) and further to a C–C triple bond (**442c**), significant differences in gelation as well as LC properties were observed. Highly stable, transparent, and birefringent gels were formed by **442a**. Transparent gels were also formed with **442b** but only at higher concentrations whereas turbid gels were formed by **442c**.

A terpyridine based organic–inorganic hybrid gelator **443** (Chart 110) possessing triethoxysilane moiety exhibited

preferential adsorption of aromatic dyes such as basic blue 41 and crystal violet from water.⁹²³ Linear and branched carbohydrate functionalized gelators **444a,b** (Chart 110) self-organized to form nanofibers and organogels at high concentrations (Figure 55).⁹²⁴ As shown in Figure 55, the reduced interfacial energy in a polar environment obtained by the stacking of hydrophobic terpyridines at the interior and hydrophilic carbohydrates at the exterior is the driving force for aggregation.

5.4.3. Phenanthrolines. Shinkai et al. reported that the cholesterol functionalized phenanthroline **445a**^{925–927} exhibits excellent gelation behavior in polar solvents whereas the gelator **445b** forms gels only in the presence of an acid (Figure 56). The sol–gel condensation of TEOS in acetic acid gels resulted in mesoporous silica nanotubes (Figure 56a).^{926,928} Interestingly, organic–inorganic hybrid materials obtained after condensation retained the fluorescence properties of the gel phase (Figure 56a).

Chart 109



The amide based phenanthroline ligands **446a,b** (Chart 111) exhibited 1D alignment through hydrogen bonding, van der Waals and π -stacking interactions leading to gelation.⁹²⁹ The characteristic features of a rigid steroidal skeleton with controllable polar and lipophilic centers have been used in combination with phenanthroline to induce aggregation and gelation.⁹³⁰ For example, the phenanthroline appended cholyl amide **447** (Chart 111) formed translucent gels in methanol–water (1:1) mixture.

Chart 110

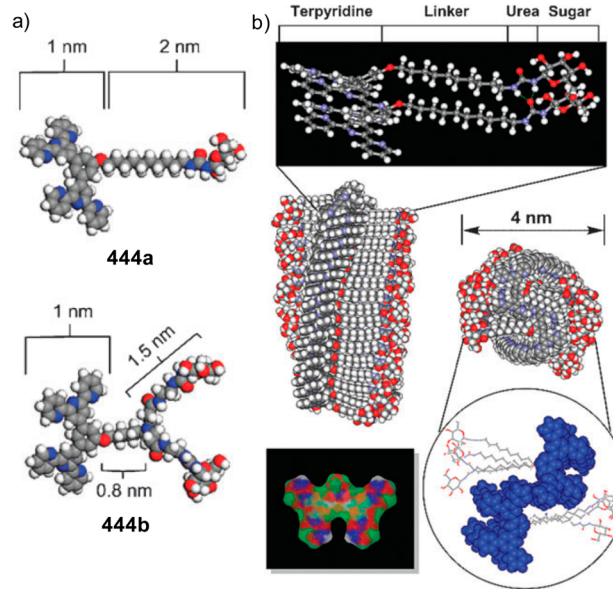
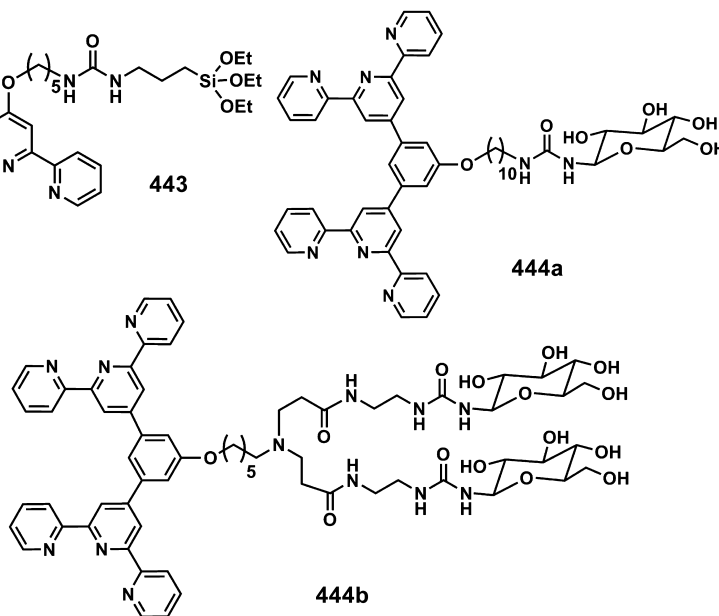


Figure 55. (a) Space-filling model of the energy minimized structures of carbohydrate functionalized terpyridines **444a,b**. (b) A proposed model of self-assembled nanofibers of **444a** and a view of the bis(terpyridine) molecular surface with mapped electron rich (red) and poor (blue) regions. (Reprinted with permission from ref 924. Copyright 2009 The Royal Society of Chemistry.)

5.4.4. Miscellaneous Pyridine Based Gelators. A simple pyridine based gelator **448** (Chart 112) exhibited strong gelation in aqueous conditions and the gel exhibited AIEE due to the protonation of the pyridine moiety.⁹³¹ Hydrogels formed at pH 7 was strongly fluorescent when compared to that at pH 2 and 13. Lehn et al. studied the gelation properties of a rigid bow shaped molecule **449** (Chart 112) bearing a self-complementary quadruple hydrogen bonding DAAD-ADDA array.⁹³² The folding induced self-assembly and gelation of the lock-washer shaped molecule **450** (Chart 112) resulted in spontaneous asymmetric generation of supramolecular chiral

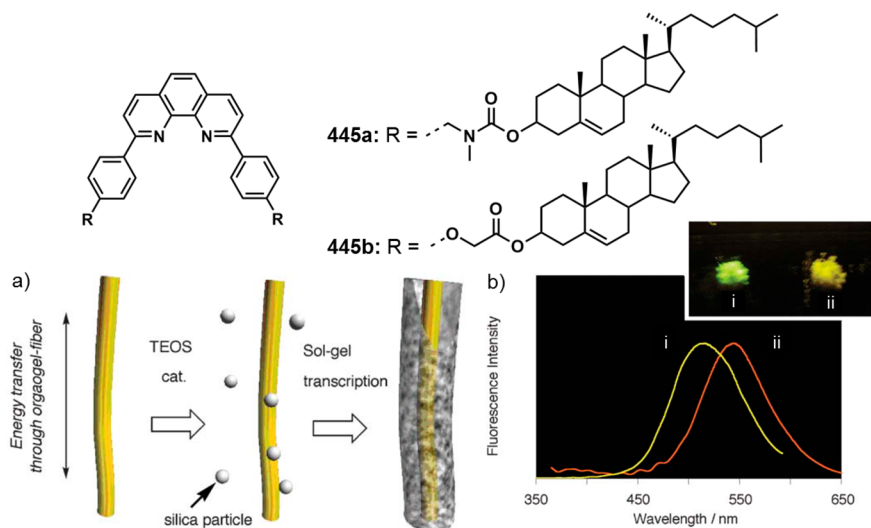


Figure 56. (a) Schematic representation of sol–gel transcription using gelators **445a,b**. (b) Fluorescence spectra and photographs (under 365 nm) of organic–inorganic hybrid materials prepared from (i) **445a** gel and (ii) **445b** gel in acetic acid. (Reprinted with permission from ref 928. Copyright 2005 The Royal Society of Chemistry.)

Chart 111

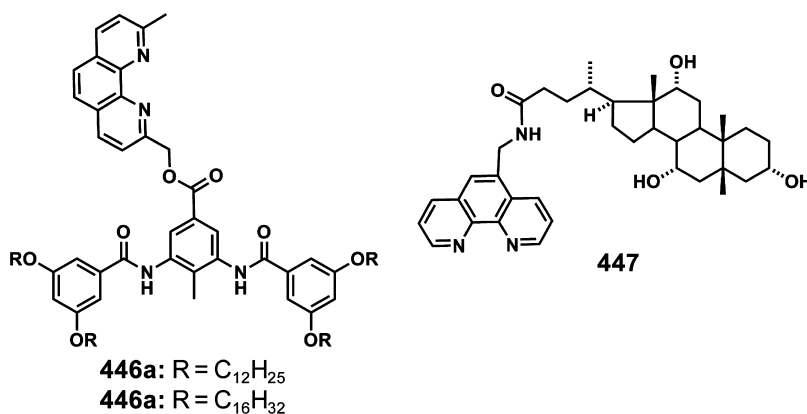
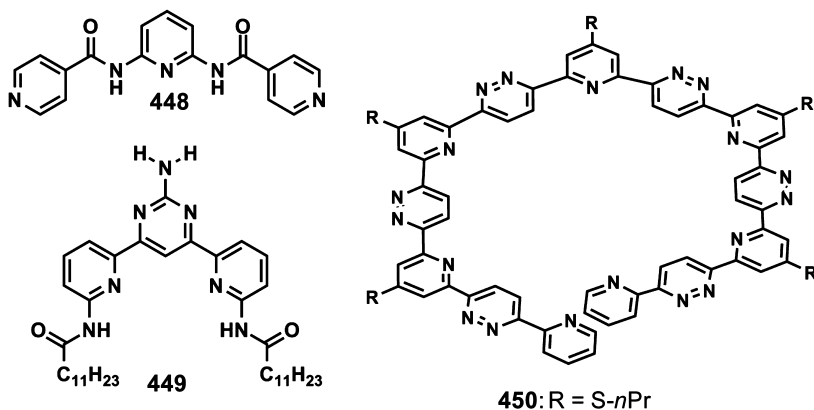


Chart 112



fibers.⁹³³ Instead of a pseudoracemic mixture, due to secondary nucleation governed ripening, **450** exhibited a preferred helical sense upon aging.

5.5. Quinolines

Ihara et al. reported the gelation of a double chain alkyl lipid **451** derived from L-glutamide with an isoquinoline head-group.⁹³⁴ Quinoline based cyclotetramer **452** (Chart 113),

upon addition of methanol to a concentrated dichloromethane solution, self-assembled to form a gel.⁹³⁵ Hydrogels of **453** (Chart 113) composed of unbranched, long and straight tubular fibers with uniform diameters can be used in drug delivery applications.⁹³⁶ On treatment with mineral acids such as sulfuric acid, hydrochloric or phosphoric acid, the *N*-cyclohexyl-2-(quinolin-8-yloxy) acetamide **454** (Chart 113)

Chart 113

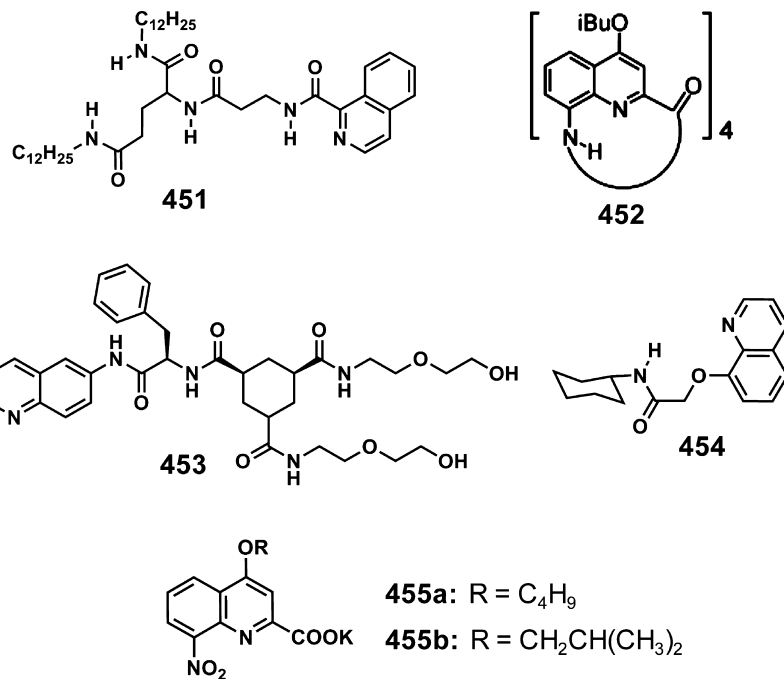
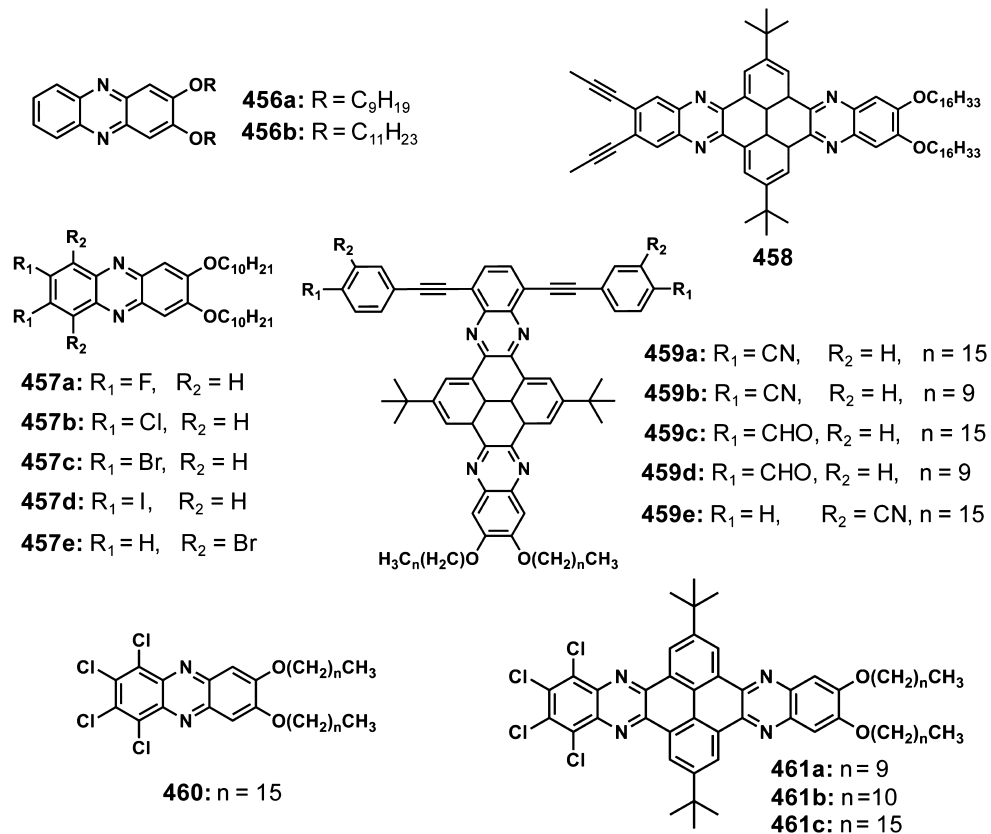


Chart 114



formed gels.⁹³⁷ It is to be noticed that in this case, acids having nonplanar anions only facilitate the gel formation. Potassium 8-nitroquinolinecarboxylates 455a,b (Chart 113) selectively formed gel in THF/MeOH mixture through π -stacking interactions.⁹³⁸

5.6. Phenazines

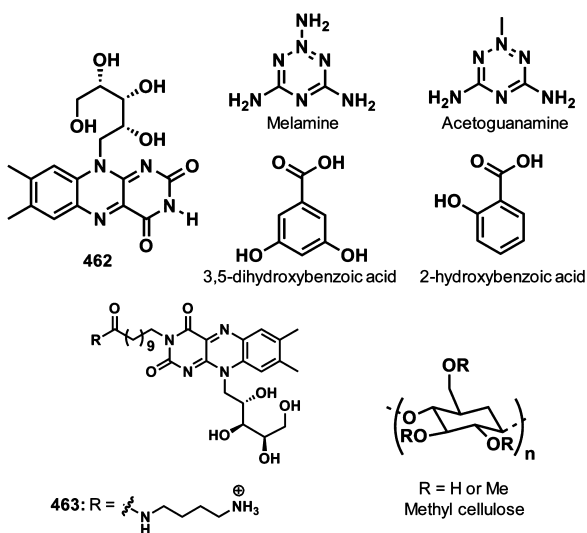
2,3-Di- n -alkoxyphenazines 456a,b (Chart 114) were shown to be acid sensitive organogelators.⁹³⁹ Pozzo et al. studied the effect of doping photochromic chromene, 3,3-diphenyl-9,10-di- n -undecyloxypyranopyrano[3,2-a]phenazine and its photochromic changes on the gel-sol transition of 2,3-di- n -undecyloxypyra-

nazine **456b**.⁹⁴⁰ The decrease in gel stability upon irradiation indicated the insertion of dopant into the gel matrix as a result of the photochromic change. The substitution of halogens at the periphery of alkyloxy substituted phenazines **457a–e** (Chart 114) produced different supramolecular structures such as torn paper-like morphology (**457a**), long straight needle-like crystals (**457b**), and 1D fibrous assemblies (**457c,d**).⁹⁴¹ The organogel of an asymmetric bisphenazine **458** (Chart 114) reported by Lee et al. exhibited colorimetric acid sensing property upon exposure of the xerogel to trifluoroacetic acid vapor.⁹⁴² A morphological control of self-assembled structures from straight strands to flexible nanofibers was observed when a cyanophenyl group was introduced to the T-shaped bisphenazine gelator **459a** (Chart 114).⁹⁴³ A detailed study revealed that the self-assembly, gelation and morphology of T-shaped bisphenazines functionalized with alkyl side groups could be tuned by peripheral cyano or aldehyde substituents as in **459a–e** (Chart 114).⁹⁴⁴ Tetrachlorophenazine **460** (Chart 114) and bisphenazines **461a–c** (Chart 114) exhibited significant difference in the morphology of the gel nanostructures.⁹⁴⁵ Straight, rigid, and bundled microbelts were formed by **460** whereas molecules **461a–c** formed entangled thinner and flexible fibers.

5.7. Riboflavins

Due to biological significance, riboflavins have been studied to form organized structures and gels. Nandi and co-workers reported the thermoreversible hydrogelation of riboflavin **462** and melamine (Chart 115) supramolecular (3:1) complex with

Chart 115



enhanced photoluminescence.⁹⁴⁶ Mechanistic pathways indicated that a spherulitic morphology was formed through the conformational ordering of the ribityl chain at lower temperature whereas at higher temperature π -stacking led to the fibrillar network morphology.⁹⁴⁷ The variation of the riboflavin-melamine compositions enabled to control the morphology from helical fiber (4:1 and 3:1) to rod (2:1) to hollow tube (1:3) (Figure 57).⁹⁴⁸ In another report, two component hydrogels of riboflavin was formed with salicylic acid, dihydroxybenzoic acid and acetoguanamine (Chart 115) in 1:1 molar ratio through the formation of tapes, bars, and helical tubes, respectively.⁹⁴⁹ Riboflavin-methyl cellulose (Chart 115) based hydrogel showed a 93-fold enhancement in photo-

luminescence when compared to that of the sol state.⁹⁵⁰ This is attributed to the entrainment of riboflavin dye in the hydrophobic environment of the gel fibers thereby inhibiting the solvent molecules mediated nonradiative decay of exitons.

Melamine exhibits excellent hydrogelation in combination with 6,7-dimethoxy-2,4[1H,3H]-quinazolininedione with a pH and temperature dependent fluorescence modulation.⁹⁵¹ At the same time, an equimolar complex of melamine and riboflavin also formed gels and the gel matrix has been used for the in situ formation of Ag nanoparticles of different size.⁹⁵² A light harvesting hydrogel consisting of a two component supramolecular complex (1:1) of melamine and 6,7-dimethoxy-2,4[1H,3H]-quinazolininedione as donor with riboflavin acceptor exhibited an increase in the emission intensity of the acceptor with a red-shifted emission maximum.⁹⁵³ A biocompatible hydrogel of riboflavin based amphiphile **463** (Chart 115) has been used to deliver VEGF-siRNA efficiently into human cells.⁹⁵⁴

5.8. Carbazoles

Carbazole is an aromatic heterocyclic compound with a tricyclic structure, consisting of two six membered benzene ring fused on either side of a five membered nitrogen containing ring. Carbazole based materials are known for their emissive features, find applications as blue emitters for LEDs and as donor in PVDs.⁹⁵⁵ Due to high charge carrier mobilities, suitable bandgaps, and orbital energies, polycarbazoles are used in PVDs and FETs.

Organogelation of the carbazole macrocycle **464** (Chart 116) in cyclohexane in which macrocycles are arranged in columnar fashion to form nanofibers is reported.⁹⁵⁶ 1D stacking of carbazole in **465** (Chart 116) assisted by L-isoleucine moiety, formed anisotropically aligned fibers in a homogeneously oriented smectic state of LC and thereby led to gelation.⁹⁵⁷ The research group of Lu have studied the properties of carbazole based organogelators.^{958–964} The dichalcone substituted carbazole gelator **466** (Chart 116) stacked into lamellar structures to form gels with red-shifted emission.⁹⁵⁸ Interestingly, bis(β -diketone)carbazole **467** (Chart 116) formed green emitting 1D nanofibers and organogels under ultrasound stimulation.⁹⁵⁹ The increased porosity of the mesh-like film of triphenylamine functionalized bis(dioxaborine)carbazole derivative **468** (Chart 116) allowed high selectivity for aniline vapor with the detection limit reaching up to 8.6 ppm.⁹⁶⁰

Unlike conventional organogels, *tert*-butyl groups have been used to modulate the self-assembling properties of carbazole gelators **469** and **470** (Chart 117) to form fibers with strong blue emission.^{961,962} The incorporation of diaryldiketopyrrolopyrrole derivative functionalized with phenothiazine moieties into the gel medium of **469** enabled tuning of gelation as well as emission properties.⁹⁶² The partial energy transfer from the excited **469** (Chart 117) to diaryldiketopyrrolopyrrole derivative resulted in a purple-white emission. In the case of dendritic oligocarbazoles, a two component organogel was formed by **471** (Chart 117) in the presence of 1,6-diaminohexane (2:1) and the gelation of **472** (Chart 117) was observed upon application of ultrasound.⁹⁶³ Another dendritic carbazole gelator **473** (Chart 117) showed AIEE due to the formation of J-type aggregates and the restricted molecular motion.⁹⁶⁴

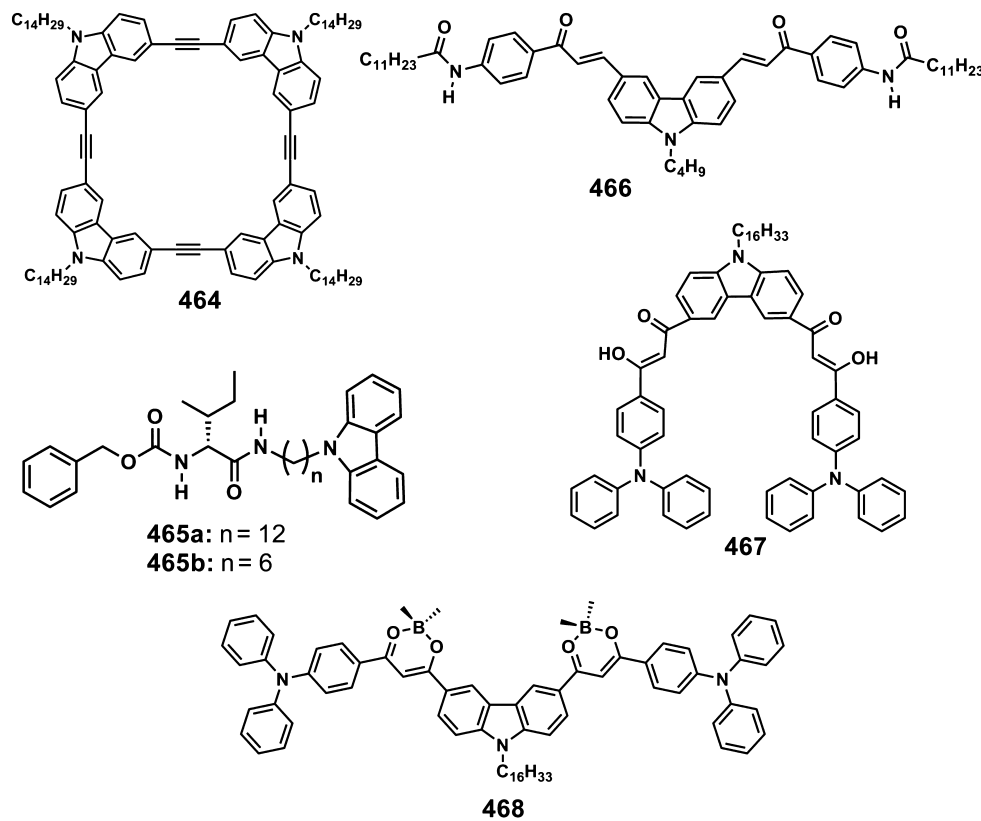
5.9. Oxadiazoles, Benzoxazoles, and Phenylisoxazoles

Park and co-workers reported GIEE in oxadiazole based benzene-1,3,5-tricarboxamide **474** (Figure 58a) through



Figure 57. SEM image of the rods (top), AFM image of the helical fibers (bottom) and the proposed molecular mode of 1:1 and 3:1 self-assembly of 462 and melamine to form tubes and helical bunched fibers. (Reprinted with permission from ref 948. Copyright 2008 The Royal Society of Chemistry.)

Chart 116

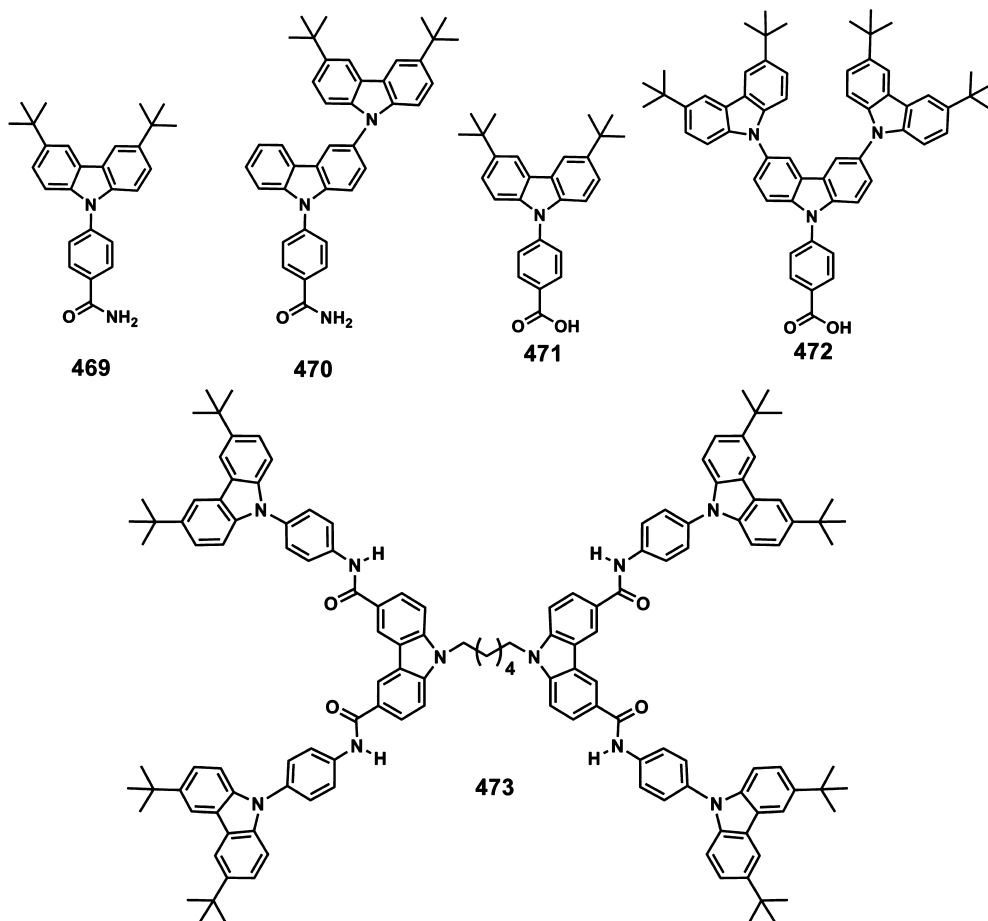


intermolecular hydrogen bonding which inactivates the non-radiative relaxation process.⁹⁶⁵ Das and co-workers have reported the slow organogelation of disk shaped octupolar oxadiazole derivative 475 (Figure 58a) which exhibited a morphological transition from clusters of spheres (H-type aggregates) to fused spheres and finally to fibrous aggregates (J-type aggregates; Figure 58b).⁹⁶⁶ Moreover, the columnar stacking of the molecules in the fibers facilitated efficient excitation energy migration between H- and J-type aggregates

of the same chromophore. An oxadiazole derivative 476a (Figure 58a) formed lyotropic LC and helical fibrous organogel.⁹⁶⁷ Twin tapered bi-1,3,4-oxadiazole derivative 476b (Figure 58a) formed highly fluorescent gel.⁹⁶⁸ Fluorinated organogelators 477a,b (Figure 58a) were obtained by substitution of 5-polyfluoroaryl-3-perfluoroheptyl-1,2,4-oxadiazoles with glycine esters.⁹⁶⁹

The benzoxazole derivative 478 (Chart 118) showed AIEE^{970,971} in the gel state and is a nerve gas sensor exclusively

Chart 117



in the gel state.⁹⁷² A color change from colorless to greenish yellow was observed upon the exposure to nerve gas stimulant such as diethylchlorophosphosphate. The benzoxazole derivatives 479–481 (Chart 118) exhibited AIEE through excited state intramolecular proton transfer.^{973–975} A dramatic enhancement in fluorescence emission of 479 in the gel state assisted by proton transfer between the hydroxyl proton of benzene ring and the nitrogen of the benzoxazole group upon aggregation was observed.⁹⁷³ The formation of a planar keto tautomer of 480 in the gel state due to intramolecular hydrogen bonding resulted in an intense long wavelength emission.⁹⁷⁴ Excited state intramolecular proton transfer in fluorescent gelators 481a,b (Chart 118) resulted in AIEE through J-type aggregated dimers formed by intermolecular hydrogen bonding.⁹⁷⁵

1,3,5-Tris(phenylisoxazolyl)benzene derivatives 482a,b (Chart 118) reported to form organogels via a weak dipole–dipole and π -stack driven columnar arrangement of chromophores into helical nanostructures.^{976,977} The coassembly of 482a,b with the chiral analogues 482d or 482e (Chart 118) controlled the overall supramolecular chirality of the helical gel nanofibers by following Majority Rule and Sergeants and Soldiers principle.^{976,977} In the case of the amphiphilic 1,3,5-tris(phenylisoxazolyl)benzene derivatives 482f,g (Chart 118) gelation was caused by lamellar type self-assembly facilitated by van der Waals interaction of the long alkyl chains and microphase separation induced by triethylene glycol groups.⁹⁷⁸ Introduction of an azobenzene moiety on the 1,3,5-tris(phenylisoxazolyl)benzene core 483 (Chart 118) resulted in the formation of photoresponsive organogels.⁹⁷⁹

5.10. Benzofurans, Benzimidazoles, and Benzothiadiazoles

The benzofuran functionalized derivative 484 (Chart 119) was found to be an efficient gelator of organic solvents.^{638,639,980} Detailed chiroptical, morphological, and molecular modeling studies revealed the formation of a helical assembly, whose helicity directly dependent on the absolute stereochemistry of the pyrrolidine moiety.^{638,639,980} Studies with enantiomers of 484 (Chart 119) suggested an enantiomeric discrimination process during the formation of the gels.⁹⁸⁰ Also, 484 was reported as an efficient excitation energy acceptor in combination with analogous organogelator functionalized with naphthalene group.⁶⁴⁰ A series of fluorescent organogelators 485a–g (Chart 119) consisting of pyridinium salts or amide derivatives of benzimidazole having long alkyl chains have been reported.⁹⁸¹ Hoffmann and co-workers reported the time dependent aggregation properties and phase behavior of aqueous mixtures of the anionic chromophore 486 (Chart 119) and the cationic surfactant cetyltrimethylammonium bromide.^{982,983} Mixing of components with an excess of 486 immediately resulted in the formation of multilamellar vesicles and were stable for many days. After a certain period of time, these turbid vesicular aggregates transformed into clear hydrogels with a tubular morphology.

Cholesterol appended benzothiadiazole dyes 487a–c (Chart 120) self-assembles to form fluorescent organogels.⁹⁸⁴ The gelator 488 exhibited AIEE and smectic LC properties.⁹⁸⁵

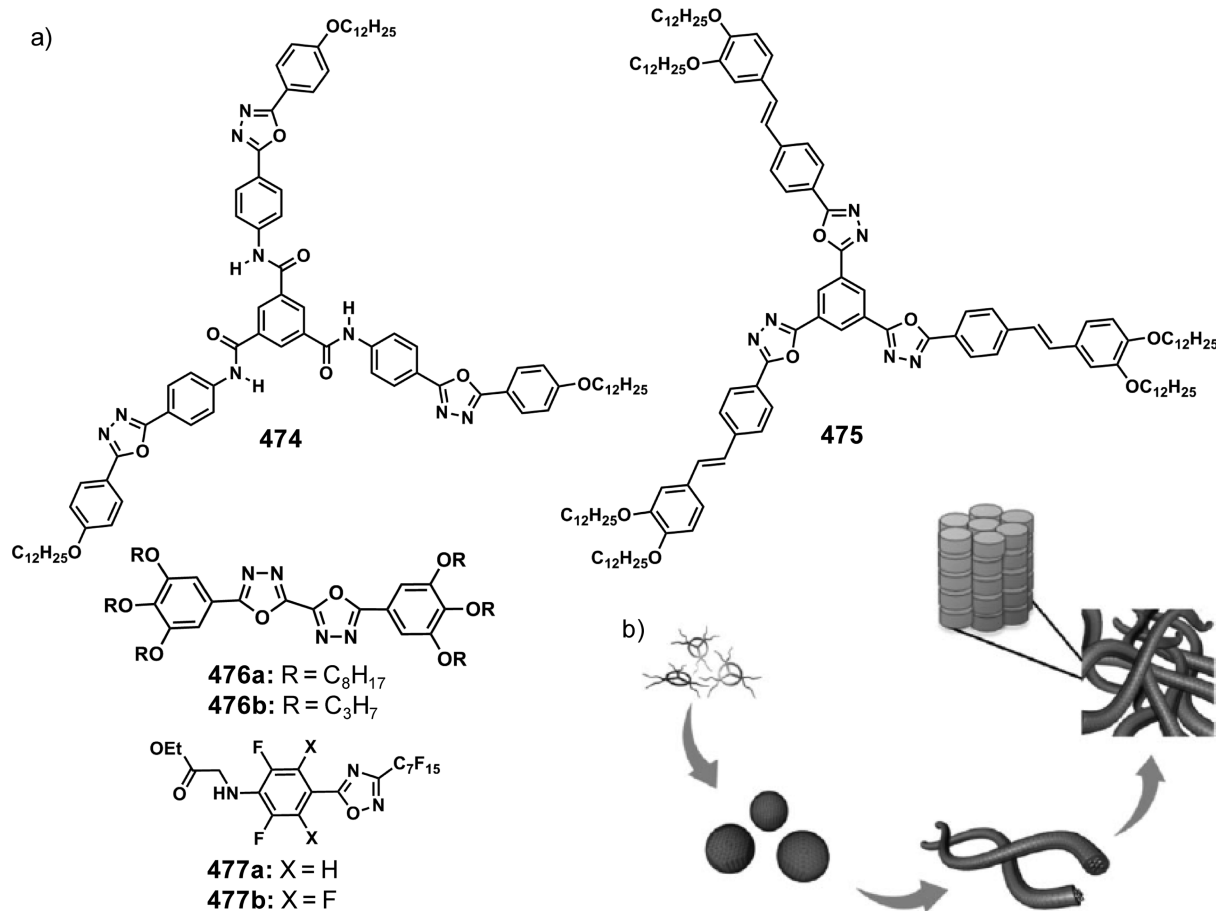


Figure 58. (a) Molecular structures of the oxadiazole derivatives 474–477. (b) Schematic representation of the hierarchical self-assembly of 475. Columnar arrangement of the molecules within the fibers is also depicted. (Reprinted with permission from ref 966. Copyright 2009 Wiley-VCH.)

5.11. Tetrathiafulvalenes

TTF is one of the extensively studied organic conductive materials showing high electron conductivity at the crystal or gel states due to π -stacked columnar structures.^{72,107,986–989} Jørgensen and Bechgaard proposed the concept of self-assembled molecular wires based on a bisarborol functionalized TTF 489a (Chart 121) gel.⁹⁹⁰ High conductivity of the dried gel on quartz plate was achieved through the required unfilled states obtained by doping of iodine to the TTF gel matrix. Bryce and co-workers reported that spin coated films of the tetraarborol functionalized TTF derivative 489b (Chart 121) bearing 24 peripheral hydroxy groups exhibited an in plane dc conductivity value (σ_{rt}) of $10^{-6} \text{ S cm}^{-1}$ which was further increased to $10^{-4} \text{ S cm}^{-1}$ for iodine doped films and $10^{-5}–10^{-4} \text{ Scm}^{-1}$ for tetrabutylammonium perchlorate or hexafluorophosphate doped films.⁹⁹¹ Self-assembly of TTF crown ether phthalocyanine gelator 182 (Figure 32a) led to helical tapes with scrolled molecular architectures and formed CT complex with TCNQ and iodine.⁴⁵⁸ Kato and co-workers reported an electroactive organogelators of TTF moieties functionalized with amino acid, L-isoleucine 490 and 491 (Chart 121) which formed stable fibrous aggregates and gel in aromatic LCs.⁹⁹² The conductivity of the fibrous aggregates of 490 showed a conductivity value of $10^{-5}–10^{-6} \text{ S cm}^{-1}$ TTF core attached to 3,4,5-tridodecyloxy benzene 492 (Chart 121) through a flexible linker containing two amide groups form aggregates and gels in *n*-hexane which upon exposure to I_2 vapor showed a

characteristic near IR absorption band assignable to the dimeric radical cation species.⁹⁹³

A combination of intermolecular hydrogen bonding and CT complex formation has been used to the formation of stable conductive TTF nanofibers. The urea functionalized TTF gelator 493 (Chart 121) could gelate organic solvents after ultrasound treatment and also formed CT gels in presence of electron acceptors such as TCNQ.⁹⁹⁴ A loose gel of 494 (Chart 121) in toluene upon addition of stoichiometric amount of the electron acceptor 2,3,5,6-tetrafluoro-TCNQ yielded a dark colored CT gel with an electrical conductivity of $5.0 \times 10^{-4} \text{ S cm}^{-1}$.⁹⁹⁵

Amabilino et al. reported an amide functionalized TTF derivative 495 (Chart 122) which forms stable gels. Upon exposure to iodine vapor, these gels exhibited characteristic bands corresponding to CT and mixed valence states.⁹⁹⁶ Current sensing AFM studies revealed *I*–*V* response corresponding to the bright areas with an apparent metallic character and the dark areas corresponding to the semiconductor character with a wide gap. By controlling the temperature of the iodine doping and post doping treatments, four different phases (α , β , γ , and δ) of TTF based nanofibers were identified.⁹⁹⁷ A hybrid gel of 495 (Chart 122) and 496 could include Au nanoparticles within the fibers having metallic behavior (10 S cm^{-1}).⁹⁹⁸ The chemical oxidation of a hybrid gel composed of 495 and oleate coated magnetic iron oxide nanoparticles by exposing to iodine vapor exhibited better electrical conductivity when the proportion of nanoparticles

Chart 118

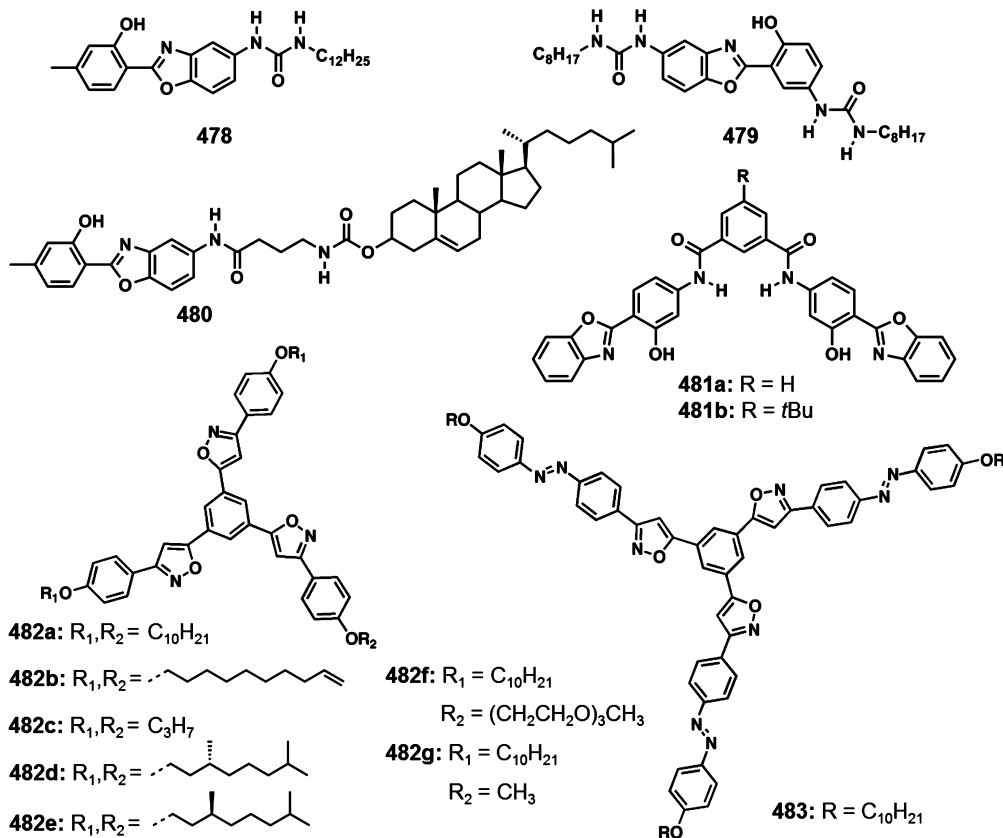
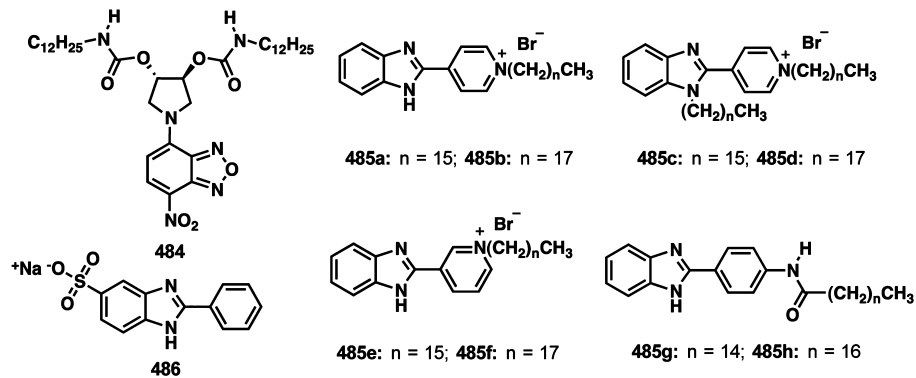


Chart 119



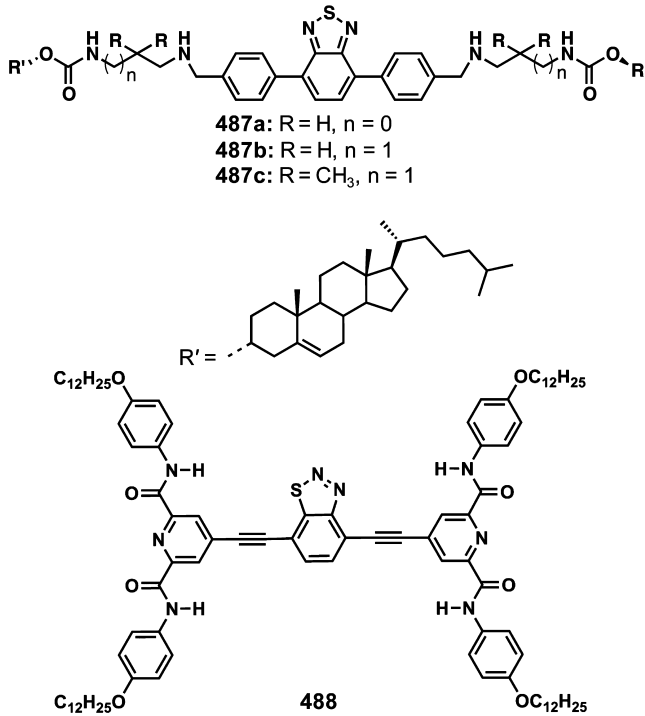
were very low.⁹⁹ In the doped xerogels of **497** (Chart 121) from (*S*)-limonene exhibited less resistance for the bulk conduction when compared to that from *n*-hexane.¹⁰⁰⁰ The dissimilar organization of molecular unit in the fibers created differences in the electrical properties.

Organogel based on C₃ symmetrical TTF derivative **498** (Chart 122) exhibited a mixed valence state capable of charge transport, when the xerogel was doped with iodine vapors.¹⁰⁰¹ Another chiral C₃ symmetrical TTF derivative **499** (Chart 122) exhibited supramolecular chirality as revealed by CD spectroscopy and morphological analysis.^{1002,1003} The CD spectra of the enantiomers of **499** showed mirror image relationship. When a solution of **499a** with a negative band CD was deposited onto quartz, the resulting CD spectrum of the solid exhibited positive bands with all the same features (Figure 59a).¹⁰⁰² The slow cooling of a solution of **499a** resulted in

precipitate with an unprecedented morphology of short scrolls. The end view showed the presence of rolled up structures made up of sheets (Figure 59b,c).¹⁰⁰² Detailed understanding of the coassemblies of **498** and **499** revealed that since the energy difference between the two helical senses becomes negligible, the presence of a wrong enantiomer in the coassembled helix nullifies the majority rule effect.¹⁰⁰³ The TTF based gelator **500** (Chart 122) forms tapes with a conductance of approximately 0.3 nS.¹⁰⁰⁴

An amphiphilic bisTTF annulated macrocycle **501** (Chart 123) is reported to form redox active organogels as well as electrically active nanostructures such as nanowires and size controllable nanodots.¹⁰⁰⁵ Iyoda et al. reported solvatochromism exhibited by the carboxylic acid derivative **502** (Chart 123) in the gel state and electrical conductivity of double and triple helical fibers of perchlorate doped bis(octadecylthio)-TTF-

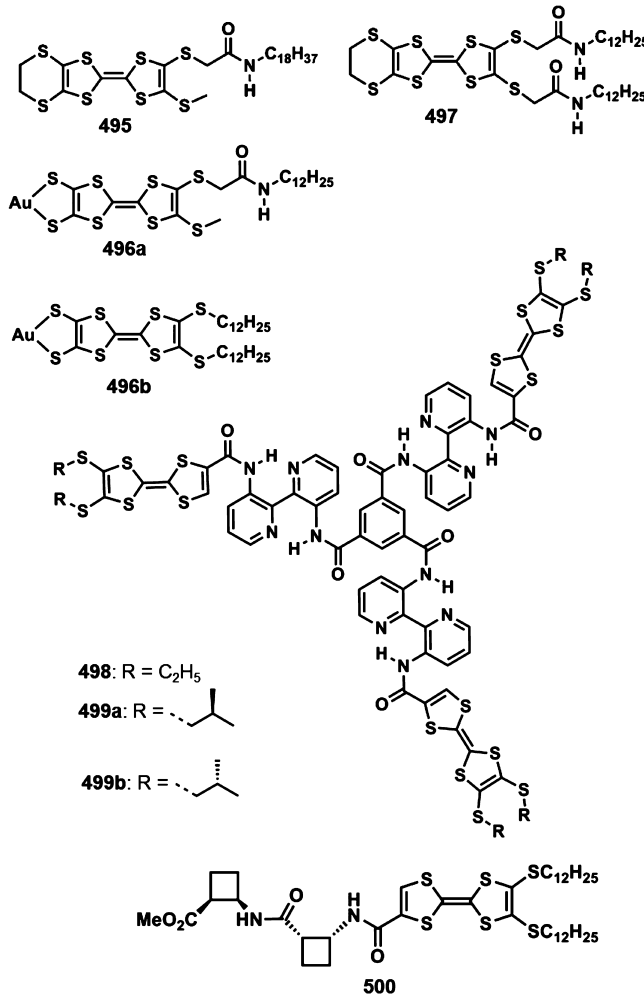
Chart 120



diamide 503 (Chart 123).^{1006,1007} Among the semiconducting TTF based gel fibers of 504 and 505 (Chart 123), the cholesterol appended gelators 504b and 505b exhibited higher thermal stability than corresponding alkoxy benzene analogues 504a and 505a.¹⁰⁰⁸ The gelator 504 bearing two TTF units exhibited enhanced gelation ability as well as higher conductivity when compared to those of the gelator 505.

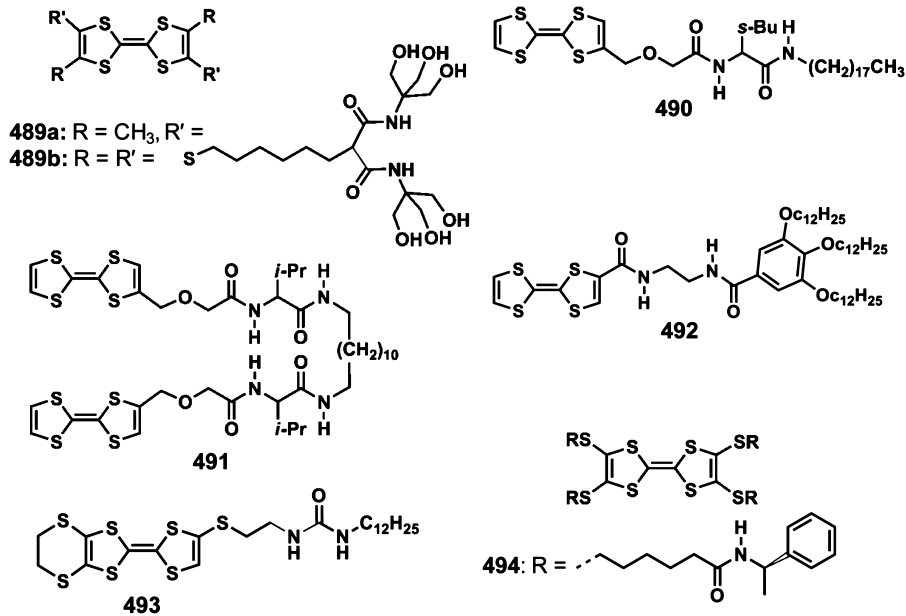
A cholesterol appended TTF derivative 506 (Chart 124) formed stimuli responsive organogels in the presence of ultrasonic sound.¹⁰⁰⁹ The redox activity of the TTF moiety has been coupled with the photochemical properties of an azobenzene moiety allowing both redox and photocontrol of

Chart 122



the electronic properties of the conducting gels.¹⁷⁴ Stoddart and co-workers investigated the switching properties, gelation

Chart 121



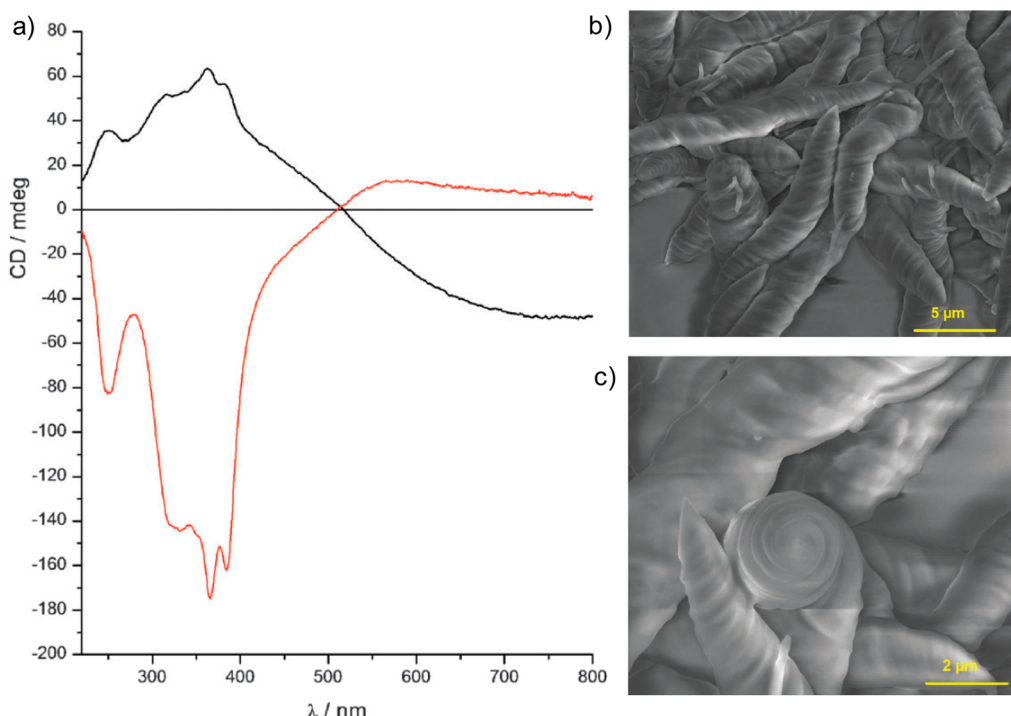
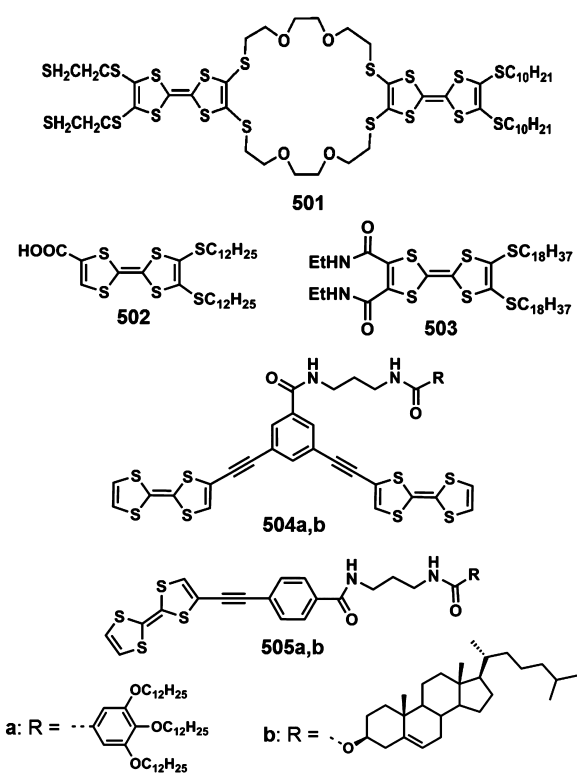


Figure 59. (a) CD spectra of **499a** in the film state (positive bands at 350 nm) and in dioxane solution state (negative band at 350 nm). (b and c) SEM images of the microcroissants formed by **499a** upon slow cooling of a dioxane solution of the compound. (Reprinted with permission from ref 1002. Copyright 2012 The Royal Society of Chemistry.)

Chart 123



addition of C₆₀ or PCBM due to the intermolecular 2:1 CT complex formation (Figure 60) and led to reproducible cathodic photocurrent.¹⁰¹⁰ It has been reported that ionically conductive gels of neutral TTF and TCNQ can be prepared by mixing and mechanical grinding in ionic liquids.¹⁰¹¹ The xerogels of TTF gelator with a dendron substituent **508** (Chart 124) exhibited rope-like frame works.¹⁰¹² As the solvent polarity was increased, the rope-like self-assembly structures of **508** changed into nanofibers.

5.12. Miscellaneous Gelators

Octahydroxypyridine[4]arenes form complexes with suitable molecules such as 2-aminonaphthyridine **509** (Chart 125) which in apolar media gave gel-like aggregates when mixed at a ratio of 1:4.¹⁰¹³ Lumichrome **510** (Chart 125) and melamine produced thermoreversible hydrogel in 3:1 and 1:1 compositions by the formation of a planar structure suitable for π-stacking through hydrogen bonds.¹⁰¹⁴ A phenothiazine based D-π-A type gelator **511** (Chart 125) formed gels upon ultrasonication, and exhibited tunable luminescence due to twisted intramolecular CT.¹⁰¹⁵ In addition, an unusual blue-shifted AIEE has been observed due to the suppression of the twisted intramolecular CT in the gel phase.

A series of monocholesterol substituted quinacridone derivatives **512a–c** (Chart 126) were reported to form organogels upon ultrasound irradiation.¹⁰¹⁶ The morphology of **512a** xerogel displayed a 3D sponge-like nanostructure, **512b** showed regular 3D fibrous network consisting of entangled bundles of fibers, and **512c** displayed partially fused and closely arranged 3D network by bundling of thinner fibers. The stimuli responsive urea functionalized quinacridone gelators **513a,b** (Chart 126) were found to form organogels under sonication.¹⁰¹⁷ The cholesterol appended quinacridone derivatives **514a,b** (Chart 114) formed stable organogels in a wide

behavior, and self-organization of a cholesterol stoppered bistable [2]rotaxane consisting of TTF and 1,S-dioxynaphthalene **278** (Chart 68) and its complex with cyclobis(paraquat-p-phenylene).⁶⁴³ The gelation ability of the ex-TTF derivative **507** (Chart 124) could be significantly improved after the

Chart 124

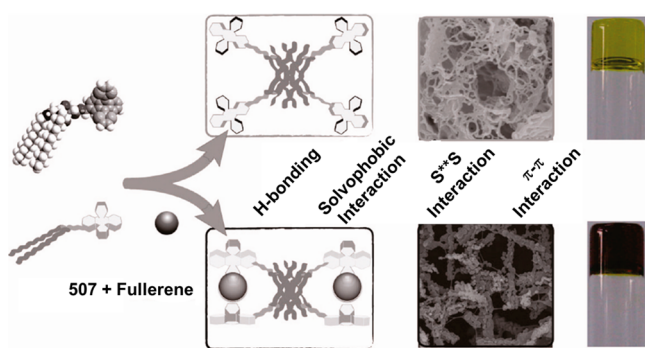
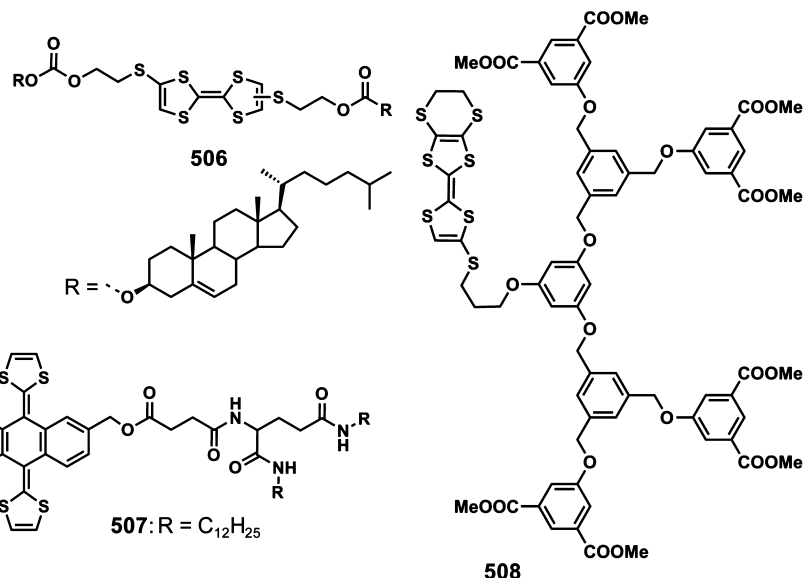
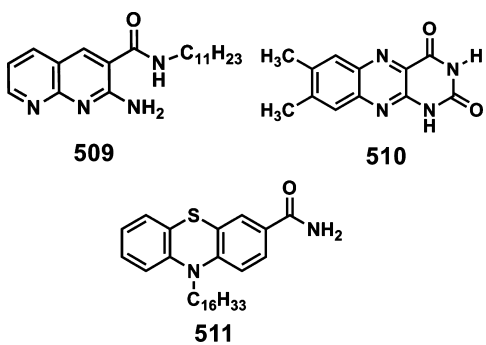


Figure 60. Schematic illustration of the possible molecular assembly mechanism for **507** in the absence and presence of C_{60} . (Reprinted with permission from ref 1010. Copyright 2010 American Chemical Society.)

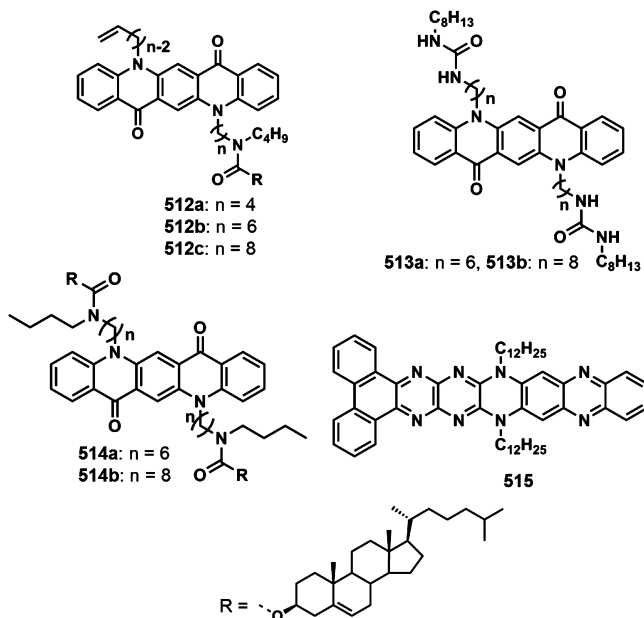
Chart 125



range of organic solvents upon ultrasound treatment and displayed reversible fluorescence switching due to mechano-chromism.¹⁰¹⁸ The large planar aromatic structure of **515** (Chart 126) assists the linear molecular stacking and as a result, organogels consisting of fibrous structures were formed.¹⁰¹⁹

The gel fibers of triphenylene fused triazatruxene **516** (Chart 127) exhibited a charge carrier mobility of $0.8 \text{ cm}^2 \text{ V}^{-1} \text{ s}^{-1}$.¹⁰²⁰ The C_3 -symmetrical heteroaromatic hexaazatrinnaphthylene gelators **517a,b** (Chart 127) are super gelators.¹⁰²¹ The hexaazatrinnaphthylenes **518a,b** (Chart 127) functionalized

Chart 126



with alkylamides afforded self-organized nanowires leading to gels through amide hydrogen bonding.¹⁰²² The self-assembled nanostructures formed on the substrate surface have been used for the creation of desired patterns by microcontact printing followed by postpolymerization.

The hexaazatriphenylene based gelator **519a** (Chart 128) exhibited excellent gelation ability and high selectivity toward Ag^+ ion.¹⁰²³ The soft regions from the flexible aromatic side chains and the hard regions of the hexaazatriphenylene core cooperatively stabilize the LC phase and the supramolecular structures of the gelators **519b-e** (Chart 128).¹⁰²⁴ In addition, chiral gels with mirror image CD signals were formed in chiral solvents such as (*R*)- and (*S*)-1-phenylethyl alcohols. Triazine derivatives containing urea motif, **520a,b** (Chart 128) showed blue fluorescence and J-aggregation in decalin whereas in CCl_4 fluorescence was quenched due to π -stacking.¹⁰²⁵ The disk shaped triazine triamides **521a-d** (Chart 128) self-assembled

Chart 127

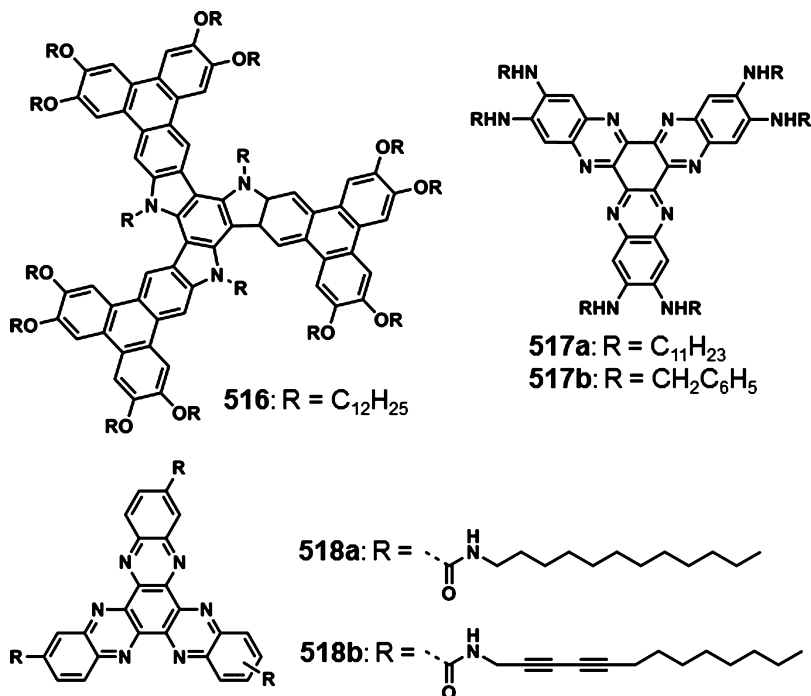
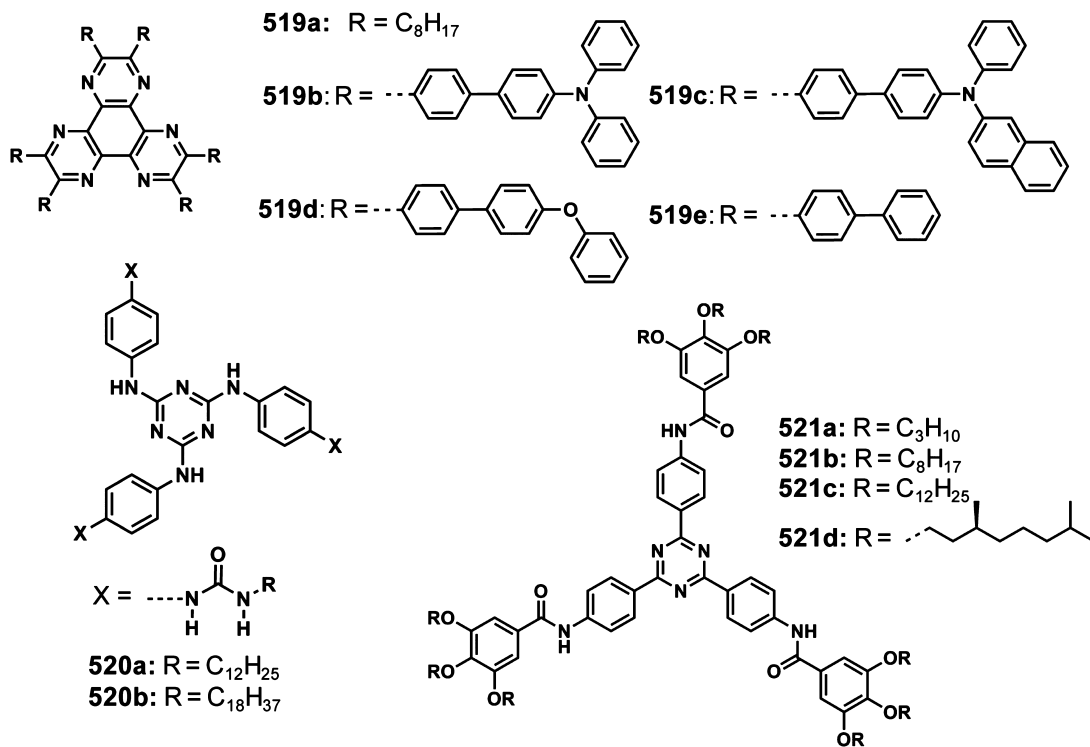


Chart 128

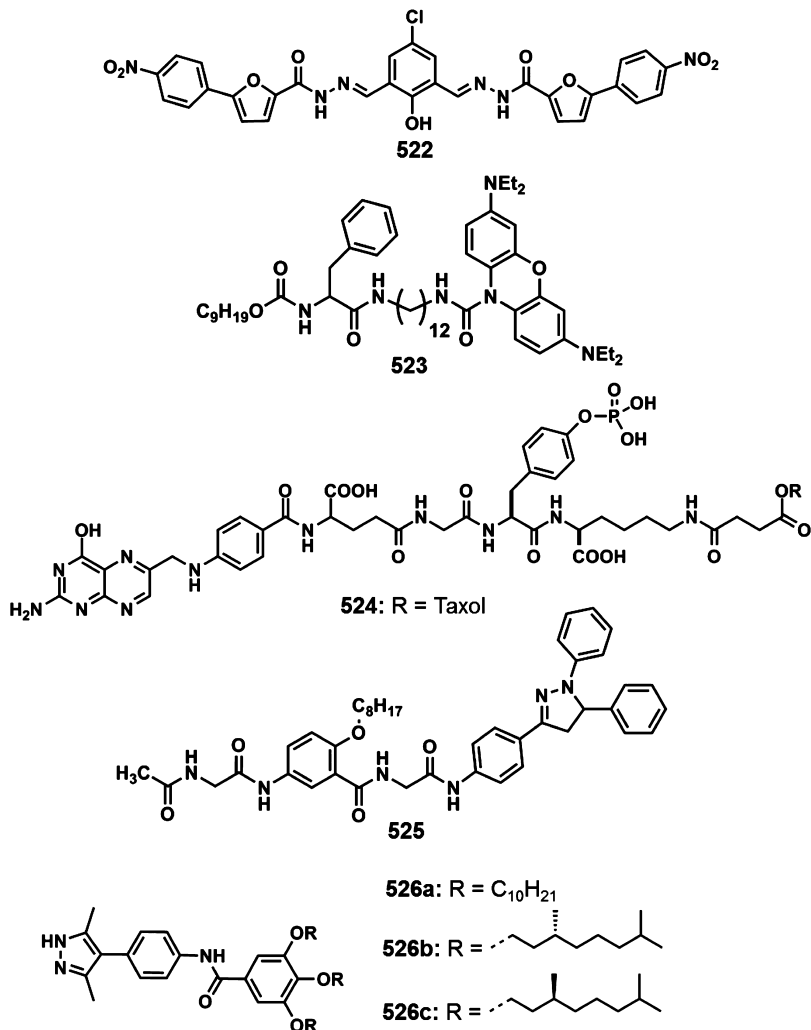


to form organogels in nonpolar solvents via helical columnar aggregates through π -stacking interactions of the triphenyltriazine moieties, hydrogen bonding interactions of the amide groups and van der Waals interactions provided by the alkyl groups.¹⁰²⁶

Wei et al. reported that the gelator 522 (Chart 129) exhibits two channel proton controlled reversible gel–sol transition and color change, due to the phenolic O–H and the acylhydrazone N–H groups.¹⁰²⁷ A leuco phenoxazine gelator containing L-

phenylalanine 523 (Chart 129) showed sensitivity to γ rays and used for imaging in heavy particle radiotherapy.¹⁰²⁸ The taxol derived gelator 524 (Chart 129) formed biocompatible hydrogels consisting of highly uniform nanospheres.¹⁰²⁹ Triarylpypyrazoline derivative 525 (Chart 129) having quadruple hydrogen bonding motif formed molecular duplex, forming a continuous 3D entangled gel network.¹⁰³⁰ LMOGs based on tialkoxybenzamide functionalized 4-arylpypyrazole derivatives 526a–c (Chart 129) showed GIEE.¹⁰³¹

Chart 129



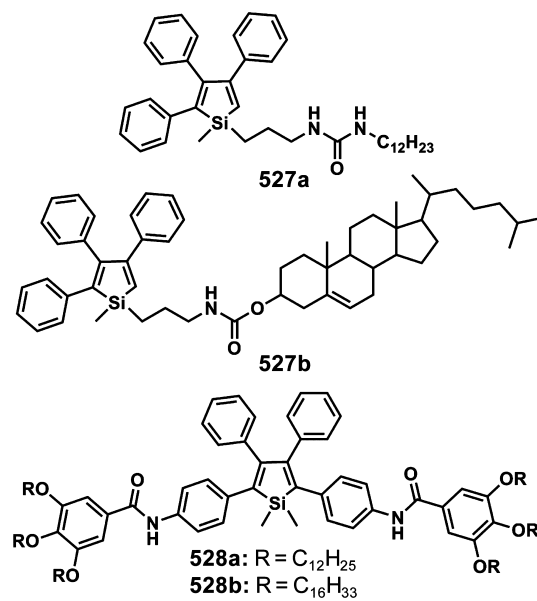
Thermally driven fluorescence switching was exhibited by the silole derivatives **527a,b** (Chart 130) due to AIEE feature.¹⁰³² The 2,3,4,5-tetraphenylsilole based organogelators **528a,b** (Chart 130) functionalized with long chain alkoxydiacylamido moiety formed stable LC phases over a wide temperature range.¹⁰³³

Bone marrow stromal cells encapsulated in the hydrogels formed by the click reaction between azido functionalized poly(ethylene glycol)-co-polycarbonate macromers and dibenzocyclooctyne functionalized poly(ethylene glycol) exhibited cellular viability.¹⁰³⁴ Upon addition of a solution of poly(butyl methacrylate) containing deazaguanosine, the clear, free-flowing solution of polystyrene with 2,7-diamido-1,8-naphthyridine became a viscous gel.^{1035,1036}

6. OLIGOMERIC π -SYSTEMS BASED GELS

The synthesis and study of linear π -conjugated systems is of great interest due to their importance in organic electronics.^{7,1037} Extended π -conjugated molecules, by virtue of the combination of delocalized π -electrons and unique nanostructures, are the integral part of organic electronic devices.^{1038,1039} A large variety of linear π -conjugated polymers and oligomers of phenylenes, phenylenevinylenes, phenyleneethynylanes and thiophenes have been extensively investigated.^{113,1040,1041} Detailed studies revealed that electron and

Chart 130



energy transport properties in these molecules are strongly influenced by the intermolecular interaction and self-assembly

of the individual molecules.^{1042,1043} One of the ways to achieve molecular alignment is through self-assembly using noncovalent forces such as hydrogen bonding, π -stacking, electrostatic and van der Waals interactions.^{7,122,1037} The appropriately functionalized monodisperse oligomers of small π -conjugated molecules are preferred for the creation of molecular self-assemblies due to the structural clarity and control over self-assembly. In recent years, a variety of supramolecular structures such as tapes, fibers, rods, helices, particles, vesicles and toroids with varying sizes (nm– μ m) of various π -conjugated molecules and their performance in electronic devices have been investigated.

6.1. Thiophenes

Thiophenes are one of the most widely studied molecules among large number of π -conjugated systems. Owing to their high charge carrier mobility and chemical stability, conjugated oligomers and polymers of thiophenes have been used in applications such FETs, LEDs, PVDs, and chemical sensors.^{1044,1045} The self-assembly and organogelation of thiophene derivatives have attracted much attention. Self-organization of thiophene based systems is more attractive due to their enhanced charge transport properties.¹⁰⁴⁵ The properties and performance of these materials not only depend on the electronic structure of the molecules, but also on the molecular packing in the resulted supramolecular assemblies.^{1046,1047} The developments in the area of thiophene based organogels enabled highly conducting nanowires.¹⁰⁴⁸ This session summarizes the self-assembly and gelation features of thiophene based systems.

The bisurea appended oligo(thiophene)s **529a,b** (Chart 131) self-assemble in solvents such as tetralin and 1,2-dichloroethane leading to the formation of organogels.¹⁰⁴⁹ The xerogels of **529a,b** showed high charge carrier mobilities of 0.001 and

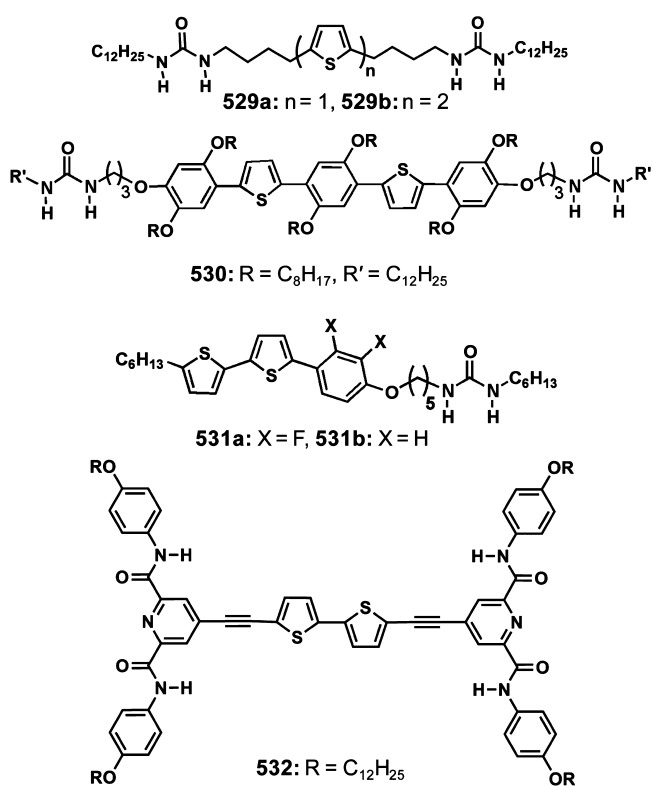
0.005 cm²/(V s), respectively. Thiophenes have been used as pendant groups with optically pure *trans*-1,2-diaminocyclohexane and 1,2-diaminobenzene.¹⁰⁵⁰ Self-assembly of these molecules through hydrogen bonded network between urea moieties form elongated and thin fibers, eventually leading to 3D network, inducing the gelation of the solvent.^{1051,1052} The extended π -system containing alternate thiophene and dialkoxybenzene moieties **530** (Chart 131) formed 1D self-assembly leading to gel formation.¹⁰⁵³ The presence of two urea groups assists the overlapping of the π -conjugated segment toward gelation with card pack orientation of the phenylenethienylene chromophores. The electrostatic force microscopy study of the self-assembled objects revealed that **530** is a good electron donor and hence can be easily oxidized. Kato and co-workers have reported fibrous aggregates formation of the laterally fluorinated phenylbithiophene molecule **531a** (Chart 131).¹⁰⁵⁴ The alignment of fibrous aggregates of **531a** under electric field resulted in the formation of aligned photoconductive fibers. In contrast, the nonfluorinated gelator **531b** (Chart 131) was not able to form aligned fibers under the AC electric field. The super gelator **532** exhibited AIEE upon self-assembly via hydrogen bonding assisted π -stacking (Chart 131).⁹⁸⁵

The microphase segregation of diblock polymers during self-assembly has been used to design electronically active gels of the oligo(thiophene) based dendron rod-coil molecule **533** (Figure 61).¹⁰⁵⁵ The iodine doped films of **533** prepared from toluene gel exhibited a conductivity value of 7.9×10^{-5} S cm⁻¹ whereas that of the monomer solution showed only 8.0×10^{-8} S cm⁻¹. Moreover, uniaxially aligned ribbon nanostructures have been obtained by the shear force alignment in the presence of an AC field (Figure 61).

Self-assembly of thiophenes can be facilitated by attaching peptides and other structure directing multiple hydrogen bonding moieties such as melamine and cyanurates. Tovar et al. have reported the self-assembly and gelation of **534** (Figure 62) in aqueous and physiologically relevant environments.¹⁰⁵⁶ The surface morphology of the gel showed entangled 1D structures of bithiophene unit in the twisted chiral environment generated by the β -sheet interactions. The aggregation mediated by the π -stacking of the thiophene moiety enabled charge transport or exciton delocalization in the resulted nanostructures. An on-resin dimerization based method has been developed to incorporate π -electron units into peptides.⁴³² The peptide appended thiophene oligomers **535a,b** (Figure 62) thus prepared were found to assemble into amyloid-like supramolecular polymers at low pH, leading to the formation of self-supporting hydrogels. Recently, Stupp and co-workers have reported a method involving the injection of a solution containing LC assembly of peptide amphiphiles into a salt solution resulting in highly aligned macrostructures over centimeter size domains.¹⁰⁵⁷ Shear force induced macroscopic alignment of the amphiphile nanostructures facilitated the formation of aligned macrostructures of **536** (Figure 62) from its hydrogel.¹⁰⁵⁸ The macrostructures thus obtained showed an anisotropy in hole mobility due to the orientation of the π -stacked channels of active organic semiconductors.

Stupp and co-workers have shown the gelation of quinque thiophenes **537** and **538** (Chart 132) functionalized with the β -sheet forming amino acid residues lysine and leucine.¹⁰⁵⁹ These gelators formed self-supporting gels in water, composed of self-assembled 1D nanofibers of a π -stacked thiophene core with amino acids on the periphery. The

Chart 131



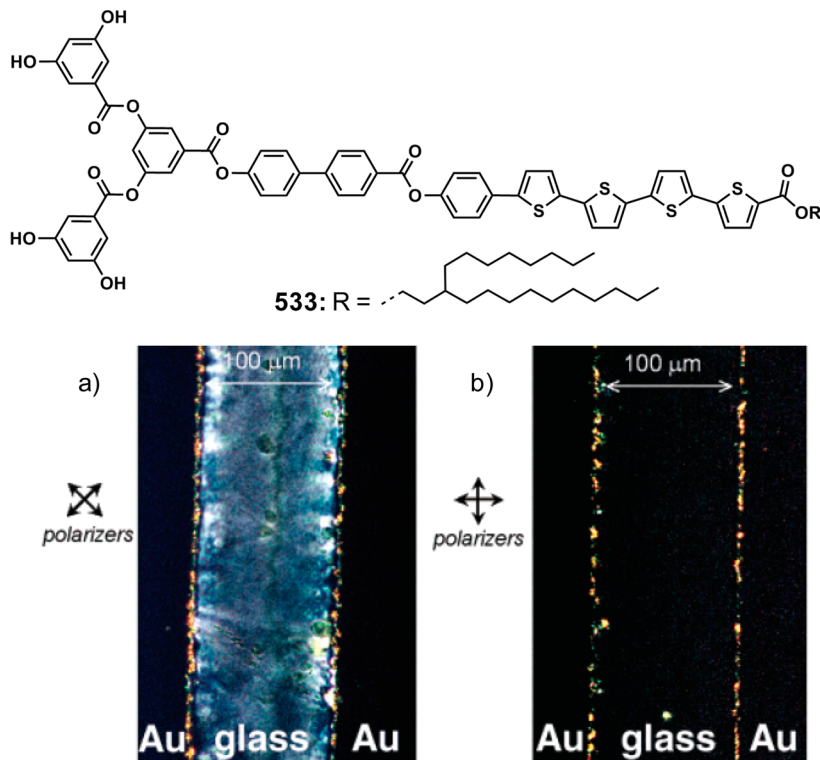


Figure 61. POM of an AC field aligned film of **533**. The film switches from light (a) to dark (b) with a 45° rotation between crossed polarizers, indicating uniaxial orientation of the optic axis of the film. (Reprinted with permission from ref 1055. Copyright 2004 American Chemical Society.)

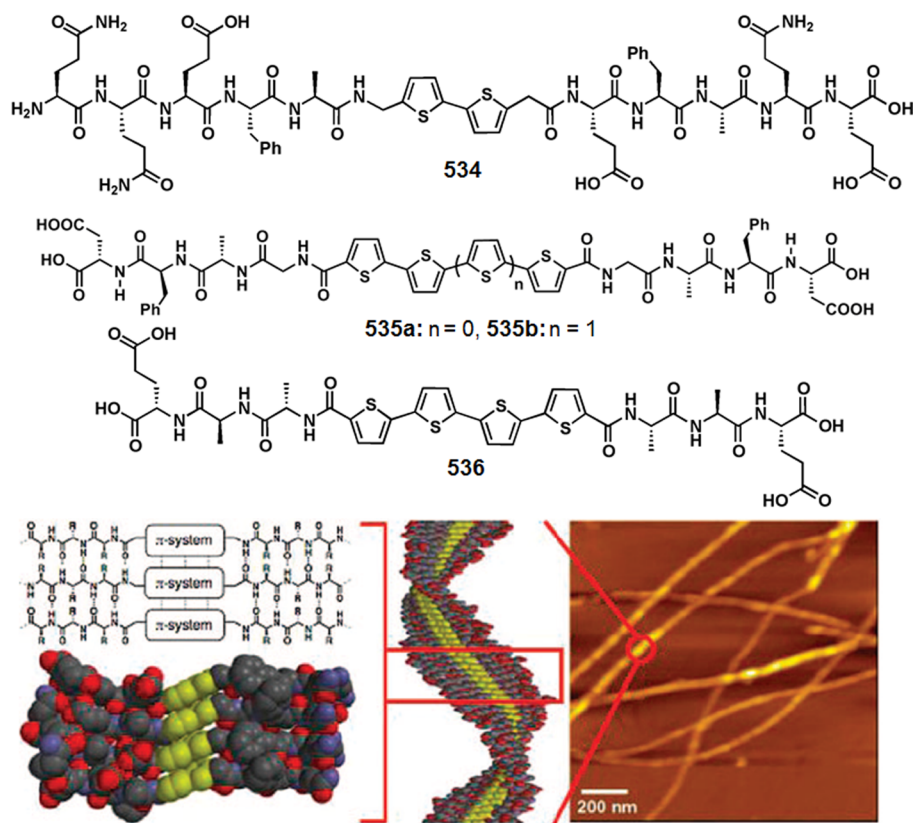
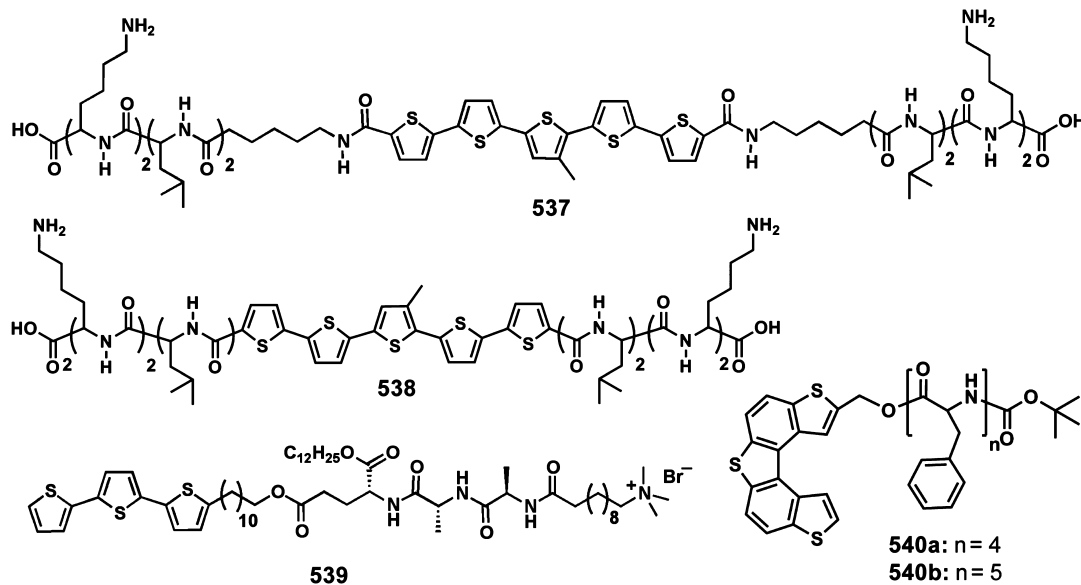


Figure 62. Energy minimized illustration of β -sheets and π -stacks of **534** as line drawings and space-filling models (left, thiophenes in yellow), the helical twist sense along a model aggregate (center) and AFM image of helical assembly (right). (Reprinted with permission from ref 1056. Copyright 2008 American Chemical Society.)

Chart 132



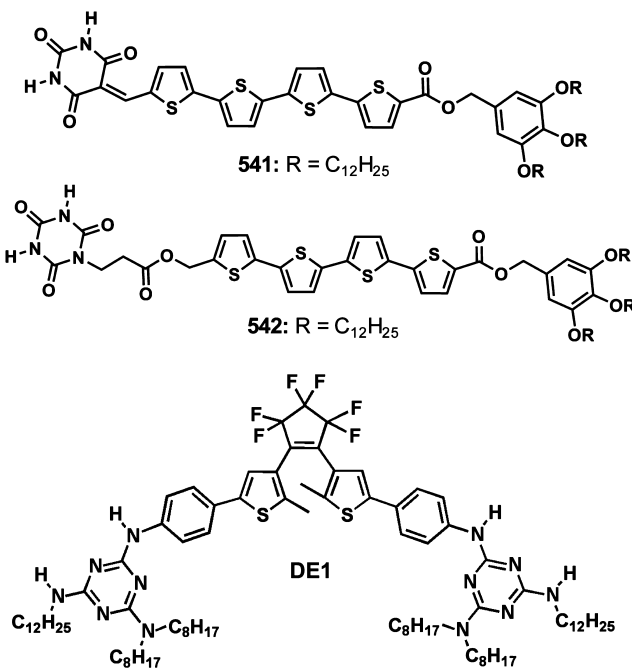
addition of a very small volume of water into a solution of 539 (Chart 132) in chlorocyclohexane resulted in a self-supporting gel composed of twisted, helical self-assembled nanofibers.¹⁰⁶⁰ The formation of β -sheet structures induce chirality in terthiophene unit and hence led to high aspect ratio left handed helical nanofibers with uniform diameter and pitch. The peptide functionalized thiaheterohelicenes 540a,b (Chart 132) formed stable transparent gels, exhibiting an interconversion of the helical sense in the gel state when compared to that in solution.¹⁰⁶¹ This could be attributed to the consequence of intra- and intermolecular interactions present in the gel and solution states, respectively.

The barbituric acid functionalized quaterthiophene based gelator 541 (Chart 133) and the complementary bismelamine

receptor BM12 (Chart 34) formed supramolecular copolymers through complementary hydrogen bonds resulting in uniform rod-like nanostructures and gels.¹⁰⁶² Irradiation of the xerogel using a laser pulse ($\lambda = 355$ nm) resulted in the generation of long-lived charge carriers showing maximum transient conductivities ($\Phi \sum \mu$) of $1.0 \times 10^{-4} \text{ cm}^2 \text{ V}^{-1} \text{ s}^{-1}$ for 541 and $0.67 \times 10^{-4} \text{ cm}^2 \text{ V}^{-1} \text{ s}^{-1}$ for the coassembly. The cyanuric acid functionalized quaterthiophene 542 (Chart 133) self-assembled to form helical ribbons which transformed into twisted ribbons upon complexation with a complementary bismelamine receptor B1 (Chart 34).¹⁰⁶³ The hierarchical self-organization of the flexible quasi 1D copolymers formed by 542 and DE1 (Chart 133) led to helical nanofibers and gels.¹⁰⁶⁴ This is due to the conformational flexibility of DE1 and the resulting supramolecular polymers to fold and intertwine into thermodynamically stable helical nanofibers.

A series of redox responsive chiral gels based on quater-, quinque-, and sexi-thiophenes 543a–c (Figure 63) bearing cholesteryl groups at the α -position have been reported.¹⁰⁶⁵ In addition to the unique thermochromic properties, sol–gel phase transition has been achieved by the addition of oxidizing and reducing reagents such as FeCl₃ and ascorbic acid, respectively. The TEM and SEM images have displayed well developed network structures composed of helical fibrous aggregates of 543a (Figure 63a–c). Addition of the corresponding perylene bisimide derivative 167a (Figure 26) into 543a resulted in a self-sorting organogel of two different π -conjugated molecules with p-n heterojunctions (Figure 63d).⁴¹⁸ The variable temperature UV-vis and CD spectral studies of the coassembly revealed that both derivatives self-assemble independently (self-sorting)¹⁰⁶⁶ and do not interfere in each other's aggregation–dissociation process. The gelation properties of the crown appended quaterthiophene derivative 544 (Figure 63) was also investigated.¹⁰⁶⁷ The helicity of the fibrous assembly of 544 has been controlled by using the crown-ammonium interaction between 544 and chiral 1,2-bisammonium guest.¹⁰⁶⁸ The chiral memory induced by the thermal gelation was found to erase completely by thixotropic gelation caused by the application of mechanical stress.

Chart 133



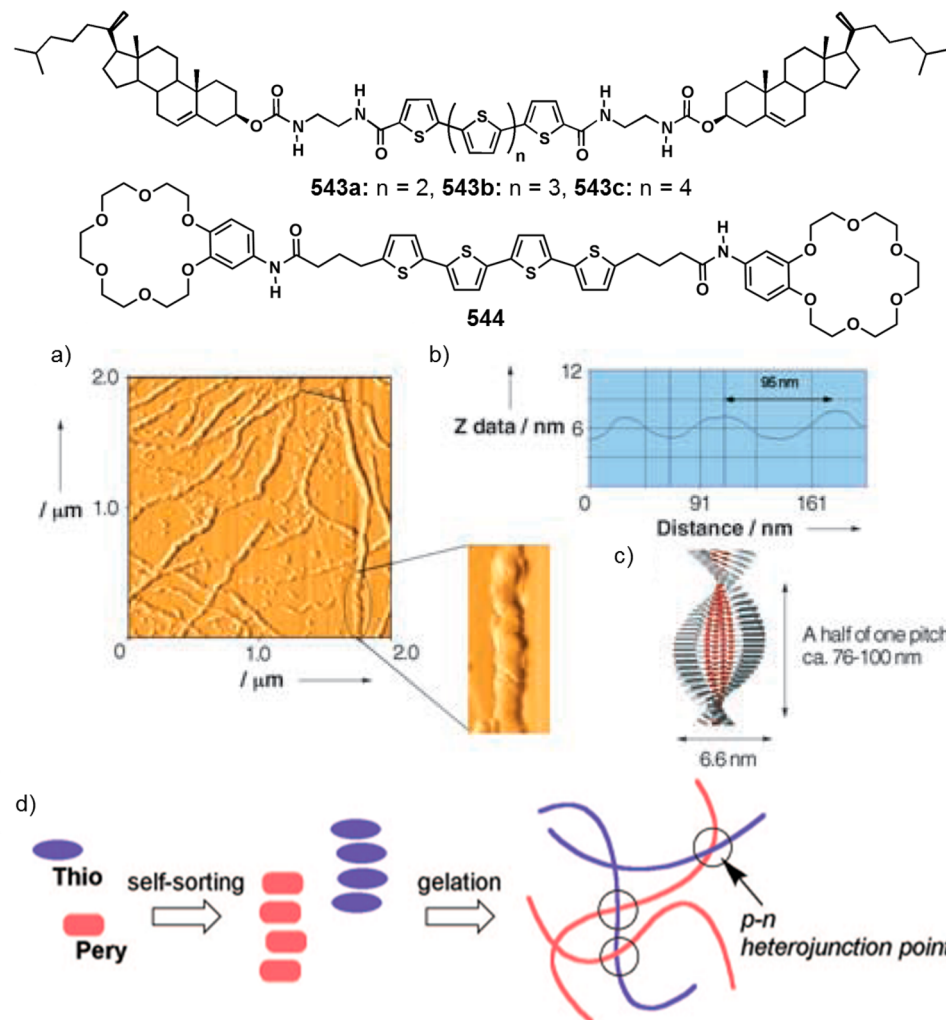


Figure 63. Chemical structures of the gelators **543** and **544**. (a) AFM image of **543a**, (b) height profile along the solid line in panel a, and (c) schematic illustration of the helical fiber of **543a**. (d) Schematic representation showing the formation of self-sorting organogel composed of **543a** and **167a** yielding p-n heterojunction points. Panels a–c reprinted with permission from ref 1065. Copyright 2005 Wiley-VCH. Panel d reprinted with permission from ref 418. Copyright 2008 American Chemical Society.)

Würthner and co-workers have reported the self-assembly and gelation of the bis(trialkoxybenzamide) functionalized quaterthiophene derivative **545** (Chart 134).¹⁰⁶⁹ The TRMC measurements of the quaterthiophene fibers showed a mobility of $4.2 \times 10^{-3} \text{ cm}^2 \text{ V}^{-1} \text{ s}^{-1}$ after annealing. Organogels of the quaterthiophene **546a** and the quinquethiophene **546b** (Chart 134) were composed of ordered 1D nanoassemblies with conducting properties.¹⁰⁷⁰ The four point probe conductivity of **546b** film was $9.9 \pm 1.7 \times 10^{-6} \text{ S cm}^{-1}$, whereas the hole mobility of **546b** in a top contact thin film transistor was $2.34 \times 10^{-7} \text{ cm}^2 \text{ V}^{-1} \text{ s}^{-1}$.

Stupp and co-workers have demonstrated that at high concentrations, **546c** (Chart 134) could gelate toluene by forming interpenetrating networks of fibers.¹⁰⁷¹ Polymorphism was shown by **546c** as rapid and slow evaporation of the solvent led to kinetically trapped fiberous mats and rhombohedra or hexagonal prisms, respectively. FETs have been fabricated from self-assembled organogels of hairpin shaped thiophene derivative **547** (Chart 134).¹⁰⁷² The interfacial contact between donor and acceptor molecules (PCBM) has been enhanced due to the grooved nature of the self-assembled nanowires of **547** and hence improved PVD efficiency after annealing.¹⁰⁷³ The self-assembled thiophene

based azomethine oligomer **548** (Chart 134) showed intrinsic charge transport properties and exhibited a value of $\Sigma \mu_{\min} = 1 \times 10^{-2} \text{ cm}^2 \text{ V}^{-1} \text{ s}^{-1}$ with a half-life time of $10 \mu\text{s}$.¹⁰⁷⁴

Park et al. have prepared high aspect ratio 1D nanowires from the fused thiophene derivative **549** (Figure 64).¹⁰⁷⁵ Space charge limited current measurement showed μ_{eff} values of 0.11 and $3.1 \text{ cm}^2 \text{ V}^{-1} \text{ s}^{-1}$ for the spin- and drop-cast films, respectively. High contrast fluorescence switching was observed when **549** was coassembled with a photochromic molecule due to highly efficient intermolecular energy transfer.¹⁰⁷⁶ The amide end-capped triphenylenevinylene gelators **550a,b** (Figure 64) exhibited epitaxial self-assembly resulting in the formation of oriented 1D fibers (**550a**) and interconnected short wires with T-junctions (**550b**; Figure 64a,b).¹⁰⁴⁸ The enhanced conductivity observed in the case of **550b** could be due to the formation of hydrogen bonded 1D assemblies and the relatively better gelation efficiency of **550b** when compared to that of **550a**. Organogels with high conductivity was obtained by extending the conjugation length of the oligo-(thienylenevinylene) gelators **550c,d** (Figure 64).¹⁰⁷⁷ Conductive AFM measurements indicated that the conductance of 0.93 nS observed for the undoped fiber bundles of **550d** was drastically increased to 7.1 nS upon doping with iodine vapors

Chart 134

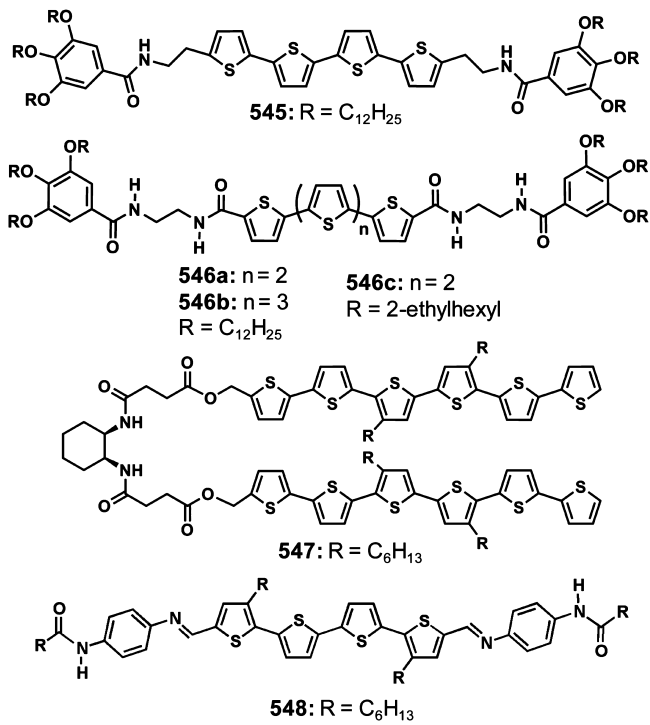


(Figure 64c,d). A nonplanar macrocycle **551** (Figure 64) obtained by unsymmetrically connecting two terthiophene skeletons with two flexible alkylene linkers formed stable organogels.¹⁰⁷⁸

A ladder type π -conjugated phosphole modified pentathienoacene **552** (Chart 135) self-assembles into 1D fibers and organogels using intermolecular π – π stacking, dipole–dipole, and van der Waals interactions.¹⁰⁷⁹ Gelators with extended

dithienophosphole derivatives **553a–c** (Chart 135) could gelate organic solvents at room temperature.¹⁰⁸⁰ The gelator **553b** with larger and rigid dendrons exhibited dramatic emission color changes from yellow to orange red upon gelation. In addition, the gelator **553b** exhibited electrochromism. The symmetrically π -extended phosphonium salts **554a–c** (Chart 135) formed emissive organogels due to the intramolecular CT from the terminal aryl groups to the phosphonium core.^{1081,1082} In contrast to other organogels with planar conjugated backbone, no red-shifted or broadened emission has been observed in the gel phase. A mechanically responsive energy transfer has been exhibited by films of **554a** and **554b** with rhodamine B and the donor emission was completely recovered by thermal annealing of the ground film.

Lee and co-workers and Stupp and co-workers^{1072,1073} have reported the fabrication of FETs from self-assembled organogels of thiophene derivatives. The FET and solar cell performance of α -helical polypeptide functionalized thiophene gelator **555** (Chart 135) and PCBM (1:2) exhibited enhanced hole mobility, efficiency and short circuit current due to the helical arrangement of the chromophores.¹⁰⁸³ Solution processed FETs of polythiophenes exhibited excellent FET characteristics with high field effect mobility.¹⁰⁸⁴ A conductive bioactive PEDOT gel was fabricated by the polymerization of the corresponding monomer in the hydrophobic environment of self-assembled peptide amphiphiles.¹⁰⁸⁵ The in situ conductivity profile of the peptide amphiphiles-PEDOT gel exhibited a finite conductivity (σ_{max}) in the forward ($5.52 \times 10^{-5} \text{ S cm}^{-1}$) and reverse sweeps ($6.57 \times 10^{-5} \text{ S cm}^{-1}$). The conductivities of the polymer hydrogels of sodium poly(4-(2,3-dihydrothieno[3,4-b][1,4]dioxin-2-yl)-methoxybutane-1-sulfonate) were in the range $100\text{--}10^2 \text{ S m}^{-1}$.¹⁰⁸⁶ The effect of morphology change and gelation of P3HT/PCBM composite at different time periods on the efficiency of the bulk heterojunction PVDs have been investigated.¹⁰⁸⁷ The molecular

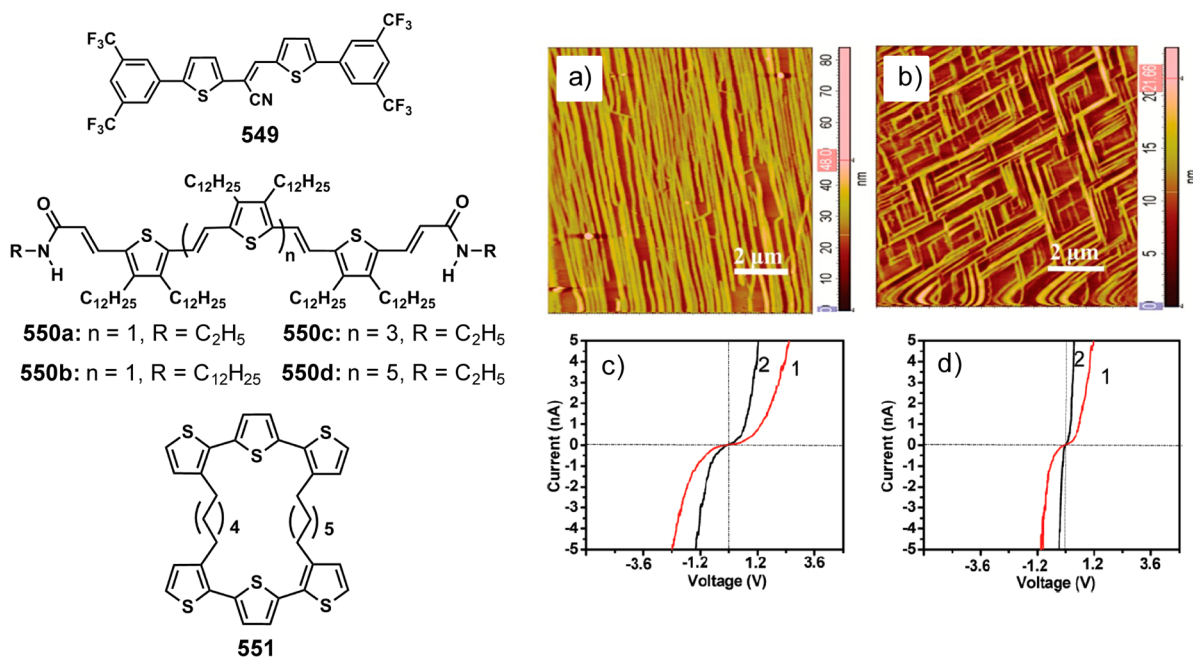


Figure 64. Chemical structures of gelators **549**–**551**. AFM images of (a) **550a** and (b) **550b** from *n*-decane drop cast on freshly cleaved mica surface. (c) I – V curves of obtained by conducting AFM measurements of (c) undoped and (d) doped xerogels from *n*-decane of **550c** (1) and **550d** (2). (Reprinted with permission from refs 1048 and 1077. Copyright 2010 American Chemical Society.)

Chart 135

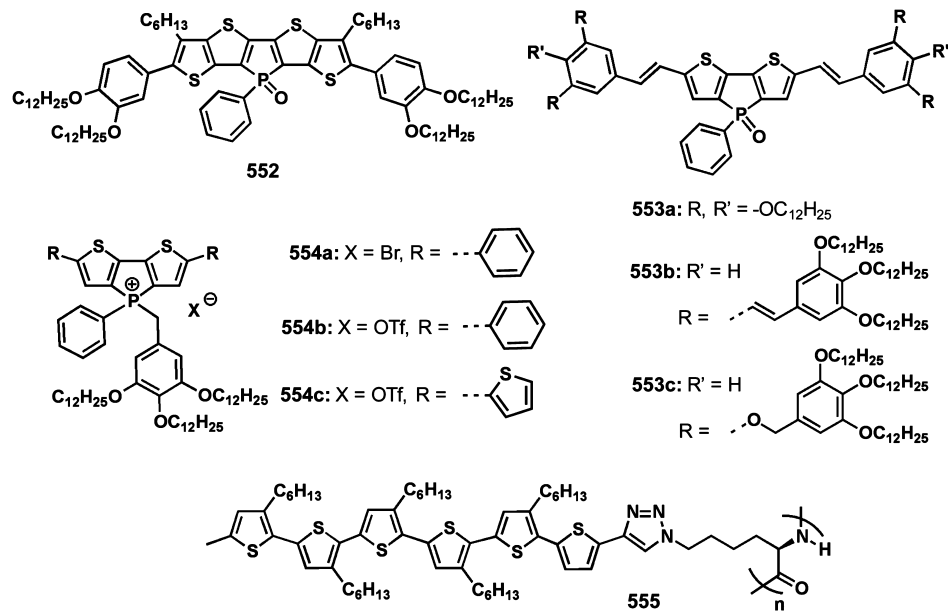
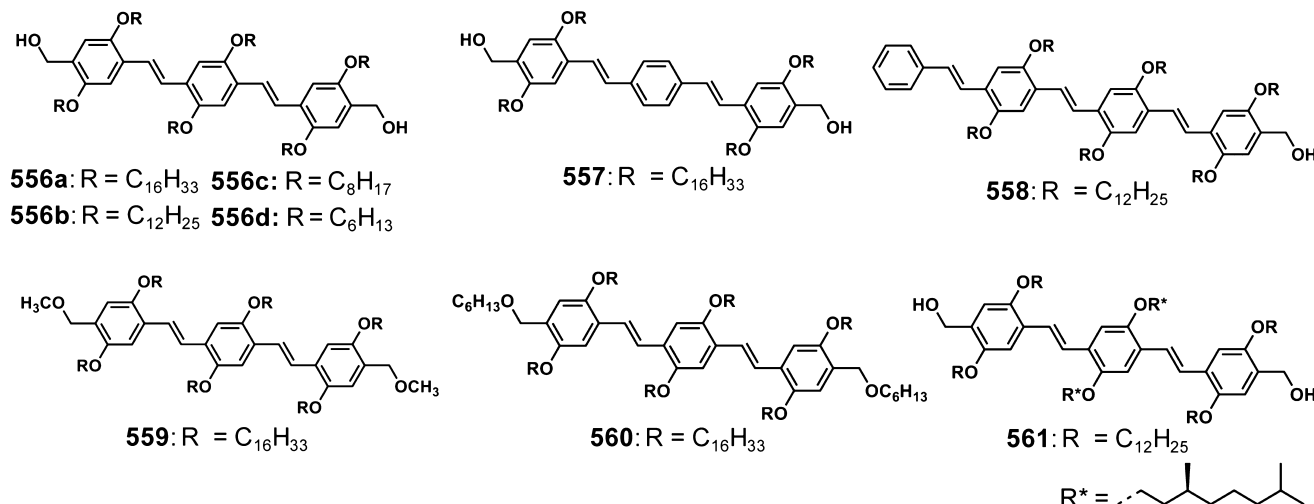


Chart 136



weight of the gelators has significant influence on the gelation behavior as demonstrated in the case of different batches of the P3HT which in turn reflect upon the device performance.¹⁰⁸⁸ Regioregular P3HT undergoes a coil to rod transformation and aggregation of the corresponding rods to form crystallites producing thermoreversible gels in xylene.^{1089–1091} A capillary method has been used to determine the gelation threshold of P3HT nanowire dispersions.¹⁰⁹² The formation of nano-whiskers of P3HT in the xylene gel was *in situ* monitored by SAXS.¹⁰⁹³ Interestingly, ice segregation induced self-assembly of PEDOT-poly(styrenesulfonate) hydrogel resulted in aligned or unaligned conducting polymer xerogels with 3D macroporous architectures.¹⁰⁹⁴ The poor solubility of ambipolar diketopyrrolopyrrolethiophene benzobisthiadiazole polymer resulted in the easy formation of inelastic gels.¹⁰⁹⁵

Poly(3-alkylthiophene)s have been investigated for their gelations assisted morphological and electronic properties.^{1096–1101} PMMA gel matrix has been used to encapsulate P3HT and the resulted composite gel enabled the crystallization of P3HT.¹⁰⁹⁶ The template effect of PMMA played a

crucial role in crystallization and thereby allowed tuning of the size and morphology of formed nanocrystals. Pozzo et al. investigated the mesoscale morphology of P3HT fibers crystallized through colloidal self-assembly and gelation.^{1097–1100} The P3HT organogel fibers exhibited different conductivity due to percolating network structure, when compared to other solution processed fibers.¹⁰⁹⁷ The rheology-SANS, dielectric-SANS, and dielectric rheology studies of P3HT gels led to an understanding of gelation induced mechanical and conductive properties.¹⁰⁹⁹ The use of nanoporous, submicrometer P3HT emulsified gel particles as solution processable inks, produced uniform thin films to use as an active layer in polymer/fullerene PVDs.¹¹⁰⁰

6.2. Phenylenevinylenes

Electronic properties of π -systems are sensitive to intermolecular interactions, particularly the way in which the chromophores are organized.^{7,1041,1102} This is more predominant in the case of linearly π -conjugated molecules which are used in the fabrication of organic electronic devices and light

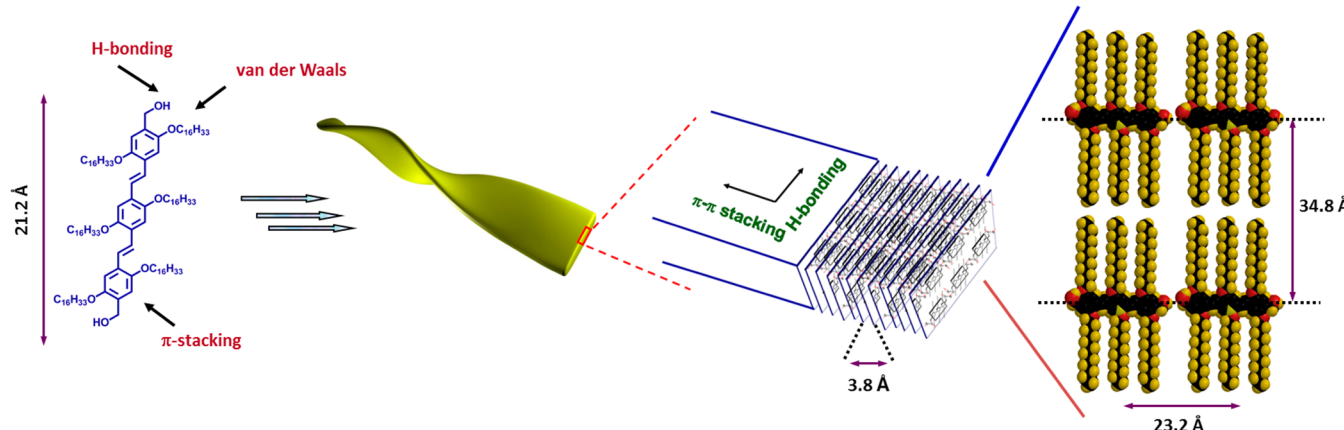


Figure 65. Schematic representation of the lamellar packing of **556b** in the gel fiber. (Reprinted with permission from ref 57. Copyright 2007 American Chemical Society.)

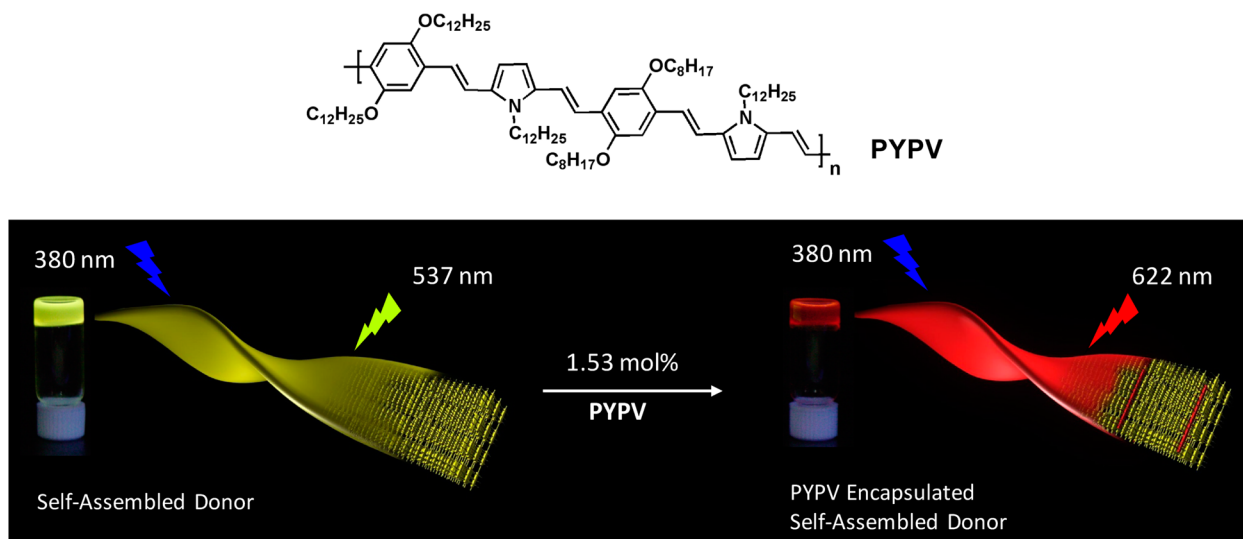


Figure 66. Schematic representation of the energy transfer process in PYPV-encapsulated within the self-assembled tapes of the gelator **556a**. (Reprinted with permission from ref 1110. Copyright 2007 Wiley-VCH.)

harvesting systems. Oligo (*p*-phenylenevinylenes) (OPVs) are one of the widely studied class of molecules due to their interesting opto-electronic properties.^{7,57} Therefore, rational approaches to the synthesis of OPVs that are functionalized with proper self-assembly directing groups are extremely crucial. In recent years, self-assembly and gelation of such OPV derivatives have been attracting much attention of interdisciplinary scientists.

Ajayaghosh and co-workers have reported that the molecule **556b** (Chart 136) spontaneously self-assembles from nonpolar hydrocarbon solvents at extremely low concentrations leading to gelation via the formation of entangled fiber network.^{57,1103,1104} Detailed studies have revealed that compounds **556–560** (Chart 136) are efficient gelators of nonpolar hydrocarbon solvents.^{1103–1106} The number of the hydrocarbon side chains present on the conjugated backbone and hydrogen bond assisted π -stacking significantly influences the gelation behavior.^{1104,1105} Morphological and XRD studies of **556b** indicated that multilayer lamellar assemblies with perpendicular arrangement of the chromophores to the long axis of the fiber have been attained through hydrogen bonding and π -stacking interactions (Figure 65).^{57,1104}

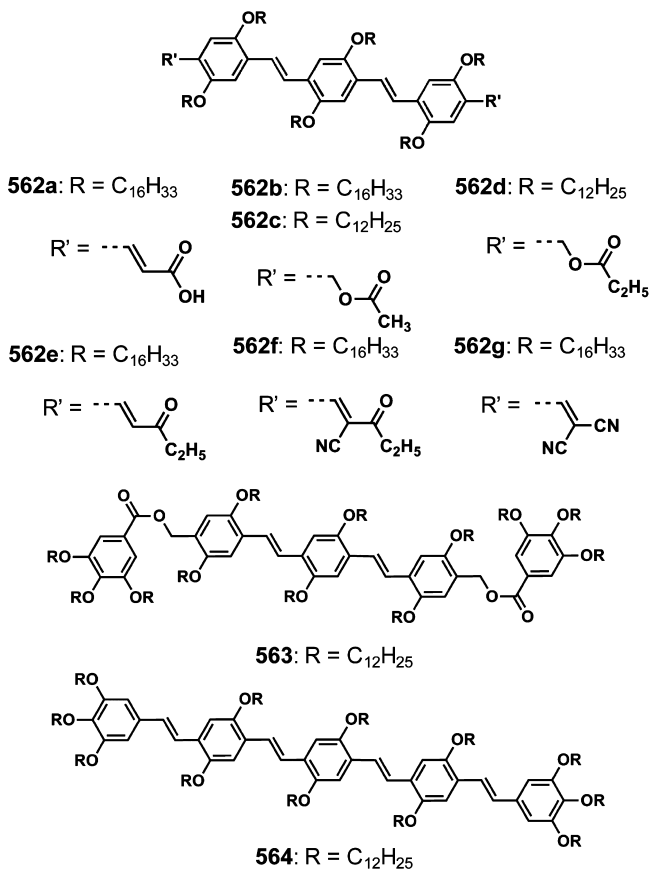
Helical nanostructures of OPV assemblies have been formed on attaching hydrocarbon chains with asymmetric carbons to the OPV backbone **561** (Chart 136).^{1107,1108} A coassembly of chiral **561** and the achiral **556b** gelators resulted in the amplification of helicity at lower concentrations (0–22 mol %) of **561**, whereas at higher concentrations, reversal of the original helicity was observed.¹¹⁰⁹ AFM studies have indicated the presence of left handed helical tapes for the homoassembly of **561**, whereas the coassembly of **556b** with 9 mol % of **561** resulted in the formation of *P*-helical tapes along with a few *M*-helical tapes. At 60 mol % **561**, a mixture of *M*-helices, *P*-helices and longitudinally fused *M*- and *P*-helices were formed.

Detailed photophysical studies have revealed that the large red shift in the emission spectrum of the OPV gel could be associated with the cascade exciton energy migration within the aggregates of different energy levels present in the self-assembled structures.^{1104,1105,1110} As a result, OPV gels of **556a** and **556b** were found excellent scaffolds for energy transfer to encapsulated energy acceptors.^{1110–1112} Thermally controlled energy transfer was observed when OPV donor gel was excited in the presence of rhodamine B.^{1111,1112} The drawback of the noncompatibility of acceptor in the donor gel scaffold has been overcome by the design of a π -conjugated

oligomer PYPV (Figure 66) as an acceptor. The fast exciton funneling in the gel scaffold facilitated highly efficient energy transfer even at very low mol % of the acceptor (Figure 66).¹¹¹⁰

The energy transfer property of OPV gelators can be controlled by the rational use of end functional groups **562–564** (Chart 137).^{1112–1116} For example, a series of OPV

Chart 137



gelators with quadrupolar type D–A substitutions (**562a–g**) have been tested for gelation as well as energy transfer with tunable emission colors.^{1113,1114} Efficient energy transfer between **562b** and **562g** in the *n*-decane gel resulted in strong quenching of the donor **562b** emission with a simultaneous onset of the acceptor **562g** emission.¹¹¹³ Another supramolecular light harvesting system was demonstrated by the coassembly between the donor **563** and the acceptor **562f**.¹¹¹² Interestingly, excitation of the *n*-decane gel of **563** in the presence of 0–2 mol % of the acceptor molecules resulted in emission corresponding to the monomeric form of the acceptor whereas upon addition of 2–20 mol %, the emission was obtained from the aggregates of the acceptor **562f**. Excitation energy migration assisted energy transfer properties of OPVs **562c**, **562d**, **563**, and **564** with different end functional groups indicated that when compared to the OPV gelators with bulky end groups (**563** and **564**), efficient energy transfer was observed in gelators functionalized with small end groups (**562c,d**) in the presence of an acceptor **562f**. The observed high efficiency in the case of the gelators **562c** and **562d** was attributed to the better self-assembly, strong gelation and efficient excitation energy migration.¹¹¹⁶

The cholesterol appended OPVs **565a,b** (Figure 67) displayed an unprecedented control on the arrangements of chromophores in the supramolecular assembly, thereby creating significant changes in the optical properties.¹¹¹⁷ The extended supramolecular assembly with twisted packing (pseudo-H aggregates, **565a**) led to twisted helical assemblies, whereas the tilted packing (pseudo-J aggregates, **565b**) resulted in a coiled helical assembly, as observed by chiroptical and AFM studies. The coassembly of the acceptor PYPV with the gelators **565a,b** resulted in distinct energy transfer properties.¹¹¹⁸ Because of the weak gelation in *n*-decane and slow exciton diffusion, a partial energy transfer occurred from the aggregates of **565a** to the acceptor PYPV, leading to white light emission. On the other hand, the strong gelation and fast exciton diffusion of **565b** facilitate efficient energy transfer to the acceptor, leading to exclusive red emission.

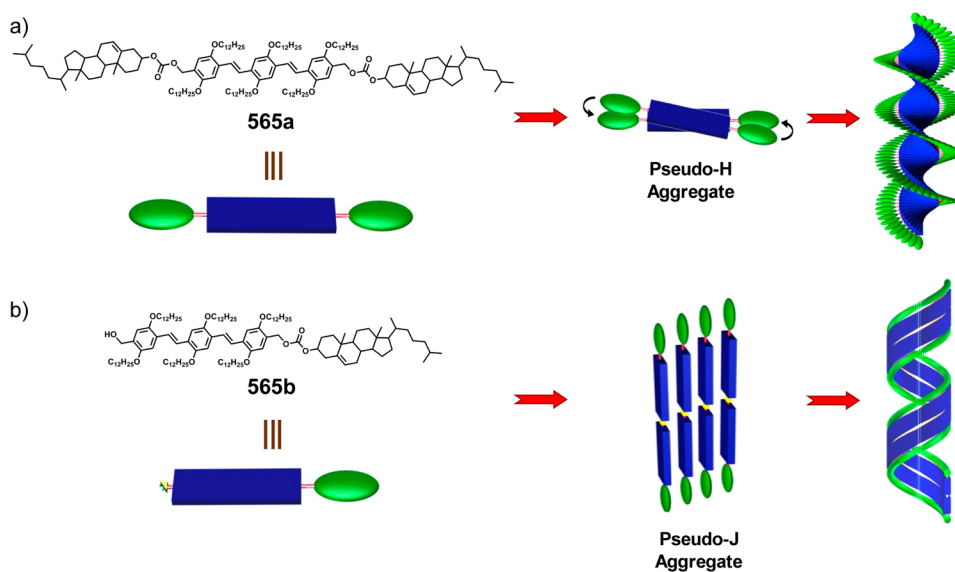


Figure 67. Probable mode of self-assembly of (a) **565a** and (b) **565b** in *n*-decane. (Reprinted with permission from ref 1117. Copyright 2006 Wiley-VCH.)

The self-organization of the Boc-alanine linked OPV amides **566a,b** (Figure 68) exhibited a periodic macroporous honey-

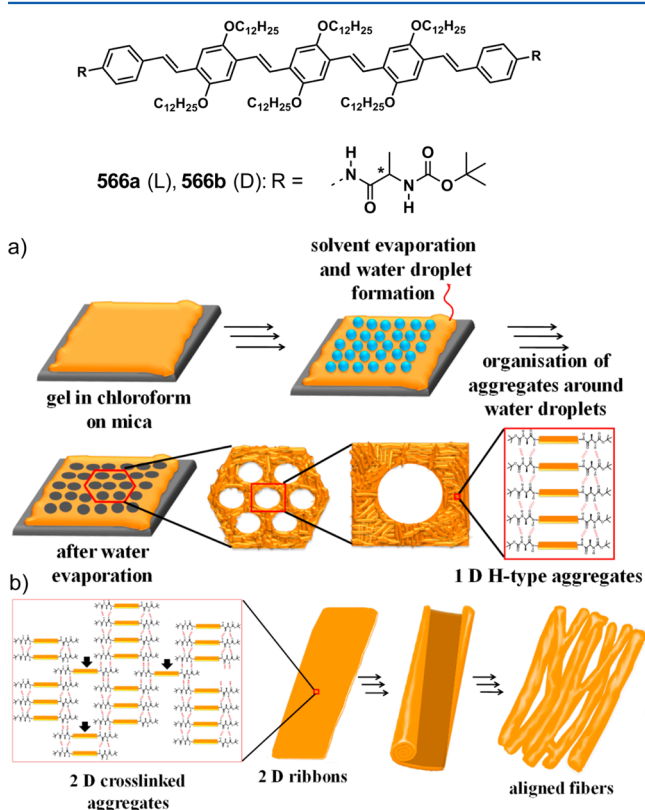


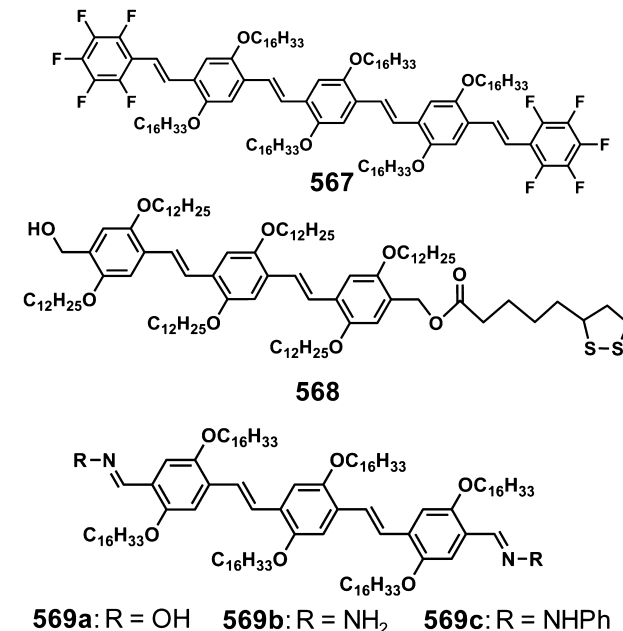
Figure 68. Schematic representation of solvent controlled self-assembly pathways of the gelator **566** leading to (a) honeycomb in chloroform and (b) aligned fibers in toluene. (Reprinted with permission from ref 1119. Copyright 2009 Wiley-VCH.)

comb structure in chloroform (Figure 68a) and aligned fiber bundles in toluene (Figure 68b).¹¹¹⁹ The OPV derivative **567** (Chart 138) undergoes hierarchical self-assembly through the arene–perfluoroarene interaction, leading to controlled longitudinal fiber growth and gelation.^{1120,1121} The supramolecular exciplex formation of **567** with *N,N*-dimethylaniline, exclusively in the gel state exhibited 3-fold enhancement in the emission intensity.¹¹²⁰

An inorganic–organic hybrid soft material has been reported using the gel scaffold of **556b** as a template for the arrangements of Au nanoparticles.¹¹²² In the presence of **568** (Chart 138), the coassembled gel fibers of **556b** and **568** can bind with Au nanoparticles leading to arrays of Au particles on the sides of the tapes. In addition, the presence of metal particles at favorable distances near to OPV tapes facilitated electronic communication between the components as indicated by the quenching of the OPV fluorescence. Subsequently, thiol protected Au nanoparticles have been used to probe the different stages of the molecular organization of the gelator **556a**.¹¹²³

It has been demonstrated that the stability of **556a** OPV gels can be improved by interacting them with CNTs.¹¹²⁴ The TEM images of the composite gels revealed that the unbundled nanotubes that are encapsulated within the OPV self-assembly appeared like fiber reinforced supramolecular tapes. Anisotropic fibrous self-assembly of **556a** in a mixture of cyanobiphenyl based nematic and smectic LCs exhibited polarized photo-

Chart 138



luminescence due to the template effect of the oriented LCs (Figure 69).¹¹²⁵ Preparation of hybrid gels using atactic and stereo regular polystyrenes and OPV gelators were shown to improve the thermal stability of the latter.¹¹²⁶ A composite of **556a** and atactic polystyrene was found to be compatible without any phase separation whereas stereoregular polystyrenes showed a very high degree of dispersion of one component into the other.

Detailed studies have been carried out to understand the effect of end functional group and the nature of the solvents on the gelation and morphology of OPV gelators.^{138,1127,1128} Report from the group of Bhattacharya has revealed the gelation properties of OPVs **569a–c** (Chart 138) end functionalized with oxime, hydrazone, and phenylhydrazone groups.¹¹²⁹ Interestingly, the gelation studies of a composite of **569a** and multiwalled boron nitride nanotubes showed a reinforced aggregation of the gelator molecules due to the wrapping of the gelator molecules on to the latter.¹¹³⁰ A mechanically stable nanocomposite has also been prepared by incorporating pristine and hexadecyl alkyl chain functionalized SWCNTs into organogels of **569a**.¹¹³¹ In addition, composite gels of **569a** with exfoliated graphene, SWCNTs, and C₆₀ showed increased electrical conductivity when compared to the organogel of **569a**.

Rod–coil type block copolymers comprising of π -conjugated moiety as a rigid rod segment have been known to self-organize to form architectures of different size and shape by taking advantage of microphase segregation between rod and coil segments.¹¹³³ This concept has been extended to design electronically active functional supramolecular architectures. Stupp and co-workers have reported the self-assembly of a series of linear π -conjugated molecules **570a,b** (Chart 139) with dendron rod–coil architectures.¹⁰⁵⁵ The added length of the biphenyl segment in **570a** increased the ability of the rod segments to form stable π -stacks.

The self-assembly and the gelation of an amphiphilic OPV **571** (Chart 139), which is asymmetrically end substituted with a hydrophilic poly(ethylene glycol) segment and a hydrophobic alkyl chains has been reported.¹¹³⁴ Strongly fluorescent self-

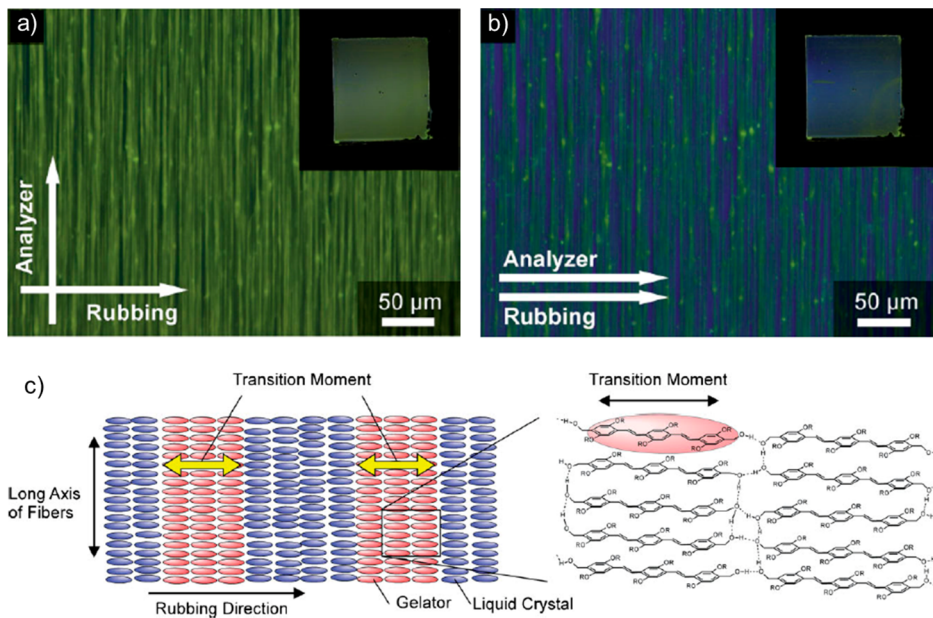
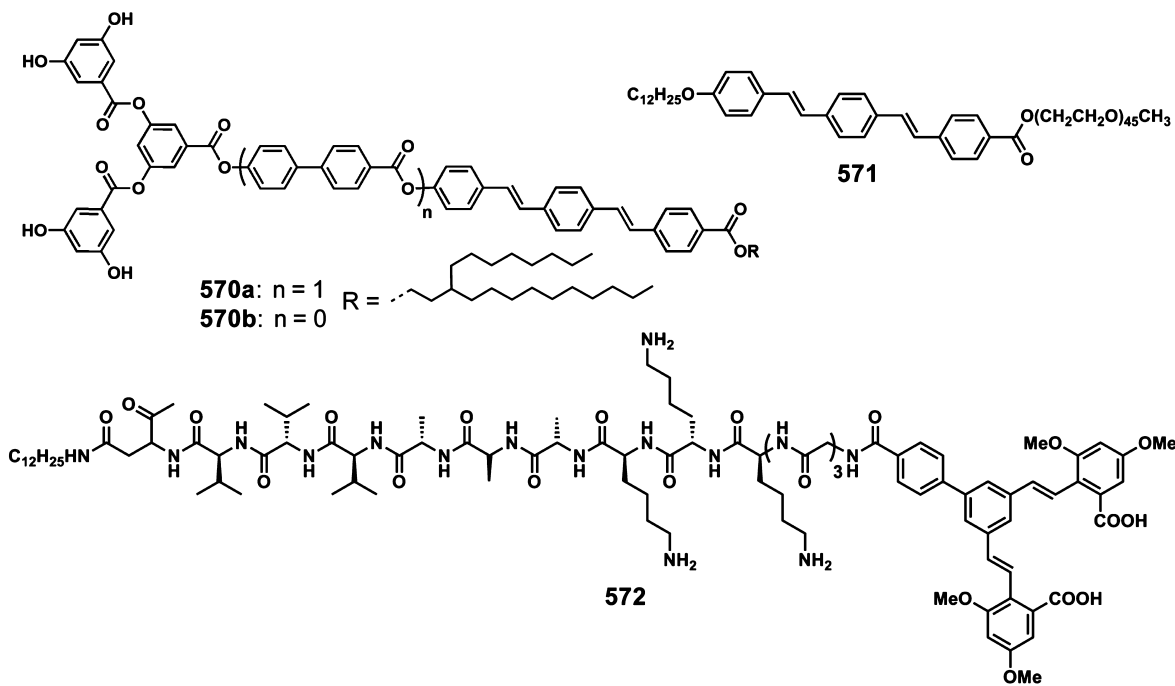


Figure 69. POM images of the LC/OPV mixtures containing 3 wt % of **556a** with the transmitting axis of the analyzer being set (a) parallel and (b) perpendicular to the long axis of the fibers. Inset: polarized photographs of aligned LC gels in 1 cm × 1 cm quartz cells. (c) Schematic illustrations of the aggregated structures of aligned OPV fibers in the smectic phase. (Reprinted with permission from ref 1125. Copyright 2009 Wiley-VCH.)

Chart 139



supporting organogels along with thermotropic and lyotropic lamellar LC phases were observed due to the bilayer arrangement of **571**. Coassembly approach has been used to modify the fluorescence intensity of the peptide amphiphile **572** (Chart 139) containing branched stilbene chromophores.¹¹³⁵ Fluorescence intensity can be tuned in these coassembled gels through efficient energy transfer to acceptors such as fluorescein which is tagged to bioactive polysaccharide heparin.

Supramolecular organization of the gelator **573** (Chart 140) in methylcyclohexane indicated the formation of micrometer long fibers which are bundled at higher concentrations to form

organogels.¹¹³⁶ Yagai and co-workers have reported the self-assembly and organogelation of bis- and monourethane appended OPVs **574a,b** and **575** (Chart 140).¹¹³⁷ The bisurea OPV derivative **574a** with a hexamethylene linker formed tape-like nanofibers that can gelate various organic solvents whereas when the length of the spacer was increased to dodecamethylene as in **574b**, the gelation ability was considerably decreased as indicated by the presence of small ill-defined nanostructures.

Self-organization and morphological features of **576a** (Chart 140), containing a monotopic D-A-D type triple hydrogen bonding melamine indicated that ill-defined structures of **576a**.

Chart 140

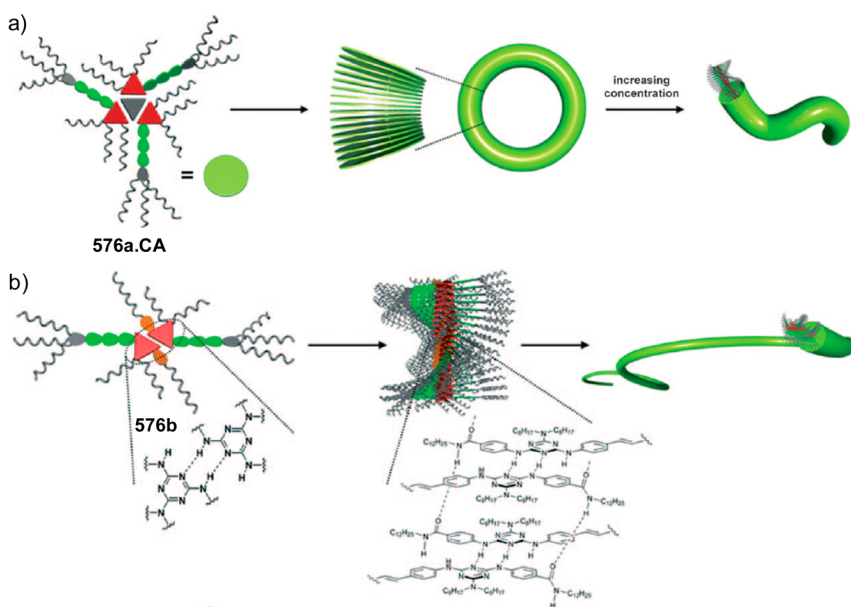
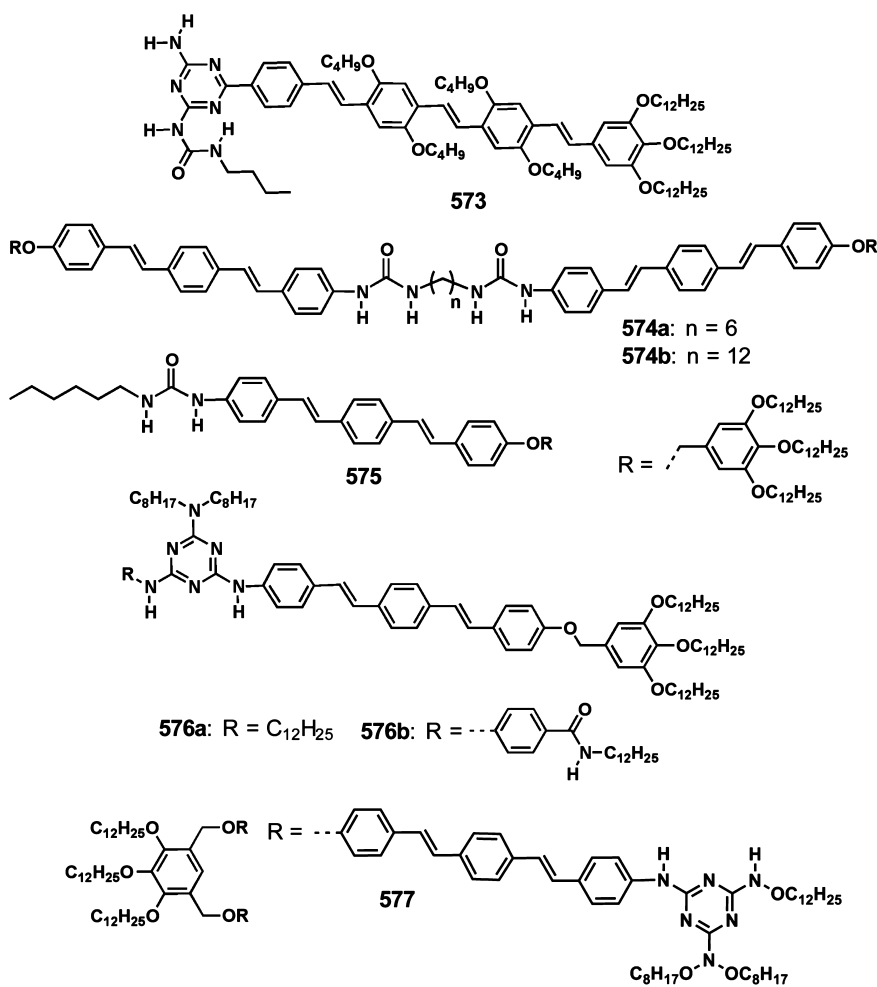


Figure 70. Schematic representation of the (a) coaggregation of **576a** with cyanuric acid (CA) and (b) self-aggregation of **576b**. (Reprinted with permission from ref 1139. Copyright 2010 Wiley-VCH.)

However, upon coassembly with complementary cyanurate CA (Chart 41), nanorings at low concentrations and open structures at high concentrations were formed, thereby leading

to the gelation (Figure 70a).^{1138,1139} In contrast, the self-aggregation of **576b** (Chart 140) showed the formation of nanofibers (Figure 70b) and its gelation ability has been

Chart 141

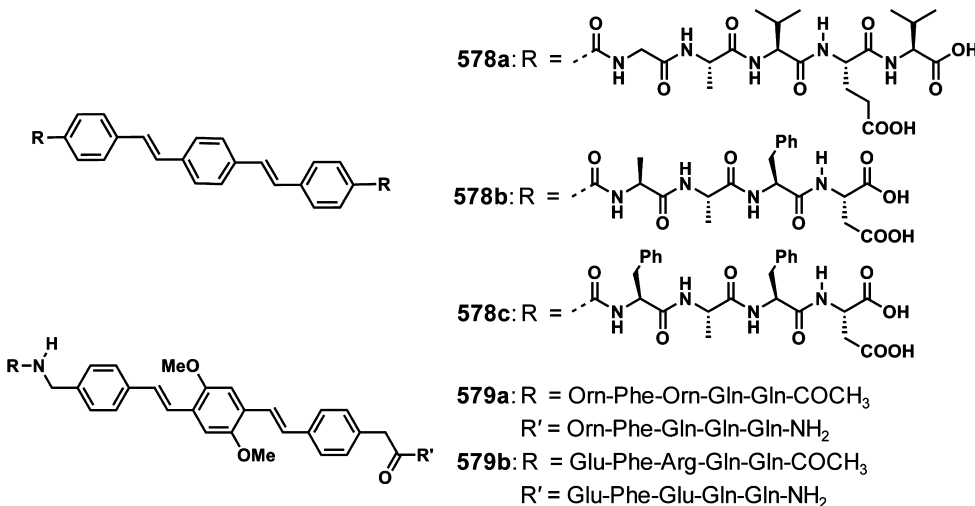
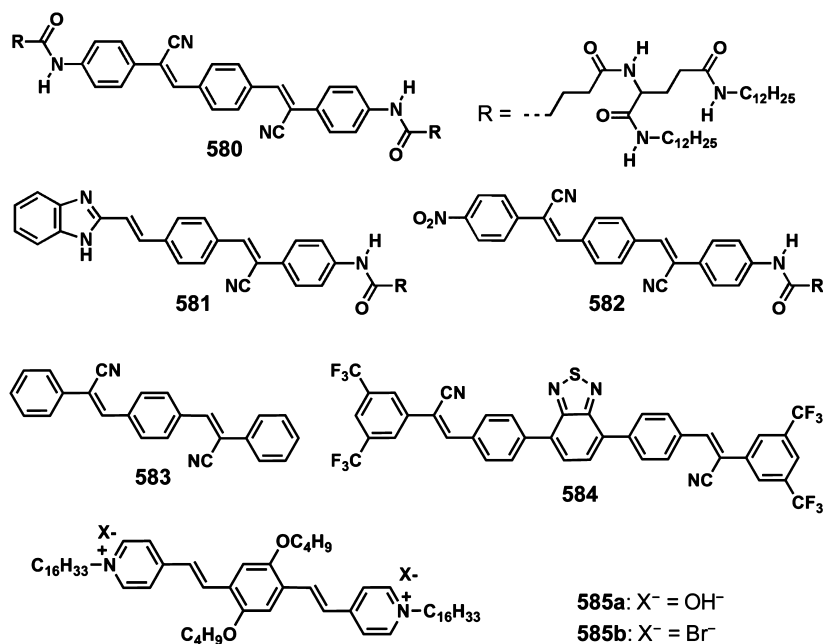


Chart 142



significantly reduced upon coassembly with CA. Interestingly, the curled, flexible nanofibers of the OPV dimer **577** (Chart 140) (gel) could be transformed into rigid nanostrips via the conformationally frozen host–guest complex **577·dCA** (sol).¹¹⁴⁰ The reverse transformation of nanostrips to nanofibers could also be possible by adding the bismelamine molecule **B1** (Chart 34) that enabled a gel phase.

In order to aid self-organization, Tovar et al. have incorporated peptides into OPV units **578a–c** (Chart 141), that formed amyloid-like supramolecular polymers resulting in stable hydrogels.^{432,1058,1141} The noodle type soft materials prepared from hydrogels of **578a** are composed of a uniform degree of macroscopically aligned individual nanostructures at the nano/micrometer scale having anisotropic optical properties.^{1058,1141} Maggini and co-workers have reported the solid phase synthesis of two OPV peptide conjugates **579a,b** (Chart 141) in which the OPV based ω -amino acid is connected to two different β -sheet forming peptide sequences.¹¹⁴² Gelation studies have shown that stable hydrogels were formed by **579a**

at pH 8 (1N aqueous NaOH) with irregular networks of highly interconnected fibers whereas the gelation of **579b** in 1 M HCl resulted in micrometer long left handed helical fibers.

In DMSO/diphenyl ether solvent mixture, the gelator **580** (Chart 142) was found to form 1D aggregates with strong exciton coupling of the aromatic units.¹¹⁴³ However, in DMSO alone these molecules self-assembled to H-type aggregates with weak exciton coupling. The formation of these two kinds of aggregates could be tuned by changing the ratio of DMSO to diphenyl ether. Interestingly, the gelator **580** exhibited two-photon fluorescence due to large intramolecular charge transfer. Xue et al. have integrated electron acceptors such as C_{60} and C_{60} acid derivatives into regular and ordered aggregates of a donor gelator **581** (Chart 142).¹¹⁴⁴ The comparison of changes in emission intensity of the gel upon addition of C_{60} and C_{60} acid derivatives to **581** revealed the relatively effective quenching of the fluorescence by the latter due to the hydrogen bonded 1:2 complex, thereby making the electron transfer more facile. Photocurrent obtained from the PVD fabricated using

Chart 143

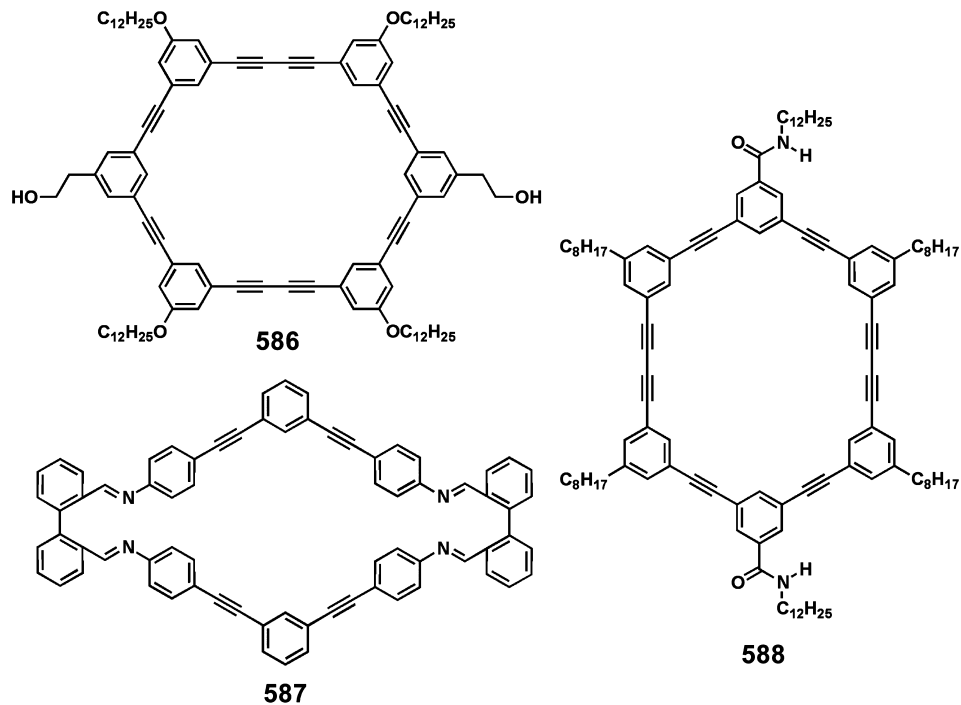
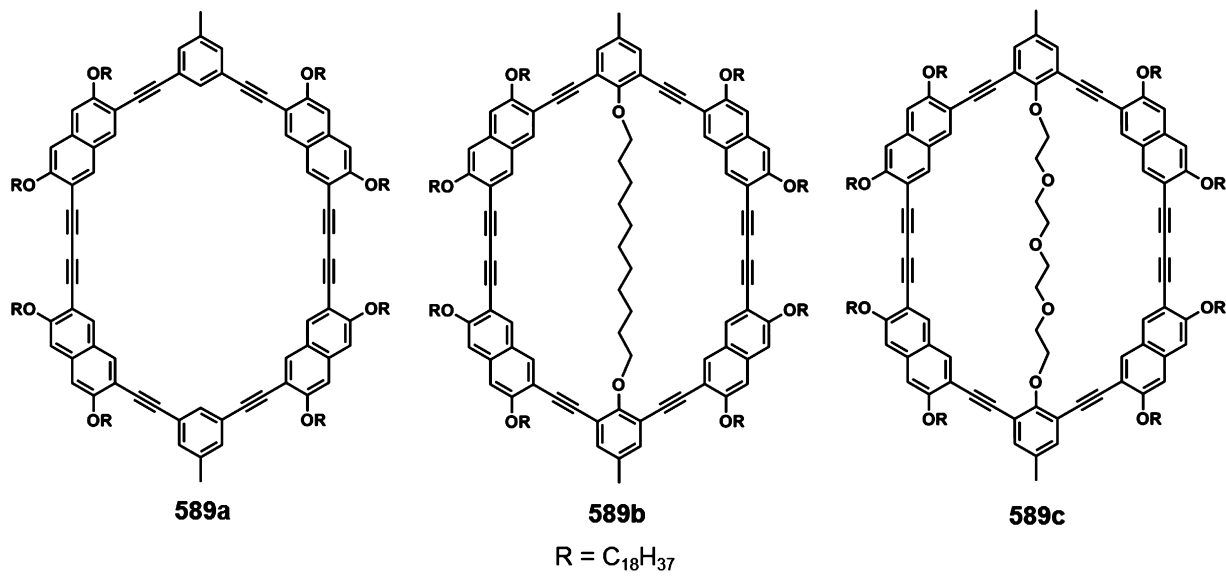


Chart 144

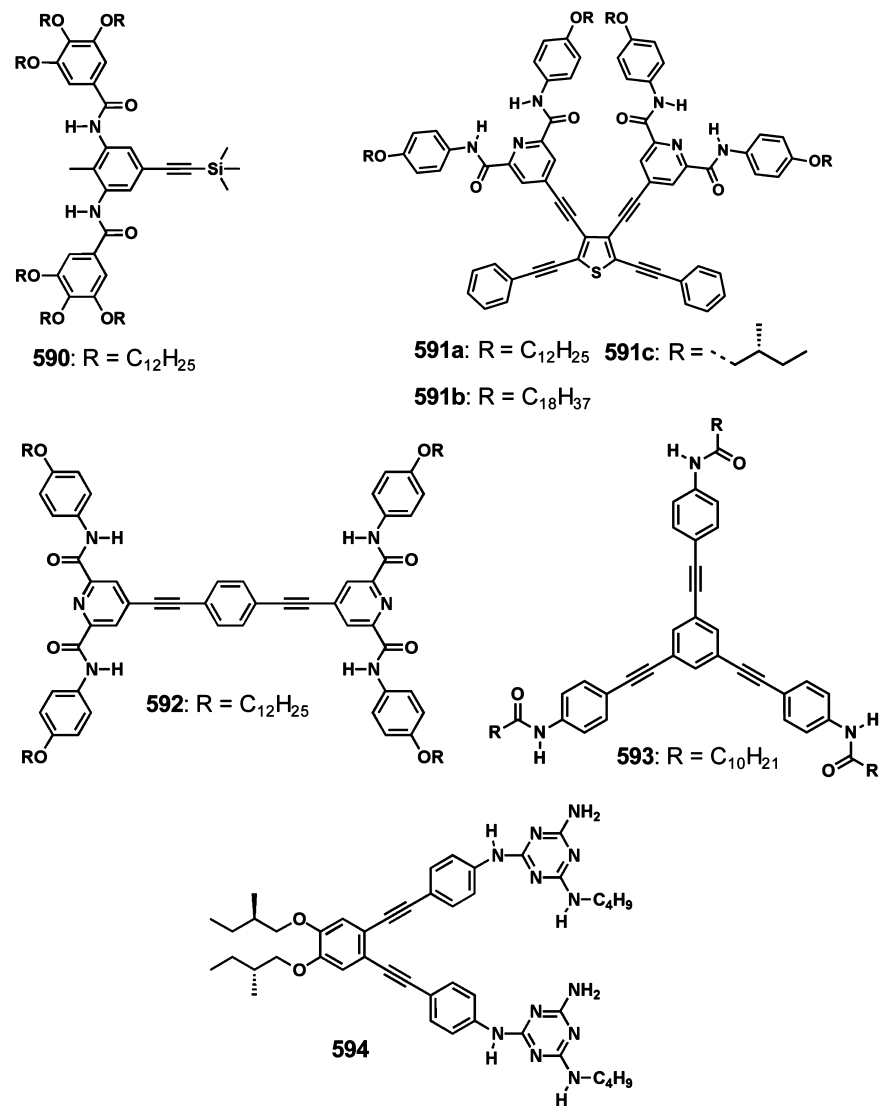


the hybrid gels of C_{60} acid and 581 (2:1) as the active layer exhibited stable and large photocurrent than a device containing pristine C_{60} in the same mixed ratio. Since the absorption and emission spectra of 581 was found to be sensitive to stimuli such as protons and anions, a chemosensor based integrated logic gate was developed.¹¹⁴⁵ The D- π -A electronic structure of the gelator 582 (Chart 142) enabled the concentration dependent tunable multicolor emission from green to red in DMSO and yellow fluorescence in *o*-dichlorobenzene.¹¹⁴⁶

In general, long alkyl chains are considered to be essential for the gelation of π -systems. In contrast to this common notion, alkyl chain free π -gelators have been recently reported.^{1147,1148} For example, Park et al. have investigated the efficient gelation

of a distyrylbenzene 583 (Chart 142) with a β -cyano substitution and found that the 1D crystalline fibrous aggregates exhibit electrical conductivity of 9.7×10^{-6} Scm^{-1} .¹¹⁴⁷ The trifluoromethyl substituted benzothiadiazole cored phenylenevinylene gelator 584 (Chart 142) displayed piezochromism, vapochromism, and thermally induced fluorescence variation in the solid phase, while sonication of a cold solution led to the formation of gels.¹¹⁴⁸ The stilbazolium derivative 585a (Chart 142) with OH^- counteranion exhibited better gelation ability than 585b (Chart 142) having Br^- as the counteranion.¹¹⁴⁹ The xerogel film of 585a showed acid sensing property by a blue shift in the emission peak from 637 to 581 nm, resulting in a gel-sol transition.

Chart 145



Apart from the above-mentioned studies of small molecules and oligomer based gelators, Chen and co-workers have reported the organogelation of poly(2-methoxy-5-(2-ethylhexyloxy)-1,4-phenylenevinylene) (MEH-PPV) in 1,3-dichlorobenzene/nonane mixture after standing at room temperature for 2 days.¹¹⁵⁰ A deuterated toluene solution of MEH-PPV was found to form soft gels upon aging at room temperature due to the nanocrystalline aggregates that serve as physical cross-links among MEH-PPV chains.¹¹⁵¹ The polymerization of the monomer in the presence of DNA resulted in fluorescent DNA poly(phenylenevinylene) hybrid hydrogels, which have been used for drug release.¹¹⁵² The microwave conductivity of poly(2-(3,7-dimethyloctoxy)-5-methoxy-1,4-phenylenevinylene) gel exhibited an order of magnitude ($2.0 \pm 0.3 \times 10^{-8} \text{ m}^2 \text{ V}^{-1} \text{ s}^{-1}$) larger when compared that in solution ($2.0 \pm 0.5 \times 10^{-9} \text{ m}^2 \text{ V}^{-1} \text{ s}^{-1}$).¹¹⁵³

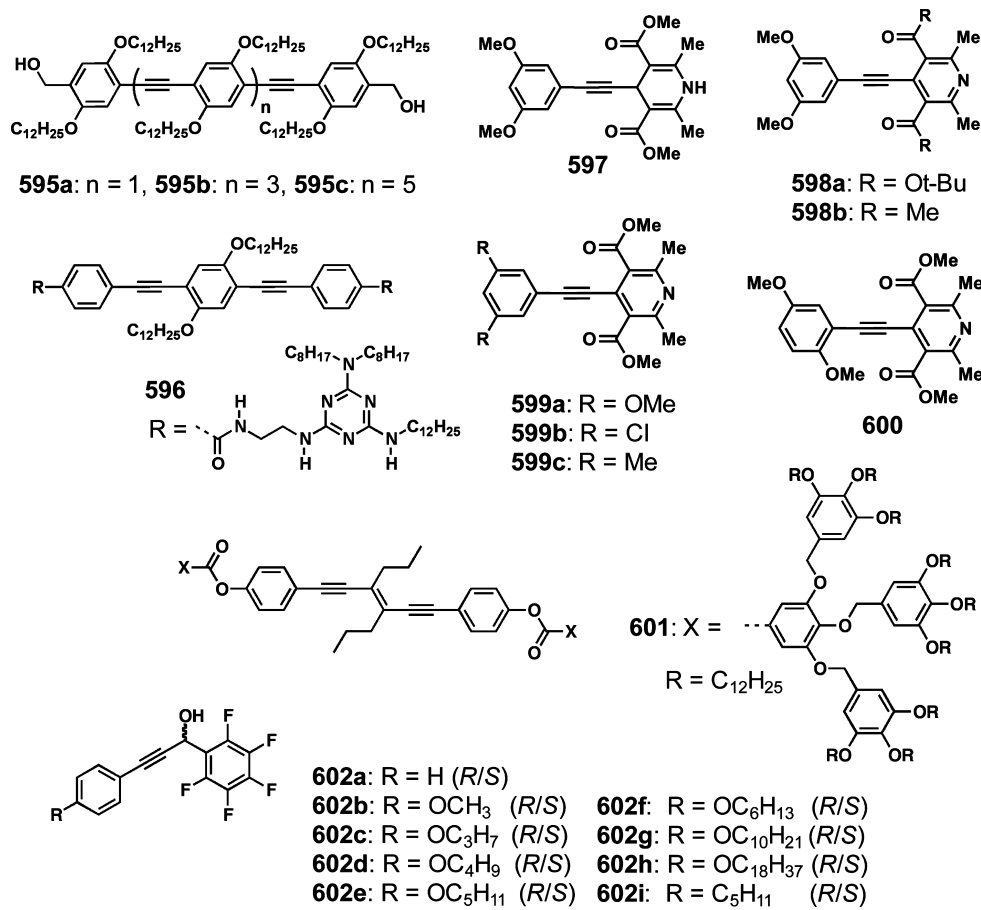
6.3. Phenyleneethynylanes

Phenyleneethynylanes are the dehydrogenated analogues of phenylenevinylanes.^{1154,1155} This section surveys gelators based on phenyleneethynylanes, with special emphasis on their physical and morphological properties. Organogels of phenyleneethynylene macrocycles have attracted much interest due to

their well-defined and noncollapsible internal channel which may provide interesting applications in nanoscale optoelectronic devices. An example for the gelation of phenyleneethynylene macrocycles was reported by Tour and co-workers.¹¹⁵⁶ The cyclophane **586** (Chart 143) formed gels through dimerization in halogenated solvents such as chloroform and dichloromethane. In this case, gelation of the macrocycle is assumed to be the cooperative effect of $\pi-\pi$ stacking and hydrogen bonding. Ultrasound irradiation of the suspension of the rhomboid macrocycle **587** (Chart 143) formed an opaque gel with fibrous aggregates obtained via $\pi-\pi$ and CH- π interactions.¹¹⁵⁷ An amide containing phenylacetylene macrocycle **588** (Chart 143) showed excellent gelation properties and formed columnar assemblies suitable for topochemical polymerization.¹¹⁵⁸

The shape persistent macrocycles **589a** with an empty cavity, **589b** with an undecyldiether strand, and **589c** with a tetraethylene glycol strand exhibited excellent aggregation leading to macroscopic gelation (Chart 144).¹¹⁵⁹ The intra-annular substitution pattern has a direct correlation with the thermal stability of the gels. Due to dipole–dipole interactions as well as solvophobic interactions, the macrocycle **589c** exhibited high gel melting temperature. The additional van der

Chart 146



Waals interactions in **589b** facilitated higher gel melting point when compared to that of **589a**.

Ziessel et al. have shown the gelation of the ambipolar gelator **590** (Chart 145) due to the formation of 3D network of interlocked fiber-like aggregates assisted by amide groups.¹¹⁶⁰ The phenyleneethynylthiophene derivatives **591a–c** (Chart 145) are good gelators due to the cooperative effect of the amide hydrogen bonding and π -stacking, resulting in the enhanced fluorescence in the gel state.^{1161,1162} The bisphenylethyneylthiophene based achiral gelator **591b** showed 1D helical morphology whereas in the case of the chiral **591c**, helical fibers were absent in the xerogel.¹¹⁶² The coassembly of the achiral gelator **591b** with the chiral gelator **591c** induced chiral amplification with increasing concentration of the latter. The phenylethynelene based gelators **592** (Chart 145) was also reported to show enhanced emission upon gelation.⁹⁸⁵ The columnar organization of the symmetric trisamide **593** (Chart 145) favored the ordered assembly to entangle the fibrils leading to organogelation.¹¹⁶³ The replacement of linear achiral alkyl chains with stereogenic centers considerably reduced the gelation ability which emphasizes the importance of interdigitation of the peripheral side chains in achieving the ordered assembly. The tweezer-like *o*-phenyleneethynylene gelator **594** (Chart 145) substituted with a melamine unit formed mesoporous and hydrophobic honeycomb structures through the breath figure process, individually and in the presence of a perylene molecule functionalized with suitable A-D-A type hydrogen bonding motif.¹¹⁶⁴

Due to the possibility of several rotamers, the fluorescence quantum yields of OPEs are relatively low when compared to the corresponding OPVs. Since OPE backbone is less planar when compared to OPV, the intermolecular π -interaction is expected to be very weak. Therefore, in contrast to the self-assembly of OPVs to supramolecular tapes, an analogous OPE **595a** (Chart 146) has been reported to form nanoparticles, microspheres, and bundled fibers, eventually leading to blue emitting organogels in *n*-decane with increasing concentration (Figure 71).^{1165–1167}

A detailed understanding of the effect of increasing the repeat units in OPEs revealed the role of concentration, substrate and humidity in controlling the assembly and gelation.¹¹⁶⁶ Instead of the vesicular assemblies of **595a**, the gelators **595b** and **595c** (Chart 146) formed entangled fibers and spiral assemblies at lower concentrations, respectively. As shown in Figure 71, a large number of polymorphic structures were obtained upon varying the gelator structure and the gelation conditions. For example, the gelator **595c** with a higher conjugation length exhibited various exotic polymorphic structures. Interestingly, the coassembly of a corresponding chiral nongelator with **595a** facilitated transcription of the molecular chirality of the former in a helical sense and resulted in a transition from vesicular assemblies to helical tubular structures.¹¹⁶⁵

The complexation of a cyanurate with the melamine linked tri(*p*-phenyleneethynylene) **596** (Chart 146) facilitated control on the physical properties and morphological features of the coassembled supramolecular gels.¹¹⁶⁸ The self-organization of **596** in aliphatic solvents lead to the formation of an opaque and

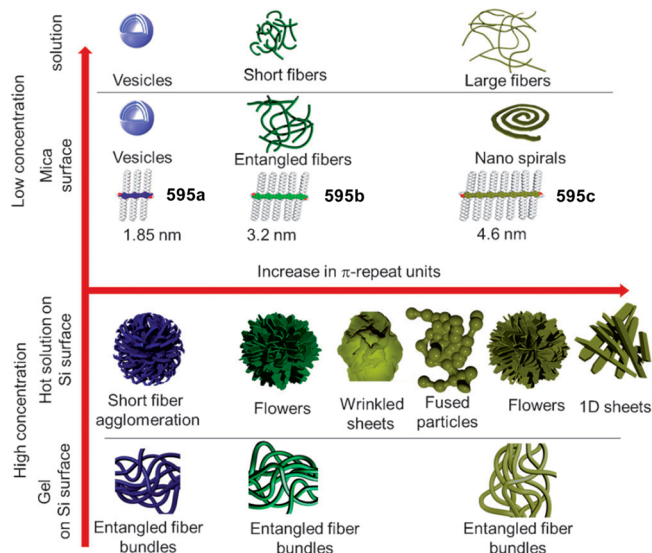


Figure 71. Schematic illustration of the polymorphic structures formed by OPEs 595a–c. (Reprinted with permission from ref 1166. Copyright 2012 Wiley-VCH.)

weak blue emitting gel which upon addition of a cyanurate dCA (Chart 41) turned into a transparent and stable gel via a 2:2 dimer during the initial stage of the self-assembly. An analyte triggered oxidation of the dihydropyridine derivative 597 (Chart 146) was known to induce gelation of solvents.¹¹⁶⁹ Detailed studies have resulted in the design and understanding of the relation between the molecular structure and gelation ability of a series of pyridine based gelators 598–600 (Chart 146).¹¹⁷⁰ A significant reduction in the critical gelator concentration and an increase in gel strength were observed

when the gelation of 598a was carried out in the presence of PAA.¹¹⁷¹ Thin fibers were formed by reducing the growth rate of the assembly thereby improving the elastic modulus and breaking stress of the gel.

The 1,6-bis(4-hydroxyphenyl)-3-hexen-1,5-diyne derivative 601 (Chart 146) with two bulky end groups self-assembled in a columnar mesomorphic organization to form fibers and gels.¹¹⁷² Gelator 602a-I (R/S) (Chart 146) capable of gelating alkane and/or silicone oil liquids have been reported.¹¹⁷³ The trimeric assemblies of 602a-I (R/S) undergone extension via hydrogen bonding to form columns, which are packed side by side using π -stacking to form the gel fibers. Two component organogel formation has been observed by mixing chiral ethynyl helicene oligomers 603(M)_n and 603(P)_n (Figure 72) forming racemic mixtures of oligomers, however optically pure oligomers did not show gelation behavior.^{1174–1176} Interestingly, depending on the difference in length of individual components, the gels formed from pseudo enantiomeric ethynyl helicene oligomers were found to exhibit different properties.¹¹⁷⁵ Transparent gels with negative cotton effect were observed for the 1:1 stoichiometric combination of oligomers with small differences between the numbers of helicenes (Type I gel, Figure 72a). In contrast, gels formed from the 1:2 stoichiometric combinations of oligomers with considerable differences in the numbers of helicenes showed the formation of turbid gels with positive cotton effect (type II gel, Figure 72a). Moreover, using this strategy, two layer gel systems were constructed from types I and II gels (Figure 72b).

Okamoto and co-workers have revealed that poly(2,5-dialkyl-p-phenyleneethynylene)s having linear alkyl side groups can form gel in toluene upon standing at room temperature for several weeks whereas polymers with branched side groups were failed to form gels.¹¹⁷⁷ The high concentration gels

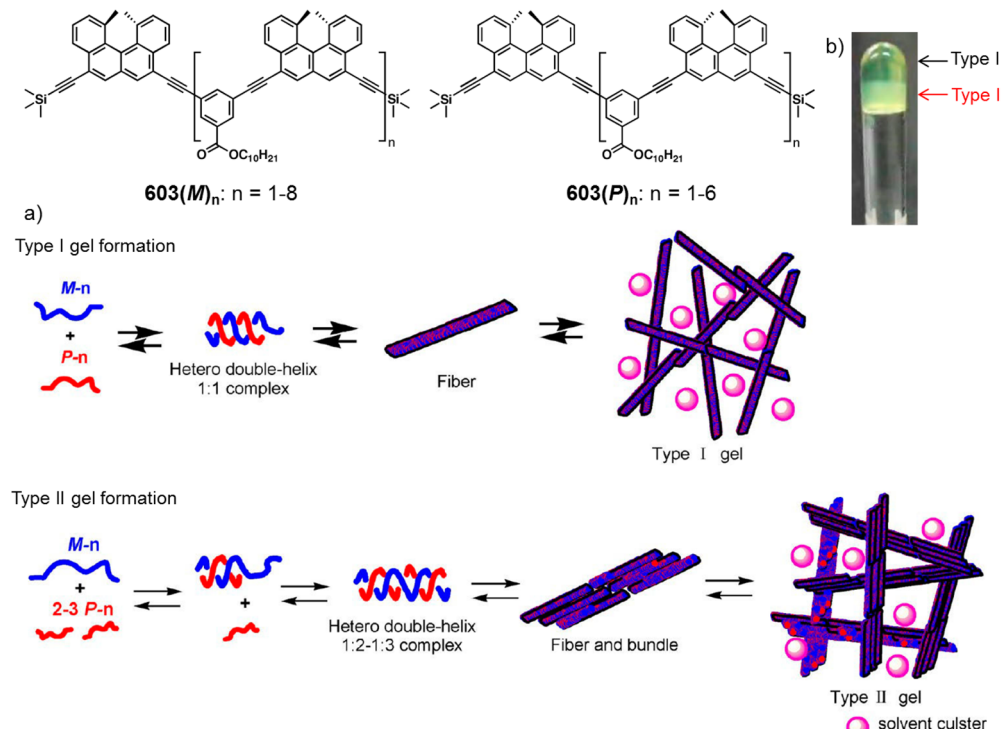
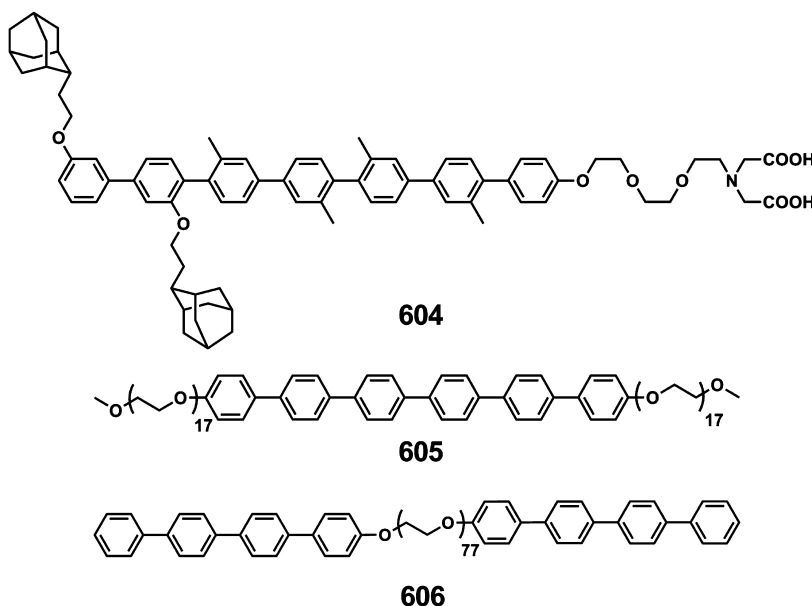


Figure 72. (a) Proposed mechanism of formation of types I and II gels. (b) Picture of two layer gel composed of the type I gel as upper layer and the type II gel as lower layer. (Reprinted with permission from ref 1175. Copyright 2012 American Chemical Society.)

Chart 147



showed birefringence and nematic LC properties. Bunz et al. have reported the change of rod-like dinonyl poly(*p*-phenyleneethynylene)s oligomers into a viscous gel in toluene.¹¹⁷⁸ The aggregates formed were large enough to induce arrest of the solvent through π - π interactions and a transformation from colorless solution to yellow gel like phase with increased viscosity was observed.

6.4. Phenlenes

Phenlenes are a class of rigid-rod type molecules which have been studied deeply in the context of their self-assembly and optical properties.¹¹⁷⁹ Since these rigid aromatic molecules have significant photonic and electronic properties, self-assembly could provide a strategy for the construction of well-defined and stable nanometer size structures with chemical functionalities and physical properties which are suitable for photonic, electronic, and biological applications. Matile et al. have discussed the self-assembly of rigid T-shaped single chain amphiphile **604** (Chart 147) in aqueous conditions to form giant vesicles, reverse micelles, and finally gels.¹¹⁸⁰

Lee and co-workers have used *p*-phenylene based rod-coil type molecules for the construction of novel supramolecular nanoscopic architectures with well-defined shapes and functions.^{1179,1181} The driving force for the self-assembly of rod-coil type molecules is microphase separation of the rod and coil blocks, thereby forming ordered periodic structures due to the mutual repulsion of the dissimilar blocks and the packing constraints imposed by the connectivity of each block.^{1179,1181} Coassembly of the amphiphilic triblock coil-rod-coil molecule **605** (Chart 147) and the rod-coil-rod molecule **606** (Chart 147) in aqueous solution resulted in cylindrical micellar structures.¹¹⁸² The addition of a small amount of **606** as a bridging agent to **605** resulted in the formation of a reversible nematic gel (Figure 73). More importantly, under this condition, selective excitation of **606** resulted in strong emission from **605** due to energy transfer from former to the latter, which is an additional evidence for the formation of the coassembly between these molecules.

The T-shaped aromatic amphiphiles **607** and **608** (Chart 148) lead to a reversible phase transition from a fluid to gel

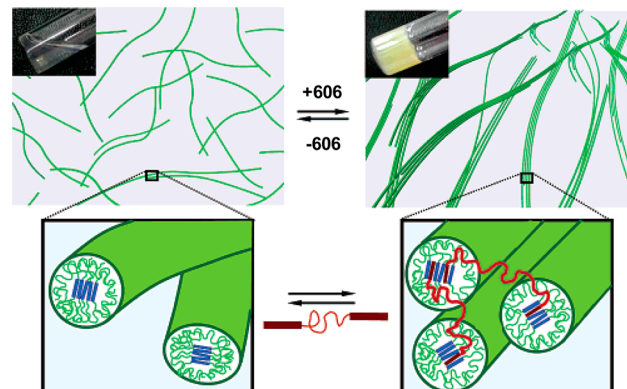


Figure 73. Schematic representation of reversible bridging between isotropic fluid and nematic gel. (Reprinted with permission from ref 1182. Copyright 2005 American Chemical Society.)

upon heating.¹¹⁸³ By adding hydrophobic guests, the gel transformed into a sol along with the transformation of the long gel fibrils to discrete micelles. Interestingly, amphiphiles **609** and **610** (Chart 148) containing oligo(ethylene oxide) dendrons and aromatic rod segments behaved in a different way to conventional gels.^{1184,1185} In these cases, anisotropic gels reversibly transformed into transparent solutions upon cooling. Helical stacks of the carbazole end-capped aromatic amphiphile **609** exhibited a preferred handedness upon addition of water into methanol solution or due to the enhanced hydrophobic interactions between the dehydrated oligo(ethylene oxide) dendrons by heating the aqueous solution.¹¹⁸⁴ Nanofibers of amphiphilic molecules **610a,b** under aqueous condition formed hydrogels, which may find applications in tissue engineering and controlled drug delivery.¹¹⁸⁵ For example, the myoblast mouse muscle adherent cells grown within these 3D gels could be released into solution upon cooling.

A series of dumbbell shaped dendritic molecules **611a-c** (Chart 149) with a stiff aromatic *p*-terphenylene core, have been shown to exhibit AIEE due to planarization of *p*-terphenylene unit in the gel state.¹¹⁸⁶ Organogelation of

Chart 148

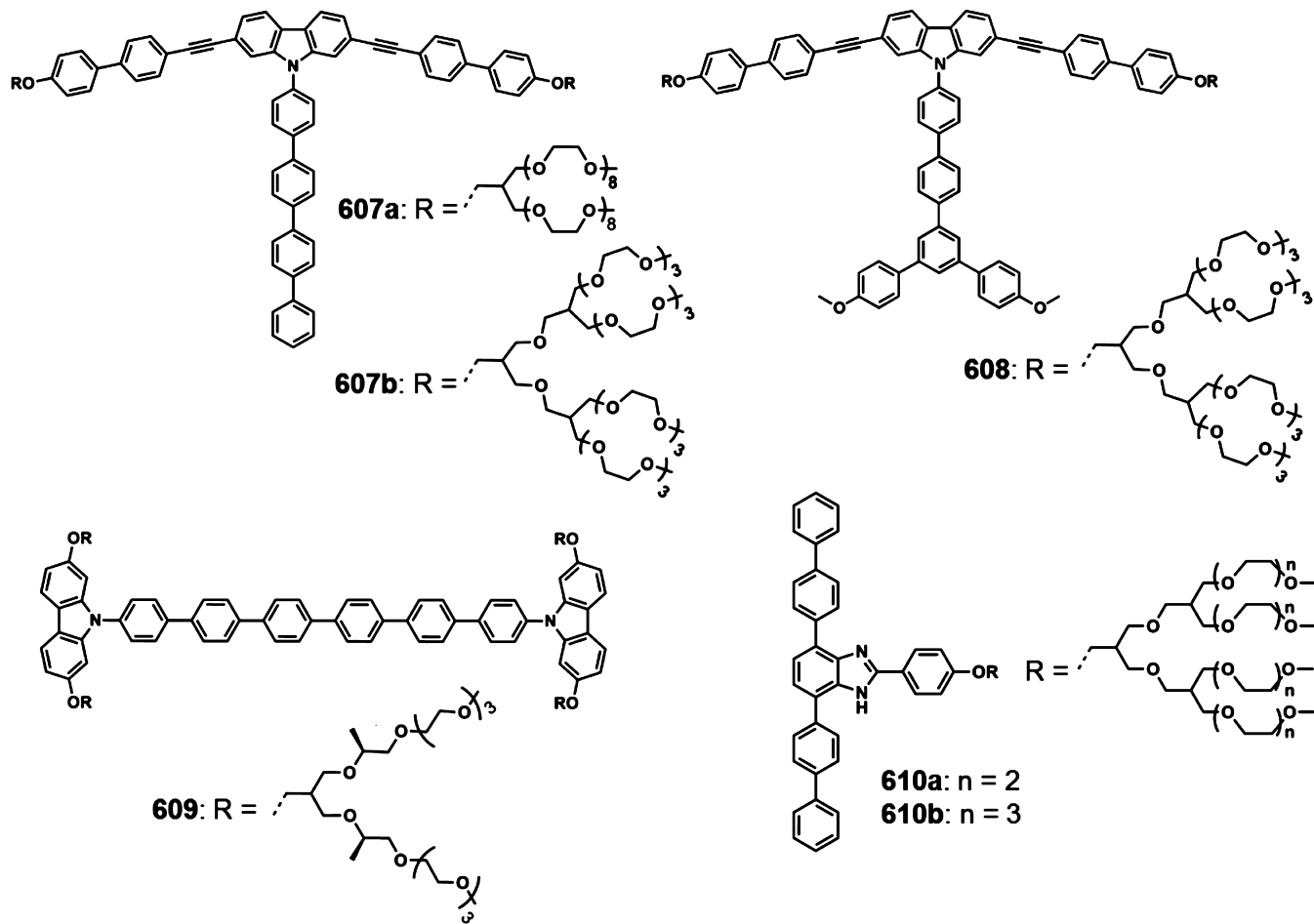
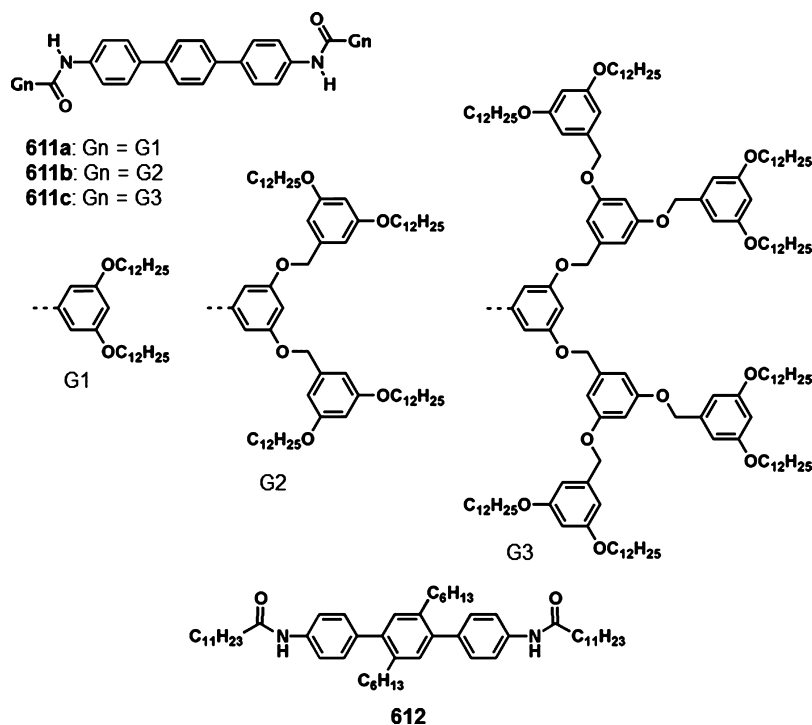


Chart 149



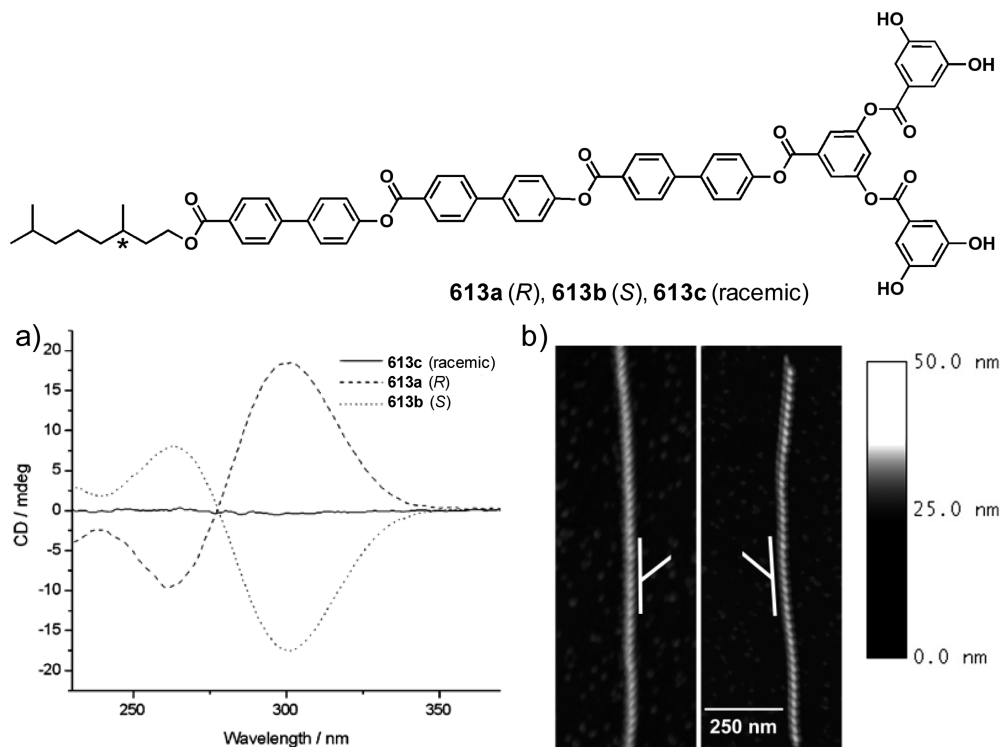
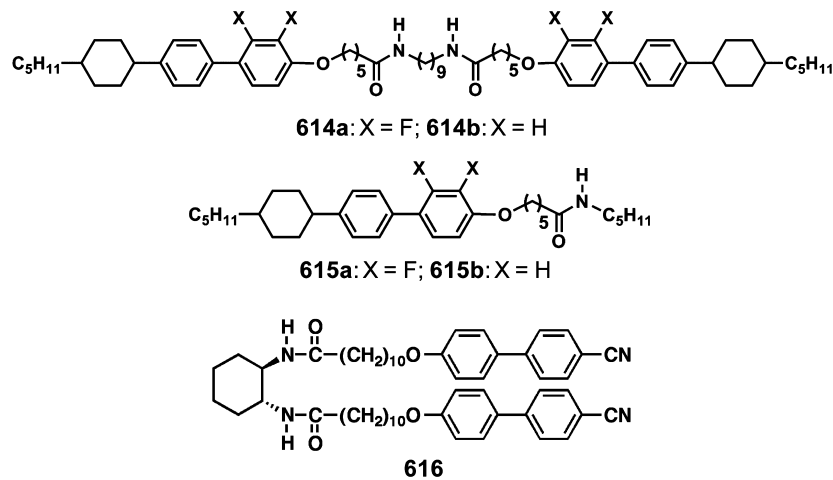


Figure 74. CD spectra of **613a** (*R*), **613b** (*S*), and **613c** (racemic) DRC. AFM images of **613a** (left) and **613b** (right). The white lines indicate handedness. (Reprinted with permission from ref 1197. Copyright 2005 American Chemical Society.)

Chart 150



terphenyl derivative **612** (Chart 149) carrying two lateral undecyl chains through amide linkages resulted in the formation of network structures composed of high aspect ratio nanoscale fibrous aggregates.¹¹⁸⁷

Stupp and co-workers have studied the self-assembly and organogelation of DRC molecules consisting of coil-like, rod-like, and dendritic segments.^{1188–1197} The use of bulky dendrons prevented the formation of 2D assemblies whereas identical aromatic rod-dendron segments enabled 1D aggregation through π - π stacking and hydroxyl groups at the periphery of the dendrons facilitated hydrogen bonding. The self-assembly of DRC molecule leads to a network of long ribbons consisting of two hydrogen bonded DRC molecules, leading to gelation in organic solvents^{1189,1190} as well as in styrene and acrylates.^{1191–1193} Further studies have utilized the

amphiphilic nature of the generated twisted DRC ribbons as templates for the fabrication of single¹¹⁹⁴ and double¹¹⁹⁵ helices of CdS. The DRC scaffold has also been used to disperse ZnO crystals at room temperature.¹¹⁹⁶ The presence of hydrogen bonding and the π -stacking interactions enabled the *R*-, *S*-, and racemic DRC molecules **613a–c** (Figure 74) to form birefringent gels.¹⁰¹⁸ Interestingly, the CD spectra of self-assembled **613a,b** showed exciton coupled signals of the biphenyl chromophore due to the influence of the chiral coil segment on the handedness of the π -stacked biphenyl rod segments (Figure 74a). AFM images of **613a,b** showed left and right handed helices indicating the formation of mirror image nanostructures (Figure 74b).

Kato and co-workers have significantly contributed to the study of LC physical gels obtained by the dispersion of gelators

Chart 151

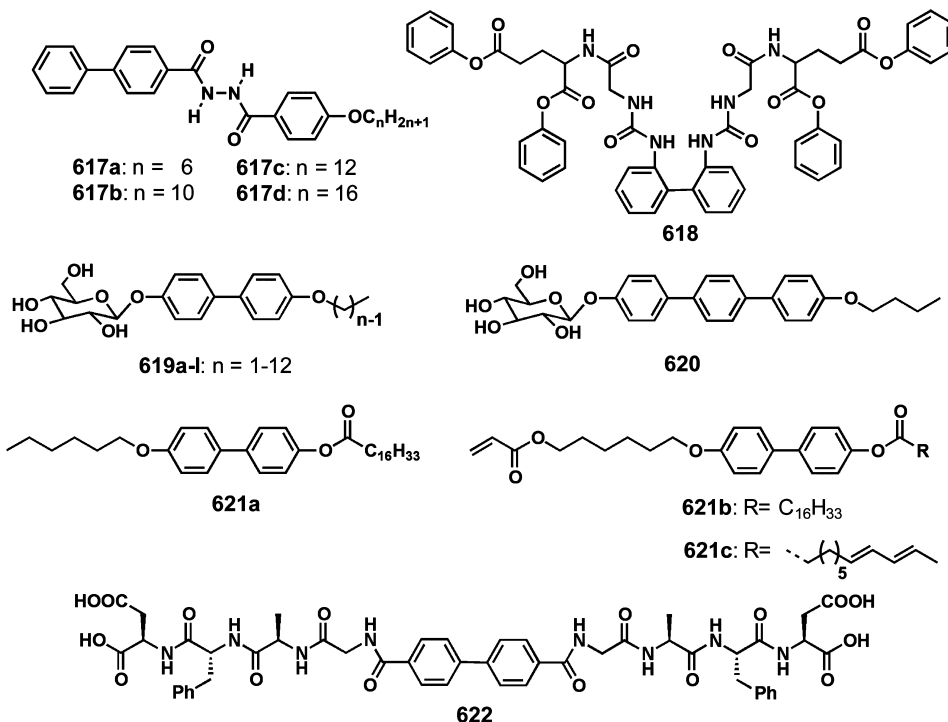
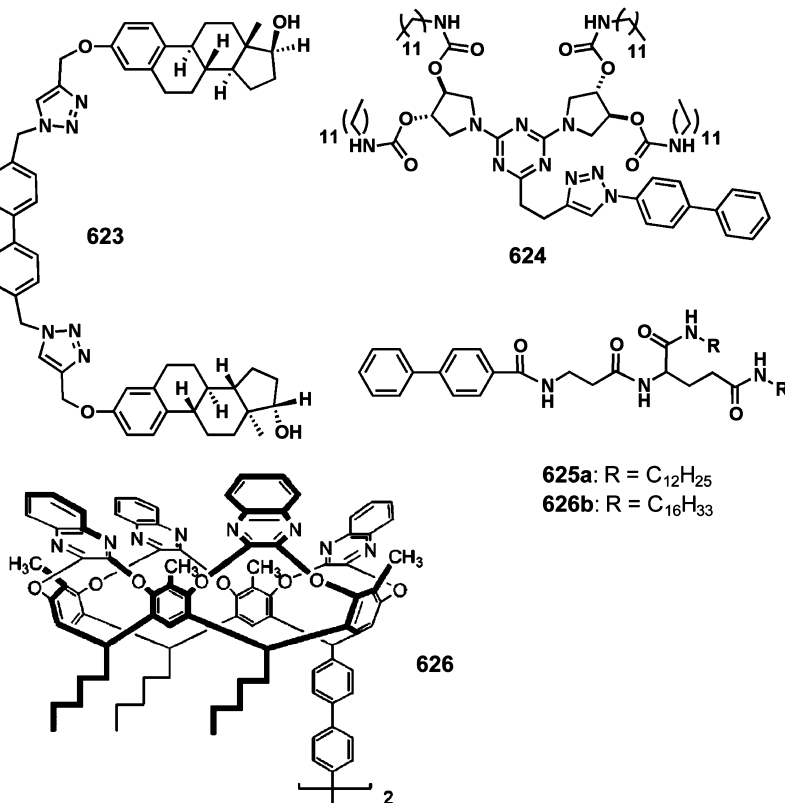


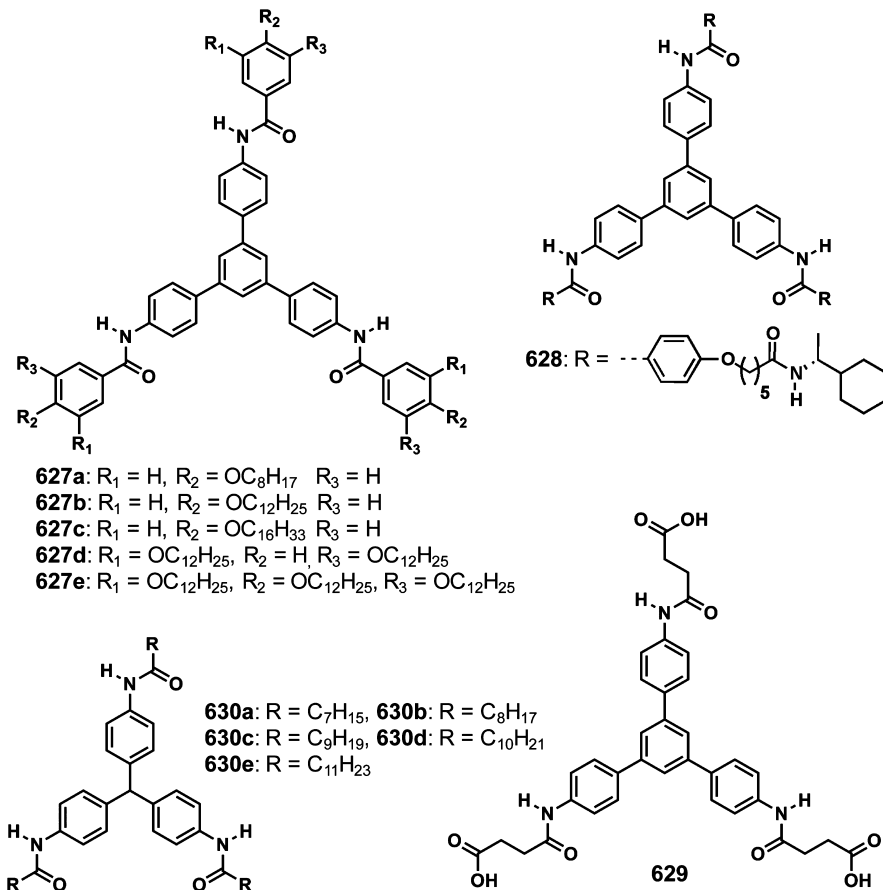
Chart 152



in LC solvents.^{101,102,1198} The concept itself is of particular importance due to the combination of two different components that form phase separated structures. The anisotropic phase separated structures retain the stimuli responsive properties of the LC and leads to the induction of enhanced electrooptical, photochemical, and electronic proper-

ties. The strong intermolecular interactions between the LC and the gelator enabled to orient the gelator molecules either in parallel or perpendicular to the molecular long axis of the LCs. Extensive studies have shown that a pool of gelators could be dispersed in LC gels to get functional assemblies with properties such as electrooptical switching, stimuli responsive

Chart 153



or photothermal control, photopolymerization, anisotropic charge carrier transport, electronic conductivity, polarized emission etc.^{342,1199–1209} Thus, the anisotropic physical gels help to the development of photo/electro active or stimuli responsive materials that are useful in advanced applications.

Control over the alignment of self-assembled fibers formed from the isotropic solution states of the gelators could be achieved by the application of AC electric fields.³⁴² The gelation abilities of **614a** and **615a** (Chart 150) with fluoro substituents were found higher than that of the nonfluorinated gelators **614b** and **615b** (Chart 150). By the application of an AC electric field, aligned fibrous aggregates were formed in the case of **614a**, in contrast to the plate like aggregates of **615a**. A *trans*-1,2-bis(acylamino)cyclohexane functionalized with biphenyl units through amide linkage **616** (Chart 150) has been reported to function as a gelling agent for isotropic and LC states of a cyanobiphenyl based LC.¹²⁰⁹

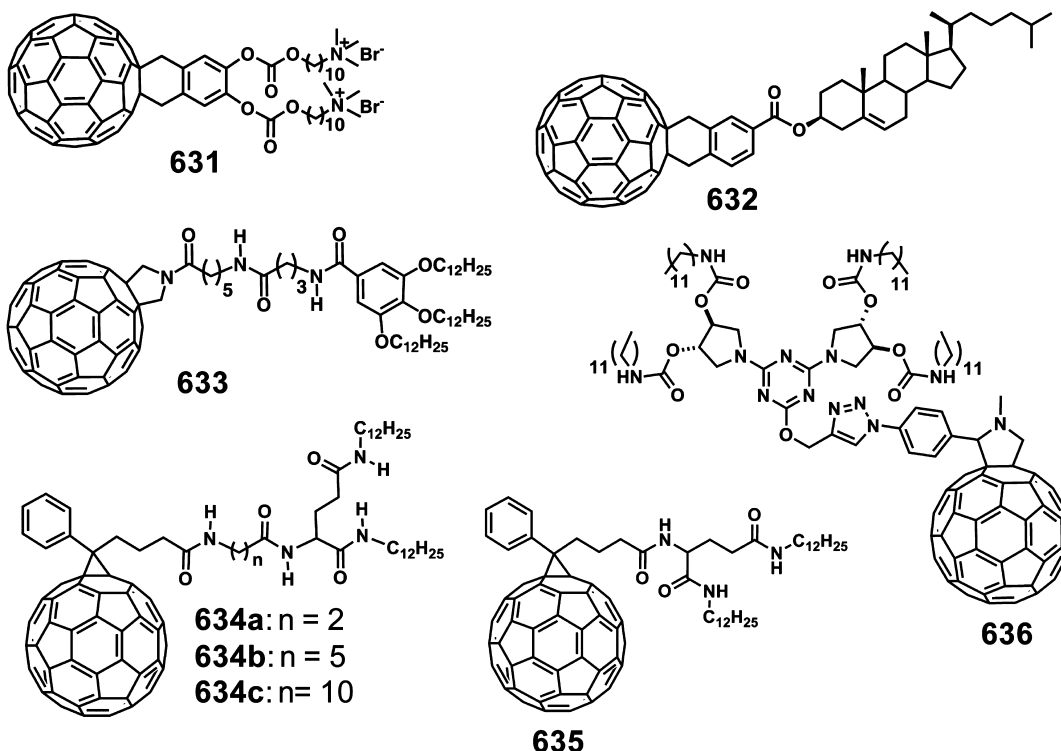
The mesomorphic dihydrazide derivatives **617a–d** (Chart 151) exhibited LC properties and gelation in organic solvents.¹²¹⁰ The biphenyl functionalized glycine-glutamic acid based dipeptide **618** (Chart 151) has been reported as a fluoride ion sensor in solution and as a sonication assisted organogelator.¹²¹¹ Another example for a biphenyl based gelator is 4-(4'-ethoxyphenyl)phenyl- β -D-glucoside **619b** (Chart 151), which formed gels by strong π - π stacking interaction assisted H-type arrangement of the biphenyl unit.¹²¹² Detailed studies indicated the formation of a 3D network made up of helical ribbons with an interdigitated bilayer structure. Later, a series of sugar appended organogelators with varying chain length of alkyl tail **619a–l** (Chart

151) has been reported.¹²¹³ Morphological studies revealed helical ribbon-like nanostructures for gels and platelet-like structures for precipitates. The terphenyl analogue **620** (Chart 151) was also found as an efficient gelator, which formed right handed ribbons on fast cooling and left handed ribbons on slow cooling.¹²¹⁴

Biphenyls **621a–c** (Chart 151) functionalized with long hydrocarbon alkyl chains and polar ester groups can gelate a range of organic solvents including polymerizable solvents such as methyl methacrylate, hexyl methacrylate and acrylonitrile.^{337,1215} Polymerization of a composite organogel consisting of an organogelator **621c** and a functional monomer resulted in the formation of molecularly imprinted organogel nanofibers.¹²¹⁵ Synthesis and gelation properties of a biphenyl moiety symmetrically end functionalized with peptide segments **622** (Chart 151) has been reported.⁴³² There are several other examples for biphenyl based gelators **623–626** (Chart 152).^{855,1216–1219} In addition, various biphenyl derivatives have been doped into organogels for making composite materials that behave as LC physical gels.^{1199,1219}

Lu et al. have reported the self-assembly and gelation properties of a series of discotic gelators **627a–e** (Chart 153) containing triphenylbenzene core and alkoxy side chain with varying length, exhibiting AIEE.¹²²⁰ The incorporation of *N,N'*-di(octadecyl)-perylene-3,4,9,10-tetracarboxylic diimide in the gel matrix of **627b** enabled tuning of the emission features through fluorescence resonance energy transfer between **627b** and perylene dye.¹²²¹ Other examples for triphenylbenzene core based discotic organogelators are **628** and **629** (Chart 153).^{1222,1223} The gelator **629** formed two component gels

Chart 154



with 4-(4-alkoxybenzoyloxy)-4'-stilbazole derivatives having varying alkyl chains.¹²²³ Morphological analysis revealed the formation of 2D sheet-like structures, nanotapes, and nanorods by the gelator **629** upon complexation with stilbazole derivatives having octyloxy, decyloxy, and dodecyloxy side chains, respectively.¹²²³ Organogel formation has been reported upon triple condensation reaction of a tribromo acid derivate of an extended triphenylbenzene with 4-*tert*-butylcatechol to give a triboronate ester, which was then linked by the 4,4'-bipyridine.¹²²⁴ The gelation in this case was due to the formation of 2D polymers, which eventually entangle into 3D-network structure. Houjou et al. have reported the gelation of a series of triphenylmethane based C₃ triamides **630a–e** (Chart 153) and correlated the dependence of gelation properties as well as morphology on the alkyl chain length.¹²²⁵

7. CARBON ALLOTROPS AND RELATED GELATORS

7.1. Fullerenes (C₆₀s)

C₆₀ is one of the most studied carbon materials in the last few decades, mainly because of its interesting optoelectronic and electrical properties.^{1226,1227} Synthetic manipulation and coassembly with other organic compounds have led to functional C₆₀ assemblies.¹²²⁸ C₆₀s find applications in FETs and PVDs, magnetic and superconducting materials, and in biology.¹²²⁸ In this context, organogelation of C₆₀ derivatives has been widely discussed due to the morphological and functional diversity of the assemblies created using spherical π-interactions supported by other noncovalent interactions.

The first report of a C₆₀ organogel came from the research group of Shinkai.¹²²⁹ Sonication of a methanol solution of a C₆₀ amphiphile **631** (Chart 154) bearing two ammonium groups, formed membrane like globular assemblies at lower concentrations and fibrous organogel aggregates upon keeping the solution for a few days. A cholesterol appended C₆₀ gelator **632**

(Chart 154) also formed transparent gel in dichloromethane.¹²³⁰ The chiral, columnar 1D packing of the cholesterol moieties enabled helical column formation, decorated with chirally oriented C₆₀ moieties outside. Nakamura and co-workers have demonstrated the formation of 1D nanostructures of C₆₀ functionalized with 3,4,5-tris(dodecyloxy)benzamide moiety **633** (Chart 154).¹²³¹ Hydrogen bonding and π–π interaction between the C₆₀ parts enabled to form a monolayered fibrous structure in the cast film at the air/water interface.

The C₆₀ linked L-glutamide **634a–c** (Chart 154) form gels in mixed organic solvents.¹²³² These gels exhibit electron transfer when coassembled with appropriate porphyrin derivatives. Interestingly, the coassembly of **635** (Chart 154) with exTTF derivative enhanced the sol–gel phase transition temperature and resulted in the formation of stable assemblies and gels.¹²³³ The steric hindrance of the pendant C₆₀ hamper the extended molecular ordering and hence only weak gels were formed in the case of gelator **636** (Chart 154).¹²³⁴ It has been proposed that C₆₀ can form single component gels, which can be identified by the slow dynamics and long-lived network structures.¹²³⁵ In addition, C₆₀ doped PMMA composite gels are also known in the literature.^{1236,1237} C₆₀/derivatives have been incorporated into gel matrix through noncovalent interaction with other host molecules, especially, porphyrins and are discussed separately (section 3.6).

7.2. Carbon Nanotubes

CNTs consist of graphitic sheets, rolled up into a cylindrical shape resulting in quasi 1D structures.¹²³⁸ The length of CNT is in the size of micrometers with diameters up to 100 nm. Because of their extraordinary properties, CNT can be considered as attractive candidates in diverse applications.¹²³⁹ CNTs can be functionalized by chemical reactions that make them more soluble for their integration into inorganic, organic,

and biological systems, however, hamper their inherent electronic properties.¹²⁴⁰ On the other hand, physical interaction with suitable molecules allow a better processing of CNTs toward the fabrication of nanodevices without compromising the electronic properties.^{1239–1241} Chemical functionalization and supramolecular physical interaction of CNTs with appropriate gelator molecules may facilitate the formation of hybrid gels. There are a few reports related to covalently functionalized CNT gels.^{1234,1242–1244} Chang and co-workers have reported the uniform distribution of CNTs in organogels of agarose by the gelation of covalently functionalized CNTs containing an organic branch having a similar structure to that of the organogelator.¹²⁴² A multiresponsive, switchable CNTs gel was prepared out of hyper branched poly(amido amine) functionalized CNTs.¹²⁴³ The organic functionalization of MWCNTs with a highly efficient organogelator allowed the production of novel and homogeneously dispersed soft nanocomposites.¹²³⁴ Oxidized SWCNTs could form viscous hydrogels due to the interaction through hydrogen bonds involving water molecules.¹²⁴⁴

π -gelators can effectively disperse CNTs in gel scaffolds. For example, the OPV gelator **556a** (Chart 136)¹¹²⁴ and tri(*p*-phenylenevinylene) bisaldoxime based gelators **569a–c** (Chart 138)^{1131,1132} have been used for the dispersion of SWCNTs and MWCNTs resulting in hybrid gels (Figure 75). These gel

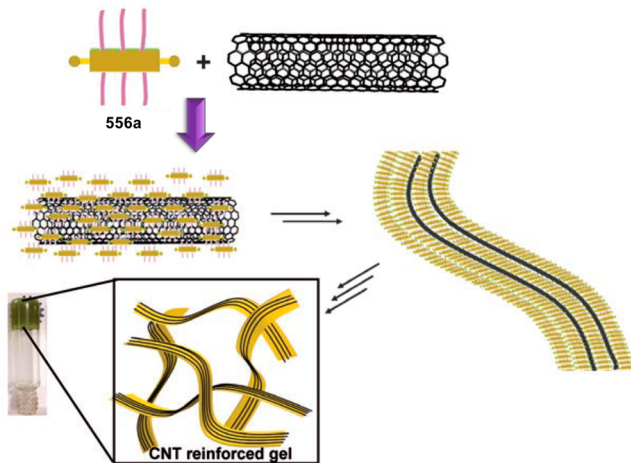


Figure 75. Schematic representation of **556a**-CNTs hybrid gel formation. (Reprinted with permission from ref 1124. Copyright 2008 Wiley-VCH.)

nanocomposites exhibited improved mechanical, thermal and electrical properties. Strong $\pi-\pi$ interactions between pyrene units of different gelators such as **235d**⁵⁷⁷ (Chart 57), **245**⁵⁹⁰ (Chart 61), and **248**^{592,593} (Chart 61) facilitated dispersion of SWCNTs leading to hybrid gel formation. SWCNTs could be effectively dispersed into the hydrogel of β -D-glucopyranoside-azonaphthol conjugate **211a** (Chart 51).⁵²¹ An L-alanine based low molecular weight gelators also interact with CNTs.¹²⁴⁵ A composite gel of CNTs with the presence of tetrakis(2-hydroxyethyl)orthosilicates was found useful as an amperometric hydrogen peroxide biosensor.¹²⁴⁶ Aqueous dispersions of surfactant stabilized SWCNTs displayed gelation as a result of 3D networks through weak physical interactions.¹²⁴⁷ The centrifugation of SWCNTs in the presence of hydroxylamine hydrochloric acid salt resulted in the dispersion of CNTs and

the lower viscous fraction obtained on redispersion in THF formed viscous nanotube gels.¹²⁴⁸

There have been significant interests in biogels of CNTs, obtained by the combination of various biorelevant molecules and CNTs.¹²⁴⁹ Lu and co-workers have reported the preparation of pH responsive and strength tunable DNA-SWCNTs hybrid hydrogel.¹²⁵⁰ A bile salt biosurfactant, sodium deoxycholate, was able to trigger the hydrogelation of SWCNTs.¹²⁵¹ In addition, electrically conductive nanowires and nanopatterns were created by direct printing using hydrogels as a solid ink. The composite gel of pristine SWCNTs and supramolecular amphiphilic dipeptide carboxylates is a good scaffold for superior peroxidase activity of cytochrome c.^{883,1252} Functionalized SWCNT and Fmoc-Phe-OH hybrid hydrogel exhibited enhanced storage modulus.⁷⁸⁸ A chemically responsive supramolecular hydrogel of SWCNTs and pyrene modified β -CDs has been reported by utilizing host–guest interaction between β -CDs and polymers carrying PAA functionalized with 2 mol % of dodecyl groups (Figure 76).¹²⁵³ Supramolecular hydrogels composed of SWCNTs

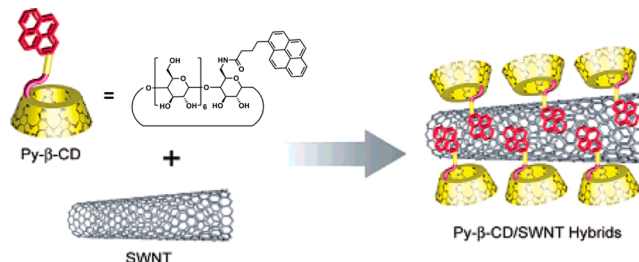


Figure 76. Schematic representation showing the noncovalent functionalization of SWCNT surface by using Pyrene appended β -CDs. (Reprinted with permission from ref 1253. Copyright 2007 American Chemical Society.)

wrapped with α -CD modified Curdlan composite and a guest polymer with an azobenzene pendant.¹²⁵⁴ UV irradiation of the supramolecular gels lead to gel–sol transition due to the association and dissociation between the α -CD unit and the azobenzene unit. There are other reports on hybrid CNT gels of cyclodextrin or gelatin based hydrogels.^{1255,1256} Wallace and co-workers have reported that the hyaluronic acid SWCNTs dispersion exhibits an increase in viscosity upon changing to a biphasic system with birefringence of nematic LC, which displayed gel-like characteristics.¹²⁵⁷ Highly conducting CNT biofibers were prepared by dispersing CNTs using biomolecules such as hyaluronic acid, chitosan, DNA etc.^{1258–1261}

MWCNTs can be effectively dispersed in 12-hydroxystearic acid gel in 1,2-dichlorobenzene.¹²⁶² Sodium dodecylsulfate-SWCNT-agarose gel composite based patterning methodology has been developed with the help of microfabricated poly(dimethylsiloxane) as a template.¹²⁶³ A peptide amphiphile containing a short hydrophobic alkyl tail and a hydrophilic peptide sequence has been used for the dispersion and hydrogelation of CNTs.¹²⁶⁴ TEM images of the composite gel confirmed the presence of an organic coating on the exterior sidewall of the outermost nanotube shell, due to the aggregation of peptide amphiphile on the surface of CNTs. Fibrous hydrogels have been prepared using β -lactoglobulin amyloid fibrils and sulfonic acid functionalized MWCNTs obtained either by diazonium reaction or by $\pi-\pi$ interaction with pyrene sulfonic acid.¹²⁶⁵

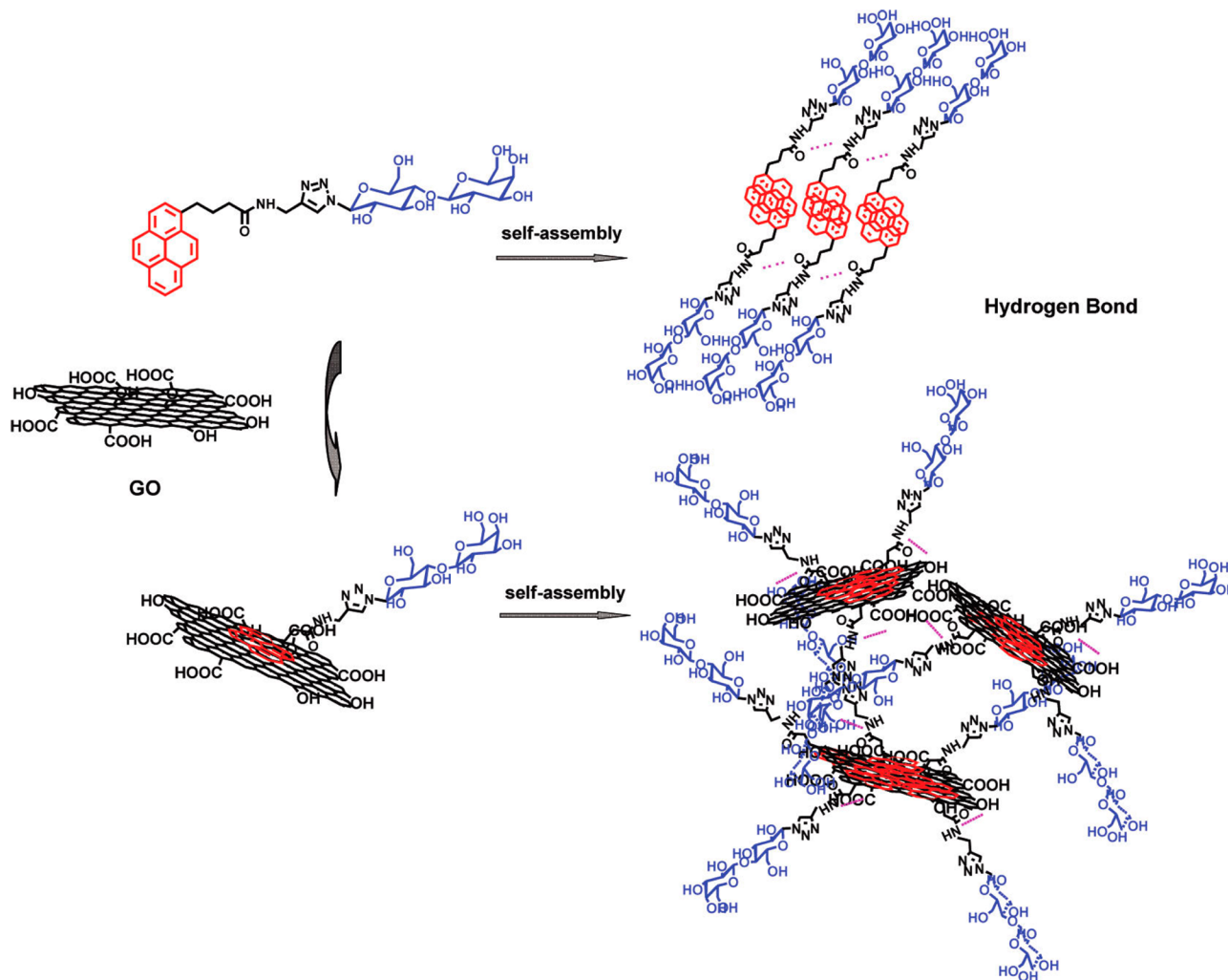


Figure 77. Schematic representation of the GO hybrid gel formation. (Reprinted with permission from ref 1297. Copyright 2012 American Chemical Society.)

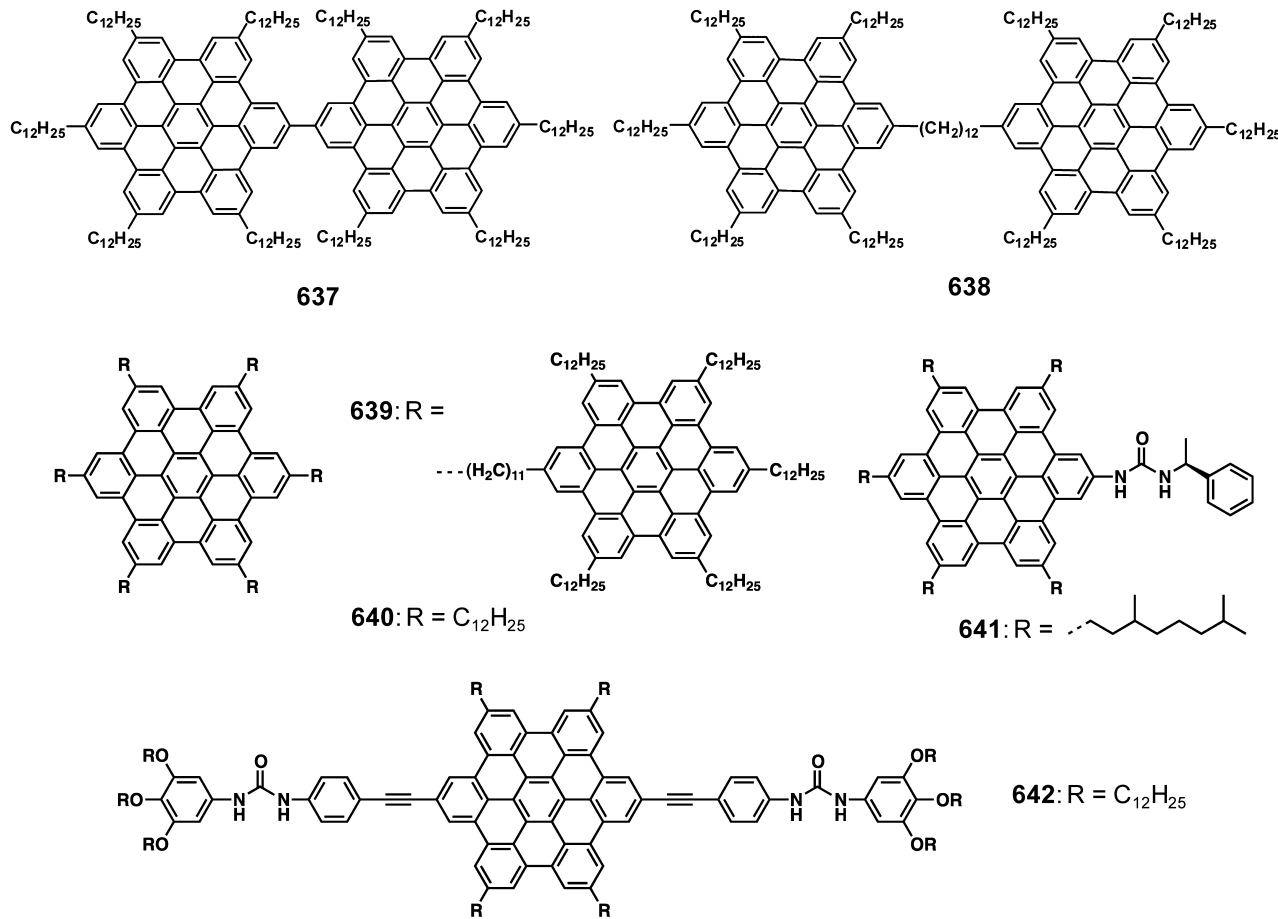
A large number of ionic liquids have also been used to disperse CNTs resulting in hybrid gels.^{31,58,67,76,1266–1274,1278} Fukushima, Aida and co-workers have reported that grinding SWCNTs in ionic solvents leads to the formation of bucky gels.¹²⁶⁷ These gels were formed by weak physical cross-linking of the nanotube bundles, mediated by local molecular ordering of the ionic liquids rather than by entanglement of the nanotubes. CNTs dispersed bucky gels have found applications as bucky plastic,¹²⁶⁸ actuator film,^{1269,1270} elastic conductor in organic FETs¹²⁷¹ and LEDs.¹²⁷² Ricci et al. have demonstrated that the performance of bucky gel actuators could be significantly enhanced by chemical modification of SWCNTs with diamines.¹²⁷⁵ The bucky gels produced using amide functionalized SWCNTs and an imidazole based ionic liquid allow preparation of low voltage bimorph actuators due to the improved charge storing ability resulted from enhanced binding between nanotubes.

An ionic oligomeric gelator has been used as a dispersant for SWCNTs.^{67,1276} A CNT-polymeric ionic liquid gel was prepared by noncovalent functionalization of oxidized SWCNTs surfaces with imidazolium based poly(ionic liquid), followed by in situ radical polymerization.¹²⁷⁷ Anion exchange process of poly(ionic liquid)s, results in the switching of hydrogels to organogels with improved thermal stability and

good electrical conductivity. An ionic liquid composite gel based electrochemical biosensor using potassium doped MWCNTs and 1-butyl-3-methylimidazolium hexafluorophosphate was developed by Xu and co-workers for the determination of superoxide anions released from cancer cells.¹²⁷⁸ A large number of SWCNT and polymers based composite gels have been prepared.^{1279–1282} Physical gelation of CNTs has also been achieved using polycarbonate, the properties of which has been studied by rheological analysis.¹²⁸³ SWCNT acrylamide gel has been used as molecular container for antineoplastic agent, doxorubicin hydrochloride, which was released into the bulk aqueous solution either by lowering the pH or by laser light irradiation.¹²⁸⁴

Design of stimuli responsive actuators has been demonstrated using composites of poly(*N*-isopropylacrylamide) hydrogel loaded with SWCNTs.¹²⁸⁵ The hydrogel of CNTs was prepared by UV curing of vertically aligned carbon nanotubes in the presence of 2-hydroxyethylmethacrylate monomer, ethyleneglycol dimethacrylate cross-linker, and a photoinitiator.¹²⁸⁶ This composite gel was useful as micro-transducers that physically direct and electrically transduce the swelling of gels. A hydrogel with superwettability was fabricated by coating vertically aligned carbon nanotube arrays with vapor deposited poly(methacrylic acid-*co*-ethylene glycol diacyr-

Chart 155



late).¹²⁸⁷ A liquid nonionic surfactant like polyoxyethylene-tridecyl ether has been used to disperse SWCNTs that formed stable gel without a solvent by mechanical grinding and subsequent ultrasonication.¹²⁸⁸ Highly conductive and transparent SWCNTs thin film was obtained by coating the gel on a surface followed by surfactant removal.

Noncovalent functionalization of SWCNTs using ferrocene linked poly(*p*-phenyleneethynylene)s resulted in free-standing organogel.¹²⁸⁹ Strong π -interaction between the aromatic functional moieties and SWCNTs surface, especially, cross-linking of the neighboring carbon nanotube surfaces by ferrocenyl groups, enabled the formation of 3D nanotube network and drove the assembly to gelation. Polymers such as aromatic polyimides,¹²⁹⁰ poly(acrylamide)¹²⁹¹ and tetrathiafulvalene vinylogues-phenylacetylene polymer,¹²⁹² etc. have also been used to disperse CNTs leading to gelation in various solvents.

7.3. Graphenes

Graphenes exhibit remarkable electronic, optical, thermal, and mechanical properties, including high Young's modulus, fracture strength, thermal conductivity, charge carrier mobility, high chemical stability, and high optical transmittance.^{1293–1296} Graphenes find applications in reinforced composites, sensors, catalysis, energy conversion and storage device, displays, PVDs and in biology.^{1293–1296} Self-assembly of graphenes with molecular systems into micro/macrosopic materials can exhibit the properties of individual graphene sheets and find numerous applications in different areas such as optoelec-

tronics, energy storage, and in biomedicine. Since graphenes lack good solubility in solvents, chemical or physical modifications are required for its use.^{1294,1295} As in the case of CNTs, gelation is a facile route to disperse graphenes into solutions and to extend the 2D structure of graphenes to supramolecular 3D structures in the gel matrix. The functional properties of graphene could be enhanced to a certain extent through gelation approach. More attention has to be paid to explore the gelation properties of graphene based materials for any potential application.

Aromatic molecules with a planar π -surface such as pyrene can effectively cross-link between graphene sheets.^{582,1297} GO gel networks were obtained by the interaction of amphiphilic molecules having polar carbohydrate head groups attached to a nonpolar pyrene group (Figure 77).¹²⁹⁷ Unfunctionalized and nonoxidized graphenes can be dispersed in an *o*-dichlorobenzene solution of the pyrene conjugated oligopeptide gelator **239e** (Chart 58) and form stable hybrid gels upon sonication of a hot solution after cooling to room temperature.⁵⁸² In recent years a large number of different graphene based hybrid gels having intriguing properties have been reported.^{1298–1320} For example, a hydrogel of metal organic framework and azobenzoic acid functionalized GO has been used as a chemosensor for the detection of TNT.¹³⁰¹

Hydrogels composed of GO and conducting polymer PEDOT:poly(styrenesulfonate) with high electrical conductivity are useful in polymer tandem solar cells.¹³²¹ The graphene/carbon composite aerogels obtained from alkali treated GO/resorcinol formaldehyde composite hydrogels exhibit low

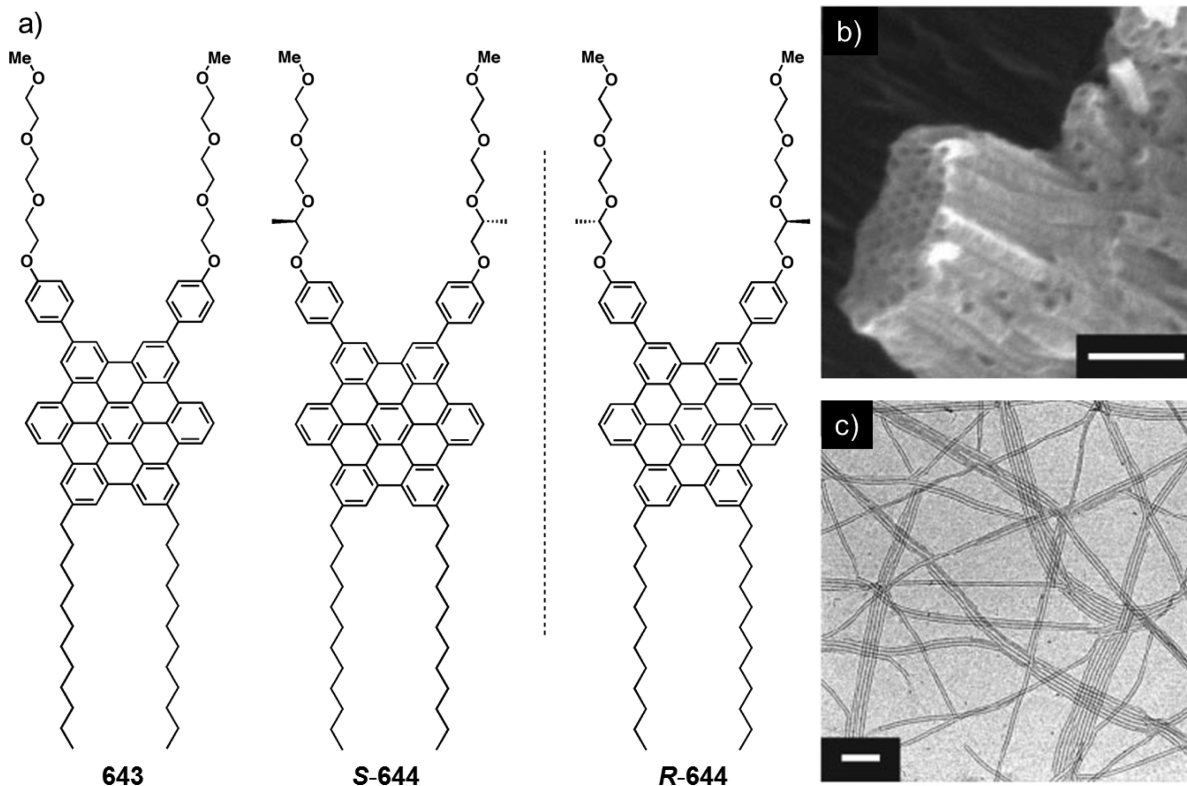


Figure 78. (a) Molecular structures of Gemini shaped amphiphilic HBCs. (b) SEM and (c) TEM micrographs of a thin film cast from a suspension of tubularly assembled **643**. The scale bar for SEM and TEM micrographs is 100 and 200 nm, respectively. (Reprinted with permission from ref 1344. Copyright 2004 American Association for the Advancement of Science.)

density, narrow pore size distribution, large specific surface area, and specific capacitance of 122 F g^{-1} that are suitable for application in supercapacitors.¹³²² Graphene hydrogels with tape-like, cylindrical, pear-shaped, and spherical 3D architectures can be obtained by a one-step mild chemical reduction and an *in situ* self-assembly.¹³²³ Sonication of a mixture of GO dispersion and CNT powder resulted in a GO/CNT hydrogel.¹³²⁴ The strong interaction between CNTs and GO leads to robust, free-standing GO/CNTs hybrid papers, useful as electrodes in supercapacitors. The use of an acetonitrile GO gel containing a quasi solid electrolyte (iodide/triiodide) in dye sensitized solar cells (1% GO gel electrolyte) achieved energy conversion efficiency (η) of 7.5%.¹³²⁵

In addition, *in situ* generated multivalent metal ions or *in situ* protonated polyamines have been employed to develop GO hydrogels with the assistance of glucono- δ -lactone promoter.¹³²⁶ The deposition of rGO hydrogel in the micropores of nickel foam enabled to fabricate a graphene hydrogel/nickel composite electrode.¹³²⁷ High conductivity and electrochemical stability of the gel as well as the 3D interpenetrating microstructure have contributed to the excellent performance of the electrode. Poly(*N*-isopropylacrylamide)-GO nanocomposite hydrogel synthesized via *in situ* γ -irradiation assisted polymerization of the monomer in the presence of GO exhibited tunable photothermal properties.¹³²⁸ Hydrogels of GO obtained in presence of polyamines have been used for the preparation of noble metal nanoparticles along with coreduction of GO.¹³²⁹ The noble metal nanoparticle-rGO hybrid hydrogel was found as an active catalyst for the reduction of aromatic nitro to amino group.

7.4. Coronenes

The polycyclic aromatic hydrocarbons such as coronenes and HBCs are considered as promising π -systems for supramolecular electronics because of their strong tendency to form 1D columnar structures via π -stacking interactions and thereby facilitating efficient electron and energy transports.^{1330–1339} HBCs consisting of thirteen fused benzene rings are considered as a smallest fragment of a graphene sheet and often called as a synthetic nanographene.^{1336,1337} Müllen and co-workers have studied the synthesis and properties of HBC derivatives.^{1332–1337} In the first report, bisHBC derivatives **637** and **638** (Chart 155) were found to gelate organic solvents such as *n*-heptane and toluene at very low concentrations.¹³⁴⁰ The broad, red-shifted absorption and emission spectra of **638** in low polar solvents indicate the strong chromophoric interaction when compared to **637**. A star shaped HBC “heptamer” **639** (Chart 155) was also found to form organogels due to the strong intermolecular π -stacking assisted aggregation of HBC units.¹³⁴¹ Very recently, gelation and solution state LC phase behaviors of a HBC derivative, substituted with six peripheral *n*-dodecyl side chains **640** (Chart 155) has been reported by Choi and co-workers.¹³⁴²

The role of intracolumnar hydrogen bonding to enhance the degree of the order of discotic molecules within a single column during the self-assembly of HBCs has also been studied.¹³⁴³ The reinforcement of the π -stacking interactions by the hydrogen bonds resulted in a supramolecular arrangement leading to LC states and fluorescent organogels of **641** and **642** (Chart 155). Morphological analysis using SEM and confocal laser scanning microscopy revealed the presence of fibrous aggregates in the gels.

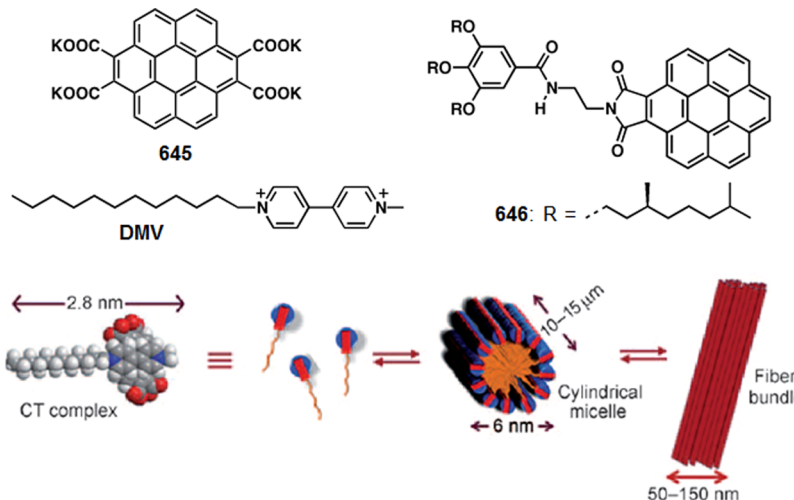


Figure 79. Schematic representation of the hierarchical self-assembly of the coronene **645**-methyl viologen derivative CT amphiphile into cylindrical micelles and fiber bundles. (Reprinted with permission from ref 1347. Copyright 2010 Wiley-VCH.)

Fukushima, Aida and co-workers have reported the self-assembly of a Gemini shaped amphiphilic HBC **643** (Figure 78) bearing two dodecyl chains on one side and two triethylene glycol chains on the other to form redox active and electroconductive nanotubes at lower concentrations.^{1338,1339,1344} At higher concentrations this molecule formed a gel in THF.¹³⁴⁴ The graphitic nanotubes formed by helical rolling of bilayer tapes composed of π -stacked HBC units exhibited an electrical resistance of $2.5\text{ M}\Omega$ which is comparable to that of the inorganic gallium nitride nanotube ($\sim 10\text{ M}\Omega$). The self-assembly of amphiphilic HBC having two chiral oxyalkylene side chains **S-644** and **R-644**, resulted in right and left handed helical graphitic nanotubular assemblies, respectively (Figure 78).¹³⁴⁵ The high level of chirality amplification as observed in CD spectra indicates a highly cooperative self-assembly process. Moreover, CD studies have revealed that the enantiomers of **644** coassembled to form nanotubes, whose helical sense was governed by the majority rule principle of supramolecular chirality. Similar to the achiral HBC **643**, cooling of the concentrated Me-THF solution of **644** to 20°C gradually turned the yellow colored solution to cloudy and finally to an organogel. Detailed XRD studies using a series of structurally similar HBC amphiphiles revealed structural parameters essential for the formation of nanotubular assembly, which involve making the discotic HBC molecule less symmetrical by incorporating two phenyl groups and the paraffinic side chains on opposite sides.¹³⁴⁶

While there are several reports on gelation of HBCs, similar studies with the parent molecule coronene are very few. George and co-workers have used the weak CT interaction between the coronene tetracarboxylate tetrapotassium salt **645** and an electron deficient dodecyl functionalized methyl viologen derivative for the creation of high aspect ratio cylindrical micelles and hydrogels through a stable 1:1 D-A CT complex (Figure 79).¹³⁴⁷ The noncovalent amphiphile like CT complex having an alternate face to face coassembly leads to cylindrical micelles which subsequently form laterally associated fiber bundles and a hydrogel (Figure 79).

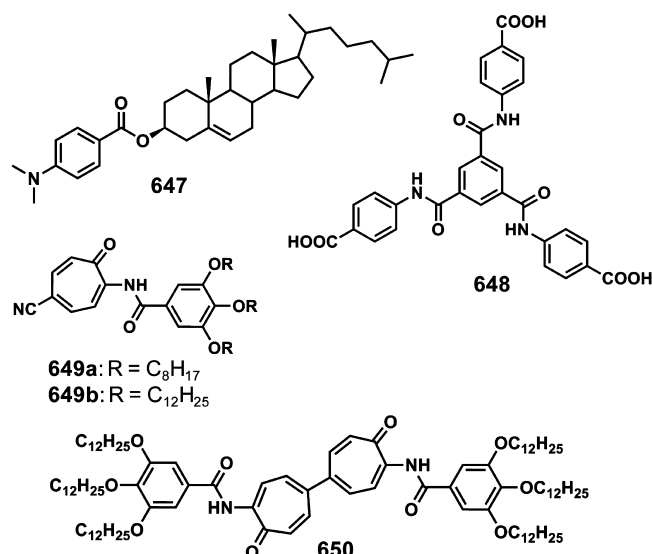
An amine terminated layered magnesium organosilicate based organoclays has been used as a template to organize **645** as donor and potassium tetracarboxylate of perylene system as acceptor, leading to hydrogels.¹³⁴⁸ The organogels

formed from the gallic amide appended coronene monoimide **646** (Figure 79) showed monomer-like emission in the aggregated state due to hydrogen bonding induced head to head frustrated dipolar assembly.¹³⁴⁹ This is an interesting method to enhance luminescent properties of chromophore assemblies through disorientation of dipolar chromophores. Lee et al. have reported the gelation of nanodiamond particles in ionic liquids.¹³⁵⁰ This is a very rare example in which imidazolium functionalized nanodiamond particles were well suspended in ionic liquids leading to a new type of soft functional material.

8. GELS FORMED BY MISCELLANEOUS CHROMOPHORES

In order to study the microenvironmental effect of gel fibrils on optical properties such as fluorescence, a twisted intramolecular CT probe, namely, dimethylaminobenzoate group was conjugated with a cholesterol group **647** (Chart 156).¹³⁵¹ Detailed studies revealed that the microenvironment around the gel fibril as well as the molecular mobility was independent

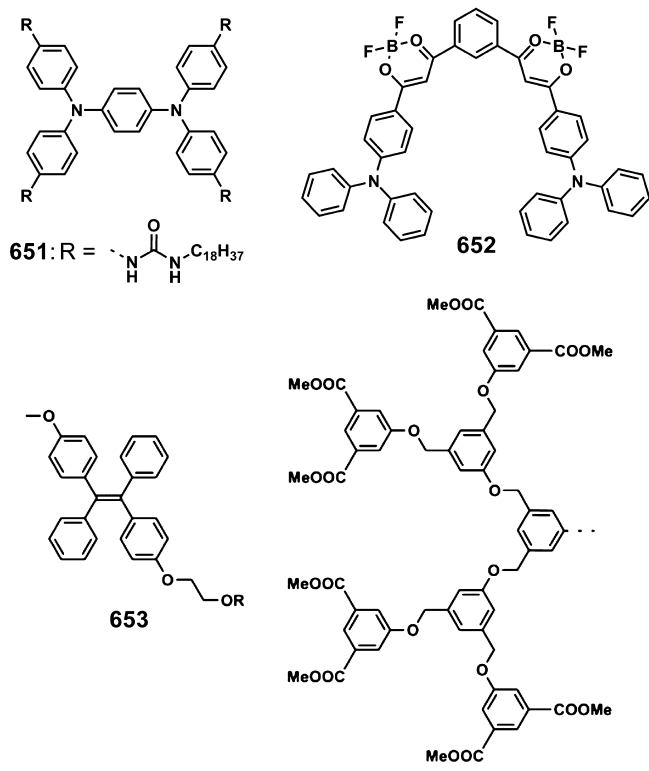
Chart 156



of the solvent polarity. pH-Sensitive hydrogelation of 1,3,5-benzene trisamide based LMOG **648** (Chart 156) resulted in tunable photoluminescence due to the formation of a supramolecular chromophore.¹³⁵² The resulted gels were fully pH reversible and thermostable up to 100 °C. The troponoid amides **649a,b** (Chart 156) exhibited hexagonal columnar phase and formed gels.¹³⁵³ In the gel state, the columnar ordering of the LC phase was retained with identical lattice parameters. A bitropone core connected with two 3,4,5-tridodecyloxybenzoylamino groups **650** (Chart 156) could gelate organic liquids using π -stacking interactions between intermolecular bitropone rings.^{1354,1355}

The triarylamine based gelator, *N,N,N',N'-tetrakis(p-octadecylido-phenyl)-p-phenylenediamine* **651** (Chart 157), ex-

Chart 157



hibits high ion conductivity of 3.5×10^{-3} S cm⁻¹ in NaClO₄/THF.¹³⁵⁶ A rigid boomerang shaped molecule **652** (Chart 157) with two β -diketone borondifluoride moieties linked to the meta positions of a benzene core exhibited good gelation ability in mixed organic solvents.¹³⁵⁷ A large Stokes shift was observed for the fluorescence when measured in polar solvents. This red shift was attributed to twisted intramolecular CT emission, which was suppressed in the gel state due to reduced conformational rotation. In addition, the fluorescence of the gel nanofibers has been quenched efficiently and rapidly upon exposure to gaseous amines and pyridine.¹³⁵⁸ The high surface/volume ratio, large interspace of nanofibrils, and intermolecular exciton diffusion enabled it as an efficient sensor for gaseous amines.

The dendron substituted gelator **653** (Chart 157) showed enhanced fluorescence due to restricted intramolecular rotation of the tetraphenylethene group in the gel phase.⁴³⁸ Energy transfer assisted fluorescence color tuning has been achieved by doping with varying amounts of perylenediimide in the gel

phase. Moreover, emission color switching by alternating UV/visible light irradiations was also observed by utilizing the photochromic transformation of spiropyran dopant. Stigmasterol containing tetraphenylethenes **654** (Chart 158) self-assembles in methanol solution to form organogels with GIEE characteristics.¹³⁵⁹

The linear nonsymmetric dihydrazide derivatives, *N*-(4-alkoxybenzoyl)-*N'*-(4'-nitrobenzoyl)hydrazines **655a-d**¹³⁶⁰ bis[(3,4-bisalkoxyphenyl)hydrozide]phenylenes **656a-d**¹³⁶¹ and salicylanilides **657a,b**¹³⁶² (Chart 158), are examples of LC based gelators. The aggregation induced planarization, the restricted intramolecular rotational motions, and J-aggregation are responsible for the enhanced emission in the organogel phase.

Depending on the substitution pattern of the alkylamido side chain, the truxene based molecules self-assembles to form vesicular (**658a**) and fibrillar (**658b**) morphologies in the gel state (Chart 159).¹³⁶³ The topochemical polymerization by irradiation of organogels of 1,8-diaryloctatetrayne **659** (Chart 159) led to a change in morphology from fibers to yellow fluorescent nanoparticles.¹³⁶⁴ Imines **660a-d** (Chart 159) obtained by the combination of two structurally simpler components could gelate alcohols because of the enhanced stacking interaction of the imine unit.¹³⁶⁵ Shigeno and Yamaguchi reported that the chiral aminohydroxyhelicene derivative **661** (Chart 159) formed a gel–liquid two layer system in THF-hexane mixture upon ultrasonication leading to diffusion controlled gelation.¹³⁶⁶ The dynamic covalent imine based oligomer surfactants obtained from water-soluble cationic bisaldehyde and various 1, ω -alkyl bisamines formed reversible stimuli responsive gels comprising of vesicular structures.¹³⁶⁷

9. APPLICATIONS OF π -GELS

While there are wide ranging applications for organogels in general, π -gels are of particular interests with respect to electronic and photonic applications.^{27,28,72,103,107} The special interests in π -gels are associated with their inherent electronic properties such as fluorescence,^{44,103} charge carrier mobilities,²⁸ electronic conductivities,^{28,1368} etc. Therefore, in recent years, considerable effort has been put in by the scientific community to the design of π -gels for specific application in the field of advanced materials.²⁵⁻²⁸ Supramolecular organization of chromophores attained through gelation approach induces strong electronic communication between the individual gelators, resulting in remarkable modulation of the electronic properties.^{44,53,103} Thus, it may be possible to impose significant control on electronic properties of π -gelators through gelation assisted self-assembly process. One of the most anticipated applications of π -gels is therefore, in the field of organic electronics. In this context, several activities have been reported during the past few years under the name of supramolecular electronics,¹⁰³⁷ which involves the use of self-assembled supramolecular architectures of nano- and micrometers in length scale as an active material in electronic devices. Even though this ambitious and challenging proposition appears attractive, a breakthrough is yet to come due to several bottlenecks associated with self-assembled organic structures. Gelation is one of the easiest and simple methods of organizing optoelectronically active π -conjugated molecules from nano to micro domains in a defined manner with precise control. The enhanced optoelectronic properties achieved through self-assembled nanostructures of oligomers are almost comparable to the performance of the polymers. Moreover, the available gel

Chart 158

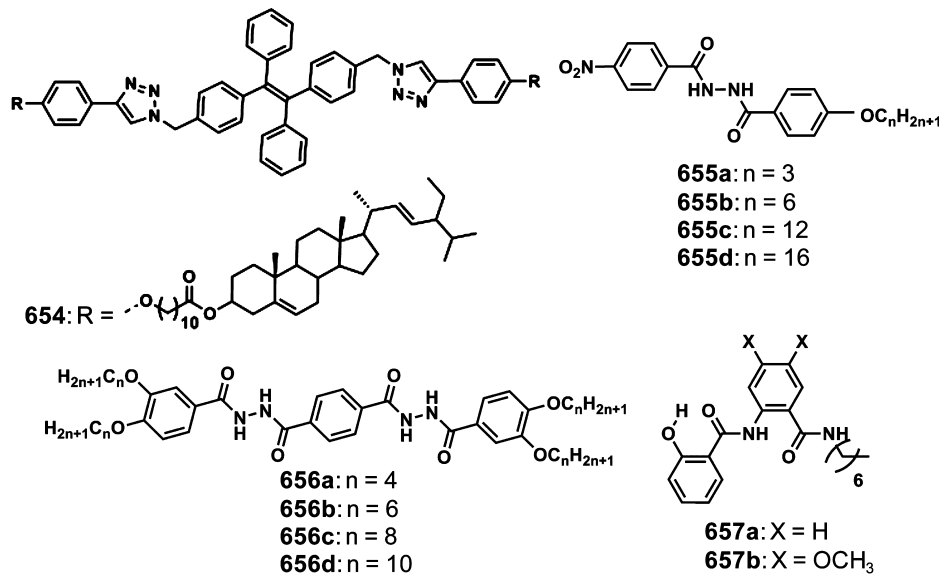
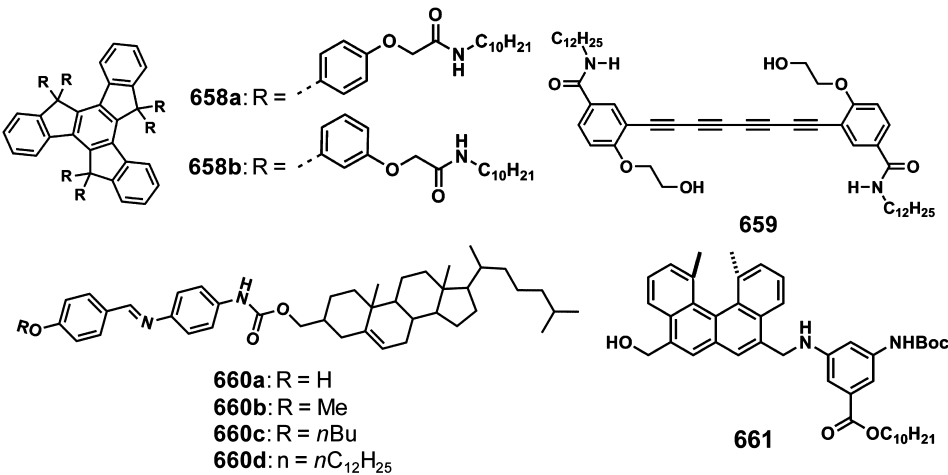


Chart 159



matrix to encapsulate organic and inorganic materials may result in various hybrid gels and thereby lead to tunable properties. The above-mentioned special features of organogels have been utilized in various applications trials, however is very limited. Nevertheless, it is important to continue the effort in this direction for which a deeper understanding of the existing knowledge is necessary and relevant. In this section we will try to address the recent developments with respect to some of the reported application of π -gelators, even though we have covered several aspects of it while discussing the different class of gelators in the previous sections.

9.1. Organic Electronics

Conducting nanowires of functional π -conjugated molecules are potential candidates in organic electronic devices.²⁸ Self-assembled 1D structures of organogelators show enhanced conductivity due to electron hopping through intermolecular interactions. In many of the cases, conducting properties of organogels were investigated in the film states as obtained from the xerogels on different substrates.

Thiophenes are one of the widely used conducting materials due to the better optoelectronic, redox, and charge transport

properties when compared to many other π -systems. Stupp and co-workers have reported that iodine doped xerogel film of the oligo(thiophene) DRC molecule 533 (Figure 61) exhibits conductivity of $7.9 \times 10^{-5} \text{ S cm}^{-1}$.¹⁰⁵⁵ The TRMC studies of xerogels of the amide end functionalized trithienylenevinylene molecular gelators (550a,b; Figure 64) from *n*-decane/chloroform mixture exhibited $\sum \mu_{\min}$ values of 6.0×10^{-2} and $7.4 \times 10^{-2} \text{ cm}^2 \text{ V}^{-1} \text{ s}^{-1}$ respectively in the presence of *N,N'*-bis(2,5-di-*tert*-butylphenyl)-3,4,9,10-PBI.¹⁰⁴⁸ The conductance of 0.93 nS observed for the undoped fiber bundles of 550d, was drastically increased to 7.1 nS upon doping with iodine vapors.¹⁰⁷⁷ Similarly, the bulk electrical conductivities (σ) of the undoped films 6.4×10^{-4} (550c) and $4.8 \times 10^{-2} \text{ Sc m}^{-1}$ (550d) measured using four probe method showed enhanced conductivities of 1.0×10^{-2} and 4.8 S cm^{-1} , respectively, after doping with iodine vapors (Figure 64).¹⁰⁷⁷

Yagai et al. have reported a barbituric acid functionalized quaterthiophene gelator 541 (Chart 133), which exhibited transient conductivity of $(\Phi \sum \mu)$ $1.0 \times 10^{-4} \text{ cm}^2 \text{ V}^{-1} \text{ s}^{-1}$. The value changed to $0.67 \times 10^{-4} \text{ cm}^2 \text{ V}^{-1} \text{ s}^{-1}$ upon coassembly with a bismelamine receptor BM12 (Chart 34).¹⁰⁶² In the case of the supramolecular complex of 144 (Chart 34) and the

complementary hydrogen bonding unit **B****Mn** (Chart 34), a higher 1D isotropic mobility (μ_{1D}) of the photogenerated charge carriers ($5.1 \times 10^{-3} \text{ cm}^2 \text{ V}^{-1} \text{ s}^{-1}$) was observed.³⁸⁰ The chiral discotic supramolecular complexes of monotonically triple hydrogen bonding melamines having two PBI chromophores **171** (Chart 41) and with tritopically triple hydrogen bonding cyanuric acid **CA** (Chart 41) showed $\Phi \sum \mu$ value of $1.4 \times 10^{-5} \text{ cm}^2 \text{ V}^{-1} \text{ s}^{-1}$ and $(\sum \mu)$ of $0.03 \text{ cm}^2 \text{ V}^{-1} \text{ s}^{-1}$.⁴²⁷

Self-assembly of amphiphilic HBCs leads to the formation of redox active, electroconductive nanotubes and gels with high charge carrier mobility.¹³⁴⁴ The electroconductivity of nanotubes of **643** (Figure 78) was found to be $2.5 \text{ M}\Omega$ upon oxidation with nitrosonium tetrafluoroborate and exhibited a p-type FET property with μ_h of $1.3 \times 10^{-4} \text{ cm}^2 \text{ V}^{-1} \text{ s}^{-1}$ and TRMC studies revealed a $\Phi \sum \mu$ value of $2.4 \times 10^{-3} \text{ cm}^2 \text{ V}^{-1} \text{ s}^{-1}$.^{1344,1369}

TTFs are another class of compounds that exhibit high electron conductivity due to π -stacked columnar structures.^{72,107,1037} Bryce et al. reported a dc conductivity value (σ_{rt}) of $10^{-6} \text{ S cm}^{-1}$ for the TTF gelator **489b** (Chart 121). Upon iodine doping, the value was further increased to 10^{-4} and 10^{-5} – $10^{-4} \text{ S cm}^{-1}$ for tetrabutylammonium perchlorate or hexafluorophosphate doped films.⁹⁹¹ Kato et al. have reported that the insulator character of the LC gelators **490** (Chart 121) having a σ_{rt} value of $<3 \times 10^{-10} \text{ S cm}^{-1}$, significantly changes after doping with I_2 ($\sigma_{rt} = 2 \times 10^{-7} \text{ S cm}^{-1}$) and TCNQ ($1 \times 10^{-5} \text{ S cm}^{-1}$).⁹⁹² An amphiphilic bisTTF annulated macrocyclic derivative **501** (Chart 123) exhibited conductance of a single nanodot with an open shell electronic structure which was 4–5 orders of magnitude higher than that of fibers with a closed shell electronic structure and fiber bundles.¹⁰⁰⁵ In the presence of 2,3,5,6-tetrafluoro-TCNQ, **494** (Chart 121) yielded a dark colored CT gel with electrical conductivity of $5.0 \times 10^{-4} \text{ S cm}^{-1}$.⁹⁹⁵ Amabilino and co-workers reported a variety of TTF based conducting gels.⁹⁹⁶–¹⁰⁰⁴ The four probe dc resistance measurements of the doped xerogel of amide functionalized TTF derivative **495** (Chart 122) exhibited conductivity (σ) of $(3\text{--}5) \times 10^{-3} \Omega^{-1} \text{ cm}^{-1}$.⁹⁹⁶ A hybrid gel of **495** and **496** (Chart 122) could incorporate Au nanoparticles within the TTF gel fibers and organized to a secondary structure with metallic conductivity of 10 S cm^{-1} .⁹⁹⁸

An interesting application of conducting gels is as actuators and capacitors. For example, the electric current profile of bucky gels indicated that it can be used as an electric double layer capacitor with a capacitance of 48 F g^{-1} .^{1269,1270,1370} The bucky gel sandwiched by metal electrodes were used as a component for electric double layer capacitors.¹³⁷⁰ The mechanically strong bucky sheets displayed large electrical conductivity (169 S cm^{-1}) and capacitance (45 F g^{-1} at a sweep rate of 1 mV s^{-1}).¹²⁷⁰ The bucky plastic film prepared from the methacrylate appended ionic liquid monomer containing 7 wt % content of SWCNTs, exhibited an electrical conductivity value of 1 S cm^{-1} .¹²⁶⁸

9.1.1. Field Effect Transistors (FETs). FETs are the key components for electronic tags, flexible circuits, electric papers, sensors, and driving circuits for active matrix displays.¹³⁷¹–¹³⁷³ The sensible design strategies and facile self-assembly conditions allow molecular π -gelators to be used as active materials in FETs.²⁸ This has resulted in the development of FETs in a cost-effective and much less complex way when compared to the inorganic counterparts. Hence the room temperature solution processing of the self-assembled organic structures could replace the highly sophisticated techniques

such as vacuum sublimation, vapor deposition, etc.¹³⁷⁴ Since charge transport mobility is a measure of how easily electrons or holes drift through a semiconductor in response to an electric field, intermolecular ordering plays a crucial role to the development of FETs with better performance.^{1374,1375} Therefore, organization of molecules using solvent assisted gelation approach has been found to be important in the design and fabrication of FETs. The strong π -orbital overlap of the stacked aggregates improves the hole/electron mobility and hence supramolecular structures obtained by organogelation are expected to improve the performance of transistors.

Lee and co-workers have fabricated the first organogel based FETs by using nano/microfibers of the organogelator **338** (Chart 82) with high mobility value up to $8.7 \text{ cm}^2 \text{ V}^{-1} \text{ s}^{-1}$.⁷⁵⁰ Stupp and co-workers have compared the FET performance and hole mobility of the self-assembled fibers of **547** (Chart 134) obtained from toluene ($3.46 \times 10^{-6} \text{ cm}^2 \text{ V}^{-1} \text{ s}^{-1}$) and from nongelating solvents such as chlorobenzene ($9.42 \times 10^{-7} \text{ cm}^2 \text{ V}^{-1} \text{ s}^{-1}$) or *o*-dichlorobenzene ($1.79 \times 10^{-7} \text{ cm}^2 \text{ V}^{-1} \text{ s}^{-1}$).¹⁰⁷² A top contact thin film transistor device, fabricated using the self-assembled 1D nanostructures of **546b** (Chart 134) exhibited hole mobility of $2.34 \times 10^{-7} \text{ cm}^2 \text{ V}^{-1} \text{ s}^{-1}$.¹⁰⁷⁰ In the case of the α -helical polypeptide functionalized thiophene gelator **555** (Chart 135) and PCBM (1:2), a hole mobility of $1.9 \times 10^{-7} \text{ cm}^2 \text{ V}^{-1} \text{ s}^{-1}$ was observed.¹⁰⁸³ FET measurements of the lamellar structures of **171d** and **BU** (Chart 41) exhibited an electron mobility value of $1.0 \times 10^{-4} \text{ cm}^2 \text{ V}^{-1} \text{ s}^{-1}$.⁴²⁸ Someya and co-workers have reported that printed elastic conductors of SWCNT-rubber composite gel on polydimethylsiloxane exhibited an extraordinarily high conductivity of 102 S cm^{-1} and has been used to construct a display comprising of organic transistors (mobility of $0.3 \text{ cm}^2 \text{ V}^{-1} \text{ s}^{-1}$ and on/off ratio of 10^6) and 16 x16 pixel organic LEDs (I_{OLED} of 1.2 mA and high luminance value of 364 cdm^{-2}).^{1271,1272}

9.1.2. Photovoltaic Devices (PVDs). The global demand for energy and the decline of fossil fuel production point out the importance of renewable energy sources and low cost solar energy conversion devices.¹³⁷⁶ In this context, solar energy conversion using organic PVDs is of particular importance.^{1377,1378} The extensive research in this area on the viability of organic molecules has resulted in the fabrication of low cost flexible PVDs with high energy conversion efficiency. The availability of large number of chemical structures, ease of processing, mechanical flexibility and low cost are the advantages which make the PVDs research attractive.¹³⁷⁹ Supramolecular assemblies have significant role to play in the design of D/A bulk heterojunction PVDs.¹³⁸⁰ The nanometer scale supramolecular ordering of D and A molecules controls the bulk separation of photoinduced excitons and high-mobility removal of electrons through the nanophase separation. Hence the structural as well as the morphological variations can significantly affect the total efficiency of the system.¹³⁸¹ The design and synthesis of various D and A molecules, new fabrication and printing technology, etc. have enabled roll to roll manufacturing of highly efficient large area PVDs. In this context, self-organization through organogelation is found to be effective in making good connection, efficient separation between D and A at the molecular level, and an efficient charge channel along the fiber direction, resulting in enhanced photocurrent.

Organogels have been used in two categories of solar cells, namely, dye sensitized solar cells and thin film solar cells. In dye sensitized solar cell, LMOGs have been used as quasi-solid

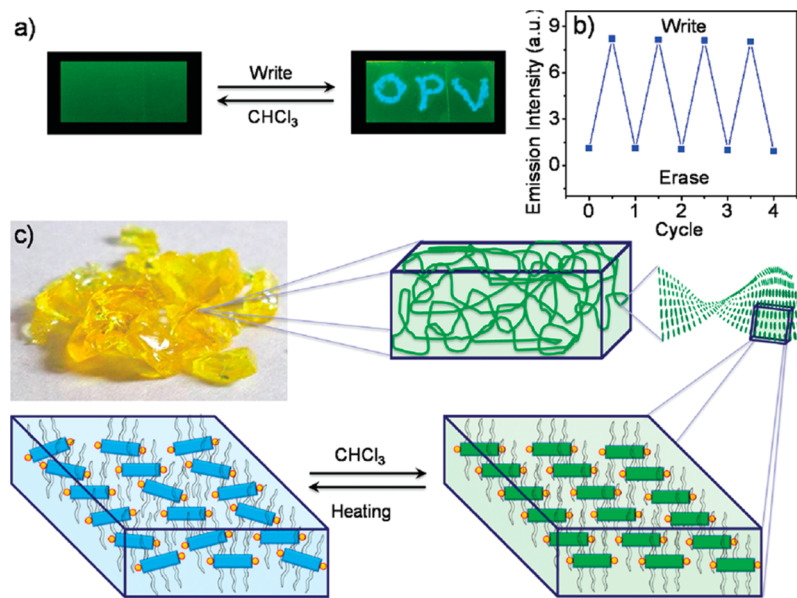


Figure 80. (a) Thermal writing and erasing on a film of **556a** in polystyrene upon exposure to 365 nm UV light. (b) Fluorescence responses of the **556a**-polystyrene film over four continuous cycles of writing and erasing. (c) Cartoonic representation of the solvent vapor assisted reversible self-assembly of **556a** in polystyrene. (Reprinted with permission from ref 1388. Copyright 2009 American Chemical Society.)

gelled electrolyte to carry the volatile organic solvent intact inside the solar cell which lead to production advantages and better performance of the device.^{1382–1384} Higher energy conversion efficiency was observed when dye sensitized solar cells were fabricated from bucky gels as electrolyte.¹³⁸⁵ The studies conducted by Huang and co-workers related to the effect of time/concentration dependent gelation and optical changes of P3HT on the performance of bulk heterojunction PVDs (P3HT/PCBM) indicate that a reasonably high power conversion efficiency of 3.78% was exhibited by the device prepared after 2 h of aging.¹⁰⁸⁷ In addition, Koppe et al. have reported significant enhancement in the PVD performance due to the controlled aggregation and gelation of P3HT by mixing low and high molecular weight samples.¹⁰⁸⁸ The bulk heterojunction devices comprised of **555** (Chart 135) and PCBM (1:2) showed enhanced efficiency due to the helical arrangement of chromophores which favors efficient charge transport.¹⁰⁸³

Shinkai et al. have reported anodic photocurrent generation from the self-sorting organogel films of the cholesterol appended thiophene **543a** (Figure 63) and the PBI **167** (Figure 26) upon visible light irradiation.⁴¹⁸ A steady and large photocurrent was observed in a PVD fabricated using hybrid gels of **581** (Chart 142) and C₆₀ acid (2:1) as the active layer.¹¹⁴⁴ The intermolecular CT complex of **507** (Chart 124) and PCBM exhibited fast generation of carriers and thereby a steady, rapid as well as reproducible cathodic photocurrent (25 nA cm⁻²) due to photoinduced electron transfer from ex-TTF to C₆₀.¹⁰¹⁰ The effect of aging time¹⁰⁸⁷ and molecular weight¹⁰⁸⁸ of the P3HT gelator on the PVD performance has been investigated. The P3HT organogel particles prepared by emulsification of gels in a water containing surfactant allowed its use as solution processable ink. The thin films thus prepared by spray coating was used as an active layer in polymer/fullerene PVDs.¹¹⁰⁰ The fabrication of PVDs using preassembled D–A acceptor suspension gel prepared from a cyano phenylenevinylene polymer containing thieno[3,2-*b*]-

thiophene units and PCBM is an efficient method to improve the overall power conversion efficiency of the device.¹³⁸⁶

9.2. Imaging and Sensing Applications

Fluorescence is one of the most useful and sensitive properties of π -systems. In many cases, fluorescence of π -gelators undergoes significant change upon gelation. Usually the change occurs in the form of a fluorescence quenching with or without shift in the peak position, while in some cases fluorescence enhancement can also occur.^{44,113,253,971,1387} Change in the surrounding medium, for example, temperature, polarity or an analyte can induce variation in the emission intensity and/or wavelength position (color). These changes have been found very predominant in the case of gels when compared to the corresponding solution. Therefore, fluorescent organogels can be used for fluorescence imaging as well as sensing various analytes such as acids, explosives, volatile organic compounds, enantiomers, etc.^{20,24,26,39} Since the excitonic interactions during gelation leads to significant changes in the optical and physical properties of the gelators, it is easier to follow the changes when used as a sensor.^{44,1121} Different types of molecular packing present in gels can induce energy or electron transfer upon entrapping of an analyte molecule leading to the fluorescence modulation.^{44,103} In addition, binding of analyte molecules may also induce disassembly of gelator molecules leading to a gel–sol transition and associated fluorescence change.

The fluorescent OPV gelator **556a** (Chart 136) has been exploited for fluorescence imaging application (Figure 80).¹³⁸⁸ A film prepared from the composite containing fluorescent OPV gelator and styrene polymer showed a green fluorescence due to the self-assembled gelator which turned light blue upon heating due to the disassembly of the gelator. The green emission could be recovered upon exposure of the film to chloroform. This has been used to create stable images which were visible only under UV light and could be erased and rewritten any number of times.

A gel composed of stilbene containing photosurfactant **57** (Figure 10) and 0.4% *N,N'*-dimethyldodecylamine has been

used for imaging applications.²⁴⁷ After irradiation through a mask, images could be created on the gel phase due to photoisomerization of the stilbene unit. Park et al. have observed high contrast fluorescence switching when the gelator **549** (Figure 64) was coassembled with a photochromic molecule exhibiting reversible and bistable photochromism.¹⁰⁷⁶ This is attributed to the highly efficient intermolecular energy transfer between **549** and the photochromic molecule. The fluorescence image (Figure 81a) created by irradiation of visible

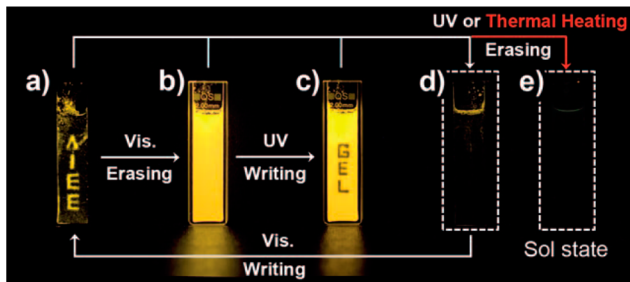


Figure 81. Reversible fluorescence imaging of a gel composite of **549** in a quartz cell under 365 nm UV light. (a) Writing, (b) erasing, (c) rewriting, (d) re-erasing, and (e) erasing by heat. (Reprinted with permission from ref 1076. Copyright 2009 Wiley-VCH.)

light through a mask was erased either to the nonfluorescent form (Figure 81e) by heating or to the fluorescent form (Figure 81b) by exposing to visible light. A write-erase-rewrite cycle and nondestructive readout system has been completed by exposing the fluorescent gel to UV light through a mask with the letters "GEL".

The acid sensitive 2,3-di-*n*-alkoxyphenazines **456a,b** (Chart 114) gelators which exhibited a reversible protonation/deprotonation induced fluorescence change has been reported by Pozzo and co-workers.⁹³⁹ The gelation ability was found significantly enhanced in the presence of trifluoroacetic acid. Shinkai and co-workers have reported a proton sensitive, fluorescent 1,10-phenanthroline appended cholesterol **445a** (Figure 56) based system showing tunable gelation and emission properties leading to energy transfer in the presence of trifluoroacetic acid (Figure 82).⁹²⁷ Interestingly, colorimetric acid sensing property has been reported for the nanofibers of **458** (Chart 114), which exhibited an yellow to red color change in the presence of trifluoroacetic acid vapor.⁹⁴² A super gelator

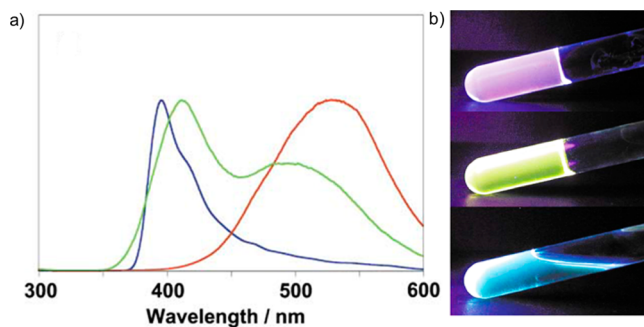


Figure 82. (a) Fluorescence spectral changes of a phenanthroline based gelator **445a** in the gel phase without TFA (blue), with TFA (2.0 equiv.) (red) and in the sol phase at 90 °C with TFA (2.0 equiv.) (green). (b) Photographs of the corresponding emission colors. (Reprinted with permission from ref 927. Copyright 2003 The Royal Society of Chemistry.)

522 (Chart 129) showed two channel anion recognition (F^- , AcO^- , and $H_2PO_4^-$) through proton controlled reversible sol-gel transition and color changes.¹⁰²⁷ Maeda et al. have reported anion responsive BF_2 complexes of aryl substituted dipyrrolyldiketone gelators **407a-d** (Figure 53).^{20,865-869} It has been reported that the fluorescent aggregates and gels of the urea based molecules are sensitive to fluoride anions, mostly through strong hydrogen bonding between bisurea and fluoride anion.^{20,24,39,43}

There has been a report on a new class of stimuli responsive gels based on NDI **161** (Chart 38) that can be used for the spontaneous colorimetric detection of various positional isomers of dihydroxynaphthalene derivatives even in minute quantities (0.2 equiv.) due to the hydrogen bonding driven recognition that significantly amplifies the binding in the gel state.⁴⁰¹ Bucky gel modified electrodes were used as electrochemical sensors, for the selective detection of dopamine.¹³⁸⁹ Lee et al. have reported the detection of nerve gas stimulant diethylchlorophosphate, by monitoring both color change from colorless to greenish yellow and disruption of gel structure upon exposure.⁹⁷²

The organogelator **567** (Chart 138) coated disposable paper strips have been used as a simple and low cost sensor for the contact mode detection of TNT (Figure 83).¹¹²¹ Filter paper strips coated with the gel showed an orange emission which exhibited superior detection capability for TNT at a record attogram (ag, 10^{-18} g) level (~ 12 ag/cm 2) with a detection limit of 0.23 ppq upon direct contact. The observed high sensitivity was attributed to the efficient energy migration

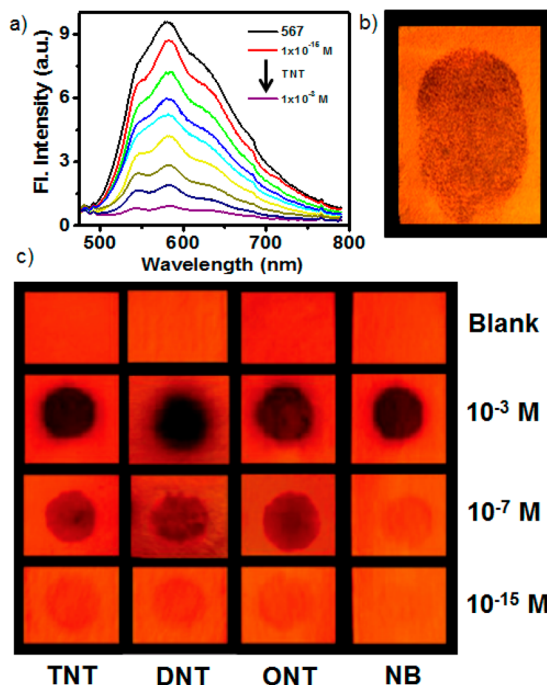


Figure 83. (a) Emission spectral change ($\lambda_{ex} = 450$ nm) of the gelator **567**-coated test strips vs concentration of added TNT ($10 \mu\text{L}$, $1 \times 10^{-15} - 1 \times 10^{-3}$ M). (b) Photograph of thumb impression after rubbing with TNT crystals on **567**-coated test strips under 365 nm UV illumination. (c) Photograph of the fluorescence quenching of **567**-coated test strips by nitroaromatics on contact mode ($10 \mu\text{L}$ of the analyte with a spot area of ~ 0.2 cm 2) under 365 nm UV illumination. (Reprinted with permission from ref 1021. Copyright 2012 American Chemical Society.)

assisted energy/electron transfer processes between 567 and TNT. Similarly, nitroaromatics based explosive materials have been detected in the gel phase using different kind of gelators.^{610,735}

10. CONCLUSION AND OUTLOOK

The large volume of literature related to supramolecular π -gel chemistry indicates the potential of this area in the field of new functional materials useful for a variety of application, particularly to the fabrication of organic electronic devices. This bottom up approach of gel design has undergone several improvements from the early stages of serendipity and uncertain molecular properties to a more defined class of soft materials with predictable behavior and properties, achieved through rational molecular design. Efforts for a deeper understanding of the processes and mechanism of gelation have helped scientists to design new and novel molecular systems that form gels comprised of exotic structures with controlled size, shape, and properties. Almost every class of molecules has been subjected to investigation in search of better gelators with improved chemical and physical properties. However, in order to compete with the inorganic counter parts and crystalline assemblies and liquid crystals, clever design strategies are needed, which may deliver better functional assemblies of π -gelators. For improved electronic properties, it is necessary to avoid/reduce the content of insulating alkyl chains in the gelator molecules, which is the key point in balancing solubility and precipitation. This will improve the 1D ordering of the gelator and thereby the charge transport properties. Postpolymerization approaches and hybrid material assemblies of gels should be further explored to obtain stable structures that can overcome ambient conditions without losing the electronic properties.

As discussed in this review, one of the promising applications of π -gelators is in organic electronics. For example, they have great potential to the development of self-assembly based bulk heterojunction solar cells, an area that needs considerable attention. A few reports have already been published in this direction. Even though some of the gelators showed excellent charge transport and related properties, their performance in real devices were not encouraging. Therefore, for improved performance, more appropriate D–A systems with absorption characteristics extendable to the near-IR and IR regions of the electromagnetic spectrum for more solar radiation coverage, improved stability and environmental compatibility are needed. In addition, since the solar cell performance is directly related to the morphology of the heterojunctions at the nano level, control of chromophore assembly in the gel state is crucial. Fluorescence of π -gelators is another property that has great potential to be tapped for application in sensing and imaging. Many of the gelator systems discussed here exhibit strong fluorescence modulation in the gel state, which can be utilized for the design of stimuli responsive systems and sensors. Even though there are a few reports on gel based sensors, this aspect of gel chemistry has not been fully exploited despite the fact that, π -gelators have the advantage of more sensitivity and selectivity when compared to their molecular building blocks in solution phase.

Anisotropic physical gels and hybrid gels are also promising materials that combine the gelator properties with other compatible materials. Especially, a combination of organic–inorganic structures within the same matrix may lead to enhanced properties for better applications. In this context,

hybrid materials of π -gels with QDs, CNTs, noble metal clusters, LCs, and polymers are of great relevance. For example, combinations of fluorescent π -gelator and LC materials may be good candidates in switchable display devices. Another potential area that needs attention is the use of hybrid gelators of organic semiconductors with CNTs and graphenes as sensors in noninvasive medical diagnostics for the early detection of diseases. Many of the volatile organic compounds formed as a result of the metabolic process during the initial stages of diseases such as cancers should be detected by using such hybrid materials. Therefore, there is immense potential for self-assembled π -gelators to remain as a forerunner in future research projects pertaining to soft functional materials. Precise design strategies and optimized experimental conditions are required to deliver exciting and useful results related to π -gels. A breakthrough in this area is yet to be realized, and therefore, we believe that young interdisciplinary scientists have great opportunities ahead of them for out of box thinking and innovative design.

APPENDIX

We have given an overview of the organogel articles published until October 2012. Since the gel chemistry is still an active and advancing area, a large number of reports have been published after submission of the manuscript. Hence the developments until August 2013 are accounted in this section. It includes articles related to general aspects of gelation,^{1390–1401} different type of gelators,^{1402–1425} azobenzene^{1426–1435} (section 2.1), stilbene^{1436–1438} (section 2.2), dithienylethenes^{1439–1441} (section 2.4), diacetylenes^{1442–1445} (section 2.7), miscellaneous photoresponsive chromophores^{1446,1447} (section 2.9), naphthalimides^{1448–1455} (section 3.2), PBI^{1456–1461} (section 3.3), squaraines^{1462–1464} (section 3.7), coumarins^{1465–1468} (section 3.9), dye doped gels^{1469–1472} (section 3.10), miscellaneous dye doped gels¹⁴⁷³ (section 3.11), pyrenes^{1474–1479} (section 4.1), naphthalenes^{1480–1499} (section 4.3.1), anthracenes^{1500–1504} (section 4.3.2), fluorenes^{1505–1513} (section 4.4), pyrroles^{1514–1516} (section 5.1), guanocines¹⁵¹⁷ (section 5.3), terpyridines¹⁵¹⁸ (section 5.4.2), miscellaneous pyridine derivatives^{1519,1520} (section 5.4.4), riboflavins¹⁵²¹ (section 5.7), carbazoles^{1522,1523} (section 5.8), oxadiazoles^{1524–1532} (section 5.9), TTFs^{1533,1534} (section 5.11), thiophenes^{1535–1537} (section 6.1), phenylenevinylenes^{1538–1553} (section 6.2), phenyleneethylenes^{1554–1560} (section 6.3), phenylenes^{1561–1564} (section 6.4), CNTs^{1565–1570} (section 7.2), graphenes^{1571–1575} (section 7.3), coronenes^{1576,1577} (section 7.4), gels formed by miscellaneous chromophores^{1578–1586} (section 8), application-FETs¹⁵⁸⁷ (section 9.1.1) and application-sensor^{1588–1590} (section 9.2).

AUTHOR INFORMATION

Corresponding Author

*E-mail: ajayaghosh@niist.res.in. Tel: 91-471-2515 306. Fax: +91-471-2491 712. <http://w3rrl.csir.res.in/photo/people/draajayaghosh/Homepage.html>.

Present Address

[†]Consiglio Nazionale delle Ricerche-Istituto per la Sintesi Organica e la Fotoreattività (CNR-ISOF), Via Gobetti 101, 40129 Bologna (Italy).

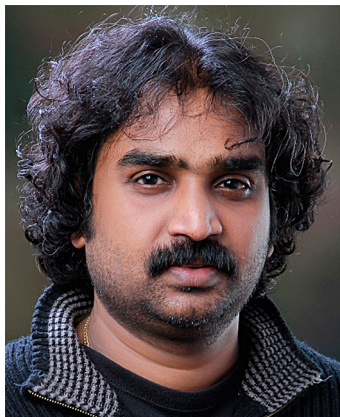
Notes

The authors declare no competing financial interest.

Biographies



Sukumaran Santhosh Babu received his Ph.D. in 2009 from National Institute for Interdisciplinary Science and Technology (NIIST), Trivandrum, India, under the guidance of Dr. A. Ajayaghosh, working on photophysical aspects of oligo(*p*-phenylenevinylene) based organogelators. Currently, he is an AUL-Marie Curie incoming postdoctoral fellow in the research group of Prof. Davide Bonifazi, University of Namur, Belgium. He started his postdoctoral research career in 2009 as a recipient of Max-Planck Institute (MPI)-National Institute for Material Science (NIMS) International Joint Laboratory fellowship at MPI of Colloids and Interfaces, Potsdam, Germany led by Prof. Dr. Helmuth Möhwald and Dr. Takashi Nakanishi, where he investigated the electronic applications of supramolecular fullerene (C_{60}) assemblies. In 2011, he moved to NIMS, Tsukuba, Japan and carried out research on luminescent nonvolatile molecular liquids in the group of Dr. Takashi Nakanishi. His research interests are self-assembly, photophysical properties of π -conjugated molecules, applications of functional assemblies and carbon nanomaterials, nonvolatile organic molecular liquids, etc.



Vakayil K. Praveen completed his Ph.D. from University of Kerala (2007) under the guidance of Dr. A. Ajayaghosh (NIIST). His Ph.D. work was focused on light harvesting supramolecular gels. Subsequently, he moved to The University of Tokyo, Japan, to work as a postdoctoral researcher in the group of Prof. Takuzo Aida on the self-assembly of amphiphilic hexabenzocoronenes. In 2011, he moved to Istituto per la Sintesi Organica e la Fotoreattività (CNR-ISOF), Italy, after receiving a grant from European Union under the Frame of Marie Curie Actions, conducting his research activities on π -electronic gel hybrids under the supervision of Dr. Nicola Armaroli. He is a recipient of Council of Scientific and Industrial Research, Government of India, Junior (2002) and Senior (2005) Research Fellowships, Japan Government Global Centers of Excellence Postdoctoral Fellowship (2007), Japan Society for the Promotion of Science (JSPS)

Postdoctoral Fellowship (2009), JSPS Science Dialogue Lecture Award (2010), and European Union Marie Curie International Incoming Fellowship (2011).



Ayyappanpillai Ajayaghosh is a CSIR-Outstanding scientist at the CSIR-NIIST Trivandrum, and Professor and Dean of Chemical Sciences, Academy of Scientific and Innovative Research (AcSIR), New Delhi, India. He is a recipient of several awards including the Shanti Swarup Bhatnagar Prize 2007, Thomson Reuters Research Excellence-India Research Front Award 2009 and the Infosys Prize 2012. He is a fellow of all of the three national science academies of India. His research interests include supramolecular and macromolecular chemistry, functional organic materials, functional dyes and fluorophores, photoresponsive materials, molecular assemblies and nanostructures, organogels, and molecular probes for sensing and imaging. He serves as an associate editor of PCCP and an international advisory board member of *Chemistry—An Asian Journal* and *RSC Advances*.

ACKNOWLEDGMENTS

A.A. is grateful to the Department of Atomic Energy, Government of India, for a DAE-SRC Outstanding Researcher Award and CSIR, Government of India, for partial financial support under TAPSUN. V.K.P. thanks European Union for Marie Curie International Incoming Fellowship (PIIF-GA-2010-276574, GELBRID). Manuscript No. PPG-342 from NIIST, Trivandrum.

ABBREVIATIONS

- A acceptor
- A/GIEE aggregation/gelation induced enhanced emission
- ANS 8-anilinonaphthalene-1-sulfonic acid
- AFM atomic force microscopy
- Boc *tert*-butyloxycarbonyl
- CT charge transfer
- CD circular dichroism
- α/β -CD α/β -cyclodextrin
- DRC dendron rod coil
- 1/2/3D one/two/three-dimensional
- DMSO dimethyl sulfoxide
- DMF dimethylformamide
- D donor
- DNT dinitrotoluene
- FETs field effect transistors
- Fmoc 9-fluorenylmethyloxycarbonyl
- GO graphene oxide
- HOPG highly ordered pyrolytic graphite
- HBC hexabenzocoronene

h-t head to tail
 h-h head to head
 IR infrared
 LCs liquid crystals
 LMOG low molecular weight organo gelator
 LEDs light emitting devices
 NDI naphthalene diimide
 NMR nuclear magnetic resonance
 OPVs oligo(*p*-phenylenevinylene)s
 OPEs oligo(*p*-phenyleneethynylene)s
 PBI perylene bisimide
 PCBM [6,6]-phenyl-C₆₁-butyric acid methyl ester
 PAA poly(acrylic acid)
 PEG poly(ethylene glycol)
 PEDOT poly(3,4-ethylenedioxythiophene)
 P3HT poly(3-hexylthiophene)
 PMMA poly(methyl methacrylate)
 PVA poly(vinyl alcohol)
 POM polarizing optical microscopy
 rGO reduced graphene oxide
 QDs quantum dots
 S/MWCNT single/multi walled carbon nanotube
 SEM scanning electron microscopy
 STM scanning tunneling microscopy
 SAN/XS small angle neutron/X-ray scattering
 SAFINs self-assembled fibrillar networks
 THF tetrahydrofuran
 TEOS tetraethoxysilane
 TTF tetrathiafulvalene
 TRMC time-resolved microwave conductivity
 TEM transmission electron microscopy
 TNF 2,4,7-trinitrofluorenone
 TNT trinitrotoluene
 UV/vis ultraviolet/visible

REFERENCES

- (1) Lehn, J.-M. *Supramolecular Chemistry: Concepts and Perspectives*; Wiley-VCH: Weinheim, Germany, 1995.
- (2) Lehn, J.-M. Supramolecular Chemistry/Science. In *Supramolecular Science: Where it is and Where it is Going*; NATO ASI Series; Ungaro, R., Dalcanale, E., Eds.; Kluwer Academic Publishers: Dordrecht, The Netherlands, 1999; Vol. 527, pp 287.
- (3) Lehn, J.-M. *Science* **1985**, *227*, 849.
- (4) Reinhoudt, D. N.; Crego-Calama, M. *Science* **2002**, *295*, 2403.
- (5) Whitesides, G. M.; Grzybowski, B. *Science* **2002**, *295*, 2418.
- (6) van Esch, J.; Schoonbeek, F.; de Loos, M.; Veen, E. M.; Kellogg, R. M.; Feringa, B. L. Low Molecular Weight Gelators for Organic Solvents. In *Supramolecular Science: Where it is and Where it is Going*; NATO ASI Series; Ungaro, R., Dalcanale, E., Eds.; Kluwer Academic Publishers: Dordrecht, The Netherlands, 1999; Vol. 527, pp 233.
- (7) Hoeben, F. J. M.; Jonkheijm, P.; Meijer, E. W.; Schenning, A. P. H. *J. Chem. Rev.* **2005**, *105*, 1491.
- (8) Aida, T.; Meijer, E. W.; Stupp, S. I. *Science* **2012**, *335*, 813.
- (9) Terech, P.; Weiss, R. G. *Chem. Rev.* **1997**, *97*, 3133.
- (10) van Esch, J. H.; Feringa, B. L. *Angew. Chem., Int. Ed.* **2000**, *39*, 2263.
- (11) Abdallah, D. J.; Weiss, R. G. *Adv. Mater.* **2000**, *12*, 1237.
- (12) Abdallah, D. J.; Weiss, R. G. *J. Braz. Chem. Soc.* **2000**, *11*, 209.
- (13) Estroff, L. A.; Hamilton, A. D. *Chem. Rev.* **2004**, *104*, 1201.
- (14) Sangeetha, N. M.; Maitra, U. *Chem. Soc. Rev.* **2005**, *34*, 821.
- (15) Hirst, A. R.; Smith, D. K. *Chem. —Eur. J.* **2005**, *11*, 5496.
- (16) de Loos, M.; Feringa, B. L.; van Esch, J. H. *Eur. J. Org. Chem.* **2005**, *3615*.
- (17) Low Molecular Mass Gelator. Fages, F., Ed.; *Top. Curr. Chem.*: Springer-Verlag: Berlin, Heidelberg, 2005.
- (18) *Molecular Gels, Materials with Self-Assembled Fibrillar Networks*; Terech, P., Weiss, R., Eds.; Kluwer Academic Publishers: Dordrecht, The Netherlands, 2005.
- (19) Fages, F. *Angew. Chem., Int. Ed.* **2006**, *45*, 1680.
- (20) Maeda, H. *Chem.—Eur. J.* **2008**, *14*, 11274.
- (21) Dastidar, P. *Chem. Soc. Rev.* **2008**, *37*, 2699.
- (22) Cravotto, G.; Cintas, P. *Chem. Soc. Rev.* **2009**, *38*, 2684.
- (23) van Esch, J. H. *Langmuir* **2009**, *25*, 8392.
- (24) Piepenbrock, M.-O. M.; Lloyd, G. O.; Clarke, N.; Steed, J. W. *Chem. Rev.* **2010**, *110*, 1960.
- (25) Hirst, A. R.; Escuder, B.; Miravet, J. F.; Smith, D. K. *Angew. Chem., Int. Ed.* **2008**, *47*, 8002.
- (26) Banerjee, S.; Das, R. K.; Maitra, U. *J. Mater. Chem.* **2009**, *19*, 6649.
- (27) Dawn, A.; Shiraki, T.; Haraguchi, S.; Tamaru, S.-i.; Shinkai, S. *Chem.—Asian J.* **2011**, *6*, 266.
- (28) Babu, S. S.; Prasanthkumar, S.; Ajayaghosh, A. *Angew. Chem., Int. Ed.* **2012**, *51*, 1766.
- (29) Zhao, F.; Ma, M. L.; Xu, B. *Chem. Soc. Rev.* **2009**, *38*, 883.
- (30) Matson, J. B.; Stupp, S. I. *Chem. Commun.* **2012**, *48*, 26.
- (31) Lee, J.; Aida, T. *Chem. Commun.* **2011**, *47*, 6757.
- (32) Terech, P. *Fullerenes, Nanotubes, Carbon Nanostruct.* **2005**, *13*, 293.
- (33) Paulusse, J. M. J.; Sijbesma, R. P. *Angew. Chem., Int. Ed.* **2006**, *45*, 2334.
- (34) Terech, P.; Gels. In *Encyclopedia of Surface and Colloid Science*, 2nd ed.; Taylor and Francis: New York, 2007; pp 2678.
- (35) van Esch, J. H.; Feringa, B. L. Gels. In *Encyclopedia of Supramolecular Chemistry*; Taylor and Francis: New York, 2007; pp 586.
- (36) Smith, D. K. *Chem. Soc. Rev.* **2009**, *38*, 684.
- (37) Bardelang, D. *Soft Matter* **2009**, *5*, 1969.
- (38) Terech, P. *Langmuir* **2009**, *25*, 8370.
- (39) Lloyd, G. O.; Steed, J. W. *Nat. Chem.* **2009**, *1*, 437.
- (40) Foster, J. A.; Steed, J. W. *Angew. Chem., Int. Ed.* **2010**, *49*, 6718.
- (41) Li, J.-L.; Liu, X.-Y. *Adv. Funct. Mater.* **2010**, *20*, 3196 and references cited therein..
- (42) John, G.; Shankar, B. V.; Jadhav, S. R.; Vemula, P. K. *Langmuir* **2010**, *26*, 17843.
- (43) Steed, J. W. *Chem. Soc. Rev.* **2010**, *39*, 3686.
- (44) Babu, S. S.; Kartha, K. K.; Ajayaghosh, A. *J. Phys. Chem. Lett.* **2010**, *1*, 3413.
- (45) Steed, J. W. *Chem. Commun.* **2011**, *47*, 1379.
- (46) Krieg, E.; Rybtchinski, B. *Chem.—Eur. J.* **2011**, *17*, 9016.
- (47) Liu, K. Q.; He, P. L.; Fang, Y. *Sci. China Chem.* **2011**, *54*, 575.
- (48) Seiffert, S.; Sprakel, J. *Chem. Soc. Rev.* **2012**, *41*, 909.
- (49) Buerkle, L. E.; Rowan, S. J. *Chem. Soc. Rev.* **2012**, *41*, 6089.
- (50) Shinkai, S.; Murata, K. *J. Mater. Chem.* **1998**, *8*, 485.
- (51) Gronwald, O.; Shinkai, S. *Chem.—Eur. J.* **2001**, *7*, 4328.
- (52) Gronwald, O.; Snip, E.; Shinkai, S. *Curr. Opin. Colloid Interface Sci.* **2002**, *7*, 148.
- (53) Ishii, T.; Shinkai, S. *Top. Curr. Chem.* **2005**, *258*, 119.
- (54) George, M.; Weiss, R. G. *Acc. Chem. Res.* **2006**, *39*, 489.
- (55) Smith, D. K. *Adv. Mater.* **2006**, *18*, 2773.
- (56) Smith, D. K. *Chem. Commun.* **2006**, *34*.
- (57) Ajayaghosh, A.; Praveen, V. K. *Acc. Chem. Res.* **2007**, *40*, 644.
- (58) Fukushima, T.; Aida, T. *Chem.—Eur. J.* **2007**, *13*, 5048.
- (59) Trickett, K.; Eastoe, J. *Adv. Colloid Interface Sci.* **2008**, *144*, 66.
- (60) Vemula, P. K.; John, G. *Acc. Chem. Res.* **2008**, *41*, 769.
- (61) Suzuki, M.; Hanabusa, K. *Chem. Soc. Rev.* **2009**, *38*, 967.
- (62) Kopeček, J.; Yang, J. *Acta Biomater.* **2009**, *5*, 805.
- (63) Terech, P.; Dourdain, S.; Bhat, S.; Maitra, U. *J. Phys. Chem. B* **2009**, *113*, 8252.
- (64) Bhattacharya, S.; Samanta, S. K. *Langmuir* **2009**, *25*, 8378.
- (65) Raghavan, S. R. *Langmuir* **2009**, *25*, 8382.
- (66) Frkanec, L.; Žinić, M. *Chem. Commun.* **2010**, *46*, 522.
- (67) Yoshida, M. *Chem. Rec.* **2010**, *10*, 230.
- (68) Yan, X.; Zhu, P.; Li, J. *Chem. Soc. Rev.* **2010**, *39*, 1877.
- (69) Suzuki, M.; Hanabusa, K. *Chem. Soc. Rev.* **2010**, *39*, 455.

- (70) Johnson, E. K.; Adams, D. J.; Cameron, P. J. *J. Mater. Chem.* **2011**, *21*, 2024.
- (71) Suzuki, Y.; Taira, T.; Osakada, K. *J. Mater. Chem.* **2011**, *21*, 930.
- (72) Yang, X.; Zhang, D.; Zhang, G.; Zhu, D. *Sci. China Chem.* **2011**, *54*, 596.
- (73) Svobodová, H.; Noponen, V.; Kolehmainen, E.; Sievänen, E. *RSC Adv.* **2012**, *2*, 4985.
- (74) Xu, X.; Jha, A. K.; Harrington, D. A.; Farach-Carson, M. C.; Jia, X. *Soft Matter* **2012**, *8*, 3280.
- (75) Jonker, A. M.; Löwik, D. W. P. M.; Van Hest, J. C. M. *Chem. Mater.* **2012**, *24*, 759.
- (76) Tunckol, M.; Durand, J.; Serp, P. *Carbon* **2012**, *50*, 4303.
- (77) Yan, X.; Wang, F.; Zheng, B.; Huang, F. *Chem. Soc. Rev.* **2012**, *41*, 6042.
- (78) Yang, X.; Zhang, G.; Zhang, D. *J. Mater. Chem.* **2012**, *22*, 38.
- (79) Tiller, J. C. *Angew. Chem., Int. Ed.* **2003**, *42*, 3072.
- (80) Yang, Z.; Xu, B. *J. Mater. Chem.* **2007**, *17*, 2385.
- (81) Yang, Z.; Liang, G.; Xu, B. *Soft Matter* **2007**, *3*, 515.
- (82) Yang, Z.; Liang, G.; Xu, B. *Acc. Chem. Res.* **2008**, *41*, 315.
- (83) Vintiloiu, A.; Leroux, J.-C. *J. Controlled Release* **2008**, *125*, 179.
- (84) Xu, B. *Langmuir* **2009**, *25*, 8375.
- (85) Gao, Y.; Yang, Z.; Kuang, Y.; Ma, M.-L.; Li, J.; Zhao, F.; Xu, B. *Peptide Sci.* **2010**, *94*, 19.
- (86) Yan, C.; Pochan, D. *J. Chem. Soc. Rev.* **2010**, *39*, 3528.
- (87) Gao, Y.; Zhao, F.; Wang, Q.; Zhang, Y.; Xu, B. *Chem. Soc. Rev.* **2010**, *39*, 3425.
- (88) Adams, D. J.; Topham, P. D. *Soft Matter* **2010**, *6*, 3707.
- (89) Tomatsu, I.; Peng, K.; Kros, A. *Adv. Drug Delivery Rev.* **2011**, *63*, 1257.
- (90) Zhang, Y.; Kuang, Y.; Gao, Y.; Xu, B. *Langmuir* **2011**, *27*, 529.
- (91) Truong, W. T.; Su, Y.; Meijer, J. T.; Thordarson, P.; Braet, F. *Chem.—Asian J.* **2011**, *6*, 30.
- (92) Wang, H.; Yang, Z. *Soft Matter* **2012**, *8*, 2344.
- (93) Li, X.; Kuang, Y.; Xu, B. *Soft Matter* **2012**, *8*, 2801.
- (94) Ryan, D. M.; Nilsson, B. L. *Polym. Chem.* **2012**, *3*, 18.
- (95) Hinze, W. L.; Uemasu, I.; Dai, F.; Braun, J. M. *Curr. Opin. Colloid Interface Sci.* **1996**, *1*, 502.
- (96) Jung, J. H.; Shinkai, S. *J. Inclusion Phenom. Macrocyclic Chem.* **2001**, *41*, 53.
- (97) van Bommel, K. J. C.; Frigeri, A.; Shinkai, S. *Angew. Chem., Int. Ed.* **2003**, *42*, 980.
- (98) Jung, J. H.; Shinkai, S. *Top. Curr. Chem.* **2004**, *248*, 223.
- (99) Llusar, M.; Sanchez, C. *Chem. Mater.* **2008**, *20*, 782.
- (100) Garretti, E.; Dei, L.; Weiss, R. G. *Soft Matter* **2005**, *1*, 17.
- (101) Kato, T.; Hirai, Y.; Nakaso, S.; Moriyama, M. *Chem. Soc. Rev.* **2007**, *36*, 1857.
- (102) Kato, T.; Tanabe, K. *Chem. Lett.* **2009**, *38*, 634.
- (103) Ajayaghosh, A.; Praveen, V. K.; Vijayakumar, C. *Chem. Soc. Rev.* **2008**, *37*, 109.
- (104) Garretti, E.; Bonini, M.; Dei, L.; Berrie, B. H.; Angelova, L. V.; Baglioni, P.; Weiss, R. G. *Acc. Chem. Res.* **2010**, *43*, 751.
- (105) Jung, J. H.; Park, M.; Shinkai, S. *Chem. Soc. Rev.* **2010**, *39*, 4286.
- (106) Escuder, B.; Rodríguez-Llansola, F.; Miravet, J. F. *New J. Chem.* **2010**, *34*, 1044.
- (107) Amabilino, D. B.; Puigmartí-Luis, J. *Soft Matter* **2010**, *6*, 1605.
- (108) Rybtchinski, B. *ACS Nano* **2011**, *5*, 6791.
- (109) Díaz, D. D.; Kühbeck, D.; Koopmans, R. J. *Chem. Soc. Rev.* **2011**, *40*, 427.
- (110) John, G.; Jadhav, S. R.; Menon, V. M.; John, V. T. *Angew. Chem., Int. Ed.* **2012**, *51*, 1760.
- (111) Das, D.; Kar, T.; Das, P. K. *Soft Matter* **2012**, *8*, 2348.
- (112) Pope, M.; Swenberg, C. E. *Electronic Processes in Organic Crystals and Polymers*, 2nd ed.; Oxford University Press: New York, 1999.
- (113) Maggini, L.; Bonifazi, D. *Chem. Soc. Rev.* **2012**, *41*, 211.
- (114) *Handbook of Conducting Polymers*; Skotheim, T. A., Elsenbaumer, R. L., Reynolds, J. R., Eds.; Marcel Dekker Inc.: New York, 1998.
- (115) *Organic Light Emitting Devices*; Müllen, K., Scherf, U., Eds.; VCH: Weinheim, Germany, 2006.
- (116) Muccini, M. *Nat. Mater.* **2006**, *5*, 605.
- (117) Mas-Torrent, M.; Rovira, C. *Chem. Rev.* **2011**, *111*, 4833.
- (118) Hains, A. W.; Liang, Z.; Woodhouse, M. A.; Gregg, B. A. *Chem. Rev.* **2010**, *110*, 6689.
- (119) *Organic Photovoltaics: Mechanisms, Materials and Devices*; Sun, S.-S., Sariciftci, N. S., Eds.; Taylor and Francis: Boca Raton, FL, 2005.
- (120) Sakakibara, K.; Hill, J. P.; Ariga, K. *Small* **2011**, *7*, 1288.
- (121) Venkataraman, D.; Yurt, S.; Venkatraman, B. H.; Gavvalapalli, N. *J. Phys. Chem. Lett.* **2010**, *1*, 947.
- (122) González-Rodríguez, D.; Schenning, A. P. H. *J. Chem. Mater.* **2011**, *23*, 310.
- (123) Hamada, D.; Yanagihara, I.; Tsumoto, K. *Trends Biotechnol.* **2004**, *22*, 93.
- (124) Jeong, Y.; Hanabusa, K.; Masunaga, H.; Akiba, I.; Miyoshi, K.; Sakurai, S.; Sakurai, K. *Langmuir* **2005**, *21*, 586.
- (125) Jonkheijm, P.; van der Schoot, P.; Schenning, A. P. H. J.; Meijer, E. W. *Science* **2006**, *313*, 80.
- (126) Zhu, G.; Dordick, J. S. *Chem. Mater.* **2006**, *18*, 5988.
- (127) Aggeli, A.; Bell, M.; Boden, M.; Keen, J. N.; Knowles, P. F.; McLeish, T. C. B.; Pitkeathly, M.; Radford, S. E. *Nature* **1997**, *386*, 259.
- (128) Raynal, M.; Bouteiller, L. *Chem. Commun.* **2011**, *47*, 8271.
- (129) Curcio, P.; Allix, F.; Pickaert, G.; Jamart-Grégoire, B. *Chem.—Eur. J.* **2011**, *17*, 13603.
- (130) Gao, J.; Wu, S.; Rogers, M. A. *J. Mater. Chem.* **2012**, *22*, 12651.
- (131) Hirst, A. R.; Coates, I. A.; Boucheteau, T. R.; Miravet, J. F.; Escuder, B.; Castelletto, V.; Hamley, I. W.; Smith, D. K. *J. Am. Chem. Soc.* **2008**, *130*, 9113.
- (132) Hirst, A. R.; Smith, D. K. *Langmuir* **2004**, *20*, 10851.
- (133) Duncan, D.; Whitten, D. *Langmuir* **2000**, *16*, 6445.
- (134) Yemloul, M.; Steiner, E.; Robert, A.; Bouquet-Bonnet, S.; Allix, F.; Jamart-Grégoire, B.; Canet, D. *J. Phys. Chem. B* **2011**, *115*, 2511.
- (135) Bouquet-Bonnet, S.; Yemloul, M.; Canet, D. *J. Am. Chem. Soc.* **2012**, *134*, 10621.
- (136) Aparicio, F.; García, F.; Sánchez, L. *Chem.—Eur. J.* **2013**, *19*, 3239.
- (137) Dasgupta, D.; Thierry, A.; Rochas, C.; Ajayaghosh, A.; Guenet, J. M. *Soft Matter* **2012**, *8*, 8714.
- (138) Stepanenko, V.; Li, X.-Q.; Gershberg, J.; Würthner, F. *Chem.—Eur. J.* **2013**, *19*, 4176.
- (139) Pieroni, O.; Fissi, A.; Angelini, N.; Lenci, F. *Acc. Chem. Res.* **2001**, *34*, 9.
- (140) Yagai, S.; Karatsu, T.; Kitamura, A. *Chem.—Eur. J.* **2005**, *11*, 4054.
- (141) Eastoe, J.; Vesperinas, A. *Soft Matter* **2005**, *1*, 338.
- (142) Tian, H.; Wang, S. *Chem. Commun.* **2007**, 781.
- (143) Zhou, W.; Li, Y.; Zhu, D. *Chem.—Asian J.* **2007**, *2*, 222.
- (144) Barrett, C. J.; Mamiya, J.-i.; Yager, K. G.; Ikeda, T. *Soft Matter* **2007**, *3*, 1249.
- (145) Yagai, S.; Kitamura, A. *Chem. Soc. Rev.* **2008**, *37*, 1520.
- (146) Das, S.; Varghese, S.; Kumar, N. S. S. *Langmuir* **2010**, *26*, 1598.
- (147) Ercole, F.; Davis, T. P.; Evans, R. A. *Polym. Chem.* **2010**, *1*, 37.
- (148) Russew, M.-M.; Hecht, S. *Adv. Mater.* **2010**, *22*, 3348.
- (149) Bléger, D.; Yu, Z.; Hecht, S. *Chem. Commun.* **2011**, *47*, 12260.
- (150) Tamai, N.; Miyasaka, H. *Chem. Rev.* **2000**, *100*, 1875.
- (151) Bouas-Laurent, H.; Dürr, H. *Pure Appl. Chem.* **2001**, *73*, 639.
- (152) Griffiths, J. *Chem. Soc. Rev.* **1972**, *1*, 481.
- (153) Murata, K.; Aoki, M.; Shinkai, S. *Chem. Lett.* **1992**, 739.
- (154) Murata, K.; Aoki, M.; Suzuki, T.; Harada, T.; Kawabata, H.; Komri, T.; Ohseto, F.; Ueda, K.; Shinkai, S. *J. Am. Chem. Soc.* **1994**, *116*, 6664.
- (155) Ono, Y.; Kanekiyo, Y.; Inoue, K.; Hojo, J.; Shinkai, S. *Chem. Lett.* **1999**, 23.
- (156) Jung, J. H.; Ono, Y.; Shinkai, S. *J. Chem. Soc., Perkin Trans. 2* **1999**, 1289.
- (157) Jung, J. H.; Ono, Y.; Shinkai, S. *Langmuir* **2000**, *16*, 1643.
- (158) Han, W. S.; Kang, Y.; Lee, S. J.; Lee, H.; Do, Y.; Lee, Y.-A.; Jung, J. H. *J. Phys. Chem. B* **2005**, *109*, 20661.

- (159) Jung, J. H.; Ono, Y.; Sakurai, K.; Sano, M.; Shinkai, S. *J. Am. Chem. Soc.* **2000**, *122*, 8648.
- (160) Jung, J. H.; Ono, Y.; Shinkai, S. *Angew. Chem., Int. Ed.* **2000**, *39*, 1862.
- (161) Jung, J. H.; Kobayashi, H.; Masuda, M.; Shimizu, T.; Shinkai, S. *J. Am. Chem. Soc.* **2001**, *123*, 8785.
- (162) Jung, J. H.; Kobayashi, H.; van Bommel, K. J. C.; Shinkai, S.; Shimizu, T. *Chem. Mater.* **2002**, *14*, 1445.
- (163) Ono, Y.; Nakashima, K.; Sano, M.; Kanekiyo, Y.; Inoue, K.; Hojo, J.; Shinkai, S. *Chem. Commun.* **1998**, 1477.
- (164) Sakurai, K.; Ono, Y.; Jung, J. H.; Okamoto, S.; Sakurai, S.; Shinkai, S. *J. Chem. Soc., Perkin Trans. 2* **2001**, 108.
- (165) Ono, Y.; Nakashima, K.; Sano, M.; Hojo, J.; Shinkai, S. *Chem. Lett.* **1999**, 1119.
- (166) Ono, Y.; Nakashima, K.; Sano, M.; Hojo, J.; Shinkai, S. *J. Mater. Chem.* **2001**, *11*, 2412.
- (167) Jung, J. H.; Ono, Y.; Shinkai, S. *Chem. Lett.* **2000**, 636.
- (168) Jung, J. H.; Shinkai, S. *J. Chem. Soc., Perkin Trans. 2* **2000**, 2393.
- (169) Jung, J. H.; Shimizu, T.; Shinkai, S. *J. Mater. Chem.* **2005**, *15*, 3979.
- (170) Jung, J. H.; Shinkai, S.; Shimizu, T. *Chem. Mater.* **2003**, *15*, 2141.
- (171) Jung, J. H.; Rim, J. A.; Lee, S. J.; Lee, S. S. *Chem. Commun.* **2005**, 468.
- (172) Jung, J. H.; Rim, J. A.; Lee, S. J.; Cho, S. J.; Kim, S. Y.; Kang, J. K.; Kim, Y. M.; Kim, Y. J. *J. Phys. Chem. C* **2007**, *111*, 2679.
- (173) Koumura, N.; Kudo, M.; Tamaoki, N. *Langmuir* **2004**, *20*, 9897.
- (174) Wang, C.; Chen, Q.; Sun, F.; Zhang, D.; Zhang, G.; Huang, Y.; Zhao, R.; Zhu, D. *J. Am. Chem. Soc.* **2010**, *132*, 3092.
- (175) Wu, Y.; Wu, S.; Tian, X.; Wang, X.; Wu, W.; Zou, G.; Zhang, Q. *Soft Matter* **2011**, *7*, 716.
- (176) Wu, Y.; Wu, S.; Zou, G.; Zhang, Q. *Soft Matter* **2011**, *7*, 9177.
- (177) Jiao, T.; Wang, Y.; Gao, F.; Zhou, J.; Gao, F. *Progr. Nat. Sci.: Mater. Int.* **2012**, *22*, 64.
- (178) Kobayashi, H.; Friggeri, A.; Koumoto, K.; Amaike, M.; Shinkai, S.; Reinhoudt, D. N. *Org. Lett.* **2002**, *4*, 1423.
- (179) Kobayashi, H.; Koumoto, K.; Jung, J. H.; Shinkai, S. *J. Chem. Soc., Perkin Trans. 2* **2002**, 1930.
- (180) Ogawa, Y.; Yoshiyama, C.; Kitaoka, T. *Langmuir* **2012**, *28*, 4404.
- (181) Rajaganesh, R.; Gopal, A.; Das, T. M.; Ajayaghosh, A. *Org. Lett.* **2012**, *14*, 748.
- (182) de Loos, M.; van Esch, J.; Kellogg, R. M.; Feringa, B. L. *Angew. Chem., Int. Ed.* **2001**, *40*, 613.
- (183) van der Laan, S.; Feringa, B. L.; Kellogg, R. M.; van Esch, J. *Langmuir* **2002**, *18*, 7136.
- (184) Guan, L.; Zhao, Y. *Chem. Mater.* **2000**, *12*, 3667.
- (185) Guan, L.; Zhao, Y. *J. Mater. Chem.* **2001**, *11*, 1339.
- (186) Zhao, Y.; Tong, X. *Adv. Mater.* **2003**, *15*, 1431.
- (187) Tong, X.; Zhao, Y. *J. Am. Chem. Soc.* **2007**, *129*, 6372.
- (188) Zhao, Y.; Guan, L. *Liq. Cryst.* **2003**, *30*, 81.
- (189) Mamiya, J.-i.; Kanie, K.; Hiyama, T.; Ikeda, T.; Kato, T. *Chem. Commun.* **2002**, 1870.
- (190) Moriyama, M.; Mizoshita, N.; Yokota, T.; Kishimoto, K.; Kato, T. *Adv. Mater.* **2003**, *15*, 1335.
- (191) Moriyama, M.; Mizoshita, N.; Kato, T. *Polym. J.* **2004**, *36*, 661.
- (192) Moriyama, M.; Mizoshita, N.; Kato, T. *Bull. Chem. Soc. Jpn.* **2006**, *79*, 962.
- (193) Deindörfer, P.; Geiger, T.; Schollmeyer, D.; Ye, J. H.; Zentel, R. *J. Mater. Chem.* **2006**, *16*, 351.
- (194) Deindörfer, P.; Eremin, A.; Stannarius, R.; Davis, R.; Zentel, R. *Soft Matter* **2006**, *2*, 693.
- (195) Deindörfer, P.; Davis, R.; Zentel, R. *Soft Matter* **2007**, *3*, 1308.
- (196) Yagai, S.; Nakajima, T.; Kishikawa, K.; Kohmoto, S.; Karatsu, T.; Kitamura, A. *J. Am. Chem. Soc.* **2005**, *127*, 11134.
- (197) Yagai, S.; Karatsu, T.; Kitamura, A. *Langmuir* **2005**, *21*, 11048.
- (198) Yagai, S.; Iwashima, T.; Kishikawa, K.; Nakahara, S.; Karatsu, T.; Kitamura, A. *Chem.—Eur. J.* **2006**, *12*, 3984.
- (199) Shu, T.; Wu, J.; Zou, Y.; Liu, K.; Chen, L.; Yi, T. *Front. Chem. China* **2010**, *5*, 184.
- (200) Lee, S. J.; Lee, S. S.; Kim, J. S.; Lee, J. Y.; Jung, J. H. *Chem. Mater.* **2005**, *17*, 6517.
- (201) Inoue, D.; Suzuki, M.; Shirai, H.; Hanabusa, K. *Bull. Chem. Soc. Jpn.* **2005**, *78*, 721.
- (202) Li, X.; Gao, Y.; Kuang, Y.; Xu, B. *Chem. Commun.* **2010**, *46*, 5364.
- (203) Matsuzawa, Y.; Ueki, K.; Yoshida, M.; Tamaoki, N.; Nakamura, T.; Sakai, H.; Abe, M. *Adv. Funct. Mater.* **2007**, *17*, 1507.
- (204) Matsuzawa, Y.; Tamaoki, N. *J. Phys. Chem. B* **2010**, *114*, 1586.
- (205) Huang, Y.; Qiu, Z.; Xu, Y.; Shi, J.; Lin, H.; Zhang, Y. *Org. Biomol. Chem.* **2011**, *9*, 2149.
- (206) Lin, Y.; Qiao, Y.; Tang, P.; Li, Z.; Huang, J. *Soft Matter* **2011**, *7*, 2762.
- (207) Ihara, H.; Hachisako, H.; Hirayama, C.; Yamada, K. *J. Chem. Soc., Chem. Commun.* **1992**, 1244.
- (208) Duan, P.; Li, Y.; Li, L.; Deng, J.; Liu, M. *J. Phys. Chem. B* **2011**, *115*, 3322.
- (209) Cao, H.; Jiang, J.; Zhu, X.; Duan, P.; Liu, M. *Soft Matter* **2011**, *7*, 4654.
- (210) Li, W.; Park, I.; Kang, S.-K.; Lee, M. *Chem. Commun.* **2012**, *48*, 8796.
- (211) Liu, Z.-X.; Feng, Y.; Yan, Z.-C.; He, Y.-M.; Liu, C.-Y.; Fan, Q.-H. *Chem. Mater.* **2012**, *24*, 3751.
- (212) Ji, Y.; Kuang, G.-C.; Jia, X.-R.; Chen, E.-Q.; Wang, B.-B.; Li, W.-S.; Wei, Y.; Lei, J. *Chem. Commun.* **2007**, 4233.
- (213) Palui, G.; Banerjee, A. *J. Phys. Chem. B* **2008**, *112*, 10107.
- (214) Kim, J. H.; Seo, M.; Kim, Y. J.; Kim, S. Y. *Langmuir* **2009**, *25*, 1761.
- (215) Srivastava, A.; Ghorai, S.; Bhattacharjya, A.; Bhattacharya, S. *J. Org. Chem.* **2005**, *70*, 6574.
- (216) Zhou, Y.; Yi, T.; Li, T.; Zhou, Z.; Li, F.; Huang, W.; Huang, C. *Chem. Mater.* **2006**, *18*, 2974.
- (217) Zhou, Y.; Xu, M.; Wu, J.; Li, T.; Han, J.; Xiao, S.; Li, F.; Huang, C. *J. Phys. Org. Chem.* **2008**, *21*, 338.
- (218) Zhou, Y.; Xu, M.; Yi, T.; Xiao, S.; Zhou, Z.; Li, F.; Huang, C. *Langmuir* **2007**, *23*, 202.
- (219) Kitahara, T.; Fujita, N.; Shinkai, S. *Chem. Lett.* **2008**, *37*, 912.
- (220) Tiefenbacher, K.; Dube, H.; Ajami, D.; Rebek, J. *Chem. Commun.* **2011**, *47*, 7341.
- (221) Suzuki, T.; Shinkai, S.; Sada, K. *Adv. Mater.* **2006**, *18*, 1043.
- (222) Zhu, L.; Ma, X.; Ji, F.; Wang, Q.; Tian, H. *Chem.—Eur. J.* **2007**, *13*, 9216.
- (223) Chen, W.; Gong, W.; Ye, J.; Lin, Y.; Ning, G. *RSC Adv.* **2012**, *2*, 809.
- (224) Ran, X.; Wang, H.; Zhang, P.; Bai, B.; Zhao, C.; Yu, Z.; Li, M. *Soft Matter* **2011**, *7*, 8561.
- (225) Kume, S.; Kuroiwa, K.; Kimizuka, N. *Chem. Commun.* **2006**, 2442.
- (226) Sahoo, P.; Chakraborty, I.; Dastidar, P. *Soft Matter* **2012**, *8*, 2595.
- (227) Delbecq, F.; Kaneko, N.; Endo, H.; Kawai, T. *J. Colloid Interface Sci.* **2012**, *384*, 94.
- (228) Kim, Y. S.; Sung, C. S. P. *Macromolecules* **1996**, *29*, 462.
- (229) Bobrovsky, A.; Shibaev, V.; Hamplova, V.; Kaspar, M.; Glogarova, M. *Colloid Polym. Sci.* **2010**, *288*, 1375.
- (230) Ikeda, T.; Nakano, M.; Yu, Y.; Tsutsumi, O.; Kanazawa, A. *Adv. Mater.* **2003**, *15*, 201.
- (231) Nakano, M.; Yu, Y.; Shishido, A.; Tsutsumi, O.; Kanazawa, A.; Shiono, T.; Ikeda, T. *Mol. Cryst. Liq. Cryst.* **2003**, *398*, 1.
- (232) Yu, Y.; Nakano, M.; Ikeda, T. *Pure Appl. Chem.* **2004**, *76*, 1467.
- (233) Chen, D.; Liu, H.; Kobayashi, T.; Yu, H. *J. Mater. Chem.* **2010**, *20*, 3610.
- (234) Takashima, Y.; Nakayama, T.; Miyauchi, M.; Kawaguchi, Y.; Yamaguchi, H.; Harada, A. *Chem. Lett.* **2004**, *33*, 890.
- (235) Tomatsu, I.; Hashidzume, A.; Harada, A. *Macromolecules* **2005**, *38*, 5223.

- (236) Tamesue, S.; Takashima, Y.; Yamaguchi, H.; Shinkai, S.; Harada, A. *Angew. Chem., Int. Ed.* **2010**, *49*, 7461.
- (237) Zhao, Y.-L.; Stoddart, J. F. *Langmuir* **2009**, *25*, 8442.
- (238) Peng, K.; Tomatsu, I.; Kros, A. *Chem. Commun.* **2010**, *46*, 4094.
- (239) Liao, X.; Chen, G.; Liu, X.; Chen, W.; Chen, F.; Jiang, M. *Angew. Chem., Int. Ed.* **2010**, *49*, 4409.
- (240) Liao, X.; Chen, G.; Jiang, M. *Langmuir* **2011**, *27*, 12650.
- (241) Liu, J.; Chen, G.; Guo, M.; Jiang, M. *Macromolecules* **2010**, *43*, 8086.
- (242) Lee, C. T.; Smith, K. A.; Hatton, T. A. *Macromolecules* **2004**, *37*, 5397.
- (243) Ueki, T.; Yamaguchi, A.; Watanabe, M. *Chem. Commun.* **2012**, *48*, 5133.
- (244) Sension, R. J.; Repinec, S. T.; Szarka, A. Z.; Hochstrasser, R. M. *J. Chem. Phys.* **1993**, *98*, 6291.
- (245) Geiger, C.; Stanescu, M.; Chen, L.; Whitten, D. G. *Langmuir* **1999**, *15*, 2241.
- (246) Wang, R.; Geiger, C.; Chen, L.; Swanson, B.; Whitten, D. G. *J. Am. Chem. Soc.* **2000**, *122*, 2399.
- (247) Eastoe, J.; Sánchez-Dominguez, M.; Wyatt, P.; Heenan, R. K. *Chem. Commun.* **2004**, 2608.
- (248) Miljanić, S.; Frkanec, L.; Meić, Z.; Žinić, M. *Langmuir* **2005**, *21*, 2754.
- (249) Miljanić, S.; Frkanec, L.; Meić, Z.; Žinić, M. *Eur. J. Org. Chem.* **2006**, *1323*.
- (250) Dautel, O. J.; Lère-Porte, J.-P.; Moreau, J. J. E.; Wong Chi Man, M. *Chem. Commun.* **2003**, 2662.
- (251) Bao, C.; Lu, R.; Jin, M.; Xue, P.; Tan, C.; Liu, G.; Zhao, Y. *Org. Biomol. Chem.* **2005**, *3*, 2508.
- (252) Hou, Q.; Wang, S.; Zang, L.; Wang, X.; Jiang, S. *J. Colloid Interface Sci.* **2009**, *338*, 463.
- (253) An, B.-K.; Gierschner, J.; Park, S. Y. *Acc. Chem. Res.* **2012**, *45*, 544.
- (254) An, B.-K.; Lee, D.-S.; Lee, J.-S.; Park, Y.-S.; Song, H.-S.; Park, S. Y. *J. Am. Chem. Soc.* **2004**, *126*, 10232.
- (255) Chung, J. W.; An, B.-K.; Kim, J. W.; Kim, J.-J.; Park, S. Y. *Chem. Commun.* **2008**, 2998.
- (256) Chung, J. W.; An, B.-K.; Park, S. Y. *Chem. Mater.* **2008**, *20*, 6750.
- (257) Tong, X.; Zhao, Y.; An, B.-K.; Park, S. Y. *Adv. Funct. Mater.* **2006**, *16*, 1799.
- (258) Tong, X.; Chung, J. W.; Park, S. Y.; Zhao, Y. *Langmuir* **2009**, *25*, 8532.
- (259) Chung, J. W.; An, B.-K.; Hirato, F.; Kim, J. H.; Jinnai, H.; Park, S. Y. *J. Mater. Chem.* **2010**, *20*, 7715.
- (260) Seo, J.; Chung, J. W.; Jo, E.-H.; Park, S. Y. *Chem. Commun.* **2008**, 2794.
- (261) Xu, Y.; Xue, P.; Xu, D.; Zhang, X.; Liu, X.; Zhou, H.; Jia, J.; Yang, X.; Wang, F.; Lu, R. *Org. Biomol. Chem.* **2010**, *8*, 4289.
- (262) Vijayakumar, C.; Tobin, G.; Schmitt, W.; Kim, M.-J.; Takeuchi, M. *Chem. Commun.* **2010**, *46*, 874.
- (263) Zhang, Y.; Jiang, S. *Org. Biomol. Chem.* **2012**, *10*, 6973.
- (264) Miura, Y.; Momotake, A.; Sato, T.; Kanna, Y.; Moriyama, M.; Nishimura, Y.; Arai, T. *Bull. Chem. Soc. Jpn.* **2011**, *84*, 363.
- (265) Hwang, I.; Jeon, W. S.; Kim, H.-J.; Kim, D.; Kim, H.; Selvapalam, N.; Fujita, N.; Shinkai, S.; Kim, K. *Angew. Chem., Int. Ed.* **2007**, *46*, 210.
- (266) Li, D.-M.; Wang, H.; Zheng, Y.-S. *Chem. Commun.* **2012**, *48*, 3176.
- (267) Kumar, N. S. S.; Varghese, S.; Narayan, G.; Das, S. *Angew. Chem., Int. Ed.* **2006**, *45*, 6317.
- (268) Abraham, S.; Vijayaraghavan, R. K.; Das, S. *Langmuir* **2009**, *25*, 8507.
- (269) Irie, M.; Uchida, K. *Bull. Chem. Soc. Jpn.* **1998**, *71*, 985.
- (270) Irie, M. *Chem. Rev.* **2000**, *100*, 1685.
- (271) Myles, A. J.; Branda, N. R. *Adv. Funct. Mater.* **2002**, *12*, 167.
- (272) Tian, H.; Yang, S. *Chem. Soc. Rev.* **2004**, *33*, 85.
- (273) Tian, H.; Feng, Y. *J. Mater. Chem.* **2008**, *18*, 1617.
- (274) Lucas, L. N.; van Esch, J.; Kellogg, R. M.; Feringa, B. L. *Chem. Commun.* **2001**, 759.
- (275) de Jong, J. J. D.; Lucas, L. N.; Kellogg, R. M.; van Esch, J. H.; Feringa, B. L. *Science* **2004**, *304*, 278.
- (276) de Jong, J. J. D.; Hania, P. R.; Pugžlys, A.; Lucas, L. N.; de Loos, M.; Kellogg, R. M.; Feringa, B. L.; Duppen, K.; van Esch, J. H. *Angew. Chem., Int. Ed.* **2005**, *44*, 2373.
- (277) Akazawa, M.; Uchida, K.; de Jong, J. J. D.; Areephong, J.; Stuart, M.; Caroli, G.; Browne, W. R.; Feringa, B. L. *Org. Biomol. Chem.* **2008**, *6*, 1544.
- (278) de Jong, J. J. D.; Tiemersma-Wegman, T. D.; van Esch, J. H.; Feringa, B. L. *J. Am. Chem. Soc.* **2005**, *127*, 13804.
- (279) de Jong, J. J. D.; van Rijn, P.; Tiemersma-Wegeman, T. D.; Lucas, L. N.; Browne, W. R.; Kellogg, R. M.; van Esch, J. H.; Feringa, B. L. *Tetrahedron* **2008**, *64*, 8324.
- (280) Green, M. M.; Park, J.-W.; Sato, T.; Teramoto, A.; Lifson, S.; Selinger, R. L. B.; Selinger, J. V. *Angew. Chem., Int. Ed.* **1999**, *38*, 3138.
- (281) Green, M. M.; Cheon, K.-S.; Yang, S.-Y.; Park, J.-W.; Swansburg, S.; Liu, W. *Acc. Chem. Res.* **2001**, *34*, 672.
- (282) Wang, S.; Shen, W.; Feng, Y.; Tian, H. *Chem. Commun.* **2006**, 1497.
- (283) Zhu, W.; Meng, X.; Yang, Y.; Zhang, Q.; Xie, Y.; Tian, H. *Chem.—Eur. J.* **2010**, *16*, 899.
- (284) Xiao, S.; Zou, Y.; Yu, M.; Yi, T.; Zhou, Y.; Li, F.; Huang, C. *Chem. Commun.* **2007**, 4758.
- (285) Rameshbabu, K.; Zou, L.; Kim, C.; Urbas, A.; Li, Q. *J. Mater. Chem.* **2011**, *21*, 15673.
- (286) Berkovic, G.; Krongauz, V.; Weiss, V. *Chem. Rev.* **2000**, *100*, 1741.
- (287) Minkin, V. I. *Chem. Rev.* **2004**, *104*, 2751.
- (288) Raymo, F. M.; Tomasulo, M. *Chem. Soc. Rev.* **2005**, *34*, 327.
- (289) Hachisako, H.; Ihara, H.; Kamiya, T.; Hirayama, C.; Yamada, K. *Chem. Commun.* **1997**, *19*.
- (290) Hachisako, H.; Nakayama, H.; Ihara, H. *Chem. Lett.* **1999**, *1165*.
- (291) Qiu, Z.; Yu, H.; Li, J.; Wang, Y.; Zhang, Y. *Chem. Commun.* **2009**, 3342.
- (292) Chen, Q.; Feng, Y.; Zhang, D.; Zhang, G.; Fan, Q.; Sun, S.; Zhu, D. *Adv. Funct. Mater.* **2010**, *20*, 36.
- (293) Shumburo, A.; Biewer, M. *Chem. Mater.* **2002**, *14*, 3745.
- (294) Lee, H.-Y.; Diehn, K. K.; Sun, K.; Chen, T.; Raghavan, S. R. *J. Am. Chem. Soc.* **2011**, *133*, 8461.
- (295) Li, Y.; Wong, K. M.-C.; Tam, A. Y.-Y.; Wu, L.; Yam, V. W.-W. *Chem.—Eur. J.* **2010**, *16*, 8690.
- (296) Delbaere, S.; Lucchioni-Houze, B.; Bochu, C.; Teral, Y.; Campredon, M.; Vermeersch, G. *J. Chem. Soc., Perkin Trans. 2* **1998**, 1153.
- (297) Ahmed, S. A.; Sallenave, X.; Fages, F.; Mieden-Gundert, G.; Müller, W. M.; Müller, U.; Vögtle, F.; Pozzo, J.-L. *Langmuir* **2002**, *18*, 7096.
- (298) Katritzky, A. R.; Sakhuja, R.; Khelashvili, L.; Shanab, K. *J. Org. Chem.* **2009**, *74*, 3062.
- (299) Ahn, D. J.; Kim, J.-M. *Acc. Chem. Res.* **2008**, *41*, 805.
- (300) Lauher, J. W.; Fowler, F. W.; Goroff, N. S. *Acc. Chem. Res.* **2008**, *41*, 1215.
- (301) Yarimaga, O.; Jaworski, J.; Yoon, B.; Kim, J.-M. *Chem. Commun.* **2012**, *48*, 2469.
- (302) Jahnke, E.; Milleroux, A.-S.; Severin, N.; Rabe, J. P.; Frauenrath, H. *Macromol. Biosci.* **2007**, *7*, 136.
- (303) Fuhrhop, J.-H.; Blumtritt, P.; Lehmann, C.; Luger, P. *J. Am. Chem. Soc.* **1991**, *113*, 7437.
- (304) Masuda, M.; Hanada, T.; Yase, K.; Shimizu, T. *Macromolecules* **1998**, *31*, 9403.
- (305) Masuda, M.; Hanada, T.; Okada, Y.; Yase, K.; Shimizu, T. *Macromolecules* **2000**, *33*, 9233.
- (306) Jung, J. H.; Rim, J. A.; Han, W. S.; Lee, S. J.; Lee, Y. J.; Cho, E. J.; Kim, J. S.; Ji, Q.; Shimizu, T. *Org. Biomol. Chem.* **2006**, *4*, 2033.
- (307) Nie, X.; Wang, G. *J. Org. Chem.* **2006**, *71*, 4734.

- (308) Wang, G.; Yang, H.; Cheuk, S.; Coleman, S. *Beilstein J. Org. Chem.* **2011**, *7*, 234.
- (309) Inoue, K.; Ono, Y.; Kanekiyo, Y.; Hanabusa, K.; Shinkai, S. *Chem. Lett.* **1999**, 429.
- (310) Fujita, N.; Sakamoto, Y.; Shirakawa, M.; Ojima, M.; Fujii, A.; Ozaki, M.; Shinkai, S. *J. Am. Chem. Soc.* **2007**, *129*, 4134.
- (311) Takahashi, R.; Nunokawa, T.; Shibuya, T.; Tomita, R.; Tatewaki, Y.; Okada, S.; Kimura, T.; Shimada, S.; Matsuda, H. *Bull. Chem. Soc. Jpn.* **2012**, *85*, 236.
- (312) Tamaoki, N.; Shimada, S.; Okada, Y.; Belaissaoui, A.; Kruk, G.; Yase, K.; Matsuda, H. *Langmuir* **2000**, *16*, 7545.
- (313) Nagasawa, J.; Kudo, M.; Hayashi, S.; Tamaoki, N. *Langmuir* **2004**, *20*, 7907.
- (314) Aoki, K.; Kudo, M.; Tamaoki, N. *Org. Lett.* **2004**, *6*, 4009.
- (315) Nagasawa, J.; Yoshida, M.; Tamaoki, N. *Eur. J. Org. Chem.* **2011**, 2247.
- (316) George, M.; Weiss, R. G. *Chem. Mater.* **2003**, *15*, 2879.
- (317) George, M.; Luo, C.; Wang, C.; Carretti, E.; Dei, L.; Weiss, R. G. *Macromol. Symp.* **2005**, *227*, 173.
- (318) Bhattacharya, S.; Acharya, S. N. G. *Chem. Mater.* **1999**, *11*, 3121.
- (319) Haridas, V.; Sharma, Y. K.; Creasey, R.; Sahu, S.; Gibson, C. T.; Voelcker, N. H. *New J. Chem.* **2011**, *35*, 303.
- (320) Löwik, D. W. P. M.; Shklyarevskiy, I. O.; Ruizendaal, L.; Christianen, P. C. M.; Maan, J. C.; van Hest, J. C. M. *Adv. Mater.* **2007**, *19*, 1191.
- (321) van den Heuvel, M.; Löwik, D. W. P. M.; van Hest, J. C. M. *Biomacromolecules* **2008**, *9*, 2727.
- (322) Hsu, L.; Cvetanovich, G. L.; Stupp, S. I. *J. Am. Chem. Soc.* **2008**, *130*, 3892.
- (323) Mata, A.; Hsu, L.; Capito, R.; Aparicio, C.; Henrikson, K.; Stupp, S. I. *Soft Matter* **2009**, *5*, 1228.
- (324) Jahnke, E.; Lieberwirth, I.; Severin, N.; Rabe, J. P.; Frauenrath, H. *Angew. Chem., Int. Ed.* **2006**, *45*, 5383.
- (325) Weiss, J.; Jahnke, E.; Frauenrath, H. *Macromol. Rapid Commun.* **2008**, *29*, 330.
- (326) Weiss, J.; Jahnke, E.; Severin, N.; Rabe, J. P.; Frauenrath, H. *Nano Lett.* **2008**, *8*, 1660.
- (327) Tian, L.; Szillar, R.; Marty, R.; Bertschi, L.; Zerson, M.; Spitzner, E.-C.; Magerle, R.; Frauenrath, H. *Chem. Sci.* **2012**, *3*, 1512.
- (328) Jahnke, E.; Severin, N.; Kreutzkamp, P.; Rabe, J. P.; Frauenrath, H. *Adv. Mater.* **2008**, *20*, 409.
- (329) Jahnke, E.; Weiss, J.; Neuhaus, S.; Hoheisel, T. N.; Frauenrath, H. *Chem.—Eur. J.* **2009**, *15*, 388.
- (330) Diegelmann, S. R.; Hartman, N.; Markovic, N.; Tovar, J. D. *J. Am. Chem. Soc.* **2012**, *134*, 2028.
- (331) Svenson, S.; Messersmith, P. B. *Langmuir* **1999**, *15*, 4464.
- (332) Miyawaki, K.; Harada, A.; Takagi, T.; Shibakami, M. *Synlett* **2003**, 349.
- (333) Kim, C.; Lee, S. J.; Lee, I. H.; Kim, K. T. *Chem. Mater.* **2003**, *15*, 3638.
- (334) Lee, S. J.; Park, C. R.; Chang, J. Y. *Langmuir* **2004**, *20*, 9513.
- (335) Perino, A.; Schmutz, M.; Meunier, S.; Mésini, P. J.; Wagner, A. *Langmuir* **2011**, *27*, 12149.
- (336) Kang, S. H.; Jung, B. M.; Chang, J. Y. *Adv. Mater.* **2007**, *19*, 2780.
- (337) Kang, S. H.; Jung, B. M.; Kim, W. J.; Chang, J. Y. *Chem. Mater.* **2008**, *20*, 5532.
- (338) Néabo, J. R.; Tohoundjona, K. I. S.; Morin, J.-F. *Org. Lett.* **2011**, *13*, 1358.
- (339) Willemen, H. M.; Vermonden, T.; Marcelis, A. T. M.; Sudhölter, E. J. R. *Langmuir* **2002**, *18*, 7102.
- (340) Dautel, O. J.; Robitzer, M.; Lère-Porte, J.-P.; Serein-Spirau, F.; Moreau, J. J. E. *J. Am. Chem. Soc.* **2006**, *128*, 16213.
- (341) Hisaki, I.; Shigemitsu, H.; Sakamoto, Y.; Hasegawa, Y.; Okajima, Y.; Nakano, K.; Tohnai, N.; Miyata, M. *Angew. Chem., Int. Ed.* **2009**, *48*, 5465.
- (342) Yoshio, M.; Shoji, Y.; Tochigi, Y.; Nishikawa, Y.; Kato, T. *J. Am. Chem. Soc.* **2009**, *131*, 6763.
- (343) Duan, P. F.; Li, Y. G.; Liu, M. H. *Sci. China Chem.* **2010**, *53*, 432.
- (344) Lee, H.-Y.; Oh, H.; Lee, J.-H.; Raghavan, S. R. *J. Am. Chem. Soc.* **2012**, *134*, 14375.
- (345) Kuang, G.-C.; Ji, Y.; Jia, X.-R.; Li, Y.; Chen, E.-Q.; Zhang, Z.-X.; Wei, Y. *Tetrahedron* **2009**, *65*, 3496.
- (346) Shi, J.; Gao, Y.; Yang, Z.; Xu, B. *Beilstein J. Org. Chem.* **2011**, *7*, 167.
- (347) Ketner, A. M.; Kumar, R.; Davies, T. S.; Elder, P. W.; Raghavan, S. R. *J. Am. Chem. Soc.* **2007**, *129*, 1553.
- (348) Kumar, R.; Raghavan, S. R. *Soft Matter* **2009**, *5*, 797.
- (349) Kumar, R.; Ketner, A. M.; Raghavan, S. R. *Langmuir* **2010**, *26*, 5405.
- (350) Sakai, H.; Taki, S.; Tsuchiya, K.; Matsumura, A.; Sakai, K.; Abe, M. *Chem. Lett.* **2012**, *41*, 247.
- (351) Trivedi, D. R.; Ballabh, A.; Dastidar, P. *Chem. Mater.* **2003**, *15*, 3971.
- (352) Trivedi, D. R.; Ballabh, A.; Dastidar, P.; Ganguly, B. *Chem.—Eur. J.* **2004**, *10*, 5311.
- (353) Sahoo, P.; Kumar, D. K.; Raghavan, S. R.; Dastidar, P. *Chem.—Asian J.* **2011**, *6*, 1038.
- (354) Koshima, H.; Matsusaka, W.; Yu, H. *J. Photochem. Photobiol. A* **2003**, *156*, 83.
- (355) Lim, G. S.; Jung, B. M.; Lee, S. J.; Song, H. H.; Kim, C.; Chang, J. Y. *Chem. Mater.* **2007**, *19*, 460.
- (356) Simon, F.-X.; Nguyen, T.-T.-T.; Schmutz, M.; Decher, G.; Nicoud, J.-F.; Mésini, P. J. *New J. Chem.* **2009**, *33*, 2028.
- (357) Ahmed, S. A.-M.; Pozzo, J.-L. *J. Photochem. Photobiol. A* **2008**, *200*, 57.
- (358) Yabuuchi, K.; Oda, N.; Inokuchi, M. *Chem. Lett.* **2009**, *38*, 1096.
- (359) Takizawa, M.; Kimoto, A.; Abe, J. *Dyes Pigm.* **2011**, *89*, 254.
- (360) Xue, P.; Lu, R.; Chen, G.; Zhang, Y.; Nomoto, H.; Takafuji, M.; Ihara, H. *Chem.—Eur. J.* **2007**, *13*, 8231.
- (361) Simalou, O.; Zhao, X.; Lu, R.; Xue, P.; Yang, X.; Zhang, X. *Langmuir* **2009**, *25*, 11255.
- (362) Datta, S.; Bhattacharya, S. *Chem. Commun.* **2012**, *48*, 877.
- (363) Frkanec, L.; Jokić, M.; Makarević, J.; Wolsperger, K.; Žinić, M. *J. Am. Chem. Soc.* **2002**, *124*, 9716.
- (364) Matsumoto, S.; Yamaguchi, S.; Ueno, S.; Komatsu, H.; Ikeda, M.; Ishizuka, K.; Iko, Y.; Tabata, K. V.; Aoki, H.; Ito, S.; Noji, H.; Hamachi, I. *Chem.—Eur. J.* **2008**, *14*, 3977.
- (365) Matsumoto, S.; Yamaguchi, S.; Wada, A.; Matsui, T.; Ikeda, M.; Hamachi, I. *Chem. Commun.* **2008**, 1545.
- (366) Komatsu, H.; Matsumoto, S.; Tamaru, S.-i.; Kaneko, K.; Ikeda, M.; Hamachi, I. *J. Am. Chem. Soc.* **2009**, *131*, 5580.
- (367) Komatsu, H.; Ikeda, M.; Hamachi, I. *Chem. Lett.* **2011**, *40*, 198.
- (368) Ikeda, M.; Ueno, S.; Matsumoto, S.; Shimizu, Y.; Komatsu, H.; Kusumoto, K.-I.; Hamachi, I. *Chem.—Eur. J.* **2008**, *14*, 10808.
- (369) *Supramolecular Dye Chemistry*. Würthner, F., Ed.; Topics in Current Chemistry; Springer-Verlag: Berlin, 2005; p 258.
- (370) Chen, Z.; Lohr, A.; Saha-Möller, C. R.; Würthner, F. *Chem. Soc. Rev.* **2009**, *38*, 564.
- (371) Würthner, F.; Kaiser, T. E.; Saha-Möller, C. R. *Angew. Chem., Int. Ed.* **2011**, *50*, 3376.
- (372) Bürckstümmer, H.; Kronenberg, N. M.; Gsänger, M.; Stolte, M.; Meerholz, K.; Würthner, F. *J. Mater. Chem.* **2010**, *20*, 240.
- (373) Lohr, A.; Gress, T.; Deppisch, M.; Knoll, M.; Würthner, F. *Synthesis* **2007**, 3073.
- (374) Würthner, F.; Yao, S.; Beginn, U. *Angew. Chem., Int. Ed.* **2003**, *42*, 3247.
- (375) Yao, S.; Beginn, U.; Gress, T.; Lysetska, M.; Würthner, F. *J. Am. Chem. Soc.* **2004**, *126*, 8336.
- (376) Schmidt, R.; Stolte, M.; Grüne, M.; Würthner, F. *Macromolecules* **2011**, *44*, 3766.
- (377) Yagai, S.; Higashi, M.; Karatsu, T.; Kitamura, A. *Chem. Mater.* **2004**, *16*, 3582.
- (378) Yagai, S.; Higashi, M.; Karatsu, T.; Kitamura, A. *Chem. Mater.* **2005**, *17*, 4392.

- (379) Yagai, S.; Kinoshita, T.; Higashi, M.; Kishikawa, K.; Nakanishi, T.; Karatsu, T.; Kitamura, A. *J. Am. Chem. Soc.* **2007**, *129*, 13277.
- (380) Yagai, S.; Nakano, Y.; Seki, S.; Asano, A.; Okubo, T.; Isoshima, T.; Karatsu, T.; Kitamura, A.; Kikkawa, Y. *Angew. Chem., Int. Ed.* **2010**, *49*, 9990.
- (381) Yagai, S.; Ishii, M.; Karatsu, T.; Kitamura, A. *Angew. Chem., Int. Ed.* **2007**, *46*, 8005.
- (382) Kira, Y.; Okazaki, Y.; Sawada, T.; Takafuji, M.; Ihara, H. *Amino Acids* **2010**, *39*, 587.
- (383) Bhosale, S. V.; Jani, C. H.; Langford, S. J. *Chem. Soc. Rev.* **2008**, *37*, 331.
- (384) Sakai, N.; Mareda, J.; Vauthay, E.; Matile, S. *Chem. Commun.* **2010**, *46*, 4225.
- (385) Avinash, M. B.; Govindaraju, T. *Adv. Mater.* **2012**, *24*, 3905.
- (386) Brosse, N.; Barth, D.; Jamart-Grégoire, B. *Tetrahedron Lett.* **2004**, *45*, 9521.
- (387) Pham, Q. N.; Brosse, N.; Frochot, C.; Dumas, D.; Hocquet, A.; Jamart-Grégoire, B. *New J. Chem.* **2008**, *32*, 1131.
- (388) Allix, F.; Curcio, P.; Pham, Q. N.; Pickaert, G.; Jamart-Grégoire, B. *Langmuir* **2010**, *26*, 16818.
- (389) Curcio, P.; Allix, F.; Pickaert, G.; Jamart-Grégoire, B. *Chem.—Eur. J.* **2011**, *17*, 13603.
- (390) Wu, J.; Yi, T.; Shu, T.; Yu, M.; Zhou, Z.; Xu, M.; Zhou, Y.; Zhang, H.; Han, J.; Li, F.; Huang, C. *Angew. Chem., Int. Ed.* **2008**, *47*, 1063.
- (391) Wu, J.; Yi, T.; Xia, Q.; Zou, Y.; Liu, F.; Dong, J.; Shu, T.; Li, F.; Huang, C. *Chem.—Eur. J.* **2009**, *15*, 6234.
- (392) Yu, X.; Liu, Q.; Wu, J.; Zhang, M.; Cao, X.; Zhang, S.; Wang, Q.; Chen, L.; Yi, T. *Chem.—Eur. J.* **2010**, *16*, 9099.
- (393) Wang, Q.; Wu, J.; Gong, Z.; Zou, Y.; Yi, T.; Huang, C. *Soft Matter* **2010**, *6*, 2679.
- (394) Zhang, M.; Sun, S.; Yu, X.; Cao, X.; Zou, Y.; Yi, T. *Chem. Commun.* **2010**, *46*, 3553.
- (395) Yu, X.; Cao, X.; Chen, L.; Lan, H.; Liu, B.; Yi, T. *Soft Matter* **2012**, *8*, 3329.
- (396) Wu, J.; Tian, Q.; Hu, H.; Xia, Q.; Zou, Y.; Li, F.; Yi, T.; Huang, C. *Chem. Commun.* **2009**, 4100.
- (397) Cao, X.; Wu, Y.; Liu, K.; Yu, X.; Wu, B.; Wu, H.; Gong, Z.; Yi, T. *J. Mater. Chem.* **2012**, *22*, 2650.
- (398) Shu, T.; Wu, J.; Lu, M.; Chen, L.; Yi, T.; Li, F.; Huang, C. *J. Mater. Chem.* **2008**, *18*, 886.
- (399) Cao, X.; Zhou, J.; Zou, Y.; Zhang, M.; Yu, X.; Zhang, S.; Yi, T.; Huang, C. *Langmuir* **2011**, *27*, 5090.
- (400) Zheng, J.; Qiao, W.; Wan, X.; Gao, J. P.; Wang, Z. Y. *Chem. Mater.* **2008**, *20*, 6163.
- (401) Mukhopadhyay, P.; Iwashita, Y.; Shirakawa, M.; Kawano, S.-i.; Fujita, N.; Shinkai, S. *Angew. Chem., Int. Ed.* **2006**, *45*, 1592.
- (402) Mukhopadhyay, P.; Fujita, N.; Takada, A.; Kishida, T.; Shirakawa, M.; Shinkai, S. *Angew. Chem., Int. Ed.* **2010**, *49*, 6338.
- (403) Molla, M. R.; Ghosh, S. *Chem. Mater.* **2011**, *23*, 95.
- (404) Molla, M. R.; Das, A.; Ghosh, S. *Chem. Commun.* **2011**, *47*, 8934.
- (405) Das, A.; Ghosh, S. *Chem. Commun.* **2011**, *47*, 8922.
- (406) Das, A.; Molla, M. R.; Ghosh, S. *J. Chem. Sci.* **2011**, *123*, 963.
- (407) Das, A.; Molla, M. R.; Banerjee, A.; Paul, A.; Ghosh, S. *Chem.—Eur. J.* **2011**, *17*, 6061.
- (408) Das, A.; Molla, M. R.; Maity, B.; Koley, D.; Ghosh, S. *Chem.—Eur. J.* **2012**, *18*, 9849.
- (409) Molla, M. R.; Ghosh, S. *Chem.—Eur. J.* **2012**, *18*, 9860.
- (410) Shao, H.; Parquette, J. R. *Chem. Commun.* **2010**, *46*, 4285.
- (411) Shao, H.; Seifert, J.; Romano, N. C.; Gao, M.; Helmus, J. J.; Jaroniec, C. P.; Modarelli, D. A.; Parquette, J. R. *Angew. Chem., Int. Ed.* **2010**, *49*, 7688.
- (412) Würthner, F. *Chem. Commun.* **2004**, 1564.
- (413) Zhan, X.; Facchetti, A.; Barlow, S.; Marks, T. J.; Ratner, M. A.; Wasielewski, M. R.; Marder, S. R. *Adv. Mater.* **2011**, *23*, 268.
- (414) Würthner, F.; Stolte, M. *Chem. Commun.* **2011**, *47*, 5109.
- (415) Görl, D.; Zhang, X.; Würthner, F. *Angew. Chem., Int. Ed.* **2012**, *51*, 6328.
- (416) Weil, T.; Vosch, T.; Hofkens, J.; Peneva, K.; Müllen, K. *Angew. Chem., Int. Ed.* **2010**, *49*, 9068.
- (417) Sugiyasu, K.; Fujita, N.; Shinkai, S. *Angew. Chem., Int. Ed.* **2004**, *43*, 1229.
- (418) Sugiyasu, K.; Kawano, S.-i.; Fujita, N.; Shinkai, S. *Chem. Mater.* **2008**, *20*, 2863.
- (419) Würthner, F.; Hanke, B.; Lysetska, M.; Lambright, G.; Harms, G. S. *Org. Lett.* **2005**, *7*, 967.
- (420) Li, X.-Q.; Stepanenko, V.; Chen, Z.; Prins, P.; Siebbeles, L. D. A.; Würthner, F. *Chem. Commun.* **2006**, 3871.
- (421) Würthner, F.; Bauer, C.; Stepanenko, V.; Yagai, S. *Adv. Mater.* **2008**, *20*, 1695.
- (422) Wicklein, A.; Ghosh, S.; Sommer, M.; Würthner, F.; Thelakkat, M. *ACS Nano* **2009**, *3*, 1107.
- (423) Ghosh, S.; Li, X.-Q.; Stepanenko, V.; Würthner, F. *Chem.—Eur. J.* **2008**, *14*, 11343.
- (424) Li, X.-Q.; Zhang, X.; Ghosh, S.; Würthner, F. *Chem.—Eur. J.* **2008**, *14*, 8074.
- (425) Yagai, S.; Monma, Y.; Kawauchi, N.; Karatsu, T.; Kitamura, A. *Org. Lett.* **2007**, *9*, 1137.
- (426) Seki, T.; Yagai, S.; Karatsu, T.; Kitamura, A. *Chem. Lett.* **2008**, *37*, 764.
- (427) Seki, T.; Asano, A.; Seki, S.; Kikkawa, Y.; Murayama, H.; Karatsu, T.; Kitamura, A.; Yagai, S. *Chem.—Eur. J.* **2011**, *17*, 3598.
- (428) Seki, T.; Maruya, Y.; Nakayama, K.-i.; Karatsu, T.; Kitamura, A.; Yagai, S. *Chem. Commun.* **2011**, *47*, 12447.
- (429) Seki, T.; Karatsu, T.; Kitamura, A.; Yagai, S. *Polym. J.* **2012**, *44*, 600.
- (430) Xue, L.; Wu, H.; Shi, Y.; Liu, H.; Chen, Y.; Li, X. *Soft Matter* **2011**, *7*, 6213.
- (431) Krieg, E.; Shirman, E.; Weissman, H.; Shimoni, E.; Wolf, S. G.; Pinkas, I.; Rybtchinski, B. *J. Am. Chem. Soc.* **2009**, *131*, 14365.
- (432) Vadehra, G. S.; Wall, B. D.; Diegelmann, S. R.; Tovar, J. D. *Chem. Commun.* **2010**, *46*, 947.
- (433) Wu, H.; Xue, L.; Shi, Y.; Chen, Y.; Li, X. *Langmuir* **2011**, *27*, 3074.
- (434) Sukul, P. K.; Asthana, D.; Mukhopadhyay, P.; Summa, D.; Muccioli, L.; Zannoni, C.; Beljonnie, D.; Rowan, A. E.; Malik, S. *Chem. Commun.* **2011**, *47*, 11858.
- (435) Ren, X.; Yu, W.; Zhang, Z.; Xia, N.; Fu, G.; Lu, X.; Wang, W. *Colloids Surf. A* **2011**, *375*, 156.
- (436) Bairi, P.; Roy, B.; Nandi, A. K. *RSC Adv.* **2012**, *2*, 264.
- (437) Khan, M. K.; Sundararajan, P. *Chem.—Eur. J.* **2011**, *17*, 1184.
- (438) Chen, Q.; Zhang, D.; Zhang, G.; Yang, X.; Feng, Y.; Fan, Q.; Zhu, D. *Adv. Funct. Mater.* **2010**, *20*, 3244.
- (439) Loudet, A.; Burgess, K. *Chem. Rev.* **2007**, *107*, 4891.
- (440) Ulrich, G.; Ziessel, R.; Harriman, A. *Angew. Chem., Int. Ed.* **2008**, *47*, 1184.
- (441) Boens, N.; Leen, V.; Dehaen, W. *Chem. Soc. Rev.* **2012**, *41*, 1130.
- (442) Camerel, F.; Bonardi, L.; Schmutz, M.; Ziessel, R. *J. Am. Chem. Soc.* **2006**, *128*, 4548.
- (443) Camerel, F.; Bonardi, L.; Ulrich, G.; Charbonnière, L.; Donnio, B.; Bourgogne, C.; Guillon, D.; Retailleau, P.; Ziessel, R. *Chem. Mater.* **2006**, *18*, 5009.
- (444) Nagai, A.; Miyake, J.; Kokado, K.; Nagata, Y.; Chujo, Y. *J. Am. Chem. Soc.* **2008**, *130*, 15276.
- (445) París, R.; Quijada-Garrido, I.; García, O.; Liras, M. *Macromolecules* **2011**, *44*, 80.
- (446) Wada, A.; Tamaru, S.-i.; Ikeda, M.; Hamachi, I. *J. Am. Chem. Soc.* **2009**, *131*, 5321.
- (447) Inabe, T.; Tajima, H. *Chem. Rev.* **2004**, *104*, 5503.
- (448) de la Torre, G.; Vázquez, P.; Agulló-López, F.; Torres, T. J. *Mater. Chem.* **1998**, *8*, 1671.
- (449) de la Torre, G.; Claessens, C. G.; Torres, T. *Chem. Commun.* **2007**, 2000.
- (450) van Nostrum, C. F.; Nolte, R. J. M. *Chem. Commun.* **1996**, *2385*.

- (451) *Phthalocyanines: Properties and Applications*; Leznoff, C. C., Lever, A. B. P., Eds.; Wiley-VCH: Cambridge, U.K., 1989–1996; Vols. 1–4.
- (452) Li, W.-S.; Aida, T. *Chem. Rev.* **2009**, *109*, 6047.
- (453) D’Souza, F.; Ito, O. *Chem. Commun.* **2009**, 4913.
- (454) van Nostrum, C. F.; Picken, S. J.; Schouten, A.-J.; Nolte, R. J. M. *J. Am. Chem. Soc.* **1995**, *117*, 9957.
- (455) Engelkamp, H.; Middelbeek, S.; Nolte, R. J. M. *Science* **1999**, *284*, 785.
- (456) Boamfa, M. I.; Christianen, P. C. M.; Engelkamp, H.; Nolte, R. J. M.; Maan, J. C. *Adv. Funct. Mater.* **2004**, *14*, 261.
- (457) Samorí, P.; Engelkamp, H.; de Witte, P.; Rowan, A. E.; Nolte, R. J. M.; Rabe, J. P. *Angew. Chem., Int. Ed.* **2001**, *40*, 2348.
- (458) Sly, J.; Kasák, P.; Gomar-Nadal, E.; Rovira, C.; Górriz, L.; Thordarson, P.; Amabilino, D. B.; Rowan, A. E.; Nolte, R. J. M. *Chem. Commun.* **2005**, 1255.
- (459) Díaz, D. D.; Torres, T.; Zentel, R.; Davis, R.; Brehmer, M. *Chem. Commun.* **2007**, 2369.
- (460) Díaz, D. D.; Cid, J. J.; Vázquez, P.; Torres, T. *Chem.—Eur. J.* **2008**, *14*, 9261.
- (461) Osada, Y.; Ohnishi, S. *Macromolecules* **1991**, *24*, 3020.
- (462) Kimura, M.; Ueki, H.; Ohta, K.; Hanabusa, K.; Shirai, H.; Kobayashi, N. *Chem.—Eur. J.* **2004**, *10*, 4954.
- (463) Rodriguez, M. E.; Diz, V. E.; Awruch, J.; Dicelio, L. E. *Photochem. Photobiol.* **2010**, *86*, 513.
- (464) Garifullin, R.; Erkal, T. S.; Tekin, S.; Ortaç, B.; Gürek, A. G.; Ahsen, V.; Yaglioglu, H. G.; Elmali, A.; Guler, M. O. *J. Mater. Chem.* **2012**, *22*, 2553.
- (465) Borovkov, V. V.; Inoue, Y. *Top. Curr. Chem.* **2006**, *265*, 89.
- (466) Drain, C. M.; Varotto, A.; Radivojevic, I. *Chem. Rev.* **2009**, *109*, 1630.
- (467) Nakamura, Y.; Aratani, N.; Osuka, A. *Chem. Soc. Rev.* **2007**, *36*, 831.
- (468) Saito, S.; Osuka, A. *Angew. Chem., Int. Ed.* **2011**, *50*, 4342.
- (469) Beletskaya, I.; Tyurin, V. S.; Tsivadze, A. Y.; Guillard, R.; Stern, C. *Chem. Rev.* **2009**, *109*, 1659.
- (470) Tashiro, K.; Aida, T. *Chem. Soc. Rev.* **2007**, *36*, 189.
- (471) Terech, P.; Gebel, G.; Ramasseul, R. *Langmuir* **1996**, *12*, 4321.
- (472) Terech, P.; Scherer, C.; Demé, B.; Ramasseul, R. *Langmuir* **2003**, *19*, 10641.
- (473) Terech, P.; Scherer, C.; Lindner, P.; Ramasseul, R. *Langmuir* **2003**, *19*, 10648.
- (474) Kimura, M.; Kitamura, T.; Muto, T.; Hanabusa, K.; Shirai, H.; Kobayashi, N. *Chem. Lett.* **2000**, 1088.
- (475) Sagawa, T.; Fukugawa, S.; Yamada, T.; Ihara, H. *Langmuir* **2002**, *18*, 7223.
- (476) Miyamoto, K.; Jintoku, H.; Sawada, T.; Takafuji, M.; Sagawa, T.; Ihara, H. *Tetrahedron Lett.* **2011**, *S2*, 4030.
- (477) Jintoku, H.; Sagawa, T.; Takafuji, M.; Ihara, H. *Org. Biomol. Chem.* **2009**, *7*, 2430.
- (478) Jintoku, H.; Sagawa, T.; Sawada, T.; Takafuji, M.; Hachisako, H.; Ihara, H. *Tetrahedron Lett.* **2008**, *49*, 3987.
- (479) Jintoku, H.; Sagawa, T.; Sawada, T.; Takafuji, M.; Ihara, H. *Org. Biomol. Chem.* **2010**, *8*, 1344.
- (480) Jintoku, H.; Sagawa, T.; Takafuji, M.; Ihara, H. *Chem.—Eur. J.* **2011**, *17*, 11628.
- (481) Jintoku, H.; Shimoda, S.; Takafuji, M.; Sagawa, T.; Ihara, H. *Mol. Cryst. Liq. Cryst.* **2011**, *539*, 63[403].
- (482) Jintoku, H.; Takafuji, M.; Oda, R.; Ihara, H. *Chem. Commun.* **2012**, *48*, 4881.
- (483) Tian, H. J.; Inoue, K.; Yoza, K.; Ishi-i, T.; Shinkai, S. *Chem. Lett.* **1998**, 871.
- (484) Ishi-i, T.; Jung, J. H.; Shinkai, S. *J. Mater. Chem.* **2000**, *10*, 2238.
- (485) Ishi-i, T.; Iguchi, R.; Snip, E.; Ikeda, M.; Shinkai, S. *Langmuir* **2001**, *17*, 5825.
- (486) Snip, E.; Shinkai, S.; Reinhoudt, D. N. *Tetrahedron Lett.* **2001**, *42*, 2153.
- (487) Tamaru, S.-i.; Nakamura, M.; Takeuchi, M.; Shinkai, S. *Org. Lett.* **2001**, *3*, 3631.
- (488) Tamaru, S.-i.; Takeuchi, M.; Sano, M.; Shinkai, S. *Angew. Chem., Int. Ed.* **2002**, *41*, 853.
- (489) Kawano, S.-i.; Tamaru, S.-i.; Fujita, N.; Shinkai, S. *Chem.—Eur. J.* **2004**, *10*, 343.
- (490) Zelenka, K.; Trnka, T.; Tišlerová, I.; Monti, D.; Cinti, S.; Naitana, M. L.; Schiaffino, L.; Venanzi, M.; Laguzzi, G.; Luvidi, L.; Mancini, G.; Nováková, Z.; Šimák, O.; Wimmer, Z.; Drašar, P. *Chem.—Eur. J.* **2011**, *17*, 13743.
- (491) Tamaru, S.-i.; Uchino, S.-y.; Takeuchi, M.; Ikeda, M.; Hatano, T.; Shinkai, S. *Tetrahedron Lett.* **2002**, *43*, 3751.
- (492) Shirakawa, M.; Kawano, S.-i.; Fujita, N.; Sada, K.; Shinkai, S. *J. Org. Chem.* **2003**, *68*, 5037.
- (493) Kishida, T.; Fujita, N.; Sada, K.; Shinkai, S. *Chem. Lett.* **2004**, *33*, 1002.
- (494) Kishida, T.; Fujita, N.; Sada, K.; Shinkai, S. *J. Am. Chem. Soc.* **2005**, *127*, 7298.
- (495) Kishida, T.; Fujita, N.; Sada, K.; Shinkai, S. *Langmuir* **2005**, *21*, 9432.
- (496) Kishida, T.; Fujita, N.; Hirata, O.; Shinkai, S. *Org. Biomol. Chem.* **2006**, *4*, 1902.
- (497) Shirakawa, M.; Fujita, N.; Shinkai, S. *J. Am. Chem. Soc.* **2005**, *127*, 4164.
- (498) Shirakawa, M.; Fujita, N.; Shinkai, S. *J. Am. Chem. Soc.* **2003**, *125*, 9902.
- (499) Shirakawa, M.; Fujita, N.; Shimakoshi, H.; Hisaeda, Y.; Shinkai, S. *Tetrahedron* **2006**, *62*, 2016.
- (500) Xiao, Z.-Y.; Hou, J.-L.; Jiang, X.-K.; Li, Z.-T.; Ma, Z. *Tetrahedron* **2009**, *65*, 10182.
- (501) Iavicoli, P.; Xu, H.; Feldborg, L. N.; Linares, M.; Paradinas, M.; Stafström, S.; Ocal, C.; Nieto-Ortega, B.; Casado, J.; Navarrete, J. T. L.; Lazzaroni, R.; De Feyter, S.; Amabilino, D. B. *J. Am. Chem. Soc.* **2010**, *132*, 9350.
- (502) Takeuchi, M.; Tanaka, S.; Shinkai, S. *Chem. Commun.* **2005**, 5539.
- (503) Tanaka, S.; Shirakawa, M.; Kaneko, K.; Takeuchi, M.; Shinkai, S. *Langmuir* **2005**, *21*, 2163.
- (504) Setnička, V.; Urbanová, M.; Pataridis, S.; Král, V.; Volka, K. *Tetrahedron: Asymmetry* **2002**, *13*, 2661.
- (505) Král, V.; Pataridis, S.; Setnička, V.; Záruba, K.; Urbanová, M.; Volka, K. *Tetrahedron* **2005**, *61*, 5499.
- (506) Xiao, Z.-Y.; Zhao, X.; Jiang, X.-K.; Li, Z.-T. *Org. Biomol. Chem.* **2009**, *7*, 2540.
- (507) van Hameren, R.; Schön, P.; van Buul, A. M.; Hoogboom, J.; Lazarenko, S. V.; Gerritsen, J. W.; Engelkamp, H.; Christianen, P. C. M.; Heus, H. A.; Maan, J. C.; Rasing, T.; Speller, S.; Rowan, A. E.; Elemans, J. A. A. W.; Nolte, R. J. M. *Science* **2006**, *314*, 1433.
- (508) van Hameren, R.; van Buul, A. M.; Castricano, M. A.; Villari, V.; Micali, N.; Schön, P.; Speller, S.; Scolaro, L. M.; Rowan, A. E.; Elemans, J. A. A. W.; Nolte, R. J. M. *Nano Lett.* **2008**, *8*, 253.
- (509) Hori, T.; Osuka, A. *Eur. J. Org. Chem.* **2010**, 2379.
- (510) Li, Y.; Wang, T.; Liu, M. *Soft Matter* **2007**, *3*, 1312.
- (511) Malik, S.; Kawano, S.-i.; Fujita, N.; Shinkai, S. *Tetrahedron* **2007**, *63*, 7326.
- (512) Law, K.-Y. *Chem. Rev.* **1993**, *93*, 449.
- (513) Ajayaghosh, A. *Acc. Chem. Res.* **2005**, *38*, 449.
- (514) Beverina, L.; Salice, P. *Eur. J. Org. Chem.* **2010**, 1207.
- (515) Stanescu, M.; Samha, H.; Perlstein, J.; Whitten, D. G. *Langmuir* **2000**, *16*, 275.
- (516) Wu, J.; Yi, T.; Zou, Y.; Xia, Q.; Shu, T.; Liu, F.; Yang, Y.; Li, F.; Chen, Z.; Zhou, Z.; Huang, C. *J. Mater. Chem.* **2009**, *19*, 3971.
- (517) Hamada, K.; Yamada, K.; Mitsuishi, M.; Ohira, M.; Miyazaki, K. *J. Chem. Soc., Chem. Commun.* **1992**, 544.
- (518) Imae, T.; Gagel, L.; Tunich, C.; Platz, G.; Iwamoto, T.; Funayama, K. *Langmuir* **1998**, *14*, 2197.
- (519) Amaike, M.; Kobayashi, H.; Shinkai, S. *Chem. Lett.* **2001**, 620.
- (520) Jung, J. H.; Shinkai, S.; Shimizu, T. *Nano Lett.* **2002**, *2*, 17.
- (521) Asai, M.; Sugiyasu, K.; Fujita, N.; Shinkai, S. *Chem. Lett.* **2004**, *33*, 120.

- (522) Guan, Y.; Antonietti, M.; Faul, C. F. J. *Langmuir* **2002**, *18*, 5939.
- (523) Faul, C. F. J.; Antonietti, M. *Chem.—Eur. J.* **2002**, *8*, 2764.
- (524) Bieser, A. M.; Tiller, J. C. *Chem. Commun.* **2005**, 3942.
- (525) Bieser, A. M.; Tiller, J. C. *J. Phys. Chem. B* **2007**, *111*, 13180.
- (526) Bieser, A. M.; Tiller, J. C. *Supramol. Chem.* **2008**, *20*, 363.
- (527) Park, J. S.; Jeong, S.; Ahn, B.; Kim, M.; Oh, W.; Kim, J. *J. Incl. Phenom. Macrocycl. Chem.* **2011**, *71*, 79.
- (528) Ranjith, C.; Vijayan, K. K.; Praveen, V. K.; Kumar, N. S. S. *Spectrochim. Acta, Part A* **2010**, *75*, 1610.
- (529) Zhang, F.; Morita, Y.; Kawabe, K.; Tasaka, T.; Okamoto, H.; Takenaka, S.; Kita, H. *Chem. Lett.* **2005**, *34*, 1156.
- (530) Morita, Y.; Kawabe, K.; Zhang, F.; Okamoto, H.; Takenaka, S.; Kita, H. *Chem. Lett.* **2005**, *34*, 1650.
- (531) Yu, H.; Mizufune, H.; Uenaka, K.; Moritoki, T.; Koshima, H. *Tetrahedron* **2005**, *61*, 8932.
- (532) Königs, P.; Neumann, O.; Hackelöer, K.; Kataeva, O.; Waldvogel, S. R. *Eur. J. Org. Chem.* **2008**, 343.
- (533) Park, M.; Jang, D.; Kim, S. Y.; Hong, J.-I. *New J. Chem.* **2012**, *36*, 1145.
- (534) Nagata, M.; Yamamoto, Y. *React. Funct. Polym.* **2008**, *68*, 915.
- (535) Nishiyama, K.; Takata, K.; Watanabe, K.; Shigematsu, H. *Chem. Phys. Lett.* **2012**, *529*, 39.
- (536) Tamaru, S.-i.; Kiyonaka, S.; Hamachi, I. *Chem.—Eur. J.* **2005**, *11*, 7294.
- (537) Ikeda, M.; Yoshii, T.; Matsui, T.; Tanida, T.; Komatsu, H.; Hamachi, I. *J. Am. Chem. Soc.* **2011**, *133*, 1670.
- (538) Lal, M.; Pakatchi, S.; He, G. S.; Kim, K. S.; Prasad, P. N. *Chem. Mater.* **1999**, *11*, 3012.
- (539) Maitra, U.; Mukhopadhyay, S.; Sarkar, A.; Rao, P.; Indi, S. S. *Angew. Chem., Int. Ed.* **2001**, *40*, 2281.
- (540) Mukhopadhyay, S.; Ira; Krishnamoorthy, G.; Maitra, U. *J. Phys. Chem. B* **2003**, *107*, 2189.
- (541) Mukhopadhyay, S.; Maitra, U.; Ira; Krishnamoorthy, G.; Schmidt, J.; Talmon, Y. *J. Am. Chem. Soc.* **2004**, *126*, 15905.
- (542) Heeres, A.; van der Pol, C.; Stuart, M.; Friggeri, A.; Feringa, B. L.; van Esch, J. *J. Am. Chem. Soc.* **2003**, *125*, 14252.
- (543) Shome, A.; Debnath, S.; Das, P. K. *Langmuir* **2008**, *24*, 4280.
- (544) Kiyonaka, S.; Sada, K.; Yoshimura, I.; Shinkai, S.; Kato, N.; Hamachi, I. *Nat. Mater.* **2004**, *3*, 58.
- (545) Yoshimura, I.; Miyahara, Y.; Kasagi, N.; Yamane, H.; Ojida, A.; Hamachi, I. *J. Am. Chem. Soc.* **2004**, *126*, 12204.
- (546) Yamaguchi, S.; Yoshimura, I.; Kohira, T.; Tamaru, S.-i.; Hamachi, I. *J. Am. Chem. Soc.* **2005**, *127*, 11835.
- (547) Zhou, S.-L.; Matsumoto, S.; Tian, H.-D.; Yamane, H.; Ojida, A.; Kiyonaka, S.; Hamachi, I. *Chem.—Eur. J.* **2005**, *11*, 1130.
- (548) Babu, P.; Chopra, D.; Row, T. N. G.; Maitra, U. *Org. Biomol. Chem.* **2005**, *3*, 3695.
- (549) Seo, S. H.; Chang, J. Y. *Chem. Mater.* **2005**, *17*, 3249.
- (550) Yu, W.; Li, Y.; Wang, T.; Liu, M.; Li, Z. *Acta Phys., Chim. Sin.* **2008**, *24*, 1535.
- (551) Das, S.; Chattopadhyay, A. P.; De, S. *J. Photochem. Photobiol., A* **2008**, *197*, 402.
- (552) Wang, H.; Zhang, W.; Dong, X.; Yang, Y. *Talanta* **2009**, *77*, 1864.
- (553) Wang, H.; Zhang, J.; Zhang, W.; Yang, Y. *Eur. J. Pharm. Biopharm.* **2009**, *73*, 357.
- (554) Ghosh, S.; Adhikari, A.; Mojumdar, S. S.; Bhattacharyya, K. J. *Phys. Chem. B* **2010**, *114*, 5736.
- (555) Okano, K.; Taguchi, M.; Fujiki, M.; Yamashita, T. *Angew. Chem., Int. Ed.* **2011**, *50*, 12474.
- (556) Bag, B. G.; Paul, K. *Asia. J. Org. Chem.* **2012**, *1*, 150.
- (557) Das, S.; de Rooy, S. L.; Jordan, A. N.; Chandler, L.; Negulescu, I. I.; El-Zahab, B.; Warner, I. M. *Langmuir* **2012**, *28*, 757.
- (558) Kitahama, Y.; Kimura, Y.; Takazawa, K.; Kido, G. *Bull. Chem. Soc. Jpn.* **2005**, *78*, 727.
- (559) Rajasekar, M.; Khan, S. M.; Devaraj, S. N.; Das, T. M. *Carbohydr. Res.* **2011**, *346*, 1776.
- (560) Ghini, G.; Lascialfari, L.; Vinattieri, C.; Cicchi, S.; Brandi, A.; Berti, D.; Betti, F.; Baglioni, P.; Mannini, M. *Soft Matter* **2009**, *5*, 1863.
- (561) Kameta, N.; Masuda, M.; Shimizu, T. *ACS Nano* **2012**, *6*, 5249.
- (562) Figueira-Duarte, T. M.; Müllen, K. *Chem. Rev.* **2011**, *111*, 7260.
- (563) Maitra, U.; Kumar, P. V.; Chandra, N.; D’Souza, L. J.; Prasanna, M. D.; Raju, A. R. *Chem. Commun.* **1999**, 595.
- (564) Bhat, S.; Valkonen, A.; Koivukorpi, J.; Ambika, A.; Kolehmainen, E.; Maitra, U.; Rissanen, K. *J. Chem. Sci.* **2011**, *123*, 379.
- (565) Maitra, U.; Potluri, V. K.; Sangeetha, N. M.; Babu, P.; Raju, A. R. *Tetrahedron: Asymmetry* **2001**, *12*, 477.
- (566) Babu, P.; Sangeetha, N. M.; Vijaykumar, P.; Maitra, U.; Rissanen, K.; Raju, A. R. *Chem.—Eur. J.* **2003**, *9*, 1922.
- (567) Das, R. K.; Kandanelli, R.; Linnanto, J.; Bose, K.; Maitra, U. *Langmuir* **2010**, *26*, 16141.
- (568) Hahma, A.; Bhat, S.; Leivo, K.; Linnanto, J.; Lahtinen, M.; Rissanen, K. *New J. Chem.* **2008**, *32*, 1438.
- (569) Moffat, J. R.; Smith, D. K. *Chem. Commun.* **2008**, 2248.
- (570) Kilbinger, A. F. M.; Grubbs, R. H. *Angew. Chem., Int. Ed.* **2002**, *41*, 1563.
- (571) Moffat, J. R.; Smith, D. K. *Chem. Commun.* **2011**, *47*, 11864.
- (572) Ihara, H.; Yamada, T.; Nishihara, M.; Sakurai, T.; Takafuji, M.; Hachisako, H.; Sagawa, T. *J. Mol. Liq.* **2004**, *111*, 73.
- (573) Takafuji, M.; Ishiodori, A.; Yamada, T.; Sakurai, T.; Ihara, H. *Chem. Commun.* **2004**, 1122.
- (574) Takafuji, M.; Kira, Y.; Ishiodori, A.; Hachisako, H.; Sawada, T.; Ihara, H. *Macromol. Symp.* **2010**, *291*–*292*, 330.
- (575) Takafuji, M.; Kira, Y.; Tsuji, H.; Sawada, S.; Hachisako, H.; Ihara, H. *Tetrahedron* **2007**, *63*, 7489.
- (576) Jintoku, H.; Ihara, H. *Chem. Commun.* **2012**, *48*, 1144.
- (577) Tian, Y.; Zhang, L.; Duan, P.; Liu, F.; Zhang, B.; Liu, C.; Liu, M. *New J. Chem.* **2010**, *34*, 2847.
- (578) Mahajan, S. S.; Paranjri, R.; Mehta, R.; Lyon, R. P.; Atkins, W. M. *Bioconjugate Chem.* **2005**, *16*, 1019.
- (579) Rajamalli, P.; Prasad, E. *Soft Matter* **2012**, *8*, 8896.
- (580) Kamikawa, Y.; Kato, T. *Langmuir* **2007**, *23*, 274.
- (581) Ma, M.; Kuang, Y.; Gao, Y.; Zhang, Y.; Gao, P.; Xu, B. *J. Am. Chem. Soc.* **2010**, *132*, 2719.
- (582) Adhikari, B.; Nanda, J.; Banerjee, A. *Chem.—Eur. J.* **2011**, *17*, 11488.
- (583) Zhang, Y.; Yang, Z.; Yuan, F.; Gu, H.; Gao, P.; Xu, B. *J. Am. Chem. Soc.* **2004**, *126*, 15028.
- (584) Xing, B.; Yu, C.-W.; Chow, K.-H.; Ho, P.-L.; Fu, D.; Xu, B. *J. Am. Chem. Soc.* **2002**, *124*, 14846.
- (585) Xing, B.; Ho, P. L.; Yu, C.-W.; Chow, K.-H.; Gu, H.; Xu, B. *Chem. Commun.* **2003**, 2224.
- (586) Bhuniya, S.; Kim, B. H. *Chem. Commun.* **2006**, 1842.
- (587) Hamachi, I.; Kiyonaka, S.; Shinkai, S. *Tetrahedron Lett.* **2001**, *42*, 6141.
- (588) Nagarajan, S.; Das, T. M. *New J. Chem.* **2009**, *33*, 2391.
- (589) Xu, H.; Rudkevich, D. M. *J. Org. Chem.* **2004**, *69*, 8609.
- (590) Kimura, M.; Miki, N.; Suzuki, D.; Adachi, N.; Tatewaki, Y.; Shirai, H. *Langmuir* **2009**, *25*, 776.
- (591) Chen, C.-Y.; Ito, Y.; Chiu, Y.-C.; Wu, W.-C.; Higashihara, T.; Ueda, M.; Chen, W.-C. *Chem. Lett.* **2012**, *41*, 92.
- (592) Canevet, D.; del Pino, Á. P.; Amabilino, D. B.; Sallé, M. *J. Mater. Chem.* **2011**, *21*, 1428.
- (593) Canevet, D.; del Pino, Á. P.; Amabilino, D. B.; Sallé, M. *Nanoscale* **2011**, *3*, 2898.
- (594) Diring, S.; Camerel, F.; Donnio, B.; Dintzer, T.; Toffanin, S.; Capelli, R.; Muccini, M.; Ziessel, R. *J. Am. Chem. Soc.* **2009**, *131*, 18177.
- (595) Cai, W.; Wang, G.-T.; Du, P.; Wang, R.-X.; Jiang, X.-K.; Li, Z.-T. *J. Am. Chem. Soc.* **2008**, *130*, 13450.
- (596) Kim, K. T.; Park, C.; Vandermeulen, G. W. M.; Rider, D. A.; Kim, C.; Winnik, M. A.; Manners, I. *Angew. Chem., Int. Ed.* **2005**, *44*, 7964.
- (597) Bhowmik, S.; Banerjee, S.; Maitra, U. *Chem. Commun.* **2010**, *46*, 8642.
- (598) Lin, C.; Gitsov, I. *Macromolecules* **2010**, *43*, 10017.

- (599) Wang, C.; Wang, Z.; Zhang, D.; Zhu, D. *Chem. Phys. Lett.* **2006**, *428*, 130.
- (600) Chen, Q.; Lv, Y.; Zhang, D.; Zhang, G.; Liu, C.; Zhu, D. *Langmuir* **2010**, *26*, 3165.
- (601) Seo, Y. J.; Bhuniya, S.; Kim, B. H. *Chem. Commun.* **2007**, 1804.
- (602) Seo, Y. J.; Bhuniya, S.; Yi, J. W.; Kim, B. H. *Tetrahedron Lett.* **2008**, *49*, 2701.
- (603) Ossipov, D. A.; Yang, X.; Varghese, O.; Kootala, S.; Hilborn, J. *Chem. Commun.* **2010**, *46*, 8368.
- (604) Rao, K. V.; Mohapatra, S.; Maji, T. K.; George, S. *J. Chem.—Eur. J.* **2012**, *18*, 4505.
- (605) Kumar, S. *Liquid Cryst.* **2004**, *31*, 1037.
- (606) Kumar, S. *Chem. Soc. Rev.* **2006**, *35*, 83.
- (607) Ikeda, M.; Takeuchi, M.; Shinkai, S. *Chem. Commun.* **2003**, 1354.
- (608) Tatewaki, Y.; Hatanaka, T.; Kimura, M.; Shirai, H. *Chem. Lett.* **2009**, *38*, 900.
- (609) Tao, K.; Wu, T.; Lu, D.; Bai, R.; Li, H.; An, L. *J. Mol. Liq.* **2008**, *142*, 118.
- (610) Bhalla, V.; Singh, H.; Kumar, M.; Prasad, S. K. *Langmuir* **2011**, *27*, 15275.
- (611) Kotlewski, A.; Norder, B.; Jager, W. F.; Picken, S. J.; Mendes, E. *Soft Matter* **2009**, *5*, 4905.
- (612) Bai, Y. F.; Zhao, K. Q.; Hu, P.; Wang, B. Q.; Shimizu, Y. *Mol. Cryst. Liq. Cryst.* **2009**, *509*, 60/[802].
- (613) Kimura, M.; Hatanaka, T.; Nomoto, H.; Takizawa, J.; Fukawa, T.; Tatewaki, Y.; Shirai, H. *Chem. Mater.* **2010**, *22*, 5732.
- (614) Mizoshita, N.; Monobe, H.; Inoue, M.; Ukon, M.; Watanabe, T.; Shimizu, Y.; Hanabusa, K.; Kato, T. *Chem. Commun.* **2002**, 428.
- (615) Hirai, Y.; Monobe, H.; Mizoshita, N.; Moriyama, M.; Hanabusa, K.; Shimizu, Y.; Kato, T. *Adv. Funct. Mater.* **2008**, *18*, 1668.
- (616) Romero, C.; Peña, D.; Pérez, D.; Guitián, E.; Termine, R.; Golemme, A.; Omenat, A.; Barberá, J.; Serrano, J. L. *J. Mater. Chem.* **2009**, *19*, 4725.
- (617) Zelzer, M.; Ulijn, R. V. *Chem. Soc. Rev.* **2010**, *39*, 3351.
- (618) Adams, D. *J. Macromol. Biosci.* **2011**, *11*, 160.
- (619) Wang, H.; Yang, Z. *Nanoscale* **2012**, *4*, 5259.
- (620) Choi, I. S.; Li, X.; Simanek, E. E.; Akaba, R.; Whitesides, G. M. *Chem. Mater.* **1999**, *11*, 684.
- (621) Terech, P.; Clavier, G.; Bouas-Laurent, H.; Desvergne, J.-P.; Demé, B.; Pozzo, J.-L. *J. Colloid Interface Sci.* **2006**, *302*, 633.
- (622) Mieden-Gundert, G.; Klein, L.; Fischer, M.; Vögtle, F.; Heuzé, K.; Pozzo, J.-L.; Vallier, M.; Fages, F. *Angew. Chem., Int. Ed.* **2001**, *40*, 3164.
- (623) Yang, Y.; Chen, T.; Xiang, J.-F.; Yan, H.-J.; Chen, C.-F.; Wan, L.-J. *Chem.—Eur. J.* **2008**, *14*, 5742.
- (624) Das, A.; Ghosh, S. *Chem.—Eur. J.* **2010**, *16*, 13622.
- (625) Nayak, M. K. *J. Photochem. Photobiol., A* **2011**, *217*, 40.
- (626) Yang, H.; Yi, T.; Zhou, Z.; Zhou, Y.; Wu, J.; Xu, M.; Li, F.; Huang, C. *Langmuir* **2007**, *23*, 8224.
- (627) Wang, C.; Zhang, D.; Zhu, D. *Langmuir* **2007**, *23*, 1478.
- (628) Lloyd, G. O.; Piepenbrock, M.-O. M.; Foster, J. A.; Clarke, N.; Steed, J. W. *Soft Matter* **2012**, *8*, 204.
- (629) Menger, F. M.; Caran, K. L. *J. Am. Chem. Soc.* **2000**, *122*, 11679.
- (630) Chen, J.; Wu, W.; McNeil, A. *J. Chem. Commun.* **2012**, *48*, 7310.
- (631) Matteucci, M.; Bhalay, G.; Bradley, M. *J. Peptide Sci.* **2004**, *10*, 318.
- (632) Li, Y.; Wang, T.; Liu, M. *Tetrahedron* **2007**, *63*, 7468.
- (633) Duan, P.; Liu, M. *Langmuir* **2009**, *25*, 8706.
- (634) Montalti, M.; Dolci, L. S.; Prodi, L.; Zaccheroni, N.; Stuart, M. C. A.; van Bommel, K. J. C.; Friggeri, A. *Langmuir* **2006**, *22*, 2299.
- (635) Tripathi, A.; Kumar, A.; Pandey, P. S. *Tetrahedron Lett.* **2012**, *S3*, 5745.
- (636) Kuang, G.-C.; Teng, M.-J.; Jia, X.-R.; Chen, E.-Q.; Wei, Y. *Chem.—Asian J.* **2011**, *6*, 1163.
- (637) Baker, M. B.; Yuan, L.; Marth, C. J.; Li, Y.; Castellano, R. K. *Supramol. Chem.* **2010**, *22*, 789.
- (638) Cicchi, S.; Ghini, G.; Lascialfari, L.; Brandi, A.; Betti, F.; Berti, D.; Ferrati, S.; Baglioni, P. *Chem. Commun.* **2007**, 1424.
- (639) Cicchi, S.; Ghini, G.; Fallani, S.; Brandi, A.; Berti, D.; Betti, F.; Baglioni, P. *Tetrahedron Lett.* **2008**, *49*, 1701.
- (640) Atsbeha, T.; Bussotti, L.; Cicchi, S.; Foggi, P.; Ghini, G.; Lascialfari, L.; Marcelli, A. *J. Mol. Struct.* **2011**, *993*, 459.
- (641) Huang, X.; Terech, P.; Raghavan, S. R.; Weiss, R. G. *J. Am. Chem. Soc.* **2005**, *127*, 4336.
- (642) Huang, X.; Raghavan, S. R.; Terech, P.; Weiss, R. G. *J. Am. Chem. Soc.* **2006**, *128*, 15341.
- (643) Zhao, Y.-L.; Aprahamian, I.; Trabolsi, A.; Erina, N.; Stoddart, J. F. *J. Am. Chem. Soc.* **2008**, *130*, 6348.
- (644) Zhao, Y.-L.; Erina, N.; Yasuda, T.; Kato, T.; Stoddart, J. F. *J. Mater. Chem.* **2009**, *19*, 3469.
- (645) He, Y.; Bian, Z.; Kang, C.; Jin, R.; Gao, L. *New J. Chem.* **2009**, *33*, 2073.
- (646) Yan, N.; He, G.; Zhang, H.; Ding, L.; Fang, Y. *Langmuir* **2010**, *26*, 5909.
- (647) Ghosh, R.; Chakraborty, A.; Maiti, D. K.; Puranik, V. G. *Org. Lett.* **2006**, *6*, 1061.
- (648) Roy, S.; Chakraborty, A.; Chattopadhyay, B.; Bhattacharya, A.; Mukherjee, A. K.; Ghosh, R. *Tetrahedron* **2010**, *66*, 8512.
- (649) Wang, G.; Cheuk, S.; Yang, H.; Goyal, N.; Reddy, P. V. N.; Hopkinson, B. *Langmuir* **2009**, *25*, 8696.
- (650) Kameta, N.; Ishikawa, K.; Masuda, M.; Asakawa, M.; Shimizu, T. *Chem. Mater.* **2012**, *24*, 209.
- (651) Chen, L.; Morris, K.; Laybourn, A.; Elias, D.; Hicks, M. R.; Rodger, A.; Serpell, L.; Adams, D. *J. Langmuir* **2010**, *26*, 5232.
- (652) Chen, L.; Revel, S.; Morris, K.; Serpell, L. C.; Adams, D. *J. Langmuir* **2010**, *26*, 13466.
- (653) Chen, L.; Pont, G.; Morris, K.; Lotze, G.; Squires, A.; Serpell, L. C.; Adams, D. *J. Chem. Commun.* **2011**, *47*, 12071.
- (654) Chen, L.; Revel, S.; Morris, K.; Adams, D. *J. Chem. Commun.* **2010**, *46*, 4267.
- (655) Chen, L.; Revel, S.; Morris, K.; Spiller, D. G.; Serpell, L. C.; Adams, D. *J. Chem. Commun.* **2010**, *46*, 6738.
- (656) Pont, G.; Chen, L.; Spiller, D. G.; Adams, D. *J. Soft Matter* **2012**, *8*, 7797.
- (657) Raeburn, J.; McDonald, T. O.; Adams, D. *J. Chem. Commun.* **2012**, *48*, 9355.
- (658) Houton, K. A.; Morris, K. L.; Chen, L.; Schmidtmann, M.; Jones, J. T. A.; Serpell, L. C.; Lloyd, G. O.; Adams, D. *J. Langmuir* **2012**, *28*, 9797.
- (659) Grigoriou, S.; Johnson, E. K.; Chen, L.; Adams, D. J.; James, T. D.; Cameron, P. *J. Soft Matter* **2012**, *8*, 6788.
- (660) Reddy, A.; Sharma, A.; Srivastava, A. *Chem.—Eur. J.* **2012**, *18*, 7575.
- (661) Yang, Z.; Liang, G.; Xu, B. *Chem. Commun.* **2006**, 738.
- (662) Yang, Z.; Liang, G.; Ma, M.; Gao, Y.; Xu, B. *J. Mater. Chem.* **2007**, *17*, 850.
- (663) Liang, G.; Yang, Z.; Zhang, R.; Li, L.; Fan, Y.; Kuang, Y.; Gao, Y.; Wang, T.; Lu, W. W.; Xu, B. *Langmuir* **2009**, *25*, 8419.
- (664) Yang, Z.; Gu, H.; Du, J.; Gao, J.; Zhang, B.; Zhang, X.; Xu, B. *Tetrahedron* **2007**, *63*, 7349.
- (665) Yang, Z.; Liang, G.; Ma, M.; Gao, Y.; Xu, B. *Small* **2007**, *3*, 558.
- (666) Yang, Z.; Liang, G.; Guo, Z.; Guo, Z.; Xu, B. *Angew. Chem., Int. Ed.* **2007**, *46*, 8216.
- (667) Ren, C.; Song, Z.; Zheng, W.; Chen, X.; Wang, L.; Kong, D.; Yang, Z. *Chem. Commun.* **2011**, *47*, 1619.
- (668) Yang, Z.; Liang, G.; Wang, L.; Xu, B. *J. Am. Chem. Soc.* **2006**, *128*, 3038.
- (669) Yang, Z.; Xu, B. *Adv. Mater.* **2006**, *18*, 3043.
- (670) Wang, H.; Ren, C.; Song, Z.; Wang, L.; Chen, X.; Yang, Z. *Nanotechnology* **2010**, *21*, 225606.
- (671) Wang, H.; Yang, C.; Tan, M.; Wang, L.; Kong, D.; Yang, Z. *Soft Matter* **2011**, *7*, 3897.
- (672) Yang, Z.; Ho, P.-L.; Liang, G.; Chow, K. H.; Wang, Q.; Cao, Y.; Guo, Z.; Xu, B. *J. Am. Chem. Soc.* **2007**, *129*, 266.

- (673) Wang, Q.; Yang, Z.; Gao, Y.; Ge, W.; Wang, L.; Xu, B. *Soft Matter* **2008**, *4*, 550.
- (674) Gao, Y.; Kuang, Y.; Guo, Z.-F.; Guo, Z.; Krauss, I. J.; Xu, B. *J. Am. Chem. Soc.* **2009**, *131*, 13576.
- (675) Zhao, F.; Weitzel, C. S.; Gao, Y.; Browdy, H. M.; Shi, J.; Lin, H.-C.; Lovett, S. T.; Xu, B. *Nanoscale* **2011**, *3*, 2859.
- (676) Yang, Z.; Xu, K.; Guo, Z.; Guo, Z.; Xu, B. *Adv. Mater.* **2007**, *19*, 3152.
- (677) Liang, G.; Xu, K.; Li, L.; Wang, L.; Kuang, Y.; Yang, Z.; Xu, B. *Chem. Commun.* **2007**, 4096.
- (678) Yang, Z.; Liang, G.; Ma, M.; Abbah, A. S.; Lu, W. W.; Xu, B. *Chem. Commun.* **2007**, 843.
- (679) Zhao, F.; Gao, Y.; Shi, J.; Browdy, H. M.; Xu, B. *Langmuir* **2011**, *27*, 1510.
- (680) Kuang, Y.; Gao, Y.; Xu, B. *Chem. Commun.* **2011**, *47*, 12625.
- (681) Li, X.; Li, J.; Gao, Y.; Kuang, Y.; Shi, J.; Xu, B. *J. Am. Chem. Soc.* **2010**, *132*, 17707.
- (682) Yang, Z.; Kuang, Y.; Li, X.; Zhou, N.; Zhang, Y.; Xu, B. *Chem. Commun.* **2012**, *48*, 9257.
- (683) Gao, Y.; Long, M. J. C.; Shi, J.; Hedstrom, L.; Xu, B. *Chem. Commun.* **2012**, *48*, 8404.
- (684) Hu, Y.; Wang, H.; Wang, J.; Wang, S.; Liao, W.; Yang, Y.; Zhang, Y.; Kong, D.; Yang, Z. *Org. Biomol. Chem.* **2010**, *8*, 3267.
- (685) Li, D.; Liu, J.; Chu, L.; Liu, J.; Yang, Z. *Chem. Commun.* **2012**, *48*, 6175.
- (686) Li, D.; Wang, H.; Kong, D.; Yang, Z. *Nanoscale* **2012**, *4*, 3047.
- (687) Wang, Z.; Wang, H.; Zheng, W.; Zhang, J.; Zhao, Q.; Wang, S.; Yang, Z.; Kong, D. *Chem. Commun.* **2011**, *47*, 8901.
- (688) Ding, L.; Wang, S.; Wu, W.; Hu, Y.; Yang, C.; Tan, M.; Kong, D.; Yang, Z. *Chin. J. Chem.* **2011**, *29*, 2182.
- (689) Liu, Q.; Ou, C.; Ren, C.; Wang, L.; Yang, Z.; Chen, M. *New J. Chem.* **2012**, *36*, 1556.
- (690) Zhang, X.; Chu, X.; Wang, L.; Wang, H.; Liang, G.; Zhang, J.; Long, J.; Yang, Z. *Angew. Chem., Int. Ed.* **2012**, *51*, 4388.
- (691) Pan, Y.; Gao, Y.; Shi, J.; Wang, L.; Xu, B. *J. Mater. Chem.* **2011**, *21*, 6804.
- (692) Shi, J.; Gao, Y.; Zhang, Y.; Pan, Y.; Xu, B. *Langmuir* **2011**, *27*, 14425.
- (693) Zhang, Y.; Li, N.; Delgado, J.; Gao, Y.; Kuang, Y.; Fraden, S.; Epstein, I. R.; Xu, B. *Langmuir* **2012**, *28*, 3063.
- (694) Matson, J. B.; Stupp, S. I. *Chem. Commun.* **2011**, *47*, 7962.
- (695) Kar, T.; Mandal, S. K.; Das, P. K. *Chem.—Eur. J.* **2011**, *17*, 14952.
- (696) Dutta, S.; Shome, A.; Debnath, S.; Das, P. K. *Soft Matter* **2009**, *5*, 1607.
- (697) Bardhan, M.; Misra, T.; Chowdhury, J.; Ganguly, T. *Chem. Phys. Lett.* **2009**, *481*, 142.
- (698) Burguete, M. I.; Izquierdo, M. A.; Galindo, F.; Luis, S. V. *Chem. Phys. Lett.* **2008**, *460*, 503.
- (699) Li, S.; John, V. T.; Irvin, G. C.; Rachakonda, S. H.; McPherson, G. L.; O'Connor, C. J. *J. Appl. Phys.* **1999**, *85*, 5965.
- (700) Waguespack, Y. Y.; Banerjee, S.; Ramannair, P.; Irvin, G. C.; John, V. T.; McPherson, G. L. *Langmuir* **2000**, *16*, 3036.
- (701) Appel, E. A.; Biedermann, F.; Rauwald, U.; Jones, S. T.; Zayed, J. M.; Scherman, O. A. *J. Am. Chem. Soc.* **2010**, *132*, 14251.
- (702) Zheng, Y.; Hashidzume, A.; Takashima, Y.; Yamaguchi, H.; Harada, A. *Langmuir* **2011**, *27*, 13790.
- (703) Becker, H.-D. *Chem. Rev.* **1993**, *93*, 145.
- (704) Lin, Y.-c.; Weiss, R. G. *Macromolecules* **1987**, *20*, 414.
- (705) Lin, Y.-c.; Kachar, B.; Weiss, R. G. *J. Am. Chem. Soc.* **1989**, *111*, 5542.
- (706) Furman, I.; Weiss, R. G. *Langmuir* **1993**, *9*, 2084.
- (707) Terech, P.; Furman, I.; Weiss, R. G. *J. Phys. Chem.* **1995**, *99*, 9558.
- (708) Terech, P.; Furman, I.; Weiss, R. G.; Bouas-Laurent, H.; Desvergne, J.-P.; Ramassuel, R. *Faraday Discuss.* **1995**, *101*, 345.
- (709) Lu, L.; Cocker, T. M.; Bachman, R. E.; Weiss, R. G. *Langmuir* **2000**, *16*, 20.
- (710) Brotin, T.; Utermohlen, R.; Fages, F.; Bouas-Laurent, H.; Desvergne, J.-P. *J. Chem. Soc., Chem. Commun.* **1991**, 416.
- (711) Terech, P.; Bouas-Laurent, H.; Desvergne, J.-P. *J. Colloid Interface Sci.* **1995**, *174*, 258.
- (712) Olive, A. G. L.; Raffy, G.; Allouchi, H.; Léger, J. M.; Del Guerzo, A.; Desvergne, J.-P. *Langmuir* **2009**, *25*, 8606.
- (713) Pozzo, J.-L.; Clavier, G. M.; Colomes, M.; Bouas-Laurent, H. *Tetrahedron* **1997**, *53*, 6377.
- (714) Desvergne, J.-P.; Brotin, T.; Meerschaut, D.; Clavier, G.; Placin, F.; Pozzo, J.-L.; Bouas-Laurent, H. *New. J. Chem.* **2004**, *28*, 234.
- (715) Placin, F.; Desvergne, J.-P.; Belin, C.; Buffeteau, T.; Desbat, B.; Ducasse, L.; Lassègues, J.-C. *Langmuir* **2003**, *19*, 4563.
- (716) Pozzo, J.-L.; Desvergne, J.-P.; Clavier, G. M.; Bouas-Laurent, H.; Jones, P. G.; Perlstein, J. *J. Chem. Soc., Perkin Trans.* **2001**, 824.
- (717) Clavier, G. M.; Pozzo, J.-L.; Bouas-Laurent, H.; Liere, C.; Roux, C.; Sanchez, C. *J. Mater. Chem.* **2000**, *10*, 1725.
- (718) Llusar, M.; Roux, C.; Pozzo, J.-L.; Sanchez, C. *J. Mater. Chem.* **2003**, *13*, 442.
- (719) Llusar, M.; Monrós, G.; Roux, C.; Pozzo, J.-L.; Sanchez, C. *J. Mater. Chem.* **2003**, *13*, 2505.
- (720) Placin, F.; Desvergne, J.-P.; Cansell, F. *J. Mater. Chem.* **2000**, *10*, 2147.
- (721) Terech, P.; Aymonier, C.; Loppinet-Serani, A.; Bhat, S.; Banerjee, S.; Das, R.; Maitra, U.; Del Guerzo, A.; Desvergne, J.-P. *J. Phys. Chem. B* **2010**, *114*, 11409.
- (722) Placin, F.; Desvergne, J.-P.; Lassègues, J.-C. *Chem. Mater.* **2001**, *13*, 117.
- (723) Lescanne, M.; Colin, A.; Mondain-Monval, O.; Fages, F.; Pozzo, J.-L. *Langmuir* **2003**, *19*, 2013.
- (724) Llusar, M.; Pidol, L.; Roux, C.; Pozzo, J.-L.; Sanchez, C. *Chem. Mater.* **2002**, *14*, 5124.
- (725) Lescanne, M.; Colin, A.; Mondain-Monval, O.; Heuze, K.; Fages, F.; Pozzo, J.-L. *Langmuir* **2002**, *18*, 7151.
- (726) Kato, T.; Kutsuna, T.; Yabuuchi, K.; Mizoshita, N. *Langmuir* **2002**, *18*, 7086.
- (727) Shklyarevskiy, I. O.; Jonkheijm, P.; Christianen, P. C. M.; Schenning, A. P. H. J.; Del Guerzo, A.; Desvergne, J.-P.; Meijer, E. W.; Maan, J. C. *Langmuir* **2005**, *21*, 2108.
- (728) Shklyarevskiy, I. O.; Jonkheijm, P.; Christianen, P. C. M.; Schenning, A. P. H. J.; Meijer, E. W.; Henze, O.; Kilbinger, A. F. M.; Feast, W. J.; Del Guerzo, A.; Desvergne, J.-P.; Maan, J. C. *J. Am. Chem. Soc.* **2005**, *127*, 1112.
- (729) Del Guerzo, A.; Olive, A. G. L.; Reichwagen, J.; Hopf, H.; Desvergne, J.-P. *J. Am. Chem. Soc.* **2005**, *127*, 17984.
- (730) Desvergne, J.-P.; Del Guerzo, A.; Bouas-Laurent, H.; Belin, C.; Reichwagen, J.; Hopf, H. *Pure Appl. Chem.* **2006**, *78*, 707.
- (731) Desvergne, J.-P.; Olive, A. G. L.; Sangeetha, N. M.; Reichwagen, J.; Hopf, H.; Del Guerzo, A. *Pure Appl. Chem.* **2006**, *78*, 2333.
- (732) Olive, A. G. L.; Del Guerzo, A.; Belin, C.; Reichwagen, J.; Hopf, H.; Desvergne, J.-P. *Res. Chem. Intermed.* **2008**, *34*, 137.
- (733) Giansante, C.; Raffy, G.; Schäfer, C.; Rahma, H.; Kao, M.-T.; Olive, A. G. L.; Del Guerzo, A. *J. Am. Chem. Soc.* **2011**, *133*, 316.
- (734) Giansante, C.; Schäfer, C.; Raffy, G.; Del Guerzo, A. *J. Phys. Chem. C* **2012**, *116*, 21706.
- (735) Giansante, C.; Olive, A. G. L.; Schäfer, C.; Raffy, G.; Del Guerzo, A. *Anal. Bioanal. Chem.* **2010**, *396*, 125.
- (736) Sangeetha, N. M.; Bhat, S.; Raffy, G.; Belin, C.; Loppinet-Serani, A.; Aymonier, C.; Terech, P.; Maitra, U.; Desvergne, J.-P.; Del Guerzo, A. *Chem. Mater.* **2009**, *21*, 3424.
- (737) Das, R. K.; Bhat, S.; Banerjee, S.; Aymonier, C.; Loppinet-Serani, A.; Terech, P.; Maitra, U.; Raffy, G.; Desvergne, J.-P.; Del Guerzo, A. *J. Mater. Chem.* **2011**, *21*, 2740.
- (738) Terech, P.; Meerschaut, D.; Desvergne, J.-P.; Colomes, M.; Bouas-Laurent, H. *J. Colloid Interface Sci.* **2003**, *261*, 441.
- (739) Kao, M.-T.; Schäfer, C.; Raffy, G.; Del Guerzo, A. *Photochem. Photobiol. Sci.* **2012**, *11*, 1730.
- (740) Nakashima, T.; Kimizuka, N. *Adv. Mater.* **2002**, *14*, 1113.

- (741) Ayabe, M.; Kishida, T.; Fujita, N.; Sada, K.; Shinkai, S. *Org. Biomol. Chem.* **2003**, *1*, 2744.
- (742) Dawn, A.; Fujita, N.; Haraguchi, S.; Sada, K.; Shinkai, S. *Chem. Commun.* **2009**, 2100.
- (743) Dawn, A.; Fujita, N.; Haraguchi, S.; Sada, K.; Tamari, S.-i.; Shinkai, S. *Org. Biomol. Chem.* **2009**, *7*, 4378.
- (744) Dawn, A.; Shiraki, T.; Haraguchi, S.; Sato, H.; Sada, K.; Shinkai, S. *Chem.—Eur. J.* **2010**, *16*, 3676.
- (745) Dawn, A.; Shiraki, T.; Ichikawa, H.; Takada, A.; Takahashi, Y.; Tsuchiya, Y.; Lien, L. T. N.; Shinkai, S. *J. Am. Chem. Soc.* **2012**, *134*, 2161.
- (746) Wang, C.; Zhang, D.; Xiang, J.; Zhu, D. *Langmuir* **2007**, *23*, 9195.
- (747) Sako, Y.; Takaguchi, Y. *Org. Biomol. Chem.* **2008**, *6*, 3843.
- (748) Zheng, Y.; Micic, M.; Mello, S. V.; Mabrouki, M.; Andreopoulos, F. M.; Konka, V.; Pham, S. M.; Leblanc, R. M. *Macromolecules* **2002**, *35*, 5228.
- (749) Wells, L. A.; Sheardown, H. *Eur. J. Pharm. Biopharm.* **2011**, *79*, 304.
- (750) Hong, J.-P.; Um, M.-C.; Nam, S.-R.; Hong, J.-I.; Lee, S. *Chem. Commun.* **2009**, 310.
- (751) Toyota, S.; Okamoto, Y.; Ishikawa, T.; Iwanaga, T.; Yamada, M. *Bull. Chem. Soc. Jpn.* **2009**, *82*, 182.
- (752) Rizkov, D.; Gun, J.; Lev, O.; Sicsic, R.; Melman, A. *Langmuir* **2005**, *21*, 12130.
- (753) Bag, B. G.; Maity, G. C.; Dinda, S. K. *Org. Lett.* **2006**, *8*, 5457.
- (754) Das, R. K.; Banerjee, S.; Raffy, G.; Del Guerzo, A.; Desvergne, J.-P.; Maitra, U. *J. Mater. Chem.* **2010**, *20*, 7227.
- (755) Kandanelli, R.; Maitra, U. *Photochem. Photobiol. Sci.* **2012**, *11*, 1724.
- (756) Isoda, K.; Yasuda, T.; Kato, T. *J. Mater. Chem.* **2008**, *18*, 4522.
- (757) Rajamalli, P.; Prasad, E. *New J. Chem.* **2011**, *35*, 1541.
- (758) Rajamalli, P.; Prasad, E. *Org. Lett.* **2011**, *13*, 3714.
- (759) Galindo, F.; Burguete, M. I.; Gavara, R.; Luis, S. V. *J. Photochem. Photobiol., A* **2006**, *178*, 57.
- (760) Liu, Y.; Yu, Y.; Gao, J.; Wang, Z.; Zhang, X. *Angew. Chem., Int. Ed.* **2010**, *49*, 6576.
- (761) Mukkamala, R.; Weiss, R. G. *J. Chem. Soc., Chem. Commun.* **1995**, 375.
- (762) Mukkamala, R.; Weiss, R. G. *Langmuir* **1996**, *12*, 1474.
- (763) Ostuni, E.; Kamaras, P.; Weiss, R. G. *Angew. Chem., Int. Ed. Engl.* **1996**, *35*, 1324.
- (764) Terech, P.; Ostuni, E.; Weiss, R. G. *J. Phys. Chem.* **1996**, *100*, 3759.
- (765) Clavier, G. M.; Brugger, J.-F.; Bouas-Laurent, H.; Pozzo, J.-L. *J. Chem. Soc., Perkin Trans. 2* **1998**, 2527.
- (766) Liu, J.-W.; Yang, Y.; Chen, C.-F.; Ma, J.-T. *Langmuir* **2010**, *26*, 9040.
- (767) Liu, J.-W.; Ma, J.-T.; Chen, C.-F. *Tetrahedron* **2011**, *67*, 85.
- (768) Kelley, T. W.; Baude, P. F.; Gerlach, C.; Ender, D. E.; Muyres, D.; Haase, M. A.; Vogel, D. E.; Theiss, S. D. *Chem. Mater.* **2004**, *16*, 4413.
- (769) Reichwagen, J.; Hopf, H.; Desvergne, J.-P.; Del Guerzo, A.; Bouas-Laurent, H. *Synthesis* **2005**, 3505.
- (770) Reichwagen, J.; Hopf, H.; Del Guerzo, A.; Belin, C.; Bouas-Laurent, H.; Desvergne, J.-P. *Org. Lett.* **2005**, *7*, 971.
- (771) Del Guerzo, A.; Bouas-Laurent, H.; Desvergne, J.-P.; Belin, C.; Reichwagen, J.; Hopf, H. *Mol. Cryst. Liq. Cryst.* **2005**, *431*, 155/[455].
- (772) Ulijn, R. V.; Smith, A. M. *Chem. Soc. Rev.* **2008**, *37*, 664.
- (773) Zhang, S. *Nat. Biotechnol.* **2003**, *21*, 1171.
- (774) Gazit, E. *Chem. Soc. Rev.* **2007**, *36*, 1263.
- (775) Carpino, L. A.; Han, G. Y. *J. Org. Chem.* **1972**, *37*, 3404.
- (776) Vegners, R.; Shestakova, I.; Kalvinsh, I.; Ezzell, R. M.; Janmey, P. A. *J. Pept. Sci.* **1995**, *1*, 371.
- (777) Zhang, Y.; Gu, H.; Yang, Z.; Xu, B. *J. Am. Chem. Soc.* **2003**, *125*, 13680.
- (778) Yang, Z.; Gu, H.; Zhang, Y.; Wang, L.; Xu, B. *Chem. Commun.* **2004**, 208.
- (779) Yang, Z.; Xu, K.; Wang, L.; Gu, H.; Wei, H.; Zhang, M.; Xu, B. *Chem. Commun.* **2005**, 4414.
- (780) Yang, Z.; Xu, B. *Chem. Commun.* **2004**, 2424.
- (781) Yang, Z.; Gu, H.; Fu, D.; Gao, P.; Lam, J. K.; Xu, B. *Adv. Mater.* **2004**, *16*, 1440.
- (782) Gao, J.; Wang, H.; Wang, L.; Wang, J.; Kong, D.; Yang, Z. *J. Am. Chem. Soc.* **2009**, *131*, 11286.
- (783) Wang, Q.; Yang, Z.; Zhang, X.; Xiao, X.; Chang, C. K.; Xu, B. *Angew. Chem., Int. Ed.* **2007**, *46*, 4285.
- (784) Wang, Q.; Yang, Z.; Ma, M.; Chang, C. K.; Xu, B. *Chem.—Eur. J.* **2008**, *14*, 5073.
- (785) Schnepf, Z. A. C.; Gonzalez-McQuire, R.; Mann, S. *Adv. Mater.* **2006**, *18*, 1869.
- (786) Wang, Q.; Li, L.; Xu, B. *Chem.—Eur. J.* **2009**, *15*, 3168.
- (787) Roy, S.; Banerjee, A. *Soft Matter* **2011**, *7*, 5300.
- (788) Roy, S.; Banerjee, A. *RSC Adv.* **2012**, *2*, 2105.
- (789) Kuang, Y.; Gao, Y.; Shi, J.; Lin, H.-C.; Xu, B. *Chem. Commun.* **2011**, *47*, 8772.
- (790) Jayawarna, V.; Ali, M.; Jowitt, T. A.; Miller, A. F.; Saiani, A.; Gough, J. E.; Ulijn, R. V. *Adv. Mater.* **2006**, *18*, 611.
- (791) Jayawarna, V.; Smith, A.; Gough, J. E.; Ulijn, R. V. *Biochem. Soc. Trans.* **2007**, *35*, 535.
- (792) Smith, A. M.; Williams, R. J.; Tang, C.; Coppo, P.; Collins, R. F.; Turner, M. L.; Saiani, A.; Ulijn, R. V. *Adv. Mater.* **2008**, *20*, 37.
- (793) Tang, C.; Smith, A. M.; Collins, R. F.; Ulijn, R. V.; Saiani, A. *Langmuir* **2009**, *25*, 9447.
- (794) Toledo, S.; Williams, R. J.; Jayawarna, V.; Ulijn, R. V. *J. Am. Chem. Soc.* **2006**, *128*, 1070.
- (795) Hughes, M.; Frederix, P. W. J. M.; Raeburn, J.; Birchall, L. S.; Sadownik, J.; Coomer, F. C.; Lin, I.-H.; Cussen, E. J.; Hunt, N. T.; Tuttle, T.; Webb, S. J.; Adams, D. J.; Ulijn, R. V. *Soft Matter* **2012**, *8*, 5595.
- (796) Bairi, P.; Roy, B.; Routh, P.; Sen, K.; Nandi, A. K. *Soft Matter* **2012**, *8*, 7436.
- (797) Patil, A. J.; Kumar, R. K.; Barron, N. J.; Mann, S. *Chem. Commun.* **2012**, *48*, 7934.
- (798) Wang, Q.; Yang, Z.; Wang, L.; Ma, M.; Xu, B. *Chem. Commun.* **2007**, 1032.
- (799) Yang, Z.; Wang, L.; Wang, J.; Gao, P.; Xu, B. *J. Mater. Chem.* **2010**, *20*, 2128.
- (800) Sadownik, J. W.; Ulijn, R. V. *Chem. Commun.* **2010**, *46*, 3481.
- (801) Hirst, A. R.; Roy, S.; Arora, M.; Das, A. K.; Hodson, N.; Murray, P.; Marshall, S.; Javid, N.; Sefcik, J.; Boekhoven, J.; van Esch, J. H.; Santabarbara, S.; Hunt, N. T.; Ulijn, R. V. *Nat. Chem.* **2010**, *2*, 1089.
- (802) Jayawarna, V.; Richardson, S. M.; Hirst, A. R.; Hodson, N. W.; Saiani, A.; Gough, J. E.; Ulijn, R. V. *Acta Biomater.* **2009**, *5*, 934.
- (803) Ryu, J.; Kim, S.-W.; Kang, K.; Park, C. B. *Adv. Mater.* **2010**, *22*, 5537.
- (804) Xu, H.; Das, A. K.; Horie, M.; Shaik, M. S.; Smith, A. M.; Luo, Y.; Lu, X.; Collins, R.; Liem, S. Y.; Song, A.; Popelier, P. L. A.; Turner, M. L.; Xiao, P.; Kinloch, I. A.; Ulijn, R. V. *Nanoscale* **2010**, *2*, 960.
- (805) Williams, R. J.; Smith, A. M.; Collins, R.; Hodson, N.; Das, A. K.; Ulijn, R. V. *Nat. Nanotech.* **2009**, *4*, 19.
- (806) Hughes, M.; Xu, H.; Frederix, P. W. J. M.; Smith, A. M.; Hunt, N. T.; Tuttle, T.; Kinloch, I. A.; Ulijn, R. V. *Soft Matter* **2011**, *7*, 10032.
- (807) Helen, W.; de Leonardis, P.; Ulijn, R. V.; Gough, J.; Tirelli, N. *Soft Matter* **2011**, *7*, 1732.
- (808) Tang, C.; Ulijn, R. V.; Saiani, A. *Langmuir* **2011**, *27*, 14438.
- (809) Liu, Y.; Kim, E.; Ulijn, R. V.; Bentley, W. E.; Payne, G. F. *Adv. Funct. Mater.* **2011**, *21*, 1575.
- (810) Roy, S.; Javid, N.; Frederix, P. W. J. M.; Lamprou, D. A.; Urquhart, A. J.; Hunt, N. T.; Halling, P. J.; Ulijn, R. V. *Chem.—Eur. J.* **2012**, *18*, 11723.
- (811) Mahler, A.; Reches, M.; Rechter, M.; Cohen, S.; Gazit, E. *Adv. Mater.* **2006**, *18*, 1365.
- (812) Orbach, R.; Adler-Abramovich, L.; Zigeron, S.; Mironi-Harpaz, I.; Seliktar, D.; Gazit, E. *Biomacromolecules* **2009**, *10*, 2646.

- (813) Orbach, R.; Mironi-Harpaz, I.; Adler-Abramovich, L.; Mossou, E.; Mitchell, E. P.; Forsyth, V. T.; Gazit, E.; Seliktar, D. *Langmuir* **2012**, *28*, 2015.
- (814) Amdursky, N.; Molotskii, M.; Aronov, D.; Adler-Abramovich, L.; Gazit, E.; Rosenman, G. *Nano Lett.* **2009**, *9*, 3111.
- (815) Amdursky, N.; Molotskii, M.; Gazit, E.; Rosenman, G. *Appl. Phys. Lett.* **2009**, *94*, 261907.
- (816) Amdursky, N.; Gazit, E.; Rosenman, G. *Adv. Mater.* **2010**, *22*, 2311.
- (817) Handelman, A.; Beker, P.; Amdursky, N.; Rosenman, G. *Phys. Chem. Chem. Phys.* **2012**, *14*, 6391.
- (818) Adhikari, B.; Banerjee, A. *Chem.—Eur. J.* **2010**, *16*, 13698.
- (819) Wang, Y.; Cao, L.; Guan, S.; Shi, G.; Luo, Q.; Miao, L.; Thistletonwaite, I.; Huang, Z.; Xu, J.; Liu, J. *J. Mater. Chem.* **2012**, *22*, 2575.
- (820) Adhikari, B.; Nanda, J.; Banerjee, A. *Soft Matter* **2011**, *7*, 8913.
- (821) Adhikari, B.; Banerjee, A. *Soft Matter* **2011**, *7*, 9259.
- (822) Nanda, J.; Banerjee, A. *Soft Matter* **2012**, *8*, 3380.
- (823) Bardelang, D.; Camerel, F.; Margeson, J. C.; Leek, D. M.; Schmutz, M.; Zaman, M. B.; Yu, K.; Soldatov, D. V.; Ziessl, R.; Ratcliffe, C. I.; Ripmeester, J. A. *J. Am. Chem. Soc.* **2008**, *130*, 3313.
- (824) Bardelang, D.; Zaman, M. B.; Moudrakovski, I. L.; Pawsey, S.; Margeson, J. C.; Wang, D.; Wu, X.; Ripmeester, J. A.; Ratcliffe, C. I.; Yu, K. *Adv. Mater.* **2008**, *20*, 4517.
- (825) Channon, K. J.; Devlin, G. L.; Magennis, S. W.; Finlayson, C. E.; Tickler, A. K.; Silva, C.; MacPhee, C. E. *J. Am. Chem. Soc.* **2008**, *130*, 5487.
- (826) Haldar, D. *Tetrahedron* **2008**, *64*, 186.
- (827) Banwell, E. F.; Abelardo, E. S.; Adams, D. J.; Birchall, M. A.; Corrigan, A.; Donald, A. M.; Kirkland, M.; Serpell, L. C.; Butler, M. F.; Woolfson, D. N. *Nat. Mater.* **2009**, *8*, 596.
- (828) Liebmann, T.; Rydholm, S.; Akpe, V.; Brismar, H. *BMC Biotechnol.* **2007**, *7*, 88.
- (829) Chronopoulou, L.; Lorenzoni, S.; Masci, G.; Dentini, M.; Togna, A. R.; Togna, G.; Bordi, F.; Palocci, C. *Soft Matter* **2010**, *6*, 2525.
- (830) Sutton, S.; Campbell, N. L.; Cooper, A. I.; Kirkland, M.; Frith, W. J.; Adams, D. J. *Langmuir* **2009**, *25*, 10285.
- (831) Adams, D. J.; Butler, M. F.; Frith, W. J.; Kirkland, M.; Mullen, L.; Sanderson, P. *Soft Matter* **2009**, *5*, 1856.
- (832) Adams, D. J.; Mullen, L. M.; Berta, M.; Chen, L.; Frith, W. J. *Soft Matter* **2010**, *6*, 1971.
- (833) Johnson, E. K.; Adams, D. J.; Cameron, P. J. *J. Am. Chem. Soc.* **2010**, *132*, 5130.
- (834) Chen, L.; Raeburn, J.; Sutton, S.; Spiller, D. G.; Williams, J.; Sharp, J. S.; Griffiths, P. C.; Heenan, R. K.; King, S. M.; Paul, A.; Furzeland, S.; Atkins, D.; Adams, D. J. *Soft Matter* **2011**, *7*, 9721.
- (835) Raeburn, J.; Pont, G.; Chen, L.; Cesbron, Y.; Lévy, R.; Adams, D. J. *Soft Matter* **2012**, *8*, 1168.
- (836) Ryan, D. M.; Anderson, S. B.; Senguen, F. T.; Youngman, R. E.; Nilsson, B. L. *Soft Matter* **2010**, *6*, 475.
- (837) Ryan, D. M.; Doran, T. M.; Nilsson, B. L. *Chem. Commun.* **2011**, *47*, 475.
- (838) Ryan, D. M.; Anderson, S. B.; Nilsson, B. L. *Soft Matter* **2010**, *6*, 3220.
- (839) Ryan, D. M.; Doran, T. M.; Anderson, S. B.; Nilsson, B. L. *Langmuir* **2011**, *27*, 4029.
- (840) Ryan, D. M.; Doran, T. M.; Nilsson, B. L. *Langmuir* **2011**, *27*, 11145.
- (841) Cheng, G.; Castelletto, V.; Moulton, C. M.; Newby, G. E.; Hamley, I. W. *Langmuir* **2010**, *26*, 4990.
- (842) Xu, X.-D.; Liang, L.; Chen, C.-S.; Lu, B.; Wang, N.-L.; Jiang, F.-G.; Zhang, X.-Z.; Zhuo, R.-X. *ACS Appl. Mater. Interfaces* **2010**, *2*, 2663.
- (843) Cheng, G.; Castelletto, V.; Jones, R. R.; Connolly, C. J.; Hamley, I. W. *Soft Matter* **2011**, *7*, 1326.
- (844) Castelletto, V.; Moulton, C. M.; Cheng, G.; Hamley, I. W.; Hicks, M. R.; Rodger, A.; López-Pérez, D. E.; Revilla-López, G.; Alemán, C. *Soft Matter* **2011**, *7*, 11405.
- (845) Castelletto, V.; Hamley, I. W.; Stain, C.; Connolly, C. *Langmuir* **2012**, *28*, 12575.
- (846) Wang, J.; Wang, Z.; Gao, J.; Wang, L.; Yang, Z.; Kong, D.; Yang, Z. *J. Mater. Chem.* **2009**, *19*, 7892.
- (847) Xu, X.-D.; Chen, C. S.; Lu, B.; Cheng, S.-X.; Zhang, X.-Z.; Zhuo, R.-X. *J. Phys. Chem. B* **2010**, *114*, 2365.
- (848) Debnath, S.; Shome, A.; Das, D.; Das, P. K. *J. Phys. Chem. B* **2010**, *114*, 4407.
- (849) Das, D.; Maiti, S.; Brahmachari, S.; Das, P. K. *Soft Matter* **2011**, *7*, 7291.
- (850) Haines-Butterick, L.; Rajagopal, K.; Branco, M.; Salick, D.; Rughani, R.; Pilarz, M.; Lamm, M. S.; Pochan, D. J.; Schneider, J. P. *Proc. Natl. Acad. Sci. U.S.A.* **2007**, *104*, 7791.
- (851) Park, S.-Y.; Jeong, H.; Kim, H.; Lee, J. Y.; Jang, D.-J. *J. Phys. Chem. C* **2011**, *115*, 24763.
- (852) Birchall, L. S.; Roy, S.; Jayawarna, V.; Hughes, M.; Irvine, E.; Okorogheye, G. T.; Saudi, N.; Santis, E. D.; Tuttle, T.; Edwards, A. A.; Ulijn, R. V. *Chem. Sci.* **2011**, *2*, 1349.
- (853) Manchineella, S.; Govindaraju, T. *RSC Adv.* **2012**, *2*, 5539.
- (854) Wang, Y.; Zhan, C.; Fu, H.; Li, X.; Sheng, X.; Zhao, Y.; Xiao, D.; Ma, Y.; Ma, J. S.; Yao, J. *Langmuir* **2008**, *24*, 7635.
- (855) Ramírez-López, P.; de la Torre, M. C.; Asenjo, M.; Ramírez-Castellanos, J.; González-Calbet, J. M.; Rodríguez-Gimeno, A.; de Arellano, C. R.; Sierra, M. A. *Chem. Commun.* **2011**, *47*, 10281.
- (856) Abbel, R.; van der Weegen, R.; Pisula, W.; Surin, M.; Leclère, P.; Lazzaroni, R.; Meijer, E. W.; Schenning, A. P. H. *J. Chem.—Eur. J.* **2009**, *15*, 9737.
- (857) Chen, J.-H.; Chang, C.-S.; Chang, Y.-X.; Chen, C.-Y.; Chen, H.-L.; Chen, S.-A. *Macromolecules* **2009**, *42*, 1306.
- (858) Justino, L. L. G.; Ramos, M. L.; Knaapila, M.; Marques, A. T.; Kudla, C. J.; Scherf, U.; Almásy, L.; Schweins, R.; Burrows, H. D.; Monkman, A. P. *Macromolecules* **2011**, *44*, 334.
- (859) Knaapila, M.; Almásy, L.; Garamus, V. M.; Ramos, M. L.; Justino, L. L. G.; Galbrecht, F.; Preis, E.; Scherf, U.; Burrows, H. D.; Monkman, A. P. *Polymer* **2008**, *49*, 2033.
- (860) Grell, M.; Bradley, D. D. C.; Long, X.; Chamberlain, T.; Inbasekaran, M.; Woo, E. P.; Soliman, M. *Acta Polym.* **1998**, *49*, 439.
- (861) Chen, C.-Y.; Chang, C.-S.; Huang, S.-W.; Chen, J.-H.; Chen, H.-L.; Su, C.-I.; Chen, S.-A. *Macromolecules* **2010**, *43*, 4346.
- (862) Lin, Z.-Q.; Shi, N.-E.; Li, Y.-B.; Qiu, D.; Zhang, L.; Lin, J.-Y.; Zhao, J.-F.; Wang, C.; Xie, L.-H.; Huang, W. *J. Phys. Chem. C* **2011**, *115*, 4418.
- (863) Falk, H. *The Chemistry of Linear Oligopyrroles and Bile Pigments*; Springer-Verlag: Vienna, 1989.
- (864) Maeda, H. *Eur. J. Org. Chem.* **2007**, 5313.
- (865) Maeda, H.; Haketa, Y.; Nakanishi, T. *J. Am. Chem. Soc.* **2007**, *129*, 13661.
- (866) Maeda, H.; Terashima, Y.; Haketa, Y.; Asano, A.; Honsho, Y.; Seki, S.; Shimizu, M.; Mukai, H.; Ohta, K. *Chem. Commun.* **2010**, *46*, 4559.
- (867) Haketa, Y.; Sasaki, S.; Ohta, N.; Masunaga, H.; Ogawa, H.; Mizuno, N.; Araoka, F.; Takezoe, H.; Maeda, H. *Angew. Chem., Int. Ed.* **2010**, *49*, 10079.
- (868) Haketa, Y.; Sakamoto, S.; Chigusa, K.; Nakanishi, T.; Maeda, H. *J. Org. Chem.* **2011**, *76*, 5177.
- (869) Maeda, H.; Terashima, Y. *Chem. Commun.* **2011**, *47*, 7620.
- (870) Lozano, V.; Hernández, R.; Ardá, A.; Jiménez-Barbero, J.; Mijangos, C.; Pérez-Pérez, M.-J. *J. Mater. Chem.* **2011**, *21*, 8862.
- (871) Debnath, S.; Shome, A.; Dutta, S.; Das, P. K. *Chem. —Eur. J.* **2008**, *14*, 6870.
- (872) Coates, I. A.; Hirst, A. R.; Smith, D. K. *J. Org. Chem.* **2007**, *72*, 3937.
- (873) Roy, S.; Dasgupta, A.; Das, P. K. *Langmuir* **2007**, *23*, 11769.
- (874) Roy, S.; Das, P. K. *Biotechnol. Bioeng.* **2008**, *100*, 756.
- (875) Dutta, S.; Shome, A.; Kar, T.; Das, P. K. *Langmuir* **2011**, *27*, 5000.
- (876) Das, D.; Dasgupta, A.; Roy, S.; Mitra, R. N.; Debnath, S.; Das, P. K. *Chem. —Eur. J.* **2006**, *12*, 5068.

- (877) Shome, A.; Dutta, S.; Maiti, S.; Das, P. K. *Soft Matter* **2011**, *7*, 3011.
- (878) Mitra, R. N.; Das, D.; Roy, S.; Das, P. K. *J. Phys. Chem. B* **2007**, *111*, 14107.
- (879) Mitra, R. N.; Das, P. K. *J. Phys. Chem. C* **2008**, *112*, 8159.
- (880) Kar, T.; Dutta, S.; Das, P. K. *Soft Matter* **2010**, *6*, 4777.
- (881) Kar, T.; Debnath, S.; Das, D.; Shome, A.; Das, P. K. *Langmuir* **2009**, *25*, 8639.
- (882) Dutta, S.; Das, D.; Dasgupta, A.; Das, P. K. *Chem.—Eur. J.* **2010**, *16*, 1493.
- (883) Mandal, S. K.; Kar, T.; Das, D.; Das, P. K. *Chem. Commun.* **2012**, *48*, 1814.
- (884) Bastiat, G.; Leroux, J.-C. *J. Mater. Chem.* **2009**, *19*, 3867.
- (885) Liu, J. *Soft Matter* **2011**, *7*, 6757.
- (886) Lena, S.; Masiero, S.; Pieraccini, S.; Spada, G. P. *Chem.—Eur. J.* **2009**, *15*, 7792.
- (887) Allain, V.; Bourgaux, C.; Couvreur, P. *Nucleic Acids Res.* **2012**, *40*, 1891.
- (888) Li, X.; Kuang, Y.; Lin, H.-C.; Gao, Y.; Shi, J.; Xu, B. *Angew. Chem., Int. Ed.* **2011**, *50*, 9365.
- (889) Li, X.; Kuang, Y.; Shi, J.; Gao, Y.; Lin, H.-C.; Xu, B. *J. Am. Chem. Soc.* **2011**, *133*, 17513.
- (890) Du, X.; Li, J.; Gao, Y.; Kuang, Y.; Xu, B. *Chem. Commun.* **2012**, *48*, 2098.
- (891) Wang, Y.; Desbat, B.; Manet, S.; Aimé, C.; Labrot, T.; Oda, R. *J. Colloid Interface Sci.* **2005**, *283*, 555.
- (892) Gottarelli, G.; Masiero, S.; Mezzina, E.; Spada, G. P.; Mariani, P.; Recanatini, M. *Helv. Chim. Acta* **1998**, *81*, 2078.
- (893) Gottarelli, G.; Masiero, S.; Mezzina, E.; Pieraccini, S.; Spada, G. *P. Liq. Cryst.* **1999**, *26*, 965.
- (894) Giorgi, T.; Grepioni, F.; Manet, I.; Mariani, P.; Masiero, S.; Mezzina, E.; Pieraccini, S.; Saturni, L.; Spada, G. P.; Gottarelli, G. *Chem.—Eur. J.* **2002**, *8*, 2143.
- (895) Lu, J.; Hu, J.; Liu, C.; Gao, H.; Ju, Y. *Soft Matter* **2012**, *8*, 9576.
- (896) Park, S. M.; Kim, B. H. *Soft Matter* **2008**, *4*, 1995.
- (897) Li, X.; Du, X.; Gao, Y.; Shi, J.; Kuang, Y.; Xu, B. *Soft Matter* **2012**, *8*, 7402.
- (898) Yoshikawa, I.; Yanagi, S.; Yamaji, Y.; Araki, K. *Tetrahedron* **2007**, *63*, 7474.
- (899) Bogliotti, N.; Ritter, A.; Hebbe, S.; Vasella, A. *Helv. Chim. Acta* **2008**, *91*, 2181.
- (900) Bogliotti, N.; Vasella, A. *Helv. Chim. Acta* **2010**, *93*, 888.
- (901) Yu, Y.; Nakamura, D.; DeBoyace, K.; Neisius, A. W.; McGown, L. B. *J. Phys. Chem. B* **2008**, *112*, 1130.
- (902) Sukul, P. K.; Malik, S. *Soft Matter* **2011**, *7*, 4234.
- (903) Park, T.; Zimmerman, S. C. *J. Am. Chem. Soc.* **2006**, *128*, 11582.
- (904) Araki, K.; Yoshikawa, I. *Top. Curr. Chem.* **2005**, *256*, 133.
- (905) Lu, J.; Hu, J.; Song, Y.; Ju, Y. *Org. Lett.* **2011**, *13*, 3372.
- (906) Godeau, G.; Barthélémy, P. *Langmuir* **2009**, *25*, 8447.
- (907) Godeau, G.; Brun, C.; Arnion, H.; Staedel, C.; Barthélémy, P. *Tetrahedron Lett.* **2010**, *51*, 1012.
- (908) Godeau, G.; Bernard, J.; Staedel, C.; Barthélémy, P. *Chem. Commun.* **2009**, *5127*.
- (909) Iwaura, R.; Yoshida, K.; Masuda, M.; Yase, K.; Shimizu, T. *Chem. Mater.* **2002**, *14*, 3047.
- (910) Moreau, L.; Barthélémy, P.; Maataoui, M. E.; Grinstaff, M. W. *J. Am. Chem. Soc.* **2004**, *126*, 7533.
- (911) Roy, B.; Bairi, P.; Nandi, A. K. *Soft Matter* **2012**, *8*, 2366.
- (912) Chhikara, B. S.; Tiwari, R.; Parang, K. *Tetrahedron Lett.* **2012**, *53*, 5335.
- (913) Sohma, J.-E. S.; Fages, F. *Chem. Commun.* **1997**, 327.
- (914) van Gorp, J. J.; Vekemans, J. A. J. M.; Meijer, E. W. *J. Am. Chem. Soc.* **2002**, *124*, 14759.
- (915) Martín-Rapún, R.; Byelov, D.; Palmans, A. R. A.; de Jeu, W. H.; Meijer, E. W. *Langmuir* **2009**, *25*, 8794.
- (916) Xue, P.; Lu, R.; Li, D.; Jin, M.; Bao, C.; Zhao, Y.; Wang, Z. *Chem. Mater.* **2004**, *16*, 3702.
- (917) Strutt, N. L.; Zhang, H.; Giesener, M. A.; Leia, J.; Stoddart, J. F. *Chem. Commun.* **2012**, *48*, 1647.
- (918) Zhu, X.; Duan, P.; Zhang, L.; Liu, M. *Chem.—Eur. J.* **2011**, *17*, 3429.
- (919) Lee, H.; Jung, S. H.; Park, S.; Jung, J. H. *New J. Chem.* **2012**, *36*, 1957.
- (920) Hanabusa, K.; Hirata, T.; Inoue, D.; Kimura, M.; Shirai, H. *Colloids Surf., A* **2000**, *169*, 307.
- (921) Camerel, F.; Ziessel, R.; Donnio, B.; Guillon, D. *New J. Chem.* **2006**, *30*, 135.
- (922) Camerel, F.; Donnio, B.; Bourgogne, C.; Schmutz, M.; Guillon, D.; Davidson, P.; Ziessel, R. *Chem.—Eur. J.* **2006**, *12*, 4261.
- (923) Cho, E. J.; Jeong, I. Y.; Lee, S. J.; Han, W. S.; Kang, J. K.; Jung, J. H. *Tetrahedron Lett.* **2008**, *49*, 1076.
- (924) Chan, Y.-T.; Moorefield, C. N.; Newkome, G. R. *Chem. Commun.* **2009**, 6928.
- (925) Accorsi, G.; Listorti, A.; Yoosaf, K.; Armaroli, N. *Chem. Soc. Rev.* **2009**, *38*, 1690.
- (926) Jung, J. H.; Nakashima, K.; Shinkai, S. *Nano Lett.* **2001**, *1*, 145.
- (927) Sugiyasu, K.; Fujita, N.; Takeuchi, M.; Yamada, S.; Shinkai, S. *Org. Biomol. Chem.* **2003**, *1*, 895.
- (928) Sugiyasu, K.; Fujita, N.; Shinkai, S. *J. Mater. Chem.* **2005**, *15*, 2747.
- (929) Ziessel, R.; Pickaert, G.; Camerel, F.; Donnio, B.; Guillon, D.; Cesario, M.; Prangé, T. *J. Am. Chem. Soc.* **2004**, *126*, 12403.
- (930) Dukh, M.; Saman, D.; Kröll, J.; Černý, I.; Pouzar, V.; Král, V.; Drasar, P. *Tetrahedron* **2003**, *59*, 4069.
- (931) Kim, T. H.; Seo, J.; Lee, S. J.; Lee, S. S.; Kim, J.; Jung, J. H. *Chem. Mater.* **2007**, *19*, 5815.
- (932) Ikeda, M.; Nobori, T.; Schmutz, M.; Lehn, J.-M. *Chem.—Eur. J.* **2005**, *11*, 662.
- (933) Azeroual, S.; Surprenant, J.; Lazzara, T. D.; Kocun, M.; Tao, Y.; Cuccia, L. A.; Lehn, J.-M. *Chem. Commun.* **2012**, *48*, 2292.
- (934) Ihara, H.; Sakurai, T.; Yamada, T.; Hashimoto, T.; Takafuji, M.; Sagawa, T.; Hachisako, H. *Langmuir* **2002**, *18*, 7120.
- (935) Jiang, H.; Léger, J.-M.; Guionneau, P.; Huc, I. *Org. Lett.* **2004**, *6*, 2985.
- (936) van Bommel, K. J. C.; Stuart, M. C. A.; Feringa, B. L.; van Esch, J. *Org. Biomol. Chem.* **2005**, *3*, 2917.
- (937) Karmakar, A.; Sarma, R. J.; Baruah, J. B. *Cryst. Eng. Commun.* **2007**, *9*, 379.
- (938) Hu, H.-Y.; Yang, Y.; Y. Xiang, J.-F.; Chen, C.-F. *Chin. J. Chem.* **2007**, *25*, 1389.
- (939) Pozzo, J.-L.; Clavier, G. M.; Desvergne, J.-P. *J. Mater. Chem.* **1998**, *8*, 2575.
- (940) Pozzo, J.-L.; Clavier, G.; Rustemeyer, F.; Bouas-Laurent, H. *Mol. Cryst. Liq. Cryst.* **2000**, *344*, 101.
- (941) Lee, D.-C.; Cao, B.; Jang, K.; Forster, P. M. *J. Mater. Chem.* **2010**, *20*, 867.
- (942) Lee, D.-C.; McGrath, K. K.; Jang, K. *Chem. Commun.* **2008**, 3636.
- (943) Jang, K.; Kinyanjui, J. M.; Hatchett, D. W.; Lee, D.-C. *Chem. Mater.* **2009**, *21*, 2070.
- (944) Jang, K.; Ranasinghe, A. D.; Heske, C.; Lee, D.-C. *Langmuir* **2010**, *26*, 13630.
- (945) Jang, K.; Brownell, L. V.; Forster, P. M.; Lee, D.-C. *Langmuir* **2011**, *27*, 14615.
- (946) Manna, S.; Saha, A.; Nandi, A. K. *Chem. Commun.* **2006**, 4285.
- (947) Saha, A.; Manna, S.; Nandi, A. K. *Langmuir* **2007**, *23*, 13126.
- (948) Saha, A.; Manna, S.; Nandi, A. K. *Chem. Commun.* **2008**, 3732.
- (949) Saha, A.; Roy, B.; Esterrani, A.; Nandi, A. K. *Org. Biomol. Chem.* **2011**, *9*, 770.
- (950) Saha, A.; Manna, S.; Nandi, A. K. *Soft Matter* **2009**, *5*, 3992.
- (951) Roy, B.; Saha, A.; Esterrani, A.; Nandi, A. K. *Soft Matter* **2010**, *6*, 3337.
- (952) Chatterjee, S.; Nandi, A. K. *Chem. Commun.* **2011**, *47*, 11510.
- (953) Bairi, P.; Roy, B.; Nandi, A. K. *Chem. Commun.* **2012**, *48*, 10850.

- (954) Patil, S. P.; Jeong, H. S.; Kim, B. H. *Chem. Commun.* **2012**, 48, 8901.
- (955) Li, J.; Grimsdale, A. C. *Chem. Soc. Rev.* **2010**, 39, 2399.
- (956) Balakrishnan, K.; Datar, A.; Zhang, W.; Yang, X.; Naddo, T.; Huang, J.; Zuo, J.; Yen, M.; Moore, J. S.; Zang, L. *J. Am. Chem. Soc.* **2006**, 128, 6576.
- (957) Yabuuchi, K.; Tochigi, Y.; Mizoshita, N.; Hanabusa, K.; Kato, T. *Tetrahedron* **2007**, 63, 7358.
- (958) Su, L.; Bao, C.; Lu, R.; Chen, Y.; Xu, T.; Song, D.; Tan, C.; Shi, T.; Zhao, Y. *Org. Biomol. Chem.* **2006**, 4, 2591.
- (959) Liu, X.; Xu, D.; Lu, R.; Li, B.; Qian, C.; Xue, P.; Zhang, X.; Zhou, H. *Chem.—Eur. J.* **2011**, 17, 1660.
- (960) Liu, X.; Zhang, X.; Lu, R.; Xue, P.; Xu, D.; Zhou, H. *J. Mater. Chem.* **2011**, 21, 8756.
- (961) Yang, X.; Lu, R.; Xu, T.; Xue, P.; Liu, X.; Zhao, Y. *Chem. Commun.* **2008**, 453.
- (962) Yang, X.; Lu, R.; Xue, P.; Li, B.; Xu, D.; Xu, T.; Zhao, Y. *Langmuir* **2008**, 24, 13730.
- (963) Yang, X.; Lu, R.; Gai, F.; Xue, P.; Zhan, Y. *Chem. Commun.* **2010**, 46, 1088.
- (964) Xu, D.; Liu, X.; Lu, R.; Xue, P.; Zhang, X.; Zhou, H.; Jia, J. *Org. Biomol. Chem.* **2011**, 9, 1523.
- (965) Ryu, S. Y.; Kim, S.; Seo, J.; Kim, Y.-W.; Kwon, O.-H.; Jang, D.-J.; Park, S. Y. *Chem. Commun.* **2004**, 70.
- (966) Varghese, S.; Kumar, N. S. S.; Krishna, A.; Rao, D. S. S.; Prasad, S. K.; Das, S. *Adv. Funct. Mater.* **2009**, 19, 2064.
- (967) Qu, S.; Wang, L.; Liu, X.; Li, M. *Chem.—Eur. J.* **2011**, 17, 3512.
- (968) Qu, S.; Wang, H.; Zhu, W.; Luo, J.; Fan, Y.; Song, L.; Zhang, H.-X.; Liu, X. *J. Mater. Chem.* **2012**, 22, 3875.
- (969) Antonio, P. P.; Guarcello, A.; Calabrese, A.; Pibiri, I.; Pace, A.; Buscemi, S. *Org. Biomol. Chem.* **2012**, 10, 3044.
- (970) Piccione, A. P.; Guarcello, A.; Calabrese, A.; Pibiri, I.; Pace, A.; Buscemi, S. *Org. Biomol. Chem.* **2012**, 10, 3044.
- (971) Hong, Y.; Lam, J. W. Y.; Tang, B. Z. *Chem. Soc. Rev.* **2011**, 40, 5361.
- (972) Kim, T. H.; Kim, D. G.; Lee, M.; Lee, T. S. *Tetrahedron* **2010**, 66, 1667.
- (973) Kim, T. H.; Choi, M. S.; Sohn, B.-H.; Park, S.-Y.; Lyoo, W. S.; Lee, T. S. *Chem. Commun.* **2008**, 2364.
- (974) Kim, T. H.; Kwon, N. Y.; Lee, T. S. *Tetrahedron Lett.* **2010**, 51, 5596.
- (975) Qian, Y.; Li, S.; Wang, Q.; Sheng, X.; Wu, S.; Wang, S.; Li, J.; Yang, G. *Soft Matter* **2012**, 8, 757.
- (976) Haino, T.; Tanaka, M.; Fukazawa, Y. *Chem. Commun.* **2008**, 468.
- (977) Tanaka, M.; Ikeda, T.; Mack, J.; Kobayashi, N.; Haino, T. *J. Org. Chem.* **2011**, 76, 5082.
- (978) Haino, T.; Saito, H. *Synth. Met.* **2009**, 159, 821.
- (979) Haino, T.; Saito, H. *Aust. J. Chem.* **2010**, 63, 640.
- (980) Cicchi, S.; Pescitelli, G.; Lascialfari, L.; Ghini, G.; Bari, L. D.; Brandi, A.; Bussotti, L.; Atsbeha, T.; Marcelli, A.; Foggi, P.; Berti, D.; Mannini, M. *Chirality* **2011**, 23, 833.
- (981) Yu, H.; Kawanishi, H.; Koshima, H. *J. Photochem. Photobiol., A* **2006**, 178, 62.
- (982) Zhai, L.; Herzog, B.; Drechsler, M.; Hoffmann, H. *J. Phys. Chem. B* **2006**, 110, 17697.
- (983) Gräßner, D.; Zhai, L.; Talmon, Y.; Schmidt, J.; Freiberger, N.; Glatter, O.; Herzog, B.; Hoffmann, H. *J. Phys. Chem. B* **2008**, 112, 2901.
- (984) Ishii, T.; Nakamura, N.; Esaki, N.; Amemori, S. *Chem. Lett.* **2008**, 37, 1166.
- (985) Shen, Y.-T.; Li, C.-H.; Chang, K.-C.; Chin, S.-Y.; Lin, H.-A.; Liu, Y.-M.; Hung, C.-Y.; Hsu, H.-F.; Sun, S.-S. *Langmuir* **2009**, 25, 8714.
- (986) Gomar-Nadal, E.; Puigmarti-Luis, J.; Amabilino, D. B. *Chem. Soc. Rev.* **2008**, 37, 490.
- (987) Hasegawa, M.; Iyoda, M. *Chem. Soc. Rev.* **2010**, 39, 2420.
- (988) Iyoda, M.; Hasegawa, M.; Enozawa, H. *Chem. Lett.* **2007**, 36, 1402.
- (989) Sallé, M.; Canevet, D.; Balandier, J.-Y.; Lyskawa, J.; Trippé, G.; Goeb, S.; Le Derf, F. *Phosphorus, Sulfur Silicon Relat. Elem.* **2011**, 186, 1153.
- (990) Jørgensen, M.; Bechgaard, K. *J. Org. Chem.* **1994**, 59, 5877.
- (991) Le Gall, T.; Pearson, C.; Bryce, M. R.; Petty, M. C.; Dahlgaard, H.; Becher, J. *Eur. J. Org. Chem.* **2003**, 3562.
- (992) Kitamura, T.; Nakaso, S.; Mizoshita, N.; Tochigi, Y.; Shimomura, T.; Moriyama, M.; Ito, K.; Kato, T. *J. Am. Chem. Soc.* **2005**, 127, 14769.
- (993) Kitahara, T.; Shirakawa, M.; Kawano, S.-i.; Beginn, U.; Fujita, N.; Shinkai, S. *J. Am. Chem. Soc.* **2005**, 127, 14980.
- (994) Wang, C.; Zhang, D.; Zhu, D. *J. Am. Chem. Soc.* **2005**, 127, 16372.
- (995) Tatewaki, Y.; Hatanaka, T.; Tsunashima, R.; Nakamura, T.; Kimura, M.; Shirai, H. *Chem.—Asian J.* **2009**, 4, 1474.
- (996) Puigmarti-Luis, J.; Laukhin, V.; del Pino, Á. P.; Vidal-Gancedo, J.; Rovira, C.; Laukhina, E.; Amabilino, D. B. *Angew. Chem., Int. Ed.* **2007**, 46, 238.
- (997) Puigmarti-Luis, J.; Laukhina, E. E.; Laukhin, V. N.; del Pino, Á. P.; Mestres, N.; Vidal-Gancedo, J.; Rovira, C.; Amabilino, D. B. *Adv. Funct. Mater.* **2009**, 19, 934.
- (998) Puigmarti-Luis, J.; del Pino, Á. P.; Laukhina, E.; Esquena, J.; Laukhin, V.; Rovira, C.; Vidal-Gancedo, J.; Kanaras, A. G.; Nichols, R. J.; Brust, M.; Amabilino, D. B. *Angew. Chem., Int. Ed.* **2008**, 47, 1861.
- (999) Taboada, E.; Feldborg, L. N.; del Pino, Á. P.; Roig, A.; Amabilino, D. B.; Puigmarti-Luis, J. *Soft Matter* **2011**, 7, 2755.
- (1000) Puigmarti-Luis, J.; del Pino, A. P.; Laukhin, V.; Feldborg, L. N.; Rovira, C.; Laukhina, E.; Amabilino, D. B. *J. Mater. Chem.* **2010**, 20, 466.
- (1001) Danila, I.; Riobé, F.; Puigmarti-Luis, J.; del Pino, Á. P.; Wallis, J. D.; Amabilino, D. B.; Avarvari, N. *J. Mater. Chem.* **2009**, 19, 4495.
- (1002) Danila, I.; Pop, F.; Escudero, C.; Feldborg, L. N.; Puigmarti-Luis, J.; Riobé, F.; Avarvari, N.; Amabilino, D. B. *Chem. Commun.* **2012**, 48, 4552.
- (1003) Danila, I.; Riobé, F.; Piron, F.; Puigmarti-Luis, J.; Wallis, J. D.; Linares, M.; Ågren, H.; Beljonne, D.; Amabilino, D. B.; Avarvari, N. *J. Am. Chem. Soc.* **2011**, 133, 8344.
- (1004) Torres, E.; Puigmarti-Luis, J.; del Pino, Á. P.; Ortúñoz, R. M.; Amabilino, D. B. *Org. Biomol. Chem.* **2010**, 8, 1661.
- (1005) Akutagawa, T.; Kakiuchi, K.; Hasegawa, T.; Noro, S.-i.; Nakamura, T.; Hasegawa, H.; Mashiko, S.; Becher, J. *Angew. Chem., Int. Ed.* **2005**, 44, 7283.
- (1006) Enozawa, H.; Honna, Y.; Iyoda, M. *Chem. Lett.* **2007**, 36, 1434.
- (1007) Ahn, S.; Kim, Y.; Beak, S.; Ishimoto, S.; Enozawa, H.; Isomura, E.; Hasegawa, M.; Iyoda, M.; Park, Y. *J. Mater. Chem.* **2010**, 20, 10817.
- (1008) Wang, X.-J.; Xing, L.-B.; Cao, W.-N.; Li, X.-B.; Chen, B.; Tung, C.-H.; Wu, L.-Z. *Langmuir* **2011**, 27, 774.
- (1009) Wang, C.; Sun, F.; Zhang, D.; Zhang, G.; Zhu, D. *Chin. J. Chem.* **2010**, 28, 622.
- (1010) Yang, X.; Zhang, G.; Zhang, D.; Zhu, D. *Langmuir* **2010**, 26, 11720.
- (1011) Mei, X.; Ouyang, J. *Langmuir* **2011**, 27, 10953.
- (1012) Yang, X.; Zhang, G.; Li, L.; Zhang, D.; Chi, L.; Zhu, D. *Small* **2012**, 8, 578.
- (1013) Gerkinsmeier, T.; Decker, B.; Schwertfeger, M.; Buchheim, W.; Mattay, J. *Eur. J. Org. Chem.* **2002**, 2120.
- (1014) Bairi, P.; Roy, B.; Nandi, A. K. *J. Phys. Chem. B* **2010**, 114, 11454.
- (1015) Yang, X.; Lu, R.; Zhou, H.; Xue, P.; Wang, F.; Chen, P.; Zhao, Y. *J. Colloid Interface Sci.* **2009**, 339, 527.
- (1016) Dou, C.; Li, D.; Gao, H.; Wang, C.; Zhang, H.; Wang, Y. *Langmuir* **2010**, 26, 2113.
- (1017) Dou, C.; Wang, C.; Zhang, H.; Gao, H.; Wang, Y. *Chem. — Eur. J.* **2010**, 16, 10744.
- (1018) Dou, C.; Li, D.; Zhang, H.; Gao, H.; Zhang, J.; Wang, Y. *Sci. China Chem.* **2011**, 54, 641.

- (1019) Richards, G. J.; Hill, J. P.; Okamoto, K.; Shundo, A.; Akada, M.; Elsegood, M. R. J.; Mori, T.; Ariga, K. *Langmuir* **2009**, *25*, 8408.
- (1020) Zhao, B.; Liu, B.; QiPing, R. Q.; Zhang, K.; Lim, K. A.; Luo, J.; Shao, J.; Ho, P. K. H.; Chi, C.; Wu, J. *Chem. Mater.* **2010**, *22*, 435.
- (1021) Velázquez, D. G.; Orive, A. G.; Creus, A. H.; Luque, R.; Ravelo, A. G. *Org. Biomol. Chem.* **2011**, *9*, 6524.
- (1022) Yip, H.-L.; Zou, J.; Ma, H.; Tian, Y.; Tucker, N. M.; Jen, A. K.-Y. *J. Am. Chem. Soc.* **2006**, *128*, 13042.
- (1023) Tao, Z.-G.; Zhao, X.; Jiang, X.-K.; Li, Z.-T. *Tetrahedron Lett.* **2012**, *53*, 1840.
- (1024) Ishii, T.; Hirayama, T.; Murakami, K.-i.; Tashiro, H.; Thiemann, T.; Kubo, K.; Mori, A.; Yamasaki, S.; Akao, T.; Tsuboyama, A.; Mukaiide, T.; Ueno, K.; Mataka, S. *Langmuir* **2005**, *21*, 1261.
- (1025) Lu, C. C.; Su, S. K. *Supramol. Chem.* **2009**, *21*, 572.
- (1026) Ishii, T.; Kuwahara, R.; Takata, A.; Jeong, Y.; Sakurai, K.; Mataka, S. *Chem.—Eur. J.* **2006**, *12*, 763.
- (1027) Zhang, Y.-M.; Lin, Q.; Wei, T.-B.; Qin, X.-P.; Li, Y. *Chem. Commun.* **2009**, 6074.
- (1028) Itoi, H.; Sekine, Y.; Sekiguchi, M.; Tachikawa, T. *Chem. Lett.* **2009**, *38*, 1002.
- (1029) Wang, H.; Yang, C.; Wang, L.; Kong, D.; Zhang, Y.; Yang, Z. *Chem. Commun.* **2011**, *47*, 4439.
- (1030) Lei, G. D.; Li, M.; Qiu, D. M.; Liu, H.; Huang, Y.; Lu, Z. Y. *Chin. Chem. Lett.* **2009**, *20*, 1419.
- (1031) Moyano, S.; Serrano, J. L.; Elduque, A.; Giménez, R. *Soft Matter* **2012**, *8*, 6799.
- (1032) Wang, M.; Zhang, D.; Zhang, G.; Zhu, D. *Chem. Phys. Lett.* **2009**, *475*, 64.
- (1033) Wan, J.-H.; Mao, L.-Y.; Li, Y.-B.; Li, Z.-F.; Qiu, H.-Y.; Wang, C.; Lai, G.-Q. *Soft Matter* **2010**, *6*, 3195.
- (1034) Xu, J.; Filion, T. M.; Prifti, F.; Song, J. *Chem.—Asian J.* **2011**, *6*, 2730.
- (1035) Li, Y.; Park, T.; Quansah, J. K.; Zimmerman, S. C. *J. Am. Chem. Soc.* **2011**, *133*, 17118.
- (1036) Park, T.; Zimmerman, S. C. *J. Am. Chem. Soc.* **2006**, *128*, 11582.
- (1037) Schenning, A. P. H. J.; Meijer, E. W. *Chem. Commun.* **2005**, 3245.
- (1038) Arias, A. C.; MacKenzie, J. D.; McCulloch, I.; Rivnay, J.; Salleo, A. *Chem. Rev.* **2010**, *110*, 3.
- (1039) Günes, S.; Neugebauer, H.; Sariciftci, N. S. *Chem. Rev.* **2007**, *107*, 1324.
- (1040) Schwab, P. F. H.; Smith, J. R.; Michl, J. *Chem. Rev.* **2005**, *105*, 1197.
- (1041) Yagai, S. *J. Photochem. Photobiol., C* **2006**, *7*, 164.
- (1042) Hoppe, H.; Sariciftci, N. S. *J. Mater. Chem.* **2006**, *16*, 45.
- (1043) Dong, L.; Li, W.; Li, W.-S. *Nanoscale* **2011**, *3*, 3447.
- (1044) Roncali, J. *Chem. Rev.* **1992**, *92*, 711.
- (1045) Mishra, A.; Ma, C.-Q.; Bäuerle, P. *Chem. Rev.* **2009**, *109*, 1141.
- (1046) Coropceanu, V.; Cornil, J.; da Silva Filho, D. A.; Olivier, Y.; Silbey, R.; Brédas, J.-L. *Chem. Rev.* **2007**, *107*, 926.
- (1047) Perepichka, I. F.; Perepichka, D. F.; Meng, H.; Wudl, F. *Adv. Mater.* **2005**, *17*, 2281.
- (1048) Prasanthkumar, S.; Gopal, A.; Ajayaghosh, A. *J. Am. Chem. Soc.* **2010**, *132*, 13206.
- (1049) Schoonbeek, F. S.; van Esch, J. H.; Wegewijs, B.; Rep, D. B. A.; de Haas, M. P.; Klapwijk, T. M.; Kellogg, R. M.; Feringa, B. L. *Angew. Chem., Int. Ed.* **1999**, *38*, 1393.
- (1050) van Esch, J.; Schoonbeek, F.; de Loos, M.; Kooijman, H.; Spek, A. L.; Kellogg, R. M.; Feringa, B. L. *Chem.—Eur. J.* **1999**, *5*, 937.
- (1051) Rep, D. B. A.; Roelfsema, R.; van Esch, J. H.; Schoonbeek, F. S.; Kellogg, R. M.; Feringa, B. L.; Palstra, T. T. M.; Klapwijk, T. M. *Adv. Mater.* **2000**, *12*, 563.
- (1052) Gesquière, A.; De Feyter, S.; De Schryver, F. C.; Schoonbeek, F.; van Esch, J.; Kellogg, R. M.; Feringa, B. L. *Nano Lett.* **2001**, *1*, 201.
- (1053) Dautel, O. J.; Robitzer, M.; Flores, J.-C.; Tondelier, D.; Serein-Spirau, F.; Lére-Porte, J.-P.; Guérin, D.; Lenfant, S.; Tillard, M.; Vuillaume, D.; Moreau, J. J. E. *Chem.—Eur. J.* **2008**, *14*, 4201.
- (1054) Shoji, Y.; Yoshio, M.; Yasuda, T.; Funahashi, M.; Kato, T. *J. Mater. Chem.* **2010**, *20*, 173.
- (1055) Messmore, B. W.; Hulvat, J. F.; Sone, E. D.; Stupp, S. I. *J. Am. Chem. Soc.* **2004**, *126*, 14452.
- (1056) Diegelmann, S. R.; Gorham, J. M.; Tovar, J. D. *J. Am. Chem. Soc.* **2008**, *130*, 13840.
- (1057) Zhang, S.; Greenfield, M. A.; Mata, A.; Palmer, L. C.; Bitton, R.; Mantel, J. R.; Aparicio, C.; de la Cruz, M. O.; Stupp, S. I. *Nat. Mater.* **2010**, *9*, 594.
- (1058) Wall, B. D.; Diegelmann, S. R.; Zhang, S.; Dawidczyk, T. J.; Wilson, W. L.; Katz, H. E.; Mao, H.-Q.; Tovar, J. D. *Adv. Mater.* **2011**, *23*, 5009.
- (1059) Stone, D. A.; Hsu, L.; Stupp, S. I. *Soft Matter* **2009**, *5*, 1990.
- (1060) Tsai, W.-W.; Li, L.-s.; Cui, H.; Jiang, H.; Stupp, S. I. *Tetrahedron* **2008**, *64*, 8504.
- (1061) Nakagawa, H.; Ohtsuka, K.; Sugahara, K.; Kobayashi, C.; Masuoka, Y.; Yamada, K.-i.; Kawase, M. *Tetrahedron: Asymmetry* **2010**, *21*, 659.
- (1062) Yagai, S.; Kinoshita, T.; Kikkawa, Y.; Karatsu, T.; Kitamura, A.; Honsho, Y.; Seki, S. *Chem.—Eur. J.* **2009**, *15*, 9320.
- (1063) Yagai, S.; Gushiken, M.; Karatsu, T.; Kitamura, A.; Kikkawa, Y. *Chem. Commun.* **2011**, *47*, 454.
- (1064) Yagai, S.; Ohta, K.; Gushiken, M.; Iwai, K.; Asano, A.; Seki, S.; Kikkawa, Y.; Morimoto, M.; Kitamura, A.; Karatsu, T. *Chem.—Eur. J.* **2012**, *18*, 2244.
- (1065) Kawano, S.-i.; Fujita, N.; Shinkai, S. *Chem.—Eur. J.* **2005**, *11*, 4735.
- (1066) Safont-Sempere, M. M.; Fernández, G.; Würthner, F. *Chem. Rev.* **2011**, *111*, 5784.
- (1067) Sobczuk, A. A.; Tamarua, S.-i.; Shinkai, S. *Chem. Commun.* **2011**, *47*, 3093.
- (1068) Sobczuk, A. A.; Tsuchiya, Y.; Shiraki, T.; Tamarua, S.-i.; Shinkai, S. *Chem.—Eur. J.* **2012**, *18*, 2832.
- (1069) Pratihar, P.; Ghosh, S.; Stepanenko, V.; Patwardhan, S.; Grozema, F. C.; Siebbeles, L. D. A.; Würthner, F. *Beilstein J. Org. Chem.* **2010**, *6*, 1070.
- (1070) Stone, D. A.; Tayi, A. S.; Goldberger, J. E.; Palmer, L. C.; Stupp, S. I. *Chem. Commun.* **2011**, *47*, 5702.
- (1071) Tevis, I. D.; Palmer, L. C.; Herman, D. J.; Murray, I. P.; Stone, D. A.; Stupp, S. I. *J. Am. Chem. Soc.* **2011**, *133*, 16486.
- (1072) Tsai, W.-W.; Tevis, I. D.; Tayi, A. S.; Cui, H.; Stupp, S. I. *J. Phys. Chem. B* **2010**, *114*, 14778.
- (1073) Tevis, I. D.; Tsai, W.-W.; Palmer, L. C.; Aytun, T.; Stupp, S. I. *ACS Nano* **2012**, *6*, 2032.
- (1074) Kiriy, N.; Bocharova, V.; Kiriy, A.; Stamm, M.; Krebs, F. C.; Adler, H.-J. *Chem. Mater.* **2004**, *16*, 4765.
- (1075) Chung, J. W.; Yang, H.; Singh, B.; Moon, H.; An, B.-k.; Lee, S. Y.; Park, S. Y. *J. Mater. Chem.* **2009**, *19*, 5920.
- (1076) Chung, J. W.; Yoon, S.-J.; Lim, S.-J.; An, B.-k.; Park, S. Y. *Angew. Chem., Int. Ed.* **2009**, *48*, 7030.
- (1077) Prasanthkumar, S.; Saeki, A.; Seki, S.; Ajayaghosh, A. *J. Am. Chem. Soc.* **2010**, *132*, 8866.
- (1078) Saito, S.; Nakakura, K.; Yamaguchi, S. *Angew. Chem., Int. Ed.* **2012**, *51*, 714.
- (1079) Wan, J.-H.; Fang, W.-F.; Li, Y.-B.; Xiao, X.-Q.; Zhang, L.-H.; Xu, Z.; Peng, J.-J.; Lai, G.-Q. *Org. Biomol. Chem.* **2012**, *10*, 1459.
- (1080) Romero-Nieto, C.; Marcos, M.; Merino, S.; Barberá, J.; Baumgartner, T.; Rodríguez-López, J. *Adv. Funct. Mater.* **2011**, *21*, 4088.
- (1081) Ren, Y.; Kan, W. H.; Thangadurai, V.; Baumgartner, T. *Angew. Chem., Int. Ed.* **2012**, *51*, 3964.
- (1082) Hong, J.-P.; Um, M.-C.; Nam, S.-R.; Hong, J.-I.; Lee, S. *Chem. Commun.* **2009**, 310.
- (1083) Kumar, R. J.; MacDonald, J. M.; Singh, T. B.; Waddington, L. J.; Holmes, A. B. *J. Am. Chem. Soc.* **2011**, *133*, 8564.
- (1084) Liu, P.; Wu, Y.; Pan, H.; Ong, B. S.; Zhu, S. *Macromolecules* **2010**, *43*, 6368.
- (1085) Tovar, J. D.; Rabatic, B. M.; Stupp, S. I. *Small* **2007**, *3*, 2024.

- (1086) Du, R.; Xu, Y.; Luo, Y.; Zhang, X.; Zhang, J. *J. Chem. Commun.* **2011**, *47*, 6287.
- (1087) Huang, W. Y.; Huang, P. T.; Han, Y. K.; Lee, C. C.; Hsieh, T. L.; Chang, M. Y. *Macromolecules* **2008**, *41*, 7485.
- (1088) Koppe, M.; Brabec, C. J.; Heiml, S.; Schausberger, A.; Duffy, W.; Heeney, M.; McCulloch, I. *Macromolecules* **2009**, *42*, 4661.
- (1089) Malik, S.; Jana, T.; Nandi, A. K. *Macromolecules* **2001**, *34*, 275.
- (1090) Malik, S.; Nandi, A. K. *J. Phys. Chem. B* **2004**, *108*, 597.
- (1091) Malik, S.; Nandi, A. K. *J. Appl. Polym. Sci.* **2007**, *103*, 2528.
- (1092) Xu, W.; Tang, H.; Lv, H.; Li, J.; Zhao, X.; Li, H.; Wang, N.; Yang, X. *Soft Matter* **2012**, *8*, 726.
- (1093) Chen, C.-Y.; Chan, S.-H.; Li, J.-Y.; Wu, K.-H.; Chen, H.-L.; Chen, J.-H.; Huang, W.-Y.; Chen, S.-A. *Macromolecules* **2010**, *43*, 7305.
- (1094) Zhang, X.; Li, C.; Luo, Y. *Langmuir* **2011**, *27*, 1915.
- (1095) Yuen, J. D.; Fan, J.; Seifter, J.; Lim, B.; Hufschmid, R.; Heeger, A. J.; Wudl, F. *J. Am. Chem. Soc.* **2011**, *133*, 20799.
- (1096) Benetti, E. M.; Causin, V.; Maggini, M. *Adv. Mater.* **2012**, *24*, 5636.
- (1097) Newbloom, G. M.; Weigandt, K. M.; Pozzo, D. C. *Macromolecules* **2012**, *45*, 3452.
- (1098) Newbloom, G. M.; Kim, F. S.; Jenekhe, S. A.; Pozzo, D. C. *Macromolecules* **2011**, *44*, 3801.
- (1099) Newbloom, G. M.; Weigandt, K. M.; Pozzo, D. C. *Soft Matter* **2012**, *8*, 8854.
- (1100) Richards, J. J.; Weigandt, K. M.; Pozzo, D. C. *J. Colloid Interface Sci.* **2011**, *364*, 341.
- (1101) Samitsu, S.; Shimomura, T.; Heike, S.; Hashizume, T.; Ito, K. *Macromolecules* **2008**, *41*, 8000.
- (1102) Ajayaghosh, A.; George, S. J.; Schenning, A. P. H. J. *Top. Curr. Chem.* **2005**, *258*, 83.
- (1103) Ajayaghosh, A.; George, S. J. *J. Am. Chem. Soc.* **2001**, *123*, 5148.
- (1104) George, S. J.; Ajayaghosh, A. *Chem.—Eur. J.* **2005**, *11*, 3217.
- (1105) Praveen, V. K.; George, S. J.; Ajayaghosh, A. *Macromol. Symp.* **2006**, *241*, 1.
- (1106) Durkut, M.; Mas-Torrent, M.; Hadley, P.; Jonkheijm, P.; Schenning, A. P. H. J.; Meijer, E. W.; George, S. J.; Ajayaghosh, A. J. *Chem. Phys.* **2006**, *124*, 154704.
- (1107) George, S. J.; Ajayaghosh, A.; Jonkheijm, P.; Schenning, A. P. H. J.; Meijer, E. W. *Angew. Chem., Int. Ed.* **2004**, *43*, 3422.
- (1108) De, M. *Curr. Sci.* **2005**, *89*, 736.
- (1109) Ajayaghosh, A.; Varghese, R.; George, S. J.; Vijayakumar, C. *Angew. Chem., Int. Ed.* **2006**, *45*, 1141.
- (1110) Ajayaghosh, A.; Praveen, V. K.; Vijayakumar, C.; George, S. J. *Angew. Chem., Int. Ed.* **2007**, *46*, 6260.
- (1111) Ajayaghosh, A.; George, S. J.; Praveen, V. K. *Angew. Chem., Int. Ed.* **2003**, *42*, 332.
- (1112) Praveen, V. K.; George, S. J.; Varghese, R.; Vijayakumar, C.; Ajayaghosh, A. *J. Am. Chem. Soc.* **2006**, *128*, 7542.
- (1113) Ajayaghosh, A.; Praveen, V. K.; Srinivasan, S.; Varghese, R. *Adv. Mater.* **2007**, *19*, 411.
- (1114) Babu, S. S.; Praveen, V. K.; Ajayaghosh, A. *Macromol. Symp.* **2008**, *273*, 25.
- (1115) Ajayaghosh, A.; Vijayakumar, C.; Praveen, V. K.; Babu, S. S.; Varghese, R. *J. Am. Chem. Soc.* **2006**, *128*, 7174.
- (1116) Vijayakumar, C.; Praveen, V. K.; Kartha, K. K.; Ajayaghosh, A. *Phys. Chem. Chem. Phys.* **2011**, *13*, 4942.
- (1117) Ajayaghosh, A.; Vijayakumar, C.; Varghese, R.; George, S. J. *Angew. Chem., Int. Ed.* **2006**, *45*, 456.
- (1118) Vijayakumar, C.; Praveen, V. K.; Ajayaghosh, A. *Adv. Mater.* **2009**, *21*, 2059.
- (1119) Babu, S. S.; Mahesh, S.; Kartha, K. K.; Ajayaghosh, A. *Chem.—Asian J.* **2009**, *4*, 824.
- (1120) Babu, S. S.; Praveen, V. K.; Prasanthkumar, S.; Ajayaghosh, A. *Chem.—Eur. J.* **2008**, *14*, 9577.
- (1121) Kartha, K. K.; Babu, S. S.; Srinivasan, S.; Ajayaghosh, A. *J. Am. Chem. Soc.* **2012**, *134*, 4834.
- (1122) van Herrikhuyzen, J.; George, S. J.; Vos, M. R. J.; Sommerdijk, N. A. J. M.; Ajayaghosh, A.; Meskers, S. C. J.; Schenning, A. P. H. J. *Angew. Chem., Int. Ed.* **2007**, *46*, 1825.
- (1123) Kumar, V. R. R.; Sajini, V.; Sreeprasad, T. S.; Praveen, V. K.; Ajayaghosh, A.; Pradeep, T. *Chem.—Asian J.* **2009**, *4*, 840.
- (1124) Srinivasan, S.; Babu, S. S.; Praveen, V. K.; Ajayaghosh, A. *Angew. Chem., Int. Ed.* **2008**, *47*, 5746.
- (1125) Hirai, Y.; Babu, S. S.; Praveen, V. K.; Yasuda, T.; Ajayaghosh, A.; Kato, T. *Adv. Mater.* **2009**, *41*, 4029.
- (1126) Dasgupta, D.; Srinivasan, S.; Rochas, C.; Ajayaghosh, A.; Guenet, J. M. *Langmuir* **2009**, *25*, 8593.
- (1127) Dasgupta, D.; Srinivasan, S.; Rochas, C.; Thierry, A.; Schröder, A.; Ajayaghosh, A.; Guenet, J. M. *Soft Matter* **2011**, *7*, 2797.
- (1128) Dasgupta, D.; Srinivasan, S.; Rochas, C.; Ajayaghosh, A.; Guenet, J. M. *Soft Matter* **2011**, *7*, 9311.
- (1129) Samanta, S. K.; Pal, A.; Bhattacharya, S. *Langmuir* **2009**, *25*, 8567.
- (1130) Samanta, S. K.; Gomathi, A.; Bhattacharya, S.; Rao, C. N. R. *Langmuir* **2010**, *26*, 12230.
- (1131) Samanta, S. K.; Pal, A.; Bhattacharya, S.; Rao, C. N. R. *J. Mater. Chem.* **2010**, *20*, 6881.
- (1132) Samanta, S. K.; Subrahmanyam, K. S.; Bhattacharya, S.; Rao, C. N. R. *Chem.—Eur. J.* **2012**, *18*, 2890.
- (1133) Lee, M.; Cho, B.-K.; Zin, W.-C. *Chem. Rev.* **2001**, *101*, 3869.
- (1134) Hulvat, J. F.; Sofos, M.; Tajima, K.; Stupp, S. I. *J. Am. Chem. Soc.* **2005**, *127*, 366.
- (1135) Behanna, H. A.; Rajangam, K.; Stupp, S. I. *J. Am. Chem. Soc.* **2007**, *129*, 321.
- (1136) George, S. J.; Tomović, Ž.; Smulders, M. M. J.; de Greef, T. F. A.; Leclère, P. E. L. G.; Meijer, E. W.; Schenning, A. P. H. J. *Angew. Chem., Int. Ed.* **2007**, *46*, 8206.
- (1137) Yagai, S.; Kubota, S.; Iwashima, T.; Kishikawa, K.; Nakanishi, T.; Karatsu, T.; Kitamura, A. *Chem.—Eur. J.* **2008**, *14*, 5246.
- (1138) Yagai, S.; Kubota, S.; Unoike, K.; Karatsu, T.; Kitamura, A. *Chem. Commun.* **2008**, 4466.
- (1139) Yagai, S.; Aonuma, H.; Kikkawa, Y.; Kubota, S.; Karatsu, T.; Kitamura, A.; Mahesh, S.; Ajayaghosh, A. *Chem.—Eur. J.* **2010**, *16*, 8652.
- (1140) Tazawa, T.; Yagai, S.; Kikkawa, Y.; Karatsu, T.; Kitamura, A.; Ajayaghosh, A. *Chem. Commun.* **2010**, *46*, 1076.
- (1141) Wall, B. D.; Tovar, J. D. *Pure Appl. Chem.* **2012**, *84*, 1039.
- (1142) MBA, M.; Moretto, A.; Armelao, L.; Crisma, M.; Toniolo, C.; Maggini, M. *Chem.—Eur. J.* **2011**, *17*, 2044.
- (1143) Xue, P.; Lu, R.; Yang, X.; Zhao, L.; Xu, D.; Liu, Y.; Zhang, H.; Nomoto, H.; Takafuji, M.; Ihara, H. *Chem.—Eur. J.* **2009**, *15*, 9824.
- (1144) Xue, P.; Lu, R.; Zhao, L.; Xu, D.; Zhang, X.; Li, K.; Song, Z.; Yang, X.; Takafuji, M.; Ihara, H. *Langmuir* **2010**, *26*, 6669.
- (1145) Xue, P.; Lu, R.; Jia, J.; Takafuji, M.; Ihara, H. *Chem.—Eur. J.* **2012**, *18*, 3549.
- (1146) Xue, P.; Zhang, Y.; Jia, J.; Xu, D.; Zhang, X.; Liu, X.; Zhou, H.; Zhang, P.; Lu, R.; Takafuji, M.; Ihara, H. *Soft Matter* **2011**, *7*, 8296.
- (1147) Yoon, S.-J.; Kim, J. H.; Chung, J. W.; Park, S. Y. *J. Mater. Chem.* **2011**, *21*, 18971.
- (1148) Dou, C.; Chen, D.; Iqbal, J.; Yuan, Y.; Zhang, H.; Wang, Y. *Langmuir* **2011**, *27*, 6323.
- (1149) Hou, J.; Wu, X.; Li, Y.-J. *Supramol. Chem.* **2011**, *23*, 533.
- (1150) Wang, P.-S.; Lu, H.-H.; Liu, C.-Y.; Chen, S.-A. *Macromolecules* **2008**, *41*, 6500.
- (1151) Chen, S. H.; Su, A. C.; Chang, C. S.; Chen, H. L.; Ho, D. L.; Tsao, C. S.; Peng, K. Y.; Chen, S. A. *Langmuir* **2004**, *20*, 8909.
- (1152) Tang, H.; Duan, X.; Feng, X.; Liu, L.; Wang, S.; Li, Y.; Zhu, D. *Chem. Commun.* **2009**, 641.
- (1153) Gelinck, G. H.; Warman, J. M.; Staring, E. G. *J. Phys. Chem.* **1996**, *100*, 5485.
- (1154) Bunz, U. H. F. *Chem. Rev.* **2000**, *100*, 1605.
- (1155) Bunz, U. H. F. *Acc. Chem. Res.* **2001**, *34*, 998.
- (1156) Lin, C.-H.; Tour, J. J. *Org. Chem.* **2002**, *67*, 7761.
- (1157) Ide, T.; Takeuchi, D.; Osakada, K. *Chem. Commun.* **2012**, *48*, 278.

- (1158) Cantin, K.; Rondeau-Gagné, S.; Néabo, J. R.; Daigle, M.; Morin, J.-F. *Org. Biomol. Chem.* **2011**, *9*, 4440.
- (1159) Vollmeyer, J.; Jester, S.-S.; Eberhagen, F.; Prangenberg, T.; Mader, W.; Höger, S. *Chem. Commun.* **2012**, *48*, 6547.
- (1160) Camerel, F.; Ulrich, G.; Ziessl, R. *Org. Lett.* **2004**, *6*, 4171.
- (1161) Tsou, C.-C.; Sun, S.-S. *Org. Lett.* **2006**, *8*, 387.
- (1162) Li, C.-H.; Chang, K.-C.; Tsou, C.-C.; Lan, Y.; Yang, H.-C.; Sun, S.-S. *J. Org. Chem.* **2011**, *76*, 5524.
- (1163) García, F.; Sánchez, L. *J. Am. Chem. Soc.* **2012**, *134*, 734.
- (1164) Yu, Y.; Ma, Y. *Soft Matter* **2011**, *7*, 884.
- (1165) Ajayaghosh, A.; Varghese, R.; Praveen, V. K.; Mahesh, S. *Angew. Chem., Int. Ed.* **2006**, *45*, 3261.
- (1166) Gopal, A.; Varghese, R.; Ajayaghosh, A. *Chem.—Asian J.* **2012**, *7*, 2061.
- (1167) Ajayaghosh, A.; Varghese, R.; Mahesh, S.; Praveen, V. K. *Angew. Chem., Int. Ed.* **2006**, *45*, 7729.
- (1168) Mahesh, S.; Thirumalai, R.; Yagai, S.; Kitamura, A.; Ajayaghosh, A. *Chem. Commun.* **2009**, 5984.
- (1169) Chen, J.; McNeil, A. *J. Am. Chem. Soc.* **2008**, *130*, 16496.
- (1170) Chen, J.; Kampf, J. W.; McNeil, A. *J. Langmuir* **2010**, *26*, 13076.
- (1171) Adhia, Y. J.; Schloemer, T. H.; Perez, M. T.; McNeil, A. *J. Soft Matter* **2012**, *8*, 430.
- (1172) Pérez, A.; Serrano, J. L.; Sierra, T.; Ballesteros, A.; de Saá, D.; Barluenga, J. *J. Am. Chem. Soc.* **2011**, *133*, 8110.
- (1173) Borges, A. R.; Hyacinth, M.; Lum, M.; Dingle, C. M.; Hamilton, P. L.; Chruszcz, M.; Pu, L.; Sabat, M.; Caran, K. L. *Langmuir* **2008**, *24*, 7421.
- (1174) Amemiya, R.; Mizutani, M.; Yamaguchi, M. *Angew. Chem., Int. Ed.* **2010**, *49*, 1995.
- (1175) Yamamoto, K.; Oyamada, N.; Mizutani, M.; An, Z.; Saito, N.; Yamaguchi, M.; Kasuya, M.; Kurihara, K. *Langmuir* **2012**, *28*, 11939.
- (1176) Saito, N.; Shigeno, M.; Yamaguchi, M. *Chem.—Eur. J.* **2012**, *18*, 8994.
- (1177) Huang, W. Y.; Matsuoka, S.; Kwei, T. K.; Okamoto, Y. *Macromolecules* **2001**, *34*, 7166.
- (1178) Perahia, D.; Traiphol, R.; Bunz, U. H. F. *J. Chem. Phys.* **2002**, *117*, 1827.
- (1179) Kim, H.-J.; Kim, T.; Lee, M. *Acc. Chem. Res.* **2011**, *44*, 72.
- (1180) Sidorov, V.; Douglas, T.; Dzekunov, S. M.; Abdallah, D.; Ghebremariam, B.; Roepe, P. D.; Matile, S. *Chem. Commun.* **1999**, 1429.
- (1181) Ryu, J.-H.; Hong, D.-J.; Lee, M. *Chem. Commun.* **2008**, 1043.
- (1182) Ryu, J.-H.; Lee, M. *J. Am. Chem. Soc.* **2005**, *127*, 14170.
- (1183) Moon, K.-S.; Kim, H.-J.; Lee, E.; Lee, M. *Angew. Chem., Int. Ed.* **2007**, *46*, 6807.
- (1184) Huang, Z.; Kang, S.-K.; Lee, M. *J. Mater. Chem.* **2011**, *21*, 15327.
- (1185) Huang, Z.; Lee, H.; Lee, E.; Kang, S.-K.; Nam, J.-M.; Lee, M. *Nat. Commun.* **2011**, *2*, 459.
- (1186) Chen, Y.; Lv, Y.; Han, Y.; Zhu, B.; Zhang, F.; Bo, Z.; Liu, C.-Y. *Langmuir* **2009**, *25*, 8548.
- (1187) Chen, Y.; Zhang, F.; Zhu, B.; Han, Y.; Bo, Z. *Chem.—Asian J.* **2011**, *6*, 226.
- (1188) Zubarev, E. R.; Pralle, M. U.; Sone, E. D.; Stupp, S. I. *J. Am. Chem. Soc.* **2001**, *123*, 4105.
- (1189) Hartgerink, J. D.; Zubarev, E. R.; Stupp, S. I. *Curr. Opin. Solid State Mater. Sci.* **2001**, *5*, 355.
- (1190) Zubarev, E. R.; Sone, E. D.; Stupp, S. I. *Chem.—Eur. J.* **2006**, *12*, 7313.
- (1191) Zubarev, E. R.; Pralle, M. U.; Sone, E. D.; Stupp, S. I. *Adv. Mater.* **2002**, *14*, 198.
- (1192) Stendahl, J. C.; Li, L.; Zubarev, E. R.; Chen, Y.-R.; Stupp, S. I. *Adv. Mater.* **2002**, *14*, 1540.
- (1193) Stendahl, J. C.; Zubarev, E. R.; Arnold, M. S.; Hersam, M. C.; Sue, H. J.; Stupp, S. I. *Adv. Funct. Mater.* **2005**, *15*, 487.
- (1194) Sone, E. D.; Zubarev, E. R.; Stupp, S. I. *Angew. Chem., Int. Ed.* **2002**, *41*, 1706.
- (1195) Sone, E. D.; Zubarev, E. R.; Stupp, S. I. *Small* **2005**, *1*, 694.
- (1196) Li, L.; Beniashi, E.; Zubarev, E. R.; Xiang, W.; Rabatic, B. M.; Zhang, G.; Stupp, S. I. *Nat. Mater.* **2003**, *2*, 689.
- (1197) Messmore, B. W.; Sukerkar, P. A.; Stupp, S. I. *J. Am. Chem. Soc.* **2005**, *127*, 7992.
- (1198) Kato, T.; Mizoshita, N.; Moriyama, M.; Kitamura, T. *Top. Curr. Chem.* **2005**, *256*, 219.
- (1199) Kato, T.; Kutsuna, T.; Hanabusa, K.; Ukon, M. *Adv. Mater.* **1998**, *10*, 606.
- (1200) Mizoshita, N.; Hanabusa, K.; Kato, T. *Adv. Mater.* **1999**, *11*, 392.
- (1201) Mizoshita, N.; Kutsuna, T.; Hanabusa, K.; Kato, T. *Chem. Commun.* **1999**, 781.
- (1202) Yabuuchi, K.; Rowan, A. E.; Nolte, R. J. M.; Kato, T. *Chem. Mater.* **2000**, *12*, 440.
- (1203) Mizoshita, N.; Suzuki, Y.; Kishimoto, K.; Hanabusa, K.; Kato, T. *J. Mater. Chem.* **2002**, *12*, 2197.
- (1204) Abe, H.; Kikuchi, H.; Hanabusa, K.; Kato, T.; Kajiyama, T. *Liq. Cryst.* **2003**, *30*, 1423.
- (1205) Abe, H.; Kikuchi, H.; Hanabusa, K.; Kato, T.; Kajiyama, T. *Mol. Cryst. Liq. Cryst.* **2003**, *399*, 43.
- (1206) Mizoshita, N.; Hanabusa, K.; Kato, T. *Adv. Funct. Mater.* **2003**, *13*, 313.
- (1207) Mizoshita, N.; Kato, T. *Adv. Funct. Mater.* **2006**, *16*, 2218.
- (1208) Mizoshita, N.; Suzuki, Y.; Hanabusa, K.; Kato, T. *Adv. Mater.* **2005**, *17*, 692.
- (1209) Kato, T.; Kondo, G.; Hanabusa, K. *Chem. Lett.* **1998**, *27*, 193.
- (1210) Xin, H.; Wang, H.; Bai, B.; Pang, D.; Li, M. *J. Mol. Liq.* **2008**, *139*, 143.
- (1211) Teng, M.; Kuang, G.; Jia, X.; Gao, M.; Li, Y.; Wei, Y. *J. Mater. Chem.* **2009**, *19*, 5648.
- (1212) Cui, J.; Shen, Z.; Wan, X. *Langmuir* **2010**, *26*, 97.
- (1213) Cui, J.; Zheng, Y.; Shen, Z.; Wan, X. *Langmuir* **2010**, *26*, 15508.
- (1214) Cui, J.; Liu, A.; Guan, Y.; Zheng, J.; Shen, Z.; Wan, X. *Langmuir* **2010**, *26*, 3615.
- (1215) Kim, W. J.; Jung, B. M.; Kang, S. H.; Chang, J. Y. *Soft Matter* **2011**, *7*, 4160.
- (1216) Ghini, G.; Lascialfari, L.; Vinattieri, C.; Cicchi, S.; Brandi, A.; Berti, D.; Betti, F.; Baglioni, P.; Manninic, M. *Soft Matter* **2009**, *5*, 1863.
- (1217) Hachisako, H.; Nakayama, H.; Ihara, H. *Chem. Lett.* **1999**, 1165.
- (1218) Ihm, H.; Ahn, J.-S.; Lah, M. S.; Ko, Y. H.; Paek, K. *Org. Lett.* **2004**, *6*, 3893.
- (1219) Kuroiwa, K.; Kikuchi, H.; Kimizuka, N. *Chem. Commun.* **2010**, *46*, 1229.
- (1220) Bao, C.; Lu, R.; Jin, M.; Xue, P.; Tan, C.; Xu, T.; Liu, G.; Zhao, Y. *Chem. — Eur. J.* **2006**, *12*, 3287.
- (1221) Simalou, O.; Zhao, X.; Lu, R.; Xue, P.; Yang, X.; Zhang, X. *Langmuir* **2009**, *25*, 11255.
- (1222) Bao, C.; Jin, M.; Lu, R.; Song, Z.; Yang, X.; Song, D.; Xu, T.; Liu, G.; Zhao, Y. *Tetrahedron* **2007**, *63*, 7443.
- (1223) Simalou, O.; Xue, P.; Lu, R. *Tetrahedron Lett.* **2010**, *51*, 3685.
- (1224) Sheepwash, E.; Krampl, V.; Scopelliti, R.; Sereda, O.; Neels, A.; Severin, K. *Angew. Chem., Int. Ed.* **2011**, *50*, 3034.
- (1225) Houjou, H.; Koga, T.; Akiizumi, M.; Yoshikawa, I.; Araki, K. *Bull. Chem. Soc. Jpn.* **2009**, *82*, 730.
- (1226) Kroto, H. W.; Heath, J. R.; O'Brien, S. C.; Curl, R. F.; Smalley, R. E. *Nature* **1985**, *318*, 162.
- (1227) Krätschmer, W.; Lamb, L. D.; Fostiropoulos, K.; Huffman, D. R. *Nature* **1990**, *347*, 354.
- (1228) Babu, S. S.; Möhwald, H.; Nakanishi, T. *Chem. Soc. Rev.* **2010**, *39*, 4021.
- (1229) Oishi, K.; Ishii-i, T.; Sano, M.; Shinkai, S. *Chem. Lett.* **1999**, *28*, 1089.
- (1230) Ishii-i, T.; Ono, Y.; Shinkai, S. *Chem. Lett.* **2000**, *29*, 808.
- (1231) Tsunashima, R.; Noro, S.-i.; Akutagawa, T.; Nakamura, T.; Kawakami, H.; Toma, K. *Chem.—Eur. J.* **2008**, *14*, 8169.

- (1232) Watanabe, N.; Jintoku, H.; Sagawa, T.; Takafuji, M.; Sawada, T.; Ihara, H. *J. Phys. Conf. Ser.* **2009**, *159*, 012016.
- (1233) Yang, X.; Zhang, G.; Zhang, D.; Xiang, J.; Yang, G.; Zhu, D. *Soft Matter* **2011**, *7*, 3592.
- (1234) Lascialfari, L.; Vinattieri, C.; Ghini, G.; Luconi, L.; Berti, D.; Mannini, M.; Bianchini, C.; Brandi, A.; Giambastiani, G.; Cicchi, S. *Soft Matter* **2011**, *7*, 10660.
- (1235) Royall, C. P.; Williams, S. R. *J. Phys. Chem. B* **2011**, *115*, 7288.
- (1236) Kawauchi, T.; Kumaki, J.; Kitaura, A.; Okoshi, K.; Kusanagi, H.; Kobayashi, K.; Sugai, T.; Shinohara, H.; Yashima, E. *Angew. Chem., Int. Ed.* **2008**, *47*, 515.
- (1237) Kawauchi, M.; Kawauchi, T.; Takeichi, T. *Macromolecules* **2009**, *42*, 6136.
- (1238) Ajayan, P. M. *Chem. Rev.* **1999**, *99*, 1787.
- (1239) Dai, H. *Acc. Chem. Res.* **2002**, *35*, 1035.
- (1240) Tasis, D.; Tagmatarchis, N.; Bianco, A.; Prato, M. *Chem. Rev.* **2006**, *106*, 1105.
- (1241) Prato, M.; Kostarelos, K.; Bianco, A. *Acc. Chem. Res.* **2008**, *41*, 60.
- (1242) Oh, H.; Jung, B. M.; Lee, H. P.; Chang, J. Y. *J. Colloid Interface Sci.* **2010**, *352*, 121.
- (1243) You, Y.-Z.; Yan, J.-J.; Yu, Z.-Q.; Cui, M.-M.; Hong, C.-Y.; Qu, B.-J. *J. Mater. Chem.* **2009**, *19*, 7656.
- (1244) Kovtyukhova, N. I.; Mallouk, T. E.; Pan, L.; Dickey, E. C. *J. Am. Chem. Soc.* **2003**, *125*, 9761.
- (1245) Pal, A.; Chhikara, B. S.; Govindaraj, A.; Bhattacharya, S.; Rao, C. N. R. *J. Mater. Chem.* **2008**, *18*, 2593.
- (1246) Zhang, L.-M.; Wang, G.-H.; Xing, Z. *J. Mater. Chem.* **2011**, *21*, 4650.
- (1247) Hough, L. A.; Islam, M. F.; Janmey, P. A.; Yodh, A. G. *Phys. Rev. Lett.* **2004**, *93*, 168102.
- (1248) Sabba, Y.; Thomas, E. L. *Macromolecules* **2004**, *37*, 4815.
- (1249) Thompson, B. C.; Moulton, S. E.; Gilmore, K. J.; Higgins, M. J.; Whitten, P. G.; Wallace, G. G. *Carbon* **2009**, *47*, 1282 and references cited therein..
- (1250) Cheng, E.; Li, Y.; Yang, Z.; Deng, Z.; Liu, D. *Chem. Commun.* **2011**, *47*, 5545.
- (1251) Tan, Z.; Ohara, S.; Naito, M.; Abe, H. *Adv. Mater.* **2011**, *23*, 4053.
- (1252) Kar, T.; Mandal, S. K.; Das, P. K. *Chem. Commun.* **2012**, *48*, 8389.
- (1253) Ogoishi, T.; Takashima, Y.; Yamaguchi, H.; Harada, A. *J. Am. Chem. Soc.* **2007**, *129*, 4878.
- (1254) Tamesue, S.; Takashima, Y.; Yamaguchi, H.; Shinkai, S.; Harada, A. *Eur. J. Org. Chem.* **2011**, *2801*.
- (1255) Wang, Z.; Chen, Y. *Macromolecules* **2007**, *40*, 3402.
- (1256) Li, H.; Wang, D. Q.; Chen, H. L.; Liu, B. L.; Gao, L. Z. *Macromol. Biosci.* **2003**, *3*, 720.
- (1257) Moulton, S. E.; Maugey, M.; Poulin, P.; Wallace, G. G. *J. Am. Chem. Soc.* **2007**, *129*, 9452.
- (1258) Lynam, C.; Moulton, S. E.; Wallace, G. G. *Adv. Mater.* **2007**, *19*, 1244.
- (1259) Granero, A. J.; Razal, J. M.; Wallace, G. G.; in het Panhuis, M. *Adv. Funct. Mater.* **2008**, *18*, 3759.
- (1260) Razal, J. M.; Gilmore, K. J.; Wallace, G. G. *Adv. Funct. Mater.* **2008**, *18*, 61.
- (1261) Bhattacharyya, S.; Guillot, S.; Dabboue, H.; Tranchant, J.-F.; Salvetat, J.-P. *Biomacromolecules* **2008**, *9*, 505.
- (1262) Moniruzzaman, M.; Sahin, A.; Winey, K. I. *Carbon* **2009**, *47*, 645.
- (1263) Miyako, E.; Nagata, H.; Hirano, K.; Hirotsu, T. *Adv. Mater.* **2009**, *21*, 2819.
- (1264) Arnold, M. S.; Guler, M. O.; Hersam, M. C.; Stupp, S. I. *Langmuir* **2005**, *21*, 4705.
- (1265) Li, C.; Mezzenga, R. *Langmuir* **2012**, *28*, 10142.
- (1266) Wang, J.; Chu, H.; Li, Y. *ACS Nano* **2008**, *2*, 2540.
- (1267) Fukushima, T.; Kosaka, A.; Ishimura, Y.; Yamamoto, T.; Takigawa, T.; Ishii, N.; Aida, T. *Science* **2003**, *300*, 2072.
- (1268) Fukushima, T.; Kosaka, A.; Yamamoto, Y.; Aimiya, T.; Notazawa, S.; Takigawa, T.; Inabe, T.; Aida, T. *Small* **2006**, *2*, 554.
- (1269) Fukushima, T.; Asaka, K.; Kosaka, A.; Aida, T. *Angew. Chem., Int. Ed.* **2005**, *44*, 2410.
- (1270) Mukai, K.; Asaka, K.; Sugino, T.; Kiyoohara, K.; Takeuchi, I.; Terasawa, N.; Futaba, D. N.; Hata, K.; Fukushima, T.; Aida, T. *Adv. Mater.* **2009**, *21*, 1582.
- (1271) Sekitani, T.; Noguchi, Y.; Hata, K.; Fukushima, T.; Aida, T.; Someya, T. *Science* **2008**, *321*, 1468.
- (1272) Sekitani, T.; Nakajima, H.; Maeda, H.; Fukushima, T.; Aida, T.; Hata, K.; Someya, T. *Nat. Mater.* **2009**, *8*, 494.
- (1273) Yu, P.; Qian, Q.; Lin, Y.; Mao, L. *J. Phys. Chem. C* **2010**, *114*, 3575.
- (1274) Aerov, A. A.; Potemkin, I. I. *J. Phys. Chem. B* **2009**, *113*, 1883.
- (1275) Biso, M.; Ansaldi, A.; Ricci, D. *Phys. Status Solidi RRL* **2010**, *4*, 64.
- (1276) Yoshida, M.; Koumura, N.; Misawa, Y.; Tamaoki, N.; Matsumoto, H.; Kawanami, H.; Kazaoui, S.; Minami, N. *J. Am. Chem. Soc.* **2007**, *129*, 11039.
- (1277) Hong, S. H.; Tung, T. T.; Trang, L. K. H.; Kim, T. Y.; Suh, K. S. *Colloid Polym. Sci.* **2010**, *288*, 1013.
- (1278) Li, X.-R.; Wang, B.; Xu, J.-J.; Chen, H.-Y. *Nanoscale* **2011**, *3*, 5026.
- (1279) Razal, J. M.; Coleman, J. N.; Muñoz, E.; Lund, B.; Gogotsi, Y.; Ye, H.; Collins, S.; Dalton, A. B.; Baughman, R. H. *Adv. Funct. Mater.* **2007**, *17*, 2918.
- (1280) Vaysse, M.; Khan, M. K.; Sundararajan, P. *Langmuir* **2009**, *25*, 7042.
- (1281) Bryning, M. B.; Milkie, D. E.; Islam, M. F.; Hough, L. A.; Kikkawa, J. M.; Yodh, A. G. *Adv. Mater.* **2007**, *19*, 661.
- (1282) Zou, J.; Liu, J.; Karakoti, A. S.; Kumar, A.; Joung, D.; Li, Q.; Khondaker, S. I.; Seal, S.; Zhai, L. *ACS Nano* **2010**, *4*, 7293.
- (1283) Liu, C.; Zhang, J.; He, J.; Hu, G. *Polymer* **2003**, *44*, 7529.
- (1284) Fujigaya, T.; Morimoto, T.; Nakashima, N. *Soft Matter* **2011**, *7*, 2647.
- (1285) Zhang, X.; Pint, C. L.; Lee, M. H.; Schubert, B. E.; Jamshidi, A.; Takei, K.; Ko, H.; Gillies, A.; Bardhan, R.; Urban, J. J.; Wu, M.; Fearing, R.; Javey, A. *Nano Lett.* **2011**, *11*, 3239.
- (1286) Volder, M. D.; Tawfick, S. H.; Copic, D.; Hart, A. J. *Soft Matter* **2011**, *7*, 9844.
- (1287) Ye, Y.; Mao, Y.; Wang, H.; Ren, Z. *J. Mater. Chem.* **2012**, *22*, 2449.
- (1288) Mei, X.; Ouyang, J. *J. Mater. Chem.* **2011**, *21*, 17842.
- (1289) Chen, J.; Xue, C.; Ramasubramaniam, R.; Liu, H. *Carbon* **2006**, *44*, 2142.
- (1290) Shigeta, M.; Komatsu, M.; Nakashima, N. *Chem. Phys. Lett.* **2006**, *418*, 115.
- (1291) Miyako, E.; Nagata, H.; Funahashi, R.; Hirano, K.; Hirotsu, T. *ChemSusChem* **2009**, *2*, 419.
- (1292) Liang, S.; Chen, G.; Peddle, J.; Zhao, Y. *Chem. Commun.* **2012**, *48*, 3100.
- (1293) Geim, A. K.; Novoselov, K. S. *Nat. Mater.* **2007**, *6*, 183.
- (1294) Rao, C. N. R.; Sood, A. K.; Subrahmanyam, K. S.; Govindaraj, A. *Angew. Chem., Int. Ed.* **2009**, *48*, 7752.
- (1295) Guo, S.; Dong, S. *Chem. Soc. Rev.* **2011**, *40*, 2644.
- (1296) Allen, M. J.; Tung, V. C.; Kaner, R. B. *Chem. Rev.* **2010**, *110*, 132.
- (1297) Cheng, Q.-Y.; Zhou, D.; Gao, Y.; Chen, Q.; Zhang, Z.; Han, B.-H. *Langmuir* **2012**, *28*, 3005.
- (1298) Adhikari, B.; Biswas, A.; Banerjee, A. *Langmuir* **2012**, *28*, 1460.
- (1299) Sui, Z.; Zhang, X.; Lei, Y.; Luo, Y. *Carbon* **2011**, *49*, 4314.
- (1300) Dan, B.; Behabtu, N.; Martinez, A.; Evans, J. S.; Kosynkin, D. V.; Tour, J. M.; Pasquali, M.; Smalyukh, I. I. *Soft Matter* **2011**, *7*, 11154.
- (1301) Lee, J. H.; Kang, S.; Jaworski, J.; Kwon, K.-Y.; Seo, M. L.; Lee, J. Y.; Jung, J. H. *Chem.—Eur. J.* **2012**, *18*, 765.
- (1302) Xu, Y.; Sheng, K.; Li, C.; Shi, G. *ACS Nano* **2010**, *4*, 4324.

- (1303) Xu, Y.; Wu, Q.; Sun, Y.; Bai, H.; Shi, G. *ACS Nano* **2010**, *4*, 7358.
- (1304) Bai, H.; Li, C.; Wang, X.; Shi, G. *Chem. Commun.* **2010**, *46*, 2376.
- (1305) Huang, C.; Bai, H.; Li, C.; Shi, G. *Chem. Commun.* **2011**, *47*, 4962.
- (1306) Sun, Y.; Wu, Q.; Shi, G. *Phys. Chem. Chem. Phys.* **2011**, *13*, 17249.
- (1307) Bai, H.; Li, C.; Wang, X.; Shi, G. *J. Phys. Chem. C* **2011**, *115*, 5545.
- (1308) Wu, Q.; Sun, Y.; Bai, H.; Shi, G. *Phys. Chem. Chem. Phys.* **2011**, *13*, 11193.
- (1309) Bai, H.; Sheng, K.; Zhang, P.; Li, C.; Shi, G. *J. Mater. Chem.* **2011**, *21*, 18653.
- (1310) Zu, S.-Z.; Han, B.-H. *J. Phys. Chem. C* **2009**, *113*, 13651.
- (1311) Sahu, A.; Choi, W. I.; Tae, G. *Chem. Commun.* **2012**, *48*, 5820.
- (1312) Sridhar, V.; Oh, I.-K. *J. Colloid Interface Sci.* **2010**, *348*, 384.
- (1313) Shen, J.; Yan, B.; Li, T.; Long, Y.; Li, N.; Ye, M. *Soft Matter* **2012**, *8*, 1831.
- (1314) Zhang, L.; Wang, Z.; Xu, C.; Li, Y.; Gao, J.; Wang, W.; Liu, Y. *J. Mater. Chem.* **2011**, *21*, 10399.
- (1315) Huang, Y.; Zeng, M.; Ren, J.; Wang, J.; Fan, L.; Xu, Q. *Colloids Surf., A* **2012**, *401*, 97.
- (1316) Liu, J.; Chen, G.; Jiang, M. *Macromolecules* **2011**, *44*, 7682.
- (1317) Jiang, X.; Ma, Y.; Li, J.; Fan, Q.; Huang, W. *J. Phys. Chem. C* **2010**, *114*, 22462.
- (1318) Pham, H. D.; Pham, V. H.; Cuong, T. V.; Nguyen-Phan, T.-D.; Chung, J. S.; Shin, E. W.; Kim, S. *Chem. Commun.* **2011**, *47*, 9672.
- (1319) Shao, J.-J.; Wu, S.-D.; Zhang, S.-B.; Lv, W.; Su, F.-Y.; Yang, Q.-H. *Chem. Commun.* **2011**, *47*, 5771.
- (1320) Yang, X.; Qiu, L.; Cheng, C.; Wu, Y.; Ma, Z.-F.; Li, D. *Angew. Chem., Int. Ed.* **2011**, *50*, 7325.
- (1321) Tung, V. C.; Kim, J.; Cote, L. J.; Huang, J. *J. Am. Chem. Soc.* **2011**, *133*, 9262.
- (1322) Meng, F.; Zhang, X.; Xu, B.; Yue, S.; Guo, H.; Luo, Y. *J. Mater. Chem.* **2011**, *21*, 18537.
- (1323) Chen, W.; Yan, L. *Nanoscale* **2011**, *3*, 3132.
- (1324) Qiu, L.; Yang, X.; Gou, X.; Yang, W.; Ma, Z.-F.; Wallace, G. G.; Li, D. *Chem.—Eur. J.* **2010**, *16*, 10653.
- (1325) Gun, J.; Kulkarni, S. A.; Xiu, W.; Batabyal, S. K.; Sladkevich, S.; Prikhodchenko, P. V.; Gutkin, V.; Lev, O. *Electrochim. Commun.* **2012**, *19*, 108.
- (1326) Huang, H.; Lü, S.; Zhang, X.; Shao, Z. *Soft Matter* **2012**, *8*, 4609.
- (1327) Chen, J.; Sheng, K.; Luo, P.; Li, C.; Shi, G. *Adv. Mater.* **2012**, *24*, 4569.
- (1328) Zhu, C.-H.; Lu, Y.; Peng, J.; Chen, J.-F.; Yu, S.-H. *Adv. Funct. Mater.* **2012**, *22*, 4017.
- (1329) Adhikari, B.; Biswas, A.; Banerjee, A. *ACS Appl. Mater. Interfaces* **2012**, *4*, 5472.
- (1330) *Polycyclic Aromatic Hydrocarbons*; Harvey, R. G., Ed.; Wiley-VCH: New York, 1997.
- (1331) Randić, M. *Chem. Rev.* **2003**, *103*, 3449.
- (1332) Watson, M. D.; Fechtenkötter, A.; Müllen, K. *Chem. Rev.* **2001**, *101*, 1267.
- (1333) Simpson, C. D.; Wu, J.; Watson, M. D.; Müllen, K. *J. Mater. Chem.* **2004**, *14*, 494.
- (1334) Grimsdale, A. C.; Wu, J.; Müllen, K. *Chem. Commun.* **2005**, *2197*.
- (1335) Wu, J.; Pisula, W.; Müllen, K. *Chem. Rev.* **2007**, *107*, 718.
- (1336) Zhi, L.; Müllen, K. *J. Mater. Chem.* **2008**, *18*, 1472.
- (1337) Chen, L.; Hernandez, Y.; Feng, X.; Müllen, K. *Angew. Chem., Int. Ed.* **2012**, *51*, 7640.
- (1338) Aida, T.; Fukushima, T. *Phil. Trans. R. Soc. A* **2007**, *365*, 1539.
- (1339) Yamamoto, Y. *Bull. Chem. Soc. Jpn.* **2011**, *84*, 17.
- (1340) Ito, S.; Herwig, P. T.; Böhme, T.; Rabe, J. P.; Rettig, W.; Müllen, K. *J. Am. Chem. Soc.* **2000**, *122*, 7698.
- (1341) Zhi, L.; Wu, J.; Müllen, K. *Org. Lett.* **2005**, *7*, 5761.
- (1342) Kim, H.-S.; Lee, J.-H.; Kim, T.-H.; Okabe, S.; Shibayama, M.; Choi, S.-M. *J. Phys. Chem. B* **2011**, *115*, 7314.
- (1343) Dou, X.; Pisula, W.; Wu, J.; Bodwell, G. J.; Müllen, K. *Chem.—Eur. J.* **2008**, *14*, 240.
- (1344) Hill, J. P.; Jin, W.; Kosaka, A.; Fukushima, T.; Ichihara, H.; Shimomura, T.; Ito, K.; Hashizume, T.; Ishii, N.; Aida, T. *Science* **2004**, *304*, 1481.
- (1345) Jin, W.; Fukushima, T.; Niki, M.; Kosaka, A.; Ishii, N.; Aida, T. *Proc. Natl. Acad. Sci. U.S.A.* **2005**, *102*, 10801.
- (1346) Jin, W.; Yamamoto, Y.; Fukushima, T.; Ishii, N.; Kim, J.; Kato, K.; Takata, M.; Aida, T. *J. Am. Chem. Soc.* **2008**, *130*, 9434.
- (1347) Rao, K. V.; Jayaramulu, K.; Maji, T. K.; George, S. *J. Angew. Chem., Int. Ed.* **2010**, *49*, 4218.
- (1348) Rao, K. V.; Datta, K. K. R.; Eswaramoorthy, M.; George, S. *J. Angew. Chem., Int. Ed.* **2011**, *50*, 1179.
- (1349) Jain, A.; Rao, K. V.; Kulkarni, C.; George, A.; George, S. *J. Chem. Commun.* **2012**, *48*, 1467.
- (1350) Park, C.-L.; Jee, A. Y.; Lee, M.; Lee, S.-g. *Chem. Commun.* **2009**, *5576*.
- (1351) Iwashita, Y.; Sugiyasu, K.; Ikeda, M.; Fujita, N.; Shinkai, S. *Chem. Lett.* **2004**, *33*, 1124.
- (1352) Bernet, A.; Albuquerque, R. Q.; Behr, M.; Hoffmann, S. T.; Schmidt, H.-W. *Soft Matter* **2012**, *8*, 66.
- (1353) Hashimoto, M.; Ujiie, S.; Mori, A. *Adv. Mater.* **2003**, *15*, 797.
- (1354) Kubo, K.; Mori, A.; Ujiie, S.; Tschierske, C. *J. Oleo Sci.* **2004**, *53*, 575.
- (1355) Kubo, K.; Mori, A. *Chem. Lett.* **2005**, *34*, 1250.
- (1356) Lu, C. C.; Su, S. K. *Supramol. Chem.* **2009**, *21*, 547.
- (1357) Zhang, X.; Lu, R.; Jia, J.; Liu, X.; Xue, P.; Xu, D.; Zhou, H. *Chem. Commun.* **2010**, *46*, 8419.
- (1358) Zhang, X.; Liu, X.; Lu, R.; Zhang, H.; Gong, P. *J. Mater. Chem.* **2012**, *22*, 1167.
- (1359) Liu, Y.; Lam, J. W. Y.; Mahtab, F.; Kwok, R. T. K.; Tang, B. Z. *Front. Chem. China* **2010**, *5*, 325.
- (1360) Wang, H.; Pang, D.; Xin, H.; Li, M.; Zhang, P.; Tian, W. *Liq. Cryst.* **2006**, *33*, 439.
- (1361) Zhang, P.; Wang, H.; Liu, H.; Li, M. *Langmuir* **2010**, *26*, 10183.
- (1362) Nayak, M. K.; Kim, B.-H.; Kwon, J. E.; Park, S.; Seo, J.; Chung, J. W.; Park, S. Y. *Chem. —Eur. J.* **2010**, *16*, 7437.
- (1363) Tseng, K.-P.; Kao, M.-T.; Tsai, T. W. T.; Hsu, C.-H.; Chan, J. C. C.; Shyue, J.-J.; Sun, S.-S.; Wong, K.-T. *Chem. Commun.* **2012**, *48*, 3515.
- (1364) Néabo, J. R.; Vigier-Carrière, C.; Rondeau-Gagné, S.; Morin, J.-F. *Chem. Commun.* **2012**, *48*, 10144.
- (1365) Wang, G.-T.; Lin, J.-B.; Jiang, X.-K.; Li, Z.-T. *Langmuir* **2009**, *25*, 8414.
- (1366) Shigeno, M.; Yamaguchi, M. *Chem. Commun.* **2012**, *48*, 6139.
- (1367) Minkenberg, C. B.; Hendriksen, W. E.; Li, F.; Mendes, E.; Elkema, R.; van Esch, J. H. *Chem. Commun.* **2012**, *48*, 9837.
- (1368) Yamamoto, Y. *Sci. Technol. Adv. Mater.* **2012**, *13*, 033001.
- (1369) Yamamoto, Y.; Jin, W.; Fukushima, T.; Minari, T.; Tsukagoshi, K.; Saeki, A.; Seki, S.; Tagawa, S.; Aida, T. *Chem. Lett.* **2009**, *38*, 888.
- (1370) Katakabe, T.; Kaneko, T.; Watanabe, M.; Fukushima, T.; Aida, T. *J. Electrochem. Soc.* **2005**, *152*, A1913.
- (1371) Tsumura, A.; Koezuka, K.; Ando, T. *Appl. Phys. Lett.* **1986**, *49*, 1210.
- (1372) *Organic Electronics: Materials, Manufacturing and Applications*; Klauk, H., Ed.; Wiley-VCH; Weinheim, Germany, 2006.
- (1373) Murphy, A. R.; Fréchet, J. M. J. *Chem. Rev.* **2007**, *107*, 1066.
- (1374) Smith, J.; Hamilton, R.; McCulloch, I.; Stingelin-Stutzmann, N.; Heeney, M.; Bradley, D. D. C.; Anthopoulos, T. D. *J. Mater. Chem.* **2010**, *20*, 2562.
- (1375) Mas-Torrent, M.; Rovira, C. *Chem. Soc. Rev.* **2008**, *37*, 827.
- (1376) Armaroli, N.; Balzani, V. *Chem.—Asian J.* **2011**, *6*, 768.
- (1377) Roncali, J. *Acc. Chem. Res.* **2009**, *42*, 1719.

- (1378) Hains, A. W.; Liang, Z.; Woodhouse, M. A.; Gregg, B. A. *Chem. Rev.* **2010**, *110*, 6689.
- (1379) *New Concepts in Solar Cells*; Somani, P. R., Umeno, M., Eds.; Wiley-VCH: Weinheim, Germany, 2009.
- (1380) Heremans, P.; Cheyns, D.; Rand, B. P. *Acc. Chem. Res.* **2010**, *42*, 1740.
- (1381) Padinger, F.; Rittberger, R. S.; Sariciftci, N. S. *Adv. Funct. Mater.* **2003**, *13*, 85.
- (1382) Kubo, W.; Murakoshi, K.; Kitamura, T.; Yoshida, S.; Haruki, M.; Hanabusa, K.; Shirai, H.; Wada, Y.; Yanagida, S. *J. Phys. Chem. B* **2001**, *105*, 12809.
- (1383) Kubo, W.; Kitamura, T.; Hanabusa, K.; Wada, Y.; Yanagida, S. *Chem. Commun.* **2002**, 374.
- (1384) Mohmeyer, N.; Wang, P.; Schmidt, H.-W.; Zakeeruddin, S. M.; Grätzel, M. *J. Mater. Chem.* **2004**, *14*, 1905.
- (1385) Usui, H.; Matsui, H.; Tanabe, N.; Yanagida, S. *J. Photochem. Photobiol., A* **2004**, *164*, 97.
- (1386) Kim, B.-G.; Jeong, E. J.; Park, H. J.; Bilby, D.; Guo, L. J.; Kim, J. *ACS Appl. Mater. Interfaces* **2011**, *3*, 674.
- (1387) Varghese, S.; Das, S. *J. Phys. Chem. Lett.* **2011**, *2*, 863.
- (1388) Srinivasan, S.; Babu, P. A.; Mahesh, S.; Ajayaghosh, A. *J. Am. Chem. Soc.* **2009**, *131*, 15122.
- (1389) Zhao, Y.; Gao, Y.; Zhan, D.; Liu, H.; Zhao, Q.; Kou, Y.; Shao, Y.; Li, M.; Zhuang, Q.; Zhu, Z. *Talanta* **2005**, *66*, 51.
- (1390) Kandanelli, R.; Bhowmik, S.; Maitra, U. *J. Indian Chem. Soc.* **2011**, *88*, 1903.
- (1391) Raghavan, S. R.; Douglas, J. F. *Soft Matter* **2012**, *8*, 8539.
- (1392) Sajisha, V. S.; Maitra, U. *Chimica* **2013**, *67*, 44.
- (1393) Raeburn, J.; Zamith Cardoso, A.; Adams, D. *J. Chem. Soc. Rev.* **2013**, *42*, S143.
- (1394) Segarra-Maset, M. D.; Nebot, V. J.; Miravet, J. F.; Escuder, B. *Chem. Soc. Rev.* **2013**, *42*, 7086.
- (1395) Sui, X.; Feng, X.; Hempenius, M. A.; Vancso, G. J. *J. Mater. Chem. B* **2013**, *1*, 1658.
- (1396) D'Aléo, A.; Del Guerzo, A.; Fages, F. Confocal Laser Scanning Microscopy: A Versatile Spectroscopic Tool for the Investigation of Molecular Gels. In *Analytical Methods in Supramolecular Chemistry*, 2nd ed.; Schalley, C. A., Ed.; Wiley-VCH: Weinheim, Germany, 2012, pp 607.
- (1397) Yu, G.; Yan, X.; Han, C.; Huang, F. *Chem. Soc. Rev.* **2013**, *42*, 6697.
- (1398) Busseron, E.; Ruff, Y.; Moulin, E.; Giuseppone, N. *Nanoscale* **2013**, *5*, 7098.
- (1399) Tu, T.; Fang, W.; Sun, Z. *Adv. Mater.* **2013**, *25*, 5304.
- (1400) *Soft Fibrillar Materials: Fabrication and Applications*; Liu, X. Y., Li, J.-L., Eds.; Wiley-VCH: Weinheim, Germany, 2013.
- (1401) Kumar, D. K.; Steed, J. W. *Chem. Soc. Rev.* **2014**, DOI: 10.1039/c3cs60224a.
- (1402) Anzenbacher, P., Jr; Liu, Y.-L.; Kozelkova, M. E. *Curr. Opin. Chem. Biol.* **2010**, *14*, 693.
- (1403) Ikeda, M.; Ochi, R.; Hamachi, I. *Lab Chip* **2010**, *10*, 3325.
- (1404) Hahn, M. E.; Gianneschi, N. C. *Chem. Commun.* **2011**, *47*, 11814.
- (1405) Huang, Y.; Wei, Z. *Chin. Sci. Bull.* **2012**, *57*, 4246.
- (1406) Bhattacharya, S.; Samanta, S. K. Graphenes in Supramolecular Gels and in Biological Systems. In *Graphene: Synthesis, Properties, and Phenomena*; Rao, C. N. R., Sood, A. K., Eds.; Wiley-VCH: Weinheim, Germany, 2012; p 339.
- (1407) Kim, S. H.; Parquette, J. R. *Nanoscale* **2012**, *4*, 6940.
- (1408) Tomasini, C.; Castellucci, N. *Chem. Soc. Rev.* **2013**, *42*, 156.
- (1409) Ikeda, M. *Bull. Chem. Soc. Jpn.* **2013**, *86*, 10.
- (1410) Dasgupta, A.; Mondal, J. H.; Das, D. *RSC Adv.* **2013**, *3*, 9117.
- (1411) Tovar, J. D. *Acc. Chem. Res.* **2013**, *46*, 1527.
- (1412) Balachandran, V. S.; Jadhav, S. R.; Vemula, P. K.; John, G. *Chem. Soc. Rev.* **2013**, *42*, 427.
- (1413) Brassinne, J.; Fustin, C.-A.; Gohy, J.-F. *J. Inorg. Organomet. Polym.* **2013**, *23*, 24.
- (1414) Jung, J. H.; Lee, J. H.; Silverman, J. R.; John, G. *Chem. Soc. Rev.* **2013**, *42*, 924.
- (1415) Zhang, J.; Su, C.-Y. *Coord. Chem. Rev.* **2013**, *257*, 1373.
- (1416) Tam, A. Y.-Y.; Yam, V. W.-W. *Chem. Soc. Rev.* **2013**, *42*, 1540.
- (1417) Lanigan, N.; Wang, X. *Chem. Commun.* **2013**, *49*, 8133.
- (1418) Knaapila, M.; Monkman, A. P. *Adv. Mater.* **2013**, *25*, 1090.
- (1419) Evans, R. C. *J. Mater. Chem. C* **2013**, *1*, 4190.
- (1420) Dong, B.; Maeda, H. *Chem. Commun.* **2013**, *49*, 4085.
- (1421) Kartha, K. K.; Mukhopadhyay, R. D.; Ajayaghosh, A. *Chimia* **2013**, *67*, 51.
- (1422) Zhao, Z.; Lam, J. W. Y.; Tang, B. Z. *Soft Matter* **2013**, *9*, 4564.
- (1423) Tsutsumi, H.; Miura, H. *Mol. BioSyst.* **2013**, *9*, 609.
- (1424) Seki, T.; Lin, X.; Yagai, S. *Asian J. Org. Chem.* **2013**, *2*, 708.
- (1425) Rao, M. R.; Sun, S.-S. *Langmuir* **2013**, DOI: 10.1021/la402449e.
- (1426) Yamaguchi, H.; Kobayashi, Y.; Kobayashi, R.; Takashima, Y.; Hashidzume, A.; Harada, A. *Nat. Commun.* **2012**, *3*, DOI: 10.1038/ncomms1617.
- (1427) Clemente, M. J.; Tejedor, R. M.; Romero, P.; Fitremann, J.; Oriol, L. *RSC Adv.* **2012**, *2*, 11419.
- (1428) Velema, W. A.; Stuart, M. C. A.; Szymanski, W.; Feringa, B. L. *Chem. Commun.* **2013**, *49*, 5001.
- (1429) Fatás, P.; Bachl, J.; Oehm, S.; Jiménez, A. I.; Cativiela, C.; Díaz Díaz, D. *Chem.—Eur. J.* **2013**, *19*, 8861.
- (1430) Zhu, L.; Li, X.; Wu, S.; Nguyen, K. T.; Yan, H.; Ågren, H.; Zhao, Y. *J. Am. Chem. Soc.* **2013**, *135*, 9174.
- (1431) Lee, S.; Oh, S.; Lee, J.; Malpani, Y.; Jung, Y.-S.; Kang, B.; Lee, J. Y.; Ozasa, K.; Isoshima, T.; Lee, S. Y.; Hara, M.; Hashizume, D.; Kim, J.-M. *Langmuir* **2013**, *29*, 5869.
- (1432) Zhou, L.; Li, J.; Luo, Q.; Zhu, J.; Zou, H.; Gao, Y.; Wang, L.; Xu, J.; Dong, Z.; Liu, J. *Soft Matter* **2013**, *9*, 4635.
- (1433) Wang, J.; Yang, G.; Jiang, H.; Zou, G.; Zhang, Q. *Soft Matter* **2013**, *9*, 9785.
- (1434) Peng, S.; Guo, Q.; Hughes, T. C.; Hartley, P. G. *Langmuir* **2013**, DOI: 10.1021/la4030469.
- (1435) Cao, X.; Gao, A.; Lv, H.; Wu, Y.; Wang, X.; Fan, Y. *Org. Biomol. Chem.* **2013**, *11*, 7931.
- (1436) Maiti, D. K.; Banerjee, A. *Chem.—Asian J.* **2013**, *8*, 113.
- (1437) Chen, Y.-C.; Wang, H.; Li, D.-M.; Zheng, Y.-S. *Eur. J. Org. Chem.* **2013**, *1521*.
- (1438) Zhang, Y.; Liang, C.; Shang, H.; Ma, Y.; Jiang, S. *J. Mater. Chem. C* **2013**, *1*, 4472.
- (1439) Yagai, S.; Ishiwatari, K.; Lin, X.; Karatsu, T.; Kitamura, A.; Uemura, S. *Chem.—Eur. J.* **2013**, *19*, 6971.
- (1440) Wan, X.; Jiang, Y.; Zeng, F.; Gong, Y.; Guo, Z.; Chen, C.-F. *Soft Matter* **2013**, *9*, 7538.
- (1441) Zhang, J.; Jin, J.; Zou, L.; Tian, H. *Chem. Commun.* **2013**, *49*, 9926.
- (1442) Shigemitsu, H.; Hisaki, I.; Senga, H.; Yasumiya, D.; Thakur, T. S.; Saeki, A.; Seki, S.; Tohnai, N.; Miyata, M. *Chem.—Asian J.* **2013**, *8*, 1372.
- (1443) Shigemitsu, H.; Hisaki, I.; Kometani, E.; Yasumiya, D.; Sakamoto, Y.; Osaka, K.; Thakur, T. S.; Saeki, A.; Seki, S.; Kimura, F.; Kimura, T.; Tohnai, N.; Miyata, M. *Chem.—Eur. J.* **2013**, *19*, 15366.
- (1444) Néabo, J. R.; Rondeau-Gagné, S.; Vigier-Carrière, C.; Morin, J.-F. *Langmuir* **2013**, *29*, 3446.
- (1445) Rondeau-Gagné, S.; Néabo, J. R.; Desroches, M.; Levesque, I.; Daigle, M.; Cantin, K.; Morin, J.-F. *Chem. Commun.* **2013**, *49*, 9546.
- (1446) Chen, C.-T.; Chen, C.-H.; Ong, T.-G. *J. Am. Chem. Soc.* **2013**, *135*, 5294.
- (1447) Xu, J.-F.; Chen, Y.-Z.; Wu, D.; Wu, L.-Z.; Tung, C.-H.; Yang, Q.-Z. *Angew. Chem., Int. Ed.* **2013**, *52*, 9738.
- (1448) Cao, X.; Zhang, M.; Liu, K.; Mao, Y.; Lan, H.; Liu, B.; Yi, T. *Chin. Sci. Bull.* **2012**, *57*, 4272.
- (1449) Kolhe, N. B.; Devi, R. N.; Senanayak, S. P.; Jancy, B.; Narayan, K. S.; Asha, S. K. *J. Mater. Chem.* **2012**, *22*, 15235.
- (1450) Kar, H.; Molla, M. R.; Ghosh, S. *Chem. Commun.* **2013**, *49*, 4220.
- (1451) Narayan, B.; Kulkarni, C.; George, S. *J. J. Mater. Chem. C* **2013**, *1*, 626.

- (1452) Collin, D.; Covis, R.; Allix, F.; Jamart-Grégoire, B.; Martinoty, P. *Soft Matter* **2013**, *9*, 2947.
- (1453) Basak, S.; Nanda, J.; Banerjee, A. *Chem. Commun.* **2013**, *49*, 6891.
- (1454) Das, A.; Maity, B.; Koley, D.; Ghosh, S. *Chem. Commun.* **2013**, *49*, 5757.
- (1455) Aparicio, F.; Sánchez, L. *Chem.—Eur. J.* **2013**, *19*, 10482.
- (1456) Peng, H.; Ding, L.; Liu, T.; Chen, X.; Li, L.; Yin, S.; Fang, Y. *Chem.—Asian J.* **2012**, *7*, 1576.
- (1457) Roy, S.; Kumar Maiti, D.; Panigrahi, S.; Basak, D.; Banerjee, A. *RSC Adv.* **2012**, *2*, 11053.
- (1458) Lin, X.; Hirono, M.; Seki, T.; Kurata, H.; Karatsu, T.; Kitamura, A.; Kuzuhara, D.; Yamada, H.; Ohba, T.; Saeki, A.; Seki, S.; Yagai, S. *Chem.—Eur. J.* **2013**, *19*, 6561.
- (1459) Datar, A.; Balakrishnan, K.; Zang, L. *Chem. Commun.* **2013**, *49*, 6894.
- (1460) Sukul, P. K.; Singh, P. K.; Maji, S. K.; Malik, S. *J. Mater. Chem. B* **2013**, *1*, 153.
- (1461) García, F.; Buendía, J.; Ghosh, S.; Ajayaghosh, A.; Sánchez, L. *Chem. Commun.* **2013**, *49*, 9278.
- (1462) Ohasedo, Y.; Miyamoto, M.; Oono, M.; Shikii, K.; Tanaka, A. *RSC Adv.* **2013**, *3*, 3844.
- (1463) Ohasedo, Y.; Miyamoto, M.; Tanaka, A.; Watanabe, H. *New J. Chem.* **2013**, *37*, 2874.
- (1464) Malicka, J. M.; Sandeep, A.; Monti, F.; Bandini, E.; Gazzano, M.; Ranjith, C.; Praveen, V. K.; Ajayaghosh, A.; Armaroli, N. *Chem.—Eur. J.* **2013**, *19*, 12991.
- (1465) Ghosh, K.; Kar, D. *Org. Biomol. Chem.* **2012**, *10*, 8800.
- (1466) Zhang, Q.; Qu, D.-H.; Wu, J.; Ma, X.; Wang, Q.; Tian, H. *Langmuir* **2013**, *29*, 5345.
- (1467) Pan, S.; Luo, S.; Li, S.; Lai, Y.; Geng, Y.; He, B.; Gu, Z. *Chem. Commun.* **2013**, *49*, 8045.
- (1468) Zhang, Q.-W.; Qu, D.; Ma, X.; Tian, H. *Chem. Commun.* **2013**, *49*, 9800.
- (1469) Cao, H.; Duan, P.; Zhu, X.; Jiang, J.; Liu, M. *Chem.—Eur. J.* **2012**, *18*, 5546.
- (1470) Edelsztein, V. C.; Jares-Erijman, E. A.; Müllen, K.; Di Chenna, P. H.; Spagnuolo, C. C. *J. Mater. Chem.* **2012**, *22*, 21857.
- (1471) D'Anna, F.; Vitale, P.; Marullo, S.; Noto, R. *Langmuir* **2012**, *28*, 10849.
- (1472) Koley, P.; Pramanik, A. *Soft Matter* **2012**, *8*, 5364.
- (1473) Cao, X.; Wang, H.; Liu, J.; Gao, A.; Yi, T.; Fan, Y. *Supramol. Chem.* **2013**, *25*, 881.
- (1474) Nanda, J.; Biswas, A.; Adhikari, B.; Banerjee, A. *Angew. Chem., Int. Ed.* **2013**, *52*, 5041.
- (1475) Nanda, J.; Biswas, A.; Banerjee, A. *Soft Matter* **2013**, *9*, 4198.
- (1476) Roy, S.; Baral, A.; Banerjee, A. *Chem. —Eur. J.* **2013**, *19*, 14950.
- (1477) Zhang, L.; Liu, C.; Jin, Q.; Zhu, X.; Liu, M. *Soft Matter* **2013**, *9*, 7966.
- (1478) Yan, N.; Xu, Z.; Diehn, K. K.; Raghavan, S. R.; Fang, Y.; Weiss, R. G. *Langmuir* **2013**, *29*, 793.
- (1479) Yan, N.; Xu, Z.; Diehn, K. K.; Raghavan, S. R.; Fang, Y.; Weiss, R. G. *J. Am. Chem. Soc.* **2013**, *135*, 8989.
- (1480) Li, X.; Du, X.; Li, J.; Gao, Y.; Pan, Y.; Shi, J.; Zhou, N.; Xu, B. *Langmuir* **2012**, *28*, 13512.
- (1481) Gao, Y.; Shi, J.; Yuan, D.; Xu, B. *Nat. Commun.* **2012**, *3*, DOI: 10.1038/ncomms2040.
- (1482) Kuang, Y.; Xu, B. *Angew. Chem., Int. Ed.* **2013**, *52*, 6944.
- (1483) Li, J.; Kuang, Y.; Shi, J.; Gao, Y.; Zhou, J.; Xu, B. *Beilstein J. Org. Chem.* **2013**, *9*, 908.
- (1484) Li, J.; Kuang, Y.; Gao, Y.; Du, X.; Shi, J.; Xu, B. *J. Am. Chem. Soc.* **2013**, *135*, 542.
- (1485) Zhang, Y.; Zhang, B.; Kuang, Y.; Gao, Y.; Shi, J.; Zhang, X. X.; Xu, B. *J. Am. Chem. Soc.* **2013**, *135*, 5008.
- (1486) Li, J.; Gao, Y.; Kuang, Y.; Shi, J.; Du, X.; Zhou, J.; Wang, H.; Yang, Z.; Xu, B. *J. Am. Chem. Soc.* **2013**, *135*, 9907.
- (1487) Zhang, Y.; Zhou, R.; Shi, J.; Zhou, N.; Epstein, I. R.; Xu, B. *J. Phys. Chem. B* **2013**, *117*, 6566.
- (1488) Kuang, Y.; Yuan, D.; Zhang, Y.; Kao, A.; Du, X.; Xu, B. *RSC Adv.* **2013**, *3*, 7704.
- (1489) Li, J.; Li, X.; Kuang, Y.; Gao, Y.; Du, X.; Shi, J.; Xu, B. *Adv. Healthcare Mater.* **2013**, DOI: 10.1002/adhm.201300041.
- (1490) Gao, Y.; Berciu, C.; Kuang, Y.; Shi, J.; Nicastro, D.; Xu, B. *ACS Nano* **2013**, *7*, 9055.
- (1491) Rasale, D. B.; Maity, I.; Das, A. K. *RSC Adv.* **2012**, *2*, 9791.
- (1492) Nakagawa, T.; Amakatsu, M.; Munenobu, K.; Fujii, H.; Yamanaka, M. *Chem. Lett.* **2013**, *42*, 229.
- (1493) Qin, S.-Y.; Pei, Y.; Liu, X.-J.; Zhuo, R.-X.; Zhang, X.-Z. *J. Mater. Chem. B* **2013**, *1*, 668.
- (1494) Rajamalli, P.; Prasad, E. *Langmuir* **2013**, *29*, 1609.
- (1495) Edwards, W.; Smith, D. K. *J. Am. Chem. Soc.* **2013**, *135*, 5911.
- (1496) Hemamalini, A.; Das, T. M. *New J. Chem.* **2013**, *37*, 2419.
- (1497) Nalluri, S. K. M.; Ulijn, R. *Chem. Sci.* **2013**, *4*, 3699.
- (1498) Majumder, J.; Das, M. R.; Deb, J.; Jana, S. S.; Dastidar, P. *Langmuir* **2013**, *29*, 10254.
- (1499) Li, Y.; Ding, Y.; Qin, M.; Cao, Y.; Wang, W. *Chem. Commun.* **2013**, *49*, 8653.
- (1500) Tsai, C.-C.; Chang, K.-C.; Ho, I.-T.; Chu, J.-H.; Cheng, Y.-T.; Shen, L.-C.; Chung, W.-S. *Chem. Commun.* **2013**, *49*, 3037.
- (1501) Banerjee, S.; Das, R. K.; Terech, P.; de Geyer, A.; Aymonier, C.; Loppinet-Serani, A.; Raffy, G.; Maitra, U.; Del Guerzo, A.; Desvergne, J.-P. *J. Mater. Chem. C* **2013**, *1*, 3305.
- (1502) Dama, M.; Berger, S. *J. Phys. Chem. B* **2013**, *117*, 5788.
- (1503) Liu, W.-T.; Tohnai, N.; Hisaki, I.; Miyata, M.; Chen, W.-T.; Wu, Y.-J.; Liu, J.-H. *J. Polym. Sci., Part A: Polym. Chem.* **2013**, *51*, 793.
- (1504) Bag, B. G.; Majumdar, R.; Dinda, S. K.; Dey, P. P.; Maity, G. C.; Mallia, V. A.; Weiss, R. G. *Langmuir* **2013**, *29*, 1766.
- (1505) Zhang, M.; Wang, B.; Jiang, T.; Jiang, M.; Yi, T. *CrystEngComm* **2012**, *14*, 8057.
- (1506) Roy, S.; Javid, N.; Sefcik, J.; Halling, P. J.; Ulijn, R. V. *Langmuir* **2012**, *28*, 16664.
- (1507) Cao, H.; Yuan, Q.; Zhu, X.; Zhao, Y.-P.; Liu, M. *Langmuir* **2012**, *28*, 15410.
- (1508) Cao, H.; Zhu, X.; Liu, M. *Angew. Chem., Int. Ed.* **2013**, *52*, 4122.
- (1509) Rodriguez, A. L.; Parish, C. L.; Nisbet, D. R.; Williams, R. J. *Soft Matter* **2013**, *9*, 3915.
- (1510) Lin, J.; Yu, Z.; Zhu, W.; Xing, G.; Lin, Z.; Yang, S.; Xie, L.; Niu, C.; Huang, W. *Polym. Chem.* **2013**, *4*, 477.
- (1511) Ding, B.; Li, Y.; Qin, M.; Ding, Y.; Cao, Y.; Wang, W. *Soft Matter* **2013**, *9*, 4672.
- (1512) Johnson, E. K.; Chen, L.; Kubiak, P. S.; McDonald, S. F.; Adams, D. J.; Cameron, P. J. *Chem. Commun.* **2013**, *49*, 8698.
- (1513) Fleming, S.; Debnath, S.; Frederix, P. W. J. M.; Tuttle, T.; Ulijn, R. V. *Chem. Commun.* **2013**, *49*, 10587.
- (1514) Maeda, H.; Chigusa, K.; Sakurai, T.; Ohta, K.; Uemura, S.; Seki, S. *Chem.—Eur. J.* **2013**, *19*, 9224.
- (1515) Bando, Y.; Sakurai, T.; Seki, S.; Maeda, H. *Chem.—Asian J.* **2013**, *8*, 2088.
- (1516) Dong, B.; Sakurai, T.; Bando, Y.; Seki, S.; Takaishi, K.; Uchiyama, M.; Muranaka, A.; Maeda, H. *J. Am. Chem. Soc.* **2013**, *135*, 14797.
- (1517) Buerkle, L. E.; von Recum, H. A.; Rowan, S. J. *Chem. Sci.* **2012**, *3*, 564.
- (1518) Griffith, A.; Bandy, T. J.; Light, M.; Stulz, E. *Chem. Commun.* **2013**, *49*, 731.
- (1519) Ahn, J.; Park, S.; Lee, J. H.; Jung, S. H.; Moon, S.-J.; Jung, J. H. *Chem. Commun.* **2013**, *49*, 2109.
- (1520) Jin, Q.; Zhang, L.; Liu, M. *Chem.—Eur. J.* **2013**, *19*, 9234.
- (1521) Bairi, P.; Roy, B.; Chakraborty, P.; Nandi, A. K. *ACS Appl. Mater. Interfaces* **2013**, *5*, 5478.
- (1522) Qian, C.; Cao, K.; Liu, X.; Zhang, X.; Xu, D.; Xue, P.; Lu, R. *Chin. Sci. Bull.* **2012**, *57*, 4264.
- (1523) Yu, X.; Li, Y.; Wu, D.; Ma, Z.; Xing, S. *New J. Chem.* **2013**, *37*, 1201.
- (1524) van Herpt, J. T.; Stuart, M. C. A.; Browne, W. R.; Feringa, B. L. *Langmuir* **2013**, *29*, 8763.

- (1525) Prabhu, D. D.; Kumar, N. S. S.; Sivadas, A. P.; Varghese, S.; Das, S. *J. Phys. Chem. B* **2012**, *116*, 13071.
- (1526) Dumur, F.; Contal, E.; Wantz, G.; Phan, T. N. T.; Bertin, D.; Gigmes, D. *Chem.—Eur. J.* **2013**, *19*, 1373.
- (1527) Zhao, C.; Bai, B.; Wang, H.; Qu, S.; Xiao, G.; Tian, T.; Li, M. *J. Mol. Struct.* **2013**, *1037*, 130.
- (1528) Zhao, C.; Wang, H.; Bai, B.; Qu, S.; Song, J.; Ran, X.; Zhang, Y.; Li, M. *New J. Chem.* **2013**, *37*, 1454.
- (1529) Zhao, C.; Wang, H.; Qu, S.; Zhang, P.; Bai, B.; Ran, X.; Liu, H.; Zhang, Y.; Li, M. *Soft Materials* **2013**, *11*, 261.
- (1530) Xu, Z.; Peng, J.; Yan, N.; Yu, H.; Zhang, S.; Liu, K.; Fang, Y. *Soft Matter* **2013**, *9*, 1091.
- (1531) Haino, T.; Hirai, Y.; Ikeda, T.; Saito, H. *Org. Biomol. Chem.* **2013**, *11*, 4164.
- (1532) Ishii, T.; Nakamura, N.; Amemori, S.; Kasatani, K.; Gorohmaru, H.; Ishida, M.; Shigeiwa, M. *Dyes Pigm.* **2013**, *99*, 14.
- (1533) Liu, Y.; Zheng, N.; Li, H.; Yin, B. *Soft Matter* **2013**, *9*, 5261.
- (1534) Tatewaki, Y.; Watanabe, T.; Watanabe, K.; Kikuchi, K.; Okada, S. *Dalton Trans.* **2013**, *42*, 16121.
- (1535) Danesh, C. D.; Starkweather, N. S.; Zhang, S. *J. Phys. Chem. B* **2012**, *116*, 12887.
- (1536) He, X.; Borau-Garcia, J.; Woo, A. Y. Y.; Trudel, S.; Baumgartner, T. *J. Am. Chem. Soc.* **2013**, *135*, 1137.
- (1537) He, X.; Lin, J.-B.; Kan, W. H.; Dong, P.; Trudel, S.; Baumgartner, T. *Adv. Funct. Mater.* **2013**, DOI: 10.1002/adfm.201302294.
- (1538) Dasgupta, D.; Srinivasan, S.; Ajayaghosh, A.; Guenet, J. M. *Macromol. Symp.* **2011**, *303*, 134.
- (1539) Dasgupta, D.; Guenet, J.-M. *Macromol. Chem. Phys.* **2013**, *214*, 1885.
- (1540) Rao, K. V.; George, S. *J. Chem.—Eur. J.* **2012**, *18*, 14286.
- (1541) Samanta, S. K.; Bhattacharya, S. *Chem.—Eur. J.* **2012**, *18*, 5875.
- (1542) Bhattacharya, S.; Samanta, S. K. *Chem.—Eur. J.* **2012**, *18*, 16632.
- (1543) Samanta, S. K.; Bhattacharya, S. *J. Mater. Chem.* **2012**, *22*, 25277.
- (1544) Samanta, S. K.; Bhattacharya, S. *Chem. Commun.* **2013**, *49*, 1425.
- (1545) Bhagat, D.; Samanta, S. K.; Bhattacharya, S. *Sci. Rep.* **2013**, *3*, DOI: 10.1038/srep01294.
- (1546) Dey, N.; Samanta, S. K.; Bhattacharya, S. *ACS Appl. Mater. Interfaces* **2013**, *214*, 1885.
- (1547) Yamauchi, M.; Kubota, S.; Karatsu, T.; Kitamura, A.; Ajayaghosh, A.; Yagai, S. *Chem. Commun.* **2013**, *49*, 4941.
- (1548) Xue, P.; Xu, Q.; Gong, P.; Qian, C.; Ren, A.; Zhang, Y.; Lu, R. *Chem. Commun.* **2013**, *49*, 5838.
- (1549) Xue, P.; Lu, R.; Zhang, P.; Jia, J.; Xu, Q.; Zhang, T.; Takafuji, M.; Ihara, H. *Langmuir* **2013**, *29*, 417.
- (1550) Xue, P.; Sun, J.; Xu, Q.; Lu, R.; Takafuji, M.; Ihara, H. *Org. Biomol. Chem.* **2013**, *11*, 767.
- (1551) zur Borg, L.; Domanski, A. L.; Berger, R.; Zentel, R. *Macromol. Chem. Phys.* **2013**, *214*, 975.
- (1552) Lin, J.; Guo, Z.; Plas, J.; Amabilino, D. B.; De Feyter, S.; Schenning, A. P. H. *J. Chem. Commun.* **2013**, *49*, 9320.
- (1553) Marciel, A. B.; Tanyeri, M.; Wall, B. D.; Tovar, J. D.; Schroeder, C. M.; Wilson, W. L. *Adv. Mater.* **2013**, *25*, 6398.
- (1554) Rondeau-Gagné, S.; Néabo, J. R.; Desroches, M.; Larouche, J.; Brisson, J.; Morin, J.-F. *J. Am. Chem. Soc.* **2013**, *135*, 110.
- (1555) Xing, L.-B.; Yang, B.; Wang, X.-J.; Wang, J.-J.; Chen, B.; Wu, Q.; Peng, H.-X.; Zhang, L.-P.; Tung, C.-H.; Wu, L.-Z. *Langmuir* **2013**, *29*, 2843.
- (1556) Pérez, A.; de Saá, D.; Ballesteros, A.; Serrano, J. L.; Sierra, T.; Romero, P. *Chem.—Eur. J.* **2013**, *19*, 10271.
- (1557) Ichinose, W.; Ito, J.; Yamaguchi, M. *Angew. Chem., Int. Ed.* **2013**, *S2*, 5290.
- (1558) Yamamoto, K.; An, Z.; Saito, N.; Yamaguchi, M. *Chem.—Eur. J.* **2013**, *19*, 10580.
- (1559) Ichinose, W.; Miyagawa, M.; Yamaguchi, M. *Chem. Mater.* **2013**, DOI: 10.1021/cm4024869.
- (1560) Banno, M.; Wu, Z.-Q.; Makiguchi, W.; Furusho, Y.; Yashima, E. *ChemPlusChem* **2013**, DOI: 10.1002/cplu.201300108.
- (1561) Grunder, S.; Valente, C.; Whalley, A. C.; Sampath, S.; Portmann, J.; Botros, Y. Y.; Stoddart, J. F. *Chem.—Eur. J.* **2012**, *18*, 15632.
- (1562) Zep, A.; Salamonczyk, M.; Vaupotič, N.; Pociecha, D.; Gorecka, E. *Chem. Commun.* **2013**, *49*, 3119.
- (1563) Sukul, P. K.; Malik, S. *RSC Adv.* **2013**, *3*, 1902.
- (1564) Rahman, M. J.; Shimizu, H.; Araki, Y.; Ikeda, H.; Iyoda, M. *Chem. Commun.* **2013**, *49*, 9251.
- (1565) Pourjavadi, A.; Doulabi, M.; Soleyman, R. *Polym. Int.* **2013**, *62*, 179.
- (1566) Sankar, R. M.; Meera, K. M. S.; Samanta, D.; Murali, A.; Jithendra, P.; Baran Mandal, A.; Jaisankar, S. N. *RSC Adv.* **2012**, *2*, 12424.
- (1567) Maggini, L.; Liu, M.; Ishida, Y.; Bonifazi, D. *Adv. Mater.* **2013**, *25*, 2462.
- (1568) Mandal, S. K.; Kar, T.; Das, P. K. *Chem.—Eur. J.* **2013**, *19*, 12486.
- (1569) Zamora-Ledezma, C.; Buisson, L.; Moulton, S. E.; Wallace, G.; Zakri, C.; Blanc, C.; Anglaret, E.; Poulin, P. *Langmuir* **2013**, *29*, 10247.
- (1570) Tunckol, M.; Fantini, S.; Malbosc, F.; Durand, J.; Serp, P. *Carbon* **2013**, *57*, 209.
- (1571) Tao, C.-a.; Wang, J.; Qin, S.; Lv, Y.; Long, Y.; Zhu, H.; Jiang, Z. *J. Mater. Chem.* **2012**, *22*, 24856.
- (1572) Gao, H.; Sun, Y.; Zhou, J.; Xu, R.; Duan, H. *ACS Appl. Mater. Interfaces* **2013**, *5*, 425.
- (1573) Srinivasan, S.; Shin, W. H.; Choi, J. W.; Coskun, A. *J. Mater. Chem. A* **2013**, *1*, 43.
- (1574) Huang, P.; Chen, W.; Yan, L. *Nanoscale* **2013**, *5*, 6034.
- (1575) Guo, W.; Cheng, C.; Wu, Y.; Jiang, Y.; Gao, J.; Li, D.; Jiang, L. *Adv. Mater.* **2013**, *25*, 6064.
- (1576) Rao, K. V.; Datta, K. K. R.; Eswaramoorthy, M.; George, S. J. *Adv. Mater.* **2013**, *25*, 1713.
- (1577) Chen, L.; Mali, K. S.; Puniredd, S. R.; Baumgarten, M.; Parvez, K.; Pisula, W.; De Feyter, S.; Müllen, K. *J. Am. Chem. Soc.* **2013**, *135*, 13531.
- (1578) Boiani, M.; Baschieri, A.; Cesari, C.; Mazzoni, R.; Stagni, S.; Zacchini, S.; Sambri, L. *New J. Chem.* **2012**, *36*, 1469.
- (1579) Jana, P.; Maity, S.; Maity, S. K.; Ghorai, P. K.; Haldar, D. *Soft Matter* **2012**, *8*, 5621.
- (1580) Wu, H.; Ni, B.-B.; Wang, C.; Zhai, F.; Ma, Y. *Soft Matter* **2012**, *8*, 5486.
- (1581) Sun, F.; Zhang, G.; Zhang, D. *Chin. Sci. Bull.* **2012**, *57*, 4284.
- (1582) Rajamalli, P.; Atta, S.; Maity, S.; Prasad, E. *Chem. Commun.* **2013**, *49*, 1744.
- (1583) Zang, L.; Shang, H.; Wei, D.; Jiang, S. *Sens. Actuators, B* **2013**, *185*, 389.
- (1584) Ochi, R.; Kurotani, K.; Ikeda, M.; Kiyonaka, S.; Hamachi, I. *Chem. Commun.* **2013**, *49*, 2115.
- (1585) Bielejewski, M.; Kowalcuk, J.; Kaszyńska, J.; Łapiński, A.; Luboradzki, R.; Demchuk, O.; Tritt-Goc, J. *Soft Matter* **2013**, *9*, 7501.
- (1586) Mattarella, M.; Haberl, J. M.; Ruokolainen, J.; Landau, E. M.; Mezzenga, R.; Siegel, J. S. *Chem. Commun.* **2013**, *49*, 7204.
- (1587) Sagade, A. A.; Rao, K. V.; Mogera, U.; George, S. J.; Datta, A.; Kulkarni, G. U. *Adv. Mater.* **2013**, *25*, 559.
- (1588) Nishiyabu, R.; Kobayashi, H.; Kubo, Y. *RSC Adv.* **2012**, *2*, 6555.
- (1589) Bhalla, V.; Arora, H.; Singh, H.; Kumar, M. *Dalton Trans.* **2013**, *42*, 969.
- (1590) Bhalla, V.; Gupta, A.; Kumar, M.; Rao, D. S. S.; Prasad, S. K. *ACS Appl. Mater. Interfaces* **2013**, *5*, 672.